TECTONOSTRATIGRAPHY, STRUCTURE AND METAMORPHISM OF THE ARCHAEAN ILANGWE GRANITE – GREENSTONE BELT SOUTH OF MELMOTH, KWAZULU – NATAL

by

Humphrey Lawrence Mbendeni Mathe

Submitted in fulfilment of the requirements
for the degree of Doctor of Philosophy
in the Department of Geology, University of Natal, Durban

November 1997

DECLARATION

I declare that all the work presented in this thesis is my own except where otherwise stated. I further declare that it has not been previously submitted to any other university for any degree or examination.

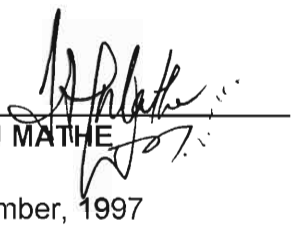

H L M MATHE

November, 1997

DEDICATION

1. I dedicate this work to the memory of my father, Moses George Manxeba Mathe, a teacher who encouraged us, his children, to get an education no matter what.

2. I also dedicate this work to all the humble and kind communities of Ilangwe and Nkandla who welcomed me and supported me in their beautiful, rugged, untamed and somewhat inhospitable land.

A B S T R A C T

TECTONOSTRATIGRAPHY, STRUCTURE AND METAMORPHISM OF THE ARCHAEAN ILANGWE GRANITE-GREENSTONE BELT SOUTH OF MELMOTH, KWAZULU-NATAL

The mapped area, measuring about 400m^2, is situated along the southern margin of the Archaean Kaapvaal Craton south of Melmoth in KwaZulu-Natal and comprises greenstones and metasediments forming a narrow, linear E-W trending and dominantly northerly inclined belt flanked to the north and south by various granitoids and granitoid gneisses which have been differentiated for the first time in this study. This belt is here referred to as the ***ILANGWE GREENSTONE BELT***.

The Ilangwe Belt rocks are grouped into the ***Umhlathuze Subgroup*** (a lower metavolcanic suite) and the ***Nkandla Subgroup*** (an upper metasedimentary suite). The former consists of :

(a) the ***Sabiza Formation***: a lower amphibolite association occurring along the southern margin of the greenstone belt;

(b) the ***Matshansundu Formation***: an eastern amphibolite-BIF association;

(c) the ***Olwenjini Formation***: an upper or northern amphibolite-banded chert-BIF association.

whereas the latter is sub-divided into :

(a) the ***Entembeni Formation***: a distinctive phyllite-banded chert-BIF association occurring in the central and the eastern parts of the belt;

(b) the ***Simbagwezi Formation***: a phyllite-banded chert-amphibolite association occurring in the western part of the belt, south-east of Nkandla;

(c) the ***Nomangci Formation***: a dominantly quartzite and quartz schist formation occurring in the western part of the belt, south-east of Nkandla.

The contacts between the six major tectonostratigraphic formations are tectonic.

In the eastern sector of the Ilangwe Belt, the lowermost metasedimentary formation, the Entembeni Formation, cuts across both the Sabiza and Matshansundu Formations (the lower formations of the Umhlathuze Subgroup) in a major deformed angular unconformity referred to as the ***Ndloziyana angular unconformity***. In the central parts of the belt, the Entembeni Formation structurally overlies the Olwenjini Formation in what seems to be a major local unconformity (disconformity). In the western sector of the belt, the Simbagwezi Formation occurs as a structural wedge between the lower and upper formations of the Umhlathuze Subgroup. That is, it structurally overlies the Sabiza Formation and structurally underlies the Olwenjini Formation. The uppermost metasedimentary unit, the Nomangci Formation occurs as a complex series of finger-like wedges cutting and extending into the Simbagwezi Formation and in each case showing that the Nomangci Formation structurally underlies the Simbagwezi Formation. This structural repetition of lithological units is suggestive of normal dip-slip duplex structures.

Palimpsest volcanic features, such as pillow structures and minor ocelli, indicate that many of the amphibolitic rocks represent metavolcanics, possibly transformed oceanic crust. This is also supported by limited major element geochemistry which suggests that the original rocks were ocean tholeiites. Evidence suggests that the talc-tremolite schists and the serpentinitic talc schists represent altered komatiites. The nature of the metasediments (represented by banded metacherts, quartzites and banded iron formations) and their similarity to those of the Barberton, Pietersburg and Nondweni greenstone complexes suggests that they were formed in relatively shallow water environments.

The Ilangwe magmatism is represented by different types of granitoids and granitoid gneisses and basic-ultrabasic intrusive bodies. Based on similar geochemical and mineralogical characteristics ***and*** on regional distribution, mutual associations and contact relationships, these granitoids and granitoid gneisses can be divided into three broad associations, viz :

(a) ***The Amazula Gneiss – Nkwalini Mylonitic Gneiss – Nkwalini Quartzo-feldspathic Flaser Gneiss Association:*** a migmatitic paragneiss and mylonitic to flaser gneiss association of ***older gneisses*** of Nondweni age occurring in several widely separated areas and intruded by younger granitoids.

(b) ***The early post-Nondweni Granitoids*** comprising the ***Nkwalinye Tonalitic Gneiss*** (a distinctive grey gneiss intrusive into the greenstones and older gneisses) and the ***Nsengeni Granitoid Suite*** (an association of three granitoid units of batholithic proportions flanking the greenstone belt and intrusive into the greenstones, older gneisses and Nkwalinye Tonalitic Gneiss).

(c) ***The late post-Nondweni Granitoids*** comprising the ***Impisi-Umgabhi Granitoid Suite***, a batholithic microcrystic to megacrystic association of five granitoid phases/units occurring to the north and south of the greenstone belt and intrusive into the greenstones, older gneisses and early post-Nondweni granitoids.

Limited major element geochemistry suggests that the granitoids and granitoid gneisses are of calc-alkaline origin and are of tonalitic, granodioritic, adamellitic and granitic composition. An igneous derivation from material located possibly at the lower crust or upper mantle is suggested.

At least three major episodes of deformation (D_1, D_2 and D_3) have been recognized in the greenstones. During D_1, a strong penetrative S_1 tectonic foliation developed parallel to the S_O primary layering and bedding. This period was characterized by intense transpositional layering, recumbent and isoclinal intrafolial folding with associated shearing,thrusting and structural repetition of greenstone lithologies. These processes took place in an essentially horizontal, high strain tectonic regime.

The first phase of deformation (D^G_1) in the migmatitic and mylonitic gneisses was also characterized by recumbent and isoclinal intrafolial folding and is remarkably similar to the D_1 deformational phase in the Ilangwe greenstones.

Structural features of the first phase of deformation suggest that it was dominated by formation of fold nappes and thrusts and was accompanied by prograde M_1 medium-grade middle to upper amphibolite facies metamorphism.

During D_2 deformation, the subhorizontal D_1 structures were refolded by new structures with steeply inclined axial planes. This resulted in the formation of superimposed Type 3 interference folding in the amphibolitic rocks and large-scale, E–W trending, doubly-plunging periclinal folds in the metasediments. These periclinal folds have steeply inclined and overturned limbs and are characterized by narrow, closed elliptical outcrop patterns well-defined by extensive banded ironstones and metacherts.

The second phase of deformation in the granitoids (D^G_2) was characterized by steeply plunging and steeply inclined small-scale tight to isoclinal ***similar*** folds. Large-scale folds are not present in the granitoids.

Evidence suggests that the second phase of deformation was a major compressional event which resulted in the large-scale upright, flattened flexural folds. It was accompanied by widespread regional greenschist metamorphism and the intrusion of the early post-Nondweni granitoids.

The third phase of deformation produced steeply plunging small-scale folds on the limbs and axial planes of the pre-existing large-scale F_2 folds and upright open folds in the granitoid terrain. This episode was characterized by the emplacement of the late post-Nondweni granitoids (along the D_2 greenstone ***boundary faults***) and is associated with two significant events of prograde M_3 upper greenschist facies metamorphism and retrograde M_3 lower greenschist facies metamorphism.

Post-D_3 deformation is characterized by late cross-cutting faults and the emplacement of younger basic - ultrabasic bodies.

CONTENTS

LIST OF PLATES

LIST OF FIGURES

LIST OF TABLES

CHAPTER 1

INTRODUCTION

1.1 PRESENT STUDY

The aim of this project was to study in detail the lithostratigraphy, tectonostratigraphy, geochemistry, structure and metamorphism of a granite-greenstone belt along the southern margin of the Kaapvaal Craton just south of Melmoth in Kwa-Zulu - Natal (Fig. 1.1).

The existence of the Archaean granite-greenstone complex in this deeply dissected and weathered terrain was first recorded by A L du Toit who carried out a pioneering geological survey of this region from 1916 to 1919 and documented it in the 2,35 miles to 1 inch Geological Survey Nkandla Sheet 109 and the accompanying explanation (du Toit, 1931). This survey revealed an extensive granitoid terrain containing a narrow, linear E-W trending and dominantly northerly inclined belt of greenstones some 3 to 4km wide extending for about 35km along strike.

Subsequent regional mapping has identified large-scale folds and faults within the greenstone belt, and major faults along its boundaries with the extensive granitic areas to the north and south (Matthews, 1972; Matthews and Charlesworth, 1981; 1:250 000 Geological Survey Dundee Sheet 2830, 1988). Recognition of these regional features clearly indicated the possibility of detailed systematic mapping of the granitoid terrain and detailed stratigraphic and structural investigation of the greenstone complex which is named the ***ILANGWE GREENSTONE BELT*** in this study. Further possible detailed studies indicated by the aforementioned regional mapping but not covered in this thesis are systematic geochronological and geophysical investigations of this Granite-Greenstone Complex.

The previous mapping had revealed that the Ilangwe greenstones form a narrow linear east-west trending and dominantly northerly-dipping belt of basaltic metalavas represented by chloritic schist, hornblende schist, actinolite schist, together with talc-, sericitic-, kyanite-, and garnet-bearing grunerite schist and subordinate basic metalavas, quartzite, cherty

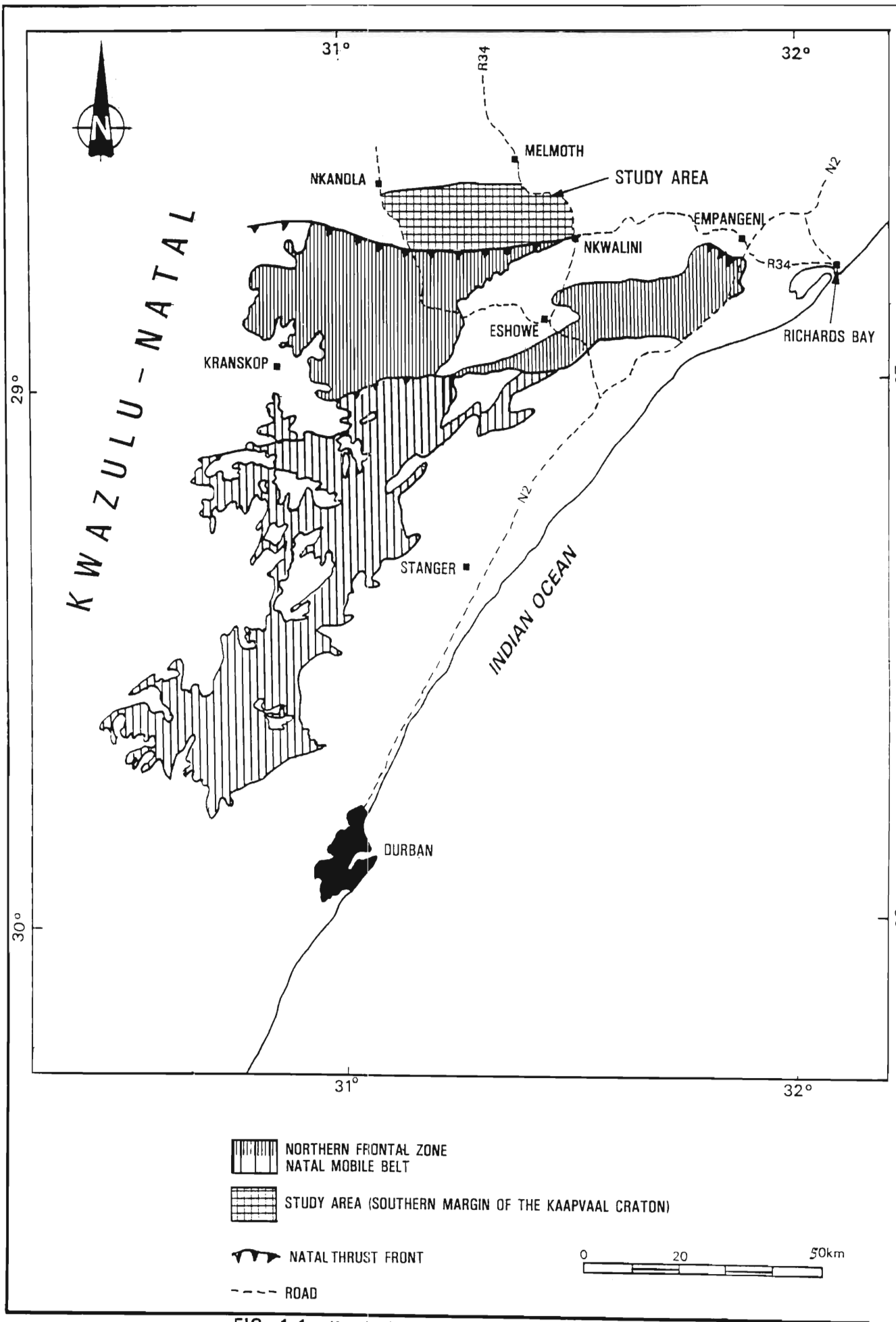

FIG. 1.1 *Map showing the location of the study area.*

quartzite, banded chert and banded iron formation. This belt is bounded on both sides by granitoids and granitoid gneisses which have been differentiated for the first time in this study.

Besides the Ilangwe greenstone belt, du Toit (1931) recognized other greenstone complexes in the southeastern Kaapvaal craton within KwaZulu-Natal, the most prominent being the Nondweni Complex in Nondweni (Nquthu district), the Buffalo Gorge greenstone*, the Mthonjaneni Complex* west of Melmoth and the Mfule greenstone complex*, southeast of Melmoth (Fig. 1.2).

The Nondweni greenstone complex consists of mafic and ultramafic metalavas with deformed pillow structures together with interbedded banded calc-silicate rock and banded chert (Linström, 1987). Subsequent to du Toit's (1913) pioneering work, the Nondweni greenstone complex has received much attention ranging from stratigraphical, sedimentological and geochemical studies (Versfeld, 1988; Wilson and Versfeld, 1992a; 1992b; 1992c; 1992d; 1994a; 1994b) to geochronological studies (Matthews et. al., 1989).

The Nondweni Greenstone Complex has been divided into three formations, namely: the Magongolozi, Toggekry and Witkop Formations (Versfeld, 1988; Wilson and Versfeld, 1992a, 1992b, 1992c, 1992d) and a minimum age of 3,29 Ga has been determined for the complex (Matthews et. al., 1989).

Versveld (1988) postulated an island-arc type environment for the Nondweni complex, citing lack of sialic sediments as suggesting deposition in a marginal interarc basin flanked by emergent volcanic arcs.

In the valley of the Buffalo River, three greenstone inliers occur in a deep ravine a few kilometres above Goodrickes' workings and in the Mganeni and Sifula streams. These inliers form part of a belt trending NNW and with near vertical strata comprising basaltic lava interbedded with thin variably coloured fine-grained chert and quartzite. These rocks are invaded by granite in the southwest (Fig. 1.2) and are overlain unconformably by the Nsuze Group (Linström, 1987). Dixon (in prep.) suggests the name Sifula Greenstone Sub-

* Names not yet approved by SACS.

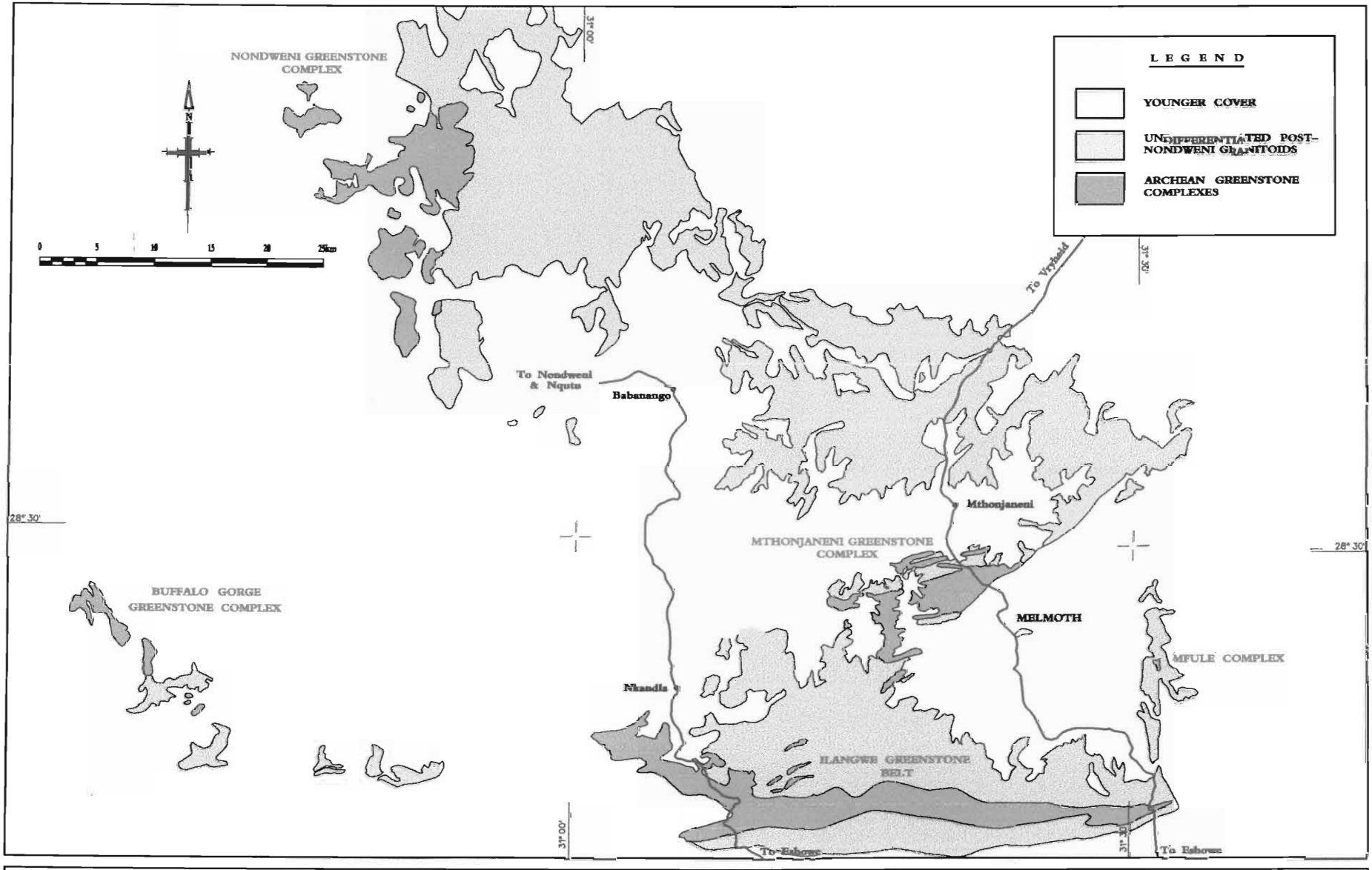

Figure 1.2 : DISTRIBUTION OF THE GRANITE-GREENSTONE COMPLEXES IN NORTHERN KWAZULU-NATAL

group for the Buffalo Gorge inlier. The subgroup is divided into two formations, viz. the Sibomvu and Mgunjane Formations.

In the inlier west of Melmoth, the rocks comprise greenstones, cherts, BIFs and quartzites. The Imfule River area comprises dark-coloured basic pillowed metalavas, BIFs and cherts. In the Imfule River pavements, southeast of Melmoth, there occurs a greyish-bluish contorted tonalitic gneiss similar to the Sand River Gneiss in Messina, Northern Province.

Other recently mapped Archaean complexes occurring in northern KwaZulu-Natal and southern Mpumalanga and extending from north of Piet Retief to south of Paulpietersburg are the Assegaai and Commondale granite-greenstone complexes (Hunter et. al., 1992). These complexes probably constitute an extension of the Swaziland granitoid terrain (Hunter et. al., 1992).

As a basis for the present study, detailed geological mapping of an area of about 400km² was carried out at a scale of 1:10 000 using orthophoto maps published in 1985. The area mapped extends east-west for 35km and is 11,5km in width (Fig. 1.1). About 28 months were spent in the field at intervals during the period March 1987 to June 1989, with subsequent short visits in October 1991 and November 1993 to April 1994.

This project was proposed and supervised by Prof. P. E. Matthews who had previously mapped the area at a scale of 1:50 000. This mapping was subsequently incorporated into the 1:250 000 Geological Survey Dundee Sheet 2830 (1988) (Linström, 1987).

1.2 PREVIOUS WORK

As mentioned previously, the first geological mapping of the Ilangwe Belt was carried out by du Toit (1931). He described a narrow linear belt extending for 35km eastward from the Nkandla forest to Ndloziyana Peak (Fig. 2), consisting of greenstones and metasediments which are flanked to the north and south by granites and granitic gneisses. Du Toit (1931) assigned these rocks to the Nondweni Series.

Detailed follow-up geological mapping of the Ilangwe Belt, done intermittently between 1960 and 1974, was carried out by Matthews whose 1:50 000 map sheets have been incorporated into the 1:140 000 map of the National Geodynamics Project of the northern margin of the Namaqua-Natal Mobile Belt in Natal (Matthews and Charlesworth, 1981) and

the 1:250 000 Geological Survey Dundee Sheet 2830 (1988) (Linström, 1987). Rocks of the Ilangwe Belt have been classified as the Nondweni Formation (Matthews, 1972), Nondweni Sequence (Matthews and Charlesworth, 1981) and Nondweni Group (Linström, 1987).

Charlesworth (1981) investigated the eastern part of the Ilangwe Greenstone Belt and the adjacent granitoid terrain to the south. He reported the occurrence of banded ironstones and amphibolites in the Entembeni area (Fig. 2) east of the Ilangwe Peak and described the pre-Nsuze granitoid complex as granodioritic to tonalitic, varying from weakly foliated fine- to medium-grained megacrystic types to mylonitic and laminar varieties.

In the Nkwalinye River (Fig. 2) he recognised granitoid gneisses intrusive into amphibolitic gneisses of the Ilangwe Belt. Northeast of Esibhudeni store he recognised the occurrence of quartz-sericite schists within granitoid gneisses.

Charlesworth (1981) also identified two phases of deformation within the southern granitoid complex of the Ilangwe Belt. The first phase is represented by tight intrafolial folds with SW to NE steeply inclined axial planes and SE or NW plunging fold axes. The regional foliation is sub-parallel to the axial planes of these early folds.

The second phase of deformation resulted in the folding of the S_1 foliation into westward-plunging folds with axial planes of variable orientation. A third phase of deformation was also recognised by Charlesworth (1981) in the Archaean granitoid gneisses to the east of the Ilangwe Belt, in the area around Empangeni (Fig. 1.1).

1.3 LOCATION AND TOPOGRAPHICAL SETTING

The study area is located 40km west of Empangeni, 20km north of Eshowe, about 15km south and southwest of Melmoth, about 20km south-southeast of Nkandla and directly east of the majestic Nkandla forest (Fig. 1.1). It consists of an area of about 400 square km, being 11,5km wide and 35km long. It is bounded to the west by the sinuous Eshowe-Nkandla gravel road passing through the Nkandla forest; in the south by the thrust front of the northern sector of the Namaqua-Natal Mobile Belt; in the east, by the Eshowe-Melmoth-Vryheid R34 road; and in the north by the Melmoth plateau (Fig. 1.1).

The area is rugged and mountainous and rises steeply from ±200m in the low-lying Umhlathuze and Nkwalini valleys to about 850m in the high ridges of the Ilangwe belt that include several peaks such as Ndloziyana (731m), Ekuthuleni (780m), Ilangwe (792m), Umgabhi (beacon 62 : 802m), Ngcengcengu (747m), Ntabandlovu (812m) and Simbagwezi (942m). The Umgabhi Peak (802m) itself overlooks the Eshowe Plateau (490m) to the south and the narrow Zululand coastal plain to the east. It is itself overlooked to the north by the high krantzes of the Melmoth Plateau (1000m) which is a fault-controlled upland surface. The Melmoth Plateau is topographically connected to the extensive Babanango Plateau (1300m) to the northwest. Westwards from the Umgabhi and Ilangwe ridges, the topography rises gradually along the granitoid and chert ridges leading to the indigenous Nkandla forest occurring at an elevation of 1150m to 1367m (Fig. 2).

The main access route, the Eshowe-Melmoth road (R34) winds its way up through the eastern and northeastern borders of the area, providing spectacular views of the rugged, mountainous nature of the region. Gravel roads descending to the area branch off from the main Eshowe-Melmoth road at Ndundulu, Zietover, Kwa-Magwaza Mission Hospital and near Kwa-Nzimela (Fig. 2). These roads require the use of a 4x4 vehicle especially on steep sections, along forestry tracks, particularly during the rainy season (November-February).

Another access route in the southwest part of the area is the scenic Eshowe-Nkandla road with branches eastwards at Esibhudeni store and further north at Vumanhlamvu. Most of the roads change into cattle tracks when followed deeper into the highly dissected mountainous belt.

Access to the southeastern parts of the area requires permission to use the road along the Goedertrouw Dam wall. However, this road becomes steep, rugged and full of dongas deeper into the Ilangwe Belt.

From east to west, the area is drained by the Nkwalinye River and its tributaries (the Memela, Safube, Fumfula and Nsengeni streams); the Amazula River and its tributaries, the Sabiza River, the Nyawoshane River and the Vungwini River and its tributary the Damuzini River. All these perennial second order streams drain into the Umhlathuze River which flows south-eastwards across the structural trend of the Ilangwe Granite Greenstone Belt. Deep dissection by these rivers has produced the present rugged valley and spur topography. Further downstream, the Umhlathuze River flows into the Goedertrouw Dam

(Fig. 2) which has been constructed to provide irrigation water to the farming communities of the lower Umhlathuze and Nkwalini valleys.

The climate of the area is subtropical with hot, humid and wet summers and warm, dry but pleasant winters. However, winter can be very cold in the mountainous regions around Nkandla and Melmoth. The whole area lies in the Natal mist belt.

The vegetation consists of Ngongoni-type grasses [*aristida junciformis and themeda triandra* - pers. comm. A. M. Zobolo, Department Botany, University of Zululand], indigenous bush along the valleys and the ubiquitous growth of noxious and exotic lantana bushes. Large trees include some wattles, acacia Karoo and the beautiful broad leaf Erythrina. Most of the hill slopes are cultivated with sugar cane and as a result outcrops are sparse. However, abundant outcrops occur along the rivers and streams. West and southwest of the Kwa-Magwaza Mission Hospital pine trees have been planted by Sappi. The Mooiplaas plantations occupy a large area stretching down to the Umhlathuze River in the south and southwest, covering areas like Spelonk, Kortbegrip, Duikerhoek and Wonderhoek. Sappi has graded numerous gravel roads on the hill flanks as access routes to the plantations.

Population distribution in the region is sparse and typical of rural areas. However, in proximity to the mission stations the population is denser than in the remote valleys. There are no industries in the area. The nearest industrial town is Richards Bay some 65km to the east (Fig. 1.1). Most of the men work in the industrial cities like Durban and Johannesburg and in nearby towns like Melmoth, Empangeni and Richards Bay. The women practise vegetable and small-scale sugar cane farming.

1.4 METHOD OF INVESTIGATION

Geological mapping at a scale of 1:10 000 was carried out using the following orthophoto maps compiled by The Air Survey Company of Africa Limited for the KwaZulu Government Department of Interior :

2831 DA21 Nkwalini	2831 DA16 Ndundulu	2831 CB16 Kortbegrip
2831 CB17 Wonderhoek	2831 CB18 Manzini	2831 CB19 Zietover
2831 CB20 Nandi Mission	2831 CB21 Reserve	2831 CB22 Reserve
2831 CB23 Ilangwe	2831 CB24 Ekuthuleni	2831 CB25 Massthansundu
2831 CA24 Sibudeni	2831 CA25 Reserve	

The 1:10 000 geological map of the area was then photographically reduced to a scale of 1:20 000. This reduced map was then digitized onto MicroStation by Mr Lynwood Hannie. This was done after hours in the drafting offices of West Rand Consolidated Mines. Figure 2 is the map presented in this thesis at a scale of 1:30 000. A rectilinear grid, spaced at 1000m intervals, is provided on the map and reference to localities using this grid is as follows: latitude is expressed as numerals and longitude as alphabetic letters and further subdivision at 100m intervals provides precise location of any point. For example, the Umgabhi Peak beacon (62; 802,8m) is located at (8.090/Y.620).

Outcrops in the Ilangwe Greenstone Complex are rather scarce due to deep weathering of steeply inclined formations and the deeply dissected rugged terrain with its dense cover of vegetation. As a result, traverses were restricted mainly to exposures along streams and rivers and on the crests of some rugged ridges and spurs. Good rock exposures occur in some road cuttings. Hill slopes and some hill crests have deep soil cover and are under sugar cane cultivation. Here outcrops are sparse or absent.

Laboratory work was conducted along conventional lines. Modal analyses were estimated using abundance charts (Terry and Chillinger, 1955; Philpotts, 1989). The accuracy of the estimation was checked in 35 randomly selected thin sections using a point counter. Plagioclase An-contents were determined by the Michel-Levy method, but in the amphibolites these determinations were checked using a four-axis universal stage and the method described by Suwa et. al., (1974).

XRF chemical analyses of 84 of the main rock units within the study area were provided by the Bophuthatswana Geological Survey, using a PW1480 X-Ray Spectrometer for the major elements and a PW1400 Sequential X-Ray Spectrometer for the trace elements.

CHAPTER 2

LITHOSTRATIGRAPHY OF THE ILANGWE GREENSTONE BELT

2.1 INTRODUCTION

The mapped area of the east-west trending Ilangwe Greenstone Belt and the associated granitoid terrain extends for a distance of about 35km from the Nkandla forest in the west through the ridges and valleys north east of Esibhudeni (Vungwini River valley), through the Umhlathuze River valley, up the ridges of Ngcengcengu and Ilangwe and past the Ekuthuleni ridges of Ndloziyana to end just beyond the R34 Eshowe - Melmoth road (Fig. 2). The structurally uppermost subgroup of the greenstone belt, the Nkandla Subgroup, extends further northwestwards (to just south of Nkandla town) and southwestwards beyond the Nkandla forest and is eventually overlain unconformably by strata of the Pongola Supergroup (Linström and Matthews, 1990a).

The Archaean geology of the study area can be divided into three distinct east-west trending zones (Fig. 2) which are separated by major east-west shear zones or faults. These zones are, from south to north :

(i) the Southern Granitoid Complex (SGC) (±2,5km wide);
(ii) the Ilangwe Greenstone Belt (IGB) (±3km wide);
(iii) the Northern Granitoid Complex (NGC) (±4,5km wide).

The Ilangwe Greenstone Belt is separated from the Southern Granitoid Complex by the major Vungwini River shear in the west and the Matshansundu Fault in the east, whereas the Entembeni Fault separates it from the Northern Granitoid Complex. The Vungwini River shear extends from the Vungwini River in the west through the tip of the U-bend in the Umhlathuze River just south of Spelonk [Fig. 2; (2.400/P.390)], straddling the southern bank of the Umhlathuze River where it flows to the east, through the point where the Sabiza River enters the Umhlathuze River (7.180/V.720) and ends NNE of Umgabhi Ridge (7.400/Y.525) where the Umgabhi Granitoid forms a WNW trending re-entrant extension

into the Sabiza amphibolites (Fig. 2; Fig. 7.1). East of the Umgabhi Granitoid wedge, the greenstones are separated from the Southern Granitoid Complex by the Matshansundu Fault which trends eastwards and is truncated by the much younger, post-Karoo, Tugela Fault just north of Nkwalini station.

The Entembeni Fault can be traced from the east, where it is truncated by the younger, post-Karoo, Tugela Fault, westwards north of Ndloziyana Peak through Entembeni and it disappears westward beneath a metagabbroic/metanoritic sheet. It reappears again west of a metanoritic sheet near the Sabiza River (Fig. 2) but is obscured by granitoids and deep weathering further westwards. It is possible that the fault bounding the amphibolites and the Ntshiweni Augen Gneiss north of Simbagwezi Peak (5/J,K) is the westward continuation of the Entembeni Fault.

The southern limit of the Southern Granitoid Complex is the southern boundary of the ***Kaapvaal Craton*** and is defined by the thrust-front of the Mid-Proterozoic Namaqua-Natal Mobile Belt. The northern margin of the Northern Granitoid Complex is covered by younger flat-lying Natal Group sandstones.

The greenstones and the associated metasediments of the Ilangwe Greenstone Belt form a narrow east-west belt ± 3,0km wide. The greenstones extend along the entire length of the belt but wedge out in a V-shape in the east whereas the associated metasediments disappear in the east just before Ndloziyana Peak (6.280/GG.590). Here the greenstones and metasediments have been intruded and cut-out by the pink Umgabhi Micrographic Granite.

The northern and southern granitoid complexes are tonalitic, granodioritic and potassic in composition. Based on similar geochemical and mineralogical characteristics ***and*** on regional distribution, mutual associations and contact relationships (which will be described in detail in Chapters 4 - 8 and Chapters 11 - 14), these granitoids and granitoid gneisses can be divided into three broad associations or suites, viz. :

(a) Amazula Gneiss - Nkwalini Mylonitic Gneiss Association;

(b) The early post-Nondweni granitoids (comprising the Nkwalinye Tonalitic Gneiss and the Nsengeni Granitoid Suite);

(c) The late post-Nondweni granitoids (comprising the Impisi-Umgabhi Granitoid Suite - an association of five granitoid phases).

2.2 STRATIGRAPHIC NOMENCLATURE

Du Toit (1931) classified the greenstones and metasediments of the Ilangwe Belt and similar rocks to the north (southeast of Nkandla and west of Melmoth), northwest (around the Nondweni village and to the west (in the Buffalo River valley) as the ***Nondweni Series***. The distinctive schistose siliceous rocks (quartz schist and quartzite) which are associated with the Nondweni Series rocks (and therefore form part of the basement) in the Vungwini valley were assigned to the Nkandla Series (Hatch, 1910; quoted in du Toit, 1931). Matthews (1959) referred to part of the Nkandla Series as the Nkandla schists and concluded that they form the lower most member of the Insuzi Series. Matthews (pers. comm.), on the basis of extensive mapping, re-classified the Nomanci quartzites of the Nkandla Series as part of the Nondweni rocks and referred to the Nondweni Series of du Toit (1931) as ***the Nondweni Sequence***. Further, Matthews and Charlesworth (1981) correlated the Ilangwe Belt rocks with the Nondweni Sequence.

The Nondweni Series of du Toit (1931) was accorded group status by Groenewald (1984) (see also Versfeld and Wilson, 1992a). Versfeld (1988) limited the Nondweni Group to the rocks in the Nondweni area. Matthews et al. (1989) referred to these rocks and those occurring in Nkandla, Melmoth and Ilangwe (see Fig. 1.2) as the ***Nondweni Greenstone Complex***. Versfeld and Wilson (1992a), following on Versfeld (1988), further proposed that the name Nondweni Group excludes all other Archaean outcrops that were previously regarded as part of the Nondweni Series/Group because their correlation with the rocks of the Nondweni area is uncertain.

In this thesis, the ***Nondweni Group*** as defined by Groenewald (1984) and Linström (1987) is adopted. This is because of the fact that, even though there is no certain correlation between the Archaean rocks of the Nondweni area with those occurring in the Nkandla, Melmoth, Buffalo River valley and Ilangwe area, there is a very close similarity in the nature of these rocks. It is further suggested here that the Nondweni Group rocks occurring 70 km southeast of Nondweni be referred to as the ***Southern Nondweni Group*** rocks. Linström (1987), on the recommendation of Matthews (pers. comm.) assigned the Ilangwe Belt rocks to two formations: the Umhlathuze and Nkandla Formations of the Nondweni Group. Rocks of the Umhlathuze Formation crop out along the Umhlathuze River (4,5/O,P) south-

east of Nkandla and south-southwest of Melmoth. The Nkandla Formation rocks crop out in the Nkandla area where they structurally and unconformably overlie the Umhlathuze Formation (Linström, 1987) and are in turn unconformably overlain by the Nsuze Group (du Toit, 1931, p.32).

Archaean greenstone belts world-wide are usually divided into an upper metasedimentary suite and a lower metavolcanic suite (Lemon, 1990 p. 443; Condie, 1981; Anhaeusser, 1973). For instance, in the Barberton Mountainland there is a three-fold subdivision into the greenstones of the Onverwacht Group and the metasediments of the Figtree and Moodies Groups (de Ronde and de Wit, 1994; de Ronde et. al., 1994; Lowe, 1994; de Wit, 1991). The Belingwe Greenstone Belt is divided into the komatiites (Reliance Formation), tholeiites (Zeederberg Formation), and the clastic sediments of the Cheshire Formation (Bickle et. al., 1994; Kusky and Kidd, 1992). Similarly, the Slave Province Greenstone Complex in Canada is grouped into mafic metavolcanic rocks, intermediate to silicic metavolcanic rocks and clastic metasediments (Kusky, 1989).

In keeping with this distinctive classification of Archaean greenstone sequences, it is proposed that the Umhlathuze and Nkandla Formations of Linström (1987) be accorded ***subgroup*** status in order that the Ilangwe Belt metavolcanics and metasediments can be sub-divided into separate lithological formations. Detailed mapping of the Ilangwe Greenstone Belt has resulted in the following classification :

(i) Mafic-ultramafic rock associations consisting of three formations (Fig. 2), viz.:

(a) the ***Sabiza Formation***: a lower amphibolite association occurring along the southern margin of the greenstone belt;

(b) the ***Matshansundu Formation***: an eastern amphibolite-BIF association;

(c) the ***Olwenjini Formation***: an upper or northern amphibolite-banded chert - BIF association.

The Sabiza Formation can be informally subdivided into the lower and upper amphibolite sequences which are locally separated by a 150m to 300m wide tectonic mélange shear zone referred to as the Umhlathuze River mélange zone consisting of tectonic slices of Amazula Gneiss and banded amphibolite.

(ii) Metasedimentary rock associations consisting of three formations, viz. :

(a) the ***Entembeni Formation***: a distinctive phyllite-banded chert-BIF association occurring in the central and the eastern parts of the belt (Fig. 2);

(b) the ***Simbagwezi Formation***: a phyllite-banded chert-amphibolite association occurring in the western part of the belt, south-east of Nkandla;

(c) the ***Nomangci Formation***: a dominantly quartzite formation occurring in the western part of the belt, south-east of Nkandla.

Table 2.1 shows the proposed lithostratigraphic subdivision of the Ilangwe Belt.

2.3 UMHLATHUZE SUBGROUP

2.3.1 INTRODUCTION

The Umhlathuze Subgroup occurs as a narrow east-west trending belt, ±2km wide, within which deformed pillow structures in metalavas clearly indicate that the subgroup as a whole youngs northwards. This evidence provides a basis for a subdivision of the subgroup into three major formations, namely the Sabiza Formation, the Matshansundu Formation and the Olwenjini Formation. The lithology of each formation is shown in ***Table 2.1***. The subgroup stretches from the Vungwini River valley (in the west) through the Umhlathuze valley, the Sabiza valley, the southern portion of the Ilangwe Peak, the Ndloziyana Peak and up to the R34 main road (in the east) (Fig. 2). In the east, the greenstones taper in a V-shape and disappear, due to faulting, near the Nkwalini mylonite zone just beyond the R34 main road between Eshowe and Melmoth (Fig. 2). In the west, they taper and wedge out in a complex manner and are unconformably and structurally overlain and underlain by metasediments of the Nkandla Subgroup (Fig. 2).

The southern boundary of the subgroup is in tectonic contact with various granitoid gneisses and granites. Evidence for this tectonic contact is provided by brecciated and recrystallized white metaquartz fault filling and quartz-sericite-talc schists which define the contact at places along the belt. In areas where these rocks are highly recrystallized, they

form positive relief and in areas where they are less recrystallized they form negative relief usually utilized by streams and rivers.

The northern limit of this subgroup is also tectonic and is defined by a sheared contact with the overlying Entembeni Formation phyllites in the central part of the belt and by various granitoid gneisses in the eastern and western parts. In the Ilangwe Peak area this shear zone consists of a number of very thin bands (0,5m to 5m) of khaki-coloured to cream-white usually sheared siliceous fine-grained argillaceous (pelitic) rock. Traced laterally, this unit occurs in a lens-like discontinuous fashion, but it is quite a distinctive horizon which signifies the end of one mafic volcanic cycle before the commencement of another volcanic cycle after which there occurs thick sedimentation of the Entembeni Formation.

Regional foliation within the Umhlathuze Subgroup is east-west with steep (60 - 90°) dips to the north. In some areas the inclination varies from north to south within a short distance. Locally, the foliation trends NW - SE and NE - SW. Younging direction is consistently to the north and northeast and is indicated by deformed pillow structures within the banded amphibolites.

The type areas where the rocks of the Umhlathuze Subgroup are developed (to varying thicknesses) are the Ekuthuleni Peak, south of Ilangwe Peak, the Sabiza valley, the Umhlathuze valley and the Vungwini valley (in the west) where they are in a structural contact with the rocks of the Nkandla Subgroup (Fig. 2). Fig. 2.1 shows the tectono-stratigraphic sections developed in these areas.

2.3.2 SABIZA FORMATION

2.3.2.1 GENERAL CHARACTERISTICS

The name Sabiza Formation is derived from the river which traverses much of the outcrop area in the central part of the Ilangwe Belt (Fig. 2).

This formation is composed mainly of amphibolites and pillowed metabasalts and occurs in an east-west narrow, linear belt extending ±30km from the R34 main road in the east to just beyond Vungwini Valley (6.800/F,G,H) in the west (Fig. 2). The formation is thickest (2185m) in the centre of the belt and thins in the east and west where it disappears under younger rocks (Fig. 2.1).

TABLE 2.1: TECTONO-LITHOSTRATIGRAPHIC SUBDIVISION OF THE ARCHAEAN ILANGWE GREENSTONE BELT

GROUP	SUBGROUP	FORMATION	LITHOLOGY	APPROX. THICKNESS
NONDWENI	NKANDLA	Nomangci	Quartzites; quartz schists; quartz-muscovite-(sericite) schists; minor phyllites; minor banded cherts	1072m
			Tectonic Contact	
		Simbagwezi	Phyllites; tremolite schists; talc schists; actinolite schists; banded metacherts and cherty quartzites, minor pillowed metabasalts.	1117m
			Tectonic Contact	
		Entembeni	Phyllites, phyllonites; banded metacherts and cherty quartzites; BIF; mica schists; minor pillowed metabasalts	1110m
			Tectonic Contact	
	UMHLATHUZE	Olwenjini	Upper or northern amphibolite-chert-BIF association: Amphibolite schists; actinolite schists, pillowed metabasalts; tremolite schists; garnetiferous amphibolite; minor gabbroic sills; quartz-biotite-cordierite-fuchsite gneiss; banded metacherts and cherty quartzites; BIF; minor magnetite quartzite; minor phyllonite.	885m
			Tectonic Contact	
		Matshansundu	Eastern amphibolite-BIF association: Amphibolite schist; tremolite schists; actinolite schists; massive metabasalts; amphibole-mica schists; BIF	468m
			Tectonic Contact	
		Sabiza	Amphibolite association: Upper Sabiza amphibolites: Banded amphibolite; pillowed metabasalts; massive metabasalts; talc tremolite schists; serpentinite talc schists; actinolite schists; minor gabbroic sheets; khaki metapelitic rock at top of sequence	2185m
			Tectonic Contact	
			Lower Sabiza amphibolites: Banded amphibolites; massive amphibolites; actinolite schists; tremolite schists	

KEY TO FIG. 2.1

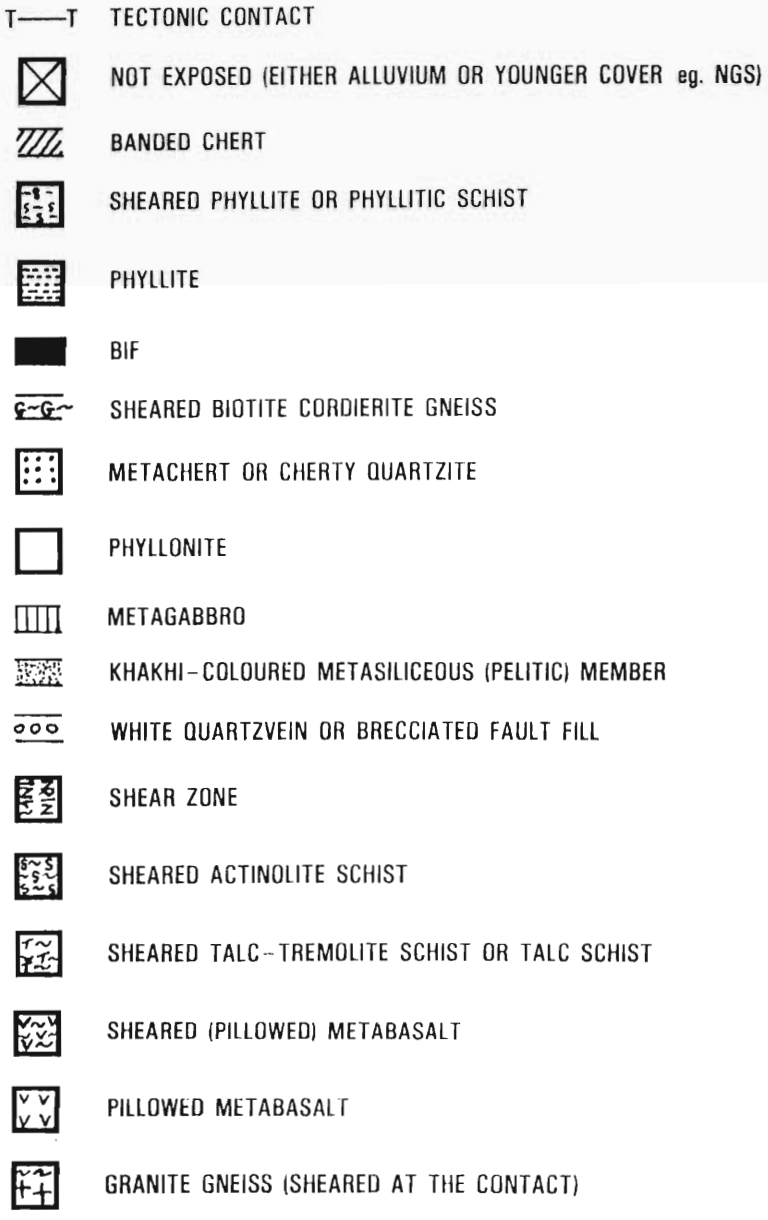
T——T TECTONIC CONTACT
NOT EXPOSED (EITHER ALLUVIUM OR YOUNGER COVER eg. NGS)
BANDED CHERT
SHEARED PHYLLITE OR PHYLLITIC SCHIST
PHYLLITE
BIF
SHEARED BIOTITE CORDIERITE GNEISS
METACHERT OR CHERTY QUARTZITE
PHYLLONITE
METAGABBRO
KHAKHI-COLOURED METASILICEOUS (PELITIC) MEMBER
WHITE QUARTZVEIN OR BRECCIATED FAULT FILL
SHEAR ZONE
SHEARED ACTINOLITE SCHIST
SHEARED TALC-TREMOLITE SCHIST OR TALC SCHIST
SHEARED (PILLOWED) METABASALT
PILLOWED METABASALT
GRANITE GNEISS (SHEARED AT THE CONTACT)

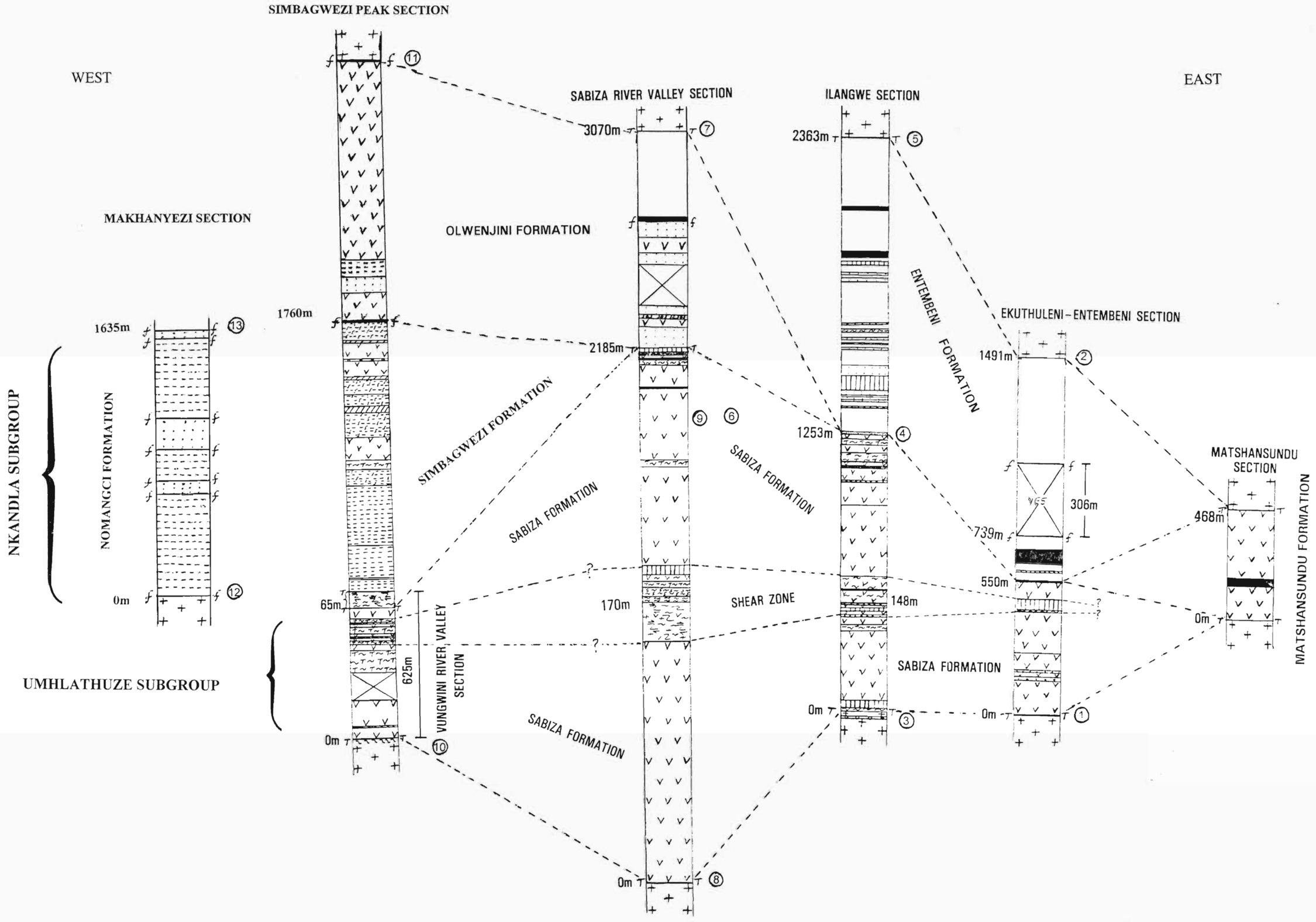

Fig. 2.1 : Tectono-stratigraphic sections of the Nondweni Group in the Ilangwe Greenstone Belt.

The southern limit of the Sabiza Formation is in tectonic contact with various granitoid gneisses and granites. The northern boundary is also tectonic, defined by the Simbagwezi shear, which, in the Ilangwe area, consists of very thin bands of a metasiliceous fine-grained argillaceous unit.

The Sabiza Formation can be informally subdivided into the lower and upper amphibolite sequences separated by a 150 - 300m wide mélange zone referred to as the Umhlathuze River shear zone (Fig. 2). This mélange zone is a strongly tectonized mixture of metavolcanic assemblages and exotic slices of Amazula Gneiss.

2.3.2.2 LOWER SABIZA BANDED AND MASSIVE AMPHIBOLITE

The lower part of the Sabiza Formation generally consists of foliated and banded amphibolite which is a fine- to medium-grained, greenish-black melanocratic rock containing thin leucocratic feldspathic lenses which give the rock its streaked banded appearance (Plate 2.1A). Predominant minerals are plagioclase, needle-like actinolite/tremolite, green hornblende with minor biotite, quartz and ore (probably pyrite). Aligned amphiboles and biotite define the foliation (Plate 2.1A). The leucocratic lenses consist of quartz and plagioclase, usually less than 10mm wide. Under the hand lens, quartz occurs in the form of thin discontinuous ribbon-like and sometimes sigmoidal veins parallel to the foliation.

In the Ilangwe section (Fig 2.1) the lower part of the Sabiza Formation consists of a thin (±10m) sheared mixture of quartz-muscovite-sericite schist (with minor feldspars which have been altered to sericite) and a talc-muscovite schist. This mixed zone weathers to a reddish-brown colour with talc giving its characteristic soapy feel and a white weathered tint. This zone is confined to the area north of the Umgabhi Peak (7.200/Y.580) and is thought to have developed due to intense shearing at the contact. Banded amphibolites overlie this sheared mixed zone.

This amphibolite weathers to a distinctive yellowish-orange to reddish-brown rich soil which is characteristic of a number of low-lying hillocks in the Ilangwe Belt. This soil colour is distinctively different from the dusky red rich soil which is derived from the weathering of gabbroic sills and dykes occurring around the Ilangwe Peak (6.000/Y,Z) and to the east of Ndloziyana in the area aptly named Matshansundu (6.490/GG,HH) ("Black stones" - literal translation).

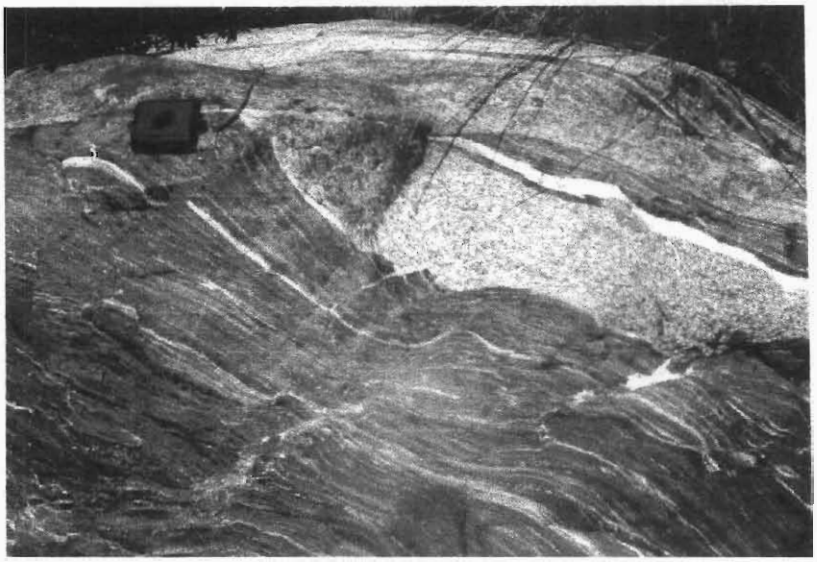

A

B

C

Plate 2.1

Further up the sequence, the banded amphibolite gives way to a slightly foliated but massive fine- to medium-grained melanocratic and pillowed metabasaltic amphibolite consisting of actinolite and plagioclase with minor quartz, hornblende, epidote, biotite, chlorite and ore. The rock varies from a dark greenish-brown colour (due to abundance of biotite?) to a dark greenish-grey colour (due to abundance of chlorite?). Chlorite, which appears to be the retrogressive product of amphiboles and biotite adds a schistose texture to the amphibolitic metabasalt and tends to be more localised along shear zones.

Well preserved pillow structures, as defined by Hyndman (1985), occur in the massive amphibolite. The pillows are visible even in the highly weathered and sheared amphibolites (Plate 2.1). The pillow structures exhibit interlobate cusps which indicate the base of the flow and are useful in determining "way up" (Hyndman, 1985; Roberts, 1984). In the Ilangwe Belt, the "way up" is consistently to the north and north east (Fig. 2).

Three types of pillow structures occur throughout the mapped area and were distinguished on the basis of size, shape, texture and degree of deformation.

Type I : Type I pillow structures are broad ellipsoidal and seemingly undeformed pillows which occur in a fine-grained massive metabasalt with a weak faint foliation. These are localised in parts of the Umhlathuze River (5.100/O.990). These pillows have well-defined cuspate shape and are of intermediate size. The pillow margins are more-or-less diffuse due to the ill-defined chill margins and the absence of textural features like ocelli (Plate 2.1B).

Type II A : These are flattened and stretched but small size pillows. They still show "way-up" and the pillow boundaries are well-defined with chilled margins or weak ocelli features and minor calcitic rims. The amphibolitic metabasalt is medium-grained and well-foliated. The tops of some pillows are crenulated and show a distinct crenulation lineation plunging at 17 to 35° in the younging direction (006 and 028) (Plate 2.1C).

Type II B : These are extremely flattened and stretched elongate closely-packed pillows which occur in a fine- to medium-grained well-foliated amphibolitic metabasalt. The interior of the pillows consists of fine-grained uniform feldspathic amphibolite and the matrix between the pillows consists of a

dark rim of very fine-grained chloritic amphibolite and minor ocelli. Their cuspate bases are still visible for "way up" determination. The Type IIA and B pillows are common in the Umhlathuze River (5.130/O.999) and in the lower reaches of the Sabiza River (7.200/W.320). ***Table 9.2*** shows some dimensions of deformed pillows at these localities.

Type III : These are extremely flattened and sheared very small pillows occurring in an extremely foliated carbonate and chlorite altered amphibolitic schist. All textural features, shape and original size of the pillows have been obliterated by intense deformation and the rock is highly talcose.

No pillow structures were observed in the banded amphibolite near tectonic contacts with the granitoids, for example in the Sabiza and Umhlathuze valleys (see Fig. 2.1 - Sabiza Section; Plate 2.1A). Here, the amphibolite is finely laminated and it is possible that the pillows were stretched and extremely attenuated parallel to the metamorphic layering during deformation (Passchier et. al., 1990).

In the Ilangwe section, the serpentinitic uppermost part of the lower Sabiza amphibolite is interspersed with a ±30m wide serpentinitic talc-tremolite schist, possibly a meta-intrusive komatiite. This is a light greenish-grey schistose rock consisting of a cluster of radiating needle-like crystals of tremolite alternating with flakes of talc, serpentine and chlorite. The rock has a soapy feel to the touch and weathers to an orange-brown colour with a tinge of grey due to talc. This weathering colour is quite diagnostic on road surfaces and the rock is quite slippery.

In the Vungwini Valley (6.700/I) the lower amphibolitic metabasalt is quite thin (Fig. 2.1).

The pillowed metabasalts of the Sabiza Formation were probably extruded in shallow subaqueous ocean floor environments as evidenced by the paucity and small-size of the vesicles (Hyndman, 1985). The dark rim of chloritic amphibolite in some of the pillows probably represents the original muddy inter-pillow matrix. Some pillows are rimmed by calcite which was probably precipitated from sea water after extrusion of the pillow basalts. Some radial fractures and veins occur within the pillows (see Plate 2.1B). These veins and micro-fractures are lined with crystals of calcite (or ankerite?) and chlorite alteration. Probably this alteration assemblage of calcite plus (ankerite?) plus chlorite resulted from fluid flow along grain boundaries and micro-fractures.

2.3.2.3 UPPER SABIZA BANDED AND MASSIVE AMPHIBOLITES

These pillowed metabasalts are well-developed in the central parts of the Ilangwe Belt where they attain thicknesses of 712m and 840m in the Ilangwe section and the Sabiza section respectively (Fig. 2.1). They thin both to the west and the east.

In the south, they are in contact with the Umhlathuze River shear zone. The northern contact varies. In the central parts of the belt, the pillowed metabasalts are in a sheared contact with phyllonites of the Entembeni Formation. In the northwest, they are in tectonic contact with the Simbagwezi Shear which also forms the southern limit of the Olwenjini Formation (Fig. 2). At some places the shear zone contains slices of serpentinitic talc schist (Fig. 2). In the extreme west just north of the Vungwini River and south of the Simbagwezi Peak at locality (6.500/J,K), they are in contact with a ±65m wide phyllonitic zone thought to represent the extensive Simbagwezi shear zone (Fig. 2; Fig. 2.1).

Younging as indicated by deformed pillow structures is consistently to the north-north east. The foliation is inclined steeply to the north.

The metabasalts are cut by a number of quartz veins ranging in thickness from a few mm up to 1m. These veins are jointed and are a dirty milky white colour with tints of red probably due to iron-rich impurities derived from the weathering of ferromagnesian minerals of the metabasalts. Towards the middle and lower top part of the sequence, the metabasalts alternate with thin (5 - 30m) concordant light greenish serpentinitic talc-tremolite schists and thin metagabbroic sheets or sills. These schists were observed in the Umhlathuze River (5.645/U.720), the Sabiza River (5.940/W.780) and in the Ilangwe area south of the Ilangwe Peak at locality (6.200/Y.480). They are composed of talc, tremolite, chlorite serpentine and minor carbonate and magnetite, typical low-grade metamorphic mineral assemblages. They are characterized by high MgO content. Relicts of olivine, orthopyroxene crystals and calcic plagioclase have been observed in thin section. The latter are mineral assemblages typical of unaltered komatiites (Arndt and Nisbet, 1982; Beswick, 1982; Pearton, 1982) and the high MgO content supports this.

It has been proposed that komatiites are the products of mantle plumes (Jarvis and Campbell, 1983; Campbell et. al., 1989; Griffiths and Campbell, 1990; Herzberg, 1992) which could possibly have risen under oceanic crust of the early Archaean. It is possible that these komatiites represent fragments of an oceanic plateaux (Storey et. al., 1991;

Kusky and Kidd, 1992). The occurrence of concordant metagabbroic sheets and altered komatiites together with pillowed metabasalts and banded amphibolites suggest that these rocks represent remnants of oceanic crust (de Wit et. al., 1987; Storey et. al., 1991; Kusky and Kidd, 1992).

Towards the top of the metabasaltic sequence, there occur two or three units of a khaki-coloured siliceous fine-grained metapelitic unit which ranges from 0,5m to about 5m in thickness. This is a distinctive horizon consisting of thin layers of sheared quartz ribbons alternating with K-feldspars. This metapelitic unit is thought to have been deposited during a period of quiescence when there was no volcanic activity. It is also significant in that its occurrence heralds the end of a major volcanic episode and the beginning of a major period of sedimentation in the Archaean Ilangwe Greenstone Belt.

2.3.3 MATSHANSUNDU FORMATION

The name Matshansundu Formation is derived from the area where the formation outcrops in the eastern part of the Ilangwe Belt. It stretches from northwest of Ndloziyana Peak (6.100/GG.320) and tapers eastwards in a V-shape and disappears beyond the R34 main road south of Mzilikazi Peak, at locality (5.400/OO.550).

The southern and northern limits of the formation are fault-bounded against the Nsengeni Granitoid Gneiss. The western limit has been diapirically intruded by the pink Umgabhi Micrographic Granite (a phase of the Impisi-Umgabhi Granitoid Suite). The northern tectonic boundary is the extensive post-tectonic Entembeni Fault. The southern fault is the post-tectonic Matshansundu Fault. Evidence of faulting is provided by quartz-breccia fault-fill observed at locality 6.210/II.130. Thin section analyses of sample H31EB from this locality showed it to contain broken brecciated crystals of cherty (amorphous) quartz in a matrix of fine-grained quartz and sericite. Some of the sericite/muscovite flakes define a planar fabric indicating the orientation of the fault.

The Matshansundu Formation is an amphibolite - BIF association consisting of deeply weathered (and at some places, poorly exposed) outcrops of massive metabasalts altered to chloritic schists, actinolite schists, amphibolite-mica schists and subordinate talc-tremolite schists. These schists are intercalated with a weathered silicate-rich cherty BIF folded into an easterly-closing synform. The ironstone consists of bands of interlocking quartz mosaics separated by bands of needle-like to fibrous stilpnomelane and grunerite and

bands of xenoblastic interlocking crystals of magnetite altered to reddish haematite. Minor rutile crystals have been observed.

A raft of amphibolite possibly part of the Matshansundu Formation occurs within the Nsengeni granitoid north of the Entembeni Kraal (4.300/EE.510). The timing of its detachment is not clear but could have happened during Nsengeni Granitoid Suite emplacement.

A detached and contorted silicate-rich cherty BIF thought to be part of this formation occurs within the contorted Nkwalinye Tonalitic Gneiss in the Zietover area (1,2/EE). It is interesting to note that both the amphibolite and the BIF rafts occur in association with metagabbroic bodies and are both enclosed in granitoids.

The amphibolites of the Matshansundu Formation are weathered into a yellowish-reddish rich soil which contrasts with the dusky red weathering of the metagabbroic rocks in the area. No pillow structures were observed in this formation and this could be due to deep weathering. The Matshansundu amphibolite-BIF association is similar to the metavolcanic - BIF association of the Rietvley area in the Pietersburg Greenstone Belt (Jones, 1990).

2.3.4 OLWENJINI FORMATION

The name of this formation is derived from the river which traverses these rocks and cuts in between the two juxtaposed fold closures in the Ngcengcengu Peak locality (4.305/Q.900).

The Olwenjini Formation is an amphibolite-banded chert-BIF association which is the upper or northern unit of the Umhlathuze Subgroup. In the south, it is bounded by the Simbagwezi shear and in the north by the western continuation of the Entembeni Fault. In the south, it is in tectonic contact with the amphibolites of the Sabiza Formation whereas in the north it is in contact with various granitoids of the Impisi and Nsengeni Granitoid Suites.

In the west, the Olwenjini Formation is structurally underlain by the Simbagwezi Formation (Fig. 2) and it wedges out where it is in a faulted contact with the Nkandla Granite and the Ntshiweni Augen Gneiss. In the east, the formation is covered by the phyllites of the Entembeni Formation and the metanoritic body occurring northwest of Ilangwe Peak (Fig. 2).

At the base, the formation consists of deformed pillowed metabasalts which are well exposed in the Umhlathuze River, south of Spelonk and north of Inhlababa Mountain , at locality (5.100/O.990). The pillowed metabasalts are about 400m thick in this area, they young to the northeast and are flattened within the axial plane foliation with the major axis of elongation parallel to the dip direction. The pillows have deformed ocelli. ***Table 9.2*** shows the dimensions of deformed pillows and ocelli in the Sabiza and Olwenjini Formations.

The pillowed metabasalts are overlain, in the Olwenjini valley (4.560/S.550), by garnetiferous amphibolites composed of intergrown actinolite fibres with high birefringence and garnet porphyroblasts ±5mm in size (in hand specimen). In thin section, some of the porphyroblasts are intergrown with actinolite and where they are fractured, also enclose actinolite. Some fractures are lined with opaque ore, probably magnetite. Accessory minerals include chlorite, epidote and biotite, all in a fine-grained actinolite matrix. The garnetiferous amphibolites are overlain by chloritic schists intercalated with folded metacherts and cherty quartzites.

The actinolite-chlorite schists are similar to those of the Sabiza Formation and the metacherts and cherty quartzites are similar to those of the Entembeni Formation in the Ilangwe area (5.580/Z.060). These hard, resistant strata are inclined steeply to the north and form the high rugged peaks of Ntabandlovu (5.200/N.260), Ngcengcengu (4.240/Q.900) and the northern slope of Simbagwezi (5.800/J.820). They can be traced along strike for a distance of about 15km.

The metacherts are massive to finely laminated fine-grained rocks of variable colour ranging from dull cream-white thick bands alternating with thin greyish-black bands (Plate 2.2B) to a uniform dull greyish-black with white discontinuous but ubiquitous stringers. The rocks can be described as banded metacherts. Under the microscope, the metachert bands alternate with very thin stringers of muscovite and sometimes with sericite and fuchsite thus giving a lepidoblastic texture. Original bedding is usually visible.

With increasing recrystallization, the metachert grades into a cherty quartzite with sugary texture. It is a massive tough and hard leucocratic rock of uniform cream-white to milky white colour and with the original banding partly or completely obliterated. In the Ngcengcengu (4/Q) and Umhlathuze (4.200/P.480) valleys, the cherty quartzite is light brown in colour and contains abundant fuchsite. In the Simbagwezi area (5.800/J.820) it is

milky white and also contains abundant fuchsite. These quartzites can be referred to as fuchsitic cherty quartzites. The rock consists mostly of quartz (60 - 90%) and minor K-feldspars, muscovite, fuchsite, sericite and minor ore minerals. In thin section the micas define the foliation which is well-developed.

The metacherts are overlain by a banded iron formation, a finely laminated moderately magnetic blackish to dark greenish rock consisting of layers of cherty quartz, grunerite, stilpnomelane and minor magnetite and haematite. The rock is similar to that occurring in the Matshansundu Formation, but the Olwenjini ironstone is sheared.

The ironstone is overlain by a thin, light to dark brown phyllonite unit containing thin subparallel quartz ribbons in a sericitic matrix. The rock is deeply weathered and crumbles easily when crushed by hand. The phyllonite is in contact with sheared chloritic amphibolite schists.

In the Sabiza River, at locality (5.180/V.820), there occurs, between the amphibolite schist and a metachert band, a distinctive quartz-biotite-cordierite-fuchsite gneiss. It is about 10-15m wide and is cut by a metanoritic body to the east. To the west, it can be traced for about 100 to 150m before it disappears. It consists of bands of quartz alternating with large flakes of dark green to black biotite wrapping light-bluish ribbon-like crystals of cordierite and quartz. Minor fuchsite and chlorite are associated with biotite. This rock occurs only in this area. It is probably similar to the carbonate fuchsite gneiss thought to represent early shears in the Pietersburg greenstone complex (Jones and de Wit, 1986; Jones, 1990).

In the Umhlathuze River, at locality (3.820/P.420), there occurs a 10 - 20m wide magnetite quartzite unit which is intercalated with the phyllonite unit. The highly magnetic magnetite quartzite occurs above the banded ironstone formation. This rock only occurs in this area.

2.4 NKANDLA SUBGROUP

2.4.1 INTRODUCTION

The Nkandla Subgroup is a predominantly metasedimentary succession of the Ilangwe Greenstone Belt (IGB). In the central to the eastern parts of the belt it occurs as a narrow ±1km wide east-west striking and northerly inclined (50° - 85°) belt within which the

deformed pillow structures indicate that "way-up" is to the north. In the west, it occurs as an easterly-tapering wedge-shaped metasedimentary unit consisting of a series of tectonic slices with a predominantly northerly dip and within which the pillow structures indicate a consistent north to northeasterly younging. It can be sub-divided into three formations (***Table 2.1***; Fig. 2.1), viz. :

(a) The ***Entembeni Formation***, which is composed of phyllites, phyllonites, banded metacherts, cherty quartzites, BIFs, muscovite schists and minor subordinate pillowed metalavas. This formation tectonically overlies rocks of the Umhlathuze Subgroup.

(b) The ***Simbagwezi Formation***, which consists of phyllites, actinolite schists, minor pillowed amphibolites, talc schists and minor chert bands. It structurally overlies and underlies the Sabiza and Olwenjini Formations of the Umhlathuze Subgroup respectively.

(c) The ***Nomangci Formation***, which is composed of quartzites, quartz schists and quartz-muscovite-(sericite) schists.

To the west of the Ilangwe Belt the Nomangci Formation is unconformably overlain by the Nsuze Group of the Pongola Supergroup (Matthews and Charlesworth, 1981; Linström, 1987; Linström and Matthews, 1990a).

In the central parts of the Ilangwe Greenstone Belt, the Nkandla Subgroup is represented by the ***Entembeni Formation*** and occupies an area extending from the Ndloziyana Peak (6.100/GG.320) in the east, where the outcrop of the metasedimentary succession is terminated by the diapiric intrusion of the pink Umgabhi Micrographic Granite, to the northwest of Ilangwe Peak where the succession is intruded by a metagabbroic body.

In the west, the Nkandla Subgroup is represented by the ***Simbagwezi and Nomangci Formations*** and occupies an eastward closing roughly V-shaped area stretching from the Vungwini River in the east with the northern arm of the V trending in the northwestern direction past the Isisusa beacon (4.400/D.245) on the northern border of the Nkandla forest through to the Nomangci Ridge just west of the Vumanhlamvu mission and disappearing beneath Nsuze Group rocks southwest of Nkandla. The southern arm of the V trends in the southwesterly direction past the Nkandla forest and terminates at the Natal

frontal thrust just near the southwestern border of the Nkandla forest (Matthews and Charlesworth, 1981). This western portion of the belt comprising the Nomangci Formation is in a rugged terrain covered by dense vegetation and thus providing very limited access. It is deeply weathered and outcrop exposure is generally poor. This part of the map was constructed from limited traverses and mapping by previous workers (Matthews, 1972; Matthews and Charlesworth, 1981; and Linström, 1987).

The type area for the Entembeni Formation is the Ilangwe Peak environs (5/Z) whereas that for the Simbagwezi Formation is in the Simbagwezi Ridge (5,6/J,K) and that for the Nomangci Formation is the Nomangci Ridge in the northwestern part of the map area, and in the area to the southeast of it.

2.4.2 ENTEMBENI FORMATION

2.4.2.1 GENERAL CHARACTERISTICS

The Entembeni Formation is named after the area to the east and southeast of Ekuthuleni Store at the localities (4,5/DD, EE,FF,GG). It occurs as a narrow (±1km wide) east-west trending belt consisting of phyllonites, phyllites, cherts, cherty quartzites, banded iron formation, muscovite schist and minor subordinate pillowed metalavas. It disappears in the east just before the Ndloziyana Peak (6.100/GG.320). In the west it is intruded by a metanoritic body and nearer locality (4.300/V.700) it is in a faulted contact with the Nsengeni granitoid. About 400m south of this locality, the Entembeni Formation tectonically overlies the Olwenjini Formation. The contact is a sinistral shear which was observed in the Sabiza River. In the Ilangwe area, the metasediments have been thickened due to folding (Fig. 2).

Along the southern boundary the metasediments of the Entembeni Formation are in sheared contact with pillowed metabasalts of the Sabiza Formation. Along the northern boundary, they are in a faulted contact with the Nsengeni Granitoid Gneiss (Fig. 2) but the quartz fault-filling is not as abundant as is the case along the southern tectonic contact between amphibolites of the Sabiza Formation and the granite-gneiss terrane.

The Entembeni metasediments form part of a large easterly-closing synformal structure. Along the southern boundary and SSW of Ilangwe Peak [(6.100/Y.770); Fig. 2; Fig. 2.2], the metasediments dip to the north at moderate angles of 40 - 60°. In the central parts, they

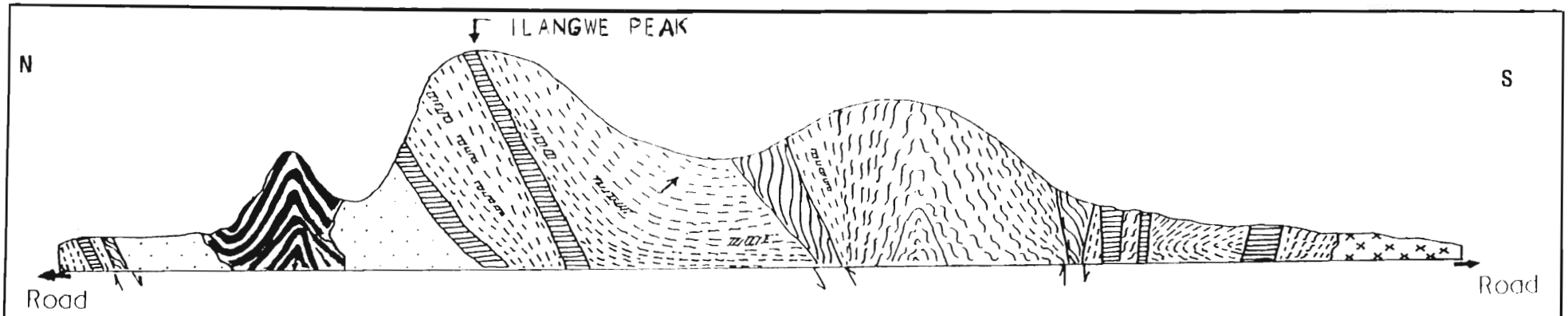

No outcrop: Subsoil of phyllitic origin

Melanorite

Quartz muscovite schist

Banded Iron Formation

Phyllonite

Banded chert

Phyllite with thin bands of chert

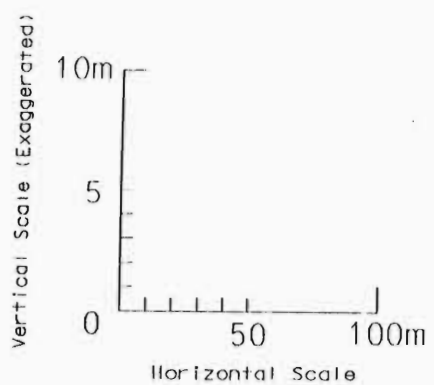

Figure 2.2 : VERTICAL ROAD SECTION OF THE ENTEMBENI FORMATION IN THE ILANGWE PEAK AREA

dip quite steeply to the north and south at 70 - 90°. Closer to the northern boundary, they are moderately to steeply inclined to the south (see Fig. 2 and Fig. 2.2).

2.4.2.2 LITHOLOGY

(a) ***Phyllites***

The phyllites of this tectono-lithostratigraphic unit are deeply weathered yellowish to orange-brown rocks consisting of quartz, sericite and chlorite. Along the southern margin, they are intercalated with thin bands of khaki-coloured siliceous pelitic rocks and greyish-black and white banded metacherts. They have a shallow (45°) northerly inclination.

In the middle section of the sequence, the phyllites are intercalated with banded metacherts, muscovite schists and minor pillowed metabasalts which young to the north-northeast. Here the rocks dip steeply (70° - 90°) to the north.

Towards the northern part of the sequence, the phyllites are intercalated with a few bands of cherty banded iron formation and metacherts or cherty quartzites. In the Ilangwe Peak area (5/Z) these rocks have a shallow (45° - 55°) southerly inclination. However, the dips are generally steeper towards the northern contacts of the formation, especially in the Ekuthuleni-Entembeni area (5/BB,CC,DD).

In the Ilangwe area the sequence is cut by local conjugate northwest-southeast and northeast-southwest faults. Some east-west faults are also present. In this area, the sequence is also intruded by a large metanoritic body which consists of altered hypersthene, calcic plagioclase and minor relicts of altered olivine, magnetite and biotite. In the Ekuthuleni area (5.100/DD,EE), the sequence is unconformably overlain by flat-lying Natal Group sandstones.

Along tectonic contacts, the phyllite has zones of phyllonite, a whitish-grey to brownish very fine-grained siliceous micaceous schist composed of quartz, muscovite, sericite and minor fuchsite. Recrystallized quartz ribbons are aligned along the foliation whereas at some places the quartz has a sugary texture. The whole rock displays a mylonitic texture. Although most of the small-scale structures within the rock have been obliterated during mylonitization, minor S and

Z folds and shear planes have survived (Plate 2.2A). These phyllonites weather to a distinctive bright brick-red to pale-reddish colour. Only the quartz/chert component of the phyllonite is obdurate and occurs as thin foliae.

The phyllonite also contains some bands of micaceous schist (with large muscovite books) alternating with thinner bands of chert and cherty quartzite and a khaki-coloured metapelitic unit quite similar to the distinctive khaki siliceous member of the Sabiza Formation.

Phyllonite is thought to have been derived from a phyllite (a rock of pelitic composition - Mason, 1986) that was subjected to phyllonitization due to cataclasis. This process was accompanied by a decrease in grain size and the development of chlorite and muscovite/sericite flakes (Turner, 1981). Some corrugated cleavage surfaces within the phyllonites, point to a phyllite protolith.

(b) ***Metacherts and Cherty Quartzites***

The rugged peaks of Ilangwe and the Ekuthuleni area (Fig. 2) are composed of resistant steeply inclined metacherts and cherty quartzites of the Entembeni Formation. These rocks can be traced from the Entembeni area (5/EE,FF) in the east to just west of the Ilangwe Peak (4,5/W,X,Y,Z), a distance of about 10km.

They are similar to those of the Olwenjini Formation but differ slightly in that they are dominantly milky-white and greyish-black in colour and contain sericite rather than fuchsite (Plate 2.2B). The greyish-black bands seem to contain carbonaceous material. Similar greyish-black layers within banded metacherts of the Pietersburg Greenstone Belt are known to contain graphite (de Wit, pers. comm., July, 1995). The greyish-black bands become obliterated with increasing recrystallization and the metachert grades into milky-white cherty quartzite with a distinct sugary texture and in which the original bedding has been completely obliterated.

A

B

C

Plate 2.2

The contacts between metacherts and phyllites are sharp and in some places (especially in the Ilangwe hook fold, locality 5.600/Y.620) are tectonic, with phyllonite along the contact zones. Within the metacherts, there occur sharp, layer-parallel detachment planes or faults, some of which contain a rusty-brown, fine-grained fault gouge (see Plate 2.2B, near the penknife). Cross-bedding is present in the metacherts (Plate 2.2B) but no graded bedding or evidence of early life forms have been observed.

(c) ***Banded Ironstone Formation (BIF)***

Banded ironstones of the Entembeni Formation can be traced discontinuously along the E-W strike for a distance of about 10km. Just east of the Ndloziyana Peak (6.100/GG.320) the ironstone splits into two or three bands. In the Entembeni area (5/EE,FF) to the northwest of Ndloziyana Peak, the ironstone shows small-scale folding and contortions. From here, the ironstone trends east-west parallel to the Entembeni fault which is the tectonic contact with the Nsengeni granitoids. North of Ilangwe Peak (5.670/Z.080), several thin bands of BIF are intercalated with phyllite, with which they have sharp contacts. To the west of the peak, a thicker band is folded but could not be traced around the hook fold of the metacherts (Fig. 2). Further to the west, the BIF is cut by a metanoritic body which is intrusive into the metasediments. To the west of the metanoritic body, no BIF was observed and the Entembeni Formation is truncated and terminated by a northeast-southwest trending fault against the Nsengeni Granitoid Gneiss and it is here where it structurally overlies the Olwenjini Formation (Fig. 2).

In general, the Entembeni Formation banded ironstones are finely-laminated strongly to moderately magnetic blackish to dark brick-red rocks consisting of thin, fine beds and laminations of microcrystalline white to grey cherty quartz, haematite and minor magnetite (Plate 2.2C). The cherty quartz layers are contorted and boudinaged (Plate 2.2C).

In the Entembeni area (5/EE,FF) the ironstone consists of thin layers of sandy sugary quartz alternating with haematite and very thin chert layers. It is brick-red to purplish-red and is intricately associated with muscovite-sericite schist and muscovite-tremolite schist.

Around the Ilangwe Peak and in the Umhlathuze valley, asymmetric ripple marks have been observed in the banded iron formations. However, the ripples are indistinct for the determination of current directions but are indicative of shallow water depositional environments (Davis, 1983; Reading, 1982). This is further evidence for deposition of Ilangwe Belt rocks in a shallow oceanic environment.

(d) ***Amphibolite Schist***

Minor pillowed amphibolites occur within the Entembeni Formation just to the southeast of Ilangwe Peak at locality (5.850/Z.170). These pillowed metavolcanics occur within the phyllites and show younging to the northeast. They consist of actinolite/tremolite and plagioclase. No ocelli are visible and the interpillow material is chlorite and calcite.

2.4.3 SIMBAGWEZI FORMATION

The Simbagwezi Formation occurs as a wedge-shaped metasedimentary sequence ±6km in strike length. The name of the formation is derived from the mountainous peak in which these rocks occur. They are confined to the western portion of the Ilangwe Belt and occupy an area bounded by the Vungwini River where it flows in a northerly and southerly direction (Fig. 2).

The formation has complex contact relationships with amphibolites of the Umhlathuze Subgroup. The southern limit of the formation structurally overlies the Sabiza Formation. At locality (6.500/K.050), the contact between the Simbagwezi phyllites and the Sabiza Formation metabasalts is sheared as evidenced by a 65m phyllonitic Simbagwezi shear zone. The foliation trends of the two formations on either side of the shear are slightly discordant and the dips of the Sabiza Formation are steeper than those of the Simbagwezi Formation.

The northern limit of the Simbagwezi Formation is in a faulted contact with the lower limit of the Olwenjini Formation. This fault is steeply inclined to the north. North of Simbagwezi Peak, the metacherts and amphibolites of the Olwenjini Formation dip steeply to the north whereas the phyllitic schists and banded cherts of the Simbagwezi Formation have moderate to steep northerly inclinations. Locally, some southerly dips have been encountered.

The Simbagwezi Formation consists of phyllites and phyllitic schists, pillowed metavolcanics, actinolite schists, talc tremolite schist and thin banded chert units intercalated with quartz sericite schist. The whole package in the Simbagwezi Ridge is about 1117m thick (Fig. 2.1). However, it is suspected that this thickness could be due to repetition and stacking of strata (Martyn, 1986) due to complex shearing and thrusting. The true thickness could be a fraction of this figure.

(a) ***Phyllites***

Phyllite is defined as a "very fine-grained schistose rock resulting from more advanced regional metamorphism than that involved in the formation of slate" (Hyndman, 1985). Phyllites are coarser-grained than slates and have a grain size of 0,1mm to 1,0mm (Best, 1982; Mason, 1986). They are the dominant rock type of the Simbagwezi Formation. They are bottle green cleaved rocks consisting of quartz, sericite and chlorite. The latter two minerals give the rock a greenish silky sheen on the cleavage surfaces. The rock also displays a characteristic wavy or refracted cleavage. Due to deformation, the cleaved surfaces have formed some kind of crude rodding lineation. The rock weathers to a light greenish-yellowish colour.

Along the Simbagwezi Ridge, the northerly inclined phyllites are truncated by a number of east-west trending faults which form pronounced topographical features as a result of the occurrence of vertically oriented, recrystallized white metaquartz fault-fill indicated as xxxxx on the geological map (Fig. 2).

The phyllites are also intercalated with two or three distinct thin (less than 4m) bands of talc-tremolite schist of limited extent. These schists probably define shear zones containing serpentinitic sills/dykes.

(b) ***Pillowed Metabasalt***

On the Simbagwezi Ridge (5.800/J.820) pillowed metavolcanics are separated from the underlying phyllites by a 20 - 30m thick unit of talc-tremolite schist. They are greenish-black and have pillow structures similar to the Type IIA structures (see Section 2.3.2.2). They are not thickly developed in the Simbagwezi Formation. They show "way-up" to the north-northeast.

(c) ***Actinolite Schist***

This is a dark greenish to bottle green rock similar to phyllite in colour but characterized by clusters of long (up to 5cm) radiating crystals/needles of actinolite. The rock itself is quite massive and the schistosity is poorly defined. The radiating needles are more spectacular on weathered surfaces. It alternates with quartz-sericite schist and weathers to a reddish-orange schistose clayey soil.

(d) ***Banded Cherts and Quartz-Sericite Schists***

Banded cherts alternate with thin quartz-sericite schists which sometimes look like cherty quartzitic schists. The banded cherts of this formation are quite distinctive and are not similar to the cherts of the underlying Umhlathuze Subgroup. The main differences are the vitreous charcoal-grey to black colour with distinct muscovite or sericite flakes that give the rock its lustrous habit, and the typical conchoidal fracture. There are no traces of cross-bedding in these cherts, probably due to recrystallization.

2.4.4 NOMANGCI FORMATION

The name of this formation is derived from the prominent ridge which occurs south of the town of Nkandla and to the northwest of the map area. The formation consists of quartzites, quartz-muscovite schists, quartz-sericite schists and minor phyllites.

Hatch (1910) (quoted in du Toit, 1931) bestowed the name Nkandla series to this sequence of rocks. Matthews (1959) described similar rocks exposed in the Nkandla forest and in the deep valleys of the Itate, Emome and Nkunzana rivers and referred to them as the Nkandla schist. In addition to the phyllites, basic schist and quartz sericite schist of the Nkandla schists, Matthews (1959) recorded the presence of kyanite within the phyllites and attributed its occurrence to the metamorphic effects of the intrusive Nkandla granite.

The Nomangci Formation occurs as a narrow easterly-tapering V-shaped outcrop wedge ±1,0km wide. The northern *"segment"* of the V trends WNW - ESE past the Isisusa beacon ridge (3/C), through the Nomangci Ridge just off the map area. The southern *"segment"* trends WSW - ENE north of Esibhudeni (6,7/A,B,C,D). These *"segments"* disappear beneath younger cover rocks to the northwest and southwest. Rafts of quartz-muscovite-

(sericite) schists and minor phyllites occur in the Nkandla Granite and the Ntshiweni Augen Gneiss to the north of the greenstone complex at localities (3,4/G,H,I,J,K).

On the eastern edge of the Nkandla forest, around locality (5.410/B.940) the Nomangci Formation is unconformably overlain by the basal formations (Hlathini and Mabaleni Formations) of the Nsuze Group (Pongola Sequence) (Linström and Matthews, 1990a,b). In the Makhanyezi area (4,5/C,D,E) to the west of the Vungwini River, the Nomangci Formation occurs in a complex relationship with the Simbagwezi phyllites. Here, the Nomangci quartzites have a steep northerly inclination whereas the Simbagwezi phyllites are inclined to the north-northeast at moderate angles (50 - 65°). The Makhanyezi Fault (Fig. 2) is the northern contact of the Nomangci Formation with the Nkandla Granite. Along this faulted contact, the quartzite is highly recrystallized and occasionally contains flakes of light-green fuchsite.

The Nomangci Formation consists mainly of thick white recrystallized fine- to medium-grained sugary or glassy pure quartzites intercalated with quartz-muscovite-(sericite) schist which appear to have been derived from micaceous or feldspathic sandstones which were less competent during deformation (Matthews, 1959). The highly recrystallized quartzites seldom show traces of bedding. Generally, the quartzites dip to the north at angles of 65° to 90°. The coarse-grained zones within the quartzites have well-defined slaty cleavage with fuchsite and white sericite flakes developed on the divisional planes (Matthews, 1959).

In the Makhanyezi ridge area (3,4/C,D,E), the quartzites have an exposed width of about 1000m. They alternate with chert bands and thin quartz-muscovite schist units. It is possible that the whole sequence consists of a series of repeated stacks of quartzitic strata whose true thickness is probably a fraction of the exposed width.

Just north of the Isisusa beacon (4.390/D.250) (Fig. 2), northwesterly trending and vertically inclined black and white banded quartzites were observed to alternate with steeply inclined phyllites. West of the Isisusa beacon, the quartzites alternate with highly weathered reddish micaceous quartz schist. Thin bands of black cherts occur discontinuously within the quartzite and schist. A thin kyanite-bearing schist band was also noticed near the road descending from the Isisusa beacon. Du Toit (1931) attributes the presence of the kyanite-bearing schist as evidence of the proximity of the contact between the quartzite and the intrusive granitoid.

Near the Vumanhlamvu mission and in the Nomangci Ridge, the northerly inclined quartzites weather into dirty white sharp and spiky ridge-like edges with distinctive light-green fuchsite bands.

The Nomangci quartz-muscovite-(sericite) schists occurring as rafts in the Nkandla Granite and, occasionally, Ntshiweni Augen Gneiss have a general NE-SW. They dip steeply to the southeast or northwest and are generally not more than 250m wide. The quartz-sericite schists in the Esibhudeni Granitoid are associated with east-west faults and shears and have similar trends. They dip steeply to the north and have a greater exposed width.

Nomangci quartz-muscovite-(sericite) schists are silvery-grey in colour and consist of fine- to medium-grained transparent rose quartz ribbons separated by minor light green and white flakes of fuchsite, muscovite and sericite. The rock forms prominent resistant thin ridges within the Nkandla Granite and, rarely, the Ntshiweni Augen Gneiss. Charlesworth (1981) mapped quartz-sericite schists on the Bope Ridge 5km northwest of Esibhudeni and suggested that they are probably a phyllonitic equivalent of the granitoid gneisses.

The protolith of the quartz-muscovite-(sericite) schists is not readily apparent, but was probably a meta-arkosic sediment. De Wit et. al., (1987a) are of the opinion that the quartz-sericite schists of the Theespruit Formation of the Onverwacht Group of the Barberton Greenstone Belt are the alteration products of ***intrusive felsic units*** which were preferentially emplaced along thrust zones. The quartz-muscovite-(sericite) schists of the Nomangci Formation have an extensive distribution and do not show evidence of occurring along shears or dykes and are probably not related to intrusive felsic units.

The Nomangci Formation is quite a distinctive unit consisting predominantly of sericitic quartzites showing complex shearing and thrusting. In this respect, it is probably analogous to the Moodies Group (of the Barberton Greenstone Belt) consisting of quartzites and conglomerates which were deposited in an emerging marine to subaerial environment (Lowe et. al., 1985; Lamb and Paris, 1988). De Ronde and de Wit (1994) regard the Moodies Group as syndepositional to a collision event.

2.5 POSSIBLE ORIGIN OF THE ILANGWE BANDED CHERTS AND BANDED IRON FORMATIONS

2.5.1 ORIGIN OF BANDED CHERTS

Most Archaean cherts are commonly interpreted as either chemical or biochemical precipitates (Condie, 1981; Hesse, 1988). The non-detrital silica is thought to be supplied in solution by hydrothermal-volcanic systems (Hesse, 1988). Some cherts are interpreted as having formed by the chertification (silicification) of tuff or greywacke (Condie, 1981; Heinrichs, 1984). Hesse (1988) contends that geological and sedimentological evidence suggests that some ancient bedded cherts owe their emplacement to deep-water re-deposition of siliceous pelagic sediments due to turbidity currents. De Ronde and de Wit (1994) believe that the convection of seawater-derived pore fluids associated with a dynamic hydrothermal system is the most likely scenario for the origin of the various cherts of the Barberton Greenstone Belt. Jones (1990), advances a similar origin for the cherts of the Pietersburg Greenstone Belt.

Based on :

(i) the probability that the pillowed metabasalts of the Ilangwe Belt, which contain rare small-sized vesicles and chloritic muddy interpillow matrix, could have been extruded in shallow subaqueous ocean-floor environments;

(ii) the fact that the metacherts occur in association with these pillowed metabasalts in the Olwenjini Formation and in association with phyllites and minor pillowed metabasalts in the Entembeni Formation;

(iii) the metacherts seem to have apparent cross-bedding and lack pelagic early life forms and deform largely in a brittle-ductile manner;

it is possible that the metacherts originated by shallow-water chemical precipitation of colloidal silica in a manner analogous to those of the Barberton and Pietersburg Greenstone Belts (de Ronde and de Wit, 1994). It is interesting to note that de Ronde and de Wit (1994) estimate (on the basis of fluid inclusion studies) the depth of the Barberton Archaean ocean to have been shallow - *"possibly as shallow as 60m"*. Versfeld (1988) also postulates a shallow water environment for the origin of the Nondweni cherts.

2.5.2 ORIGIN OF BANDED IRON FORMATIONS

Much has been written on the origin and genetic models of iron formations (Dimroth, 1977; Kimberley, 1978; 1979; 1989; Isley, 1995). BIF and associated chert units in greenstone belts have commonly been interpreted as the product of sea-floor-related hydrothermal activity and chemical exhalative processes (Viljoen and Viljoen, 1969a; Anhaeusser, 1973; Fripp, 1976; Boyle, 1976; de Ronde et. al., 1994). However, other workers such as de Wit et. al., (1982); Lowe et. al., (1985) and Paris et. al., (1985) in the Barberton Mountain Land, Boulter et. al., (1987) in the Pilbara Block (Australia) and Dimroth (1977) in Canada, have all documented BIF and chert units that were originally interpreted as chemical exhalative sediments, but were shown to be silicified and ferruginized sediments and simatic rocks. The reinterpretations were based on the presence of remnant sedimentary structures and igneous textures in the rocks.

From an extensive compilation of recent research concerning the origin of iron-formations, Kimberley (1989) concluded that all iron-formations can be attributed to exhalation of Fe-rich fluids into sea water. The fluids are enriched in Fe because of water/rock interaction. Kimberley (1989) suggested that most of the available data point to a "shallow" body of water within which the iron-formations accumulated. Isley (1995) supports the notion that the iron of the BIF's was supplied by hydrothermal plumes but further argues that during the Archaean to Early Proterozoic period, iron deposition rates were as high as 10^{12}gm/y. Therefore, to satisfy these high deposition rates, another significant source of iron was involved. The most viable source is thought to be the iron remobilized from marine sediments (Isley, 1995).

The Ilangwe belt iron-formations are spatially associated with metavolcanic rocks and are probably of the Algoma-type. It is probable that they were derived from sea-floor hydrothermal processes taking place in a relatively "shallow" body of water (Kimberley, 1989).

CHAPTER 3

TECTONOSTRATIGRAPHY OF THE ILANGWE GREENSTONE BELT

3.1 INTRODUCTION

In this chapter, a detailed description of contact relationships ***between*** and ***within*** the six mappable formations of the Umhlathuze and Nkandla Subgroups will be given. This discussion will ***not*** include description of contacts between the greenstones and the granitoid complexes to the north and south of the Ilangwe Belt. This aspect will be dealt with in subsequent chapters on the granitoids. The purpose of this chapter is to present evidence for a possible ***structural succession*** for the six mappable formations which were described in Chapter 2. In order to achieve this I will first describe the nature of ***intra-formational*** contacts and thereafter, the nature of ***inter-formational*** contacts and the possible structural succession.

The contacts between the six major lithostratigraphic formations of the Ilangwe Greenstone Belt are tectonic (Fig. 2.1; ***Table 2.1***). In addition, exposures of these contacts are rather scarce due to deep weathering of steeply inclined formations and deeply dissected rugged terrain with its dense cover of vegetation. As mentioned previously, good outcrop exposure occurs in stream sections, road cuttings and in deeply dissected areas.

The Ilangwe rocks are complexly deformed and show primary layering and foliation to be vertical to sub-vertical. Moreover, detailed mapping has provided evidence for polyphase folding with an early episode of near isoclinal folding. Due to this high degree of deformation, it may be expected, in theory, that all initial angular discordances will have been obliterated by rotation parallel or sub-parallel to the regional steep axial planar foliation (Turner and Weiss, 1963; Ramsay, 1967; Hobbs et. al., 1976; Davis, 1984; Price and Cosgrove, 1990). Therefore, it is unlikely that any direct evidence of original angular unconformities will be found within this greenstone belt.

3.2 NATURE OF INTRA-FORMATIONAL CONTACTS

3.2.1 SABIZA FORMATION

The banded amphibolites form the lower limit of the Sabiza Formation and the Vungwini River shear together with the Matshansundu Fault are the tectonic contacts with the Southern Granitoid Complex. In the Ilangwe section (Fig. 2.1) just north of Umgabhi Peak (7.200/Y.580), this contact is characterized by a ±10m wide mixed zone consisting of tectonized quartz-muscovite-sericite schist and talc-muscovite schist. These schists are overlain by the banded amphibolites. Elsewhere along the contact (for example in the Umhlathuze Valley [7.000/V.100]), the banded amphibolites are in direct tectonic contact with the granitoids (see Plate 2.1). The banded amphibolites extend from the Vungwini Valley (6/G,H,I,J) in the west to the Ekuthuleni/Entembeni area (6/FF) in the east – a distance of about 27km. Their thickness varies, being greatest in the middle of the belt.

The banded amphibolites are overlain by pillowed metabasalts. The contact, observed in the Vungwini River locality (6.900/J.410), is sharp and concordant; elsewhere, the contact is diffuse and obscured by deep weathering. The foliation of both units is inclined steeply to the north and the pillow structures indicate younging to the NNE. The pillowed amphibolites are truncated by thin discontinuous units of transgressive serpentinitic talc schists which are thought to represent shears (see Fig. 2, locality [6,7/Y]).

In the mid-sections of the Sabiza Formation, the massive and pillowed amphibolites are cut by the extensive and semi-concordant Umhlathuze River shear zone which consists of exotic slices of Amazula Gneiss, Nkwalinye Tonalitic Gneiss and greenstones (amphibolites). To the north and south of this shear zone, the amphibolites young to the NNE and are inclined to the north at angles between 60° and 85°. The significance of the Umhlathuze River shear zone and the shears represented by serpentinitic talc schists is not known but it is probable that these structures were important in the possible stacking and accretion (Howell, 1995) of greenstones during Sabiza times.

North of the Umhlathuze River shear zone, the massive and pillowed metabasalts are interbedded with thin concordant and northerly inclined serpentinitic talc-tremolite schists and thin metagabbroic sills. These rocks extend from the Umhlathuze River valley in the west to the Ekuthuleni area in the east (Fig. 2). The contacts are sharp and locally show discordant relationships with the amphibolites. This thin assemblage of serpentinic talc

tremolite schists (ultramafic units), metagabbroic sills and pillowed amphibolites can be regarded as a possible "ophiolitic sliver" (Bernstein - Taylor, et. al., 1992).

The top of the Sabiza sequence is characterized by thin units of a distinctive khaki-coloured siliceous pelitic rock of sedimentary origin. This unit is usually quite discontinuous, dips to the north and has sharp semi-concordant contacts with the amphibolites. These contacts possibly represent a local disconformity.

3.2.2 MATSHANSUNDU FORMATION

The Matshansundu Formation occurs to the east of the Sabiza Formation but it is not in contact with it. It comprises an amphibolite – BIF association whereas the Sabiza Formation is mainly an amphibolite association. Although no contact relationships between the two formations have been observed, it is thought that the Matshansundu Formation either structurally overlies the Sabiza Formation or it is contemporaneous with it. Way up evidence as indicated by pillow structures in the Sabiza Formation suggests the former.

Its southern and northern boundaries are in tectonic contact with the Nsengeni Granitoid Gneiss. It thins eastwards and it is cut out by the Tugela Fault in the Mzilikazi Peak – Nkwalini area. Its western limit (in the Ndloziyana Peak area - Fig. 3.1) has been diapirically intruded by the Umgabhi Micrographic Granite. In this locality (Fig. 3.1), the deformed phyllites and BIFs of the Entembeni Formation (the lowermost unit of the Nkandla Subgroup) are in a sharp and transgressive contact with the western limit of the Matshansundu Formation and the eastern limit of the Sabiza Formation (the two lowermost units of the Umhlathuze Subgroup) ***and*** the northern limit of the Umgabhi Micrographic Granite (a late post-Nondweni granitoid). In this area, the Matshansundu Formation trends NNE-SSW and dips to the NW, the Sabiza Formation trends E-W and dips steeply to the north, the Entembeni Formation is complexly folded and the micrographic granite shows some weak E-W foliation along the contact. This contact therefore represents a major deformed ***angular unconformity***.

The amphibolites of the Matshansundu formation are schistose, deeply weathered and contact relationships are difficult to see. No pillow structures were observed. A folded silicate BIF occurs within the amphibolites and the contacts are sharp and semi-concordant to slightly discordant. The Matshansundu Formation is laterally extensive (±10km). In the Entembeni area (3,4/EE), a detached segment of the amphibolites occurs within Nsengeni

Granitoid Gneiss and further to the north (1,2/EE), a silicate BIF segment, thought to be part of the Matshansundu Formation, occurs within the Nkwalinye Tonalitic Gneiss. The timing of the dislocation of these segments is not clear.

3.2.3 OLWENJINI FORMATION

This formation is the upper or northern unit of the Umhlathuze Subgroup and it structurally overlies the Sabiza Formation. In the west, it structurally overlies the Simbagwezi Formation and in the east it is overlain by the Entembeni Formation. It extends from the Simbagwezi Peak area (5/J) in the west to the Sabiza valley (4/V,W) in the east, a distance of about 14km.

Deformed and north-northeasterly younging pillowed metabasalts (amphibolites) form the lower limit of this formation and are well exposed in the Umhlathuze River at locality (5.100/O.990) south of Spelonk. The pillowed amphibolites extend the whole length of the lower part of the formation but thicknesses vary. In the Umhlathuze River area where they are well-exposed, widths of up to 400m have been estimated. They thin considerably to the east (Fig. 2).

In the Olwenjini valley (4.560/S.550), the pillowed amphibolites are overlain by garnetiferous amphibolites. The contact is diffuse and ill-defined but is characterized by the occurrence of red garnets. Both units are inclined to the north but the garnetiferous amphibolites are not laterally extensive. They have not been observed in the Umhlathuze River to the west nor in the Sabiza River to the east. Their vertical extent is not known and they seem to be confined to the Olwenjini valley in the Ngcengcengu Peak area.

The garnetiferous amphibolites are overlain by chloritic schists intercalated with folded metacherts and cherty quartzites. The contacts are sharp and concordant. These schists and metacherts are extensive (Fig. 2). Amphibolitic schists form the northern limit of the Olwenjini Formation. However, at the locality (4.300/U,V,W), the BIFs form the northern boundary. It is possible that the amphibolites in this locality were eroded because in the Sabiza valley (4.600/V), the BIF, amphibolite and metacherts show an off-lap relationship which suggests erosion of material just before the deposition of the Entembeni Formation. This evidence suggests that the contact between the Olwenjini Formation and the Entembeni Formation possibly represents a local unconformity.

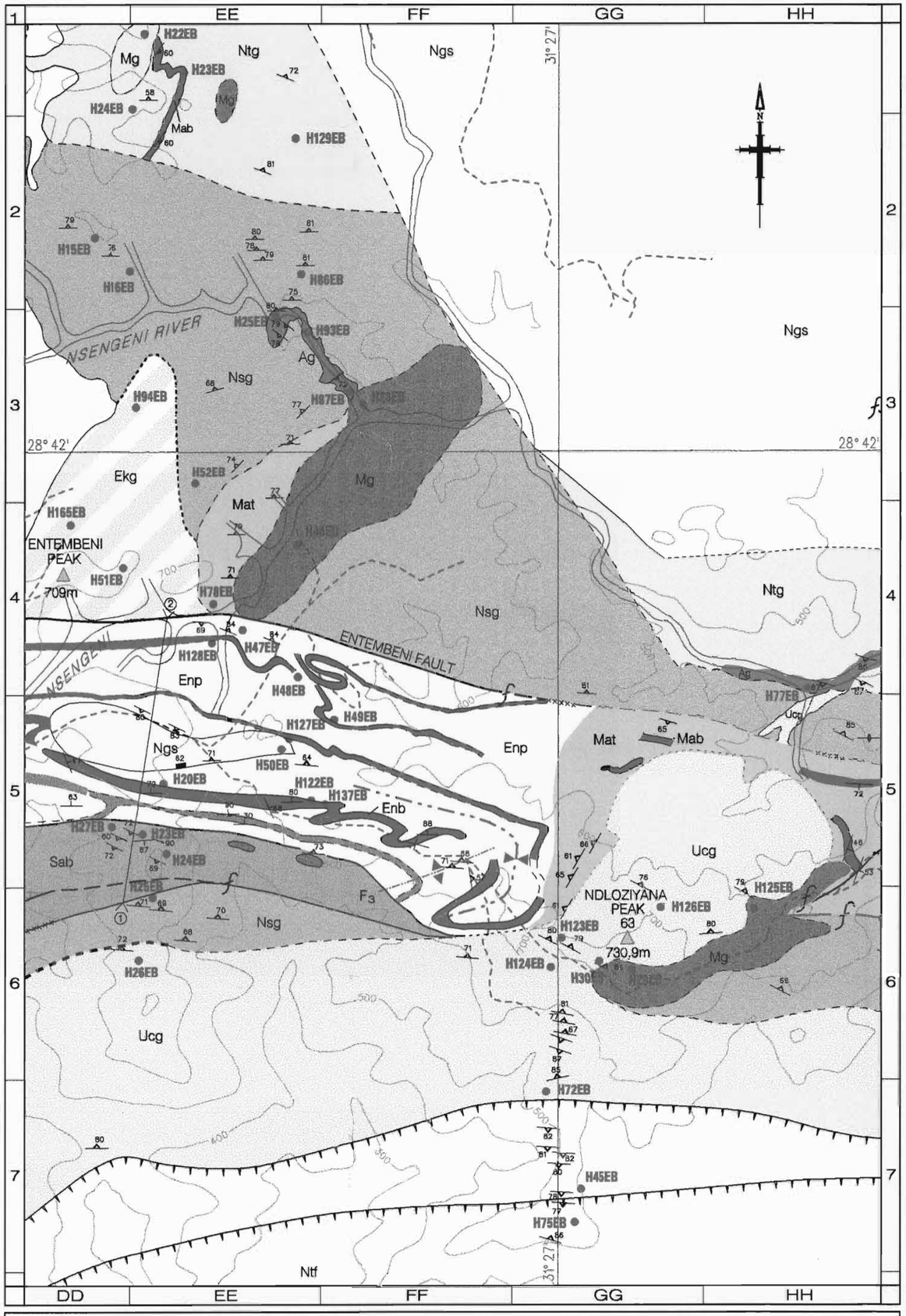

Figure 3.1 UNCONFORMITY BETWEEN THE SABIZA, MATSHANSUNDU AND ENTEMBENI FORMATIONS.

L E G E N D

Entembeni Formation	Enb / Enp / Enc	Phyllite (phyllonitic in the shear zones and along fault contacts) and minor pillowed metavolcanics (Enp), intercalated with cherty BIF (Enb), metacherts and cherty quartzite bands (Enc).
Matshansundu Formation	Mat / Mab	Actinolite–tremolite schist; amphibole–mica schist; massive metabasalt (Mat) intercalated with cherty silicate BIF (Mab).
Sabiza Formation	Sbc / Sab / Sbt	Pillowed metabasalt; banded amphibolite; massive amphibolite; actinolite–tremolite schist (Sab); talc–tremolite schist; serpentinite–talc schist (Sbt); with thin metachert bands (Sbc) and a khakhi-coloured siliceous pelitic rock towards the top of the sequence
	Sat	Transgressive serpentinite–talc schists
	Mg	Metagabbro; metanorite; metagabbroic amphibolite
Umgabhi Granitoid Suite	Ucg	Umgabhi Micrographic Granite
	Esg / Esq	Esibhudeni Granitoid Gneiss (with quartz–sericite schist)
	Umg	Umgabhi Granitoid Gneiss
Nsengeni Granitoid Suite	Ekg	Ekuthuleni Granite
	Nsg	Nsengeni Granitoid Gneiss
	Nts	Ntshiweni Augen Gneiss
Nkwalinye Tonalitic Gneiss	Ntg	Nkwalinye Tonalitic Gneiss
	Ag	Amazula Paragneiss

0 1000 2000

M E T R E S

Of particular interest in the Olwenjini Formation, is the local occurrence of a 15-25m wide quartz-biotite-cordierite-fuchsite gneiss in the Sabiza valley (5.180/V.820). This gneiss has short lateral extent and is thought to be of tectonic origin and probably occurs within a bedding-parallel shear zone in the Olwenjini Formation. It has sharp sheared contacts with chert to the north and amphibolite to the south.

3.2.4 ENTEMBENI FORMATION

This formation tectonically overlies the Sabiza Formation along its southern contact, the Matshansundu Formation in the east and the Olwenjini Formation in the west. Its northern boundary with the Nsengeni Granitoid Gneiss is the Entembeni Fault. The greenstones and metasediments of this formation form part of a large easterly-closing synformal structure.

The lower limit of this formation consists of phyllites which are phyllonitic along the sheared contact with the Sabiza Formation. These phyllites extend the whole strike length of the formation and dip to the north at angles between 45° and 85°. They have sharp concordant contacts with various inter-layered complexly folded metacherts which dip steeply to the north, but in the central areas of the formation, steep southerly dips are encountered (Fig. 2; Fig. 2.2). The metacherts can be traced for a considerable distance along strike and vary in thickness. In some localities (for example in the Ilangwe Peak area) the contacts between the phyllites and metacherts are sheared, resulting in phyllites being phyllonitic near the contact with mylonitic and highly recrystallized metacherts.

Cherty banded iron formations occur along the northern or outer flank of the large synformal fold. Their contacts with the phyllites are sharp, concordant and generally dip steeply to the north. These ironstones are complexly folded. In the Ilangwe Peak road section (Fig. 2.2) they are folded into a tight WNW shallow plunging antiform. They extend eastwards and in the Entembeni/Ndloziyana area they are in contact with structurally underlying Sabiza and Matshansundu Formations of the Umhlathuze Subgroup. The fact that the BIFs occur along the outer flank of the large synform and that they are in contact with the structurally underlying formations indicates that they occur towards the ***base*** of the Entembeni Formation. Moreover, the fact that the Entembeni Formation cuts across the Sabiza and Matshansundu Formations in the Entembeni/Ndloziyana area (Fig. 3.1), suggests that this represents a deformed angular unconformity, as mentioned previously.

East of Ekuthuleni Peak, the phyllites and BIFs are unconformably overlain by an outlier of flat-lying Natal Group sandstones.

3.2.5 SIMBAGWEZI FORMATION

This formation is confined to the western portion of the study area. As mentioned previously, it occurs as a structural wedge between the Olwenjini and Sabiza Formations (see section A – B, Fig. 2). Its southern and northern boundaries are tectonic. It consists mainly of northerly inclined phyllites which are intercalated with pillowed amphibolites, actinolite schists and serpentinitic talc-chlorite schists.

In the vicinity of the southern boundary of this formation, the phyllites contain a number of thin (10-30cm) semi-concordant white quartz veins which represent foliation – parallel faults. The quartz veins are lenticular. Further to the north, the phyllites are in contact with thin steep northerly-inclined concordant lenses of siliceous and serpentinized talc-tremolite-chlorite schists. These serpentinized talc-tremolite-chlorite schists are thought to represent altered ultramafic sheets probably intruded along bedding – parallel faults or shears.

The pillowed amphibolites of the Simbagwezi Formation have sharp concordant contacts with talc-tremolite-chlorite schists and show younging to the NNE. Their foliation dips to the north at angles of 60° to 80°. Towards the northern limits of the Simbagwezi Formation, there occur banded cherts associated with thin cherty quartzitic schists. All these units dip to the north and show concordant contacts with the amphibolites. These rocks occur along the crest of the Simbagwezi Ridge and can be followed intermittently along strike for up to 3km.

3.2.6 NOMANGCI FORMATION

This formation, like the Simbagwezi Formation, occurs only in the northwest portion of the Ilangwe Greenstone Belt. It is a dominantly quartzitic unit with thin quartz schists, quartz-muscovite-(sericite) schists, minor metachert bands and minor phyllites. This formation occurs as wedges extending eastward into the Simbagwezi Formation (5,6/F,G,H). These Nomangci Formation wedges show sharp, concordant tectonic contacts with the Simbagwezi Formation.

The quartzites are clean and massive, and in less recrystallized areas show steep northerly-inclined bedding. Their contacts with the quartz-muscovite-(schists) are concordant. These units are laterally extensive but wedge out eastward into the phyllites of the Simbagwezi Formation. The quartz-muscovite schists probably represent meta-arkosic sediments.

Near Isisusa Peak (4.400/D.280), the quartzites are intercalated with thin discontinuous black metachert bands and minor kyanite-bearing schists. These rocks are inclined steeply to the north and show concordant contacts with the quartzites. The Nomangci Formation is a dominantly meta-arkosic unit and in this respect it is similar to the Moodies Group of the Barberton Greenstone Belt.

3.3 NATURE OF INTER-FORMATIONAL CONTACTS AND STRUCTURAL SUCCESSION

The Ilangwe Greenstone Belt consists of the Umhlathuze and Nkandla Subgroups which are each divided into three formations. In general, the contacts between the six major stratigraphic formations are tectonic, denoted either by semi-concordant faults or shear zones. These structures extend for a long distance along the belt. Faults are denoted by brecciated quartz veins and shears are represented by phyllonites and serpentinitic talc schists.

The Sabiza Formation is the basal unit of the greenstones and extends from the Esibhudeni area north of Isibuta Peak (6.960/E.480) in the west to just west of the Ndloziyana Peak (6.260/FF.720) in the east. The Simbagwezi shear zone forms its northern contact with the Entembeni Formation in the east, the Olwenjini Formation in the central parts of the belt and the Simbagwezi Formation in the west (Fig. 2). South of Simbagwezi Peak, at locality (6.500/J,K,L), the Simbagwezi shear is represented by a 65m wide phyllonitic zone which extends for over 2km. Further to the east, where the Sabiza Formation is overlain by the Olwenjini Formation, the Simbagwezi shear is represented by concordant to slightly transgressive serpentinitic talc schists. Further eastwards, the Simbagwezi shear is phyllonitic and extremely schistose and represents the contact between the Sabiza amphibolite schists and Entembeni phyllites. In the Entembeni/Ndloziyana area, the Simbagwezi shear is cut out by the Umgabhi Micrographic Granite re-entrant. It is at this locality where the Entembeni Formation cuts across both the Sabiza and Matshansundu Formations. The foliation of the Sabiza and Entembeni

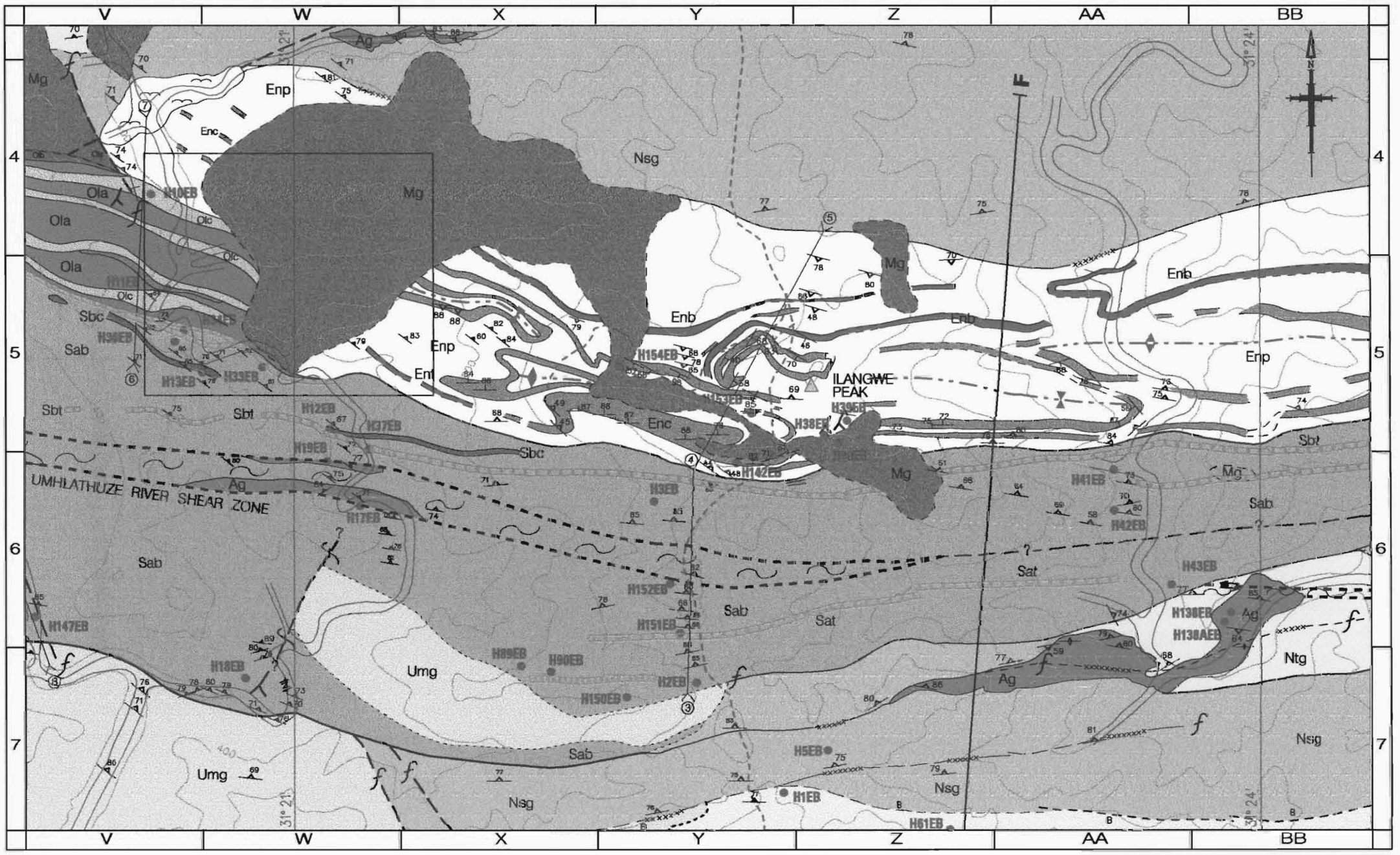

Figure 3.2 : MAP OF THE ANGULAR UNCONFORMITY BETWEEN THE SABIZA, OLWENTINI AND ENTEMBENI FORMATIONS IN THE SABIZA AREA

L E G E N D

Entembeni Formation

Enb, Enp, Enc — Phyllite (phyllonitic at the shear zones and fault contacts) (Enp) intercalated with cherty BIF (Enb), mtacherts and cherty quartzite bands (Enc).

Olwenjini Formation

Ola, Olb, Olm, Olg, Olp, Olc — Pillowed metabasalt; garnetiferous amphibolite; actinolite–tremolite schist (Ola); minor phyllite (Olp); banded cherty quartzite, banded metacherts, fuchsitic quartzites (Olc), silicate BIF (Olb), magnetite quartzite (Olm) and a quartz–biotite cordierite fuchsite gneiss (Olg).

Sabiza Formation

Sbc, Sab, Sbt — Pillowed metabasalt; banded amphibolite; massive amphibolite; actinolite–tremolite schist (Sab); talc–tremolite schist; serpentinite–talc schist (Sbt); with thin metachert bands (Sbc) and a khakhi–coloured siliceous pelitic rock towards the top of the sequence

Sat — Discordant serpentinite–talc schists

Mg — Metagabbro; metanorite; metagabbroic amphibolite

Umgabhi Granitoid Suite

Umg — Umgabhi Micrographic Granite

Esg, Esq — Esibhudeni Granitoid Gneiss (with quartz–sericite schist)

Umg — Umgabhi Granitoid Gneiss

Nsengeni Granitoid Suite

Ekg — Ekuthuleni Granite

Nsg — Nsengeni Granitoid Gneiss

Nts — Ntshiweni Augen Gneiss

Nkwalinye Tonalitic Gneiss

Ntg — Nkwalinye Tonalitic Gneiss

Ag — Amazula Paragneiss

0 1000 2000 3000

METRES

Figure 3.2

Formations is steeply inclined to the north whereas that of the Matshansundu Formation is steeply inclined to the northwest. The fact that the Entembeni Formation cuts across structurally underlying formations at this locality, suggests that this represents a deformed angular unconformity.

In the Sabiza Valley (4,5/V,W), the Entembeni Formation (of the Nkandla Subgroup) is in contact with both the Olwenjini and Sabiza Formations, i.e. the upper and lower formations of the Umhlathuze Subgroup. When followed westward, it seems to be transgressively overlapping the underlying Olwenjini Formation (Fig. 3.2). The pillowed amphibolites of the Olwenjini and Sabiza Formations indicate younging to the NNE and all three formations show steep north-easterly inclined foliations. The contact of the Entembeni Formation with the underlying Olwenjini and Sabiza Formations seem to represent a deformed angular unconformity.

In the Simbagwezi Peak area, the Simbagwezi Formation occurs as a structural wedge between the upper and lower formations of the Umhlathuze Subgroup, i.e. the Olwenjini Formation in the north and the Sabiza Formation in the south (see Section A – B in Fig. 2). Its southern contact with the Sabiza Formation is the Simbagwezi shear zone and its northern contact with the Olwenjini Formation is faulted with brecciated quartz veins occurring at various places along the contact. This means that it is structurally underlain by the Sabiza Formation and is structurally overlain by the Olwenjini Formation with all units younging northwards in the direction of the structural dip. This suggests that the Simbagwezi Formation has been overthrust from the north by a segment of the Umhlathuze Subgroup with the implication that the Simbagwezi Formation was originally at a higher level in the structural succession.

The Nomangci Formation, which is located to the west of the Vungwini River, occurs as a series of finger-like wedges cutting and extending into the Simbagwezi Formation. At locality (3,4,5/D,E,F,G,H), there occurs about five to six E-W or NW-SE trending contacts between Simbagwezi Formation on the north side and Nomangci Formation on the south side of these contacts. The contacts are sharp, concordant and tectonic. In each case, bedding in the Nomangci Formation dips steeply (70° - 87°) to the north or northeast towards, and therefore, below a contact with the Simbagwezi Formation. It follows, therefore, that in each case, the Nomangci Formation structurally underlies the Simbagwezi Formation. This has the implication that the Nomangci Formation was originally at the highest level in the structural sequence.

CHAPTER 4

THE ILANGWE GRANITOID AND METABASIC INTRUSIVE COMPLEX

4.1 GRANITOIDS

Ilangwe magmatism is represented by different types of granitoids and granitoid gneisses and minor basic-ultrabasic bodies, mainly metagabbros, metanorites and metadolerites. The term "granitoid" is used here in a general sense to refer to a whole range of granitic rocks (Best, 1982; Clarke, 1992).

The ***granitoids***, which bound the greenstones and metasediments, can be divided into the Northern Granitoid Complex (NGC) and the Southern Granitoid Complex (SGC).

These northern and southern granitoid complexes can be divided into three broad associations based on similar geochemical and mineralogical characteristics and on three kinds of important ***field relationships***, namely: regional distribution, mutual associations and contact relationships. These associations are :

(a) ***The Amazula Gneiss, Nkwalini Mylonitic Gneiss and Nkwalini Quartzo-feldspathic Flaser Gneiss Association:*** a paragneiss and mylonitic to flaser gneiss association of older gneisses occurring in several widely separated areas and intruded by younger granitoids.

(b) ***The early post-Nondweni granitoids*** comprising -

(i) ***Nkwalinye Tonalitic Gneiss:*** a grey contorted tonalitic gneiss occurring together with the Amazula Gneiss in several widely separated areas and intrusive into the greenstones, the Amazula Gneiss and the Nkwalini mylonitic and flaser gneisses. It is itself intruded by younger granitoids; and

(ii) ***the Nsengeni Granitoid Suite:*** an association of three granitoid phases of similar geochemical-mineralogical characteristics occurring to the north and south of the Ilangwe Greenstone Belt (IGB).

(c) ***the late post-Nondweni*** granitoids consisting of the ***Impisi-Umgabhi Granitoid Suite:*** a microcrystic/megacrystic association of five granitoid phases of similar geochemical and mineralogical characteristics and occurring to the north and south of the Ilangwe Greenstone Belt.

Table 4.1 gives the various phases of these granitoid associations/suites and their general characteristics.

The above classification of post-Nondweni granitoids is derived from field evidence and the recognition and delineation of intrusive and faulted contacts with the Ilangwe greenstones and Nondweni older gneisses (Amazula Gneiss and Nkwalini Mylonitic and flaser gneisses). These observations, supported by geochemical and mineralogical data, mutual association and distribution, suggest that there were ***two*** major episodes of granitoid emplacement with an intervening period of regional faulting - (that is, faults forming the greenstone boundaries).

The early post-Nondweni Nkwalinye Tonalitic Gneiss occurs in both the Northern and Southern Granitoid Complexes but it is more extensive in the former. It is a migmatitic orthogneiss showing intense deformation. It is discussed in more detail in Chapters 6 and 12.

The early post-Nondweni Nsengeni Granitoid Suite consists of :

(i) the Ntshiweni Augen Gneiss which occurs in the western part of the Northern Granitoid Complex;

(ii) the Nsengeni Granitoid Gneiss which occurs in both the Northern and Southern Granitoid Complexes; and

(iii) the Ekuthuleni Granite, a minor unit confined to the Northern Granitoid Complex in the Ekuthuleni area.

TABLE 4.1: THE GRANITOID ASSOCIATIONS OF THE ILANGWE BELT AND THEIR CHARACTERISTICS

GRANITOID ASSOCIATION OR SUITE	PHASES OF THE GRANITOID SUITE	GENERAL CHARACTERISTICS
3. THE LATE POST-NONDWENI GRANITOIDS *IMPISI-UMGABHI GRANITOID SUITE*	5. Zietover Granite 4. Nkandla Granite 3. Umgabhi Micrographic Granite 2. Esibhudeni Granitoid 1. Umgabhi Granitoid	4 and 5 occur in the Northern Granitoid Complex; 1, 2 and 3 occur in the Southern Granitoid Complex. They have similar chemical and mineralogical compositions but varying grain sizes. They are in mutual contact and show gradational relationships with each other. They are intrusive into the greenstone complex, the Amazula paragneiss, the Nkwalini mylonitic and flaser gneisses and the early post-Nondweni granitoids. The above features suggest a genetic relationship and that the Impisi-Umgabhi Granitoid Suite is a young post-Nondweni batholith.
2. THE EARLY POST-NONDWENI GRANITOIDS (ii) *NSENGENI GRANITOID SUITE*	3. Ekuthuleni Granite 2. Nsengeni Granitoid Gneiss 1. Ntshiweni Augen Gneiss	They occur to the south and north of the Ilangwe Greenstone Belt. 1 and 3 occur only in the Northern Granitoid Complex. They have similar major element geochemistry and mineralogy including megacrysts. They show gradational contact relationships; however, 1 has not been found in contact with the others. They are intrusive into the greenstones, the Amazula paragneiss, the Nkwalini mylonitic and flaser gneisses and the Nkwalinye Tonalitic Gneiss. The above features suggest that the Nsengeni Granitoid Suite is a post-Nondweni intrusive of batholithic proportions.
(i) *NKWALINYE TONALITIC GNEISS*		This tonalitic gneiss occurs in several widely separated areas and mostly occurs together with the Amazula Gneiss. It contains rafts of BIF and greenstones and is intrusive into the Amazula Gneiss and the Nkwalini mylonitic and flaser gneisses. The above suggest that the tonalitic gneiss is an early intrusive into the major crustal framework of Ilangwe greenstones and the migmatitic and mylonitic gneisses and is post-Nondweni in age.
1. THE NONDWENI GRANITOIDS *AMAZULA GNEISS - NKWALINI MYLONITIC AND FLASER GNEISSES ASSOCIATION*	A variety of migmatitic, mylonitic and flaser gneisses of widespread distribution.	The Amazula Gneiss occurs as rafts in the Nkwalinye Tonalitic Gneiss or as rafts together with the Nkwalinye Tonalitic Gneiss in younger post-Nondweni granitoids. It also occurs as tectonic slices within the greenstones. The Nkwalini mylonitic and flaser gneisses occur in more extensive but isolated units to the north of the Greenstone Belt. These older gneisses originally formed part of a framework that represents the oldest recognizable gneissic metamorphic complex in this region. (This wording does not mean that these gneisses are older than the Nondweni Greenstones).

These granitoids are discussed in detail in Chapters 7 and 12.

The early post-Nondweni granitoids contain rafts and xenoliths of greenstones and older gneisses and have faulted contacts against the Ilangwe Greenstone Belt (Fig. 2). A feature that they have in common (except the Ekuthuleni Granite) is a well-developed regional foliation. These granitoids are ***pre-boundary faults*** * in age.

The late post-Nondweni Impisi Granitoid Suite is confined to the western and northern parts of the Northern Granitoid Complex whereas the Umgabhi Granitoid Suite is confined to the Southern Granitoid Complex. The former consists of the Nkandla and Zietover Granites and the latter consists of the Umgabhi Granitoid, the Esibhudeni Granitoid and the Umgabhi Micrographic Granite. These granitoid suites are discussed in detail in Chapters 8 and 13.

The late post-Nondweni granitoids also contain rafts and xenoliths of greenstones and older gneisses. The Nkandla Granite contains rafts of quartz-muscovite-(sericite) schists whereas the Umgabhi and Esibhudeni granitoids have rafts of Amazula Gneiss and Nkwalinye Tonalitic Gneiss respectively. The late post-Nondweni granitoids have intrusive contacts against the Ilangwe greenstones and boundary faults. A feature that all these granitoids have in common is a lack of foliation or, rarely, development of a very weak foliation near the contacts with older rocks and near the tectonic contact with the mid-Proterozoic Natal Thrust Front. The late post-Nondweni granitoids are ***post-boundary faults*** in age.

Evidence suggesting that the late post-Nondweni granitoids are intrusive into the early post-Nondweni granitoids is shown by a biotite selvage - an enrichment in biotite - along the contact between the pre-faulting Nsengeni Granitoid Gneiss and the post-faulting Umgabhi Granitoid and Micrographic Granite (7,8/X to CC).

In the Northern Granitoid Complex, the Nkandla Granite is intrusive into the Ntshiweni Augen Gneiss. This is suggested by the northeast trending contact of the Nkandla Granite which is oblique and transgressive to the general E-W to NW-SE trend of foliation in the augen gneiss.

---

*The ***boundary faults*** are the faults bounding the Ilangwe Greenstone Belt.

In Chapter 9 it will be shown that the emplacement of the Nsengeni Granitoid Suite produced the complex folding of an earlier foliation in the Nkwalinye Tonalitic Gneiss; and, in turn, the emplacement of the late post-Nondweni granitoids resulted in the uniform foliation in the Nsengeni Granitoid Gneiss, the augen gneissic texture in the Ntshiweni Augen Gneiss and a superimposed deformation in the Nkwalinye Tonalitic Gneiss.

4.2 METABASIC INTRUSIVES

The Ilangwe Belt is intruded at various places by numerous metabasic/ultrabasic dykes and sills of varying sizes ranging from a few centimetres to hundreds of metres. Only the largest mappable bodies are shown in Fig. 2.

These metabasic intrusions are generally similar in mineralogy and chemistry. They range from fine-grained to coarse grained in texture and they are mainly undeformed, with minor incipient layering at the contacts with the rocks they intrude.

They weather to a rich dusky red soil and onion skin weathering (exfoliation) is characteristic of some weathered surfaces.

Three types of metabasic/ultrabasic intrusions have been observed:

(i) coarse-grained dark green ***metagabbroic*** rocks consisting of coarse-grained white plagioclase feldspars and dark greenish-black pyroxenes, and amphiboles (mainly hornblende);

(ii) coarse-grained dark greenish-black ***metanorite*** with whitish-grey plagioclase, dark green to black pyroxenes and red-brown biotite;

(iii) fine-grained ***porphyritic amphibolitic dykes*** with square/cubic light green microcline porphyroblasts ranging in size from a few mm to about 30mm. In river sections, these porphyritic dykes have been observed to intrude older migmatitic and mylonitic gneisses and the contact margins are chilled and have no porphyroblasts, signifying rapid cooling. A few mm from the contact, the porphyroblasts occur and their size increases away from the contact (see Plate 5.1).

These metabasic intrusions will be discussed in detail in Chapter 15.

The following chapters will be concerned with the lithology, distribution and contact relationships of the various granitoid phases themselves ***and*** those of the granitoids and other lithologies (greenstones and metasediments). The aim is to examine relationships between the phases in an attempt to establish age relationship with the greenstones and other granitoid suites

CHAPTER 5

MIGMATITIC AND MYLONITIC GNEISSES

5.1 INTRODUCTION

These gneisses comprise the migmatitic Amazula Gneiss, the mylonitic Nkwalini Gneiss and the Nkwalini quartzo-feldspathic flaser gneiss. They have wide-spread occurrences within a complex of tonalitic and granitic gneisses.

The Amazula Gneiss, the oldest lithological unit of the granitoid terrain, outcrops as pavements in the Nkwalinye, Nsengeni, Amazula and Umhlathuze Rivers (Fig. 2). Deep weathering obscures the lateral extent of this gneiss but it has been intruded by, and generally occurs as rafts in the Nkwalinye Tonalitic Gneiss or as rafts together with the Nkwalinye Tonalitic Gneiss in younger post-Nondweni granitoids both to the north and south of the Ilangwe Greenstone Belt. It also occurs as small tectonic slices within pillowed amphibolites of the Sabiza Formation.

In contrast, the Nkwalini mylonitic and flaser gneisses occur in more extensive but isolated units to the north of the Greenstone Belt. In the eastern part of the study area, in the Nkwalini area and the Nkwalinye valley, the Nkwalini Mylonitic Gneiss and the Nkwalini Quartzo-feldspathic Flaser Gneiss occur together in association with the Nkwalinye Tonalitic Gneiss and the Amazula Gneiss. In the western areas of Mooiplaas and Mfanefile (Fig. 2) the Nkwalini Flaser Gneiss is absent. The Nkwalini Mylonitic and Flaser Gneisses share a common stratigraphic feature with the Amazula Gneiss in that they are intruded by the Nkwalinye Tonalitic Gneiss and the younger post-Nondweni granitoids. These important features will be discussed in the next sections.

A

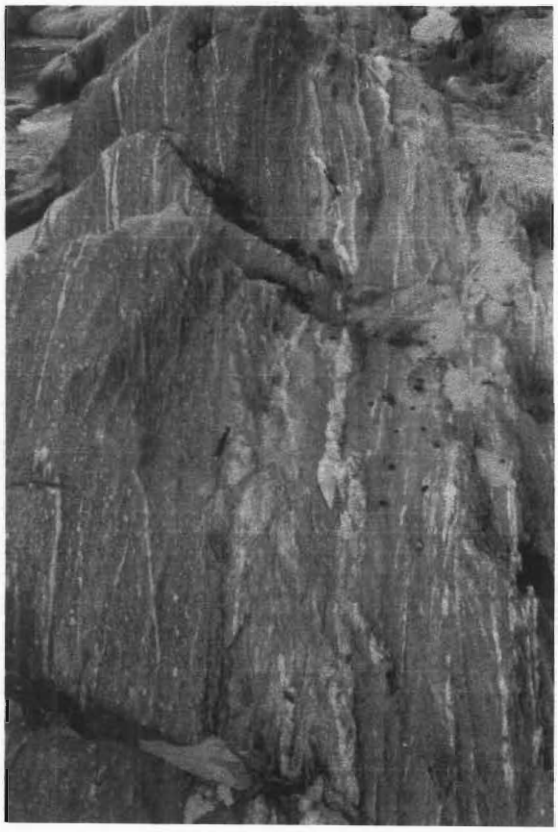

B

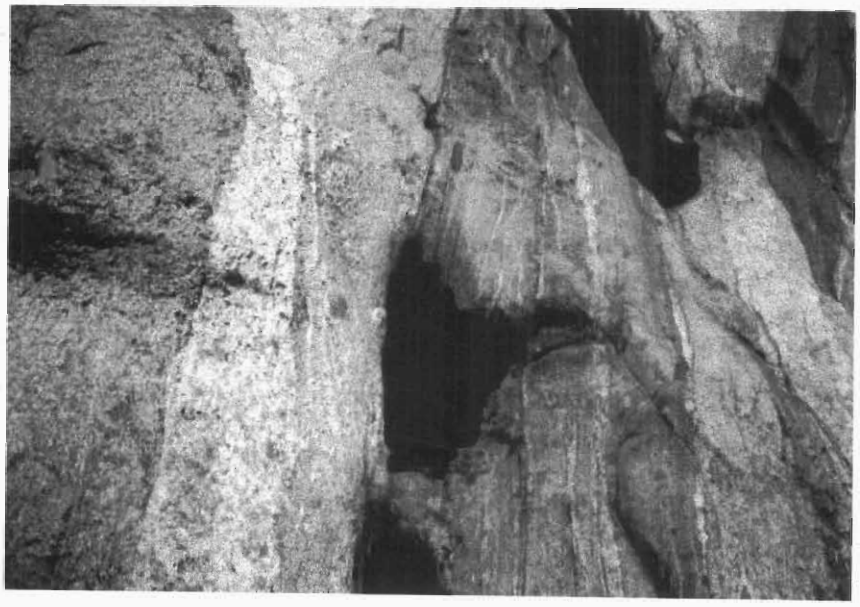

C

Plate 5.1

5.2 AMAZULA MIGMATITIC GNEISS

5.2.1 LITHOLOGY

The Amazula Gneiss consists of crystalline quartzitic and dark greenish amphibolitic bands, fine- to medium- grained, well foliated or finely banded and deformed into complex superimposed folds and sheath folds

The quartzitic - amphibolitic gneiss contains two types of mafic enclaves :

Type A: Type A enclaves are lenticular and on average 2cm wide and about 10cm to 30cm long and most of them parallel the foliation of the gneiss and some are folded. They are described further in the text below.

Type B: Type B enclaves occur as large rafts (schollens) of amphibolite or pyroxenite within the gneiss. The amphibolite schollens are foliated whereas the ultramafic (pyroxenite) schollens are structureless and could represent an original ultramafic component of the greenstones which is now totally lacking or completely altered to talcose serpentinitic schists in the Ilangwe Belt.

In the lower sections of the Nkwalinye River (5/LL,MM) (Fig. 2) (which is the most accessible area where typical exposures of the Amazula quartzitic-amphibolitic gneiss occur) the gneiss consists of greyish-black bands of crystalline quartzitic material alternating with dark green to black bands of hornblendic amphibolite. The gneiss contains dismembered, detached and boudinaged Type A mafic enclaves ranging in size from a few mm to >20cm and are elongated in the foliation direction with the foliation being wrapped around them. Some enclaves have been folded (Plate 5.2).

The gneiss is mylonitic at some places due to intense shearing, contains disseminated pyrite mineralization and is intruded by late stage pegmatite veins (with black tourmaline-schorl) and quartzo-feldspathic sheets deformed into ptygmatic folds cutting across the gneissic foliation (see Plate 5.1).

A

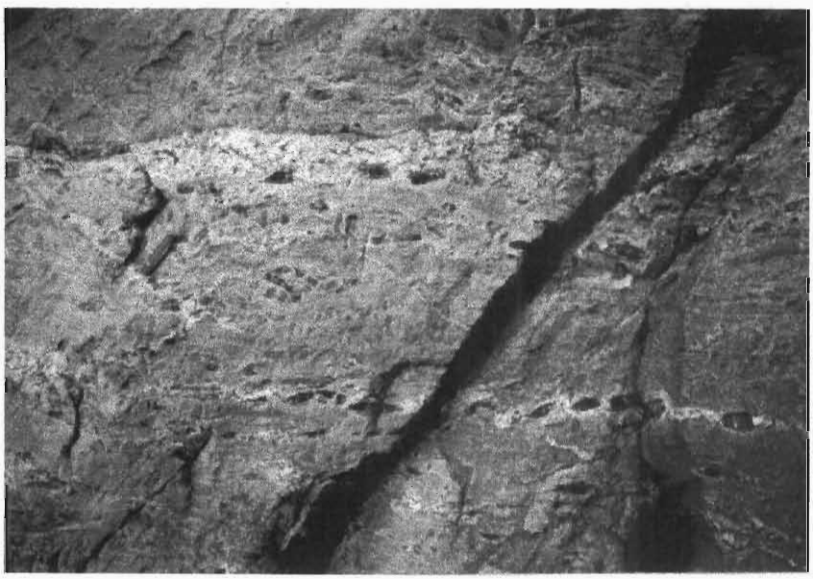

B

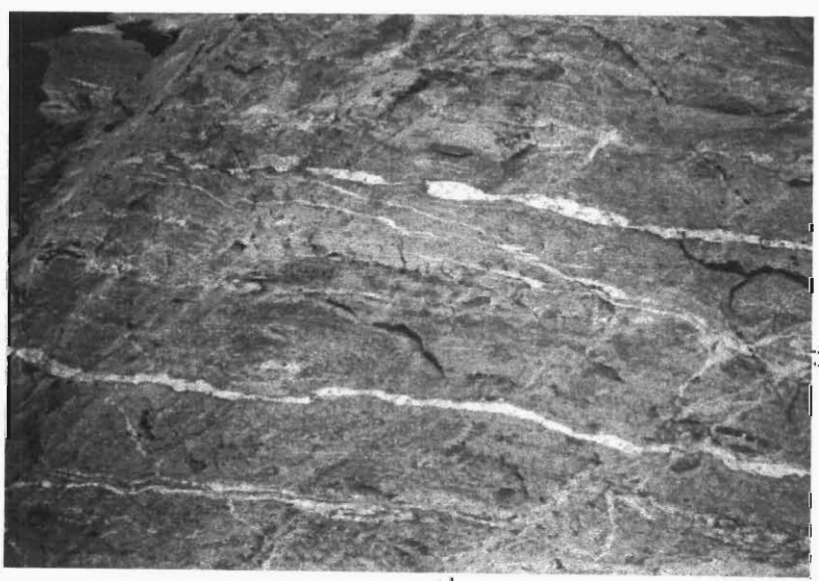

C

Plate 5.2

The gneiss is also intruded by mafic porphyritic dykes and by metagabbroic dykes and sills. The porphyritic dykes contain large phenocrysts of light green microcline ranging from a few mm to about 30mm in size and have sharp contacts with the gneiss (Plate 5.1A). The phenocrysts become finer or even lacking near the contact, indicating a chilled margin. The porphyritic dyke is itself intruded by late stage quartzo-feldspathic sheets of Nsengeni granitoid, indicating that the dyke is at least of pre-Nsuze age.

At some places, the gneiss is intruded by porphyritic dykes which have assimilated some of the gneissic material (Plate 5.1A). Here, it is also intruded by sheets of Nkwalinye Tonalitic Gneiss which displays tight inclined isoclinal folds plunging steeply to the east.

Further upstream in the Nkwalinye River, the Amazula Gneiss is brecciated with amphibolite blocks cemented by quartz and calcite (Plate 5.3C). This breccia is also intruded by pink quartzo-feldspathic sheets of the Nsengeni Granitoid Gneiss and the grey contorted Nkwalinye Tonalitic Gneiss with which it has sharp contacts (Plate 5.3C).

In the upper sections of the Nkwalinye River (4.5/HH,II) just NNE of the Ndloziyana Peak (6.550/GG.570) (Fig. 2.), the Amazula Gneiss consists of thick cream-white bands of quartz and feldspar alternating with dark greenish-grey bands of biotite-rich amphibolite. It has tightly appressed intrafolial isoclinal folds with steep WSW and NNW plunges. The foliation here trends NW -SE and dips steeply to the SW. In general, this gneiss shows transposition of the foliation.

In the Nsengeni River (3.350/EE.750), just before it enters the Nkwalinye River, there is a small pavement of the Amazula Gneiss intruded by the Nsengeni quartz-feldspar-biotite gneiss of the Nsengeni Granitoid Suite. The contact is sharp but transgressive to the foliation of the Amazula Gneiss.

In the Amazula River at the type locality (6,7/Z,AA,BB,CC,DD) (Fig. 2), the paragneiss is spectacularly exposed and to the south it is truncated by the Natal Thrust Front (7.990/CC.990). Here the amphibolite bands of the gneiss contain red garnets which are aligned along the foliation. The gneiss is intruded by the Nsengeni Granitoid Gneiss

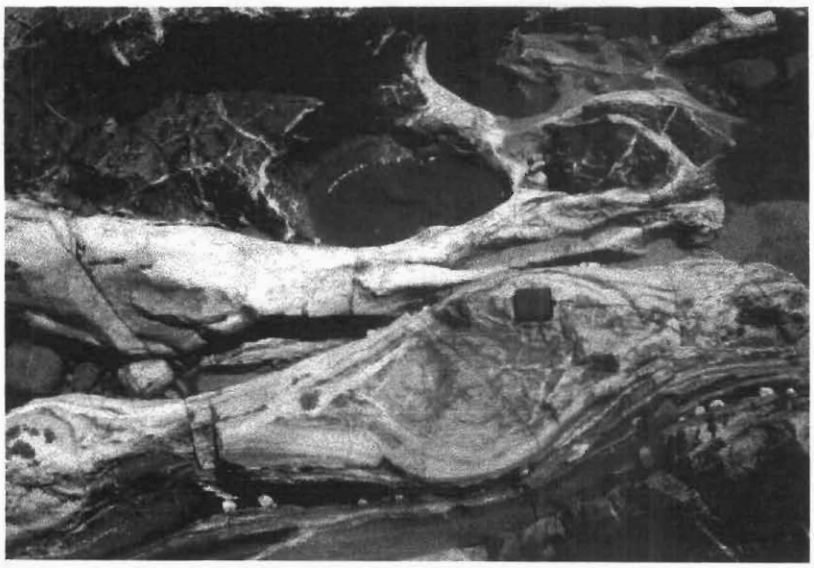

A

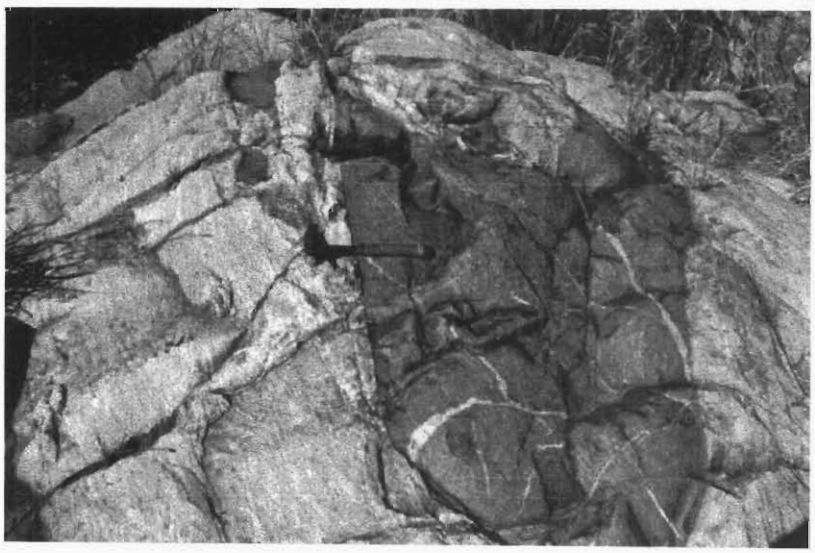

B

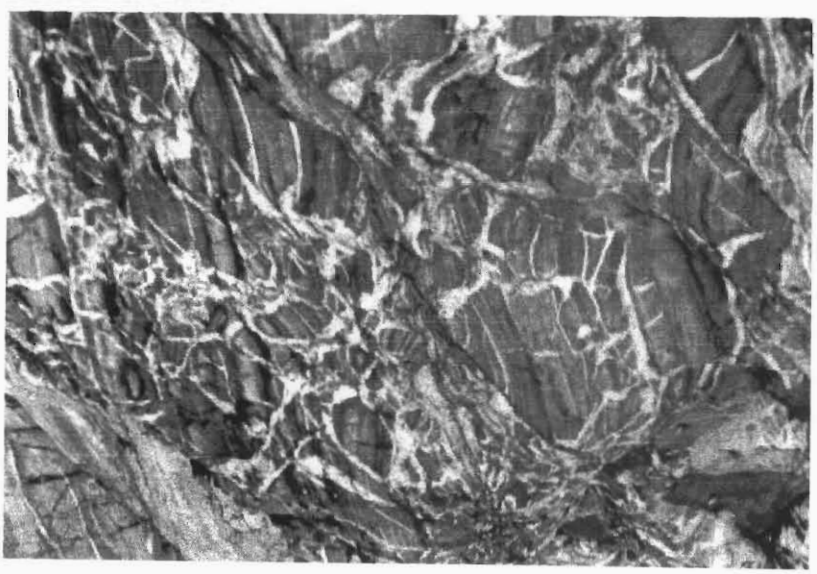

C

Plate 5.3

and the Umgabhi Micrographic Granite. The contacts are sharp and sheeted. Late stage pegmatite veins with black tourmaline (schorl) and quartzo-feldspathic sheets which have been deformed into ptygmatic folds occur in the Amazula Gneiss a few metres from the contacts with the Nsengeni Granitoid Gneiss.

In the central sections of the Amazula River (7.000/BB.300) where it flows in an easterly direction, the Amazula Gneiss is intensely deformed to form sheath folds (Plate 5.4A and B) and it contains Type B deformed mafic enclaves ranging from 10cm to 60cm in size (Fig. 5.1). Late pegmatite veins have been boudinaged (Plates 9.1 and 9.4). The gneiss has been intruded by the Nkwalinye Tonalitic Gneiss and metagabbroic dykes.

In the Umhlathuze River (5.000/Q.250) (Fig. 2), the Amazula Gneiss consists of dark greyish-black crystalline quartzitic bands alternating with dark green amphibolite bands. It is in thrust contact with pillowed metabasaltic lavas of the Sabiza Formation (Fig. 5.2). The thrust plane is concave to the south decreasing in dip from vertical to about 42° in that direction. The Amazula Gneiss structurally overlies sheared mica schists and banded amphibolite slices which form part of the thrust mélange. The thrust structures are syn- or post-D_2 in age as the amphibolite and mica schists show D_2 fold structures.

In the upper sections of the Umhlathuze River where it completes a circular loop, and just west of Spelonk in the Mooiplaas Sappi forest (2/N.O) (Fig. 2), the Amazula quartzitic-amphibolitic gneiss is similar to that in the Nkwalinye River (5/LL,MM) containing rafts of Type B mafic enclaves (Plate 5.3A). Further downstream it is brecciated, with the breccias being cemented by quartz and calcite. The gneiss is deformed into a north-northeasterly inclined steeply plunging antiformal structure (Plate 9.8). The hinge of the antiform is sheared by a major dextral shear. The gneiss is intruded by sheets of the Ntshiweni Augen Gneiss and further down-stream the two rock units are well-foliated with trends parallel to a slightly wavy contact (Plate 5.1B). The augens have been flattened in the plane of foliation.

The Amazula Gneiss is clearly a ***migmatite*** with a quartzitic leucosome and an amphibolitic melanosome and conforms in all respects to the definition of a migmatite (Ashworth, 1985). Field observations from the limited outcrop areas suggest that the Amazula Gneiss

A

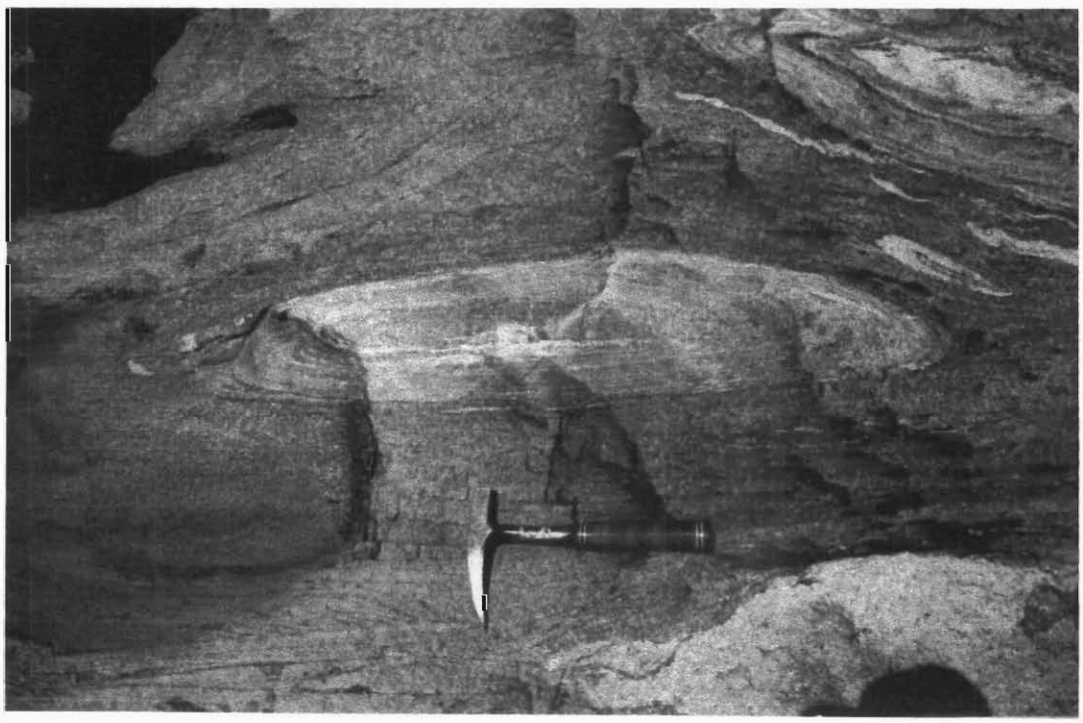

B

Plate 5.4

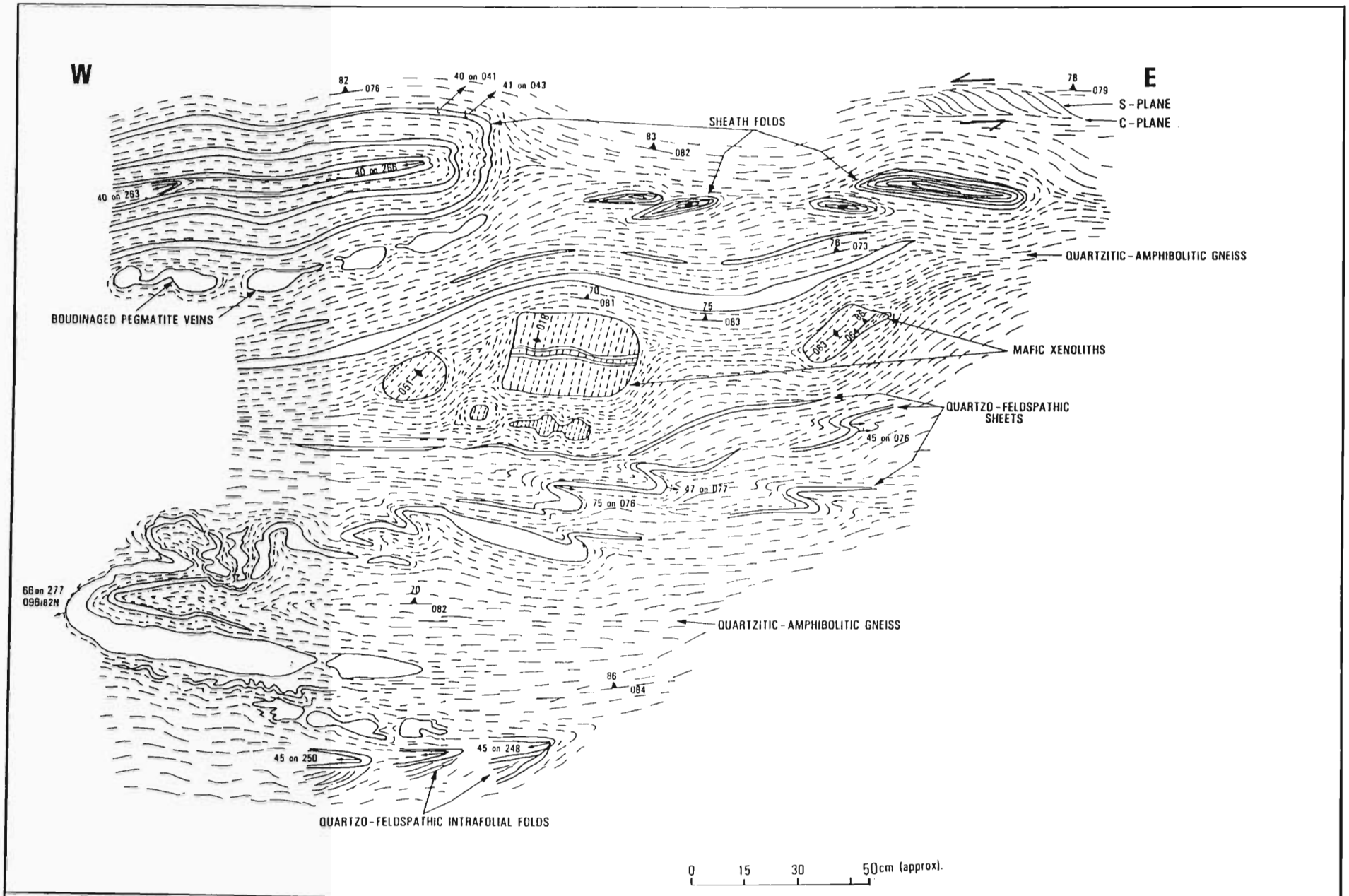

FIG. 5.1 SKETCH MAP OF THE SINISTRAL SHEAR ZONE IN THE AMAZULA RIVER

Author : H Mathe | Date : May 1994 | Scale : As Shown
Drawn By: M. Daubermann | Drawing No :

was derived from pre-existing rocks by diatexis and is therefore a diatexite (Ashworth, 1985). Structures and textures present within the gneiss are :

(i) agmatitic breccias;

(ii) Type A and Type B enclaves, e.g. Plates 5.2 and 5.3;

(iii) ptygmatic folding, boudinage, pinch and swell structures and early intrafolial folds in the quartzo-feldspathic veins and sheets e.g. Plate 5.2B and C ***and*** Plate 5.3A and C;

(iv) intense shearing and bulk flow within the gneiss e.g. Plate 5.1B and Plate 5.4A and B, suggest that it originated by a combination of the following processes (Hyndman, 1985) :

(a) injection of magma to form quartzo-feldspathic veins which usually show dilation. The magma was probably injected into sialic host rocks (Anhaeusser et. al., 1969, p2178);

(b) metasomatism is indicated by some quartzo-feldspathic veins showing no dilation;

(c) metamorphic differentiation, resulting in the distinctive layering of the paragneiss;

(d) extensive partial melting.

The angular enclaves within the quartzitic-amphibolitic gneiss can be interpreted as being derived from pre-existing mafic dykes and/or sills by brittle fracture. The dismembered, ellipsoidal (at some places) and foliation - parallel enclaves probably resulted from post-melt mechanical deformation that affected both the enclave and the host gneiss (Clarke, 1992). Clarke (1992) is of the opinion that the shape and orientation of the enclave represents, in part, the effects of a ductility contrast between the host rock and the enclave.

5.2.2 DISTRIBUTION AND CONTACT RELATIONSHIPS

As mentioned previously, the Amazula Gneiss is exposed in river pavements where it occurs as rafts in younger granitoids both to the north and south of the Ilangwe Greenstone Belt. It also occurs within the greenstones as tectonic slices.

To the north of the greenstone belt, the gneiss is found in the Nkwalinye River, Nsengeni River, a tributary of the Sabiza River and in the Umhlathuze River west of Spelonk (2/O,P).

In the lower sections of the Nkwalinye River, at locality (5.500/MM.480), a raft of Amazula Gneiss occurs in the Nsengeni Granitoid Gneiss. The contacts are transgressive and sharp. To the north and northwest of this raft in the section where the river flows eastwards (centred on [5.300/MM.160]), the Amazula Gneiss is in a transgressive and sharp contact with the Nsengeni Granitoid Gneiss to the south and west ***and*** with the Nkwalini quartzo-feldspathic gneiss to the north. Further to the northwest, at locality (4.930/LL.370), the gneiss is intruded by the Nkwalinye Tonalitic Gneiss to the southwest and by the Nkwalini quartzo-feldspathic flaser gneiss to the northeast. The tonalitic gneiss also intrudes the Nkwalini flaser gneiss near this locality. The contacts are discordant and transgressive, characterized by thin slivers and rafts of boudinaged quartzo-feldspathic flaser gneiss within the tonalitic gneiss (Plate 6.1B). Near this same locality, the Amazula Gneiss is also intruded by a number of small porphyritic dykes (Plate 5.1A).

At the confluence of the Safube River and the Nkwalinye River (4.420/KK.925), a raft of Amazula Gneiss occurs in Nkwalinye Tonalitic Gneiss. The contacts are transgressive and sharp. The foliation of the Amazula Gneiss trends E-W whereas that of the Nkwalinye Tonalitic Gneiss trends NE-SW.

North-northeast of Ndloziyana Peak and in the Nkwalinye River (4.900/HH,II), a raft of Amazula Gneiss occurs in Nkwalinye Tonalitic Gneiss. The southern limit of the raft is a sharp transgressive contact with the intrusive Nsengeni Granitoid Gneiss. At this locality, the raft is also intruded by the Umgabhi Micrographic Granite.

In the Nsengeni River (3/FF), a tributary of the Nkwalinye River, a raft of pyrite-rich Amazula amphibolitic gneiss occurs in the Nsengeni Granitoid Gneiss. Along the transgressive contacts, pegmatoid sheets of Nsengeni gneiss cut across the Amazula Gneiss. A metagabbroic body

intrudes the Amazula Gneiss along its southern boundary and amphibolites of the Matshansundu Formation along the eastern boundary.

Further westwards, at locality (3.840/X.050), and to the northwest of Ilangwe Peak, a raft of Amazula Gneiss occurs within Nsengeni gneiss in a pavement of the tributary of the Sabiza River. The contacts are transgressive.

In the upper sections of the Umhlathuze River and west of Spelonk (2/N,O), a raft of Amazula Gneiss occurs in Ntshiweni Augen Gneiss. The contacts are sharp and slightly wavy and both gneisses are well-foliated with trends parallel to sub-parallel to the wavy contact.

To the south of the Ilangwe Greenstone Belt and within the Southern Granitoid Complex, the Amazula Gneiss occurs in the type area of the Amazula River and also in the Umhlathuze River just to the north of the Umhlathuze gorge. Both these localities are not easily accessible. In the lower sections of the Amazula River (centred on [7.600/CC.790]), a raft of Amazula Gneiss occurs within Umgabhi Micrographic Granite. The contact is slightly discordant and transgressive with a number of feldspathic pegmatoid sheets cutting the gneiss at various places along the contact. Further to the north and northwest (6,7/Z,AA,BB,CC), the Amazula Gneiss is intruded by the Nsengeni Granitoid Gneiss to the south and Nkwalinye Tonalitic Gneiss to the north. The transgressive contacts are sharp and semi-concordant to slightly discordant. Transgressive sheets of a pegmatoid of Nsengeni Granitoid Gneiss occur in both the Amazula Gneiss and the tonalitic gneiss.

In the lower sections of the Umhlathuze River just north of the gorge, slivers of Amazula Gneiss and Nkwalinye Tonalitic Gneiss occur in a shear zone within the Umgabhi Granitoid which has semi-concordant possibly syn-intrusive sheared contacts with the older gneisses.

Within the Ilangwe Greenstone Belt itself, thrust slices of Amazula Gneiss occur in the Umhlathuze River locality (5.000/Q.250) (Fig. 5.2), just south-southwest of Ngcengcengu Peak. The contact between the gneiss and the pillowed amphibolites of the Sabiza Formation is thrusted. Further to the east and just west of the Amazula River, at locality (7.000/AA.290), the apparent faulted contact between the Amazula Gneiss and the Sabiza amphibolites is obscured by a deeply dissected fault gully.

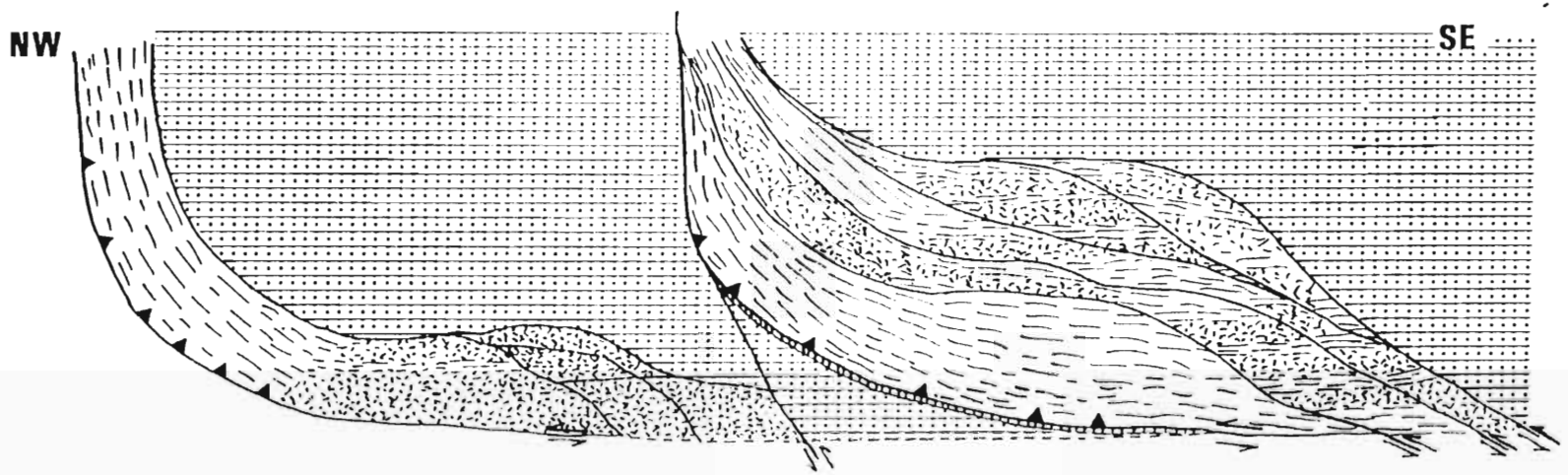

THIN CALCITE (MARBLE) BAND

BANDED AND SHEARED AMPHIBOLITE

MICA SCHIST

FINELY BANDED CHERTY QUARTZITIC - AMPHIBOLITIC GNEISS. (AMAZULA GNEISS)

THRUST: SERATIONS POINT TO OVERTHRUST BLOCK.

FIG. 5.2 : SCHEMATIC SKETCH MAP OF THE AMAZULA GNEISS THRUST SLICES.

Author : H. Mathe	Date : June 1994	Scale : As Shown
Drawn by: M. Daubermann	Drawing No :	

5.3 NKWALINI MYLONITIC AND FLASER GNEISSES

5.3.1 LITHOLOGY

Extensive exposures of ***Nkwalini Mylonitic Gneiss*** occur in the eastern, central and western parts of the study area. The eastern exposures occur in the Mzilikazi Peak area (5/MM,NN,OO) with excellent outcrops in road cuttings along the Nkwalini Pass. The exposures in the central parts of the study area are located in the Mfanefile area (3.600/X,Y) whereas those in the western parts occur in the Sappi Mooiplaas forest plantation east of Spelonk (1,2,3/Q,R,S).

In these widely separated areas, these gneisses are a product of intense deformation (Hobbs et. al., 1976; Ramsay, 1980; Ramsay and Huber, 1987). They consist of alternating bands of fine-grained melanocratic biotite-amphibole schist and leucocratic pinkish-red mylonitic quartzo-feldspathic gneiss (Fig. 5.3; Plate 5.5).

The biotite-amphibole schist consists of dark greenish-black biotite and needle-like to lath-like crystals of hornblende and actinolite with a preferred orientation defining an E-W foliation, which is inclined to the south at about 50°-75°.

The mylonitic quartzo-feldspathic gneiss consists of a fine-grained thin ribbon-like and laminated bands of quartz alternating with bands of pink K-feldspars and white creamy plagioclase. The quartz ribbons define a mineral stretching lineation plunging at 60° to the south-southeast in the foliation which dips to the south at 50° to 65°.

In the road section below Mzilikazi Peak (5.210/NN.500) (Fig. 5.3) the mylonites consist of alternating biotite-hornblende schist, mylonitic quartzo-feldspathic gneiss, a unit of quartzo-feldspathic gneiss containing thin melanocratic amphibolite-biotite lenses (schlieren), amphibolitic schist/gneiss alternating with thin (2mm -20mm) quartzo-feldspathic bands and pink moderately foliated Umgabhi Micrographic Granite which is intrusive into the mylonitic gneisses at this locality. These units are in sheared contact with each other and have been intruded by metagabbroic sheets along shear and foliation planes. The contact margins of metagabbros are fine-grained and chilled, and these metagrabbos show a faint foliation due possibly to shear reactivation. They are cut by a number of sub-horizontal and sub-vertical joints (Fig. 5.3).

PLATE 5.5 : NKWALINI MYLONITES IN THE NKWALINI AREA (5.430/NN.490).

PLATE 5.5A : Southerly-dipping mylonites. South is to the left of the photograph. Note the sheared duplexes in the centre of the photograph.

PLATE 5.5B : D_1 tightly appressed reclined isoclinal folds and intrafolial folds within the Nkwalini mylonites (to the left of the tip of the pencil). The folds plunge to the WSW (right of photo) with axial planes inclined to the southeast.

PLATE 5.5C : Minor reclined F^G_3 small-scale asymmetric S-folds in the mylonites. The "s - c" planes show a down-dip sense of movement (i.e. a southerly vergence).

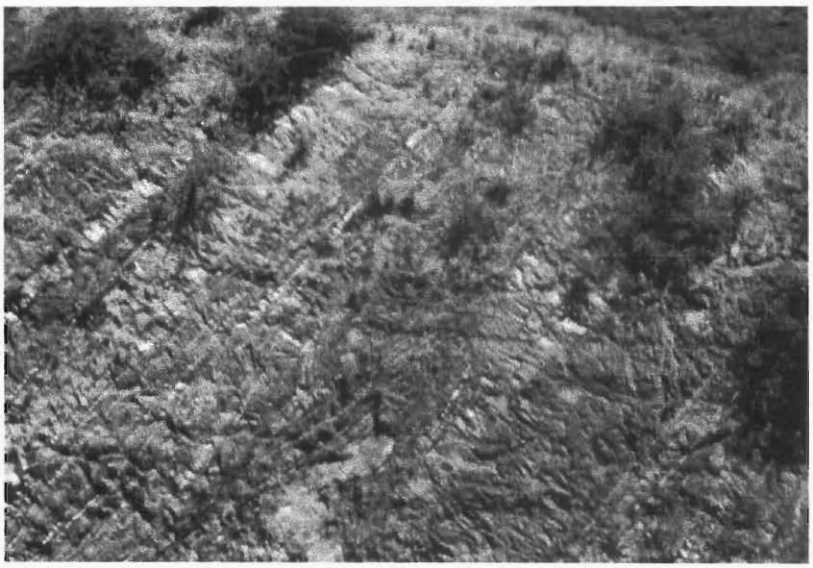

A

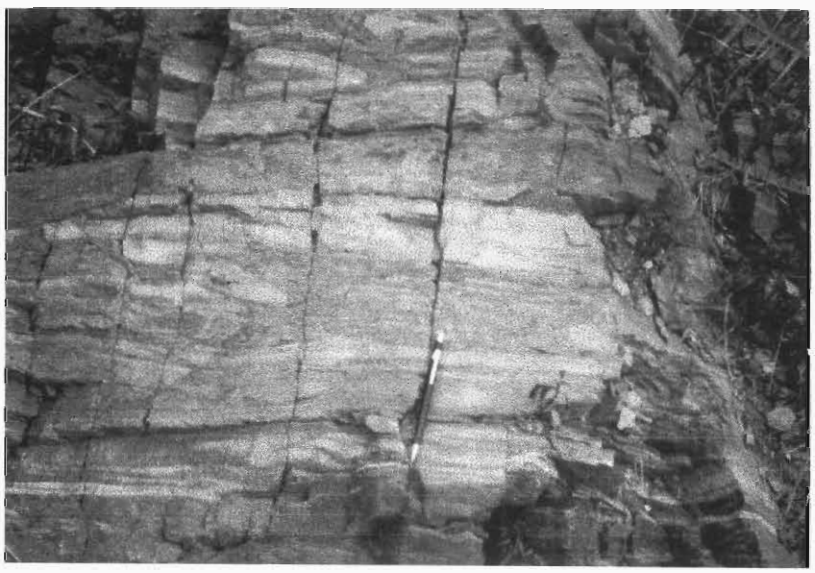

B

C

Plate 5.5

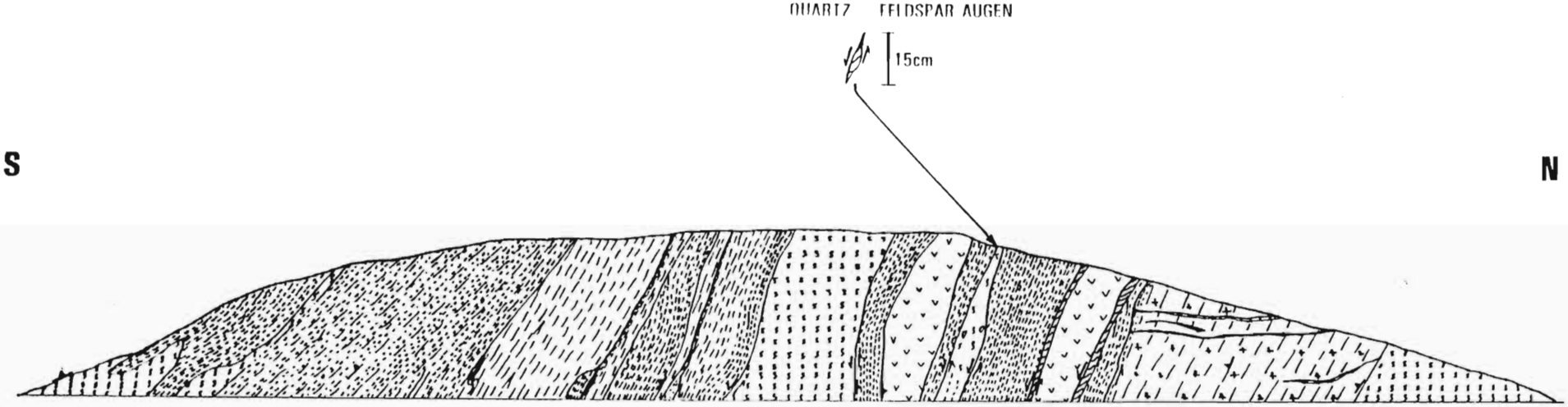

MYLONITIC BIOTITE-AMPHIBOLITE SCHIST WITH BOUDINAGED QUARTZ-FELDSPAR AUGENS

PINK MYLONITIC QUARTZ-FELDSPAR ROCK (PROBABLY DERIVED FROM A MICROGRAPHIC GRANITE)

AMPHIBOLITE WITH THIN (2-20mm) QUARTZ FELDSPAR BANDS

FOLIATED PINK MICROGRAPHIC GRANITE

METAGABBRO

SUBHORIZONTAL GREYISH-WHITE FIBROUS QUARTZ (DISPLACING FOLIATION ON THE GRANITE)

0 5 10m

FIG. 5.3 SECTION ON THE R34 ROAD CUTTING THROUGH THE NKWALINI MYLONITE ZONE

Author : H. Mathe	Date June 1994	Scale As Shown
Drawn by: M. Daubermann		Drawing No :

In the eastern [Nkwalini-Mzilikazi Peak (5/NN.500)] and central [Mfanefile (3.600/X,Y)] areas, the mylonites have an E-W foliation and are inclined steeply to the south. In the western [Mooiplaas (1,2,3/Q,R,S)] area, the foliation is NW-SE and dips steeply to the southwest. In the Nkwalini area, the gneisses are deformed into early D_1 intrafolial and isoclinal folds with axial planes trending E-W and inclined to the south at 50° to 75°. The S_2 foliation is axial planar to these early folds. Vergence, as determined from small-scale asymmetric D_2 folds is down-dip to the SSW (Plate 5.5C). S-C structures also show the same sense of movement (Fig. 5.3).

The ***pink Nkwalini Quartzo-Feldspathic Flaser Gneiss*** is confined to the eastern parts of the study area. It occurs to the north and south of the Ilangwe Greenstone Belt and is intruded by the Nsengeni Granitoid Gneiss and the Nkwalinye Tonalitic Gneiss.

Along the Nkwalini pass, the slightly less deformed pink quartzo-feldspathic granitoid gneiss occurs together with Nkwalini mylonites (see Fig. 5.3).

It is dominantly pinkish-red and contains pink K-feldspars alternating with streaked and elongated transparent quartz ribbons and creamy to milky white plagioclase giving the rock its intensely foliated flaser texture. Where it is mylonitic, it also contains flaky biotite and sericite (from the alteration of feldspars). In less deformed areas along the Nkwalinye River, this granitoid has a weak (or even lacks) foliation.

In the Nkwalinye River (5.570/LL.860) this flaser gneiss is intrusive into the Amazula Gneiss and in some areas the intrusive contact is characterized by abundant hydrothermal brecciation (auto brecciation ?) of the Amazula amphibolitic gneiss. The amphibolite breccias are cemented by calcite in a quartz-feldspar matrix. The flaser gneiss is itself intruded by a fine-grained mafic dyke which contains detached quartzo-feldspathic flaser gneiss xenolithic rafts and by the Nkwalinye tonalitic gneiss.

5.3.2 DISTRIBUTION AND CONTACT RELATIONSHIPS

The Nkwalini mylonitic and flaser gneisses occur mainly to the north of the Ilangwe Greenstone Belt. A thin wedge of flaser gneiss occurs to the south of the greenstones. Whereas the flaser gneiss is confined to the eastern parts of the study area in the Nkwalini area and Nkwalinye valley, the Nkwalini Mylonitic Gneiss occurs in three widely separated areas as mentioned previously.

In the type area around Mzilikazi Peak and the Nkwalini Pass (4,5/MM,NN), the mylonites and flaser gneisses are intruded by the Nsengeni Granitoid Gneiss along their western boundaries. The contacts are discordant and transgressive. In this locality, these gneisses are also intruded by the Nkwalinye Tonalitic Gneiss along their northern boundary. A transgressive wedge of tonalitic gneiss also separates the mylonites from the flaser gneiss.

Thirty kilometres to the west, in the Mooiplaas area (2/R,S), a similar relationship is observed, with the Nsengeni Granitoid Gneiss transgressing across the foliation around the eastern limit of the Nkwalini mylonites. The Nkwalinye Tonalitic Gneiss in this area extends as a wedge into the mylonites, cutting transgressively across the foliation of the mylonites along both boundaries of the wedge. The mylonites are also cut transgressively by the Ntshiweni Augen Gneiss along the western and northern boundaries.

In the Mfanefile area (3/Y), a raft of Nkwalini Mylonitic Gneiss occurs in the Nsengeni Granitoid Gneiss, whereas in the Mooiplaas area (1/Q,R), a triangular raft of mylonitic gneiss is intruded by the Zietover Granite along its western limit and by the Ntshiweni Augen Gneiss along the eastern and southern boundaries. The contacts are sharp and transgressive.

CHAPTER 6

THE EARLY POST-NONDWENI GRANITOIDS (PART I) NKWALINYE TONALITIC GNEISS

6.1 INTRODUCTION

The most widespread occurrence of the Nkwalinye Tonalitic Gneiss is to the north of the Ilangwe Greenstone Belt, within the ***Northern Granitoid Complex***. The tonalitic gneiss extends from the Ndundulu Peak area in the east, to the Sappi Mooiplaas Forest Plantation area in the west, a distance of about 24km. In the Mzilikazi Peak - Nkwalini area and along the Nkwalinye River, the tonalitic gneiss occurs together with the older migmatitic and mylonitic gneisses. In the Mooiplaas area, it intrudes the mylonitic gneisses. In the Zietover area, rafts of BIF and metagabbroic sheets occur within the tonalitic gneiss; whereas to the west of Mfanefile area, only metagrabboic rafts occur within the gneiss.

Minor widely separated outcrops of this tonalitic gneiss occur within the ***Southern Granitoid Complex***. These exposures are found along the lower sections of the Amazula and Umhlathuze River and occur together with the Amazula Gneiss. These exposures are not easily accessible. Towards the western limit of the Southern Granitoid Complex, a small raft of Nkwalinye Tonalitic Gneiss occurs within the Esibhudeni Granitoid Gneiss.

Relatively few tonalitic gneiss exposures are found within the ***Ilangwe Greenstone Belt*** and these occur in shear zones as tectonic slices within sheared amphibolites. These occurrences are found in isolated areas in the Sabiza, Umhlathuze and Olwenjini Rivers.

In the following description of the Nkwalinye Tonalitic Gneiss, only intrusive contacts with older gneissic and greenstone formations will be considered. The contacts with younger granitoids will be described later.

6.2 LITHOLOGY

The ***Nkwalinye Tonalitic Gneiss*** consists of leucocratic bands of megacrystic to microcrystic leucosome of quartz and feldspars with a perthitic texture and melanocratic melanosome bands of foliated amphiboles and biotite (Plate 6.1) (Ashworth, 1985). It can be classified as a ***migmatitic orthogneiss***. It is characterized by transposed foliation, a distinctly layered to stromatic structure, a quartzo-feldspathic leucosome and a ferromagnesian melanosome and a K_2O/Na_2O ratio of less than unity.

Generally, the gneiss is medium- to coarse-grained but becomes fine-grained in high strain areas (e.g. Nkwalinye River and Olwenjini River shear zone) and also near sharp, intrusive contacts with the Amazula Gneiss. The tonalitic gneiss has E-W trending foliations with variable steep northerly or southerly dips. It is frequently folded into tight intrafolial and isoclinal folds (Plate 6.1C) with steep easterly plunges. In the Umgabhi shear zone (in the Umhlathuze River near the gorge) the tonalitic gneiss has been deformed into tight isoclinal folds and it is intrusive into the Amazula Gneiss with which it occurs in this locality. In the lower sections of the Nkwalinye River (5.190/LL.340), it has an extreme mylonitic texture and transposed foliations resulting in natural back-rotated layer segments - Type IIB asymmetrical pull-aparts of Hanmer and Passchier (1991) (Plate 6.1A and B).

In the Nkwalinye River (4.950/LL.260) and the Safube tributary of the Nkwalinye River (4.020/KK.420) the tonalitic gneiss is intruded by several fine- to medium-grained non-foliated mafic dykes which contain, near the sharp transgressive intrusive contact, large xenolithic rafts (schollens) of contorted gneiss. The dyke cuts obliquely across the tonalitic gneiss foliation and as it intruded it ripped off and assimilated blocks (of varying size) of tonalitic gneiss. These tonalitic rafts, which lie in an orientation sub-perpendicular to the gneissic foliation, "float" in the mafic dyke near the sharp contact with the gneiss.

In the Zietover area (1.440/EE.480) the tonalitic gneiss is fine-grained (microcrystic) and mylonitic (Plate 6.2A). It is deformed into D_2 tight isoclinal s-fold structures plunging steeply to the east with F_2 axial planes inclined to the north (Plate 6.2A). The mylonitic nature of the gneiss is possibly due to an E-W fault which is thought to be the contact between this gneiss and the Zietover Granite.

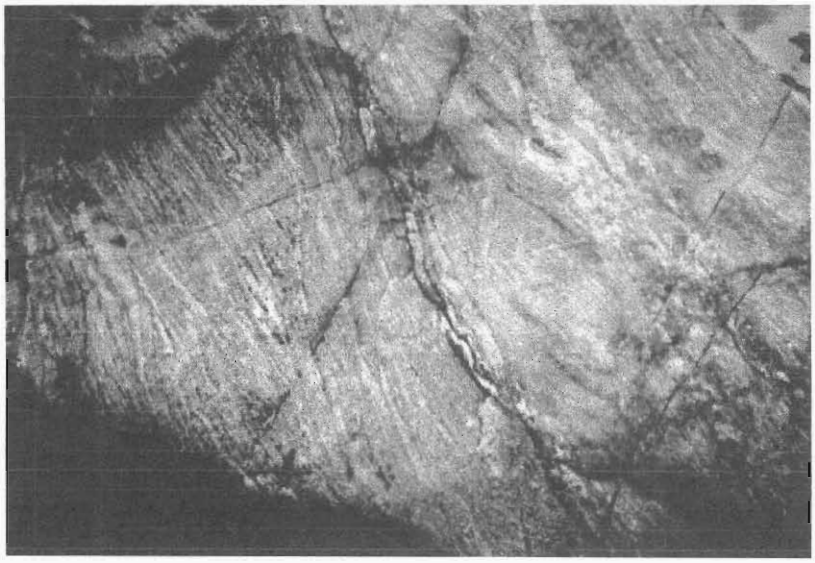

A

B

C

Plate 6.1

In the upper sections of the Nkwalinye River (4.950/HH.995), the tonalitic gneiss is also microcrystic and mylonitic and is deformed into a D_2 easterly-closing upright fold (Plate 6.2B). The northern limb of this fold is intruded obliquely by pinkish-red quartzo-feldspathic sheets of the Nsengeni Granitoid Gneiss (Plate 6.2B). The contact is diffuse and discordant but the colour contrast is obvious.

In the Olwenjini valley (4.250/S.500), the Umhlathuze valley (5.950/U.870) and the Sabiza valley (6.200/W.700), the Nkwalinye Tonalitic Gneiss is in tectonic contact with amphibolite schists of the Umhlathuze Subgroup. The gneiss is fine-grained and completely sheared and schistose in texture.

6.3 CONTACT RELATIONSHIPS

As mentioned previously, the Nkwalinye Tonalitic Gneiss occurs mainly to the north of the Ilangwe Greenstone Belt. To the south of the belt, it occurs in the Amazula River and also to the northeast of Esibhudeni (7.200/G.820) in the Esibhudeni Granitoid Gneiss. Minor occurrences are found as thrust slices within the greenstones of the Umhlathuze Subgroup.

In the lower sections of the Nkwalinye River, the tonalitic gneiss transgressively intrudes the south-western boundary of the Amazula Gneiss and forms a wedge into the western limit of the Nkwalini quartzo-feldspathic flaser gneiss and the Nkwalini mylonitic gneiss at Mzilikazi Peak.

In the upper sections of the Nkwalinye River just north of the Matshansundu area, the tonalitic gneiss contains a number of rafts of Amazula Gneiss. The contacts are sharp and transgressive.

Further to the west, in the Mooiplaas area, a re-entrant extension of the tonalitic gneiss cuts across the foliation of the Nkwalini Mylonitic Gneiss.

To the south of the Ilangwe Greenstone Belt within the Southern Granitoid Complex, the tonalitic gneiss shows discordant transgressive contacts with the Amazula Gneiss which it intrudes in the Amazula River (6,7/Z,AA,BB,CC). It shows similar intrusive contact relationships with the Sabiza Formation amphibolites at this locality but the contacts are

A

W

E

B

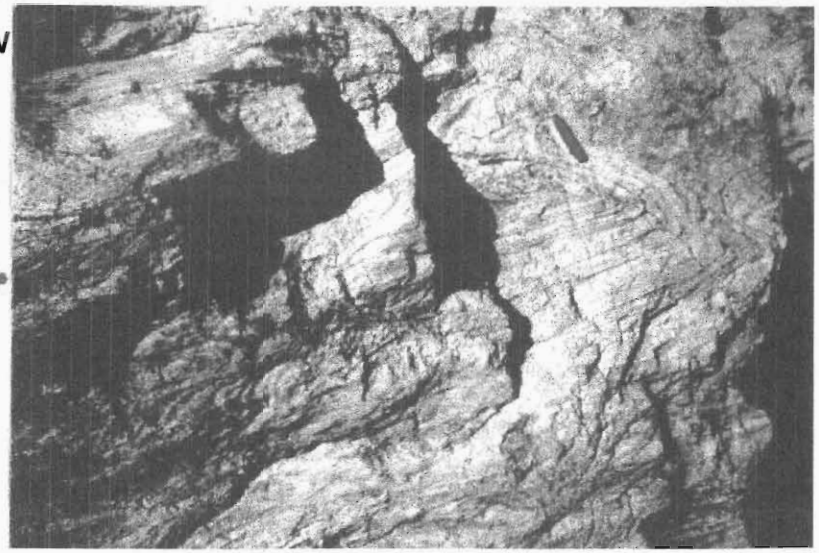

C

Plate 6.2

deeply weathered and obscured by alluvium. The contact relationships between the Nkwalinye Tonalitic Gneiss on the one hand, and the older gneisses and greenstones on the other, indicate that the tonalitic gneiss is an early intrusive into the major crustal framework of the Ilangwe greenstones, the Amazula Gneiss and mylonitic to flaser gneisses. It is therefore of post-Nondweni age.

In the Sabiza and Umhlathuze Rivers and within the Umhlathuze River shear zone (5,6/U,V,W,X), thrust slices of tonalitic gneiss occur within schistose amphibolites of the Sabiza Formation. The tonalitic gneiss contains quartz veins with black tourmaline and cataclastic structures like agmatitic breccias containing amphibolite blocks (Plate 6.2C). The contact with the Sabiza amphibolites are slightly discordant to semi-concordant. Within the Olwenjini Formation in the Olwenjini valley, the tonalitic gneiss is structurally deformed and has a mylonitic fabric.

CHAPTER 7

THE EARLY POST-NONDWENI GRANITOIDS (PART II) NSENGENI GRANITOID SUITE

7.1 INTRODUCTION

The Nsengeni Granitoid Suite is an association of three megacrystic and well foliated granitoid units with gradational contacts, similar mineralogical and geochemical characteristics. This suite occurs to the north and south of the Ilangwe Greenstone Belt. The general characteristics of the granitoids of the Nsengeni Suite are listed in ***Table 4.1***.

To the north of the greenstone belt, the suite stretches from just north of the Simbagwezi Peak (3,4/J,K) in the west to the Nkwalinye-Nkwalini area in the east – a distance of about 30 km. To the south of the greenstone belt, the suite extends from west of Umgabhi Ridge (7,8/W,X) in the west to west of Nkwalinye valley (5,6/LL,MM) in the east, a distance of about 16km.

This granitoid suite consists of the following units (***Table 4.1***) :

(i) ***Ntshiweni Augen Gneiss*** which occurs only in the western part of the Northern Granitoid Complex. It is intensely deformed but probably less evolved than the Nsengeni Granitoid Gneiss and hence it may represent an earlier phase of the Nsengeni Granitoid Suite;

(i) ***Nsengeni Granitoid Gneiss*** which occurs on both sides of the Ilangwe Greenstone Belt; and

(iii) ***Ekuthuleni Granite***, a minor megacrystic unit confined to the Northern Granitoid Complex in the Ekuthuleni area (3,4/DD,EE). It shows gradational contacts with the Nsengeni Granitoid Gneiss.

Evidence presented later indicates that these granitoids are intrusive into the greenstones, the migmatitic and mylonitic Amazula and Nkwalini gneisses and the Nkwalinye Tonalitic Gneiss. These aspects and the extensive distribution of the Nsengeni Suite suggest that this granitoid association represents an early post-Nondweni intrusive of batholithic proportions.

7.2 LITHOLOGIES AND CONTACTS BETWEEN GRANITOID UNITS

The ***Nsengeni Granitoid Gneiss*** is the most wide-spread granitoid in the study area and it is well developed in the Nsengeni valley in the north central parts of the study area (2,3,4/W to FF), where the river itself traverses granitic terrain until it enters the Nkwalinye River. The northern Nsengeni Granitoid Gneiss extends from the Nkwalinye River valley (5/NN) in the east to the Sappi Mooiplaas forest plantation (3/Q,R) in the west. The southern Nsengeni Granitoid Gneiss also extends westwards from the Nkwalinye River valley (5/NN) to just west of Umgabhi Peak (8.345/Y.000).

It is a fine- to medium-grained rock consisting of transparent to milky white quartz, pinkish-orange perthitic K-feldspars and creamy white perthitic plagioclase which form the leucocratic component of the granitoid. The melanocratic component is composed of fine-grained greenish-brown-black biotite flakes, which define the foliation where it is developed. The foliation dips dominantly to the north at 60 - 90° but steep southerly dips also occur. Foliation is well-developed near the faulted contact with the greenstones and also near the E-W trending faults cutting the granitoid gneiss northeast of Umgabhi Ridge (7/Y,Z,AA). The well-foliated portions of the granitoid gneiss are characterized by the reduction in grain size, largely by recrystallization and in part by grain breakage especially near faults where there is abundant brecciation (areas marked xxxxx in Fig. 2). In these localities, biotite is altered to chlorite whereas plagioclase is altered to epidote and sericite. However, no S-C foliations have been observed in this granitoid, but they do occur in the Nkwalinye Tonalitic Gneiss which it intrudes.

In non-foliated parts of the granitoid, very weak magmatic foliations occur. These are in the form of aligned K-feldspars and biotite. In thin section, deformation is characterized by undulose extinction and the recrystallization of quartz and, occasionally, the development of myrmekite along grain boundaries (Plate 12.1 B-D). No folding of the foliation has been observed in this granitoid.

The Nsengeni granitoid weathers into a characteristic orange-brown sandy soil.

In the Umgabhi Peak area (8/Y), the granitoid gradually becomes porphyroblastic with the occurrence of large greenish-black biotite flakes and porphyroblasts of plagioclase feldspar. There is a marked enrichment in biotite along the contact between the Nsengeni Granitoid Gneiss and the intrusive Umgabhi Granitoid and Umgabhi Micrographic Granite. This biotite selvage is due to the intrusion of these late post-Nondweni granitoids. Biotite from these sites usually exhibits undulose extinction and minor kinking and is slightly altered to chlorite and epidote.

At locality (5.200/MM.210), a rounded wedge of Nsengeni Granitoid Gneiss shows discordant transgressive contacts with the Nkwalini Quartzo-feldspathic Flaser Gneiss. In the Nkwalinye River (4.780/KK.920), near an intrusive contact with the pink Nkwalini Quartzo-feldspathic Flaser Gneiss, the Nsengeni Granitoid Gneiss contains pinkish-red K-feldspar porphyroblasts and ribbon-like quartz resulting in the gradual development of a flaser texture, mimicking that of the Nkwalini Flaser Gneiss. Discordant transgressive contacts are shown with Amazula Gneiss and Nkwalini Mylonitic Gneiss in the Nkwalinye Valley. These contact relationships have been discussed previously.

The ***Ntshiweni Augen Gneiss*** extends from the eastern Mandaba area in the west to just beyond the Sappi Mooiplaas forest plantation in the east. The granitoid is spectacularly exposed in the area where the Umhlathuze River forms a circular loop (2,3/N,O). Accessible outcrops are in the Umhlathuze River just west of Spelonk (2.200/P/105). It is a lensoid-shaped greyish-blue granitoid consisting of cream white quartz and drawn-out porphyroclasts of feldspars and greenish-black biotite and minor hornblende. The feldspar porphyroclasts are up to 20mm in diameter and are set in a fine- to medium-grained matrix of biotite and quartz, and the biotite tends to wrap itself around the augens.
In the Umhlathuze River just south of Spelonk and west of Ntshiweni Peak (Fig. 2) the megacrystic Ntshiweni Augen Gneiss intrudes the banded Amazula Gneiss and the feldspar porphyroclasts are flattened and elongated in the foliation and the augen gneiss becomes a flaser gneiss. To the north of Spelonk, the augen gneiss is intruded by the Zietover Granite. The E-W trending contact of the Zietover Granite is discordant and transgressive to the NW-SE trend of foliation of the augen gneiss. A similar discordant transgressive contact relationship can be observed further to the southwest (1,2,3/K,L,M) where the NE trend of the intrusive Nkandla Granite is transgressive to the E-W to NW-SE foliation trend of the Ntshiweni Augen Gneiss. Another significant characteristic of this contact is the significant biotite enrichment in the augen gneiss.

In the northeastern flanks of the Simbagwezi Peak (6/K) the augen gneiss contains a raft of Nomangci Formation quartz-muscovite-(sericite) schist. Near these schists there occur a number of very thin white metaquartz fault fillings which define NE - SW trending micro faults cutting the augen gneiss. Foliations generally dip to the north at 60 - 80°.

In some deformed areas, for example near the confluence of the Damuzini and Vungwini Rivers (3.600/M) and also in the Umhlathuze River at locality (3.840/O.620), the augen gneiss shows a very prominent lineation - an L-tectonite - which is displayed by quartz and plagioclase feldspars. The augen in this gneiss probably developed by gradual grain size reduction during dynamic recrystallization of quartz and feldspars (Tullis et. al., 1982).

The ***Ekuthuleni Granite*** phase of the Nsengeni Granitoid Suite is restricted in occurrence to the Entembeni area to the east of the Ekuthuleni store and school (4/DD,EE). It is a light grey to dark grey megacrystic granite consisting of greyish perthitic feldspars and megacrystic quartz grains set in a fine-grained matrix of quartz and feldspar. The feldspar porphyroclasts are up to 15 - 20mm in diameter. The granite is structureless and shows no signs of deformation. However, under the microscope quartz shows undulatory extinction, which is indicative of deformation. Another characteristic deformation indicator is the fracturing of feldspars and the breakdown of plagioclase to epidote and sericite (Paterson et. al., 1990; Morand, 1992).

To the north and east it grades into the Nsengeni Granitoid Gneiss and in the southeast it is intrusive into an amphibolitic schist raft of the Matshansundu Formation (3,4/EE,FF). Its western limits cannot be established because it is overlain by sandstones of the Natal Group. It is possibly a local megacrystic variant of the Nsengeni Granitoid Gneiss which shows no foliation and contains very little biotite.

7.3 CONTACTS WITH NKWALINYE TONALITIC GNEISS

The contact relationships between the Nsengeni Granitoid Suite of rocks and the migmatitic and mylonitic gneisses have been described in Chapter 5. In this section, only those between the Nsengeni Granitoid Suite and the Nkwalinye Tonalitic Gneiss will be described.

To the north of the Ilangwe Greenstone Belt, the southern boundary of the Nkwalinye Tonalitic Gneiss is in contact with the northern limit of the Nsengeni Granitoid Gneiss. The

contact is slightly discordant to semi-discordant and in some places it shows evidence of post-intrusive deformation with mylonitic fabrics in the Nsengeni granitoid near the contact with the tonalitic gneiss; for example at locality (4/II,JJ,KK) in the Nkwalinye Valley and at locality (2.500/EE.940) in the Zietover area.

In the lower sections of the Nkwalinye River (5.130/LL.195), the Nsengeni Granitoid Gneiss shows a discordant, transgressive intrusive contact across the western limit of the tonalitic gneiss. The eastern limit of this tonalite gneiss shows a discordant transgressive intrusive contact with the Amazula Gneiss and the tonalite extends eastwards as a thin wedge intrusive into the Nkwalini Quartzo-feldspathic Flaser Gneiss.

From the Nkwalinye valley, the Nsengeni Granitoid Gneiss extends westwards as a broad sheet and its northern limit forms an E-W trending slightly discordant to semi-concordant sharp intrusive contact with the Nkwalinye Tonalitic Gneiss occurring to the north. This contact can be followed westwards for a distance of about 15km with a break occurring in the Ndloziyana area northeast of the peak (5.100/HH.490) where the northeasterly trending thin sheet of Umgabhi Micrographic Granite intrudes the Nsengeni Granitoid Gneiss.
In the Entembeni area (2,3,4/EE,FF), the Nsengeni Granitoid Gneiss contains rafts or xenoliths of greenstone, metagabbro and Amazula Gneiss. West of these rafts, the gneiss shows gradational contacts with the locally developed Ekuthuleni Granite.

To the west of Mfanefile area (2,3/W,X), the Nsengeni gneiss transgressively intrudes the tonalitic gneiss forming horizontal v-shaped re-entrant extensions into the tonalitic gneiss. Further to the west, in the Sappi Mooiplaas forest plantation and to the northeast of Ngcengcengu Peak (1,2,3/S,T,U), the Nsengeni Granitoid Gneiss forms a northwesterly trending discordant sharp transgressive intrusive contact with the Nkwalinye Tonalitic Gneiss. Near this locality, the Nsengeni gneiss also intrudes the eastern limit of the Nkwalini Mylonitic Gneiss. The contact is discordant and transgressive.

To the south of the greenstones, in the Amazula valley (6,7/BB,CC), the Nsengeni Granitoid Gneiss forms a transgressive re-entrant extension into the Nkwalinye Tonalitic Gneiss along its eastern limits. Its southern semi-concordant contact with the Nsengeni gneiss shows evidence of post-intrusive deformation as indicated by fault-fill quartz veining along the contact.

7.4 CONTACTS WITH ILANGWE GREENSTONES

7.4.1 INTRODUCTION

Two different types of contacts occur between the granitoid units of the Nsengeni Granitoid Suite and the Ilangwe greenstones. These are :

(i) discordant, transgressive intrusive contacts; and

(ii) concordant to semi-concordant tectonic contacts, some of which may be of syn-intrusive age.

Fig. 2 shows different ornamentations for these types of contacts. Rafts and xenoliths of greenstones also occur within Nsengeni granitoids. Fig. 2 only shows the bigger mappable rafts. In some localities, for example, Umhlathuze River localities (7.000/V.100) and (5.710/P.220), Ekuthuleni locality (6.100/EE.000) and Vungwini River locality (6.850/I.270) very small unmappable xenoliths occur in the granite (see Plate 2.1A).

7.4.2 DISCORDANT CONTACTS

Nsengeni granitoids show discordant contacts transgressive to bedding and foliation in the Ilangwe greenstones in two widely separated areas. In the upper Sabiza valley (4/V), the contact between Nsengeni Granitoid Gneiss and the Entembeni Formation and part of the Olwenjini Formation shows a cross-cutting intrusive relationship (Fig. 7.1). This contact trends roughly NE-SW to E-W. The foliation on either side of the contact trends NW-SE and dips steeply to the north. Thin slivers of Entembeni and Olwenjini lithologies occur in the Nsengeni gneiss near the contact with the greenstones. There is no development of a contact aureole in this area. Minor S-C structures have been observed in the Entembeni phyllites not far from the contact but no such structures occur in the granitoid gneiss. The prominent foliation shown by the gneiss seems to be related to solid-state deformation (Guineberteau et. al., 1987; Paterson et. al., 1990; Morand, 1992) and is characterized by grain size reduction, recrystallization of quartz and a moderate gneissic layering.

The second area where cross-cutting intrusive contact relationships are found is in the Entembeni area (3,4/EE) where the contact of the Ekuthuleni Granite and the Matshansundu amphibolite schist trends N-S cross-cutting the E-W foliation of the amphibolite schists (Fig. 3.1). The contact is sharp and no xenoliths of amphibolite schist occur in the granite. Visually, the granite is non-foliated and massive but in thin section there is incipient alignment of plagioclase feldspars along a preferred orientation whilst quartz exhibits undulose extinction.

Just northeast of the above contact (Fig. 3.1), there occurs a NNE trending contact between Nsengeni Granitoid Gneiss and Matshansundu amphibolite schist. This contact cross-cuts the E-W foliation of the amphibolite schist. The foliation of the granitoid gneiss trends sub-parallel to the contact and is discordant to the E-W foliation of the amphibolite schist. Further away from the contact, the foliation of the gneiss trends E-W. No evidence of amphibolite schist xenoliths was found in the vicinity of the contact.

The N-S trending contact of the Nsengeni Granitoid Gneiss and the Ekuthuleni Granite is gradational (Fig. 3.1). This probably suggests that the Ekuthuleni Granite is a non-foliated coeval variant of the Nsengeni Granitoid Gneiss or alternatively the granite was emplaced immediately after the emplacement of the gneiss and it probably contributed in the weak deformation of the gneiss.

In the Mandaba area, north of Simbagwezi Peak (4.740/J,K), a NE-SW trending raft of Nomangci quartz-muscovite-(sericite) schist is intruded by the Ntshiweni Augen Gneiss. The gneiss has an E-W foliation which is discordant to both the trend of the contact and the foliation of the quartz-muscovite-(sericite) schist. At locality (4.600/J.880) the augen gneiss forms a re-entrant extension into the Nomangci quartz-muscovite-(sericite) schist. This wedge of augen gneiss contains thin xenoliths of quartz-muscovite-(sericite) schist. The contact of the augen gneiss and the schist is discordant and transgressive.

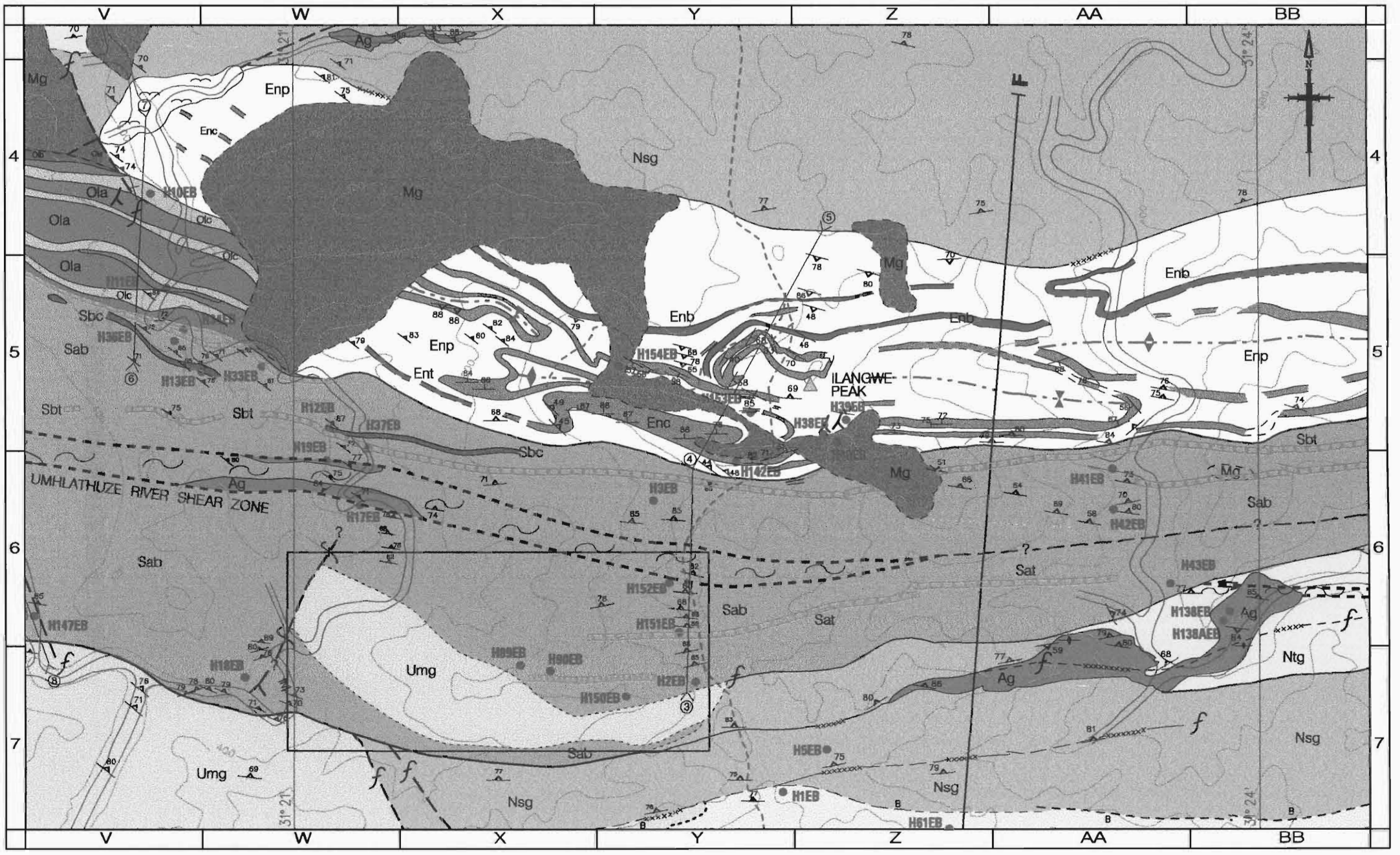

Figure 7.1 : UMGABHI GRANITOID RE-ENTRANT EXTENSION

L E G E N D

Entembeni Formation

Enb / Enp / Enc — Phyllite (phyllonitic at the shear zones and fault contacts) (Enp) intercalated with cherty BIF (Enb), metacherts and cherty quartzite bands (Enc).

Olwenjini Formation

Ola / Olm / Olp / Olb / Olg / Olc — Pillowed metabasalt; garnetiferous amphibolite; actinolite–tremolite schist (Ola); minor phyllite (Olp); banded cherty quartzite, banded metacherts, fuchsitic quartzites (Olc), silicate BIF (Olb), magnetite quartzite (Olm) and a quartz–biotite cordierite fuchsite gneiss (Olg).

Sabiza Formation

Sbc / Sab / Sbt — Pillowed metabasalt; banded amphibolite; massive amphibolite; actinolite–tremolite schist (Sab); talc–tremolite schist; serpentinite–talc schist (Sbt); with thin metachert bands (Sbc) and a khakhi–coloured siliceous pelitic rock towards the top of the sequence

Set — Discordant serpentinite–talc schists

Mg — Metagabbro; metanorite; metagabbroic amphibolite

Umgabhi Granitoid Suite

Ugg — Umgabhi Micrographic Granite

Esg / Eeg — Esibhudeni Granitoid Gneiss (with quartz–sericite schist)

Umg — Umgabhi Granitoid Gneiss

Nsengeni Granitoid Suite

Ekg — Ekuthuleni Granite

Nsg — Nsengeni Granitoid Gneiss

Nts — Ntshiweni Augen Gneiss

Nkwalinye Tonalitic Gneiss

Ntg — Nkwalinye Tonalitic Gneiss

Ag — Amazula Paragneiss

0 1000 2000 3000

M E T R E S

7.4.3 POST-INTRUSIVE CONTACTS

The Nsengeni Granitoid Suite bounds the Ilangwe greenstones to the north and south. The northern boundary is the extensive Entembeni Fault which is a major E-W trending dislocation. It extends from the Nkwalini-Mzilikazi area (5/NN,OO) in the east to just north of Simbagwezi Peak in the west, a distance of about 32km. In the upper Sabiza valley (3,4/U,V) this fault is obscured by metagabbroic intrusions. The contact is sharp, slightly discordant to semi-concordant and tectonic. It is characterized by brecciated white quartz fault-filled material which has been identified in a number of localities along the contact (areas marked xxxxx in Fig. 2). In these areas, the faulted contact is a positive feature. In areas along major streams, the fault expression is a negative feature. This can be observed in the Nsengeni River at Entembeni (4.600/DD,EE) and in the Umhlathuze River south of Ntshiweni Peak (3.750/O,P). Another negative feature (fault gully) not associated with streams occurs along the pre-fault intrusive contact of the Ntshiweni Augen Gneiss with the Olwenjini Formation north of Ntabandlovu Peak (4.680/L,M,N). This contact is a sharp, steep and deep gully.

The foliation of the granitoids in the vicinity of the contact trends E-W sub-parallel to the trend of the greenstones and the fault. Locally, slightly discordant foliation trends occur. Foliation is characterized by gneissic layering and the alignment of biotite and slightly flattened plagioclase feldspars along the foliation trend. Intense grain-breakage and recrystallization of quartz in the granitoids is evident near the contact. The greenstones usually show intense schistosity and S-C structures (Plate 2.2A) near the faulted contact. Near Ilangwe Peak (4.950/Z.260) small-scale asymmetric folds have been observed in the phyllites not very far from the faulted contact.

The southern boundary between the Nsengeni Granitoid Gneiss and the Ilangwe greenstones is the Matshansundu Fault which extends from the Nkwalinye valley (where it is cut by the younger Tugela Fault) in the east to north of Umgabhi Ridge (7.180/Y.730) in the west, a distance of about 15km. Evidence of faulting is shown by brecciated quartz fault-fill material. To the north of Umgabhi Ridge (6.900/Z,A) the fault expression is a prominent gully which extends eastwards and cuts through the Amazula Gneiss and Nkwalinye Tonalitic Gneiss in the Amazula valley. In the Matshansundu area, near Ndloziyana Peak, the fault is obscured by intrusive metagabbroic sheets.

The foliation of the Matshansundu amphibolite schists north of the post-intrusive fault trends NW-SE to WNW-SSE whereas that of the Nsengeni Granitoid Gneiss trends roughly E-W slightly oblique to semi-concordant to that of the greenstones. The Matshansundu amphibolite is strongly schistose near the contact. Minor S-C structures indicating a south-side down sense of movement also occur. The granitoid gneiss shows structures similar to those of the northern Nsengeni Granitoid Gneiss. Further to the west, the contact between the Nsengeni Granitoid Gneiss and the greenstones is sharp and semi-concordant. Northeast of Umgabhi Ridge, both the Nsengeni gneiss and the Sabiza amphibolites are intruded by the late post-Nondweni Umgabhi Granitoid.

7.4.4 GREENSTONE RAFTS WITHIN THE EARLY POST-NONDWENI GRANITOIDS

Ilangwe greenstone rafts occur within early post-Nondweni granitoids. In the Zietover area (1/EE), a N-S trending deformed raft of Matshansundu BIF occurs within Nkwalinye Tonalitic Gneiss. The BIF is intruded by a slightly foliated metagabbroic sheet on its western limit (Fig. 3.1). The iron formation is the silicate facies type consisting of alternating bands of quartz and fibrous to massive stilpnomelane and grunerite. Thin bands of xenoblastic magnetite are associated with bands of brown chert. Some magnetite shows effects of recrystallization. The iron formation is similar to the Matshansundu BIF and is correlated with it.

The Nkwalinye Tonalitic Gneiss shows sharp discordant and transgressive contacts with the iron formation. The foliation in the tonalitic gneiss trends E-W and is inclined steeply to the north whereas that of the iron formation trends N-S and dips to the west. However, further to the north, the foliation is variable due to folding (Fig. 3.1).

Further to the south, in the Entembeni area (3,4/EE,FF), a raft of Matshansundu amphibolite schist occurs within Nsengeni Granitoid Gneiss. The western and northern limits of the schist are intruded by Ekuthuleni Granite and Nsengeni Granitoid Gneiss respectively. The eastern limit of the schist is intruded by a slightly foliated metagabbroic sheet. The foliation in the metagabbro probably mimics that of the schist because further away from the contact, the metagabbro is massive. However, evidence of solid-state deformation has been observed in thin section. This is in the form of undulose extinction and nematoblastic textures (see Plate 13.1). The contact relationships between the Nsengeni Suite granitoids and the amphibolite schists have been discussed previously in Section 7.4.2.

7.4.5 POSSIBLE MODE OF EMPLACEMENT OF THE EARLY POST-NONDWENI GRANITOIDS

It has been shown that the magmatic foliations and solid-state structures of the early post-Nondweni granitoids strike E-W and dip steeply to the north or south, roughly parallel to the long dimensions of the granitoids and also parallel to sub-parallel to the linear greenstone belt.

The Nkwalinye Tonalitic Gneiss is the earliest of the early post-Nondweni granitoids. It is a highly deformed granitoid showing migmatitic structures. It is characterized by S-C fabrics indicating dextral strike-slip and these grade into mylonitic fabrics (Plate 6.1 and Plate 6.2) closer to the contact with the older gneisses, greenstones and, to a lesser extent, the Nsengeni Granitoid Gneiss which intrudes it. The tonalitic gneiss also shows complex structures like foliation transposition and natural back-rotated layer segments (Hanmer and Passchier, 1991). In the lower section of the Nkwalinye River, it intrudes the Amazula Gneiss along F_1 axial planar regions. These features suggest that the tonalitic gneiss was emplaced as a passive sheet-like body probably along earlier pre-existing (but now obscured) faults or shears or along the gneissic layering of older lithologies. This is further supported by the observation that foliations in the older lithologies are rarely deflected near the margin of the tonalitic gneiss. This indicates passive emplacement similar to the emplacement of the tonalitic and granodioritic sheets of the Fiskenaesset region, west Greenland (Myers, 1976) or the Wyangala Batholith, SE Australia (Paterson et. al., 1990).

The Nsengeni Granitoid Suite was emplaced shortly after the emplacement of the tonalitic gneiss, probably as a sheet-like batholithic body. Emplacement commenced in the western part of the study area with the passive intrusion of the Ntshiweni Augen Gneiss sub-concordant to the layering and foliation in the greenstones and Nkwalinye Tonalitic Gneiss. The Nsengeni Granitoid Gneiss was emplaced at comparable temperatures in the central and eastern parts of the study area. It is possible that the augen gneiss is an earlier, less evolved phase of the Nsengeni Granitoid Gneiss because they both show similar geochemical and mineralogical features. The Ekuthuleni Granite is probably a local variant of the Nsengeni Granitoid Gneiss.

The significance of the emplacement of the Nkwalinye Tonalitic Gneiss together with the Nsengeni Granitoid Suite is that they produced complex superimposed deformation in the migmatitic and mylonitic gneisses ***and*** greenstones, whereas the emplacement of the

Nsengeni Granitoid Suite produced the complex folding of an earlier foliation in the Nkwalinye Tonalitic Gneiss.

7.4.6 POST-NONDWENI AGE OF THE NSENGENI GRANITOID SUITE

Field evidence suggests that the possible sequence of emplacement of the Nsengeni Granitoid Suite is :

1. Ntshiweni Augen Gneiss;
2. Nsengeni Granitoid Gneiss;
3. Ekuthuleni Granite.

The Ekuthuleni Granite could possibly be coeval with the Nsengeni Granitoid Gneiss but it is massive and structureless.
The granitoids of the Nsengeni Suite show similar geochemical and mineralogical characteristics and evidence already presented in this chapter shows that they are intrusive into :

(a) the migmatitic and mylonitic gneisses (Amazula Gneiss and Nkwalini mylonites);

(b) the greenstones of the Umhlathuze Subgroup and the metasediments of the Entembeni Formation;

(c) the Nkwalinye Tonalitic Gneiss (which is itself intrusive into (a) and (b) above).

The intrusive contact relationships with these older formations were discussed in the previous chapters. The fact that the Nkwalinye Tonalitic Gneiss and the granitoids of the Nsengeni Suite are intrusive into the older formations specified in (a) and (b) above, suggests that they are of ***post-Nondweni*** age and their widespread occurrence implies that they are of batholithic proportion.

CHAPTER 8

THE LATE POST-NONDWENI GRANITOIDS: IMPISI-UMGABHI GRANITOID SUITE

8.1 INTRODUCTION

The Impisi-Umgabhi Granitoid Suite is an association of two granitoid suites comprising the Impisi Granitoid Suite and the Umgabhi Granitoid Suite. The former occurs in the northwestern portion of the study area and consists of two granitoid units (the Nkandla Granite and the Zietover Granite) whereas the latter occurs in the Southern Granitoid Complex and consists of three granitoid units, viz. the Umgabhi Granitoid, Esibhudeni Granitoid and the Umgabhi Micrographic Granite. These granitoids are all megacrystic, have gradational contacts and similar geochemical and mineralogical characteristics (Table 4.1).

The Impisi Granitoid Suite extends from southwest of Nkandla in the west to beyond the Sappi Mooiplaas forest plantation in the east, a distance of about 17km. Further to the east, in the Zietover area (1/DD,EE) and in the Safube area (2/JJ,KK,LL) exposures of the Zietover Granite occur.

The Umgabhi Granitoid Suite extends from west of Esibhudeni area in the west to just west of the Nkwalinye River valley (6/LL,MM) in the east, a distance of about 39km.

8.2 LITHOLOGIES AND GRADATIONAL CONTACTS BETWEEN GRANITOID UNITS

The ***Nkandla Granite*** extends from the Vumanhlamvu area (1/A,B) in the west to just east and northeast of the Mandaba area (1,2/L,M,N) in the east. It is the most extensive granitoid occupying the northwestern portion of the study area. The granite is well-exposed next to the road between Vumanhlamvu and Mandaba. It is a reddish-grey, massive to poorly foliated, granoblastic medium- to coarse-grained granite which is porphyritic. It consists of megacrysts of reddish microcline, white plagioclase, small quartz grains and

minor greenish-black biotite flakes. In the Mandaba area (3,4/G,H,I,J), it contains rafts of quartz-muscovite-(sericite) schist of the Nomangci Formation. The granite shows no foliation near the contacts. The biotite is often altered to chlorite and is locally replaced by hornblende. To the east of Mandaba area (1,2,3,4/J,K,L,M) it transgressively intrudes the Ntshiweni Augen Gneiss. A network of granitic dykes and sheets have been observed to truncate the augen gneiss in the vicinity of the contact. The contact of the Nkandla Granite and the Zietover Granite is gradational. At locality (1/N) this contact is characterized by the gradual colour change of the feldspars from pinkish-red to white and the occurrence of black biotite flakes. Generally, the Zietover Granite becomes yellowish-grey.

The ***Zietover Granite*** occurs in the northwestern part of the Sappi Mooiplaas forest plantation (1/O,P,Q). It also occurs in the Zietover area (1.200/DD,EE) and at the Safube area to the west of Ndundulu Peak (2/JJ,KK,LL) where its southern limit is a contact with the Nkwalinye Tonalitic Gneiss and its northern limit is obscured by the overlying younger, flat-lying Natal Group sandstones. It is a light yellowish-grey medium- to coarse-grained granite consisting of megacrystic transparent and milky white quartz, white plagioclase feldspars and dispersed large flakes of greenish-black biotite. It is possibly intrusive into the Nsengeni Granitoid Gneiss and the Nkwalinye Tonalitic Gneiss but the contact relationships are obscured by deep weathering and sugar cane/tree plantation.

The ***Umgabhi Granitoid*** only occurs in the Southern Granitoid Complex and is well-developed in the Umgabhi Peak area (8/W,X,Y). It extends from the Umgabhi Ridge (8/Y) in the east, to east of Inhlababa Mountain (7,8/Q,R) in the west. In this area it grades into the Esibhudeni Granitoid. It is a coarse-grained granitoid consisting of large transparent quartz grains, creamy white perthitic plagioclase, pink perthitic potash feldspars all surrounded by large greenish-black flakes of biotite which become books in some places.

The granitoid has a subordinate very weak E-W trending foliation which is inclined to the north at 50 - 85°. To the south of the beacon at the Umgabhi Peak, it is truncated by the southerly dipping basal thrust units of the Natal Mobile Belt. This is one accessible area where the Natal Mobile Belt and foreland contact relationships are spectacularly exposed. To the west, the granitoid grades into the finer grained Esibhudeni grey biotite granitoid. To the east, it grades into the pink Umgabhi Micrographic Granite. The contact area is characterized by a gradual decrease in the amount of biotite and a corresponding gradual increase in the amount of pinkish K-feldspars.

The Umgabhi granitoid weathers to a brownish-black sandy, to loamy soil.

Near the confluence of the Sabiza and Umhlathuze Rivers (7.420/V) this granitoid intrudes banded amphibolite of the Sabiza Formation. The contact is sharp (Plate 2.1A) with detached xenoliths of the banded amphibolite "floating" in the granitoid not far from the contact. A number of small-scale post-intrusive detachment planes cut the amphibolite and the granitoid at an oblique angle to the contact (Plate 2.1A). The granitoid itself is very fine-grained and mylonitic near the contact and shows intense steep northerly-inclined foliation subparallel to that of the banded amphibolite. A few metres south of the contact, the granitoid is almost massive with a weakly developed foliation (Fig. 2).

Some features of the Umgabhi Granitoid such as its elongate shape adjacent to the Vungwini River Shear, its steep boundaries and mylonitic margins are similar to the Mortagne Pluton in France (Guineberteau et. at., 1987) and the Doctors Flat Pluton of Victoria, Australia (Morand, 1992) which are interpreted as having been emplaced into a pull-apart along a shear zone.

The ***Esibhudeni Granitoid*** is an extensive unit (10-15 km) which is found only to the south of the Ilangwe Greenstone Belt. It extends from east of Inhlababa Mountain (6,7/S,T,U) in the east to the western limit of the map area (Fig. 2). It is dark grey, fine- to medium-grained and consists of creamy white quartz and plagioclase feldspars and greyish-black biotite. Weakly developed foliations generally dip to the north at 50 - 80°. Steep southerly dips occur in the Esibhudeni area in the western portions of the study area.

It has similar weathering characteristics to the Umgabhi Granitoid.

West-southwest of Inhlababa Mountain (7,8/M,N) , in local stream sections, the Esibhudeni biotite granitoid is highly deformed and contains interbanded flaser gneiss and mylonitic gneiss in a zone of extreme deformation that strikes northeast-southwest and is inclined steeply to the northwest. It is truncated by the Natal Thrust Front (NTF - Fig. 2) to the south.

To the west of this area, thin zones of quartz-sericite schists occur within the granitoid. These schists have steep northeasterly-inclined foliations which are perpendicular to those of the gneissic granitoid. These schists are associated with shear zones in the granitoid

and represent retrograde assemblages related to M_3 dislocation metamorphism. Charlesworth (1981) interprets them as phyllonites along shear zones in the granitoid.

To the southeast of Inhlababa Mountain the granitoid is medium-grained and contains creamy-white (with a tint of rose-pink) porphyroblasts up to 15mm in diameter set in a fine- to medium-grained matrix of biotite, plagioclase feldspar and quartz. Further to the east, the biotite becomes coarser-grained (and greenish-black in colour) and the granitoid grades into the Umgabhi Granitoid.

The pink ***Umgabhi Micrographic Granite*** occurs to the east of Umgabhi Peak (8.120/Y.600) and extends eastwards as far as the Nkwalinye Valley where it is truncated by the ENE-WSW trending Tugela Fault. It consists of pink potash feldspars with intergrowths of quartz in a sub-graphic granitic texture. It has no observable foliation. It grades into the Umgabhi quartz-feldspar biotite granitoid. In the vicinity of the gradational contact, there is a gradual increase in the biotite content and a gradual decrease in the pink potash feldspar content. The K-feldspars in the granite weather to a pinkish-white kaolin-rich material with loose granular quartz grains. In the Ndloziyana Peak area, it diapirically intrudes the greenstones and metasediments. It is also intrusive into the Nsengeni Granitoid Gneiss.

8.3 CONTACTS WITH ILANGWE GREENSTONES

As mentioned previously, the granitoids of the Impisi Suite are in contact with the northern limits of the Ilangwe greenstones and metasediments represented by the Nomangci, Simbagwezi and Olwenjini Formations whereas the Umgabhi and Esibhudeni granitoids are in contact with the southern limit of the Sabiza Formation amphibolites. Two types of contacts are found, namely :

(i) discordant transgressive contacts with re-entrant extensions into the greenstones and metasediments; and

(ii) semi-concordant intrusive contacts.

The Nkandla Granite has discordant transgressive contacts with Nomangci quartzites and phyllites at localities (1,2,3/B,C,D,E) and (3/G,H,I). At localities (3.820/D.710) and (5.000/E,F), the Nkandla Granite forms re-entrant extensions into the quartzites and

phyllites. At the latter locality, the northern limit of the re-entrant extension is in contact with the quartzites of the Nomangci Formation and the southern boundary is in contact with the phyllites of the Simbagwezi Formation. Just WNW of Simbagwezi Peak (5.400/J.400), a wedge of Nkandla Granite is in contact with the Simbagwezi and Olwenjini Formations on its southern and northern boundaries respectively. The southern boundary trends E-W slightly discordant to the WNW foliation trend of the Simbagwezi phyllites. Northwest of Simbagwezi Peak (5.500/J.160) the contact area is intruded by a sill of metagabbro. In the Vungwini River (5.300/H.770), thin slivers of phyllite occur in the granite just close to the contact. Elsewhere they were not observed and the contact is sharp and slightly discordant to semi-concordant. The northern post-intrusive contact is sharp and tectonic as shown by the schistose and sheared nature of the amphibolites at this locality.

To the north of Isisusa Peak (3.700/D.235), a circular mass of Nklandla Granite occurs within quartzites and phyllites. The edges of this granite are irregular, indicating the intrusive nature of the contact.

Rafts of Nomangci Formation quartz-muscovite-(sericite) schists occur in the Nkandla Granite. The granite shows discordant transgressive contacts with the NE trending slivers of Nomangci quartz-muscovite-(sericite) schist. The foliation of the schist also trends NE-SW and dips steeply to the northwest. In the Mandaba area, the intrusion of the Nkandla Granite resulted in M_3 prograde metamorphism of the Nomangci quartz-muscovite-(sericite) schist with the resultant occurrence of kyanite in the Nomangci schists. At locality (1/D), two of these rafts have their eastern limits bounded by N-S trending thin shear zones.

The Zietover Granite does not intrude the Ilangwe greenstones and metasediments but is intrusive into older gneisses. The contact features of the granitoids of the Impisi Suite and the older granitoid gneisses have been discussed previously.

In the Southern Granitoid Complex, concordant to semi-concordant intrusive contacts between the Umgabhi Granitoid Suite rocks and the Ilangwe greenstones are characterized by flow foliation and highly ductile, migmatitic structures with aligned xenoliths at various localities along the southern flank of the greenstone belt between the Sabiza amphibolites and the granitoids.

Along the Vungwini River at localities (6.800/I.070) and (7.000/J.400) the contact is characterized by intense flow foliation and aligned amphibolite xenoliths in the marginal

Esibhudeni Granitoid. The amphibolite itself is finely banded and sheared. This sheared contact is referred to as the Vungwini River Shear. Similar characteristics are found at various localities along the Umhlathuze River, for example, locality (5.720/P.220) just to the north of Inhlababa Mountain, locality (5.780/R.165) northeast of Inhlababa Mountain and locality (7.000/V.100) near the confluence with the Sabiza River (Plate 2.1A). At the first two localities, the contact granitoid is the Esibhudeni Granitoid whereas at the last locality, the granitoid is the Umgabhi Granitoid. All these localities occur in deep river valleys and are not easily accessible.

Northwest of Umgabhi Ridge (6,7/W,X,Y) in the lower Sabiza valley, an extensive WNW-ESE trending re-entrant of the Umgabhi Granitoid cuts through the Sabiza amphibolites. This wedge of granitoid contains disorientated xenoliths of amphibolites. The southern and northern contacts are transgressive. The western contact is a sharp post-intrusive fault characterized by a schistose fabric in the amphibolite. The eastern boundary is a NNE trending discordant transgressive intrusive contact with the Nsengeni Granitoid Gneiss (Fig. 7.1).

Around Ndloziyana Peak (5,6/GG,HH), the pink Umgabhi Micrographic Granite diapirically intrudes the Matshansundu and Entembeni Formations. The regional foliation of the greenstones trends NNE-SSW but is inclined to the west along the western contact with the granite and is inclined to the east along the eastern contact. The weakly developed foliation in the granite is inclined to the north.

8.4 POSSIBLE MODE OF EMPLACEMENT OF THE LATE POST-NONDWENI GRANITOIDS

No detailed study of the possible mode of emplacement of the granitoids was undertaken. The following short discussion is conjecture based on the features of the contact relationships between the granitoids and the Ilangwe greenstones and older gneisses. These relationships are compared to those of other well-studied granitoids in France, Australia and Greenland. Conclusions on possible mode of emplacement are based on similarities with known granitoids.

The late post-Nondweni granitoids show two types of intrusive contacts with the Ilangwe greenstones and the boundary faults, viz. discordant transgressive intrusive contacts and semi-concordant intrusive contacts. The former are characterized by re-entrant extensions

into greenstones and by the oblique nature of both the contact and foliations on either side of the contact. The semi-concordant intrusive contacts are characterized by flow foliation and highly ductile migmatitic structures with aligned or disorientated xenoliths in the marginal granitoids (Plate 2.1A). These features are absent further away from the contact. Further, the granitoids are elongate in shape and their weak foliation is parallel to the boundary faults and the foliation in the greenstones. These features suggest that the granitoids were emplaced as sheet-like bodies (Hutton and Reavy, 1992; Paterson, et. al., 1990; Myers, 1976) probably along a pull-apart structure formed along a jog in the Vungwini River Shear, similar to the Mortagne pluton in France (Guineberteau et. al., 1987) and the Doctors' Flat Pluton in Australia (Morand, 1992).

In the Ndloziyana Peak area (Fig. 3.1), there is evidence of the Umgabhi Micrographic Granite forcefully intruding the greenstones and metasediments. This diapiric intrusion is spectacularly exposed in this easily accessible area. Foliations on the intruded Matshansundu amphibolite schists trend NNE-SSW and dip steeply to the west on the western contact with the granite and dip to the east on the eastern contact. Foliation on the granite trends E-W, perpendicular to that in the schist, and dips steeply to the north. The micrographic granite also cuts out the Nsengeni Granitoid Gneiss, the Sabiza Formation and the Entembeni Formation in this area.

The significant implication of the intrusion of the late post-Nondweni granitoids is that they were responsible for the regional deformation of the earlier granitoids. This resulted in the rather uniform foliation in the granitoids of the Nsengeni Granitoid Suite and, in addition, a superimposed deformation in the Nkwalinye Tonalitic Gneiss. These structures will be discussed in detail in the next chapter.

8.5 POST-NONDWENI AGE OF THE IMPISI-UMGABHI GRANITOID SUITE

The sequence of emplacement of the Impisi granitoids is possibly Nkandla Granite, followed by Zietover Granite, whereas that of the Umgabhi granitoids is: Umgabhi Granitoid, followed by Esibhudeni Granitoid and finally the Umgabhi Micrographic Granite. In the preceding discussion these granitoid suites were treated as separate but probably coeval events mainly because they occur on opposite sides of the Ilangwe greenstone belt. However, it is possible that they form a combined association probably derived from a single magmatic event. This is supported by geochemical and mineralogical similarities of

these granitoid suites. In Chapter 13 these granitoid suites will be discussed as a single association, referred to as the Impisi-Umgabhi Granitoid Suite.

As mentioned previously, the lithologies of the Impisi-Umgabhi granitoids show that they are all megacrystic to microcrystic and contain quartz and K- and plagioclase feldspars with varying amounts of biotite. They can be classified as K-rich granitoids and have K_2O/Na_2O ratios greater than 1:5. They have weak generally E-W trending foliations which only become pronounced in intensely deformed areas. These granitoids are in mutual contact with each other, are intrusive into greenstones, boundary faults and older granitoids ***and*** occur in the northwestern and southern portions of the study area.

All these features seem to imply that the emplacement of these granitoids represents related events of a young post-Nondweni composite intrusive mass of batholithic proportions.

CHAPTER 9

STRUCTURAL GEOLOGY OF THE ILANGWE GRANITE-GREENSTONE COMPLEX

PART 1

9.1 GENERAL

During the study of the structural geology of the Ilangwe Granite-Greenstone Complex, it was apparent that a suitable method to present and analyse the structural data would be in several ***parts***, with each part dealing with a specific and major topic. This method will provide a more systematic and detailed description of the structural features of the study area. Therefore, ***Chapter 9*** has been divided into ***four parts***. The first part deals with the general introduction on the structural geology of the granite-greenstone complex. This short part lays the foundation for the ensuing parts. ***Part 2*** of Chapter 9 considers the structural analysis and interpretation of the Ilangwe Greenstone Belt (i.e. D_1 to post-D_3 deformation), including the ductile shear zones within the greenstone belt and the faults bounding the greenstones. ***Part 3*** is concerned with the structural features of the Ilangwe Granitoid Complex comprising D^G_1 to D^G_3 deformation and ductile shear zones. The final part (***Part 4***) deals with the tectonic synthesis.

As mentioned previously, the Archaean geology of the Ilangwe complex can be divided into three broad east-west trending zones (Fig. 2) which are separated by major dislocations (faults and shears). These zones are, from north to south :

(a) the Northern Granitoid Complex;
(b) the Ilangwe Greenstone Belt;
(c) the Southern Granitoid Complex.

The northern and southern granitoid complexes are composed of similar granitoid lithologies of different ages and can therefore be regarded as a major ***granitoid terrain***,

whereas the Ilangwe Belt consists of variably deformed greenstones and metasediments. Field observations indicate a regional sequence of major structural and magmatic events which will be described and analysed in this chapter.

The method used in the structural study of the Ilangwe complex will be to examine structures in order of inferred development, ***first*** in the Ilangwe Greenstone Belt and ***thereafter*** in the granitoid terrain. This means that D_1, D_2 and D_3 structures in the greenstone belt will be examined first and thereafter D^G_1 to D^G_3 structures of the granitoid terrain will be considered. This method will provide a sequential examination of the structural and magmatic development of the Ilangwe Granite-Greenstone Complex in an attempt to elucidate the complex polyphase geological evolution of this region.

This method is adopted because it will lead to an attempt to correlate deformational events in different terrains or sequences in the Ilangwe Granite-Greenstone Complex. The validity of this method is further supported by the following observations :

(i) A sequence of deformational events can be recognised in the greenstone complex whereas the sequence in the granitoid terrain was interrupted by major episodes of granitic intrusions.

(ii) Large-scale folds defined by bedding/primary layering in BIFs and metacherts occur in the greenstone complex whereas no such folds have been identified in the granitoid terrain.

(iii) In contrast to the greenstone complex, primary layering (bedding, S_o) cannot be recognised in the granitoid terrain. Thus, although a D_1 episode can be established in the greenstones, this cannot be correlated ***directly*** with the D_1 episode in the granitoid terrain because it does not involve primary layering (S_o).

The terminology used to describe the different events of deformation and the related planar and linear elements is summarised in ***Table 9.1***.

All structural data gathered during this study were plotted on lower hemisphere Schmidt equal area nets.

Table 9.1 : Summary of Structural Nomenclature

Description	Terminology		
Bedding and original banding/layering	S_0		
Co-planar S, S_0 and S_1	S_{01}		
Deformation phase (in the Ilangwe Belt) Deformation phase (in the granitoid terrain)	D_1 D_1^G	D_2 D_2^G	D_3 D_3^G
Metamorphic phase	M_1	M_2	M_3
(Axial planar) ***foliation***[1]	S_1	S_2	S_3
Fold axis	F_1	F_2	F_3
Lineation[2]	L_1	L_2	L_3

1. *Foliation is used here as a general term for all mesoscopically penetrative planar surfaces of metamorphic origin such as axial planar cleavage/foliation, strain-slip cleavage/foliation, slaty cleavage, schistosity and gneissosity (Turner and Weiss,1963). It is indicated by S_1, S_2, ... S_n where the subscripts denote the relative age or order of development. In the case of granitoids, the different foliation planes will be referred to as S^G_1, S^G_2, ... S^G_n.*

2. *Lineation refers to any kind of linear structure related to deformation. It includes structures like mineral stretching lineation, preferred orientation of mineral grains, aligned mineral aggregates, S-surface intersections, crenulation lineations and larger linear structures like fold axes of megascopic folds, mullions, boudins and rods (Turner and Weiss, 1963; Smalley, 1980; Charlesworth, 1981; Park, 1983). L_1, L_2, ... L_n designates the lineations and F_1, F_2, ... F_n represents the fold axes. The subscripts refer to the relative order of development. In the cast of granitoids of the Ilangwe Complex, lineations will be designated L^G_1, L^G_2, ... L^G_n and fold axes will be designated F^G_1, F^G_2, ... F^G_n.*

PART 2

9.2 STRUCTURE OF THE ILANGWE GREENSTONE BELT

9.2.1 INTRODUCTION

The Ilangwe greenstones and metasediments form a narrow, linear E-W trending and predominantly northerly inclined belt 3 to 4 km wide, extending for about 35 to 40 km along strike and flanked by granitoids and granitoid gneisses. In the western sector, the belt trends WSW-ENE and then swings to trend WNW-ESE in the west central and central sectors and finally trends E-W in the eastern sector (Fig. 2). It is bounded by the Entembeni Fault in the north and the Vungwini shear and Matshansundu Fault in the south. In the western sector, the northern and southern boundaries comprise transgressive and semi-concordant intrusive contacts between late post-Nondweni granitoids and the greenstones.

The Ilangwe complex is structurally disrupted by granitoid and metagabbroic intrusives of different ages. In the Ndloziyana Peak area (4,5/GG,HH) of the eastern sector, the belt is diapirically intruded by the Umgabhi Micrographic Granite whose southeastern boundary is also intruded by the Matshansundu metagabbroic body. It is in this area where a major deformed angular unconformity has been recognized.

In the central area just northwest of Umgabhi Ridge (6,7/W,X,Y), the Sabiza Formation is disrupted by the Umgabhi Granitoid which forms a re-entrant extension into the Sabiza amphibolites. WNW of Ilangwe Peak (2,3,4/U,V,W,X,Y), the greenstones are structurally disrupted by the intrusion of the metanoritic and metagabbroic bodies. In the western sector near Simbagwezi Peak (5,6/I,J), the greenstones have been intruded semi-concordantly by a metagabbroic sill.

Polyphase deformation has been recognized in the Ilangwe Greenstone Belt. Direct evidence of D_1 fold-systems is provided by refolded folds in which the F_1 axial plane cleavage is also folded about the F_2 fold axes (Fig. 9.1). Where F_1 fold closures are not present in outcrops, the most distinguishing criterion used was the folding of primary layering and an associated parallel or slightly oblique cleavage wrapped around the hinges

of the later F_2 folds. Another distinguishing feature of D_1 deformation is the occurrence of intrafolial folds in transposed foliations – this is especially significant in the granitoid gneisses and amphibolites. Indirect evidence is provided by analysis of structural data from small-scale folds.

The most important diagnostic feature of the D_2 fold system is a near constant orientation of the axial plane cleavage and the fact that the F_2 fold axes generally show a systematic great – or small-circle spread and/or two or more point maxima in a stereoplot. Similar characteristics were recognized for the later (D_3) fold systems.

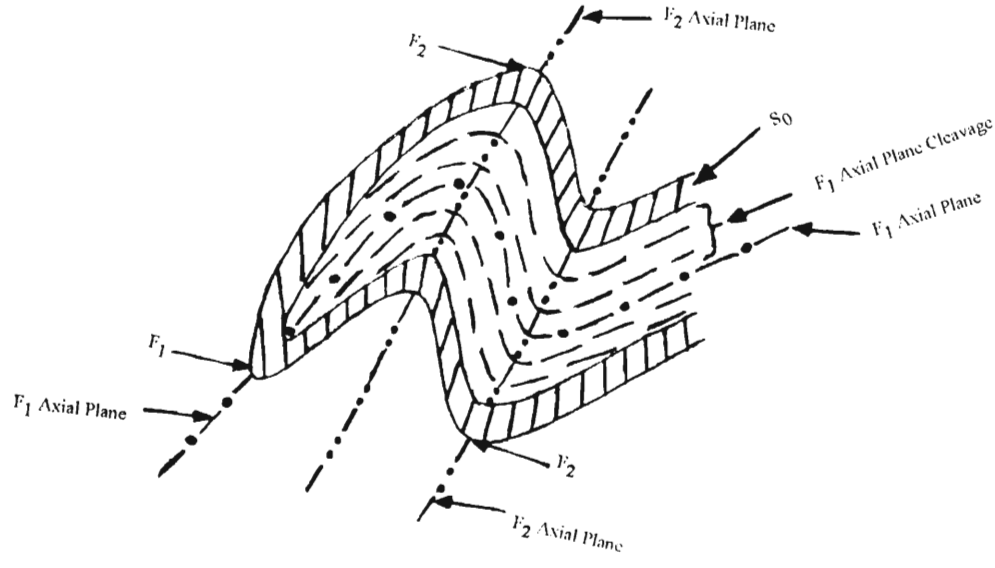

Fig. 9.1: A diagrammatic representation of a refolded F_1 fold showing the criteria used in the field to distinguish between various fold phases

The most prominent structures within the Ilangwe Greenstone Belt are the large-scale E-W trending, tightly appressed, upright folds with sub-vertical axial planes that are well-defined by banded ironstones and metacherts which can be traced around the fold closures and along the steeply-dipping fold limbs for distances of 4 to 10 km (see Fig. 2). In many cases, the plunge of the folds cannot be established because the bedding in the BIFs and metacherts have been obliterated by brecciation and almost total recrystallization (see Plate 9.2 and Plate 9.9C). The fold limbs have narrow, elliptical outcrop pattern (see Plate 9.2C). Evidence from the study of small-scale folds belonging to the same fold system, and described later in Section 9.2.3.2, indicates that these large folds are doubly-plunging structures which generally have an en-echelon arrangement (Fig. 2; Plate 9.2C). Further, this evidence suggests that these folds were produced during the D_2 phase of deformation.

Another prominent structural feature of the greenstone belt as a whole is a penetrative E-W trending foliation that is axial planar to the large-scale folds and coplanar to the vertical to steeply inclined limb of the large folds. This relationship is shown in Figs. 9.2 A-J.

Major shear zones, to be described later, have been recognized within the Ilangwe Belt.

9.2.2 D_1 PHASE OF DEFORMATION IN THE ILANGWE GREENSTONE BELT

9.2.2.1 GENERAL

F_1 structures are predominantly isoclinal intrafolial folds occurring in $S_1//S_o$ transposed foliation, which is the dominant structure. The common geometric varieties of intrafolial folds are *rootless intrafolial folds, tightly reclined intrafolial folds* and *tightly appressed isoclinal folds*. These folds are usually distinguished from later isoclinal folds by the absence of folded cleavage in the F_1 fold hinges. Asymmetric isoclinal folds and rootless intrafolial folds usually show sharp slightly thickened hinges with narrow "limbs" whereas symmetric isoclinal folds and reclined intrafolial folds have slightly rounded but tightly appressed and steeply plunging fold hinges. Some steeply plunging reclined folds can be classified as neutral folds.

D_1 folds occur in widely separated areas within the ***Umhlathuze and Nkandla Subgroups*** of the Ilangwe Greenstone Belt. In the eastern sector of the greenstone belt just southeast of Ekuthuleni Peak (5.760/EE.150) and within ***Sabiza amphibolites***, steep southerly

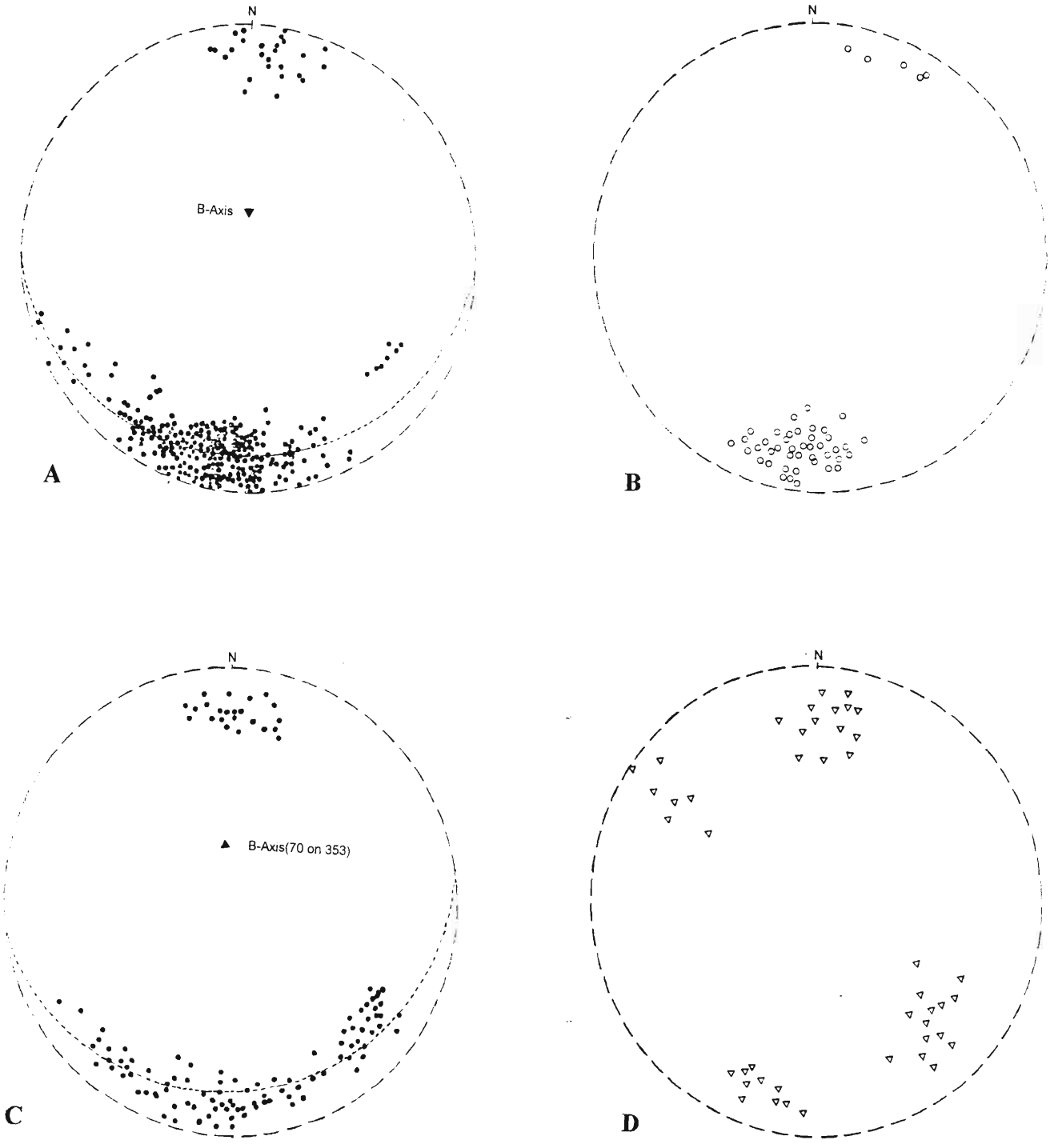

Fig. 9.2A : Poles to undifferentiated foliation in the Sabiza amphibolites (n=295).

Fig. 9.2B : Poles to bedding in the Sabiza metacherts (n=47).

Fig. 9.2C : Poles to undifferentiated foliation in the Matshansundu amphibolites (n=119).

Fig. 9.2D : Poles to bedding in the Matshansundu BIFs (n=45).

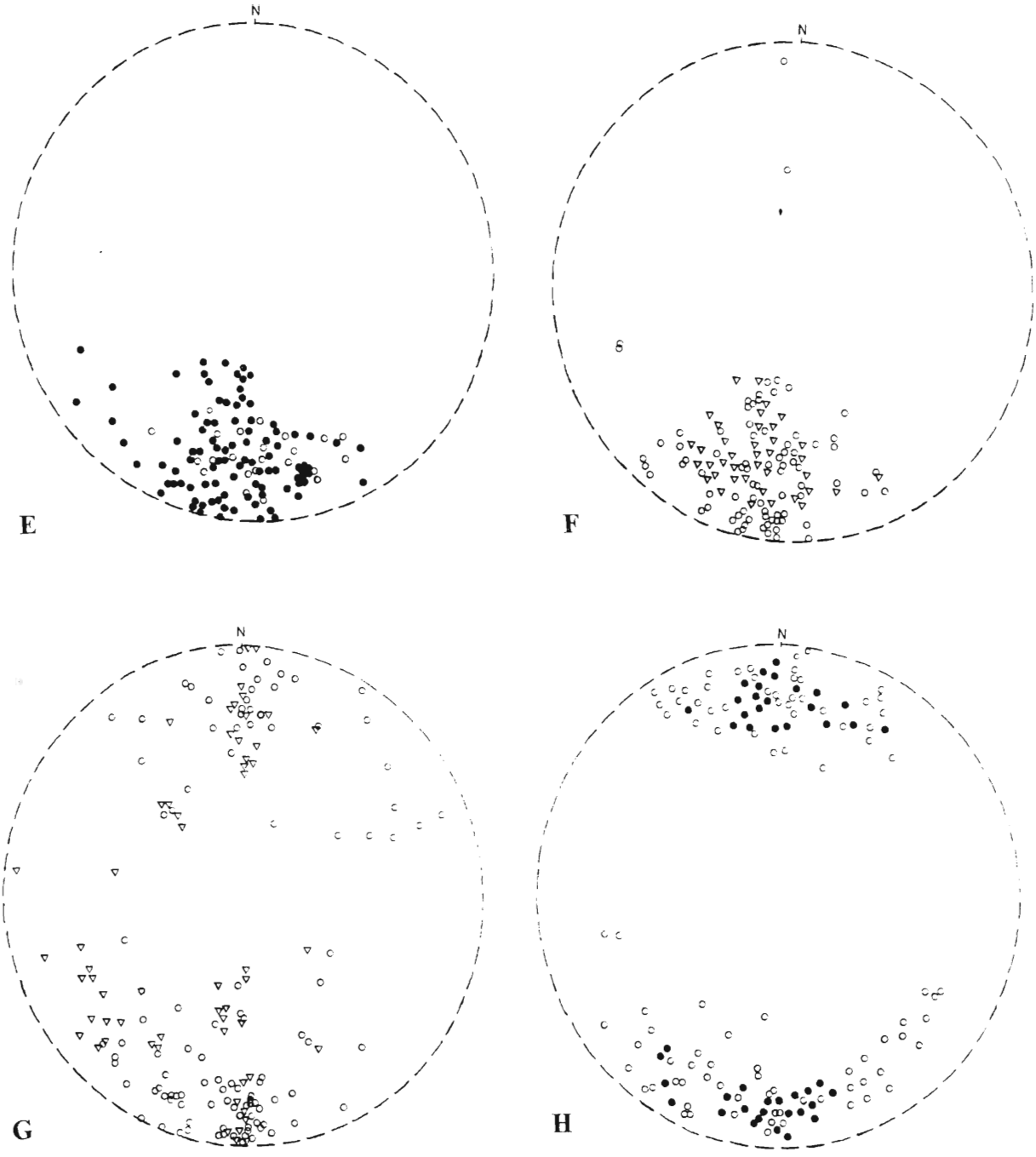

Fig. 9.2E : Poles to undifferentiated foliation in the Olwenjini amphibolites and phyllites.
- ● = Amphibolites (n=89).
- O = Phyllites (n=24).

Fig. 9.2F : Poles to bedding in the BIFs and metacherts of the Olwenjini Formation.
- O = Metacherts (n=77).
- ∇ = BIFs (n=36).

Fig. 9.2G : Poles to bedding in the BIFs and metacherts of the Entembeni Formation.
- O = Metacherts (n=108).
- ∇ = BIFs (n=58).

Fig. 9.2H : Poles to undifferentiated foliation in the Entembeni amphibolites and phyllites.
- ● = Amphibolites (n=45).
- O = Phyllites (n=94).

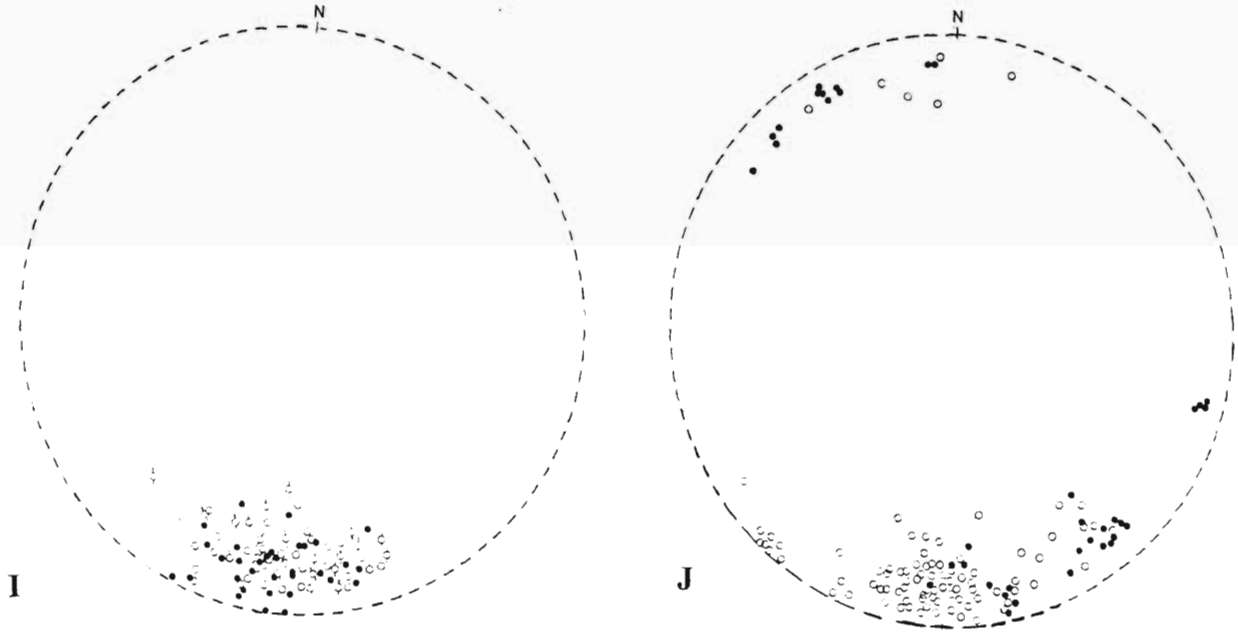

Fig. 9.2I : Poles to bedding and undifferentiated foliation in the lithologies of the Simbagwezi Formation.

- ● = Poles to foliation in the amphibolites (n=33).
- ℘ = Poles to foliation in the phyllites (n=24).
- o = Poles to bedding in the metacherts (n=28).

Fig. 9.2J : Poles to bedding and undifferentiated foliation in the lithologies of the Nomangci Formation.

- ● = Poles to foliation in the quartz-muscovite schists (n=37).
- o = Poles to bedding in the quartzites and metacherts (n=86).

inclined and easterly-closing steeply plunging isoclinal reclined folds (almost neutral folds) are found (Fig. 9.3). They have steep southerly inclinations.

In the east-central sector, west-central sector and the western sector of the Ilangwe greenstones of the Sabiza Formation, isoclinal intrafolial folds have identical orientations showing a bimodal distribution with moderate to steep WSW and ENE plunges and northerly or southerly inclined axial planes (Figs. 9.4, 9.5, 9.6). In the Umhlathuze River locality (6.210/U.860) of the west-central sector of the belt, a Type 3 superimposed interference fold (Ramsay, 1967; Ramsay and Huber, 1987) occurs within banded amphibolites of the Sabiza Formation (Plate 9.1A). This is one of the few exposures in the Ilangwe Belt where superimposed folding is well-preserved. Here D_1 folds plunge WNW at about 60-70° with axial planes inclined 80°N (Fig. 9.5). Minor L_1 lineations are subparallel to the F_1 fold axes (Plate 9.1A). The F_1 folds are refolded into NW plunging F_2 folds.

In the eastern sector of the greenstone just east of Ndloziyana Peak (5.900/II.710), reclined intrafolial folds in ***Matshansundu amphibolite schists*** plunge moderately to the WSW. The theoretical mean pole of the axial planes is inclined steeply to the SW (Fig. 9.7). Tightly appressed isoclinal folds in this area plunge steeply to the NE and SW and are inclined steeply to the north and rarely to the south (Fig. 9.7). These isoclinal folds show a bimodal distribution similar to those of the Sabiza Formation (Figs. 9.4, 9.5, 9.6).

Near Entembeni Kraal (4.550/EE.530), the ***Matshansundu Formation*** enclave displays isoclinal folds with a shallow plunge to the southwest and steep southerly dipping axial planes (Fig. 9.8). The shallow plunge of these folds is attributed to rotation during the displacement of the enclave.

In the west-central sector and within the ***Olwenjini Formation*** (Fig. 9.9), D_1 isoclinal folds have a bimodal distribution similar to that of the Sabiza Formation (Figs. 9.4, 9.5, 9.6) and the Matshansundu Formation (Fig. 9.7). In the Umhlathuze River locality (4.805/P.110) (Fig. 9.9), small-scale D_1 isoclinal intrafolial folds plunge steeply to the WSW and ENE and are inclined steeply to the north and very rarely to the south (Fig. 9.10). All along the Umhlathuze River in this area, the plunge of the intrafolial folds varies from 45° to 70° (Fig. 9.10).

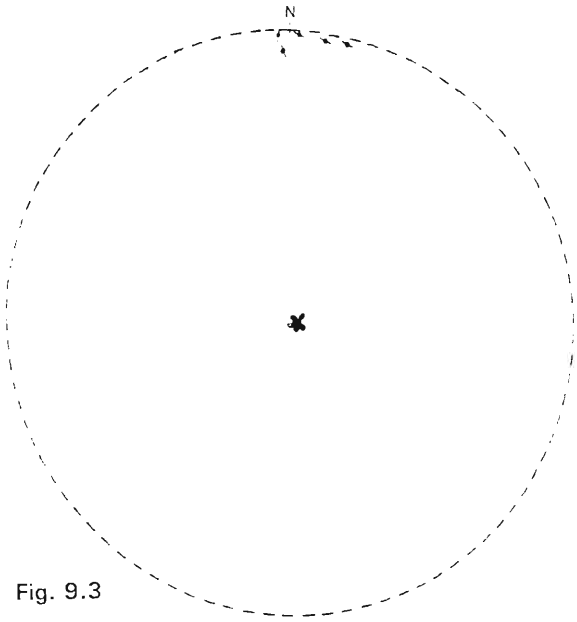

Fig. 9.3

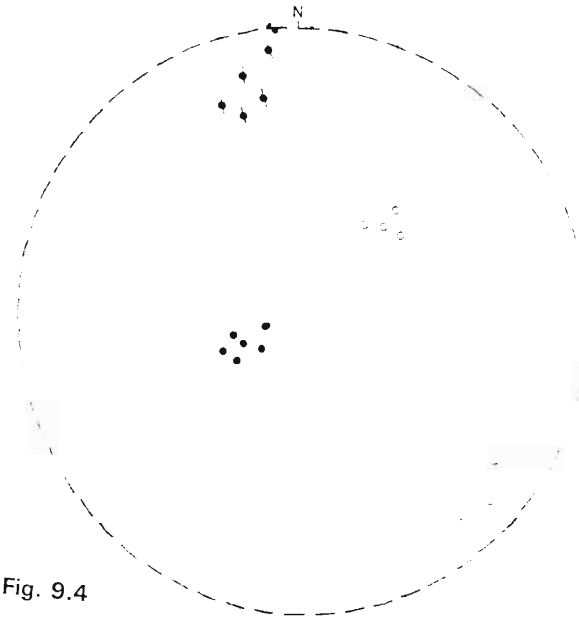

Fig. 9.4

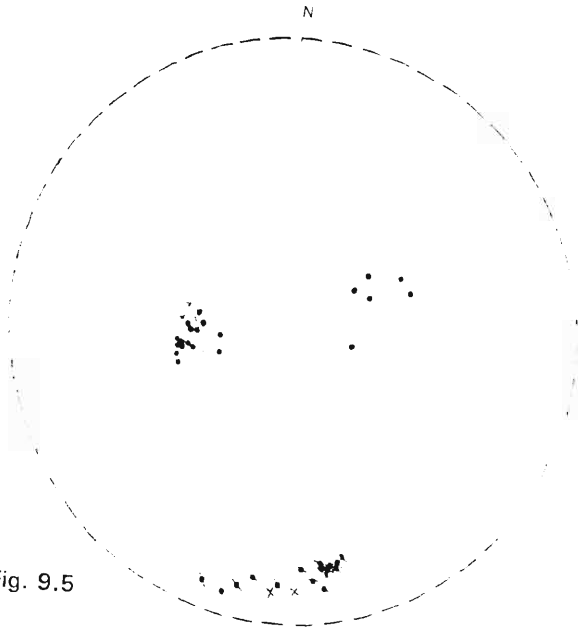

Fig. 9.5

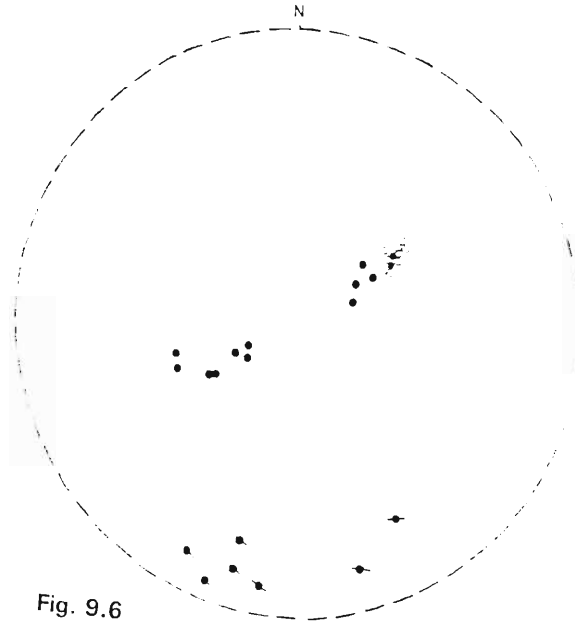

Fig. 9.6

Fig. 9.3 : Orientation data of D_1 folds in the Sabiza Formation of the Entembeni area in the eastern sector of the Ilangwe belt.
- ● = Plunge of F_1 axes of the neutral fold (n=7).
- = Poles to F_1 axial planes (n=5).

Fig. 9.4 : Orientation data of D_1 structures in the Sabiza banded amphibolites of the Amazula River area in the east-central sector of the Ilangwe belt.
- ● = Plunge of F_1 axes of intrafolial folds (n=6).
- = Poles to F_1 axial planes of intrafolial folds (n=5).
- ○ = Plunge of F_1 axes of isoclinal folds (n=4).
- = Poles to F_1 axial planes of isoclinal folds (n=4).

Fig. 9.5 : Orientation data of D_1 structures in the Sabiza banded amphibolites of the Umhlathuze and Sabiza valleys in the west-central sector of the Ilangwe belt.
- ● = Plunge of F_1 axes of isoclinal folds (n=22).
- ● = Poles to F_1 axial planes of isoclinal folds (n=16).
- ✱ = Plunge of F_1 axes of Type 3 interference fold (n=3).
- × = Poles to F_1 axial planes of Type 3 interference fold (n=2).
- ○ = Plunge of L_1 lineations (n=5).

Fig. 9.6 : Orientation data of D_1 structures in the Sabiza banded amphibolites of the Vungwini River valley in the western sector of the Ilangwe belt.
- ● = Plunge of F_1 axes of isoclinal folds (n=13).
- = Poles to F_1 axial planes of isoclinal folds (n=7).
- ○ = Plunge of L_1 mineral stretching lineations (n=9).

A

B

C

D

Plate 9.1

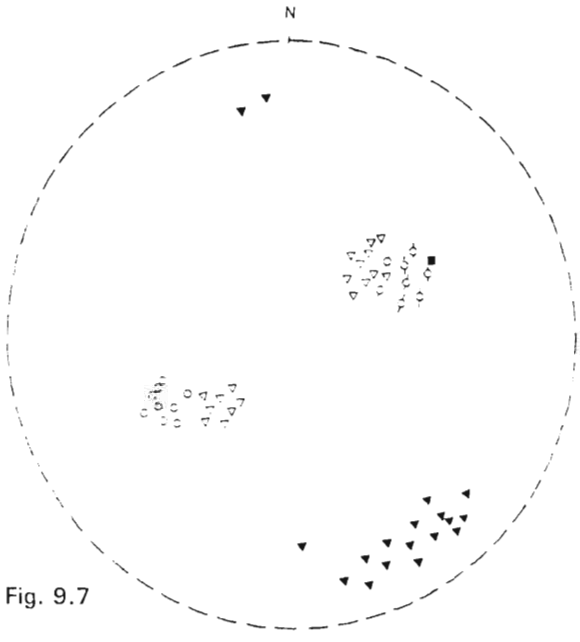

Fig. 9.7

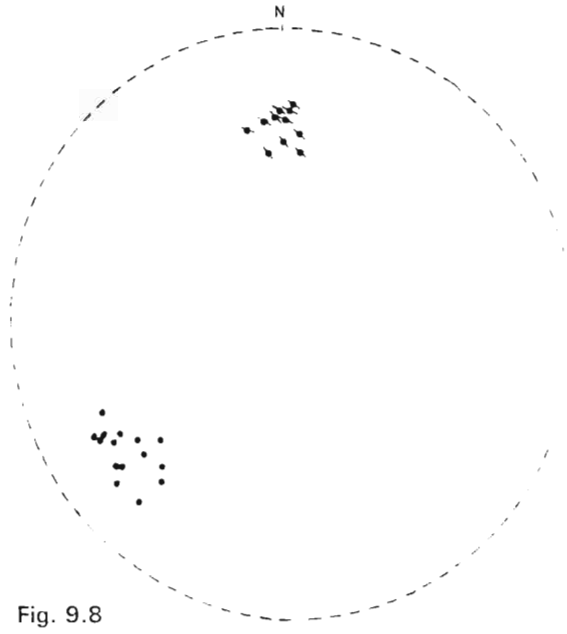

Fig. 9.8

Fig. 9.7 : Orientation data of D_1 structures of the Matshansundu Formation in the eastern sector of the Ilangwe belt.

- O = Plunge of F_1 axes of reclined folds (n=9).
- ⌀ = Poles to F_1 axial planes of reclined folds (n=8).
- ▽ = Plunge of F_1 axes of isoclinal folds (n=18).
- ▼ = Poles to F_1 axial planes of isoclinal folds (n=18).
- ■ = Theoretical mean pole to F_1 reclined axial plane.

Fig. 9.8 : Orientation data of D_1 structures in the Matshansundu raft of the Entembeni area in the eastern sector of the Ilangwe belt.

- ● = Plunge of F_1 fold axes (n=15).
- ⌀ = Poles to F_1 axial planes (n=11).

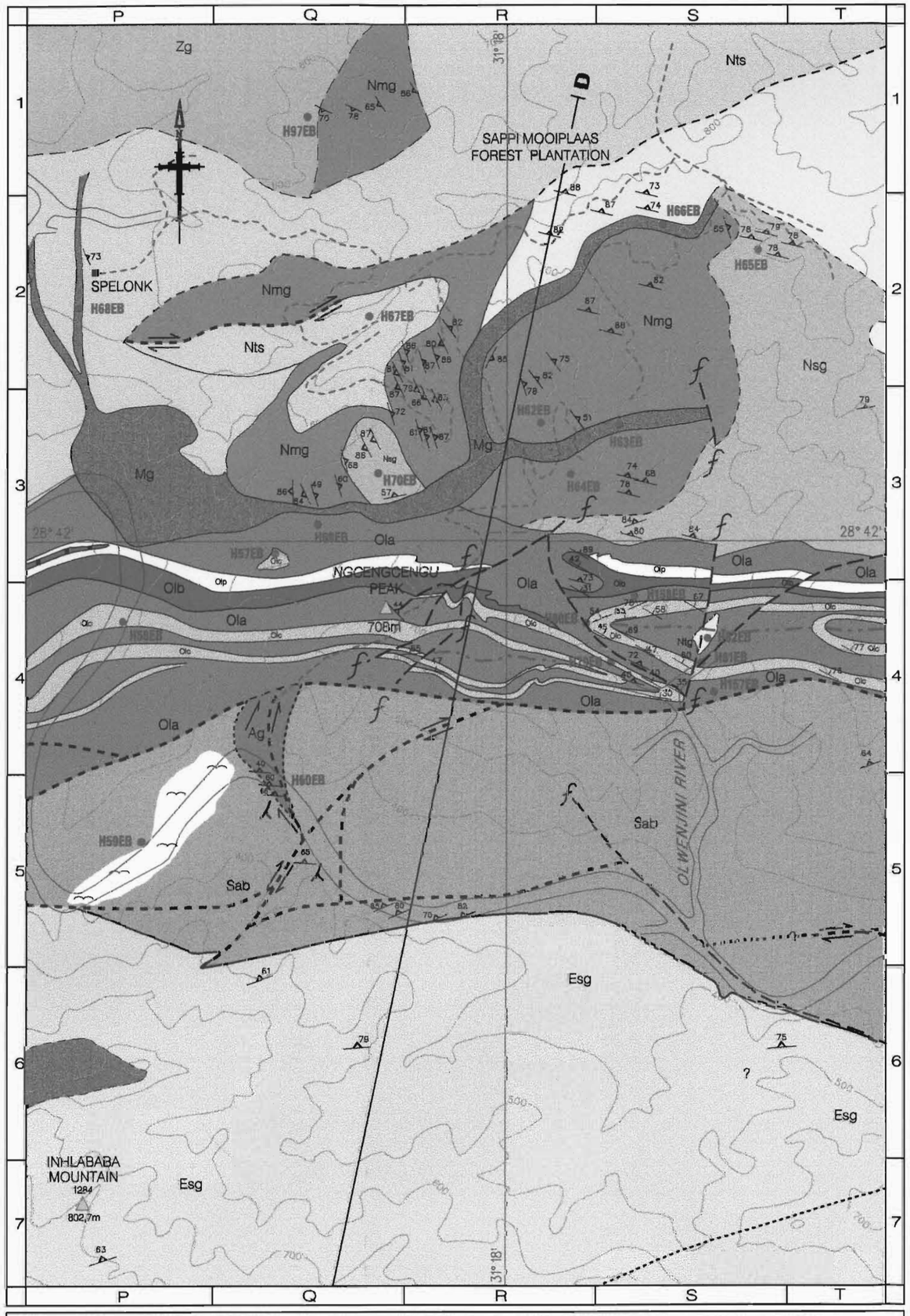

Figure 9.9 : MYLONITIC GNEISSES IN THE MOOIPLAAS AREA AND FOLDED METACHERTS OF THE OLWENJINI FORMATION IN THE NGCENGCENGU PEAK AREA

L E G E N D

Olwenjini Formation

Olb, Olm, Olp, Olg, Olc, Ola — Pillowed metabasalt; garnetiferous amphibolite; actinolite–tremolite schist (Ola); minor phyllite (Olp); banded cherty quartzite, banded metacherts, fuchsitic quartzites (Olc), silicate BIF (Olb), magnetite quartzite (Olm) and a quartz–biotite cordierite fuchsite gneiss (Olg).

Sabiza Formation

Sbc, Sab, Sbt — Pillowed metabasalt; banded amphibolite; massive amphibolite; actinolite–tremolite schist (Sab); talc–tremolite schist; serpentinite–talc schist (Sbt); with thin metachert bands (Sbc) and a khakhi–coloured siliceous pelitic rock towards the top of the sequence

Sat — Discordant serpentinite–talc schists

Ntg — Metagabbro; metanorite; metagabbroic amphibolite

Impisi Granitoid Suite

Zg — Zietover Granite

Nkg — Nkandla Granite

Umgabhi Granitoid Suite

Ucg — Umgabhi Micrographic Granite

Esg, Esq — Esibhudeni Granitoid Gneiss (with quartz–sericite schist)

Umg — Umgabhi Granitoid Gneiss

Nsengeni Granitoid Suite

Ekg — Ekuthuleni Granite

Nsg — Nsengeni Granitoid Gneiss

Nts — Ntshiweni Augen Gneiss

Nkwalinye Tonalitic Gneiss

Ntg — Nkwalinye Tonalitic Gneiss

Nmg — Nkwalini Mylonitic Gneiss

Ag — Amazula Paragneiss

0 1000 2000

M E T R E S

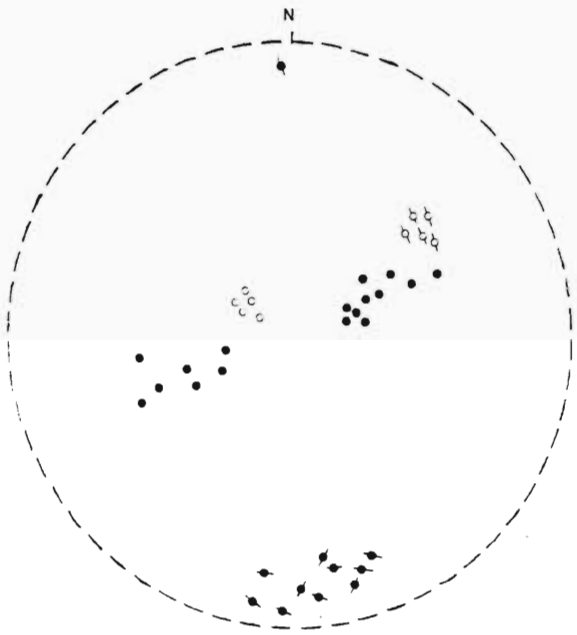

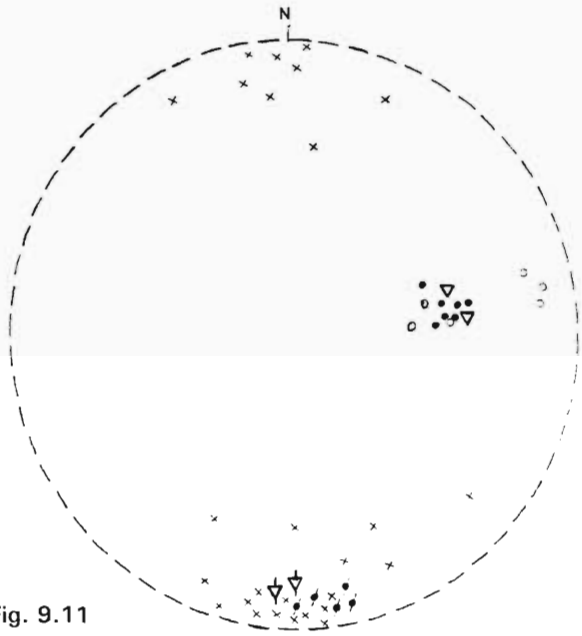

Fig. 9.11

Fig. 9.10 : Orientation data of D_1 structures in the Olwenjini amphibolites of the west-central sector of the Ilangwe belt.

- ● = Plunge of F_1 axes of reclined interfolial folds (n=17).
- ◢● = Poles to F_1 axial planes of reclined folds (n=10).
- ○ = Plunge of F_1 axes of isoclinal intrafolial folds (n=5).
- ◢○ = Poles to F_1 axial planes of intrafolial folds (n=5).

Fig. 9.11 : Orientation data of D_1 structures in the Olwenjini BIFs and metacherts of the west-central sector of the Ilangwe belt.

- ● = Plunge of F_1 fold axes in Bifs (n=7).
- ◢● = Poles to F_1 axial planes (n=5).
- ▽ = Plunge of F_1 fold axes in metacherts (n=2).
- ▽ = Poles to F_1 axial planes in metacherts (n=2).
- × = Poles to bedding in metacherts (n=27).
- ○ = Plunge of L_1 lineation (n=6).

In the Mooiplaas forest plantation area about 1 km due east of Ngcengcengu Peak (3.930/R.980), two juxtaposed isoclinal folds in Olwenjini BIFs plunge at about 45° to the ENE with axial planes inclined to the north (Fig. 9.11). Poles to bedding of the BIFs are inclined steeply to the north and south.

D_1 structures occur in BIFs, phyllites and amphibolites of the ***Entembeni Formation***. They have been rarely found in the Entembeni metacherts. The fold style is mainly isoclinal. In the Entembeni area west of Ndloziyana Peak (6/FF) (Fig. 9.12), small-scale tight isoclinal folds in BIF and phyllites plunge moderately to the ENE and WSW and are inclined to the north and south (Fig. 9.13A and Fig. 9.13B). An L_1 lineation is subparallel to the F_1 fold axes. Some of the shallow plunges here (Fig. 9.13A) can be attributed to tilting due to the diapiric intrusion of the Umgabhi Micrographic Granite and to creep in this hilly area.

On both limbs of the extensive F_2 BIF synform shown on Fig. 9.12, small-scale F_1 isoclinal folds verge to the NE, suggesting that they are earlier than the synform. In one area, an F_1 isoclinal fold has been refolded into an F_2 close to tight isoclinal structure with the same orientation as the large-scale BIF synform which will be described in Section 9.2.3.1.

The similarity of the F_1 and F_2 isoclinal fold styles is evident in a loose block of cherty BIF from Ilangwe Peak area (5.380/Y.910) (Plate 2.2C). This plate shows a tight F_1 isoclinal fold refolded into a tight F_2 isoclinal fold. The chert limbs of the F_1 fold show boudinage and pinch-and-swell structures which can be attributed to a ductility contrast between the chert and Fe-rich layers.

In the Ilangwe Peak area (Fig. 9.14), isoclinal folds in BIF and asymmetric s- and z-folds in metacherts show a moderate plunge to the WSW and ENE and are inclined to the north and south (Fig. 9.15A). This bimodal distribution is also depicted by Ilangwe phyllites and metabasalts occurring to the SSE of Ilangwe Peak (Fig. 9.15B).

In the western sector of the belt and within the ***Simbagwezi Formation***, isoclinal intrafolial folds occur in amphibolites and phyllites. The folds plunge steeply to the NE and SW and are steeply inclined to the north (Fig. 9.16). This distribution is similar to that of the Entembeni Formation (Figs. 9.13 A and B; Fig. 9.15) and Umhlathuze Subgroup structures

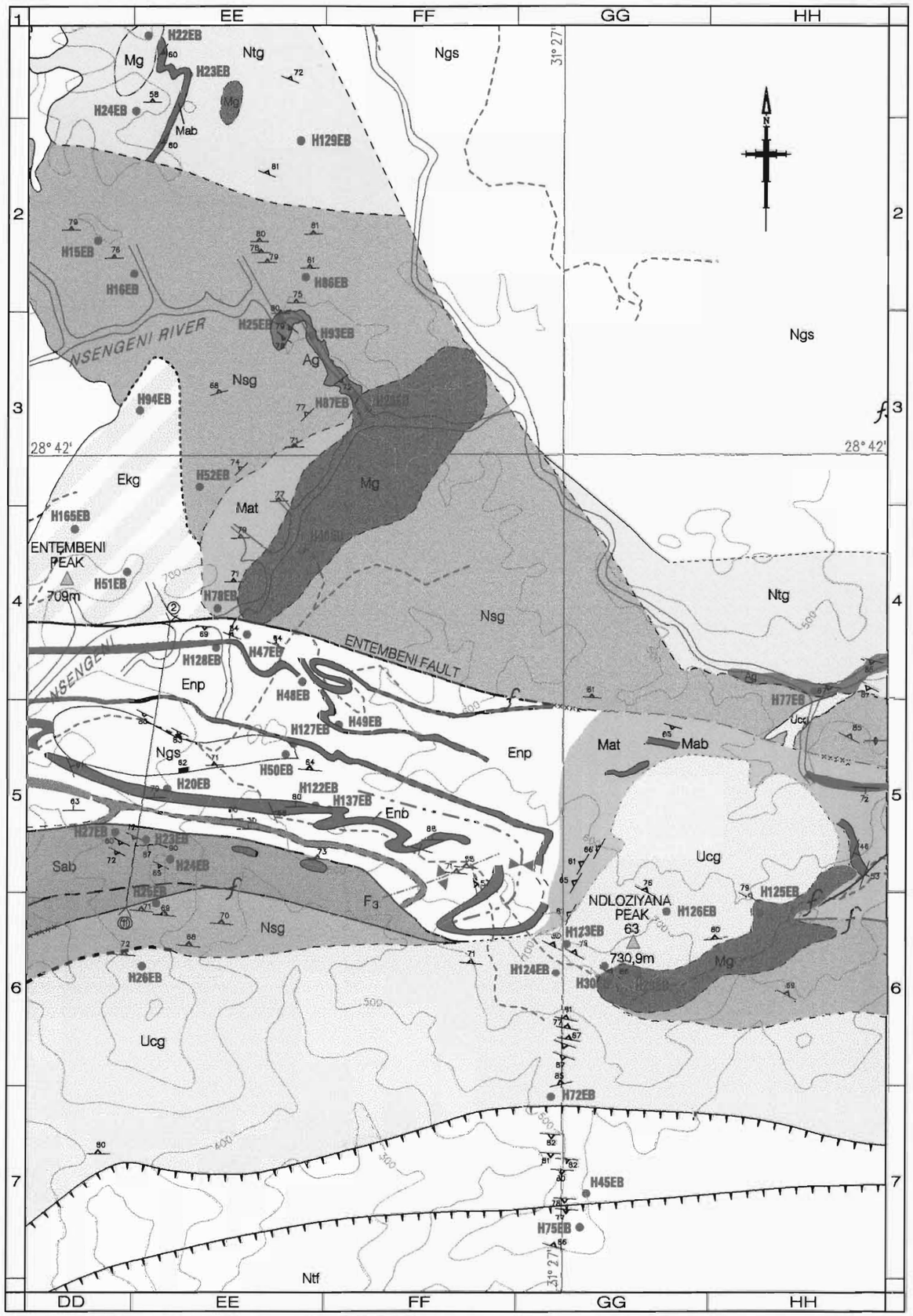

Figure 9.12 **Complexly folded BIFs of the Entembeni Formation and the diapiric intrusion of the Umgabhi Micrographic Granite in the Ndloziyana Peak area.**

LEGEND

Entembeni Formation — Enb / Enp / Enc — Phyllite (phyllonitic in the shear zones and along fault contacts) and minor pillowed metavolcanics (Enp), intercalated with cherty BIF (Enb), metacherts and cherty quartzite bands (Enc).

Matshansundu Formation — Mat / Mab — Actinolite–tremolite schist; amphibole–mica schist; massive metabasalt (Mat) intercalated with cherty silicate BIF (Mab).

Sabiza Formation — Sbc / Sab / Sbt — Pillowed metabasalt; banded amphibolite; massive amphibolite; actinolite–tremolite schist (Sab); talc–tremolite schist; serpentinite–talc schist (Sbt); with thin metachert bands (Sbc) and a khakhi-coloured siliceous pelitic rock towards the top of the sequence

Sat — Transgressive serpentinite–talc schists

Mg — Metagabbro; metanorite; metagabbroic amphibolite

Umgabhi Granitoid Suite
- Ucg — Umgabhi Micrographic Granite
- Esg / Esq — Esibhudeni Granitoid Gneiss (with quartz–sericite schist)
- Umg — Umgabhi Granitoid Gneiss

Nsengeni Granitoid Suite
- Ekg — Ekuthuleni Granite
- Nsg — Nsengeni Granitoid Gneiss
- Nts — Ntshiweni Augen Gneiss

Ntg — Nkwalinye Tonalitic Gneiss

Ag — Amazula Paragneiss

0 1000 2000

METRES

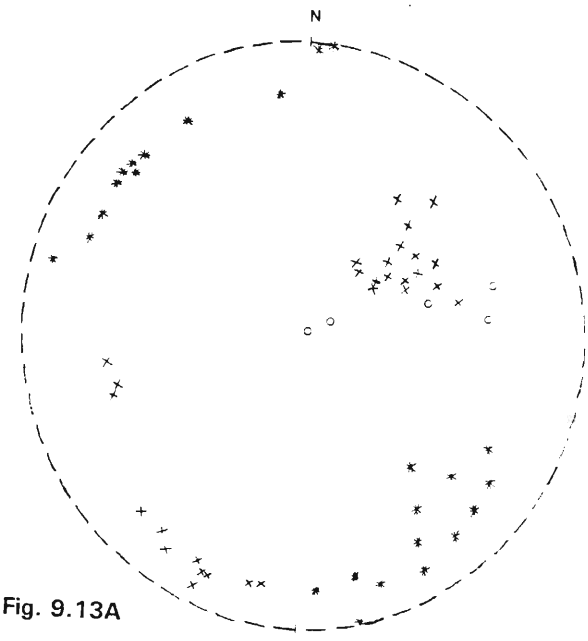

Fig. 9.13A

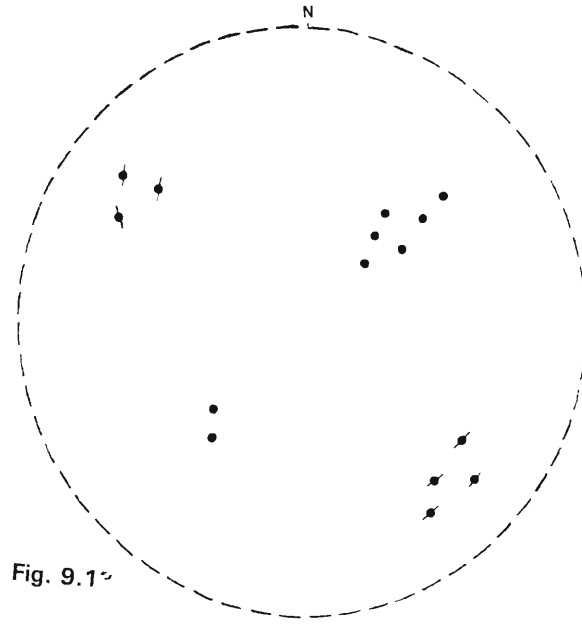

Fig. 9.1

Fig. 9.13A : Orientation data of D_1 structures in the Entembeni BIFs of the eastern sector of the Ilangwe belt.

× = Plunge of F_1 fold axes (n=29).
✳ = Poles to F_1 axial planes (n=25).
○ = Plunge of L_1 lineation (n=5).

Fig. 9.13B : Orientation data of D_1 structures in the Entembeni phyllites of the eastern sector of the Ilangwe belt.

● = Plunge of F_1 fold axes (n=8).
◢ = Poles to F_1 axial planes (n=7).

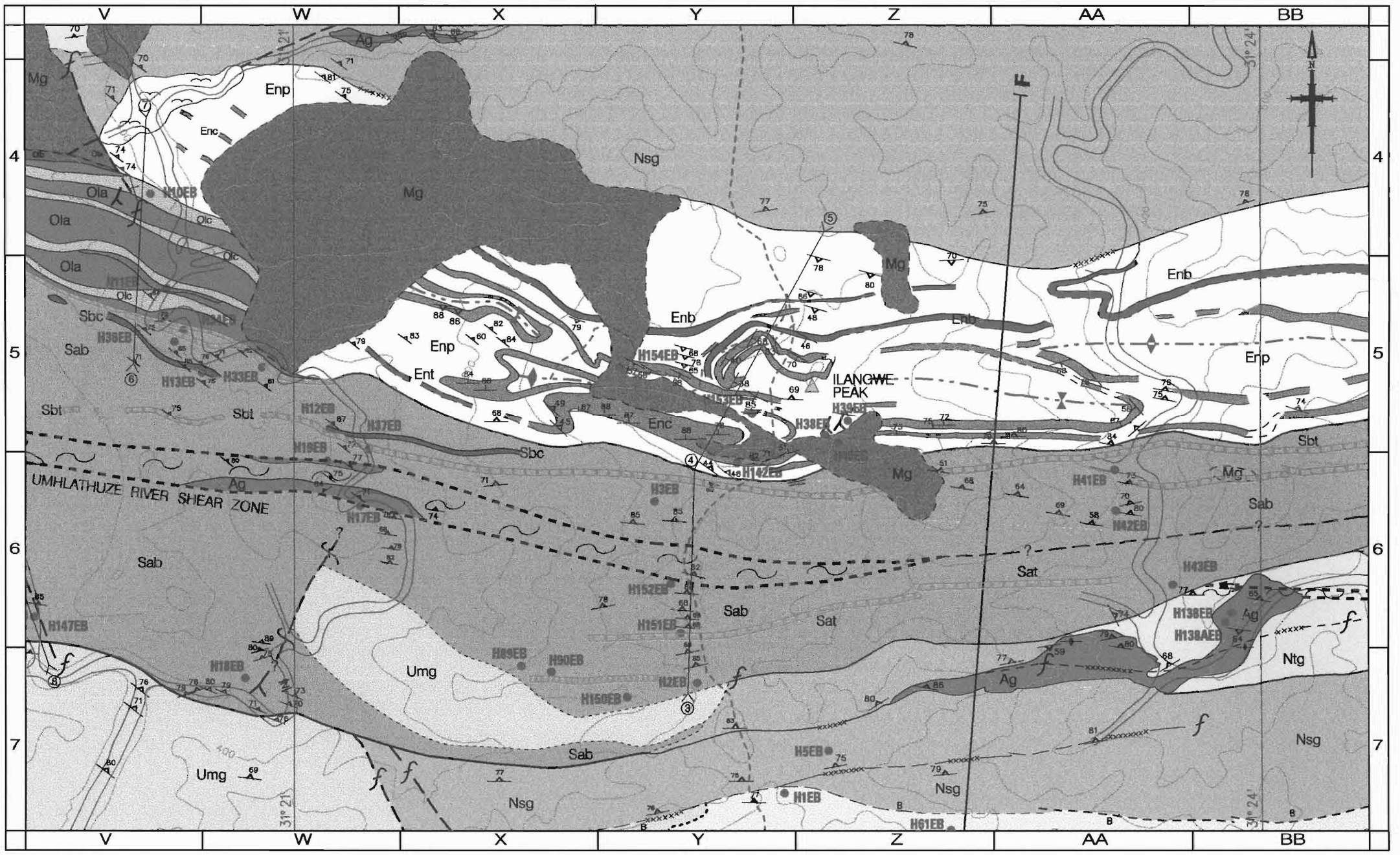

Figure 9.14 : THE GEOLOGY OF THE ENTEMBENI FORMATION IN THE ILANGWE PEAK AREA

L E G E N D

Entembeni Formation

Enb / Enp / Enc — Phyllite (phyllonitic at the shear zones and fault contacts) (Enp) intercalated with cherty BIF (Enb), mtacherts and cherty quartzite bands (Enc).

Olwenjini Formation

Ola / Olb / Olm / Olg / Olp / Olc — Pillowed metabasalt; garnetiferous amphibolite; actinolite–tremolite schist (Ola); minor phyllite (Olp); banded cherty quartzite, banded metacherts, fuchsitic quartzites (Olc), silicate BIF (Olb), magnetite quartzite (Olm) and a quartz–biotite cordierite fuchsite gneiss (Olg).

Sabiza Formation

Sbc / Sab / Sbt — Pillowed metabasalt; banded amphibolite; massive amphibolite; actinolite–tremolite schist (Sab); talc–tremolite schist; serpentinite–talc schist (Sbt); with thin metachert bands (Sbc) and a khakhi–coloured silceous pelitic rock towards the top of the sequence

Sat — Discordant serpentinite–talc schists

Mg — Metagabbro; metanorite; metagabbroic amphibolite

Umgabhi Granitoid Suite

Ucg — Umgabhi Micrographic Granite

Esg / Esq — Esibhudeni Granitoid Gneiss (with quartz–sericite schist)

Umg — Umgabhi Granitoid Gneiss

Nsengeni Granitoid Suite

Ekg — Ekuthuleni Granite

Nsg — Nsengeni Granitoid Gneiss

Nts — Ntshiweni Augen Gneiss

Ntg — Nkwalinye Tonalitic Gneiss

Ag — Amazula Paragneiss

0 1000 2000 3000

M E T R E S

Figure 9.14

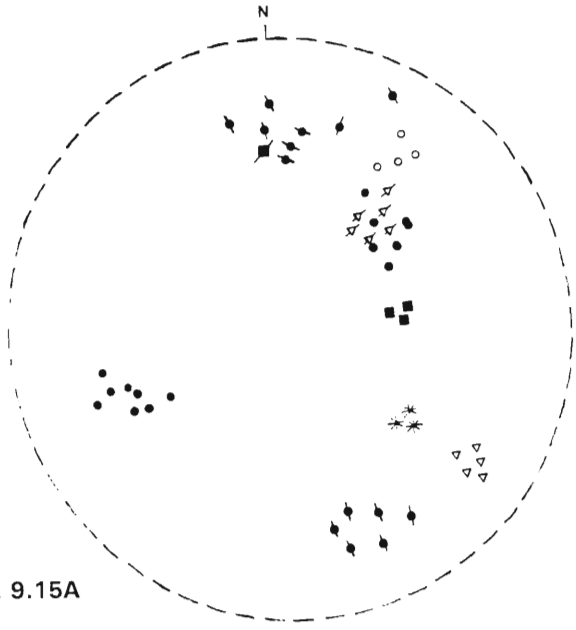

Fig. 9.15A

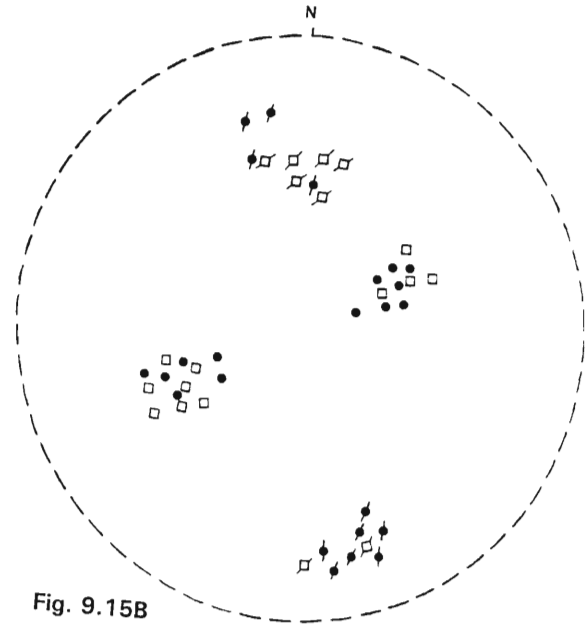

Fig. 9.15B

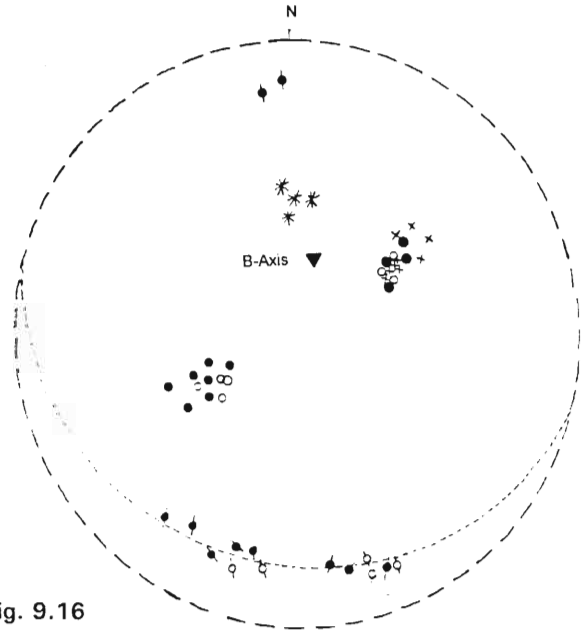

Fig. 9.16

Fig. 9.15A : Orientation data of D_1 structures in the Entembeni metacherts of the Ilangwe Peak area in the central sector of the belt.

- = Plunge of F_1 axes of s-folds (n=6).
- = Poles to F_1 axial planes of s-folds (n=5).
- = Plunge of F_1 axes of z-folds (n=3).
- = Pole to F_1 axial plane of z-folds (n=1).
- = Plunge of L_1 rodding (n=3).
- = Plunge of F_1 isoclinal fold axes (n=15).
- = Poles to F_1 axial planes (n=14).

Fig. 9.15B : Orientation data of D_1 structures in the Entembeni amphibolites and phyllites of the Ilangwe Peak area in the central sector of the Ilangwe belt.

- = Plunge of F_1 axes of isoclinal folds in amphibolites (n=13).
- = Poles to F_1 axial planes in amphibolites (n=11).
- = Plunge of F_1 axes of isoclinal folds in phyllites (n=11).
- = Poles to F_1 axial planes in phyllites (n=8).

Fig. 9.16 : Orientation data of D_1 structures in the Simbagwezi Formation of the western sector of the Ilangwe belt

- = Plunge of F_1 axes of interfolial folds in amphibolites (n=11).
- = Poles to F_1 axial planes in amphibolites (n=10).
- = Plunge of F_1 fold axes in phyllites (n=7).
- = Poles to F_1 axial planes in phyllites (n=5).
- = Plunge of F_1 axes of reclined folds (n=3).
- = Plunge of L_1 mineral stretching lineation and quartz rods (n=9).

(Figs. 9.4, 9.5, 9.6, 9.7 and 9.8) but shows a northerly inclined axial planar distribution with a subhorizonal girdle declaring a steep northerly plunging B-axis (Fig. 9.16).

The ***Nomangci Formation*** shows a predominant E-W trending bedding and foliation (Figs. 9.2I and 9.2J). Transposed foliation has been observed but intrafolial folds are absent. Although the Nomangci metacherts and quartzites are intensely recrystallized, traces of original bedding have been observed. In some metacherts, a semblance of transpositional layering is present (Plate 2.2).

9.2.2.2 ANALYSIS OF STRUCTURAL DATA FROM F_1 FOLDS

Compilations of all the data on the orientations of F_1 fold axes and axial planes are shown in the lower hemisphere stereo projections of Figs. 9.17 and 9.18, respectively, and the combined plot is shown in Fig. 9.19. These plots show a remarkable close correspondence of the maxima for the amphibolites, on the one hand, and the BIFs and metacherts, on the other, and thus suggest that the amphibolite banding is a primary layering S_o.

It is apparent from Fig. 9.17 that the F_1 fold axes show a remarkable symmetric, bimodal distribution in a vertical plane with azimuth 070°. One set of folds plunge NE at a mean angle of ±60° and the other set plunges SW also at a mean angle of about 60°. The axial plane poles show a major concentration around the N and S poles.

When the bimodal concentration of the F_1 fold axes is examined in relation to the elements of the large-scale folds, it is found that each of the F_1 fold axes maxima falls on a great circle trace representing the mean orientation of the steeply dipping north or south limbs of the large-scale folds. The preferred best-fit configuration with axial plane azimuth of 100° is shown in Fig. 9.20A and Fig. 9.21A. Several other possible arrangements with slightly different axial plane azimuths (060° to 110°) are shown in Figs. 9.22A, 9.23A and 9.24A. It is also apparent that the north and south concentrations of poles to the F_1 axial planes correspond rather closely with the mean poles to the limbs of the large folds (Figs. 9.21, 9.22, 9.23 and 9.24).

This remarkable concentration of structural relationships must be extremely uncommon, because it corresponds almost exactly with one of the well-known theoretical models of polyphase or superposed folding. This model is the ***flexural fold*** model in which any initial lineation is deformed along a conical locus about the B tectonic fold-axis (Ramsay, 1967).

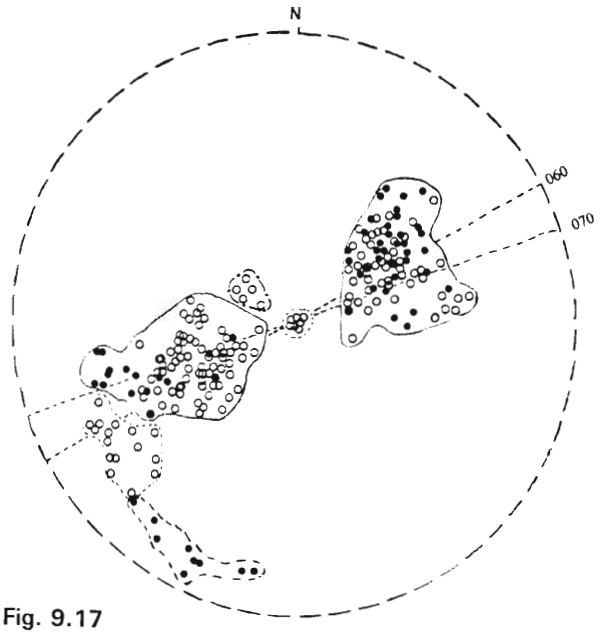

Fig. 9.17

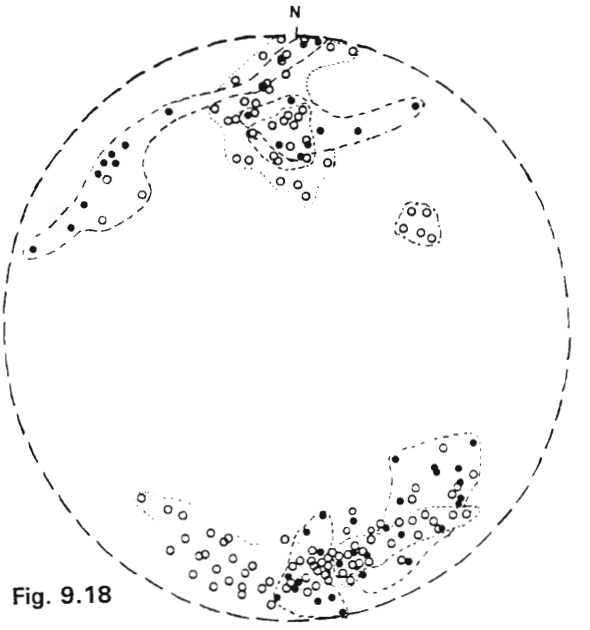

Fig. 9.18

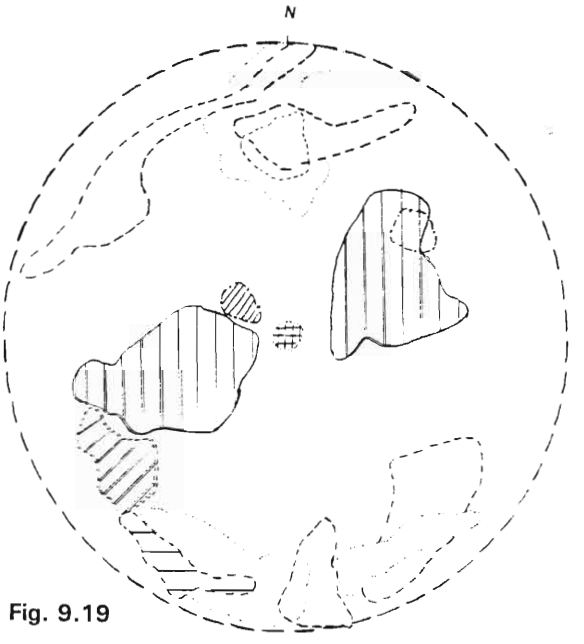

Fig. 9.19

Fig. 9.17 : Compilation of F_1 fold axes in the different lithologies of the Ilangwe Greenstone Belt.
- O = Plunge of F_1 fold axes in amphibolites and phyllites.
- ● = Plunge of F_1 fold axes in BIFs and metacherts.

Fig. 9.18 : Compilation of F_1 axial planes in the different lithologies of the Ilangwe Greenstone Belt.
- O = Poles to axial planes in the amphibolites and phyllites.
- ● = Poles to axial planes in the BIFs and metacherts.

Fig. 9.19 : A combined plot of F_1 fold axes and axial planes in the different formations of the Ilangwe Greenstone Belt.

- = BIF and amphibolite fold axes.
- = Amphibolites in Matshansundu raft.
- = BIF and amph. Axial planes.
- = Axial planes in Matshansundu raft.
- = Axial planes of intrafolial folds in amphibolite.
- = BIF fold axes only.
- = Intrafolial folds in amphibolite.
- = Axial planes in amphibolite.
- = Plunge of neutral folds.

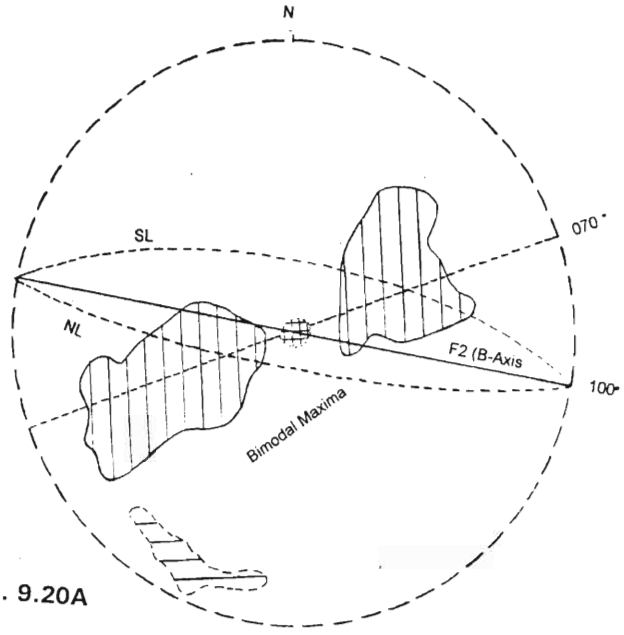

Fig. 9.20A

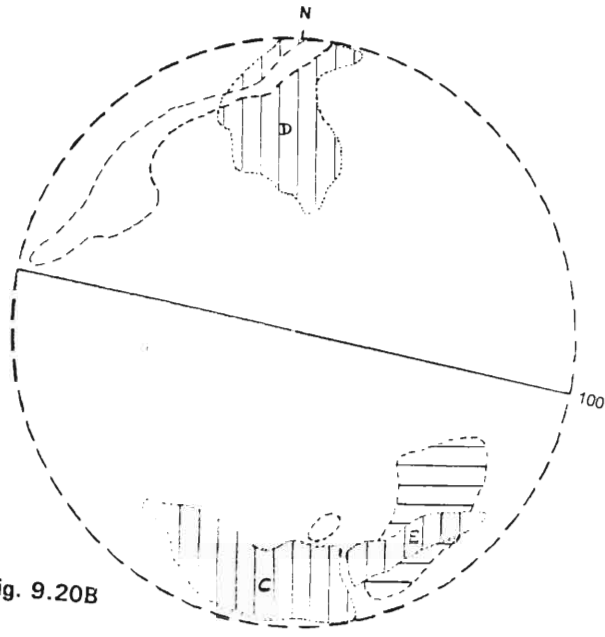

Fig. 9.20B

Fig. 9.20A : Preferred best-fit configuration plot of F_1 fold axes with axial plane (B_2-axis) azimuth of 100 degrees.

Fig. 9.20B : Preferred best-fit configuration plot of F1 axial planes with B_2 tectonic axis azimuth of 100 degrees.

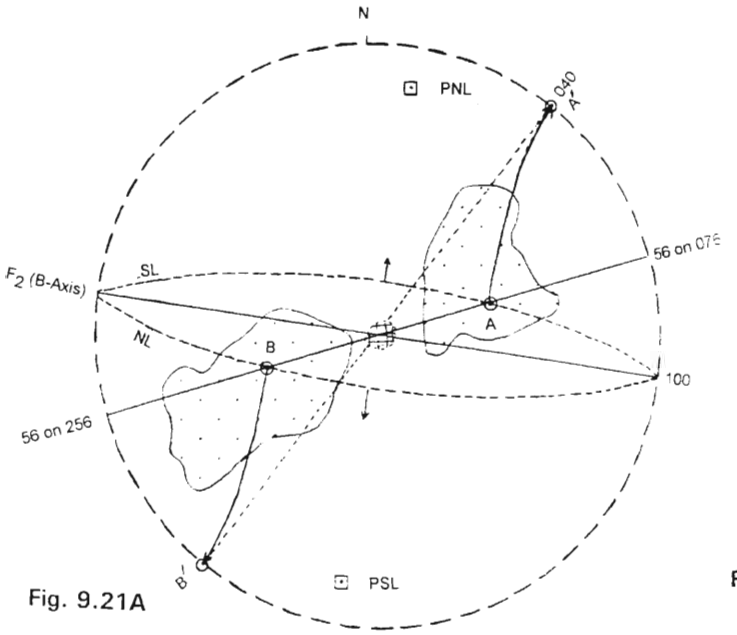

Fig. 9.21A

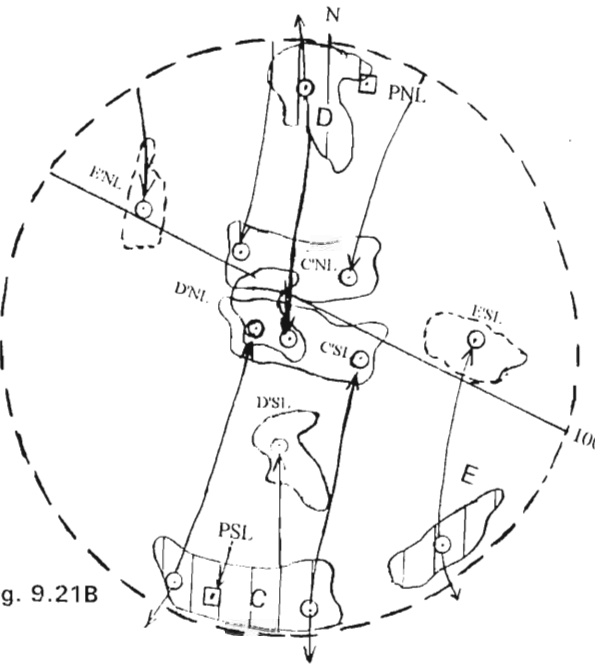

Fig. 9.21B

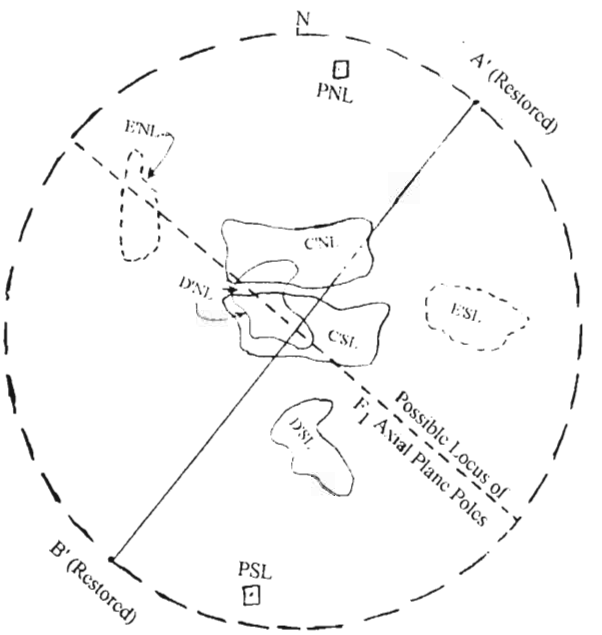

Fig. 9.21C

Fig. 9.21A : Unfolding of the north and south limbs of the D_2 large-scale syncline and rotation of deformed F_1 folds about the F_2 tectonic axis (100 degrees).

Fig. 9.21B : Unfolding of the poles to F_1 axial planes.

Fig. 9.21C : The final pattern of unfolded F_1 axial planes.

Application of the model with the B-axis horizontal on an azimuth of 100° is shown in Figs. 9.21A, B and C. Fig. 9.21A represents unfolding of the north (NL) and south (SL) limbs of a large-scale syncline. Each limb contains the mean orientation pole (A or B) of the bimodal F_1 fold axes distributions. The pole A is located on the great circle trace of the south limb (SL) and pole B on the trace of the north limb (NL). As the limbs are unfolded the poles A and B rotate with the respective fold-limbs and follow small circle arcs to points A' and B' on the peripheral circle which represents the horizontal plane. The poles A' and B' are now coincident and define a single, initial F_1 fold orientation with an azimuth of 040°. At this stage the analysis suggests that the D_1 compression acted in a NW-SE direction, but the vector is not defined. This direction should be indicated by undeforming the axial planes of the F_1 folds.

A diagrammatic 3D representation of the model at this stage is shown in Fig. 9.46A and B.

Unfolding of the poles to the F_1 axial planes is shown in Fig. 9.21B. The various initial pole-maxima are labelled C, D and E. These poles unlike the F_1 fold-poles, are not attached to particular D_2 fold limbs, so it is necessary to carry out the unfolding procedure ***by tracing two small-circle arcs for each pole of the F_1 axial planes***. One of these arcs will follow the pole during unfolding of the north limb (NL) of the D_2 syncline, and the other will follow the south limb (SL). In each case the necessary rotation angle is 80°-85° to bring the D_2 fold limbs to the horizontal (i.e. to rotate the limb-poles NLP and SLP to the centre of the stereoplot. The final rotated positions of the poles are labelled C'NL, C'SL; D'NL, D'SL; and E'NL, E'SL.

The final pattern of unfolded F_1 axial plane poles is shown in Fig. 9.21C. This shows a major concentration of poles at the centre of the stereoplot which, of course, indicates that the F_1 folds had a predominantly recumbent style.

Minor concentrations of axial-plane poles occur in a symmetrical pattern about the possible locus of poles defined by the 040° azimuth of the F_1 fold axis in Fig. 9.21A. This suggests a genetic relationship due, perhaps, to slight cross-warping prior to the D_2 folding. In general, this part of the analysis allows formulation of two important ***preliminary conclusions*** :

(a) That the F_1 folding took place in an essentially horizontal tectonic regime and was characterized by recumbent folding that was directed either to the SE or to the NW. Unfortunately, the subhorizontal orientation of the undeformed F_1 axial planes does not provide evidence for the direction of tectonic transport. Nevertheless, the conclusion that F_1 folds were recumbent in style is supported by the occurrence of the Type 3 interference fold (Plate 9.1A) previously described in Section 9.2.2.1. Type 3 interference folding is commonly developed where initially recumbent folds are refolded by new structures with steeply inclined axial planes (Ramsay, 1967).

(b) That the large-scale folds, forming a prominent feature of the Ilangwe Greenstone Belt (Fig. 9.9; Fig. 9.12; Fig. 9.14; Fig. 9.51) are of D_2 age and were essentially the product of flexural folding. This conclusion is in accord with later considerations concerning the classification and mode of development of these large folds.

These are preliminary conclusions because it is necessary to examine a few implications that arise from any acceptance of the interpretation of the large-scale folds as the product of flexural folding.

Briefly, the ***first implication*** is that the occurrence of a well-developed axial-planar foliation/cleavage to the large upright folds indicates that substantial flattening must have been involved in the evolution of these folds. Additional evidence of D_2 flattening is provided by the high axial ratios of deformed pillow structures (Table 9.2) that are elongated and flattened in a sub-vertical foliation which is axial planar to the large-scale F_2 folds.

The ***second implication***, which will be considered in section 9.2.3.2 under D_2 phase of deformation, is the theoretical probability that the development of the large flexural folds will generate sub-horizontal second order small-scale s, z and m folds (see Fig. 9.46B).

9.2.2.3 EXTENDED ANALYSIS FOR A COMPONENT OF PURE SHEAR

The first implication mentioned above concerning the evidence for flattening provided by the occurrence of axial-planar cleavage to the large-scale flexural folds, suggests that the analysis should be extended to take account of this feature.

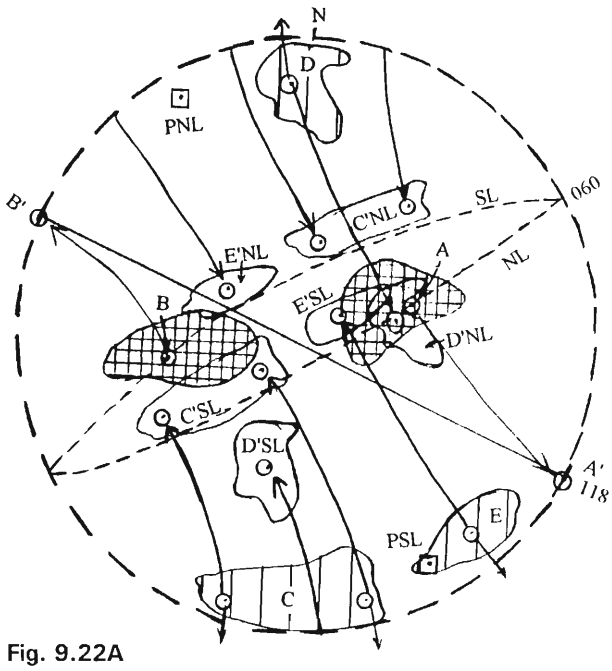

Fig. 9.22A

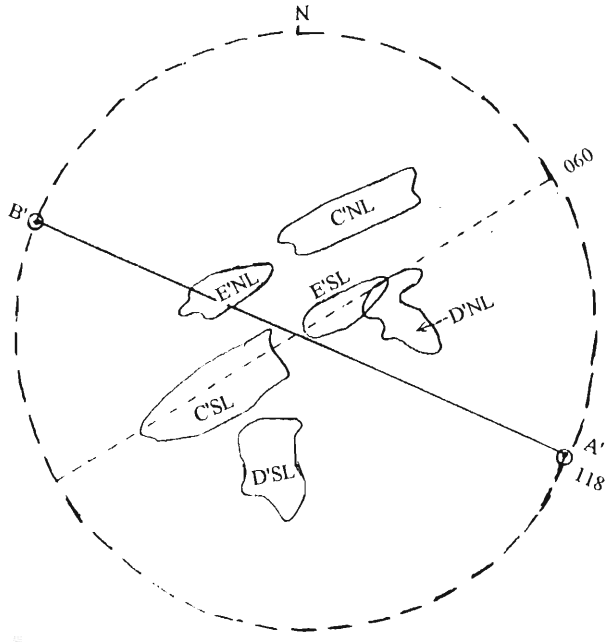

Fig. 9.22B

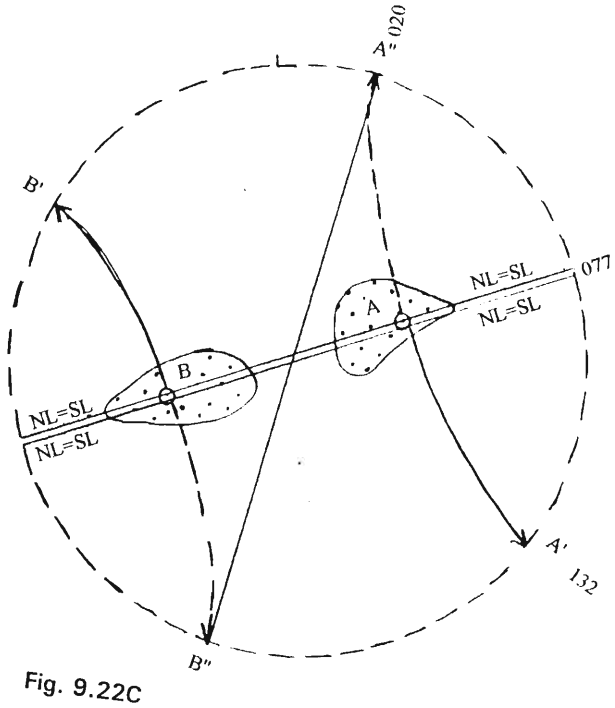

Fig. 9.22C

Fig. 9.22A : Unfolding of the north and south limbs of the large-scale syncline and rotation of deformed F_1 fold elements about the F_2 tectonic axis azimuth of 60 degrees.

Fig. 9.22B : The final pattern of F_1 axial planes.

Fig. 9.22C : Orientation of the north and south limbs after unfolding of the F_1 fold axes.

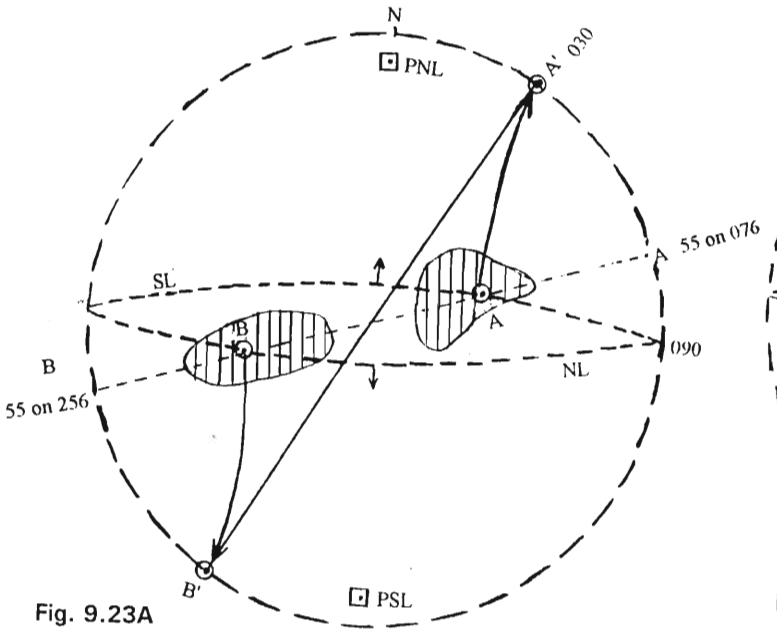

Fig. 9.23A

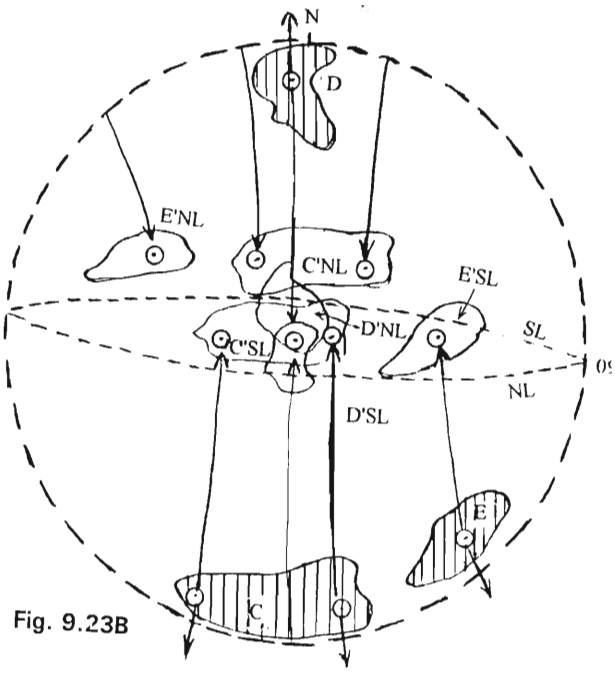

Fig. 9.23B

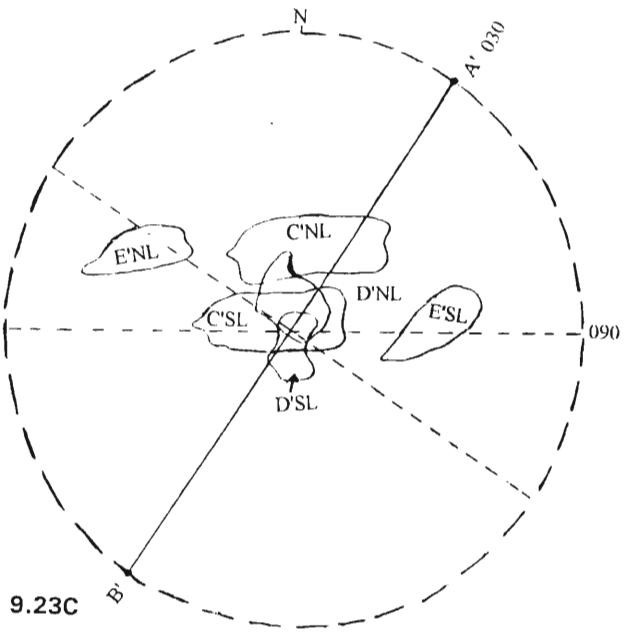

Fig. 9.23C

Fig. 9.23A,B,C : Unfolding of the north and south limbs of the large-scale syncline and rotation of deformed F_1 fold elements about the F_2 tectonic axis azimuth of 90 degrees.

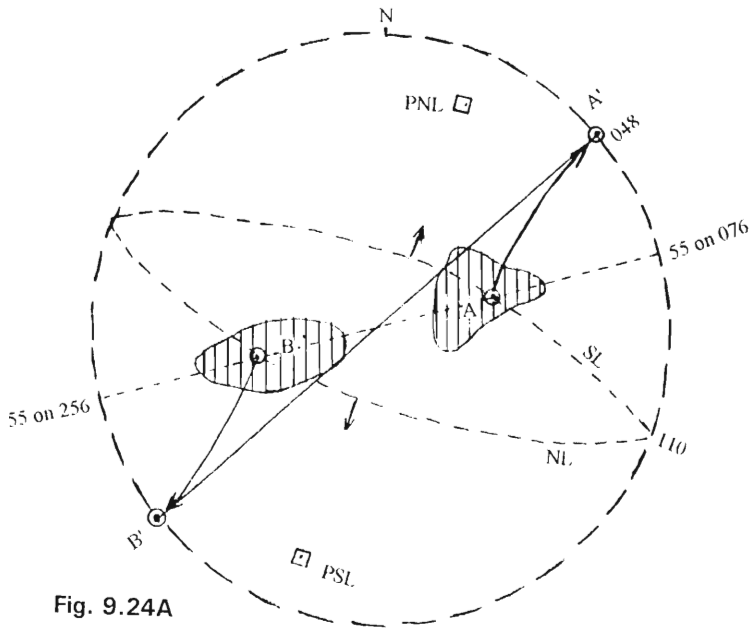

Fig. 9.24A

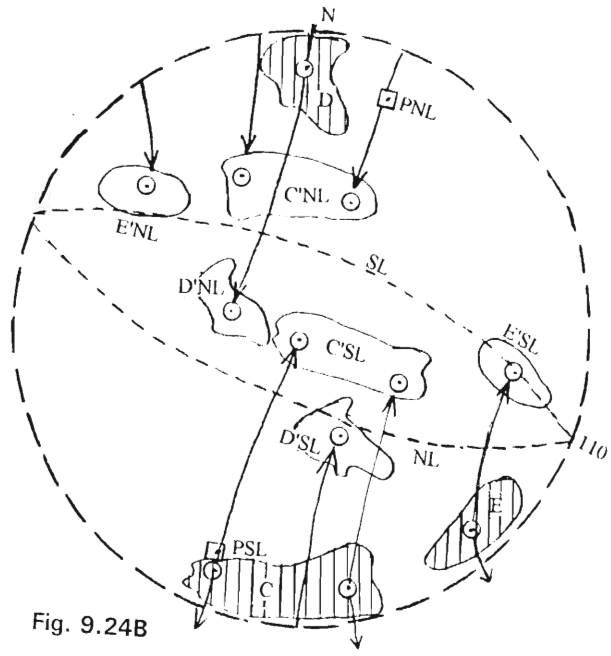

Fig. 9.24B

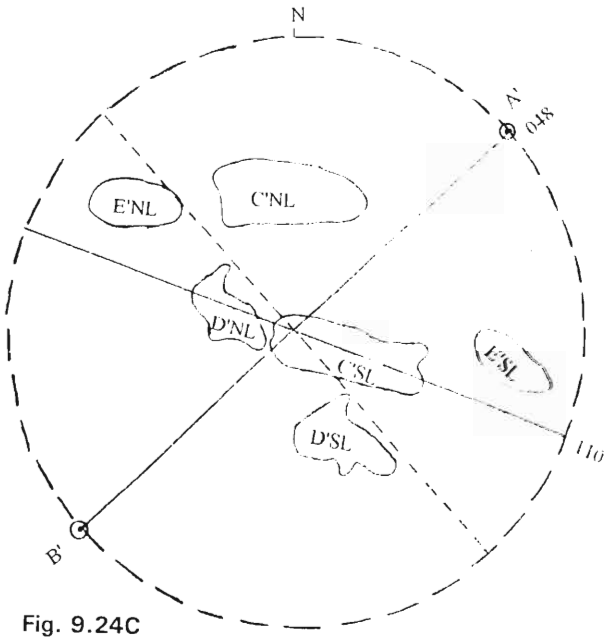

Fig. 9.24C

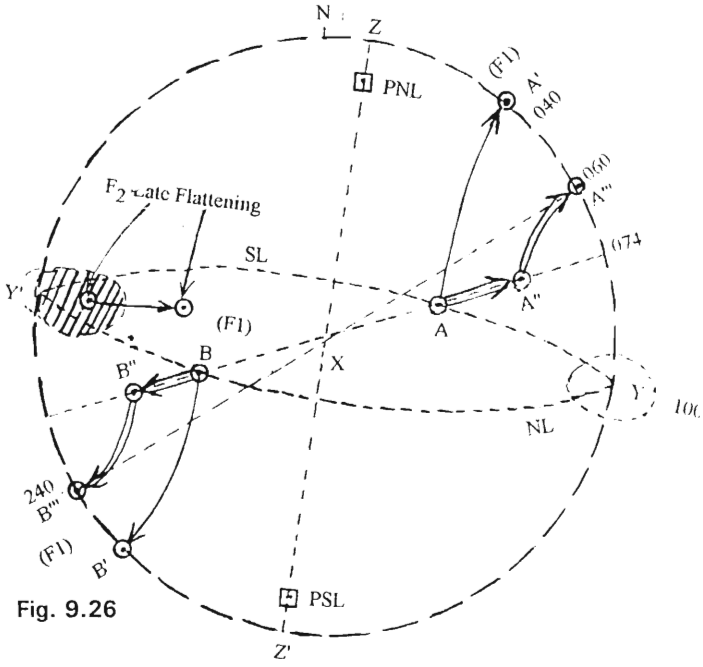

Fig. 9.26

Fig. 9.24A,B,C : Unfolding of the north and south limbs of the large-scale syncline and rotation of deformed F_1 fold elements about the F_2 tectonic axis azimuth of 110 degrees.

Fig. 9.26 : Modified analysis of the flexural fold model with a component of flattening introduced normal to the vertical axial plane of the F_2 large-scale syncline with the B-axis azimuth at 100 degrees.

Fig. 9.26 shows a modified analysis of the flexural fold model with a component of flattening introduced normal to the vertical axial plane of the postulated D_2 syncline with the B-axis azimuth of 100°. The small-circle rotations A to A' and B to B' are the unmodified paths of the first analysis for reference.

In the modified model it should be noted that a pure shear flattening has the effect of steepening the plunge of line-elements towards the X-tectonic axis (vertical in this case) in a plane defined by this axis and the line-element.

The modified version involves a two stage undeforming process. This is shown, for example, by the F_1 fold-axis pole labelled A. In the first stage of undeforming, a component of flattening which is post-D_1 folding, moves the pole from A to A" within a vertical plane X-A. In the second stage, D_2 folding about the B-tectonic axis (azimuth 100°) rotates the A" pole to A"' on the peripheral circle (that is to the horizontal). A similar set of movements moves the pole B to B" and B"' together with the north limb (NL) of the syncline. Poles A"'and B"' are coincident with an azimuth of 060° in contrast to the first analysis where the fold azimuth was 040°.

This extended analysis is probably more realistic than the first, but it does not alter the preliminary conclusions mentioned previously, except for the fact that the inferred direction of compression of the D_1 deformation was not NW-SE but NNW-SSE. This is closer to the N-S D_2 direction of compression that produced the general E-W structural trend of the Ilangwe Greenstone Belt.

9.2.2.4 AN INTERPRETATION OF D_1 TECTONICS

In summary, the preceding analysis suggests that the D_1 deformation of the Ilangwe Greenstone sequence took place in an essentially horizontal tectonic regime which was characterized by widespread recumbent folding with fold axes aligned in a more or less ENE (060°) direction. This conclusion is in accord with the observed isoclinal and intrafolial forms of the F_1 folds, which point to deformation in a regional high strain environment.

Unfortunately, the preceding analysis has not revealed an initial, asymmetric F_1 fold geometry which would have indicated a direction of tectonic transport. On the contrary, the undeformed orientation of the F_1 axial planes is sub-horizontal. Further detailed field work

with a focus on meticulously searching for superimposed small-scale folding will be required in an attempt to resolve this problem.

9.2.3 D_2 PHASE OF DEFORMATION IN THE ILANGWE GREENSTONE BELT

9.2.3.1 LARGE-SCALE FOLDS

The Olwenjini and Matshansundu Formations of the Umhlathuze Subgroup and the Entembeni Formation of the Nkandla Subgroup contain a series of en echelon large-scale folds which form the most prominent structural features within the Greenstone Belt. These folds occur as a series of E-W trending, tightly appressed, upright folds, with sub-vertical axial planes, and are well-defined by extensive outcrops of banded ironstones and metacherts. These banded units can be traced continuously along the steeply-dipping fold-limbs for distances of 4 to 10 km (see Fig. 2). Although these units can also be traced around the fold-closures, the plunge of the folds cannot be determined because the orientation of bedding is obscured by the falling of outcrops due to creep, brecciation of the ironstones and almost total recrystallization of the metacherts to massive quartz (Plate 9.2A). However, the lack of substantial thickening of the ironstones and metacherts around the fold closures suggests that the mechanism of folding was ***flexural-slip***. Nevertheless, the well-developed sub-vertical axial plane cleavage (foliation) suggests that this folding was accompanied by considerable flattening.

Recognition of antiforms and synforms is limited by several factors, such as the lack of way-up indicators with only a few determinations from deformed pillow structures at widely spaced localities [5.250/J.850); (5.900/J.910); (5.880/K.190); (6.660/K.190); (5.920/K.510); (5.070/O.940); 5.200/Q.290); 5.520/Q.540); (4.600/S.550); (5.620/U.570); (4.700/V.570); (7.200/W.290); (5.900/Z.195)] and the overturned nature of some of the fold limbs. Other limitations are the near vertical dip of the fold-limbs and the associated cleavage, a relationship that prohibits the use of Pumpelly's Rule. There is also the previously mentioned problem of not being able to directly establish the plunge of individual folds. However, the characteristic elliptical outcrop pattern shows an en echelon arrangement of adjacent fold-closures which suggests alternating antiforms and synforms (see Plate 9.2C).

In quite a number of localities within the belt, the dip of the fold-limbs suggests some antiformal and synformal structures. For example, in the eastern sector around the Matshansundu area, the northern limb of the Matshansundu BIF dips steeply to the south

and the southern limb dips steeply to the north thus suggesting a synformal structure (Fig. 2). Similarly, the deformed BIF structure west of Ndloziyana Peak (Fig. 9.12) has a form of a synform refolded into a D_3 antiform.

Around the Ekuthuleni area (Fig. 9.51), the brecciated BIFs and recrystallized metacherts are overturned and lack of way-up structures makes recognition of antiforms and synforms difficult.

East of Ilangwe Peak (Fig. 9.14), a synformal structure is recognized by the fact that the bedding around the fold hinge (5.800/AA.620) dips towards the fold core (Fig. 9.14). In the Ilangwe Peak area (Fig. 9.14), a pair of en echelon fold structures in BIF and metacherts form an antiform and a synform respectively (Plate 9.2C). The synformal metachert structure has been refolded (probably during D_3) into a hook fold (Fig. 9.14; Plate 9.2C). The structures in Plate 9.2C show a characteristic elliptical pattern.

Recognition of antiformal and synformal structures is difficult in some of the large folds WNW of Ilangwe Peak (Fig. 9.14) and those in the Ngcengcengu Peak area (Fig. 9.9). These folds generally trend E-W with steeply inclined and overturned limbs and have narrow closed elliptical outcrops forming a typical pattern of right-hand en echelon folding (Campbell, 1958) but for the reasons already described, the plunge of the fold-closures cannot be established.

However, elliptical patterns are a typical feature of commonly occurring ***periclinal folds*** which are simply doubly-plunging synformal and antiformal structures. Furthermore, periclinal folds generally have an en echelon arrangement which is exactly the pattern of the elliptical folds WNW of Ilangwe Peak. Some periclinal folds of this type are initiated with this built-in 3D pattern as second order folds on the flanks of larger structures (Campbell, 1958). For this reason they are known in the literature as En Echelon (or Elliptical) Folds.

In the absence of evidence of the plunge of the large folds, it is customary to rely on small-scale folds as possible indicators of the plunge of the larger folds, provided these structures belong to the same fold-system (similar axial-plane orientations). This aspect will be discussed in the following section on the second-order F_2 folds.

A

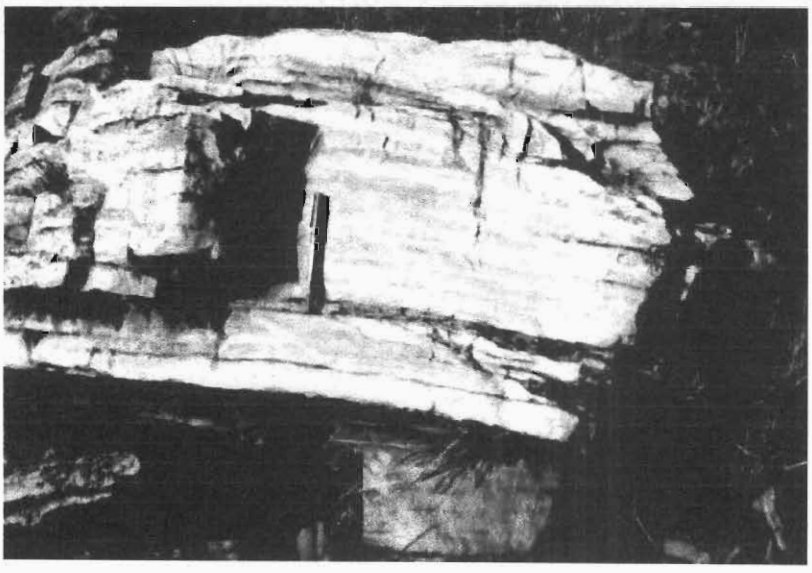

B

C

Plate 9.2

9.2.3.2 DESCRIPTION AND ANALYSIS OF STRUCTURAL DATA FROM SECOND-ORDER F_2 FOLDS

Geological mapping revealed a large number of tightly appressed, small- to medium-scale folds with cleavage wrapped around the hinges of the folds. As this is one of the conventional criteria for the recognition of superposed folding, folds of this type were classified as F_2 folds. These folds will be briefly discussed hereunder.

In the ***Umhlathuze Subgroup***, D_2 folds are more common in the Sabiza and Olwenjini Formations and less common in the Matshansundu Formation.

In the Matshansundu Formation raft of the Entembeni area (4.220/EE.585) (Fig. 9.12), there occurs a D_2 tight similar fold with F_2 axis plunging steeply (68°) to the NW and axial plane dipping steeply to the north (Fig. 9.27A). In the Ndloziyana Peak area, the foliation of the Matshansundu amphibolite and the bedding of the Matshansundu BIF show similar fold orientation (Fig. 9.27A).

In the Sabiza Formation, D_2 folds differ slightly in style from east to west. In the eastern sector around Ekuthuleni Peak, D_2 folds are broadly isoclinal in style. In the central parts of the Sabiza Formation, in the area around the Sabiza and Umhlathuze Rivers, D_2 folds are mainly tight isoclinal class 2 folds whereas in the western sector around Vungwini River area, D_2 folds are close to tight in style and have sharp hinges.

In the Ekuthuleni area, isoclinal folds plunge steeply to the WNW and are inclined steeply to the SSW (Fig. 9.27B). These folds were formed as a result of the refolding (about B_2 tectonic axis) of the F_1 vertical isoclinal folds in this area.

In the Sabiza and Umhlathuze Rivers of the central sector, D_1 folds have been refolded about F_2 into tight isoclinal class 2 similar folds (Ramsay, 1967; Plate 9.1A). These folds plunge moderately to the NW and are inclined steeply to the NE. An L_2 lineation subparallels the F_2 fold axes (Fig. 9.28). Within the Umhlathuze River Shear Zone, sheath folds in Sabiza banded amphibolites plunge northwesterly and southeasterly at about 45° (Fig. 9.28). The same orientation of folds is found in the Vungwini River area (Fig. 9.29).

In the upper reaches of the Sabiza River [(5.050/V.910); Fig. 3.2], D_2 isoclinal s-folds occur in the amphibolite schists of the Olwenjini Formation. These folds plunge to the SE at

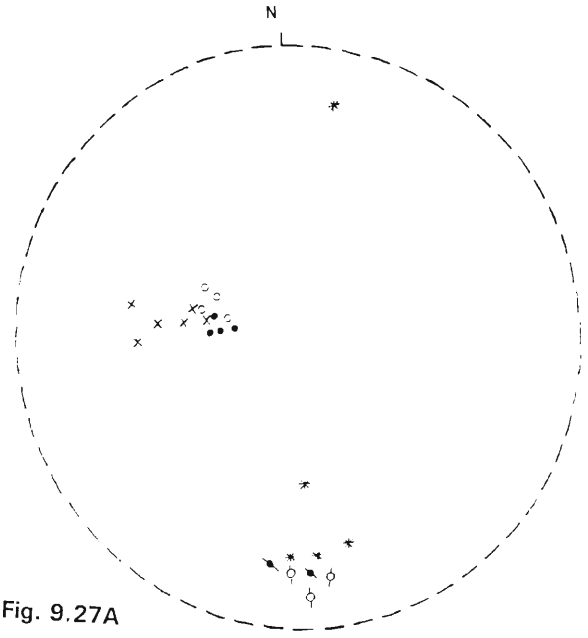

Fig. 9.27A

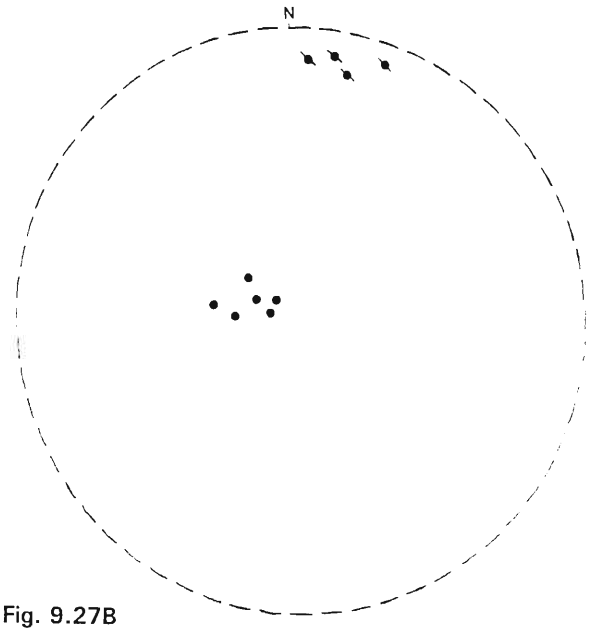

Fig. 9.27B

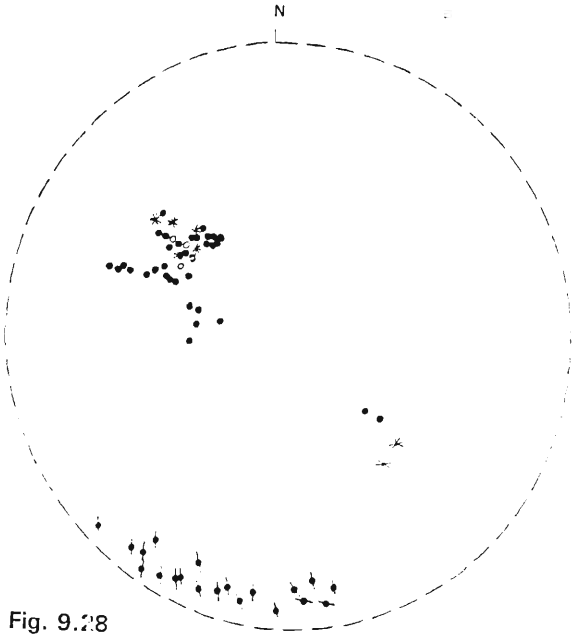

Fig. 9.28

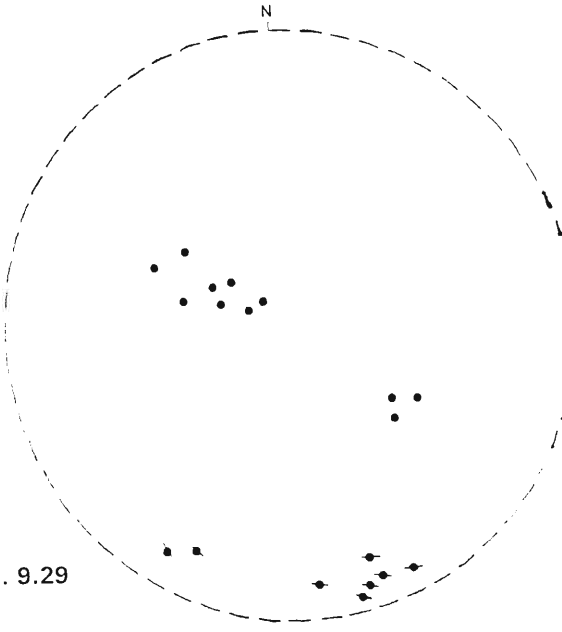

Fig. 9.29

Fig. 9.27A : Orientation data of D_2 structures in the Matshansundu Formation of the Entembeni-Ndiozivana area in the eastern sector of the Ilangwe belt.

- O = Plunge of F_2 axes of tight similar fold in Matshansundu raft (n=4).
- = Poles to F_2 axial planes of tight similar fold in Matshansundu raft (n=3).
- ● = Plunge of F_2 axes of tight folds in amphibolites (n=4).
- = Poles to F_2 axial planes in amphibolites (n=2).
- × = Plunge of F_2 fold axes in BIFs (n=7).
- ✳ = Poles to F_2 axial planes in BIFs (n=5).

Fig. 9.27B : Orientation data of D_2 structures in the Sabiza banded amphibolites of the Ekuthuleni area in the eastern sector of the Ilangwe belt.

- ● = Plunge of F_2 fold axes (n=6).
- = Poles to F_2 axial planes (n=4).

Fig. 9.28 : Orientation data of D_2 structures in the Sabiza banded amphibolites of the Umhlathuze and Sabiza valleys in the central sector of the Ilangwe belt.

- ● = Plunge of F_2 fold axes (n=34).
- = Poles to F_2 axial planes (n=20).
- ✳ = Plunge of F_2 sheath folds (n=7).
- O = Plunge of L_2 lineation (n=4).

Fig. 9.29 : Orientation data of D_2 structures in the Sabiza banded amphibolites of the Vungwini River valley in the western sector of the Ilangwe belt.

- ● = Plunge of F_2 fold axes (n=11).
- = Poles to F_2 axial planes (n=8).

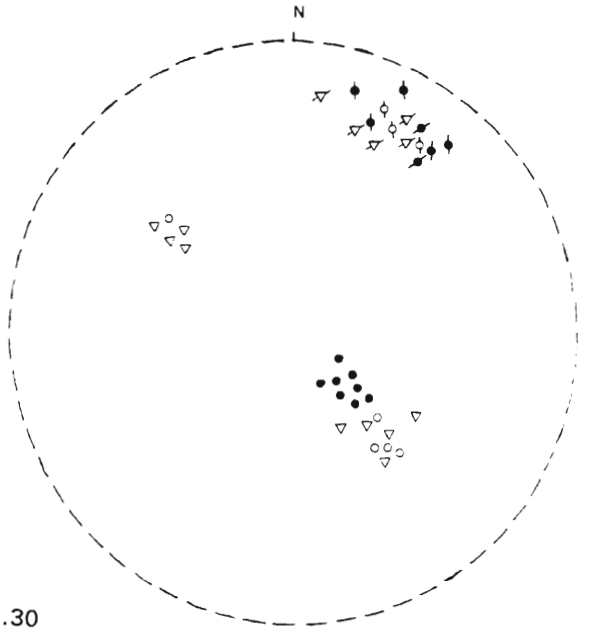

Fig. 9.30

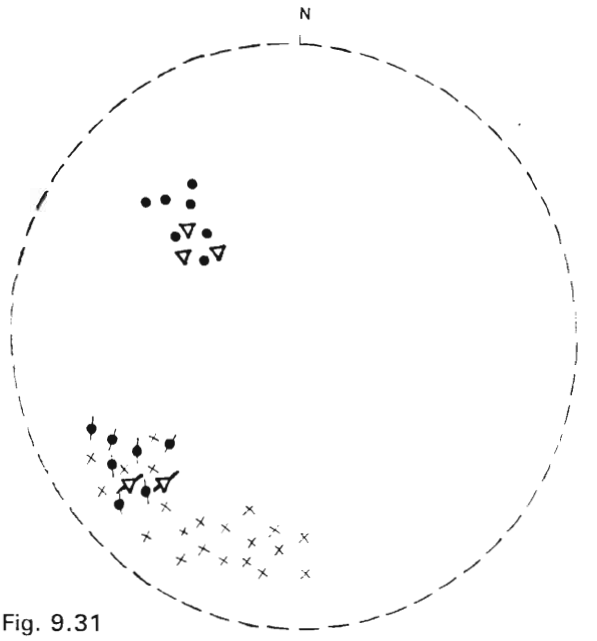

Fig. 9.31

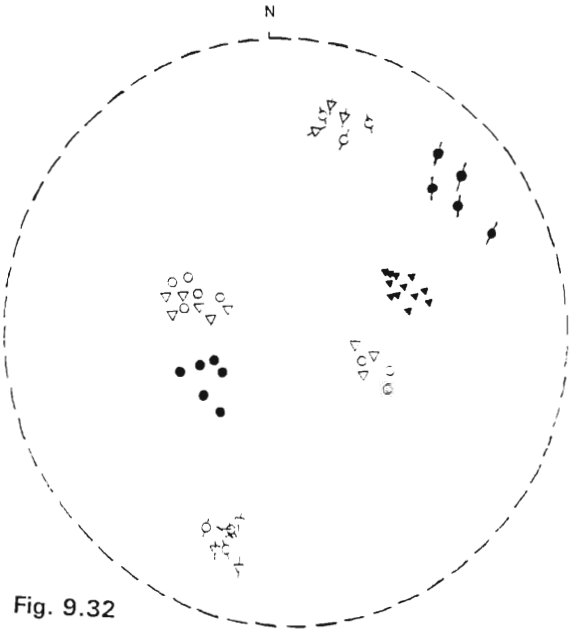

Fig. 9.32

Fig. 9.30 : Orientation data of D_2 structures in the Olwenjini Formation of the upper Sabiza River valley in the west-central sector of the Ilangwe belt.

- ● = Plunge of F_2 fold axes in amphibolite schist (n=8).
- ◢ = Poles to F_2 axial planes in amphibolite schist (n=7).
- ○ = Plunge of F_2 fold axes in phyllites (n=5).
- ◡ = Poles to F_2 axial planes in phyllites (n=3).
- ▽ = Plunge of F_2 fold axes in metacherts (n=9).
- ◢ = Poles to F_2 axial planes in metacherts (n=5).

Fig. 9.31 : Orientation data of D_2 structures in the BIFs and metacherts of the Ngcengcengu Peak area of the west-central sector of the Ilangwe belt.

- ● = Plunge of F_2 fold axes in metacherts (n=7).
- ◢ = Poles to F_2 axial planes in metacherts (n=7).
- ▽ = Plunge of F_2 fold axes in BIF (n=3).
- ◢ = Poles to F_2 axial planes in BIF (n=2).
- × = Poles to bedding in BIFs and metacherts (n=21).

Fig. 9.32 : Orientation data of D_2 structures in the Olwenjini Formation of the Umhlathuze River area south of Spelonk in the western sector of the Ilangwe belt.

- ○ = Plunge of F_2 fold axes in amphibolite (n=8).
- ◡ = Poles to F_2 axial planes in amphibolite (n=6).
- ● = Plunge of F_2 axes of reclined folds (n=6).
- ◢ = Poles to F_2 axial planes of reclined folds (n=5).
- ▽ = Plunge of F_2 fold axes in metacherts (n=9).
- ◢ = Poles to F_2 axial planes in metacherts (n=7).
- ▼ = Plunge of L_2 rodding in metacherts and quartzites (n=12).

about 65° and have axial planes inclined at 75° to the SSW (Fig. 9.30). Small-scale isoclinal folds in the metacherts of this area show a bimodal distribution (Fig. 9.30) similar to that found in the amphibolites of the Sabiza-Umhlathuze River valleys (Fig. 9.28) and the Vungwini River valley (Fig. 9.29),

In the Ngcengcengu Peak area [(4/R,S,T) (Fig. 9.9)], mesoscopic folds in metacherts plunge to the NW and are inclined steeply to the NE (Fig. 9.31). However, these folds do not show a bimodal distribution and from the analysis that will follow, it will be shown that the spread of data in Fig. 9.31 (and also in those stereograms which show a NW–SE orientation) is probably due to D_3 deformation.

Further to the west, in the Umhlathuze River south of Spelonk [(4/P) - Fig. 9.9], small-scale D_2 reclined s-folds and minor tight isoclinal folds in amphibolites plunge to the SW and WNW respectively. The isoclinal folds in banded amphibolites have the same orientation as the metacherts and show a bimodal distribution with fold axes plunging to the WNW and ESE with axial planes inclined steeply to the NNE and SSW (Fig. 9.32). To the west of Spelonk and just north of Simbagwezi Peak, L_2 rodding and fold mullion structures in metacherts and quartzites of the Olwenjini Formation plunge to the ENE at moderate angles (Fig. 9.32).

In the ***Nkandla Subgroup***, D_2 folds are more common in the Entembeni Formation than in the Simbagwezi and Nomangci Formations.

In the eastern part of the Ilangwe Greenstone Belt around Entembeni west of Ndloziyana Peak (Fig. 9.12), the large-scale and small-scale BIFs are folded into D_2 isoclinal synformal folds plunging moderately to steeply to the ENE with axial planes inclined steeply to the NNW (Fig. 9.33A). A similar orientation is found in small-scale isoclinal folds in phyllites (Fig. 9.33B). The large-scale BIF synform occurring west of Ndloziyana Peak (Fig. 9.12) has formed a distorted accommodation structure due to the emplacement of the Umgabhi Micrographic Granite.

In the east central parts of the belt, west of Ekuthuleni Peak and east of Ilangwe Peak (Fig. 9.14), D_2 small-scale asymmetric folds associated with the large-scale metachert and BIF periclinal folds plunge moderately to steeply to the WNW and ESE and have steep axial planes inclined to the south and north (Fig. 9.34A). The phyllites and minor amphibolites in this area also show similar orientations (Fig. 9.34B).

In the central area of the Ilangwe Belt, south of Ilangwe Peak [(5.850/Z.200); (Fig. 9.14)], dark green olivine-rich amphibolites and phyllites show small-scale F_1 isoclinal folds which have been refolded into F_2 isoclinal folds plunging to the WNW with axial planes inclined steeply to the north (Fig. 9.35A). Assymetric D_2 folds in metacherts of the Ilangwe area show a bimodal distribution with moderate plunges to the WNW and ESE and axial planes inclined moderately to steeply to the north and south (Fig. 9.35B). This orientation is similar to that found in the east around Entembeni and Ekuthuleni (Figs. 9.33A and B; 9.34A and B).

In the western part of the Ilangwe belt south of Simbagwezi Peak (5,6/J,K), small-scale D_2 isoclinal folds occur in phyllites and amphibolites of the Simbagwezi Formation. They plunge steeply to the WNW and are inclined to the NNE (Fig. 9.36). The southern limbs of some of the folds are truncated by thin E-W trending faults. Occasionally, these faults also truncate the F_2 axial planar regions of the folds. This E-W faulting is probably related to the deformation which resulted in the Simbagwezi Formation being wedged between the Olwenjini Formation to the north and the Sabiza Formation to the south. The L_2 rodding lineation in this area plunges steeply to the ESE (Fig. 9.36). The quartz-muscovite-sericite schists of the Nomangci Formation show minor F_2 folds plunging steeply to the ENE (Fig. 9.36). This orientation is similar to that found in the BIFs and phyllites of the Entembeni area (Fig. 9.33 A and B).

Hereunder follows the analysis of the F_2 structural data. As mentioned previously, this analysis suggests that only a limited group of these folds can be regarded as F_2, with the implication that the other folds are probably D_3 age.

Examination of the orientation patterns of the small-scale F_2 folds is of particular interest in view of the two contrasting implications of the previous analysis of the F_2 large-scale folds. In the first place, an implication of the flexural-fold model presented in Section 9.2.2.2 has been that the pattern of orientations should be a sub-horizontal concentration of fold axes on an azimuth of either 100° and/or 280° with vertical to near vertical axial planes.

The second and alternative implication from the previous analysis suggests that the small-scale folds should display a bimodal distribution of fold axes in conformity with the interpretation of the large-scale F_2 folds as doubly-plunging, periclinal structures with vertical to near vertical axial planes on an azimuth of 100°.

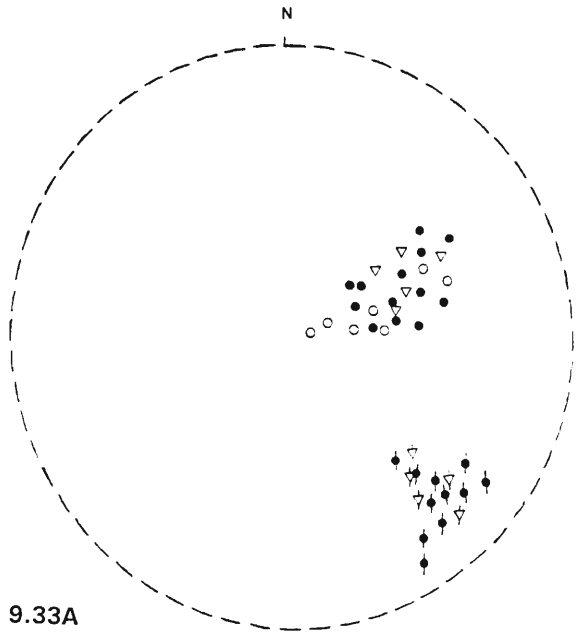

Fig. 9.33A

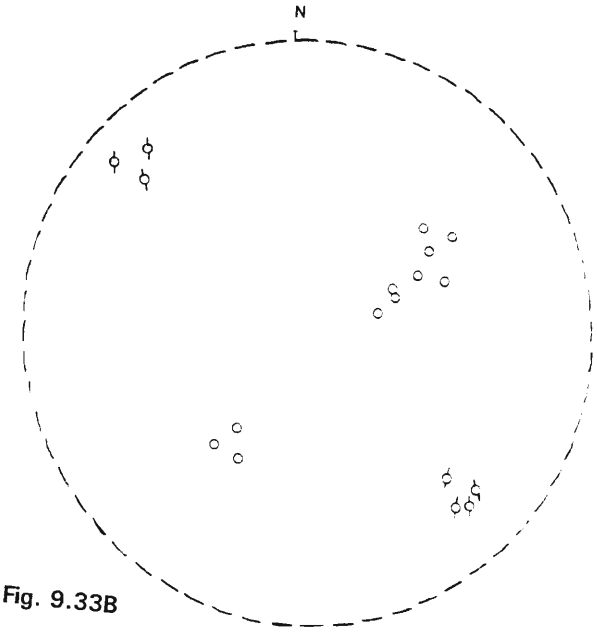

Fig. 9.33B

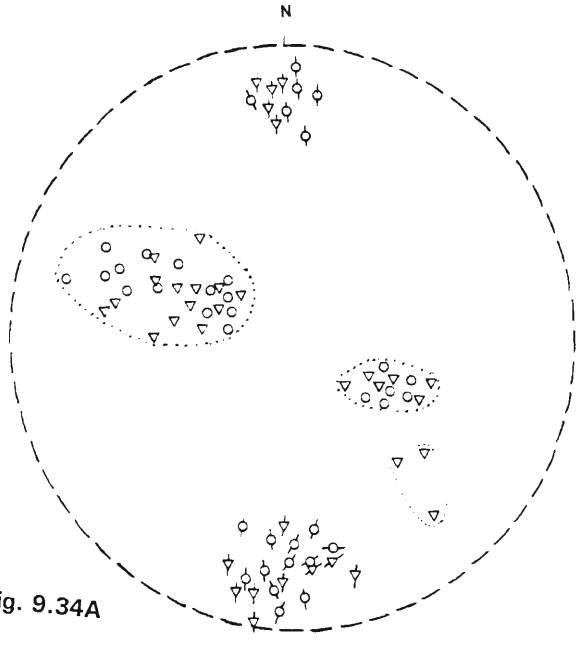

Fig. 9.34A

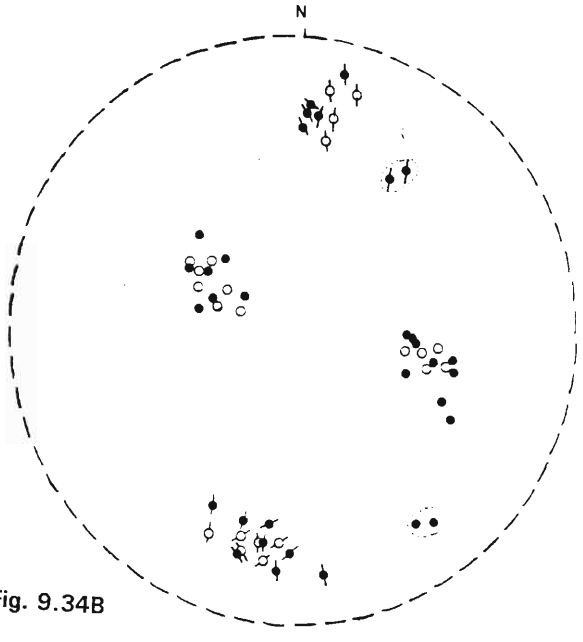

Fig. 9.34B

Fig. 9.33A : Orientation data of D_2 structures in the BIFs and metacherts of the Entembeni area west of Ndloziyana in the eastern sector of the Ilangwe belt.

- ● = Plunge of F_2 fold axes in BIFs (n=13).
- ◪ = Poles to F_2 axial planes in BIFs (n=11).
- ▽ = Plunge of F_2 Fold axes in metacherts (n=5).
- ◪ = Poles to F_2 axial planes in metacherts (5).
- o = Plunge of L_2 rodding and stretching lineation (n=7).

Fig. 9.33B : Orientation data of D_2 structure in the phyllites of the Entembeni area in the eastern sector of the Ilangwe belt.

- o = Plunge of F2 folds in phyllites (n=11).
- ◪ = Poles to F2 axial planes in phyllites (n=6).

Fig. 9.34A : Orientation data of D_2 structures in the BIFs and metacherts of the Entembeni Formation in the east-central sector of the Ilangwe belt.

- o = Plunge of F_2 fold axes in BIFs (n=20).
- ◪ = Poles to F_2 axial planes in BIFs (n=18).
- ▽ = Plunge of F_2 small-scale fold axes in metacherts (n=23).
- ◪ = Poles to F_2 axial planes in metacherts (n=14).

Fig. 9.34B : Orientation data of D_2 structures in the amphibolites and phyllites of the Entembeni Formation in the east-central sector of the Ilangwe belt.

- ● = Plunge of F_2 fold axes in amphibolites (n=18).
- ◪ = Poles to F_2 axial planes in amphibolites (n=15).
- o = Plunge of F_2 fold axes in phyllites (n=12).
- ◪ = Poles to F_2 axial planes in phyllites (n=10).

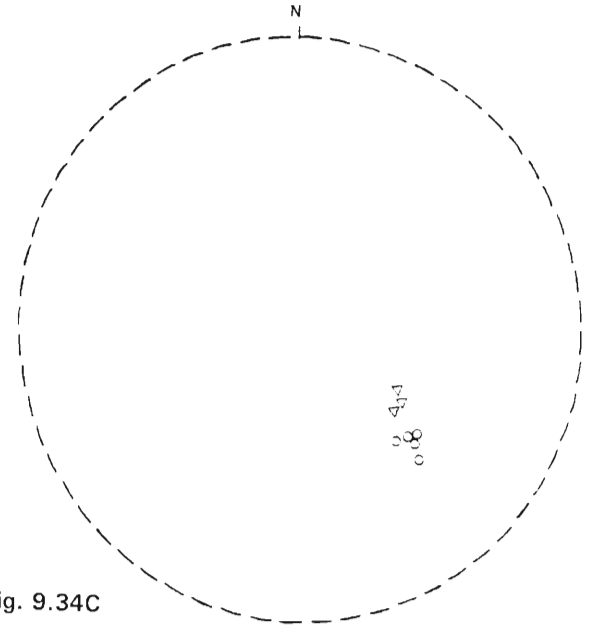

Fig. 9.34C

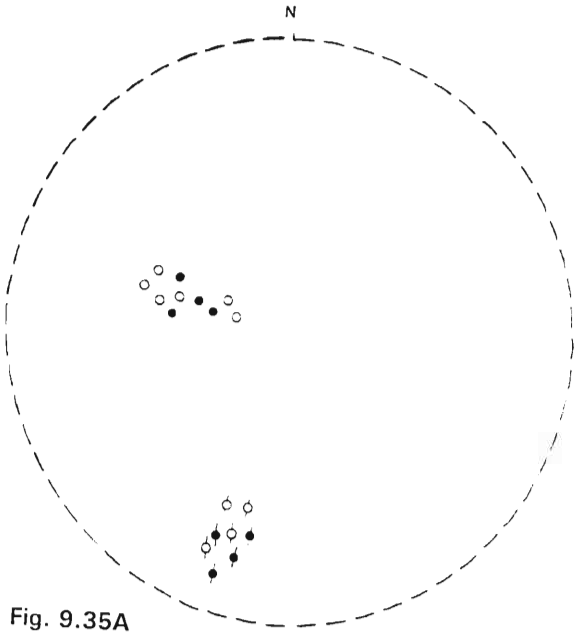

Fig. 9.35A

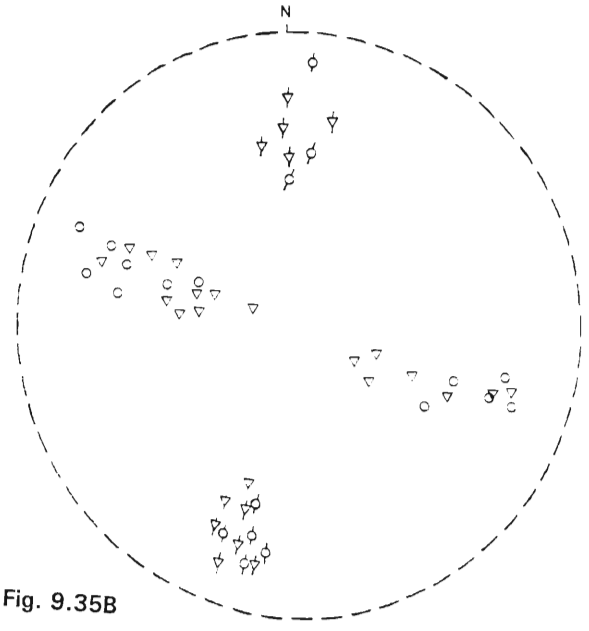

Fig. 9.35B

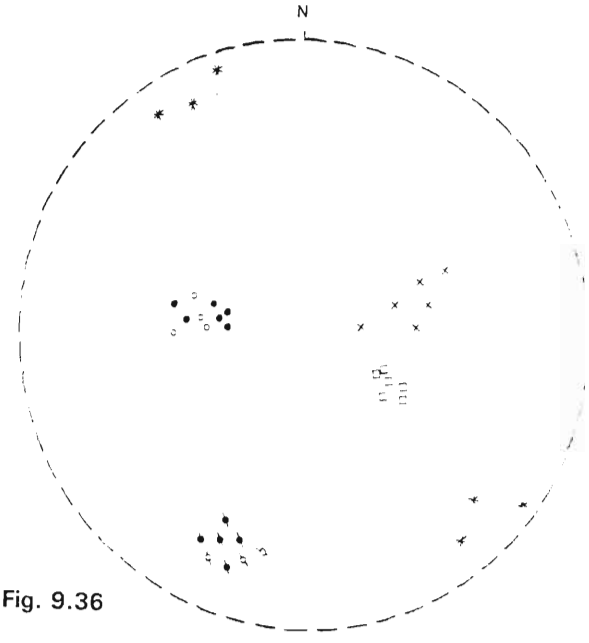

Fig. 9.36

Fig. 9.34C : Orientation data of D_2 rodding and stretching lineation in the metacherts of the Entembeni Formation in the east-central sector of the Ilangwe belt.

- o = Plunge of L_2 roddind lineation (n=5).
- ▽ = Plunge of L_2 stretching lineation (n=3).

Fig. 9.35A : Orientation data of D_2 structures in the amphibolites and phyllites of the Entembeni Formation in the Ilangwe Peak area of the central sector of the Ilangwe belt.

- ● = Plunge of F_2 axes of tight folds in amphibolites (n=4).
- ◢ = Poles to F_2 axial planes in amphibolites (n=4).
- o = Plunge of F_2 fold axes in phyllites (n=6).
- ◜ = Poles to F_2 axial planes in phyllites (n=4).

Fig. 9.35B : Orientation data of D_2 structures in the BIFs and metacherts of the Entembeni Formation in the Ilangwe Peak area of the central sector of the Ilangwe belt.

- o = Plunge of F_2 fold axes in BIFs (n=12).
- ◜ = Poles to F_2 axial planes in BIFs (n=8).
- ▽ = Plunge of F_2 fold axes in metacherts (n=17).
- ◢ = Poles to F_2 axial planes in metacherts (n=12).

Fig. 9.36 : Orientation data of D_2 structures in the Simbagwezi and Nomangci Formations of the western sector of the Ilangwe belt.

- ● = Plunge of F_2 fold axes in amphibolites (Simbagwezi) (n=6).
- ◢ = Poles to F_2 axial planes in amphibolites (n=6).
- o = Plunge of F_2 fold axes in Simbagwezi phyllites (n=4).
- ◜ = Poles to F_2 axial planes in phyllites (n=3).
- × = Plunge of F_2 fold axes in Nomangci quartz-muscovite schist (n=6).
- ✳ = Poles to F_2 axial planes in quartz-muscovite schist (n=6).
- □ = Plunge of L_2 rodding lineation (n=6).

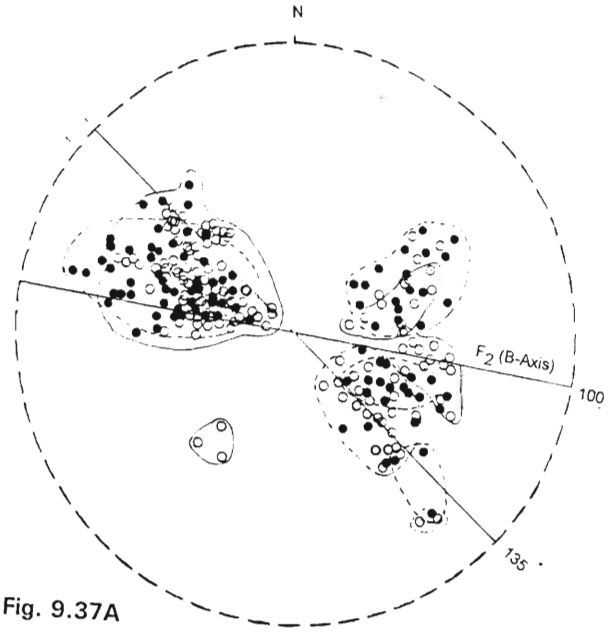

Fig. 9.37A

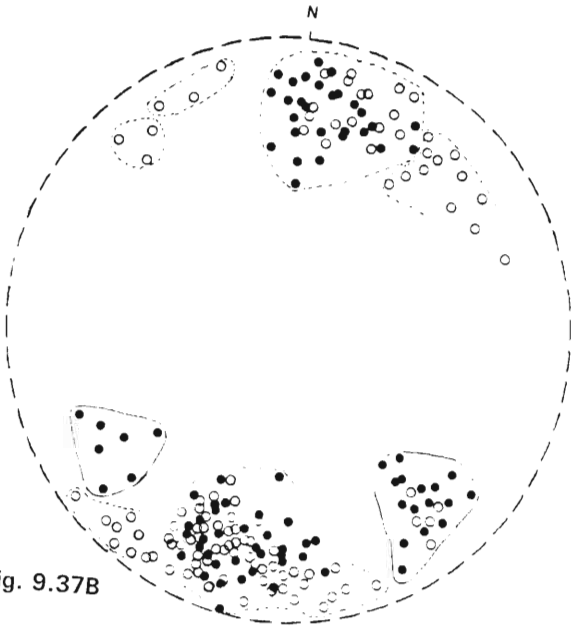

Fig. 9.37B

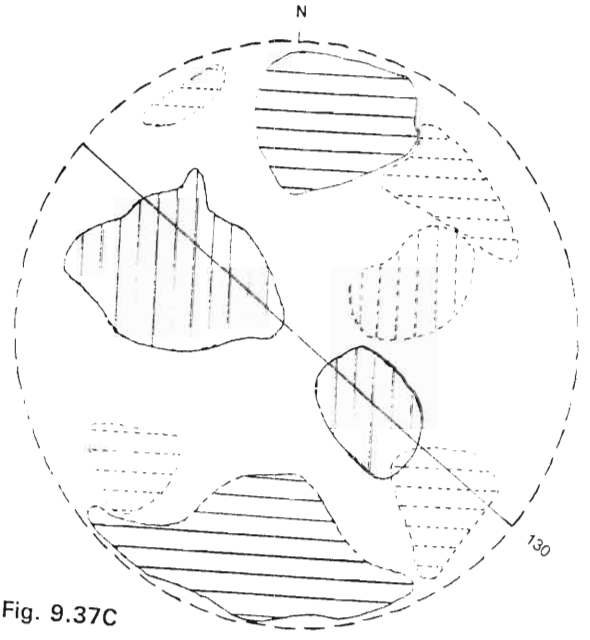

Fig. 9.37C

Fig. 9.37A : Compilation of data from the F_2 fold axes in the different lithologies of the Ilangwe Greenstone Belt.

- ● = Plunge of F_2 fold axes in BIFs and metacherts.
- o = Plunge of F_2 fold axes in amphibolites and phyllites.

Fig. 9.37B : Compilation of data from the F_2 axial planes of the different lithologies of the Ilangwe Greenstone Belt.

- ● = Poles to F_2 axial planes in BIFs and metacherts
- o = Poles to F_2 axial planes in amphibolites and phyllites.

Fig. 9.37C : A combined plot of F_2 fold axes and axial planes in the different formations of the Ilangwe Greenstone Belt.

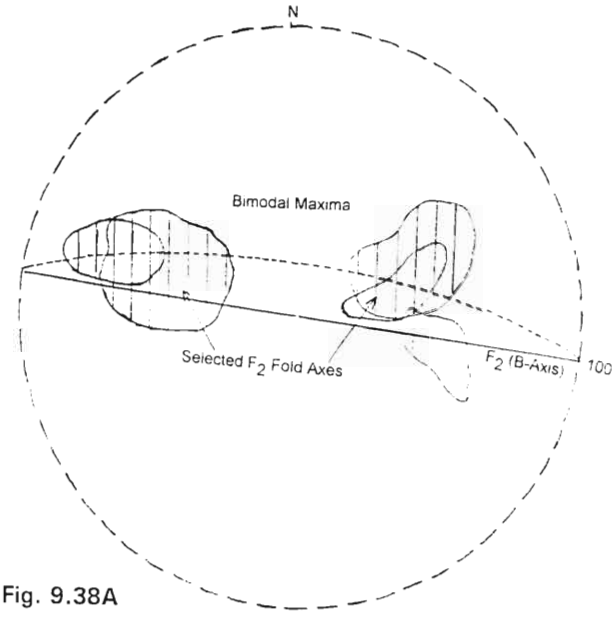

Fig. 9.38A

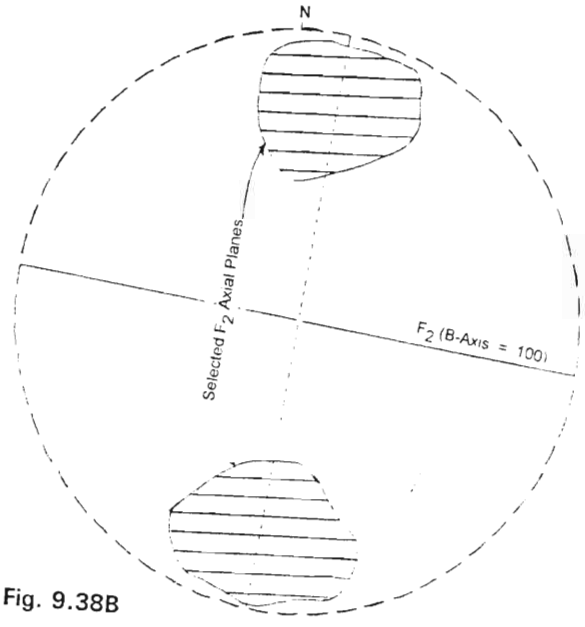

Fig. 9.38B

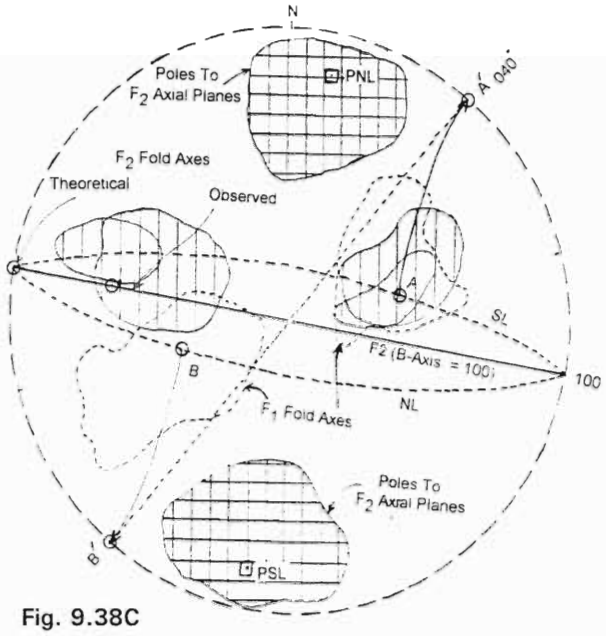

Fig. 9.38C

Fig. 9.38A : Plot of selected F_2 fold axes in the different formations of the Ilangwe Greenstone Belt.

Fig. 9.38B : Plot of selected F_2 axial planes in the different formations of the Ilangwe Greenstone Belt.

Fig. 9.38C : A combined plot of F_2 fold elements in the Ilangwe Greenstone Belt.

It should be emphasized that these implications simply represent alternative interpretations of the geometric shape of the large-scale F_2 folds, which are regarded in both cases as the product of flexural folding.

A compilation of all the data from the orientations of F_2 fold axes and axial planes is shown in Figs. 9.37A and 9.37B respectively and the combined plot is shown in Fig. 9.37C. It must be noted that Fig. 9.37A contains two distinct sets of fold axes orientations. As was mentioned previously, the NW–SE fold axes orientations are probably due to D_3 deformation. This aspect will be considered further in Sections 9.2.4.1 and 9.2.4.2 where reasons will be given for the reclassification of these folds as belonging to the D_3 deformation event.

Although the major concentration of axial-plane poles (Fig. 9.37B) is consistent with both interpretations from the previous analysis (Sections 9.2.2.2 and 9.2.2.3), there is no evidence of any concentration of sub-horizontal fold-axes in Fig. 9.37A, an aspect that does not seem to support the implication of the first analysis unless a major component of pure shear flattening has caused a significant rotation of the fold axes.

Before discussing this possibility, it is important to note that the assemblage of fold-axes orientations shown in Fig. 9.37A contains groups of axes that could define a bimodal pattern of the type required by the alternative hypothesis of periclinal geometry. The two significant groups have been extracted from the composite diagram and are shown in Fig. 9.38A. The bimodal distribution defined by these fold axes is located on a great-circle arc inclined steeply at about 80°-85° to 010°, which is approximately the mean orientation defined by the major concentration of axial-plane poles (Fig. 9.37B and Fig. 9.38B). However, the mean plunge angle of these two groups of folds is of the order of 30°-40° to the NE and NW respectively. It is unlikely that these rather steep angles can represent the final plunges of an associated group of larger periclinal folds, unless these angles have been steepened by rotation in response to a pure-shear flattening normal to the axial planes.

As mentioned already, evidence for substantial flattening within the Ilangwe greenstones is provided by measurements of the X/Z axial ratios of deformed pillow structures which show an upper range of values of 9 to 14 (***Table 9.2***). These high axial ratios could be partitioned into an initial shape factor (say R = 3) and then to a factor for the intense D_1

deformation (isoclinal folding) under an essentially horizontal tectonic regime, before the effect of the postulated D_2 flattening in a vertical plane.

Steepening of a fold-plunge by pure-shear flattening normal to an associated vertical axial plane is illustrated in Fig. 9.39 and the results of some calculations, based on the relationships derived in Fig. 9.39, are listed in ***Table 9.3***.

In this table, an axial ratio of R = 4 means a vertical extension factor of α = 2 which probably represents an upper limit for a realistic vertical uplift. In view of this limitation it is evident from this table that the rotation of a fold axis from an initial sub-horizontal orientation (say 10°) to an angle of 30° to 40° would require extension factors far in excess of any realistic value. For this reason the first of the implications discussed previously, that the second-order F_2 folds were formed with shallow plunging axes, is untenable.

In contrast, in the case of the second implication, the fold geometry is periclinal, so the expected bimodal plunge of the second-order folds could reach values of 20° 30° without rotation due to coaxial flattening. However, from the values listed in ***Table 9.3*** it is evident that the effect of flattening with α = 2 would be to increase an initial angle of plunge of 20° to 36°, and an angle of 30° to 49°. These initial and final values are compatible with the observed range of small-scale, F_2 fold-axes orientations (Fig. 9.38A) and hence this evidence supports the concept that the large-scale, double-plunging F_2 folds can be regarded as flattened, periclinal, flexural folds.

9.2.3.3 INTERPRETATION OF D_2 TECTONICS

The evidence and analysis presented in the preceding section suggests that the D_2 phase of deformation was a major compressional event which produced the large-scale upright, flattened flexural folds that are the most prominent structural feature of the Ilangwe Greenstone Belt. These folds are well-defined by units of banded ironstones and metacherts and, in some cases, the outcrops form narrow elliptical shapes which clearly indicate a doubly plunging geometry.

TABLE 9.2: DIMENSIONS OF DEFORMED PILLOWS AND OCELLI IN THE AMPHIBOLITES OF THE UMHLATHUZE SUBGROUP

FORMATION	LOCALITY	DIMENSIONS OF DEFORMED PILLOWS (in mm)			AXIAL RATIO *X/Z* or Y/Z	DIMENSIONS OF DEFORMED OCELLI (in mm)		AXIAL RATIO Y/Z
		Major Axis (X)	Intermediate Axis (Y)	Minor Axis (Z)		Intermediate Axis (Y)	Minor Axis (Z)	
Olwenjini	Sabiza River *(4.840/V.940)*		500 700 500 750 800 650	150 200 130 120 150 130	3.33 3.50 3.85 6.25 5.33 5.00			
Olwenjini	Umhlathuze River *(5.000/P.010)*	 1820 1804 1795	900 600 - - -	175 145 200 197 205	5.14 4.14 *9.10* *9.16* *8.76*	20 25 28	2 3 3	10.00 8.33 9.33
Sabiza	Sabiza River *(7.050/W.440)*	2000 1500 1765	- - -	150 131 122	*13.33* *11.45* *14.47*			
Sabiza	Umhlathuze River *(5.580/U.690)*		596 605 651 637	217 177 171 167	2.75 3.42 3.81 3.81	16 18 20	1.5 2 3	10.67 9.00 6.67

Unfortunately, the fold plunges cannot be determined directly from the fold-closures because the trend of bedding has been obscured by brecciation of the ironstone, and almost total recrystallization of the metacherts. However, indirect evidence provided by the orientations of the associated small-scale folds supports the view that the large-scale folds are doubly plunging, periclinal, en echelon structures. Substantial flattening normal to the axial planes produced a penetrative axial-planar foliation, and rotated the initial bimodal plunge of the periclinal folds to steeper angles.

9.2.4 D_3 PHASE OF DEFORMATION IN THE ILANGWE GREENSTONE BELT

9.2.4.1 GENERAL

D_3 structures are difficult to recognize in the amphibolites of the Sabiza and Matshansundu Formations. This is probably due to lack of colour contrast and the deep level of weathering. Small-scale F_3 folds commonly show an earlier cleavage deformed around the fold hinges. These folds show two types of profile shapes, being chevron-type folds or close similar folds. In the case of the latter, the closure is slightly thickened but the similar profile shape is maintained.

In common with the F_2 folds, some of the F_3 folds are tightly appressed. Reasons have been given previously for the view that some small-scale folds originally regarded as D_2 structures should now be classified as F_3. Further justification for this reclassification will be discussed in the next section. In this section, a brief description of the occurrence, distribution and orientation of the F_3 folds in the Ilangwe Belt will be given.

As mentioned previously, D_3 folds are easily observable in the Olwenjini Formation (and to a lesser extent, the Sabiza Formation) of the Umhlathuze Subgroup and in the Entembeni and Simbagwezi Formations of the Nkandla Subgroup.

In the central sector around the Sabiza and Umhlathuze valleys (Fig. 9.14) and within the Sabiza amphibolites, small-scale z-folds of probable D_3 age occurring on the limbs of the F_2 synform (Plate 9.1D) plunge steeply to the NNW and are inclined steeply to the W or WSW (Fig. 9.40).

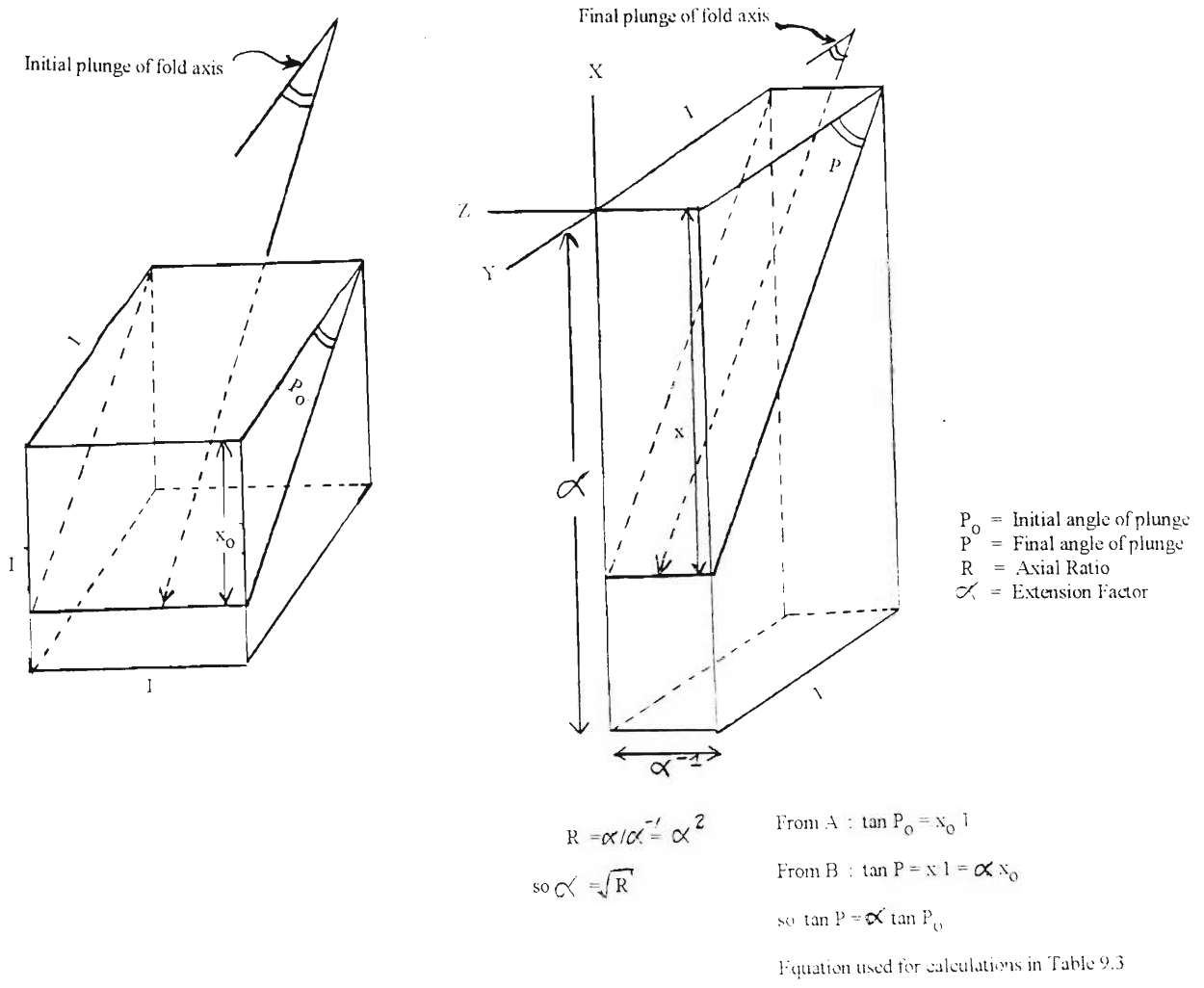

Fig. 9.39 : Steepening of a fold axis by pure-shear flattening.

TABLE 9.3:

STEEPENING OF A FOLD PLUNGE BY PURE-SHEAR FLATTENING

(Symbols defined in Fig. 9.39)

R	α	P_0 = 10	P_0 = 20	P_0 = 30	P_0 = 40
		P	P	P	P
2	1.414	14.00	27.23	39.23	49.88
4	2.00	19.43	36.05	49.11	59.21
6	2.45	23.36	41.72	54.74	64.06
8	2.83	26.52	45.85	58.53	67.16
10	3.16	29.13	49.00	61.27	69.34

West of Ilangwe Peak (5.500/Y) (Fig. 9.14), the D_2 hook folded antiformal periclinal fold has been refolded into an open to close steep northerly-plunging structure. Similarly deformed structures in metacherts and phyllites around this area can be recognized (Fig. 9.14) and plunge steeply to the north and are inclined to the west or NW and rarely to the east (Fig. 9.41). Minor L_3 lineations are subparallel to the F_3 fold axes (Fig. 9.41).

In the west central sector of the belt around Ngcengcengu Peak (Fig. 9.9) and within Olwenjini amphibolites, metacherts and BIFs, D_3 structures are recognizable as close chevron-type to similar folds plunging steeply to the N or NNW with axial planes inclined to the W or WNW. Some minor folds also plunge to the south and are inclined steeply to the east (Figs. 9.42). These folds are cut by post-D_3 NNE-SSW trending faults which are subparallel to the F_3 axial planes (see Fig. 2). In the vicinity of the fold closures, fractures subparallel to the axial planes occur. The development of these fractures is probably sympathetic to faulting.

In the western part of the greenstone belt, south and southeast of Simbagwezi Peak (5.950/J,K), D_3 structures in the Simbagwezi Formation show the same orientations as in the Olwenjini and Entembeni Formations (Figs. 9.40; 9.41; 9.42) but have slightly shallower angles (Fig. 9.43). An L_3 crenulation lineation on pillowed amphibolites plunges shallowly to the north (Fig. 9.43). This northerly plunge direction is parallel to the younging directions indicated by pillow structures (Fig. 2).

9.2.4.2 ANALYSIS OF STRUCTURAL DATA FROM SMALL-SCALE F_3 FOLDS

Structural data on the small-scale folds now classified as F_3 are shown in Figs. 9.44A and B.

Also shown in these figures is the data of other small-scale D_3 folds which trend NNW–SSE. This distinct F_3 distribution is thought to be due to clockwise rotation of fold elements as a result of transpression or possibly in response to the intrusion of the late post-Nondweni granitoids. This resulted in the remarkable arcuate shape of the greenstone belt as shown in Fig. 2. An interesting aspect of Fig. 9.44A and especially Fig. 9.45 is an obvious bimodal distribution of fold axes orientations in a vertical plane with azimuth 130°-135°. One set of fold axes plunge NW at 40° to 70° and the other set plunge to the SE at 60° to 70°. The existence of this remarkable pattern can be regarded as some justification for the classification of this assemblage of folds as a distinct group from the F_2 folds. This

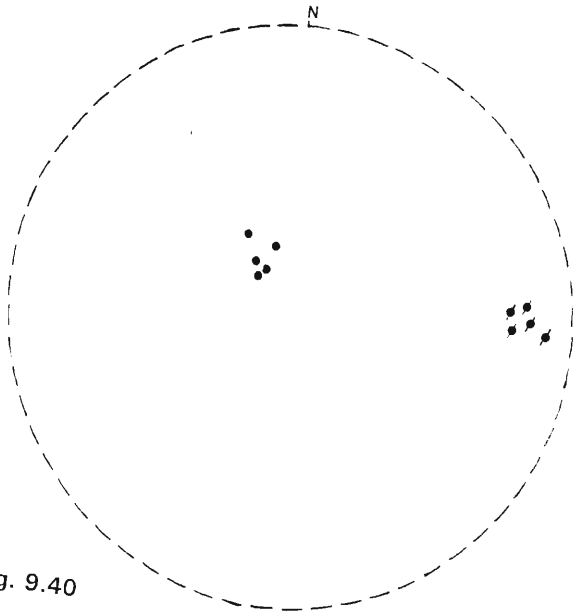

Fig. 9.40

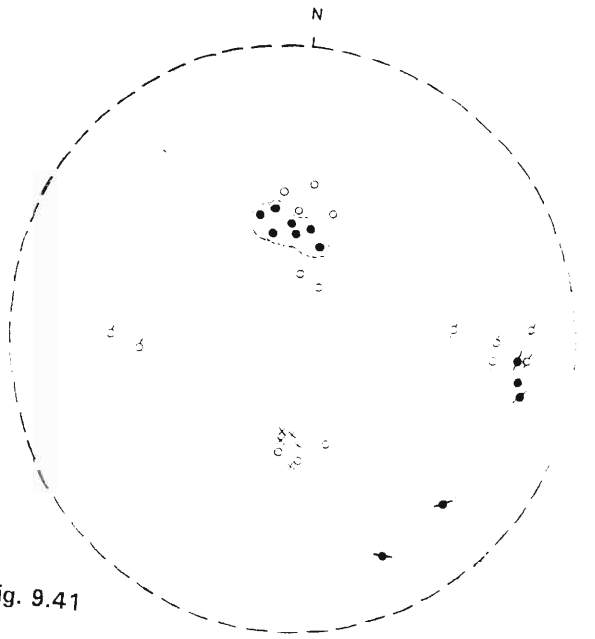

Fig. 9.41

Fig. 9.40 : Orientation data of D_3 structures in the Sabiza amphibolites of the Sabiza and Umhlathuze valleys of the central sector of the Ilangwe belt.

- ● = Plunge of D_3 fold axes (n=5).
- ⌐ = Poles to D_3 axial planes (n=5).

Fig. 9.41 : Orientation data of D_3 structures in the Entembeni Formation of the Ilangwe Peak area in the central sector of the Ilangwe belt.

- ● = Plunge of F_3 fold axes in amphibolites (n=7).
- ⌐ = Poles to F_3 axial planes in amphibolites (n=5).
- ○ = Plunge of F_3 fold axes in metacherts (n=9).
- ⌐ = Poles to F_3 axial planes in metacherts (n=7).
- × = Plunge of L_3 stretching lineations (n=5).

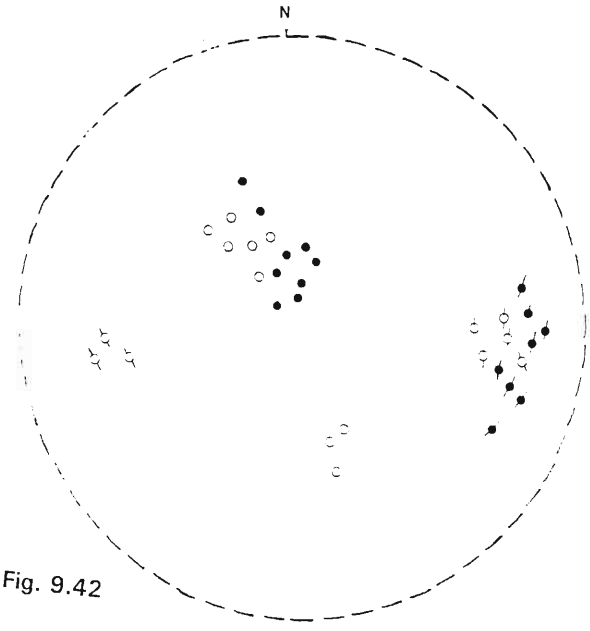

Fig. 9.42

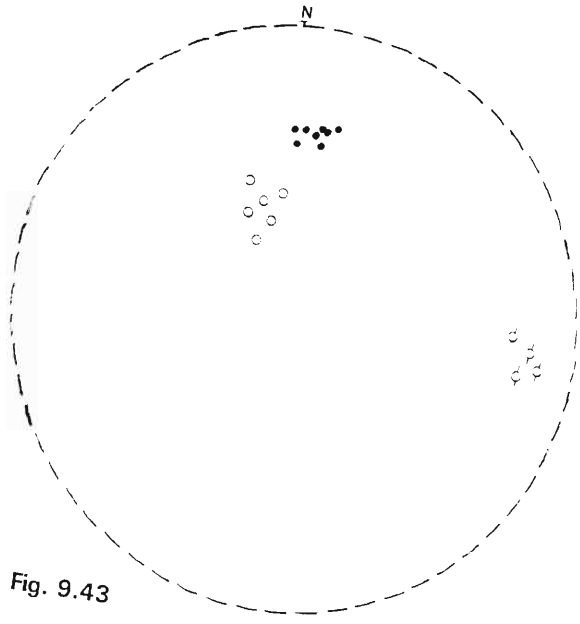

Fig. 9.43

Fig. 9.42 : Orientation data of D_3 structures in the Olwenjini Formation of the Ngcengcengu Peak area in the west-central sector of the belt.

- ● = Plunge of F_3 fold axes in amphibolites (n=9).
- ⌀ = Poles to F_3 axial planes in amphibolites (n=8).
- o = Plunge of F_3 fold axes in metacherts (n=9).
- ⌀ = Poles to F_3 axial planes in metacherts (n=8).

Fig. 9.43 : Orientation data of D_3 structures in the Simbagwezi Formation of the western sector of the Ilangwe belt.

- o = Plunge of F_3 fold axes in amphibolites (n=6).
- ⌀ = Poles to F_3 axial planes in amphibolites (n=4).
- ● = Plunge of L_3 crenulation lineation (n=8).

concept is supported by the fact that the bimodal pattern of the fold axes of these F_3 folds appears to be directly related to the orientations of the steeply inclined limbs of the large-scale F_2 folds. This relationship is shown in Fig. 9.44A and Fig. 9.45 where the trace of a steep north dipping limb contains the NW plunging F_3 fold axes, and the steep south dipping limb contains the SE plunging F_3 folds. The average plunge of the folds on the northern limb is 63° on 287° whereas on the southern limb it is 61° on 108°.

These relationships conform exactly with a well-known model of superposed folding in which the fold axes of the later phase (F_3 in this case) are generated parallel to the lines of intersection of the later XY tectonic plane (axial plane) with the limbs and the axial planar foliation of the earlier folds. A schematic representation of these features is shown in Fig. 9.46C.

9.2.4.3 INTERPRETATION OF D_3 TECTONICS

In terms of the preceding analysis, the D_3 deformation produced steeply plunging small-scale folds on the limbs and axial planes of the pre-existing larger-scale F_2 folds. The axial planes of these later folds are subvertical and have an azimuth of about 135° which is oblique to the 100° orientation of the F_2 axial planes in the central and eastern sectors of the Ilangwe Greenstone Belt. In the Ilangwe Peak area of the central sector, minor folds in the hinge region of the larger periclinal fold have been observed. They trend clockwise of the major hinge as schematically depicted in Fig. 9.46C. Perhaps this inferred oblique relationship could be attributed to a D_3 transpressional deformation with a left-lateral component of shear in response to a slight clockwise rotation of the regional compressive stress. This aspect will be considered in Part 4, Section 9.4.3.

9.2.5 POST D_3 DEFORMATION

Post-D_3 deformation is not widespread in the Ilangwe Granite-Greenstone Complex. It comprises the voluminous intrusion of metabasic bodies in different areas of the complex; the occurrence of faults which truncate both the D^G_2 Nsengeni Suite rocks and the D^G_3 Umgabhi Suite rocks; and, finally, the buckling of the weak S^G_3 foliation in the Umgabhi Granitoid Suite.

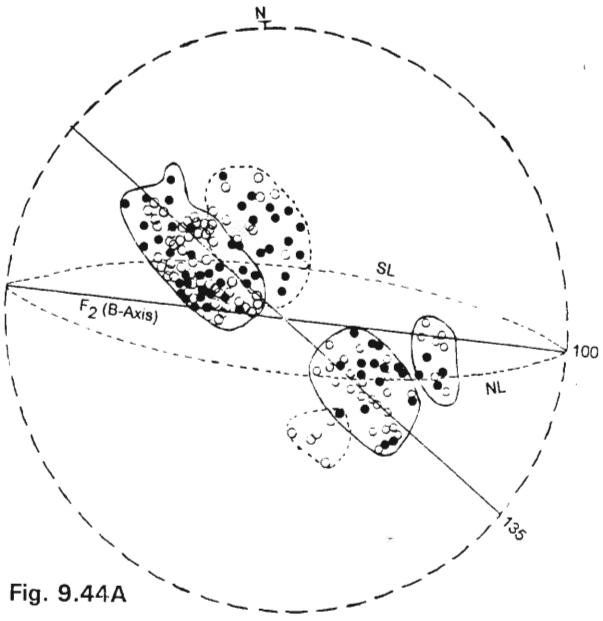

Fig. 9.44A

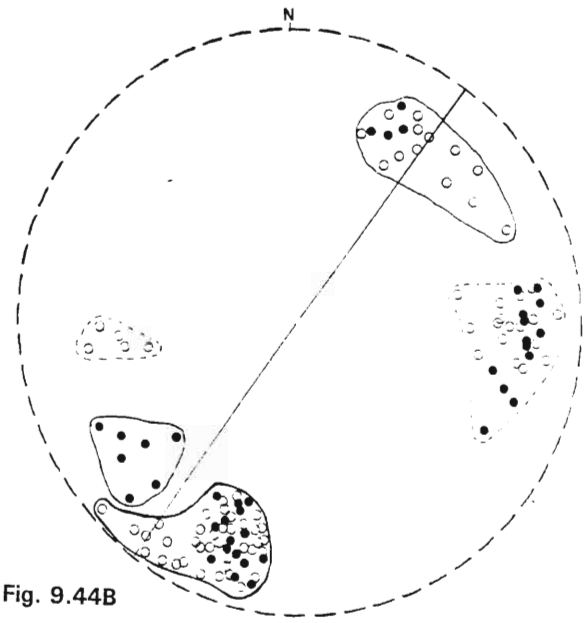

Fig. 9.44B

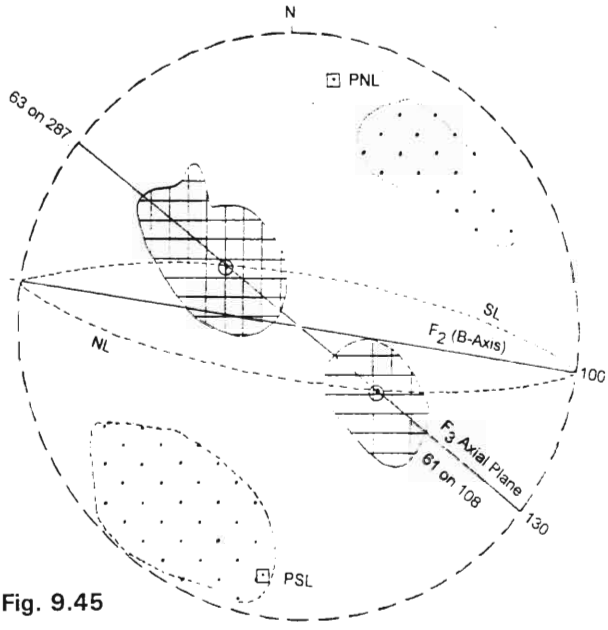

Fig. 9.45

Fig. 9.44A and B : Compilation of the structural data of F_3 small-scale folds in the Ilangwe Greenstone Belt. Fig. 9.44A = fold axes. Fig. 9.44B = axial planes.

- ● = BIFs and metacherts.
- o = Amphibolites and phyllites.

Fig. 9.45 : A combined plot of selected F_3 fold axes and F3 axial planes contained on the limbs of steeply dipping F_2 large-scale syncline.

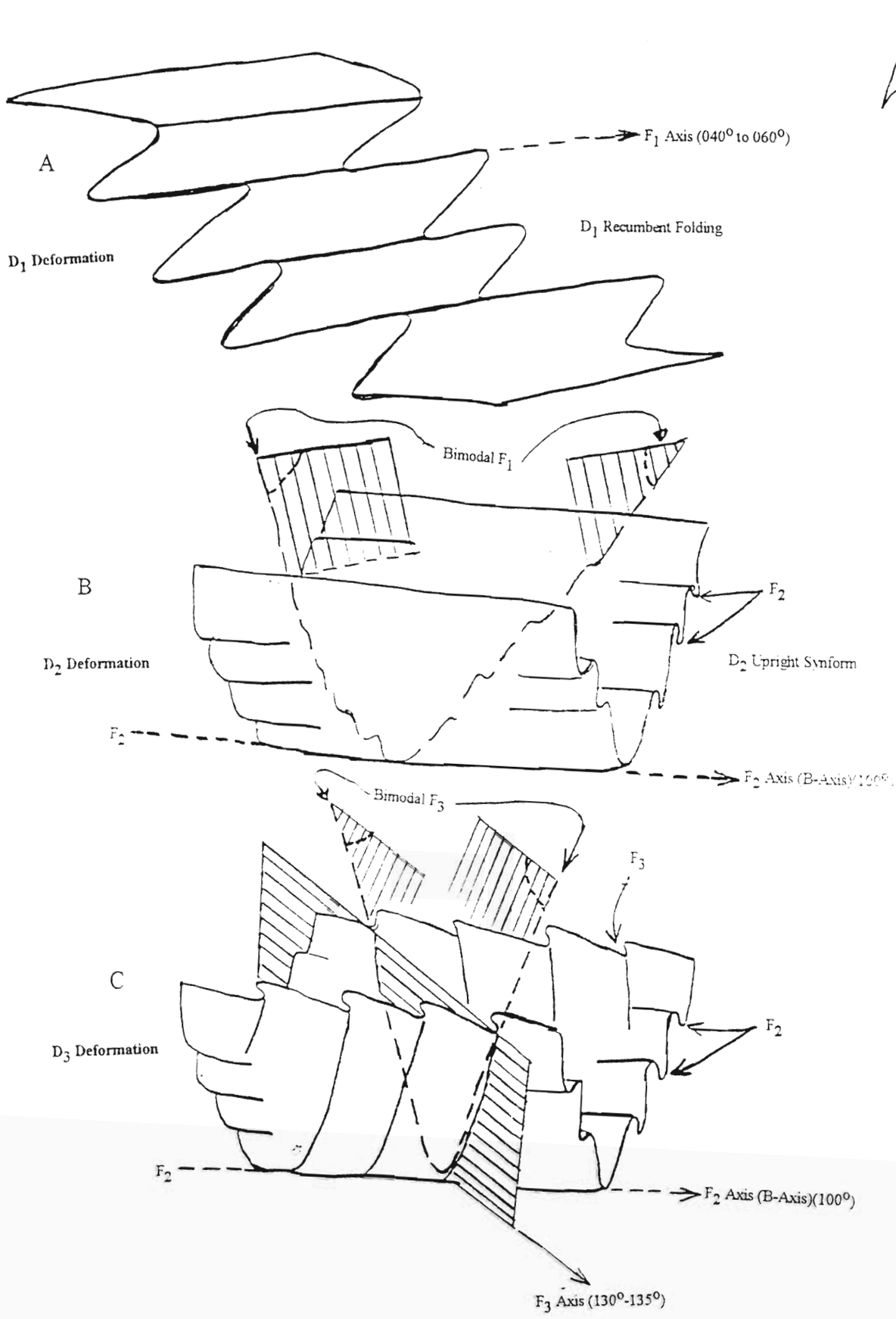

Fig. 9.46 : A schematic representation of D_1 to D_3 structural features of the Ilangwe Greenstone Belt.

in the eastern sector of the granite-greenstone complex around the Entembeni area (3,4,5/EE,FF,GG,HH,II) and particularly the Ndloziyana Peak area (5,6/GG,HH,II), dark green metagabbroic bodies intrude the Matshansundu Formation, the Nsengeni Granitoid Gneiss and the Umgabhi Micrographic Granite. The metagabbroic body is concentrated around the Matshansundu Fault thus suggesting that the fault was used as a conduit. East of Entembeni Peak (4.420/DD.710), a large NE-SW trending metagabbroic body intrudes the Matshansundu Formation and the Nsengeni Granitoid Gneiss.

In the central sector around Ilangwe Peak (2,3,4,5/U to Z), a large metanoritic body intrudes the Sabiza Formation, Olwenjini Formation, Entembeni Formation and the early post-Nondweni granitoids. West of Ilangwe Peak, this metanorite obscures the contact between the Olwenjini Formation and the overlying Entembeni Formation. Several small metagabbroic bodies occur in the Sabiza Formation close to the tectonic contact with the Entembeni Formation.

In the western sector, several minor metagabbroic bodies intrude the Simbagwezi Formation and the Nkandla Granite, the Esibhudeni Granitoid (around Inhlababa Mountain) and the Ntshiweni Augen Gneiss and the greenstones east of Ntshiweni Peak.

Two dominant orientations of post-D_3 faults are found in the Ilangwe Complex. In the western sector, faults of NE-SW and NW-SE trends occur. Faults with a NE-SW orientation show a right-lateral displacement whereas those with a NW-SE trend show a left-lateral sense of displacement. Minor faults in this area show an E-W orientation.

In the west central sector around Ngcengcengu Peak, both the NE-SW and the NW-SE trending faults show a dextral sense of movement. In the central sector, post-D_3 faults have a predominantly NW-SE trend. These faults are splays of the boundary faults and truncate the Nsengeni Granitoid Gneiss and the Umgabhi Granitoid. In the eastern sector around Matshansundu area, two conjugate faults with a NE-SW and NW-SE orientation truncate the greenstones and the Nsengeni Granitoid Gneiss.

Finally, buckling of the weak S_3 foliation can be observed in the area around Inhlababa Mountain (7,8/M to U). In this area, the foliation in the Umgabhi and Esibhudeni granitoids forms a wide open fold plunging to the north. This buckling has also affected the greenstone belt and it shows an arcuate form convex to the north. Buckling also occurs

locally in the Nkwalinye River where the Amazula Gneiss shows northerly plunging open buckle folds (Plate 2.1A).

9.2.6 DUCTILE SHEAR ZONES WITHIN THE ILANGWE GREENSTONE BELT

A number of shear zones occur within the Ilangwe Greenstone Belt. The most prominent are the Simbagwezi Shear Zone (6.500/I,J,K,L,M) and the Umhlathuze River Shear Zone (6.00/T,U,V,W,X,Y,Z). A series of thin but extensive units of serpentinitic talc schists and talc chlorite schists thought to be representing probable shears occur within the Sabiza amphibolites and the Simbagwezi Formation respectively (see Fig. 2). These schists occur as highly deformed concordant or discordant units within less deformed amphibolites and phyllites. In most cases it was not possible to determine the sense of shear in these units. Although they are interpreted as representing shears, they could also represent thin concordant to discordant faults intruded by deformed and altered ultramafic sills and dykes. However, the latter interpretation is dubious because no significant apparent displacement has been observed in the country rocks.

The Simbagwezi Shear Zone stretches from the Esibhudeni area (8/A) in the western sector of the belt to east of Ngcengcengu Peak (4.510/T.450) in the west central sector of the belt – a distance of about 20 km. In the western sector, it forms the contact between the Simbagwezi Formation and the Sabiza Formation whereas in the west central sector, it forms the contact between the Olwenjini Formation and the Sabiza Formation. Around the upper reaches of the Sabiza River (5/V), this shear is represented by sheared serpentinitic talc schists which occur along the contact of the Olwenjini and Sabiza Formations. Kinematic indicators (s–c planes) in the schist show a right-lateral sense of movement.

In the western sector of the belt just south of Simbagwezi Peak (6.450/J,K,L), the Simbagwezi shear has a maximum width of 65 metres and comprises yellowish-red mica schists. Within the shear zone, an anastomosing extensional crenulation cleavage is oblique to the zone boundaries and to the older foliation of the amphibolites and phyllites in the Sabiza and Simbagwezi Formations, respectively. The shear has a dextral sense of movement. The age of the shear zone could not be conclusively resolved in the field but seems to be post-D_1.

The Umhlathuze River Shear Zone extends from east of the Olwenjini River (5.800/S.940) in the west central sector of the belt to just west of the Amazula River (6.520/Z.790) in the

central sector of the belt. In the Umhlathuze and Sabiza valleys, the shear zone has a width ranging between 150 metres and 300 metres and comprises a mélange of strongly tectonized metavolcanic assemblages and Amazula Gneiss. It occurs tectono-stratigraphically above the banded amphibolites and pillowed metabasalts of the Sabiza Formation. East of the Olwenjini River, small s–c structures in deformed amphibolites indicate a right-lateral sense of shear. However, in the Umhlathuze–Sabiza valleys where Amazula Gneiss and Sabiza amphibolite slices occur, the sense of shear is left-lateral and is denoted by a NW–SE orientation of foliation within the zone and an E–W foliation outside the shear zone boundaries (Fig. 9.14). This conflict in shear sense can be attributed to later rejuvenation.

The presence of Amazula Gneiss slices in the Umhlathuze River Shear Zone suggests that this structure is an originally low-angle D_1 thrust zone associated with the D_1 isoclinal folding. The observed lateral movement fabric patterns within the zone probably represent an oblique component during D_1 or a later D_3 oblique rejuvenation of the folded thrust zone.

Another possible D_1 thrust zone containing slices of quartzitic Amazula Gneiss and Sabiza amphibolites occurs southwest of Ngcengcengu Peak (4,5/Q) in the Umhlathuze River (Fig. 5.2; Fig. 9.9).

Small-scale shears in phyllites and metacherts also occur within the Ilangwe Belt (Plate 2.2A; Plate 9.2; Fig. 2.2). A 10 cm wide shear zone in the phyllites north of Ilangwe Peak (5.440/Z.000) shows a north over south sense of movement, i.e. a southward vergence. The banded metacherts of Ilangwe show small-scale bedding parallel shears (Plate 9.2B) which show a sinistral sense of movement.

9.2.7 ILANGWE GREENSTONE BOUNDARY FAULTS AND ASSOCIATED STRUCTURES.

The structures bounding the Ilangwe Greenstone Belt can be divided into two, viz :

(i) those that developed subsequent to the intrusion of the Early post-Nondweni granitoids but prior to the intrusion of the Late post-Nondweni granitoids;

(ii) those that developed during or even after the intrusion of the Late post-Nondweni granitoids – syn to post Late post-Nondweni granitoids.

The structures falling under the first category are the Entembeni and Matshansundu Faults whereas the Vungwini River Shear falls under the second category.

The Ilangwe Greenstone Belt is bounded by the Entembeni Fault in the north whereas in the south it is bounded by the Matshansundu Fault. The Entembeni Fault extends from the Nkwalini area (5/OO) in the east to the Mandaba area (4/J) in the west – a distance of about 32 km. The Matshansundu Fault extends for about 17 km from the Nkwalini area in the east to just north of Umgabhi Ridge (7/Y) in the west central sector of the belt. The Entembeni Fault extends the 32 km length of the belt almost uninterrupted (except by late minor NW–SE and NE–SW faults) whereas the Matshansundu Fault is interrupted in the Ndloziyana Peak area (Fig. 9.12) and to the NW of the Umgabhi Ridge (Fig. 9.14), by re-entrant extensions of later granitoids into the greenstones. In the Nkwalini–Mzilikazi Peak area (5/MM,NN,OO) both faults are truncated by the post–Karoo Tugela Fault (Fig. 9.48).

In the western and west-central sectors of the belt, the greenstones are bounded in the south by the Vungwini River Shear which extends from the Umgabhi area (7/Y) in the east to the Esibhudeni area north of Isibuta Peak (6,7/E) in the west (Fig. 2).

The Entembeni and Matshansundu Faults are dominated by brecciation and cataclasis of the country rocks – areas marked xxxx in Fig. 2. They are characterized by vertical fault planes, a predominantly horizontal movement direction (strike-slip) and a generally non-linear trace at the surface. In areas where brecciated quartz veining occurs, the faults show a positive relief [e.g. in the Ndloziyana area (Fig. 9.12) and in the Sabiza Valley (Fig. 9.14)]. In the western sector southeast of the Mandaba area (5.000/K,L), the Entembeni Fault appears as a positive feature with brecciated quartz and then becomes a negative topographical feature (a gully) eastwards towards the sinuous Vungwini River (Fig. 2).

Various secondary structures are associated with these regional first order strike-slip faults. East of Ndloziyana Peak (6.060/HH.525), a second-order divergent splay of the Matshansundu Fault cuts and displaces the Entembeni Fault. The sense of movement is right-lateral. West of Ndloziyana Peak (5,6/AA to FF), there occurs a number of convergent second-order strike-slip faults associated with the first-order Matshansundu Fault. It is in this area where a possible pull-apart formed which resulted in the emplacement of the Umgabhi Micrographic Granite and the Matshansundu metagabbroic body (Fig. 9.12). Such pull-apart (void) or overlap (pressure ridge) structures are thought to

be due to strike-slip movement on a vertical, curved or kinked (i.e. non-linear) fault plane (Guineberteau et. al., 1987; Price and Cosgrove, 1990; Morand, 1992).

North of Umgabhi Ridge (7.300/Y.560), a similar void occurred which resulted in the intrusion of the Umgabhi Granitoid. It is also in this area where the Matshansundu Fault seems to terminate. Further west of Umgabhi Ridge and south of Ngcengcengu Peak (5,6/P to X), a number of faults which seem to form divergent splays from the Vungwini River Shear occur. Some of these faults show extensive brecciation and quartz-fault-fill material.

Structures associated with the Entembeni Fault are found in two localities in the Northern Granitoid Complex. NNE of Ndloziyana Peak (5/HH), an outcrop of Umgabhi Micrographic Granite is thought to occupy a possible void resulting from the kink in the Entembeni Fault. No secondary strike-slip or splay faults were recognized in this locality.

In the Sabiza River valley northwest of Ilangwe Peak (4/V,W), a conjugate pair of divergent splay faults are associated with the Entembeni Fault. The NE–SW trending divergent splay forms the western limit of the Entembeni Formation; whereas the NW–SE trending splay forms the eastern boundary of the metagabbroic body intruding the early post-Nondweni granitoids.

As mentioned previously, the Vungwini River shear bounds the southern limit of the greenstone belt in the western sector. In the Vungwini River shear, there is evidence of extensive grinding and comminution of fragments of granitoid and amphibolite along the shear planes. This fluxion structure (Roberts, 1984) is in the form of mylonitic schists and gneisses in the Umhlathuze River locality (5.700/P.280), in the Vungwini River locality (6.820/H,I) and in the area around the confluence of the Umhlathuze River and the Sabiza River (6,7/U,V,W). In these localities, the granitoids (Umgabhi and Esibhudeni) and the Sabiza amphibolites are extremely mylonitic. At the locality (6.960/V.130) there is a sharp and discordant intrusive relationship between the mylonitic Umgabhi granitoid and Sabiza amphibolite (Plate 2.1A). A similar relationship is observed between the Esibhudeni granitoid and the Sabiza amphibolite. These relationships suggest that the Vungwini River shear post-dates the intrusion of the late post-Nondweni granitoids.

The Entembeni and Matshansundu Faults post-date the early post-Nondweni granitoids but pre-date the late post-Nondweni granitoids. In all these first-order and second-order faults,

the amount of strike-slip displacement is difficult to determine due to the lack of displaced distinctive marker horizons in the dull blackish to greenish amphibolites; or even due to lack of displaced granitic plutons, sedimentary facies, zones of high grade metamorphism and tectonic zones.

PART 3

9.3 STRUCTURAL FEATURES OF THE GRANITOID TERRAIN

9.3.1 INTRODUCTION

The major deformed granitoid units comprise the migmatitic and mylonitic gneisses (older gneisses) and the Nkwalinye Tonalitic Gneiss. These units have a wide distribution within the granitoid complex. The migmatitic and mylonitic gneisses comprise the Amazula Gneiss, the Nkwalini Mylonitic Gneiss and the Nkwalini Quartzo-feldspathic Flaser Gneiss. They occur together in the Nkwalinye-Nkwalini area (3,4,5/LL,MM,NN,OO) (Fig. 9.48), Mfanefile area (2,3/W,X,Y) and in the Sappi Mooiplaas forest plantation area (1,2,3/O,P,Q,R,S) (Fig. 9.9). The Amazula Gneiss further occurs (together with the Nkwalinye Tonalitic Gneiss) as rafts in younger granitoids in the upper reaches of the Nkwalinye River, just north of Ndloziyana Peak (4,5/HH,II), in the Nsengeni River (2,3/EE,FF), in the type area of the Amazula River (6,7/Z,AA,BB,CC) (Fig. 9.51) and in the Umhlathuze River near the gorge (8/U,V,W). Slices of the Amazula Gneiss occur together with the Sabiza amphibolites in shear zones within the Sabiza Formation in the Umhlathuze River Shear Zone (6.000/T,U,V,W,X) and in the Umhlathuze River locality (4,5/Q) south-southwest of Ngcengcengu Peak (Fig. 9.9). The Nkwalinye Tonalitic Gneiss further covers an extensive area in the Northern Granitoid Complex (Fig. 2).

Steep to vertical (and usually transposed) foliation characterizes the major deformed units of the granitoid terrain. This characteristic feature, together with the occurrence of intrafolial folds in transposed foliations, was used as the main distinguishing feature of D^G_1 deformation. Another most common diagnostic feature for the existence of D^G_1 folds (especially in the case where F^G_1 closures are not present in outcrop) is the characteristic folding of what is regarded as primary metamorphic banding and associated parallel or slightly oblique cleavage wrapped around the hinges of the later isoclinal F^G_2 folds. In rare instances, direct evidence of D^G_1 folding was provided by refolded folds in which the F^G_1

axial plane cleavage is also folded about the F^G_2 fold axis (see Fig. 9.49B). The most important diagnostic feature of D^G_2 folding is a near constant orientation of the axial plane cleavage (point maximum of poles). The D^G_2 fold axes generally show a systematic great- or small-circle spread and/or two or more point maxima in a stereoplot. The characteristic feature of D^G_3 folding is the steep northerly or southerly plunge.

As mentioned previously, the sequence of deformational events in the granitoid complexes was interrupted by episodes of granitoid emplacement. These plutonic events can be broadly divided into :

(i) the early post-Nondweni granitoids; and
(ii) the late post-Nondweni granitoids.

The early post-Nondweni granitoids comprise the Nkwalinye Tonalitic Gneiss and the Nsengeni Granitoid Suite. The tonalitic gneiss occurs together with older gneisses (migmatitic and mylonitic gneisses) whereas the Nsengeni Granitoid Suite occurs to the north and south of the Ilangwe Greenstone Belt. The Nsengeni Suite is an association of three megacrystic and well foliated granitoid units with gradational contacts and similar mineralogical and geochemical characteristics. These granitoid units are the Ntshiweni Augen Gneiss, the Nsengeni Granitoid Gneiss and the Ekuthuleni Granitoid.

Field evidence suggests that the Nkwalinye Tonalitic Gneiss is intrusive into the early crustal framework comprising the Ilangwe Greenstones and the migmatitic and mylonitic gneisses (older gneisses). Further, the Nsengeni Granitoid Suite is intrusive into the greenstones, older gneisses and the Nkwalinye Tonalitic Gneiss.

The late post-Nondweni granitoids were emplaced onto the older gneisses, greenstones and boundary faults and the early post-Nondweni granitoids. They comprise an association of two granitoid suites – the Impisi Granitoid Suite and the Umgabhi Granitoid Suite. The former occurs in the northwestern portion of the Northern Granitoid Complex and consists of the Nkandla Granite and the Zietover Granite, whereas the latter occurs in the Southern Granitoid Complex and consists of the Umgabhi Granitoid, Esibhudeni Granitoid and the Umgabhi Micrographic Granite. The late post-Nondweni granitoids are all megacrystic, have gradational contacts and similar geochemical and mineralogical characteristics (see ***Table 4.1***).

As mentioned previously, a conspicuous feature of the older gneisses is the steep to vertical foliation which is defined by the alignment of platy micaceous minerals, alignment of deformed and ribbon-like quartz, augen textures and metamorphic layering and banding. Frequently it is difficult in the field to differentiate the various foliation surfaces as S^G_0 and S^G_1 are brought to parallelism. S^G_1 is the dominant regional foliation. Generally, foliation trends E–W and dips steeply to the north or south. However, NE–SW and NNW–SSE trending foliations do occur (Fig. 2).

The foliation of the older gneisses in various localities is shown in Figs. 9.47 A - H.

In the Northern Granitoid Complex, the older gneisses show a slightly variable foliation distribution. In the Nkwalinye–Nkwalini area (3,4,5/LL,MM,NN,OO) and in the Nsengeni River area (2,3/EE,FF), a well-defined E–W trending foliation shows a predominantly steep south to SSE dipping distribution (Figs. 9.47A and B) scattered about a great circle declaring a B axis plunging steeply to the south; whereas in the Nkwalinye River area NNE of Ndloziyana Peak (Fig. 9.12) (4,5/HH,II), foliation is inclined steeply to the SSW (Fig. 9.47C).

In the Mfanefile area (2,3/W,X,Y), the Amazula Gneiss has a predominantly northerly to north-northeasterly distribution whereas the Nkwalini mylonites have a well-defined southerly dipping planar distribution (Fig. 9.47D).

In the Mooiplaas Forest Plantation area (Fig. 9.9) (1,2,3/O,P,Q,R,S), the older gneisses trend predominantly to the NNW–SSE and dip steeply to the NE or SW (Fig. 9.47E). Minor E–W trending and southerly dipping foliations do occur. Generally, the distribution forms a partial horizontal girdle (Fig. 9.47E) which implies that deformation assumed steep to vertical rotation axis similar to the Nkwalinye-Nkwalini area (30 km to the east) (Fig. 9.47A). However, in the Mooiplaas Forest plantation area, the B axis declared by the great circle plunges steeply to the north (Fig. 9.47E).

The migmatitic and mylonitic gneisses occurring in the Southern Granitoid Complex show a uniform foliation distribution. In the Amazula River section (6,7/Z,AA,BB,CC) and in the Umhlathuze River locality near the gorge (8/U,V,W), the Amazula Gneiss shows a predominantly northerly to north-northeasterly inclination (Figs. 9.47F and G). In the Umhlathuze River southwest of Ngcengcengu Peak (4,5/Q), the foliation of the Amazula Gneiss shows two distinct distributions (Fig. 9.47H) which indicate a progressive change

from northerly to southwesterly inclinations depicting the northerly-directed thrusting of the Amazula Gneiss onto the Sabiza Formation amphibolites (see Fig. 5.2).

The steep to vertical foliation and metamorphic layering of the migmatitic and mylonitic gneisses is thought to be a transposed regional foliation (S^G_O // S^G_1). This is supported by the occurrence of intrafolial folds in these lithologies (Plates 9.3A, 9.4C, 9.5B and Fig. 9.50). (*See next section.*) This transposed foliation implies a very high degree of deformation and associated high grade metamorphism during D^G_1 and, most significantly, it provides evidence for an early period of possible ***horizontal tectonics***.

9.3.2 D^G_1 PHASE OF DEFORMATION IN THE GRANITOID TERRAIN

9.3.2.1 D^G_1 FOLDING

D^G_1 structures within the migmatitic and mylonitic gneisses are not common but do occur and differ significantly in orientation but are predominantly isoclinal in style. These structures were formed in response to intense D^G_1 deformation under conditions of prograde medium grade middle to upper amphibolite facies metamorphism (M_1). The most conspicuous structures are isoclinal intrafolial folds, rootless intrafolial folds and tightly reclined intrafolial folds. The D^G_1 deformation, together with the associated M_1 metamorphism, caused intense tectonic transposition (Turner and Weiss, 1963; Hobbs et. al., 1976; Passchier et. al., 1990) resulting in the ubiquitous co-planar S^G_O // S^G_1 axial planar foliation. D^G_1 fold closures are difficult to measure in the field because of the parallelism of the fold limbs (see Plate 9.3A and Plate 9.4C).

In the ***Northern Granitoid Complex***, D^G_1 isoclinal folds occur in the Nkwalinye–Nkwalini area, the Nkwalinye River area NE of Ndloziyana Peak and in the Nsengeni River area.

In the Nkwalinye-Nkwalini area (3,4,5/LL,MM,NN,OO) (Fig. 9.48), D^G_1 folds vary from tightly appressed isoclinal to rootless intrafolial folds having steep plunges to the NE and SW with southeasterly inclined F^G_1 axial planes (Plate 9.3A; Plate 9.6A; Fig. 9.49A). The fold axes show an asymmetrical distribution about the vertical. The asymmetry is skewed to the southwest. At one locality in the mylonites, a D^G_1 steeply plunging tightly appressed isoclinal fold has been refolded into a tight to isoclinal fold with a moderate plunge to the west-southwest (Fig. 9.49B). The F^G_1 axial plane has been folded about S^G_2 (Fig. 9.49B). In the Nkwalinye River (5.405/LL.730) (Fig. 9.48), attenuated rootless intrafolial folds occur in

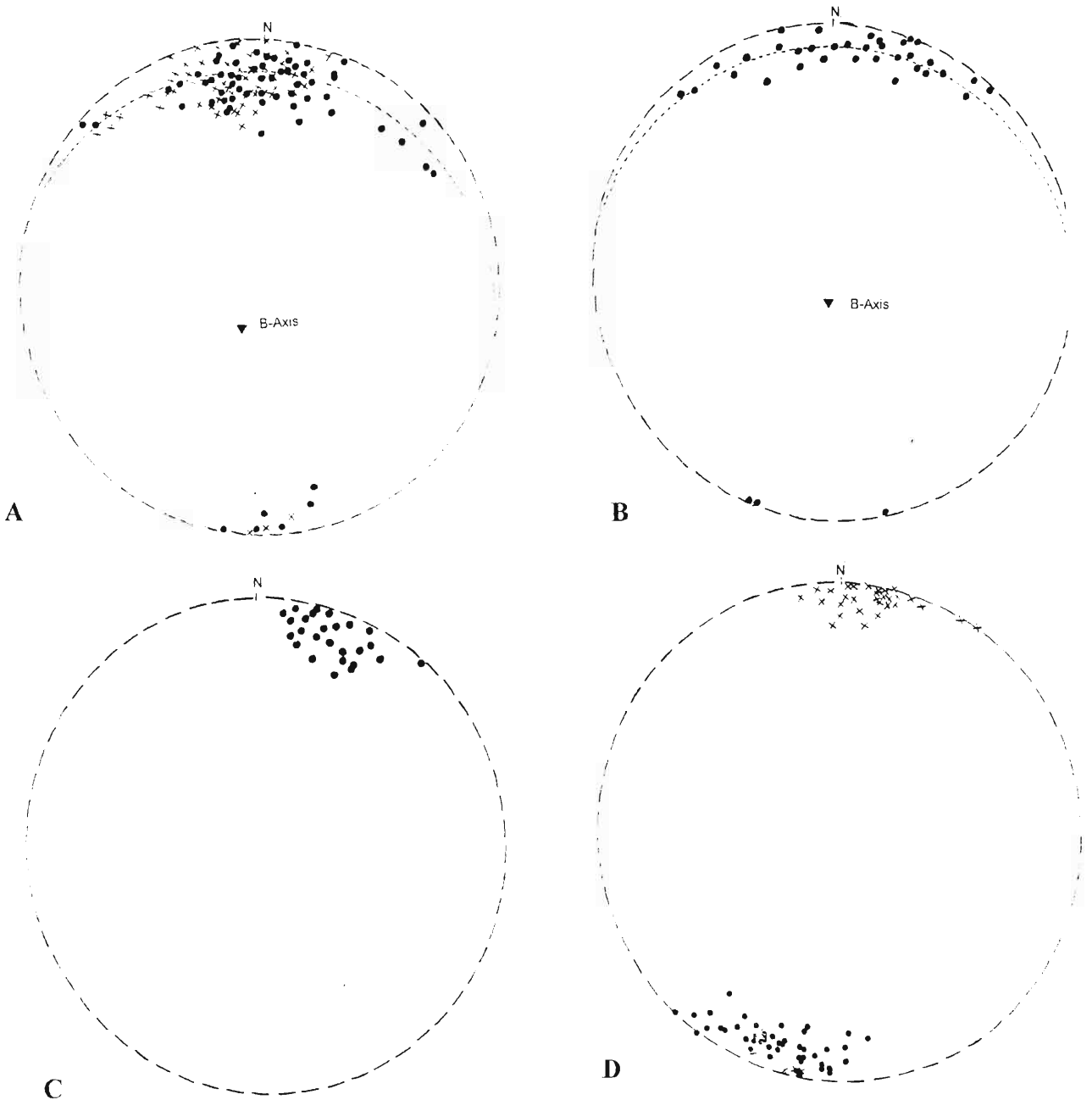

Fig. 9.47A : Distribution of poles to undifferentiated foliations of the migmatitic and mylonitic gneisses of the Nkwalinye-Nkwalini area.

● = Amazula Gneiss (n=67).

X = Nkwalini mylonitic and flaser gneisses (n=59).

Fig. 9.47B : Distribution of poles to undifferentiated foliations of the Amazula Gneiss in the Nsengeni River area (n=37).

Fig. 9.47C : Distribution of poles to undifferentiated foliations of the Amazula Gneiss in the Nkwalinye River area, northeast of Ndloziyana Peak (n=27).

Fig. 9.47D : Distribution of poles to undifferentiated foliations of the migmatitic and mylonitic gneisses of the area to the northeast of Ilangwe Peak.

● = Amazula Gneiss (n=47).

X = Nkwalini Mylonitic Gneiss (n=39).

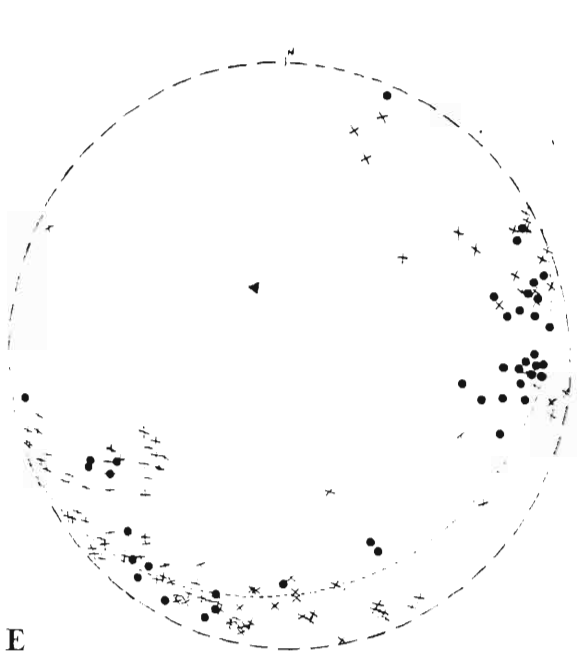

E

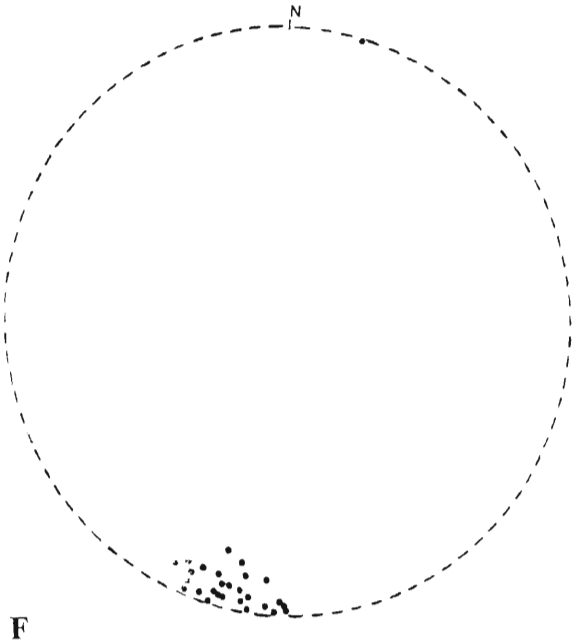

F

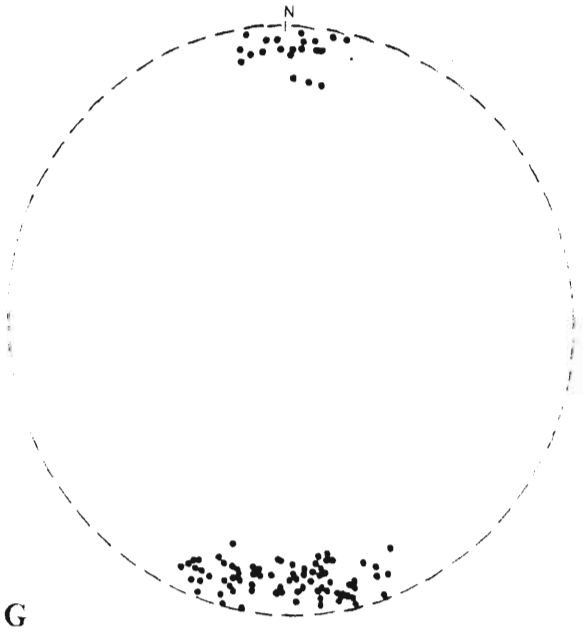

G

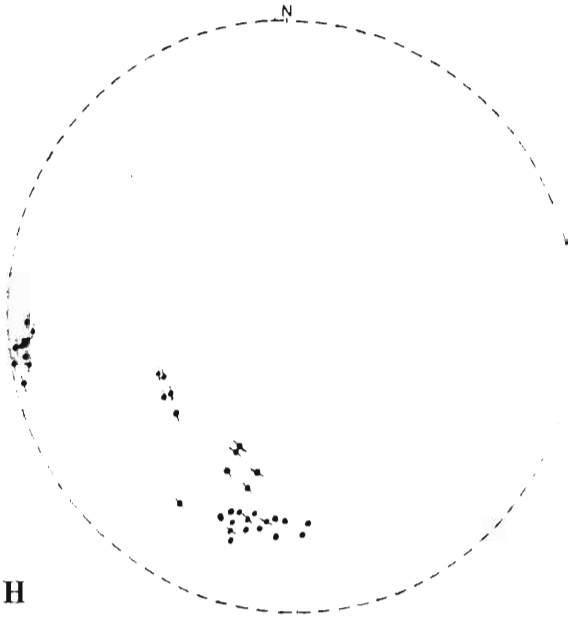

H

Fig. 9.47E : Distribution of poles to undifferentiated foliations of the migmatitic and mylonitic gneisses of the Mooiplaas Forest Plantation area.

● = Amazula Gneiss (n=43).

X = Nkwalini Mylonitic Gneiss (n=108).

Fig. 9.47F : Distribution of poles to undifferentiated foliations of the Amazula Gneiss in the lower sections of the Umhlathuze River near the gorge (n=29).

Fig. 9.47G : Distribution of poles to undifferentiated foliations of the Amazula Gneiss in the Amazula River area (n=105).

Fig. 9.47H : Distribution of poles to undifferentiated foliations of the Amazula Gneiss in the Umhlathuze River near Ngcengcengu Peak area. For comparison, the poles to foliation of the Sabiza amphibolite are shown.

● = Sabiza amphibolites.

= Amazula Gneiss.

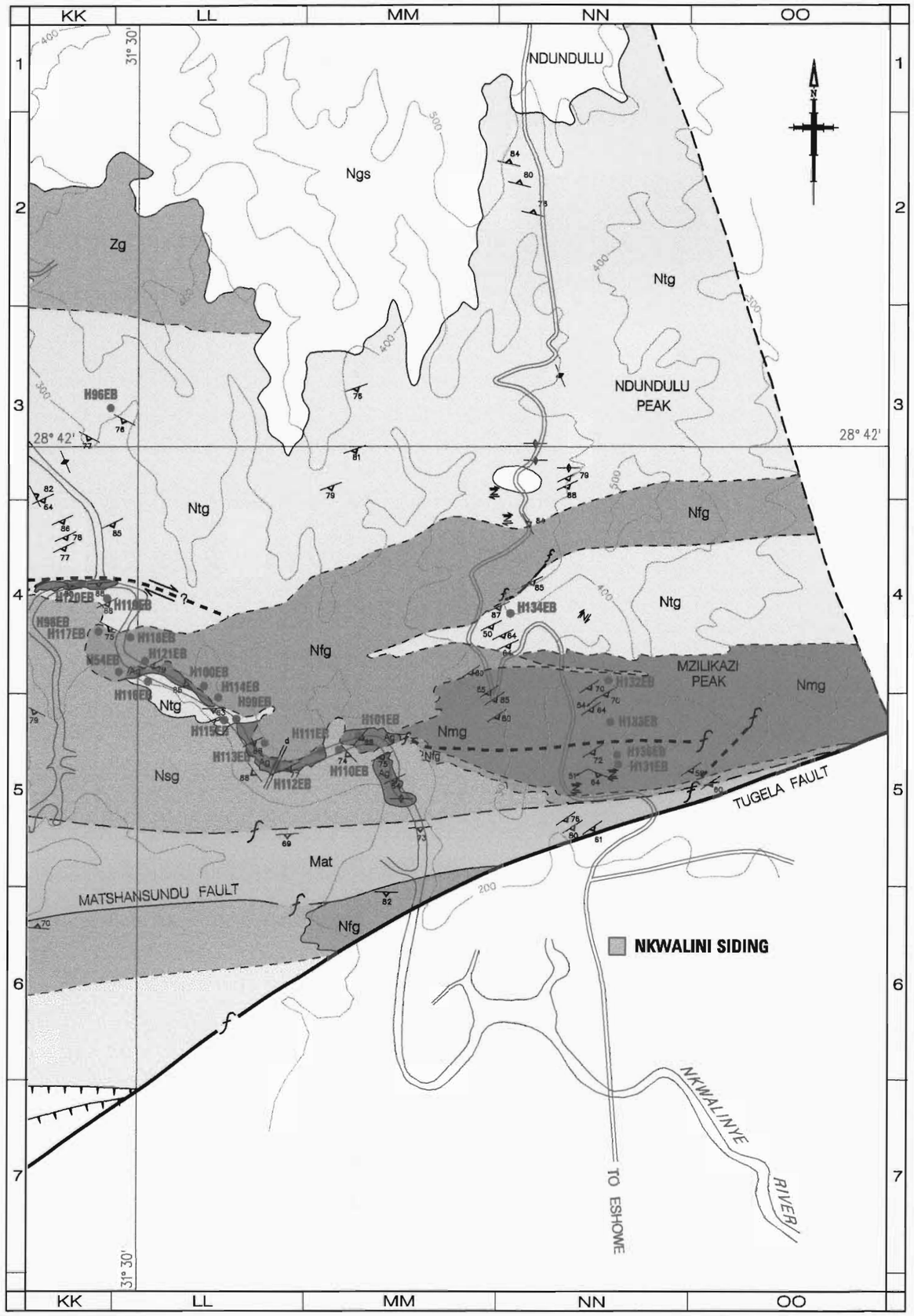

Figure 9.48 MIGMATITIC AND MYLONITIC GNEISSES IN THE NKWALINYE–NKWALINI AREA

LEGEND

Matshansundu Formation	Mat / Mab	Actinolite–tremolite schist; amphibole–mica schist; massive metabasalt (Mat) intercalated with cherty silicate BIF (Mab).
	Sat	Transgressive serpentinite–talc schists
	Mg	Metagabbro; metanorite; metagabbroic amphibolite
Impisi Granitoid Suite	Zg	Zietover Granite
	Nkg	Nkandla Granite
Umgabhi Granitoid Suite	Ucg	Umgabhi Micrographic Granite
	Esg / Esq	Esibhudeni Granitoid Gneiss (with quartz–sericite schist)
	Umg	Umgabhi Granitoid Gneiss
Nkwalinye Tonalitic Gneiss	Ntg	Nkwalinye Tonalitic Gneiss
	Nfg	Nkwalini Quartzo–Feldspathic Flaser Gneiss
	Nmg	Nkwalini Mylonitic Gneiss
	Ag	Amazula Paragneiss

0 1000 2000

METRES

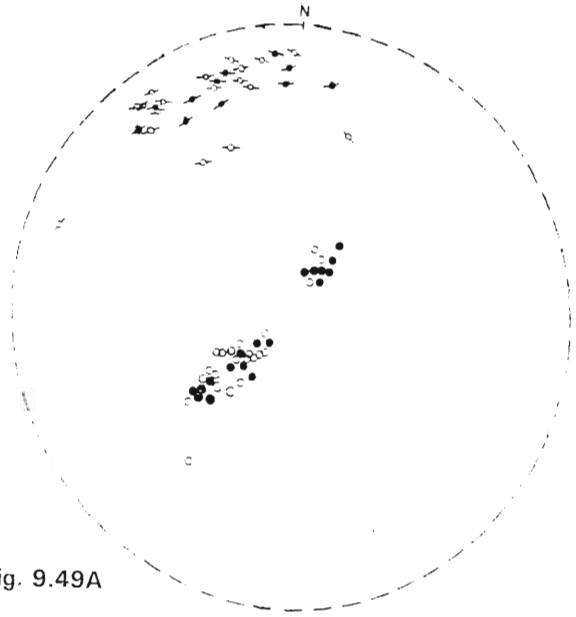

Fig. 9.49A

Fig. 9.49A : Orientation data of D^G_1 structures in the migmatitic and mylonitic gneisses of the Nkwalinye-Nkwalini area.

- = Plunge of F^G_1 axes of isoclinal folds in the mylonitic gneisses (n=23).
- = Poles to F^G_1 axial planes of isoclinal folds (n=21).
- = Plunge of F^G_1 axes of isoclinal folds in Amazula Gneiss (n=18).
- = Poles to F^G_1 axial planes in the Amazula Gneiss (n=13).

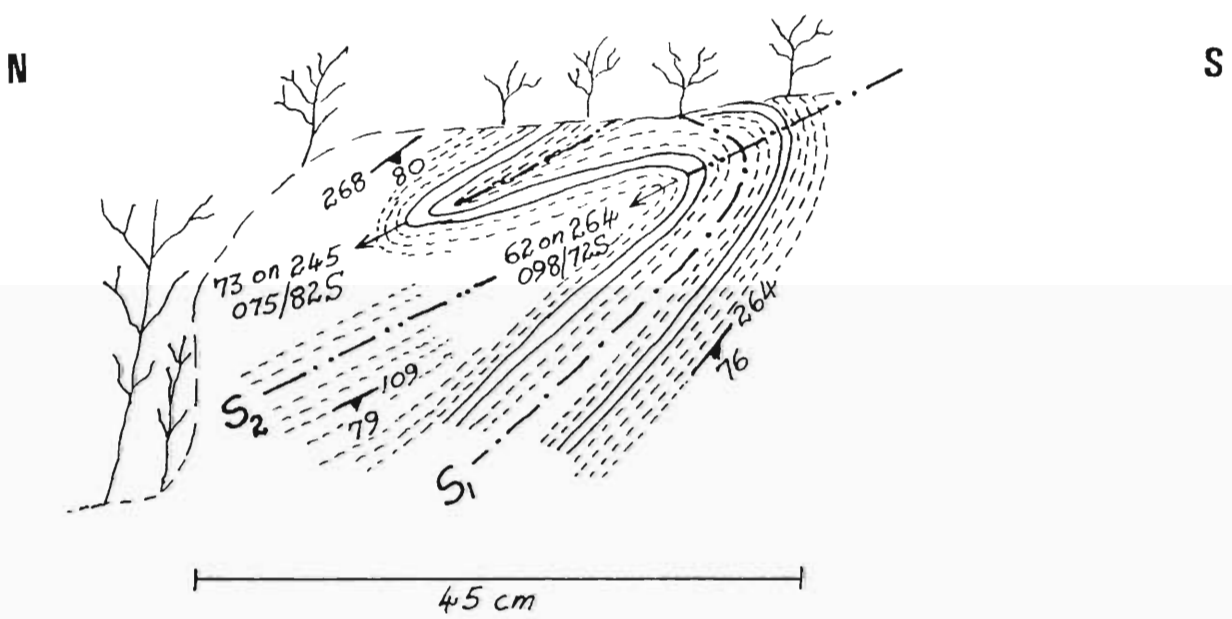

Fig. 9.49B : Field sketch of a refolded D^G_1 isoclinal fold in the Nkwalini mylonites just north of Nkwalini siding station.

PLATE 9.3 : STRUCTURES IN THE NKWALINI MYLONITIC GNEISS IN THE NKWALINI – MZILIKAZI PEAK AREA (4,5/MM,NN,OO).

PLATE 9.3A : D^{G}_{1} tightly appressed isoclinal folds and D^{G}_{2} isoclinal folds. The D^{G}_{1} folds are transposed to the S^{G}_{2} axial planar foliation.

PLATE 9.3B : D^{G}_{2} isoclinal composite similar folds. The competent quartz layers form Class 1B folds whereas the incompetent layers which are less resistant to deformation thicken into the fold hinges to form Class 3 folds. Note the boudinaged limbs of the fold.

PLATE 9.3C : Minor reclined D^{G}_{3} s-folds in the Nkwalini mylonites. The folds verge to the south and their S^{G}_{3} axial planes are slightly oblique to the S^{G}_{2} axial planar foliation. These D^{G}_{3} folds are sometimes difficult to differentiate from the D^{G}_{2} minor s-folds.

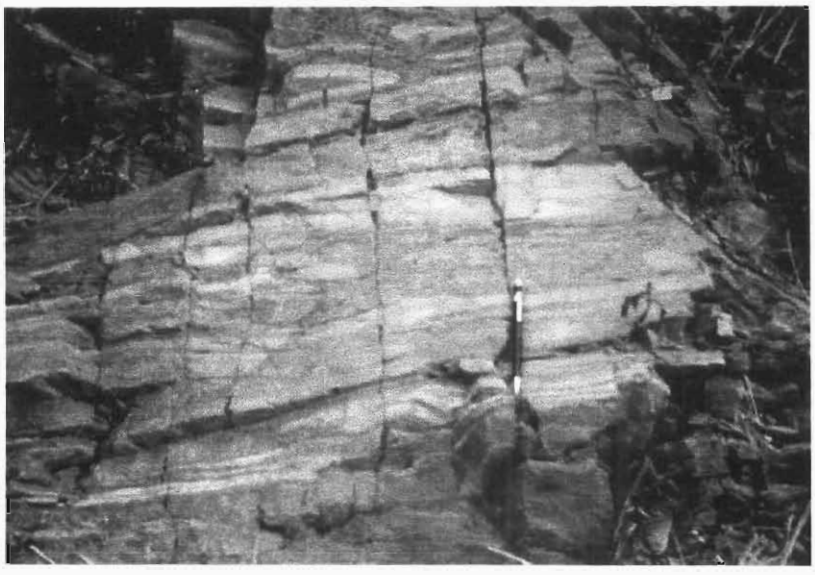

A

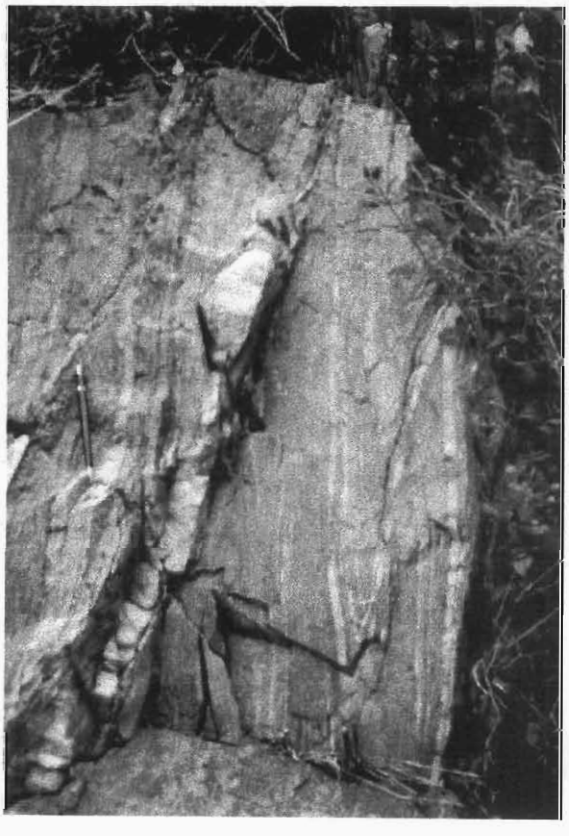

B

C

Plate 9.3

the Amazula Gneiss (Plate 9.6A) and plunge steeply to the north-east and southwest (Fig. 9.49A). The Nkwalini mylonitic and flaser gneisses also show a similar orientation (Fig. 9.49A).

Northeast of Ndloziyana Peak, in the Nkwalinye River (5.120/HH.800) (Fig. 9.12), D^G_1 intrafolial folds are found within the Amazula Gneiss and plunge WSW and ENE at about 60° to 70° with steep southerly-inclined axial planes (Fig. 9.50 A and B). This bimodal distribution is similar to that found in the Nkwalinye–Nkwalini area (Fig. 9.49A), and the Amazula River area (Fig. 9.52).

In the Nsengeni River (2,3/EE,FF) (Fig. 9.12), D^G_1 isoclinal intrafolial folds occur in the amphibolitic variety of the Amazula Gneiss. Some pyrite mineralization occurs in the fold closures and minor disseminated pyrite occurs along the attenuated limbs. No reliable measurements were taken in this area, due to the nature of the erosion surface of the outcrop.

Due to deep weathering and intense transposition, no D^G_1 fold structures were observed in the Mfanefile and Sappi Mooiplaas forest plantation areas. Steep southerly to southwesterly or northerly to northeasterly inclined foliations trend E-W and NNW-SSE in these areas (Figs. 9.47D and 9.47E).

In the ***Southern Granitoid Complex***, D^G_1 isoclinal folds are found in the Amazula River area (Fig. 9.51) and in the Umhlathuze River near the gorge (Fig. 2).

In the Amazula River [(7.140/AA.940) (Fig. 9.51; Fig. 2], complex superimposed folding (Ramsay, 1967; Ramsay and Huber, 1987) has been observed in the Amazula Gneiss (Plate 9.4A). Here, D^G_1 folds have fold axes plunging to the ENE and WSW at about 50°-80° with axial planes inclined steeply to the north or south (Fig. 9.52). A tightly appressed westerly plunging D^G_1 isoclinal intrafolial fold is shown in Plate 9.4C. This plate also shows a refolded D^G_1 tightly appressed isoclinal fold which plunges steeply to the east. The limbs of this fold show pinch-and-swell and boudinage.

Isoclinal intrafolial folds of quartzo-feldspathic veins (Fig. 5.1; Plate 9.4C; Plate 9.5A and B) show steep ENE and WSW plunges (Fig. 9.52). The deformation pattern on these folded veins (Plate 9.5) shows that they were first extended along the S^G_{O1} foliation direction (XY plane of the finite strain ellipsoid) to form boudins and pinch-and-swell structures and then

they were shortened to form isoclinal folds and intrafolial folds. The quartz vein at the bottom of Plate 9.5A shows the F^G_1 axial surface. The asymmetry of the veins show a sinistral sense of shear whilst the deformation is that of a general non-coaxial flow type (Passchier et. al., 1990). The stubby vein (sv) on Plate 9.5A defines a stair-step geometry (Lister and Snoke, 1984) and its development can be explained in terms of general non-coaxial flow (Hanmer and Passchier, 1991; Passchier et. al., 1990).

Also notable on the veins in Plates 9.5A and B is the fact that the open folds have thickened short limbs whilst the tight to isoclinal folds have thinned short limbs. Further, the axial surface of the tight to isoclinal folds makes a smaller angle with the main S^G_{01} foliation than the axial surface of the open folds. Fossen and Rykkelid (1990) found a similar relationship for the folded layers of the Toftoy, Øygarden tectonite.

In the Amazula River locality [(6,7/Z,AA,BB,CC); (Fig. 9.51)], there occur other less obvious but quite common types of isoclinal intrafolial folds not involving quartzo-feldspathic veins but rather the amphibolitic mylonitic gneiss. These are folds of the mylonitic foliation itself and have axial planes subparallel to or making a smaller angle with those of the quartzo-feldspathic veins. These folds show development of new mylonitic foliation on their limbs due to the intense D^G_1 transpositional layering (Plate 9.5A and B; Bell and Hammond, 1984). Such folds are said to be quite common in mylonitic zones and are apparently confined to them (Bell and Hammond, 1984; Cobbold and Quinquis, 1980; Bell, 1978; Williams, 1978; Rhodes and Gayer, 1977). Classification of the different groups of mylonitic foliations is difficult as they anastomose and terminate abruptly, no doubt, due to intense deformation which tends to align all structural elements towards parallelism with the regional S^G_1 foliation. Multiple generations of mylonitic foliation are thought to form during a single extended period of mylonitization (Bell and Hammond, 1984).

North of the Umhlathuze River gorge and within the Amazula Gneiss [Fig. 2; (8/U,V,W)] small-scale D^G_1 intrafolial tightly reclined folds plunge steeply (65°) to the NE (Fig. 9.53). Charlesworth (1981) observed similar folds within "pre-Nsuze granitoid gneisses" near the contact with the Natal Thrust Front.

No D^G_1 structures were observed in the thrust slices of the Amazula Gneiss in the Umhlathuze River [Fig. 9.9; (4,5/Q); Fig. 2].

PLATE 9.4 : COMPLEX FOLDING IN THE AMAZULA GNEISS OF THE AMAZULA RIVER.

PLATE 9.4A : Complex interference folding in the Amazula Gneiss of the Amazula River. [Locality: (7.150/AA.900)].

PLATE 9.4B : Steep westerly-plunging and steep northerly-inclined overturned D^{G}_{2} antiform of the Amazula Gneiss with the attenuated and boudinaged northern limb.

PLATE 9.4C : Boudinaged and folded D^{G}_{2} antiformal structure in the Amazula Gneiss. The structure plunges steeply to the west and is steeply inclined to the north. Note the tightly appressed D^{G}_{1} isoclinal fold in the boxed area.

A

B

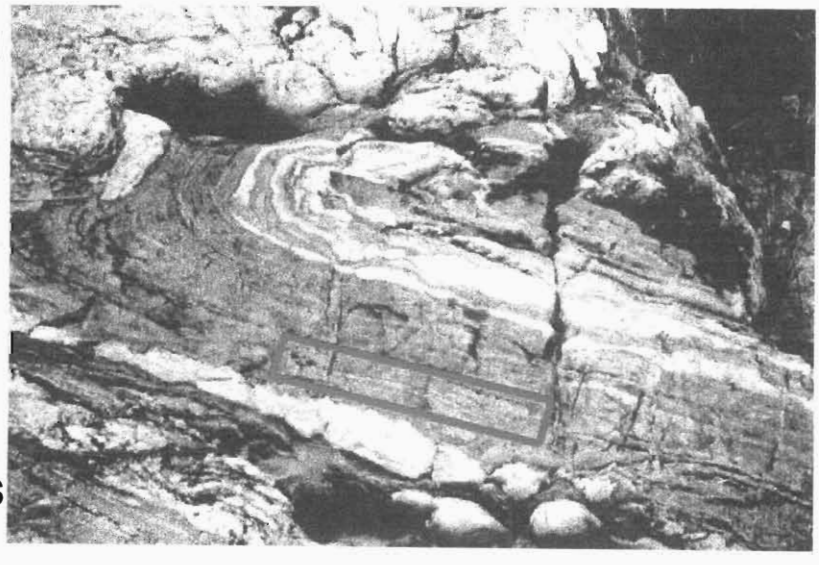

C

Plate 9.4

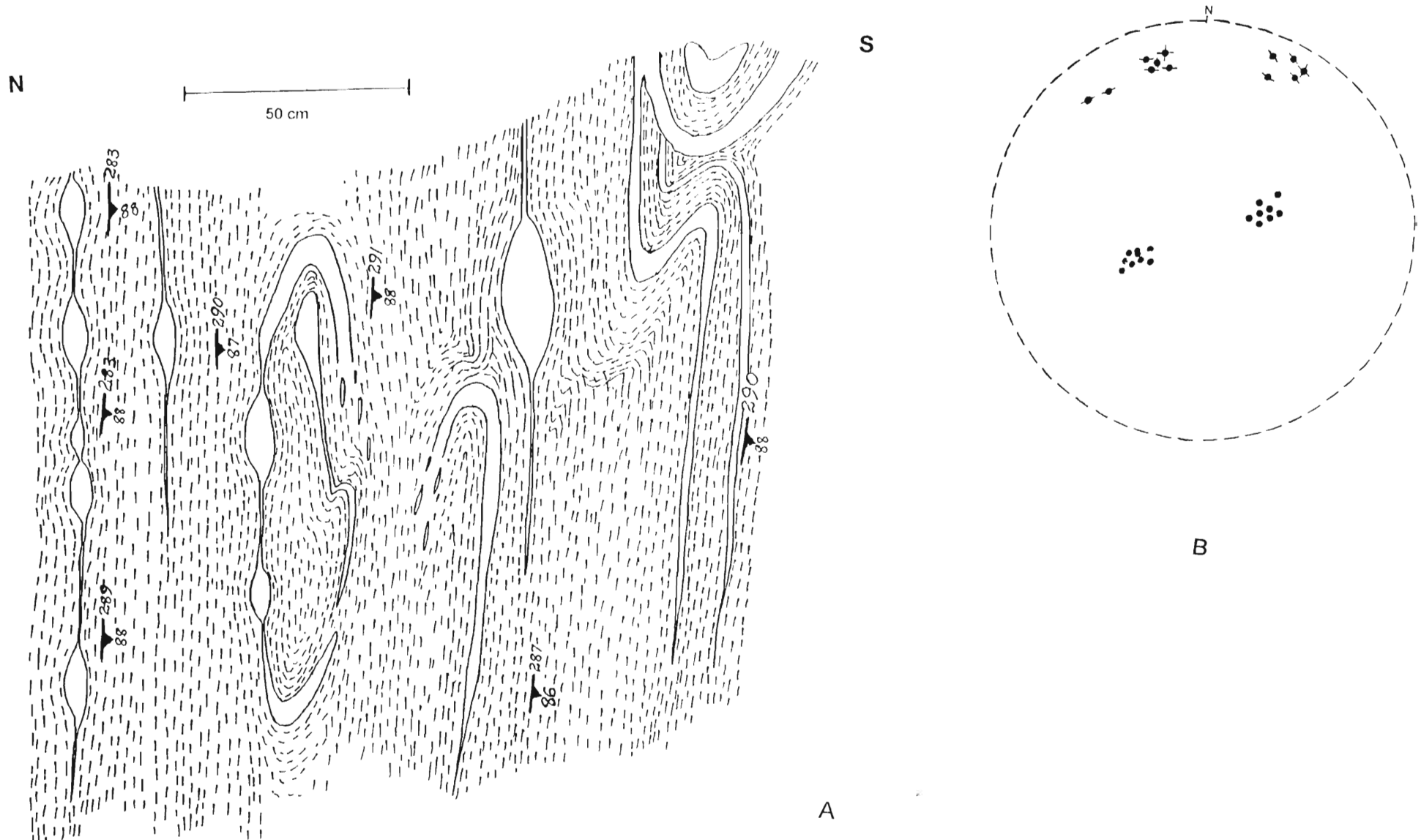

Fig. 9.50A : Superimp osed D^G_2 folding on D^G_1 isoclinal intrafolial folding in the finely banded Amazula Gneiss in the Nkwalinye River NE of Ndloziyana Peak.

Fig. 9.50B : Orientation data of F^G_1 isoclinal folds in the Nkwalinye River NE of Ndloziyana Peak.
- ● = Plunge of F^G_1 axes of isoclinal folds in the Amazula Gneiss (n=17).
- = Poles to F^G_1 axial planes of isoclinal folds in the Amazula Gneiss (n=12).

PLATE 9.5 : STRUCTURES IN THE AMAZULA GNEISS OF THE AMAZULA RIVER AREA (6/BB).

PLATE 9.5A : D^{G}_{1} and D^{G}_{2} fold structures on quartzo-feldspathic veins. Note the stubby vein (sv) defining a sinistral stair-step geometry (Lister and Snoke, 1984), the anastomosing mylonitic foliation on the amphibolitic gneiss and the detachment plane running through the centre of the photograph from the lower left hand corner to the upper right hand corner. The arrows indicate ***anvil***-shaped folds. The cross-section of the anvil folds suggest a steep plunge into the outcrop. This implies that the direction of transport was sub-vertical. See also Plate 5.4B.

PLATE 9.5B : Boudinaged and folded quartzo-feldspathic veins. The isoclinal intrafolial folds are D^{G}_{1} age. Note the detachment plane near the sharp tip of the hammer.

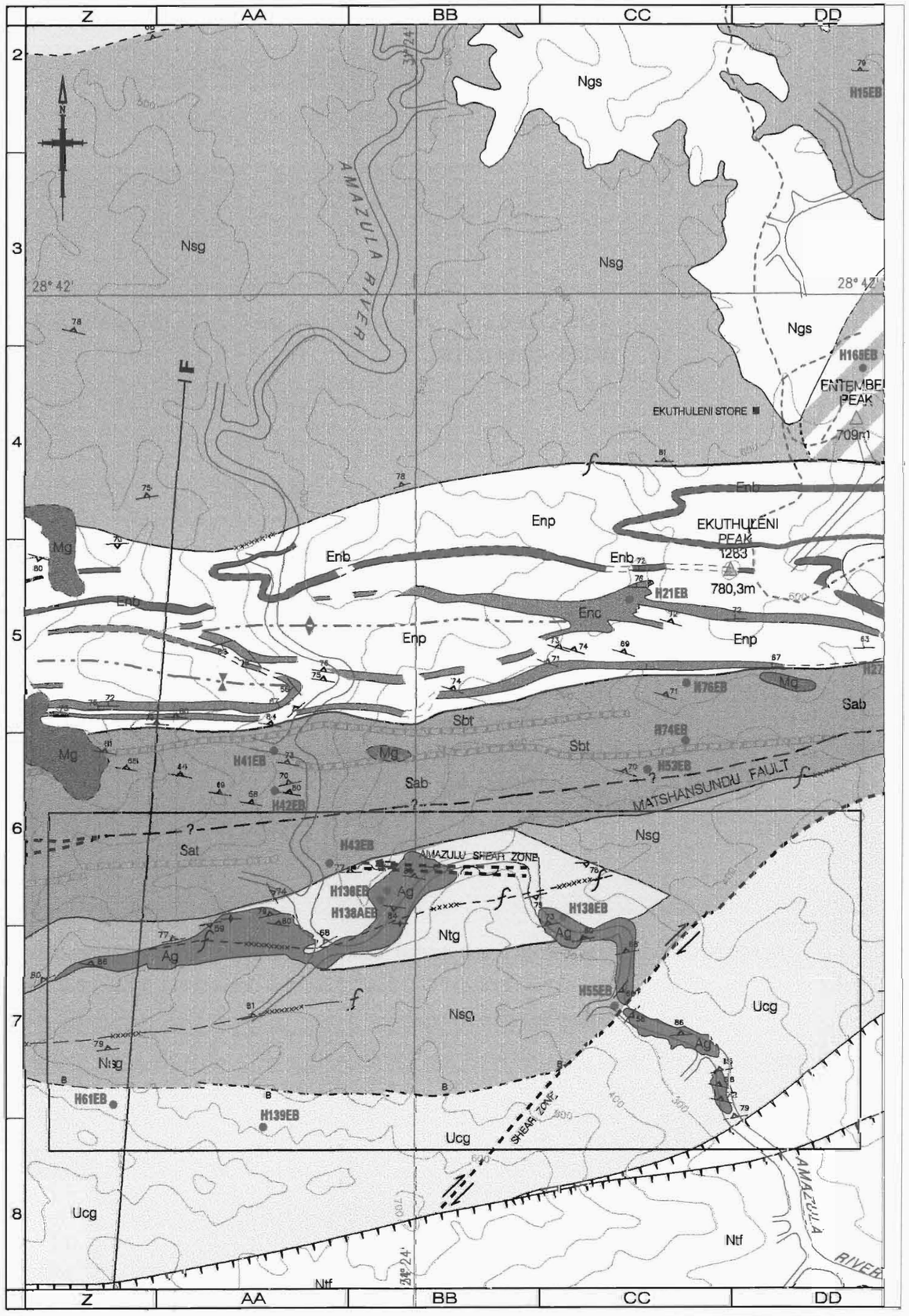

Figure 9.51 : MIGMATITIC AND MYLONITIC GNEISSES IN THE AMAZULA RIVER AREA

L E G E N D

Entembeni Formation	Enb, Enp, Enc	Phyllite (phyllonitic in the shear zones and along fault contacts) and minor pillowed metavolcanics (Enp), intercalated with cherty BIF (Enb), metacherts and cherty quartzite bands (Enc).
Sabiza Formation	Sbc, Sab, Sbt	Pillowed metabasalt; banded amphibolite; massive amphibolite; actinolite–tremolite schist (Sab); talc–tremolite schist; serpentinite–talc schist (Sbt); with thin metachert bands (Sbc) and a khakhi-coloured siliceous pelitic rock towards the top of the sequence
	Sat	Transgressive serpentinite–talc schists
	Mg	Metagabbro; metanorite; metagabbroic amphibolite
Umgabhi Granitoid Suite	Ucg	Umgabhi Micrographic Granite
	Esg < Esq	Esibhudeni Granitoid Gneiss (with quartz–sericite schist)
	Umg	Umgabhi Granitoid Gneiss
Nsengeni Granitoid Suite	Ekg	Ekuthuleni Granite
	Nsg	Nsengeni Granitoid Gneiss
	Nts	Ntshiweni Augen Gneiss
Nkwalinye Tonalitic Gneiss	Ntg	Nkwalinye Tonalitic Gneiss
	Ag	Amazula Paragneiss

0 1000 2000

M E T R E S

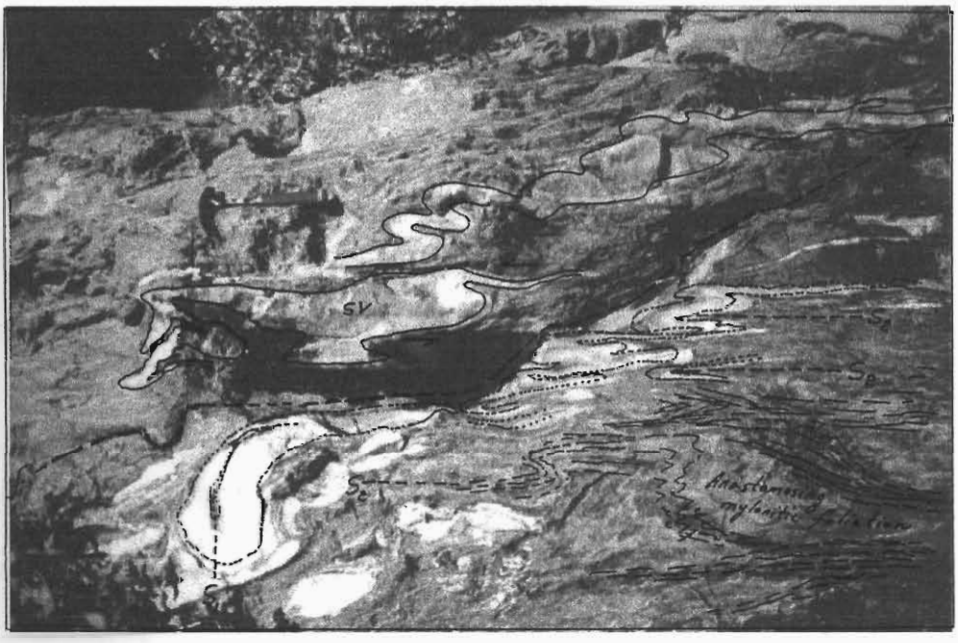

A

B

Plate 9.5

9.3.2.2 ANALYSIS AND INTERPRETATION OF STRUCTURAL DATA FROM F^G_1 FOLDS

Fig. 9.54 and Fig. 9.55 show a compilation of the data on the orientation of F^G_1 fold axes and axial planes in the Northern Granitoid Complex and the Southern Granitoid Complex

respectively. The combined plot is shown in Fig. 9.56. Figures 9.54 and 9.55 depict a close correspondence of the fold elements of the migmatitic and mylonitic gniesses in the Northern and Southern Granitoid Complexes.

The fold axes show a symmetric bimodal distribution in a vertical plane with azimuth 056°. One set of folds plunge to the WSW at about 65° and the other set plunges to the ENE also at about 65° (see Figs. 9.54A and 9.55A). The axial plane poles of the ***older gneisses*** in the Northern Granitoid Complex are steeply inclined to the south and southeast and form a horizontal girdle distribution which suggests that deformation assumed a steep rotation axis (Fig. 9.54B). The axial plane poles of the Amazula Gneiss in the Southern Granitoid Complex show a major concentration around the south pole with a minor concentration around the north pole (Fig. 9.55B).

Fig. 9.56 shows a remarkable similarity to Figs. 9.19 and 9.20 of the structural elements in the Ilangwe Greenstone Belt. However, in contrast to the greenstones, primary layering has not been unequivocally determined in the gneissic terrain. This suggests that even though the D_1 structural elements are similar in the gneisses and the greenstones, those of the gneisses probably do not involve S_O. This also suggests that the primary layering in the gneisses (especially the Amazula paragneiss) could have been obliterated and what is now observed is induced metamorphic layering which is probably similar to that of the Sabiza amphibolites. Therefore, although the D^G_1 episode in the gneisses cannot be ***directly*** correlated with the D_1 episode of the greenstones, there is nevertheless a close correspondence between the two earliest deformation episodes and they are probably synchronous. They both took place in a horizontal tectonic regime characterized by recumbent folding and possible thrusting. The recumbent folds have their axes aligned in an ENE–WSW direction with axial planes inclined steeply to the SSE and NNW. The occurrence of transposed foliation in the older gneisses and the Sabiza amphibolites is further evidence of horizontal tectonics during D_1 deformation. This is the case because transposition is the product of extreme deformation involving very high strain and

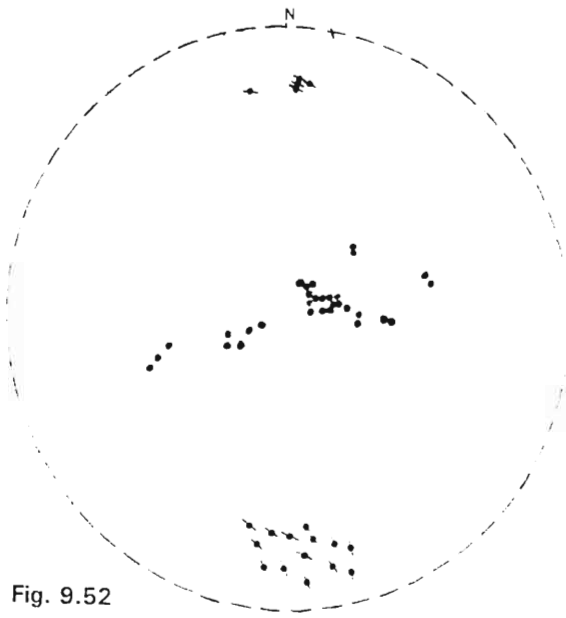

Fig. 9.52

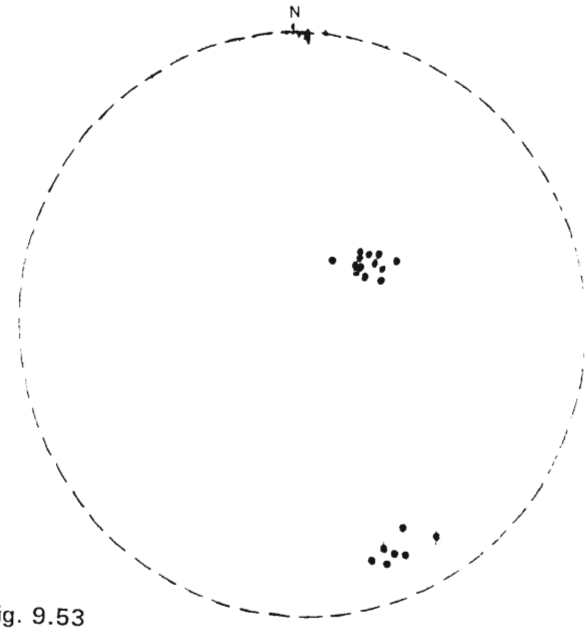

Fig. 9.53

Fig. 9.52 : Orientation data of F^G_1 structures in the Amazula Gneiss of the Amazula River.

- = Plunge of F^G_1 axes of isoclinal folds (n=31).
- = Poles to F^G_1 axial planes of isoclinal folds (n=17).

Fig. 9.53 : Orientation data of F^G_1 reclined folds in the Umhlathuze River near the gorge.

- = Plunge of F^G_1 reclined fold axes (n=13).
- = Poles to F^G_1 axial planes of reclined folds (n=7).

PLATE 9.6 : STRUCTURES IN THE AMAZULA GNEISS.

PLATE 9.6A : D^{G}_{1} attenuated rootless intrafolial folds (near the knife) of the Amazula Gneiss in the Nkwalinye River (5.340/LL.790). The folds are tightly appressed and are transposed onto the regional S^{G}_{1} foliation.

PLATE 9.6B : Keel-shaped sheath fold (boxed) in the Amazula River. The sheath fold plunges to the WSW at about 40°. [Locality: (6.720/BB.480)].

PLATE 9.6C : Photomicrograph of the quartzitic leucosome of the Amazula Gneiss showing a quartz-feldspar porphyroblast delta structure indicating a sinistral sense of shearing.

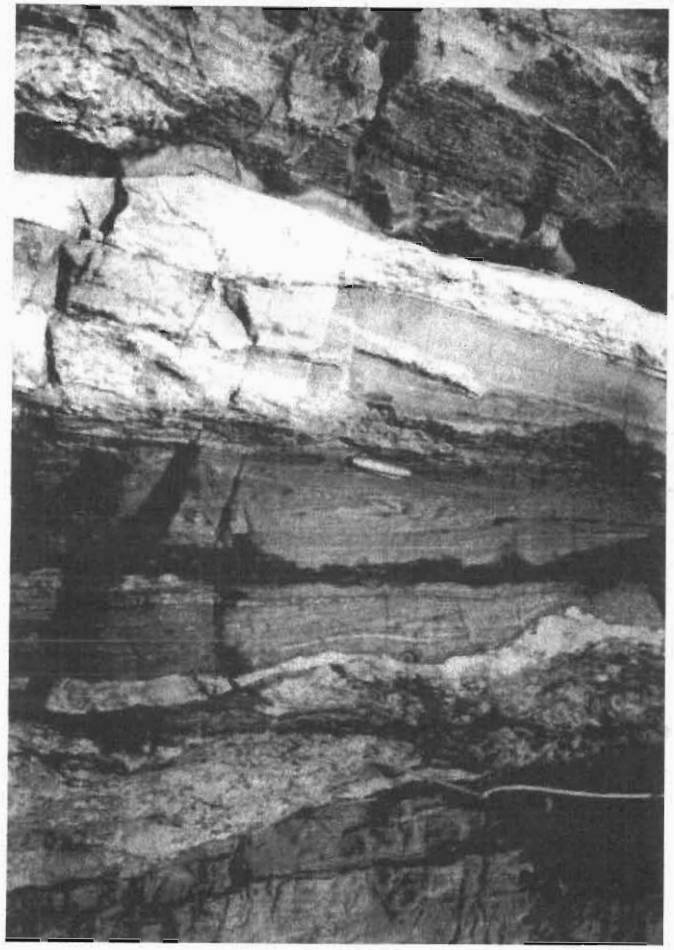

A

B

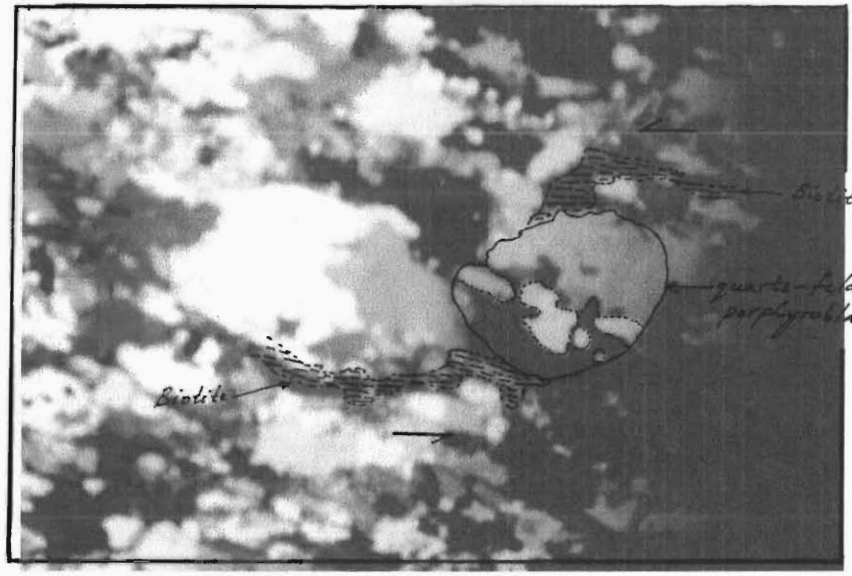

C

Plate 9.6

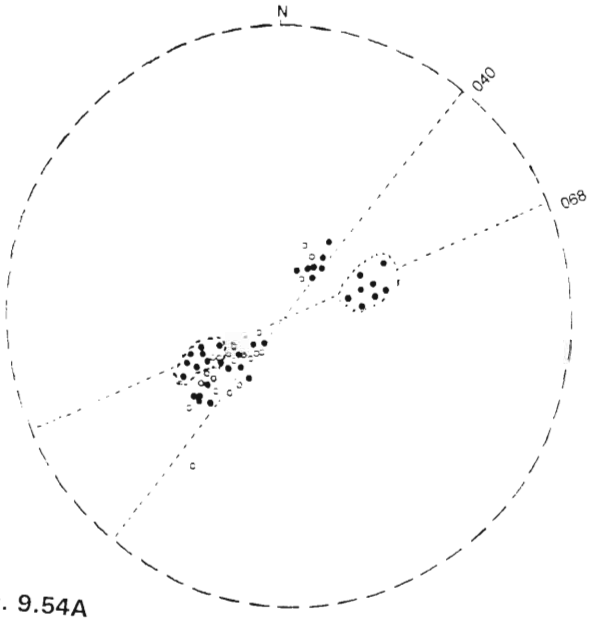

Fig. 9.54A

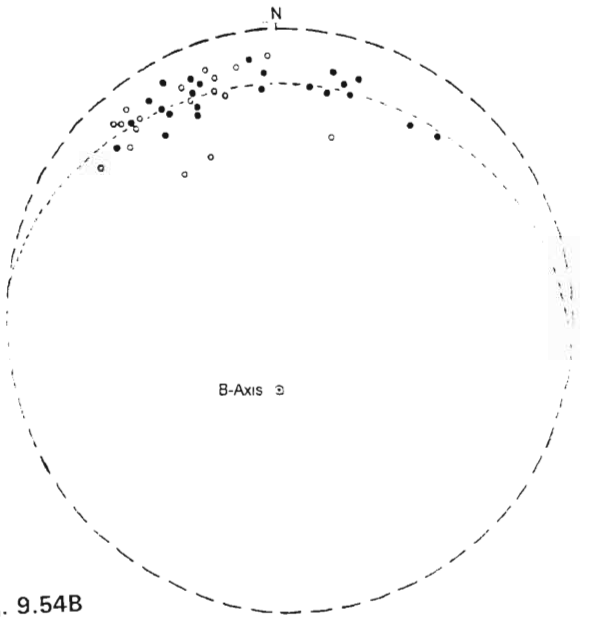

Fig. 9.54B

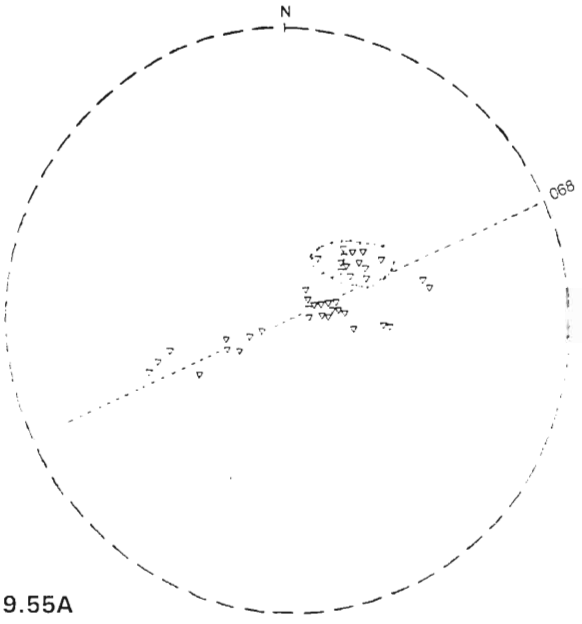

Fig. 9.55A

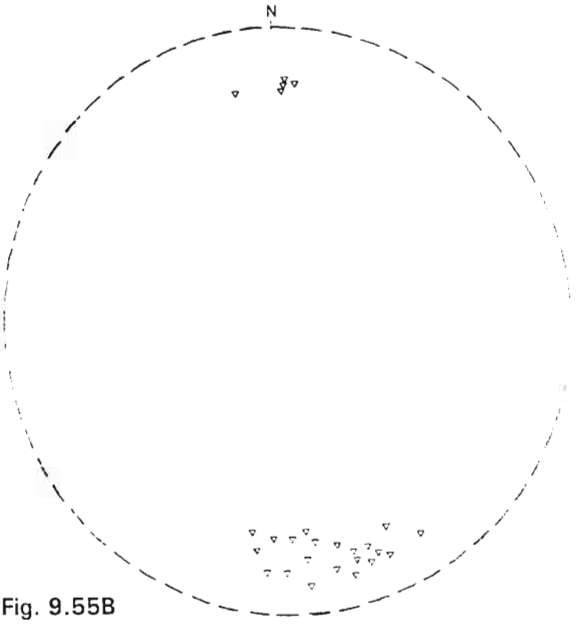

Fig. 9.55B

Fig. 9.54A : Compilation of structural data from the F^{G}_{1} fold axes in the migmatitic and mylonitic gneisses of the Northern Granitoid Complex.

- ● = Plunge of fold axes in Amazula Gneiss.
- O = Plunge of fold axes in the mylonitic gneisses.

Fig. 9.54B : Compilation of structural data from the F^{G}_{1} axial planes of the migmatitic and mylonitic gneisses in the Northern Granitoid Complex.

- ● = Poles to axial planes in Amazula Gneiss.
- O = Poles to axial planes in the mylonitic gneisses.

Fig. 9.55A : Compilation of structural data from the F^{G}_{1} fold axes in the Amazula Gneiss of the Southern Granitoid Complex.

Fig. 9.55B : Compilation of structural data from the F^{G}_{1} axial planes of the Amazula Gneiss in the Southern Granitoid Complex.

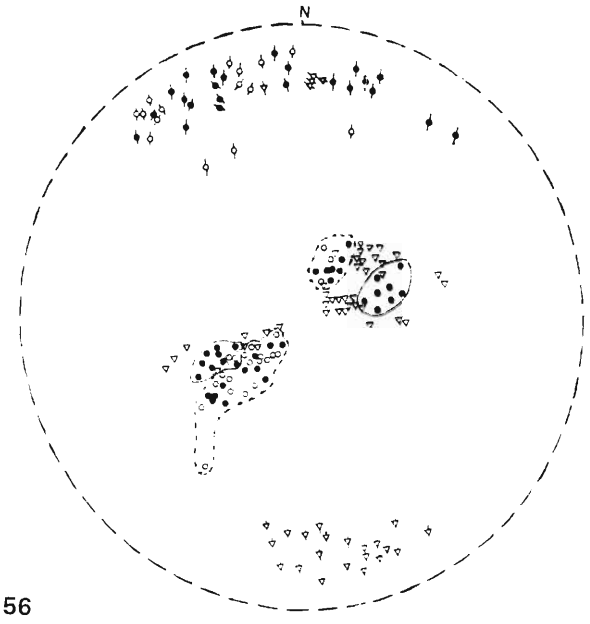

Fig. 9.56

Fig. 9.56 : A combined plot of F^{G}_{1} fold axes and axial planes in the migmatitic and mylonitic gneisses of the Ilangwe Granitoid Complex.

elongation. The migmatitic and mylonitic nature of these rocks is testimony to the high strain regime.

9.3.3 D^G_2 PHASE OF DEFORMATION

9.3.3.1 D^G_2 FOLDING

D^G_2 deformation is widespread in the granitoid terrain. It was characterized by tight to isoclinal folding together with widespread retrogressive metamorphism from middle/upper amphibolite facies to lower amphibolite/greenschist facies.

The D^G_1 folds in the older gneisses have been intruded along their axial planes by the Nkwalinye Tonalitic Gneiss or its pegmatitic phase (Plate 9.4A) which were subsequently deformed together with the older gneisses during D^G_2 deformation. The tonalitic gneiss is also migmatitic, which implies that there was a second episode of migmatization which was possibly induced during the emplacement of the Nkwalinye Tonalitic Gneiss.

Small-scale tight to isoclinal folds of D^G_2 age are abundant in the migmatitic and mylonitic gneisses (Fig. 9.49B). In the Nkwalini mylonite zone of the Nkwalinye-Nkwalini area (Fig. 9.48), isoclinal similar folds occur (Plate 9.3B; Plate 9.7A; Fig. 9.57) and have a moderate (45°-55°) plunge to the WNW to NW and their F^G_2 axial planes are steeply inclined to the SSW. Locally, these folds become upright isoclinal folds (Plate 9.3B; Plate 9.7A) and are associated with a mineral stretching lineation which occurs on the foliation plane striking 088° and inclined to the south at 60° to 70°. This L^G_2 lineation (Fig. 9.57) plunges to the southeast at 40° to 55°. It is denoted by stretched quartz stringers. Fig. 9.57 shows a bimodal distribution and the L^G_2 lineation is perpendicular to one maximum and parallel to another.

In the Nkwalinye Valley (4,5/LL,MM) (Fig. 9.48), D^G_2 folds occur in both the Amazula Gneiss and the Nkwalinye Tonalitic Gneiss. The folds are isoclinal with steep westerly-plunging F^G_2 fold axes and steep southerly inclined axial planes (Fig. 9.58). The fold geometry of these litho types is identical and this suggests that the tonalite gneiss was emplaced after D^G_1 folding, probably during the late stages of D^G_1 deformation or very early during D^G_2 deformation.

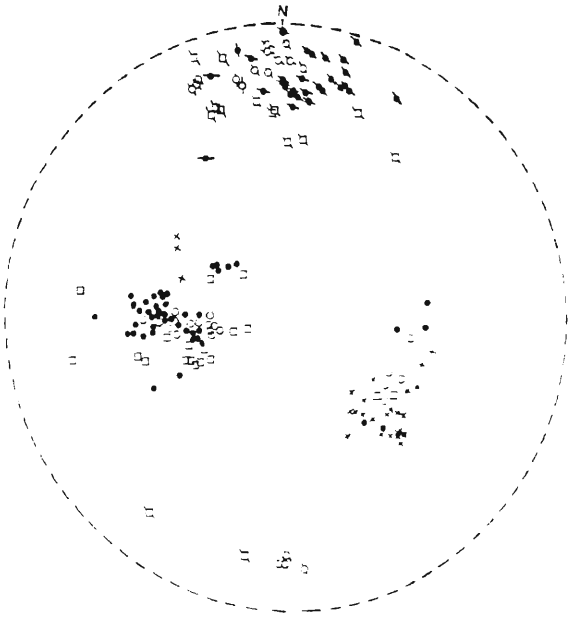

Fig. 9.57

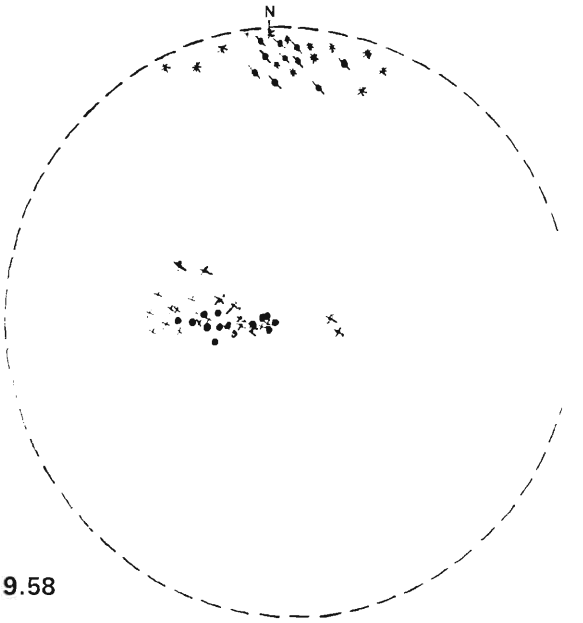

Fig. 9.58

Fig. 9.57 : Orientation data of D^G_2 structures in the granitoids of the Nkwalinye-Nkwalini area.

- ● = Plunge of F^G_2 fold axes in the Nkwalini mylonites (n=71).
- ◐ = Poles to F^G_2 axial planes in the Nkwalini mylonites (n=49).
- □ = Plunge of F^G_2 fold axes in the Nkwalini flaser gneisses (n=18).
- ◫ = Poles to F^G_2 axial planes in the flaser gneisses (n-14).
- o = Plunge of F^G_2 fold axes in the Amazula Gneiss (n=19).
- ◯ = Poles to F^G_2 axial planes in the Amazula Gneiss (n=17).
- × = Plunge of L^G_2 mineral stretching lineation in the Nkwalini mylonites (n=26)

Fig. 9.58 : Orientation data of D^G_2 structures in the granitoids of the lower section of the Nkwalinye River valley.

- ● = Plunge of F^G_2 fold axes in the Amazula Gneiss (n=15).
- ◐ = Poles to F^G_2 axial planes in the Amazula Gneiss (n=10).
- × = Plunge of F^G_2 fold axes in the Nkwalinye Tonalitic Gneiss (n=23).
- ✳ = Poles to F^G_2 axial planes in the Nkwalinye Tonalitic Gneiss (n=14).

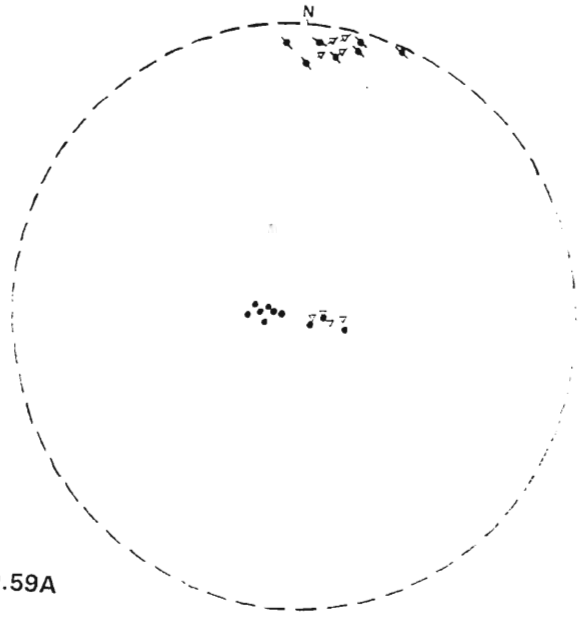

Fig. 9.59A

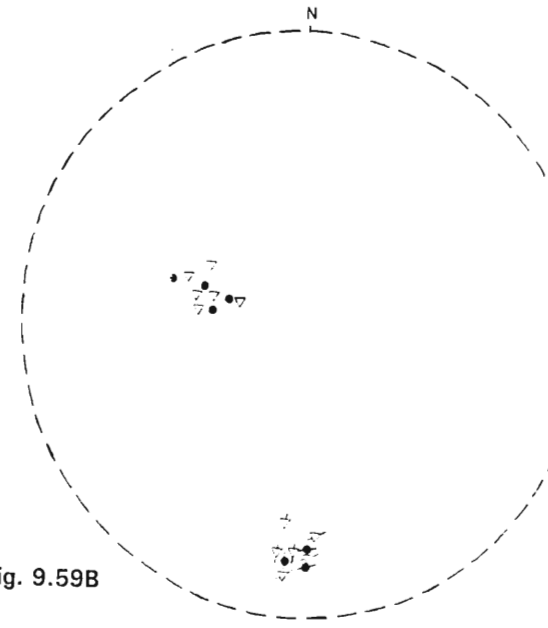

Fig. 9.59B

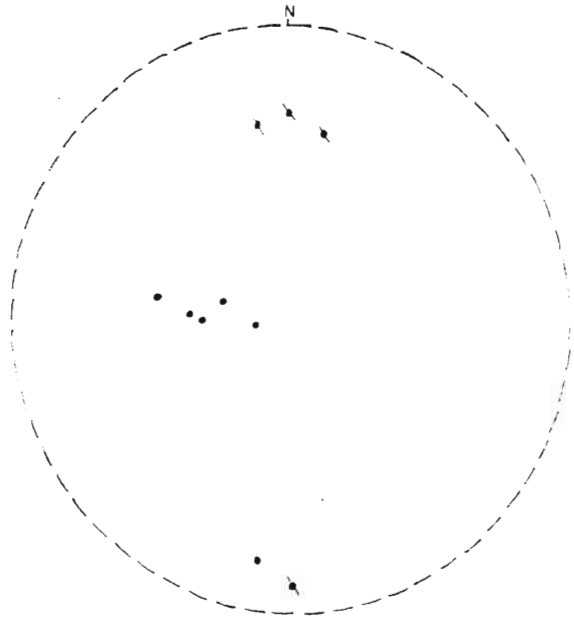

Fig. 9.59A : Orientation data of D^G_2 structures in the granitoids of the Nkwalinye River valley NE of Ndloziyana Peak.

- ● = Plunge of F^G_2 fold axes in the Amazula Gneiss (n=10).
- ◐ = Poles to F^G_2 axial planes of folds in the Amazula Gneiss (n=7).
- △ = Plunge of F^G_2 fold axes in the Nkwalinye Tonalitic Gneiss (n=4).
- ◺ = Poles to F^G_2 axial planes in the Nkwalinye Tonalitic Gneiss (n=4).

Fig. 9.59B : Orientation data of D^G_2 structures in the granitoids of the Umhlathuze River area near the gorge.

- ● = Plunge of F^G_2 fold axes in the Amazula Gneiss (n=4).
- ◐ = Poles to F^G_2 axial planes in the Amazula Gneiss (n=3).
- △ = Plunge of F^G_2 fold axes in the Nkwalinye Tonalitic Gneiss (n=6).
- ◺ = Poles to F^G_2 axial planes in the Nkwalinye Tonalitic Gneiss (n=6).

Fig. 9.59C : Orientation data of D^G_2 structures in the Nkwalinye Tonalitic Gneiss of the Zietover area.

- ● = Plunge of F^G_2 axes of s-folds (n=5).
- ◐ = Poles to F^G_2 axial planes of s-folds (n=5).

Similar distributions as the one in the Nkwalinye Valley are found in widely separated areas, e.g. the Nkwalinye River NE of Ndloziyana Peak (Fig. 9.59A), the Umhlathuze River near the gorge (Fig. 9.59B) and in the Zietover area (1.420/EE.580) (Fig. 9.59C).

In the upper reaches of the Nkwalinye River, just below Ndloziyana Peak (4.800/HH,II) (Fig. 9.12; Fig. 9.59A), the tonalitic gneiss is deformed into a steep easterly plunging reclined fold whose geometry is close to a neutral fold (Plate 6.2B). This plate also shows that the northern limb of the neutral fold is dextrally sheared and is intruded (near the red knife) by pink quartzo-feldspathic veins of Nsengeni Granitoid Gneiss. This implies that the Nsengeni Granitoid Suite is post-D^G_2 folding and was emplaced during the terminal stages of D^G_2 deformation.

No D^G_2 folds were observed in the Amazula Gneiss in the Nsengeni River raft (2,3/EE,FF) (Fig. 9.12) and on the raft occurring in the tributary of the Sabiza River northwest of Ilangwe Peak (3/W,X). In these localities, the gneiss shows a predominantly steep south-dipping planar foliation (Fig. 9.47B and Fig. 9.47D).

In the Sappi Mooiplaas forest plantation area (1,2,3/O,P,Q,R,S) (Fig. 9.9), D^G_2 folds occur in exposures in streams and on the side walls of gravel roads constructed by Sappi. The rocks are deeply weathered in this area. In the Umhlathuze River west of Spelonk (2/O), minor D^G_2 folds occur in the Amazula Gneiss. They are isoclinal in style and have axes plunging to the NW at about 60° with F^G_2 axial planes inclined steeply to the northeast (Fig. 9.60). An L^G_2 stretching lineation also plunges to the NW.

In the Amazula River (6,7/Z,AA,BB,CC) (Fig.9.51), D^G_1 folds were refolded during D^G_2 into tight to isoclinal folds (Plate 9.4B and C; Fig. 9.12) with axes plunging steeply (60° - 80°) to the WNW and ESE with axial planes inclined to the north or south (Fig. 9.61). A steeply plunging L^G_2 intersection lineation (Pencil lineation - Davis, 1984) is associated with these F^G_2 folds (Plate 9.8B; Fig. 9.61). Further to the south, at locality (7.500/CC.520), D^G_2 isoclinal folds have the same orientation as those in the north-northwest.

At the Amazula River locality (6.650/BB.200), a D^G_1 isoclinal fold (Plate 9.4B and C; Fig. 5.1) has been refolded into a steep (71°) westerly plunging D^G_2 antiformal ***similar*** fold with the southern limb overturned to the north and the northern limb ptygmatically folded, tightly appressed and attenuated (Plate 9.4B; Platt, 1983). The tight stacking of the

boudins on this limb (Plate 9.5) is testimony to the intensity of the D^G_2 compressional regime. Fig. 9.61 gives the orientation data of this fold.

Another important D^G_2 fold style which has been observed to deform the banded Amazula Gneiss (which contains F^G_1 intrafolial folds in transposed foliation) and, to a lesser extent, the migmatitic Nkwalinye Tonalitic Gneiss, is ***sheath folding***. The term sheath fold was introduced by Carreras et. al. (1977) and defined by Ramsay and Huber (1987) as a fold with a hinge line variation of more than 90°. Skjernaa (1989) suggested a geometric definition of a sheath fold as a fold with the hinge line angle T <90° and x:y ratio >0,25. She further suggested the name tubular fold for a sheath fold variant with a tight hinge and geometrically defined it as a fold with a hinge line angle T <20° and x:y ratio <1.

A lot has been written about the occurrence of sheath folds (including the tubular folds of Skjernaa, 1989) in shear regimes (Mies, 1993; Fossen and Rykkelid, 1990; Skjernaa, 1989; Ramsay and Huber, 1987; Henderson, 1981; Mattauer et. al., 1981; Cobbold and Quinquis 1980; Minnigh, 1979; Quinquis et. al., 1978; Carreras, et al., 1977; Rhodes and Gayer, 1977)

Sheath folds in the Amazula Gneiss occur in the Amazula River (Fig. 5.1; Plate 5.4; Plate 9.6B) (6.720/BB.480) and in the lower reaches of the Umhlathuze River near the Umhlathuze gorge (8.300/U.880). In the former locality, sheath folds plunge moderately to the west and ENE. They are associated with an oblique mineral stretching lineation plunging moderately to the NE (Fig. 9.62). In the latter locality, D^G_2 sheath folds plunge moderately to the ESE and WNW (Fig. 9.63). The sheath folds in these localities are symmetrical about the vertical and show a bimodal distribution (Figs. 9.62 and 9.63). These folds have not been observed in the migmatitic and mylonitic gneisses of the Nkwalinye River.

In the Amazula River (6.720/BB.480), a large sheath fold has a keel-like shape (Fig. 5.1; Plate 9.6B). To the east of the keel-like structure, in the river pavement, the sheath folds appear as eye-like structures or "eye-folds" (Plate 5.4B; Fig. 5.1) (Dalziel and Bailey, 1968; Lacassin and Mattauer, 1985) with elliptical patterns with no common centre (Plate 5.2B; Mies, 1993). These ellipses share a plane of approximate bilateral symmetry, similar to those in the Moretti-Harrah Quarry (Mies, 1993).

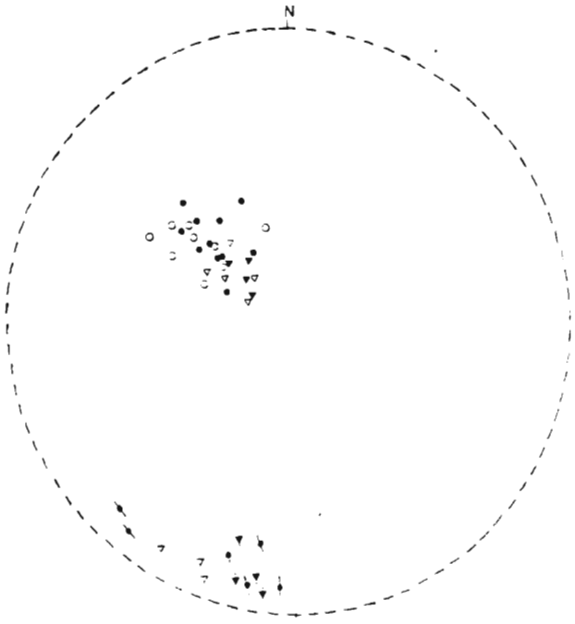

Fig. 9.60

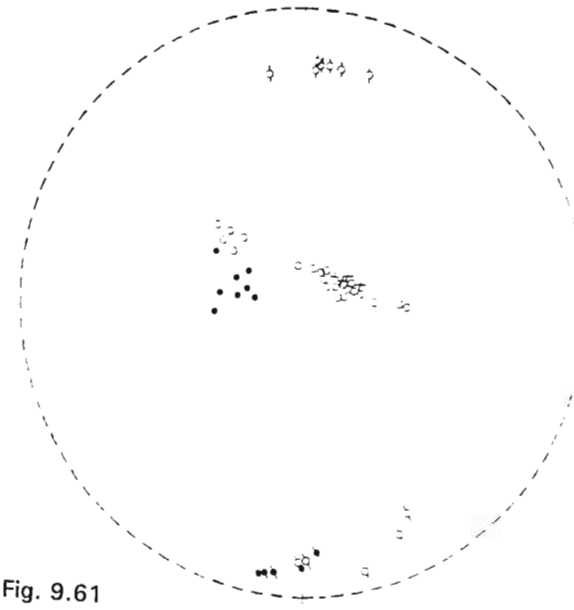

Fig. 9.61

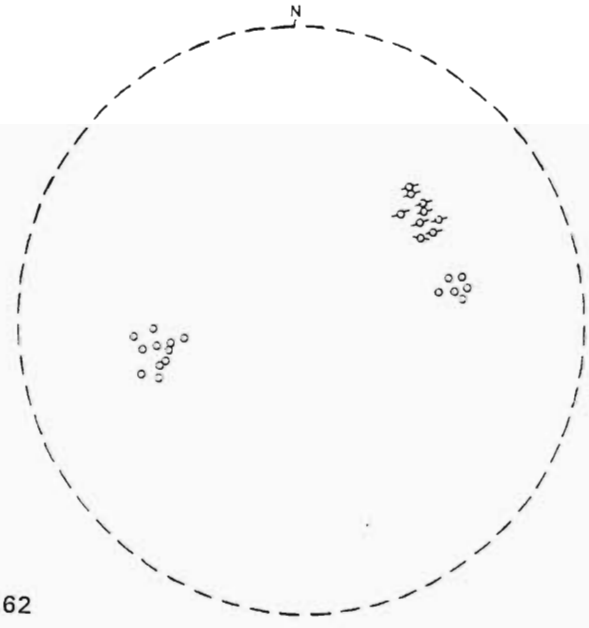

Fig. 9.62

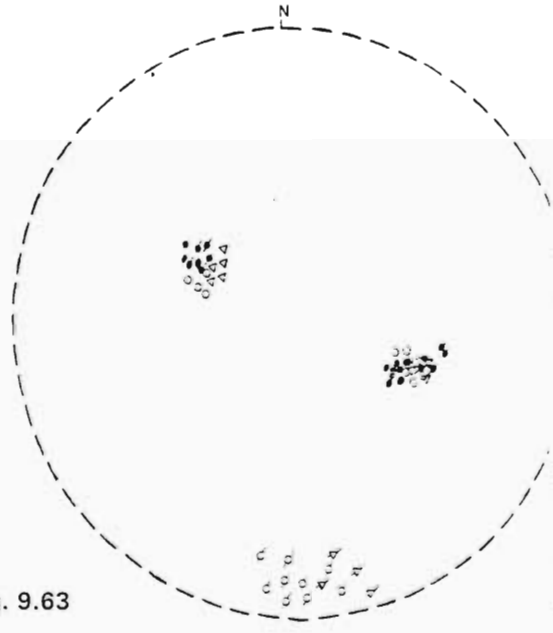

Fig. 9.63

Fig. 9.60 : Orientation data of D^G_2 structures in the migmatitic and mylonitic gneisses of the Mooiplaas Forest Plantation area.

- ● = Plunge of F^G_2 fold axes in the Nkwalini mylonites (n=10).
- ◐ = Poles to F^G_2 axial planes in the Nkwalini mylonites (n=9).
- △ = Plunge of F^G_2 fold axes in the Amazula Gneiss (n=5).
- ◺ = Poles to F^G_2 axial planes in the Amazula Gneiss (n=3).
- ▲ = Plunge of F^G_2 fold axes in the Nkwalinye Tonalitic Gneiss (n=4).
- ◤ = Poles to F^G_2 axial planes in the Nkwalinye Tonalitic Gneiss (n=4).
- o = Plunge of L^G_2 lineation (n=9).

Fig. 9.61 : Orientation data of D^G_2 structures in the Amazula Gneiss of the Amazula River area.

- ● = Plunge of F^G_2 axes of the antiformal similar fold (n=9).
- ◐ = Poles to F^G_2 axial planes of the antiformal similar fold (n=5).
- o = Plunge of other F^G_2 isoclinal fold axes (n=23).
- ⌀ = Poles to F^G_2 axial planes of isoclinal folds (n=12).
- X = Plunge of L^G_2 intersection lineations (n=4).

Fig. 9.62 : Orientation data of D^G_2 sheath folds in the Amazula Gneiss of the Amazula River area.

- o = Plunge of F^G_2 axes of sheath folds (n=17).
- ⌀ = Plunge of L^G_2 oblique lineation (n=9).

Fig. 9.63 : Orientation data of D^G_2 sheath folds in the Amazula Gneiss of the Umhlathuze River valley near the gorge.

- ⊙ = Plunge of F^G_2 axes of tight folds in Amazula Gneiss (n=10).
- ⌀ = Poles to F^G_2 axial planes of tight folds in Amazula Gneiss (n=9).
- △ = Plunge of F^G_2 fold axes in the Nkwalinye Tonalitic Gneiss (n=5).
- ◺ = Poles to F^G_2 axial planes in the Nkwalinye Tonalitic Gneiss (n=4).
- ◐ = Plunge of F^G_2 axes of sheath folds in the Amazula Gneiss (n=6).
- ● = Plunge of L^G_2 rodding lineation (n=8).

Measurements taken in the field on the keel-like structure (Plate 9.6B) and on other sheath folds (Plate 5.4) show these folds to plunge at an average angle of 40° to the ENE and WSW (Fig. 9.62). The mineral stretching lineation on the flanks of the keel-like structure occurs on a foliation plane of 268/79°N and plunges at about 43° on 046° (Fig. 9.62). It is defined by stretched slightly rodded quartz, mica streaking and elongated mineral aggregates. The presence of sheath folds with axes oblique to the lineation has been observed elsewhere (Fossen and Rykkelid, 1990; Bell and Hammond, 1984). Coward and Potts (1983) are of the opinion that these structures are formed by complex strains related to frontal or lateral tips of shear zones whereas Ridley (1986) invokes shear strain gradients perpendicular to the movement direction. Fossen and Rykkelid (1990) give a purely geometric explanation for the formation of fold axes oblique to the mineral stretching lineation.

9.3.3.2 ANALYSIS AND INTERPRETATION OF STRUCTURAL DATA FROM F^G_2 FOLDS

Compilations of structural data on the orientations of F^G_2 fold axes and axial planes of the migmatitic and mylonitic gneisses and the Nkwalinye Tonalitic Gneiss of the Northern Granitoid Complex are shown in Figs. 9.64A and B ***and*** Figs. 9.65A and B, whereas those of the Southern Granitoid Complex are shown in Figs. 9.66A and B.

The migmatitic gneisses (including the Nkwalinye Tonalitic Gneiss) and the mylonitic and flaser gneisses have been plotted separately for both the Northern Granitoid Complex and the Southern Granitoid Complex in order to see if there was any significant variation in the D^G_2 deformation in these lithologies on either side of the Ilangwe Greenstone Belt.

Figs. 9.64, 9.65 and 9.66 show remarkable similarities which are compiled in Fig. 9.67. An obvious aspect of Fig. 9.67 is the poorly-developed bimodal distribution of fold axes orientations in a vertical plane with azimuth 094°. One set of fold axes plunges westerly to WNW at about 30° to 85° and the other set (which is not strongly developed) plunges E to ESE at 40° to 80°. The axial planes of these folds are steeply dipping and are concentrated around the north and south poles (Fig. 9.67).

Another aspect of Fig. 9.67 is the steep NW plunge of the lithologies in the Mooiplaas Forest plantation area. The fold axes show a unimodal distribution in a vertical plane with azimuth 139°. This orientation is thought to be due to local rotation of fold axes probably as a result of the intrusion of the Nsengeni Granitoid Suite (see Fig. 2). It is of interest to

note that this orientation is similar to that which was assigned to D_3 deformation in the Ilangwe greenstones (compare with Fig. 9.44A and Fig. 9.45).

In the Southern Granitoid Complex, F^G_2 axes of sheath folds and isoclinal folds show slightly different orientations in the Amazula River area (6,7/AA,BB,CC,DD) and the Umhlathuze River area near the gorge (8.200/U,V,W). In the former locality, sheath folds in the Amazula Gneiss show a symmetric bimodal distribution about the vertical plane with azimuth 080° (Fig. 9.66A). They plunge to the WSW and ENE at about 40° and are not co-axial with the F^G_2 isoclinal folds which plunge to the E and W at steeper angles (Fig. 9.66A).

In the Umhlathuze River area near the gorge, the F^G_2 sheath folds plunge to WNW and ESE at a mean angle of 55° and show a symmetric bimodal distribution about the vertical plane with azimuth 115° (Fig. 9.66A).

Comparison of the compilations of D^G_1 fold elements (Fig. 9.55) and D^G_2 fold elements (Fig. 9.67) shows that the angle between the F^G_1 fold axes and the F^G_2 fold axes is approximately 10° to 20°. This suggests that the D^G_1 and D^G_2 deformations were approximately co-axial. Moreover, when the D^G_2 axes of the sheath folds of the Amazula Gneiss in the Amazula River are examined against the D^G_1 axes of isoclinal folds, it is found that they are also co-axial (compare Fig. 9.66A with Fig. 9.50B. Fig. 9.52, Fig. 9.53).

However, the F^G_2 sheath folds of the Amazula Gneiss in the Umhlathuze River area near the gorge (Fig. 9.66A) are ***not*** co-axial with the F^G_1 fold axes. They are in fact co-axial with the F^G_2 isoclinal fold axes. As was previously mentioned, an oblique mineral stretching lineation plunging at about 43° on 046° is associated with the sheath folds of the Amazula River area (Fig. 9.62).

The presence of D^G_2 sheath folds in the Amazula Gneiss of the Amazula River indicates a local history of plastic, non-coaxial deformation (probably developed under retrograde M_2 dislocation metamorphic conditions). This is supported by the presence of sigmoidal delta structures in thin section (Plate 9.6C). Many authors have demonstrated that sheath folds form under progressive non-coaxial simple shear where rocks have deformed plastically in ductile or semi-ductile shear zones (Mies, 1993; Fossen and Rykkelid, 1990; Skjernaa, 1989; Lacassin and Mattauer, 1985; Henderson, 1981; Cobbold and Quinquis, 1980; Carreras et. al., 1977; Rhodes and Gayer, 1977; Escher and Watterson, 1974).

PLATE 9.7 : D^G_2 AND D^G_3 STRUCTURES IN THE GRANITOIDS.

PLATE 9.7A : Tight D^G_2 isoclinal similar folds in the Nkwalini Mylonite Zone (5.400/NN.580). Note the shearing along the axial planar regions of the antiformal structure (i.e. from the right-hand top corner of the photograph to the right-hand bottom corner).

PLATE 9.7B : Ntshiweni Augen Gneiss intruding Amazula Gneiss in the Umhlathuze River west of Spelonk (2.380/P.040). Note the sharp intrusive contact. Also note the prominent quartz-feldspar augens which define a conspicuous L^G_3 lineation (L-tectonite).

PLATE 9.7C : D^G_3 dextral Nkwalinye River Shear Zone (below the red penknife – 84mm) in the Nkwalinye River (4.430/LL.130). The knife is subparallel to the shear zone boundary (c-plane) which is parallel to the S^G_2 foliation.

A

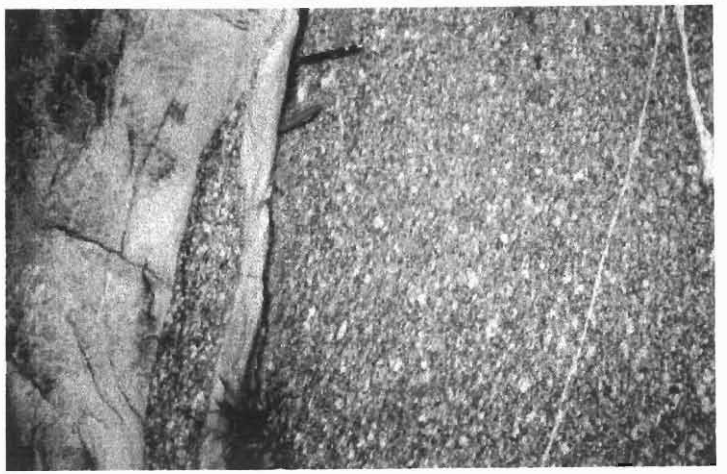

B

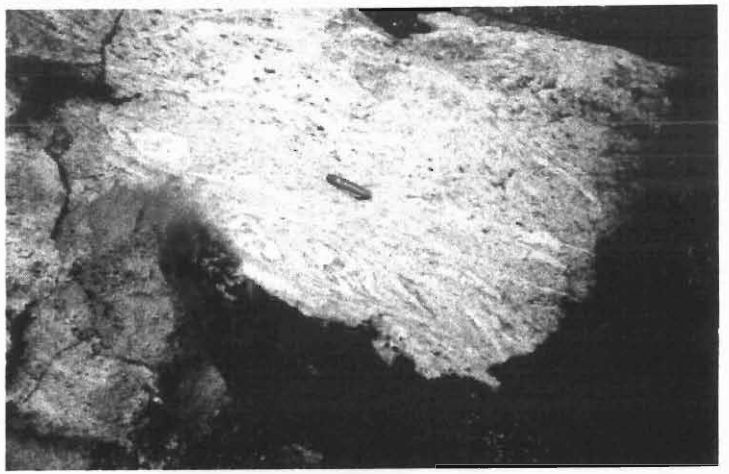

C

Plate 9.7

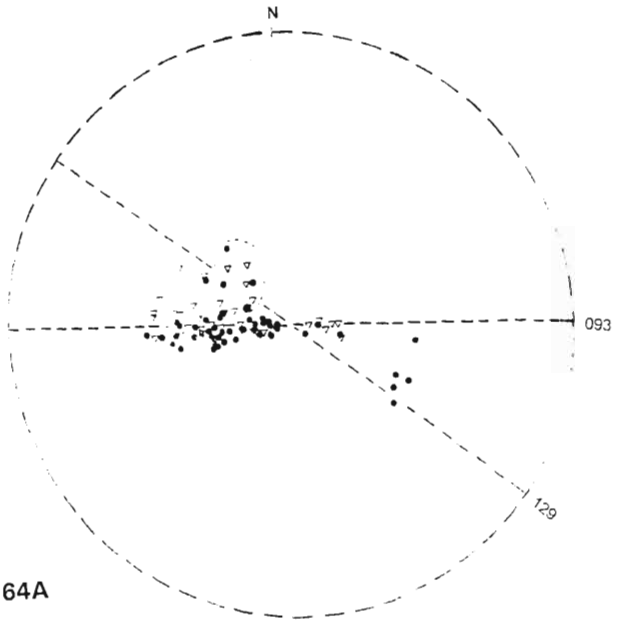

Fig. 9.64A

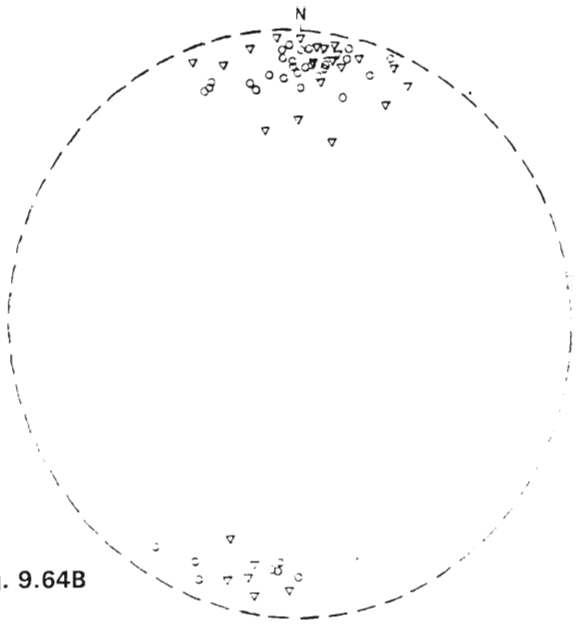

Fig. 9.64B

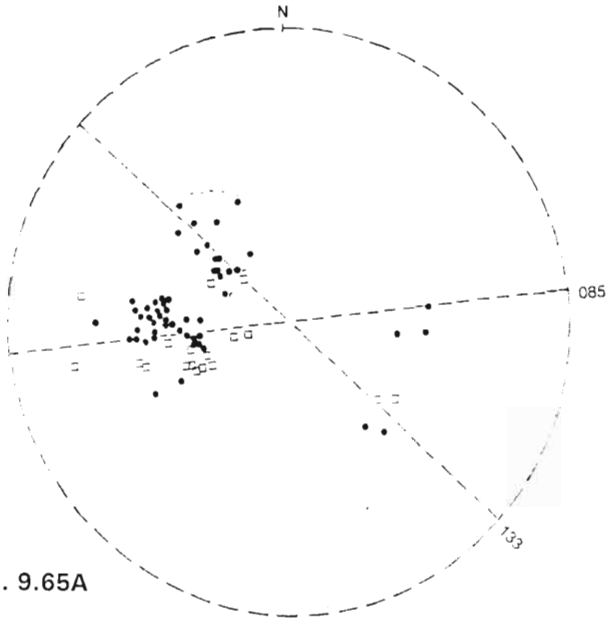

Fig. 9.65A

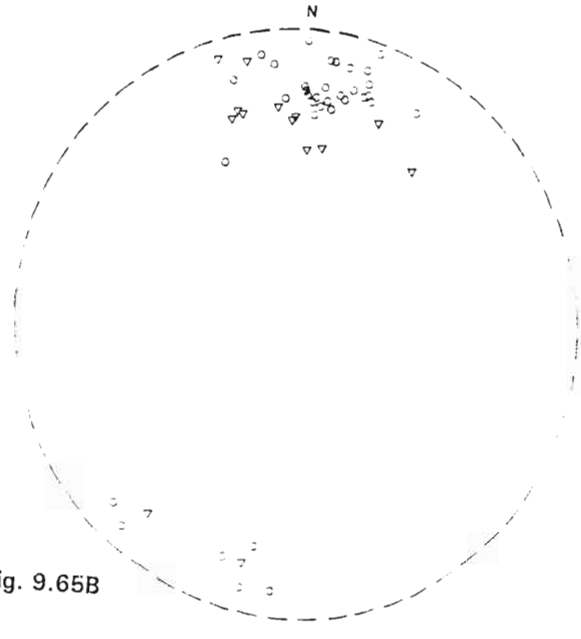

Fig. 9.65B

Fig. 9.64A : Compilation of structural data on theF^G_2 fold axes of the Amazula Gneiss and Nkwalinye Tonalitic Gneiss of the Northern Granitoid Complex

- ● = Plunge of fold axes in the Amazula Gneiss (n=29).
- ○ = Plunge of fold axes in the Nkwalinye Tonalitic Gneiss (n=31).

Fig. 9.64B : Compilation of the structural data on the F^G_2 axial planes of the Amazula Gneiss and Nkwalinye Tonalitic Gneiss of the Northern Granitoid Complex.

- ○ = Poles to axial planes in the Amazula Gneiss (n=35).
- △ = Poles to axial planes in the Nkwalinye Tonalitic Gneiss (n=26).

Fig. 9.65A : Compilation of structural data on the F^G_2 fold axes of the mylonitic gneisses in the Northern Granitoid Complex.

- ● = Plunge of fold axes in the Nkwalini Mylonitic Gneiss (n=55).
- □ = Plunge of fold axes in the Nkwalini flaser gneiss (n=18).

Fig. 9.65B : Compilation of structural data on the F^G_2 axial planes of the mylonitic gneisses of the Northern Granitoid Complex.

- ○ = Poles to axial planes in the Nkwalini mylonites (n=35).
- △ = Poles to axial planes in the Nkwalini flaser gneiss (n=14).

Further scrutiny of the F^G_2 fold elements of the granitoids reveals that they developed according to well-established geometrical principles (Ramsay, 1967 pp 538–545). ***Firstly***, Fig. 9.67 shows that the axial planes of the F^G_2 folds have a fairly constant northerly or southerly inclination even despite the variable orientation of the different linear structures (Fig. 9.68). For example, the Amazula Gneiss and to a lesser extent the Nkwalinye Tonalitic Gneiss in the Northern Granitoid Complex (Fig. 9.64A) and the Amazula Gneiss of the Amazula River (Fig. 9.66A) show a great variation in axial direction of the F^G_2 folds whereas their axial planes are constantly oriented (Fig. 9.64B and Fig. 9.66B). ***Secondly***, the dip of the F^G_1 fold limbs must have been subperpendicular to the steep to vertical F^G_2 axial planes in order to produce symmetric similar folds (Plate 9.3B; Plate 9.7A; Fig. 9.3). This geometry suggests that folding probably took place by heterogeneous simple shear (Price and Cosgrove, 1990; Ramsay and Huber, 1987; Ramsay, 1967). In the Nkwalini mylonites of the Nkwalini–Mzilikazi Peak area (4,5/MM,NN,OO), the F^G_2 similar folds are nearly coaxial with F^G_1 isoclinal folds (Fig. 9.3). The boudinaged and pinch-and-swell structure of the competent units in Plate 9.3B imply that boudinage and folding occurred during a single episode of deformation (Price and Cosgrove, 1990). This plate shows that the boudin lengths are parallel to the fold axis thus suggesting that the boudins formed because the limbs of the folds rotated into the extension field as the folds amplified (Price and Cosgrove, 1990).

Thirdly, because the F^G_1 folds were predominantly recumbent and isoclinal, it is observed that only one dominant F^G_2 axial direction developed (Figs. 9.65A and 9.66A). However, in the Umhlathuze River area near the gorge, the F^G_2 folds have two dominant axial directions which were controlled by the well-developed F^G_1 fold limbs and narrow hinge zones (Ramsay, 1967) and the fact that the distribution of the surfaces in the F^G_1 folds of this area does not show a large range (Fig. 9.53).

The D^G_2 deformation produced folds of a composite ***similar*** geometry which resulted from intense compression and flattening with associated widespread regional metamorphism accompanied by recrystallization, mineral growth and emplacement of the Nsengeni Granitoid Suite during the terminal stages of D^G_2 deformation, Composite similar folds are said to be common in the most strongly deformed zones of orogenic belts (Ramsay, 1967; Roberts, 1984). This F^G_2 fold geometry is consistent with the heterogeneous simple shear model (Ramsay, 1967; Ramsay and Huber, 1987).

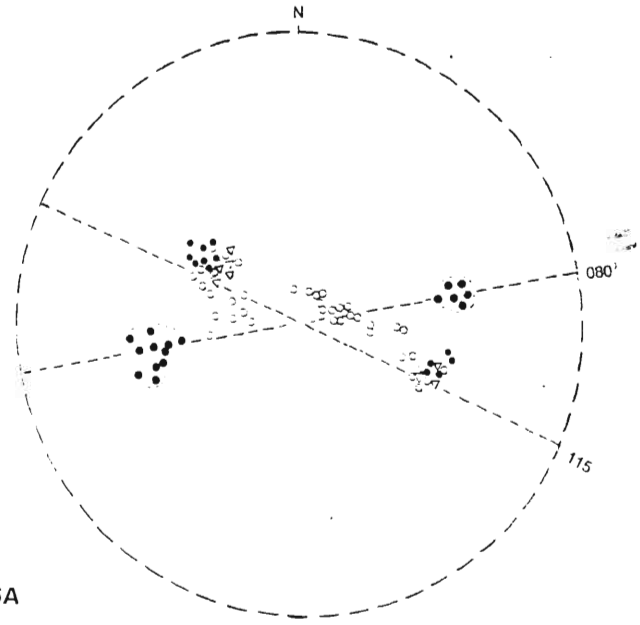

Fig. 9.66A

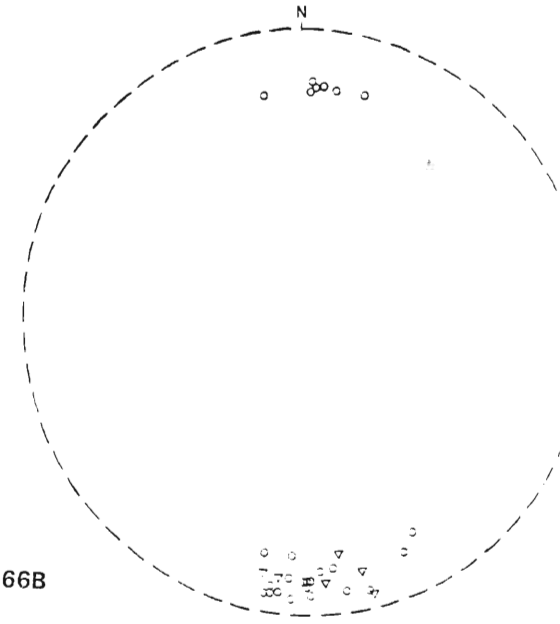

Fig. 9.66B

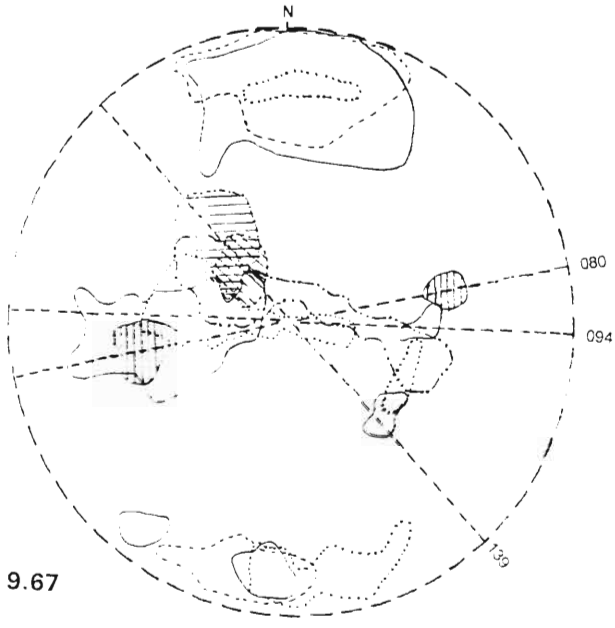

Fig. 9.67

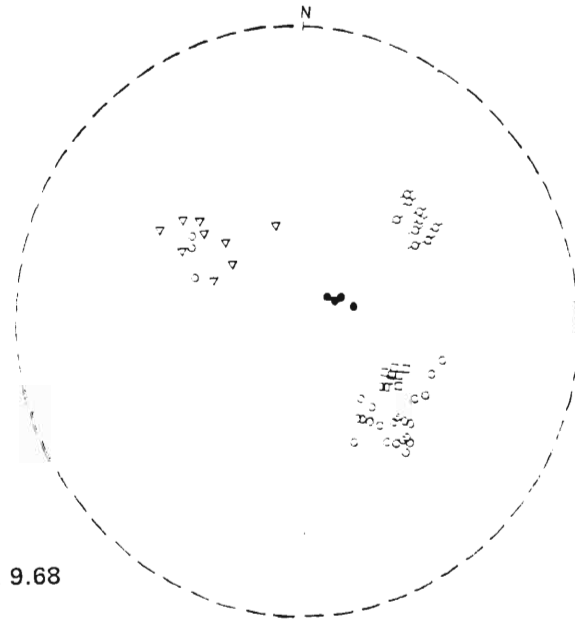

Fig. 9.68

Fig. 9.66A : Compilation of structural data on the F^G_2 fold axes of the Amazula Gneiss and Nkwalinye Tonalitic Gneiss of the Southern Granitoid Complex.

- o = Plunge of fold axes in the Amazula Gneiss.
- ● = Plunge of sheath fold axes in the Amazula Gneiss.
- △ = Plunge of fold axes in the Nkwalinye Tonalitic Gneiss.

Fig. 9.66B : Compilation of structural data on the F^G_2 axial planes of the Amazula Gneiss and Nkwalinye Tonalitic Gneiss of the Southern Granitoid Complex.

- o = Poles to axial planes in the Amazula Gneiss.
- △ = Poles to axial planes in the Nkwalinye Tonalitic Gneiss.

Fig. 9.67 : A combined plot of F^G_2 structural data of the migmatitic and mylonitic gneisses.

Fig. 9.68 : Orientation data of D^G_2 lineations in the Ilangwe Granitoid Complex.

- ⌀ = Plunge of L^G_2 mineral elongation lineation in the Amazula River.
- ● = Plunge of L^G_2 intersection lineation in the Amazula River.
- △ = Plunge of L^G_2 lineation in the Mooiplaas Forest Plantation area.
- o = Plunge of L^G_2 stretching lineation in the Nkwalinye-Nkwalini area.
- □ = Plunge of L^G_2 rodding in the Umhlathuze River near the gorge.

PLATE 9.8 : PENCIL AND INTERSECTION LINEATIONS IN THE AMAZULA GNEISS AND IN THE BANDED AMPHIBOLITE OF THE SABIZA FORMATION.

PLATE 9.8A : Steeply-plunging L_2 pencil lineation in the banded amphibolite of the Sabiza Formation in the Amazula River (6.740/AA.820).

PLATE 9.8B : Steeply plunging L^G_2 intersection lineation on the nose of the fold in the Amazula Gneiss of the Amazula River (7.160/AA.910). Note the sharp contact between the amphibolite (dark) and the Amazula Gneiss (light).

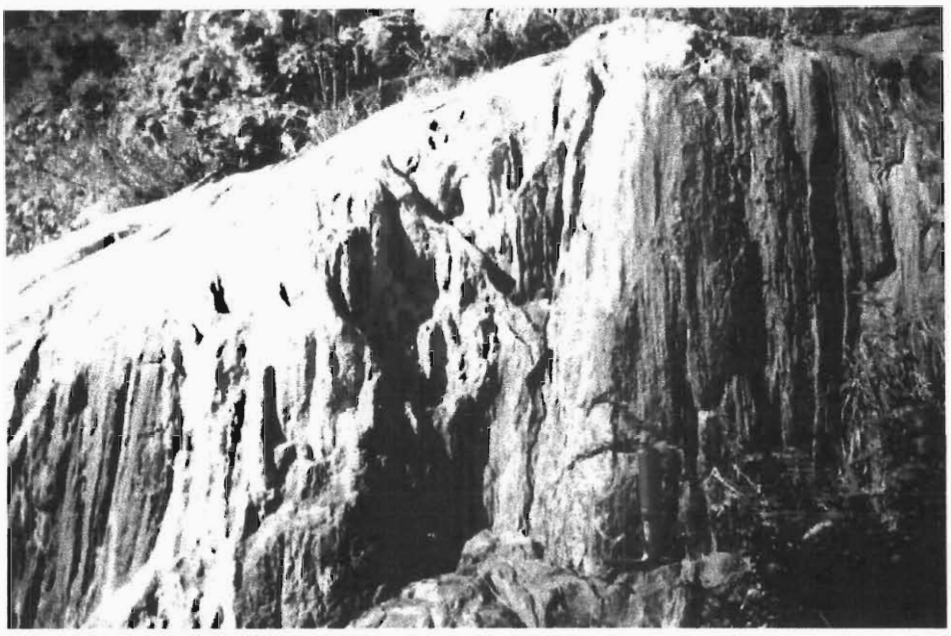

A

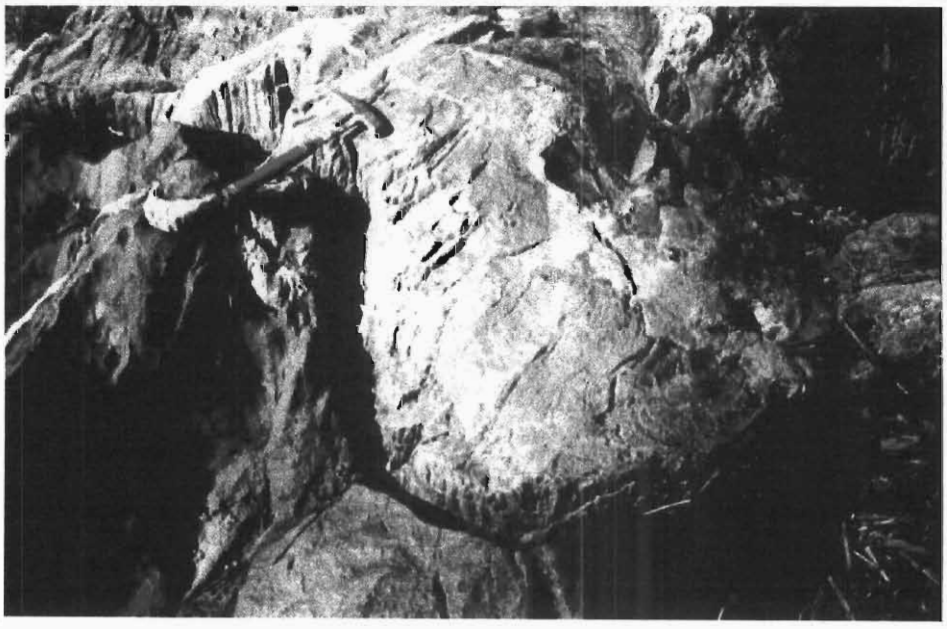

B

Plate 9.8

9.3.4 D^{G}_{3} PHASE OF DEFORMATION

9.3.4.1 GENERAL

D^{G}_{3} structures occur mostly in the Northern Granitoid Complex and are found in the Amazula Gneiss, Nkwalini Mylonitic Gneiss and the Nkwalinye Tonalitic Gneiss. In the Southern Granitoid Complex, D^{G}_{3} structures have been observed in the Amazula Gneiss of the Amazula River.

These structures comprise open folds (including reclined small-scale s-folds – Plate 9.3C), lineation and rodding. D^{G}_{3} folding has an open to close geometry which is characterized by round hinge zones which rarely show substantial thickening thus suggesting that the folding mechanism was due to flexural-slip. D^{G}_{3} folding is easily recognized in areas where F^{G}_{2} tight to isoclinal folds have been refolded. No penetrative S^{G}_{3} axial planar cleavage is associated with these folds. In areas where no refolded F^{G}_{2} isoclinal folds have been recognized, indirect evidence of D^{G}_{3} folding was observed from later classification of D^{G}_{3} folds and lineations with others that have a similar pattern of orientations of fold axes and the poles to axial planes. The more obvious support for D^{G}_{3} folding is the general arcuate nature of the Ilangwe Granite–Greenstone Complex which is evident from Fig. 2.

The D^{G}_{3} episode was also characterized by :

(i) the intrusion of the late post-Nondweni granitoids into the Ilangwe greenstones, the migmatitic and mylonitic gneisses ***and*** the early post-Nondweni Granitoids; and

(ii) the occurrence of shearing affecting the migmatitic and mylonitic gneisses and the early post-Nondweni granitoids.

These shears will be described in Section 9.3.4.3.

D^{G}_{3} structures are confined to the Nkalinye-Nkwalini area (1,2,3,4,5/KK,LL,MM,NN), the Sappi Mooiplaas forest plantation area (1,2,3/N,O,P,Q,R,S and the Amazula River area (6,7,8/AA,BB,CC). In these three localities, the Amazula Gneiss and the Nkwalinye Tonalitic Gneiss show similar orientations whereas the Nkwalini Mylonites have slightly

different orientations in the two localities where they occur, i.e. in the Nkwalinye-Nkwalini area and in the Sappi Mooiplaas forest plantation area.

The Amazula Gneiss and the Nkwalinye Tonalitic Gneiss have D^G_3 folds plunging steeply to the north to NNW and south with steep westerly to southwesterly inclined F^G_3 axial planes (Figs. 9.69, 9.70 and 9.71).

In the Nkwalini Mylonite zone (5/MM,NN), D^G_3 reclined asymmetric s-folds verge to the south (Plate 9.3C). They have fold axes plunging moderately to the south and F^G_3 axial planes inclined to the SSE at about 60° (Fig. 9.69). No associated L^G_3 lineation nor S^G_3 penetrative axial planar cleavage has been observed.

In the Nkwalini-type mylonites of the Sappi Mooiplaas forest plantation area (Fig. 9.9), D^G_3 folds are parallel vertical and upright plunging to the NNE and inclined steeply to the WNW (Fig. 9.72). An L^G_3 mineral stretching lineation is sub-parallel to the fold axis. This lineation occurs along the crests or troughs of the vertical folds and parallels the fold axis. It is denoted by quartz-feldspar minerals which, in some places, are rod-like

No D^G_3 folding was observed in the granitoids of the Nsengeni Suite. Foliation (Figs. 9.73A and B) is the only dominant structural feature of these granitoids. It trends predominantly E–W and dips steeply to the north and locally to the south. The Ntshiweni Augen Gneiss also shows a NNW–SSE trend with a southwesterly inclination. A prominent L^G_3 lineation (L-tectonite) occurs in the augen gneiss (Fig. 9.73B; Plate 9.7B).

As mentioned previously, the D^G_3 phase of deformation was characterized by the intrusion of the late post-Nondweni granitoids comprising the Umgabhi Granitoid Suite and the Impisi Granitoid Suite. These granitoids occur in the Southern Granitoid Complex and the Northern Granitoid Complex respectively and were emplaced subsequent to the development of the post-Nsengeni Suite greenstone boundary faults (i.e. the Entembeni and Matshansundu Faults).

A weakly-developed foliation is the only dominant feature in the Umgabhi Granitoid Suite. It is formed by aligned biotite-flakes and plagioclase feldspars. It is quite enhanced in the vicinity of the contacts with the country rocks but poorly-developed further away from the contacts. It was probably induced during emplacement because it parallels the foliation of the country rocks.

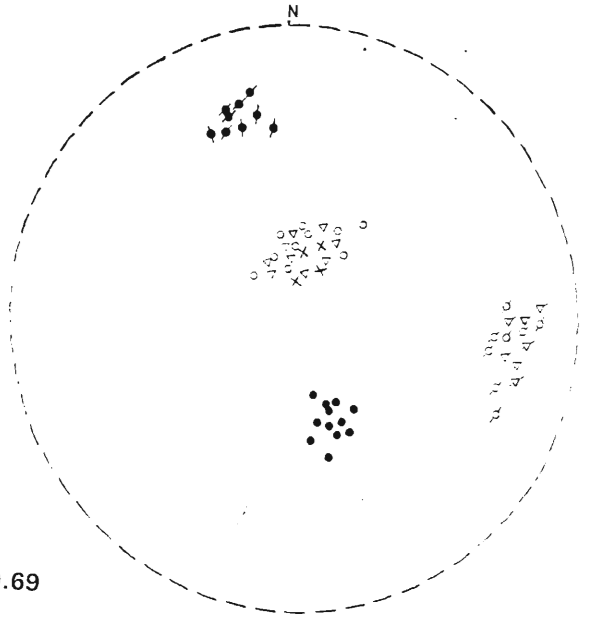

Fig. 9.69

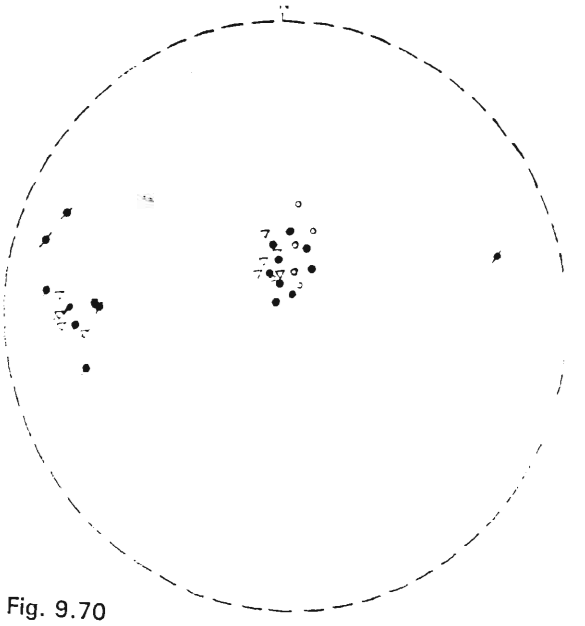

Fig. 9.70

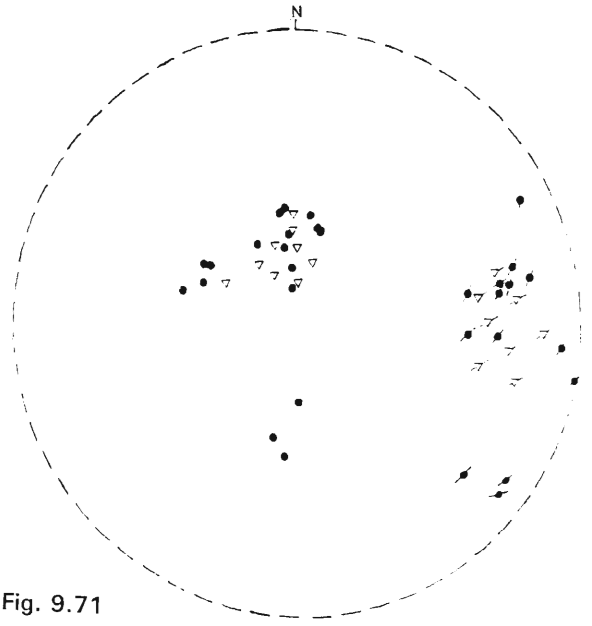

Fig. 9.71

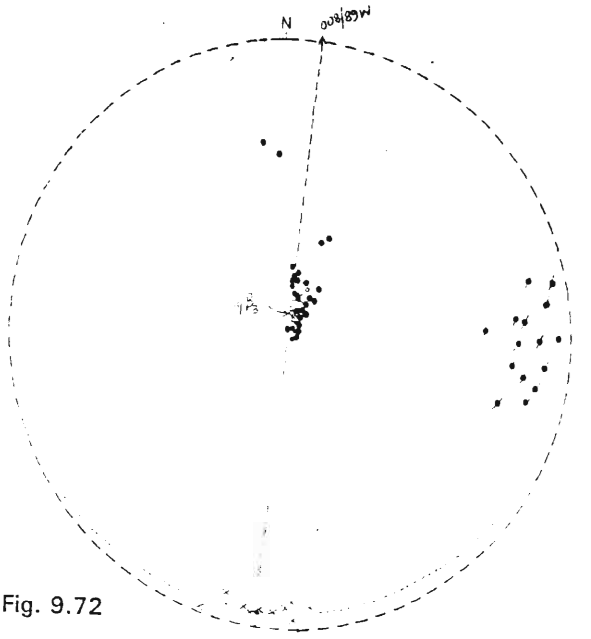

Fig. 9.72

Fig. 9.69 : Orientation data of F^G_3 structures in the Amazula Gneiss and Nkwalinye Tonalitic Gneiss of the Nkwalinye-Nkwalini area in the Northern Granitoid Complex.

- ● = Plunge of F^G_3 fold axes in the Nkwalinye mylonites (n=12).
- ◪ = Poles to F^G_3 axial planes in the Nkwalinye mylonites (n=9).
- ○ = Plunge of F^G_3 fold axes in the Amazula Gneiss (n=10).
- ◪ = Poles to F^G_3 axial planes in the Amazula Gneiss (n=8).
- △ = Plunge of F^G_3 fold axes in the Nkwalinye Tonalitic Gneiss (n=9).
- △ = Poles to F^G_3 axial planes in the Nkwalinye Tonalitic Gneiss (n=7).
- ✕ = Plunge of L^G_3 lineation (n=4).

Fig. 9.70 : Orientation data of F^G_3 structures in the Amazula Gneiss and Nkwalinye Tonalitic Gneiss of the Mooiplaas Forest Plantation area in the Northern Granitoid Complex.

- ● = Plunge of F^G_3 fold axes in the Amazula Gneiss (n=9).
- ◪ = Poles to F^G_3 axial planes in the Amazula Gneiss (n=9).
- △ = Plunge of F^G_3 fold axes in the Nkwalinye Tonalitic Gneiss (n=5).
- ◪ = Poles to F^G_3 axial planes in the Nkwalinye Tonalitic Gneiss (n=4).
- ○ = Plunge of L^G_3 lineation (n=6).

Fig. 9.71 : Orientation data of F^G_3 structures in the Amazula Gneiss and Nkwalinye Tonalitic Gneiss of the Amazula River in the Southern Granitoid Complex.

- ● = Plunge of F^G_3 fold axes in the Amazula Gneiss (n=17).
- ◪ = Poles to F^G_3 axial planes in the Amazula Gneiss (n=14).
- △ = Plunge of F^G_3 fold axes in the Nkwalinye Tonalitic Gneiss (n=9).
- ◪ = Poles to F^G_3 axial planes in the Nkwalinye Tonalitic Gneiss (n=8).

Fig. 9.72 : Orientation data of F^G_3 structures in the Nkwalini mylonites of the Sappi Mooiplaas Forest Plantation area in the Northern Granitoid Complex.

- ● = Plunge of F^G_3 fold axes in the mylonites (n=29).
- ◪ = Poles to F^G_3 axial planes in the mylonites (n=15).
- ○ = Plunge of L^G_3 lineation (n=8).
- ✕ = Poles to foliation in the gneisses (n=10).

PLATE 9.9 : STRUCTURES IN THE ENTEMBENI FORMATION META-SEDIMENTS OF THE ILANGWE PEAK AREA (5/Y).

PLATE 9.9A : A diagrammatic representation of a D_3 wedge-shaped or "keystone" uplift structure in the Entembeni Formation. The structure was formed as a result of the near-surface effect of D_3 transpression.

PLATE 9.9B : Sheared duplex-like structures in phyllonites of the Entembeni Formation on the southern margin of the Ilangwe "keystone" uplift structure (6.100/Y.490). The tectonic contact with the Sabiza amphibolites (not on photo) is just to the bottom left of the photograph. The northern contact of the structure is depicted on Plate 2.2A.

PLATE 9.9C : Intensely recrystallized Entembeni metachert in the Ilangwe Peak area. The plate shows the development of bedding-parallel cleavage (parallel to pen). Bedding is barely visible. The photograph was taken near the periclinal fold closure.

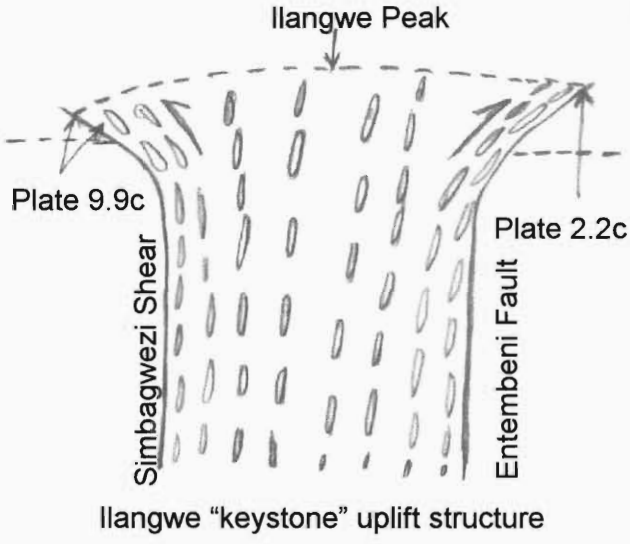
Ilangwe Peak
Plate 9.9c
Plate 2.2c
Simbagwezi Shear
Entembeni Fault
Ilangwe "keystone" uplift structure

A

C

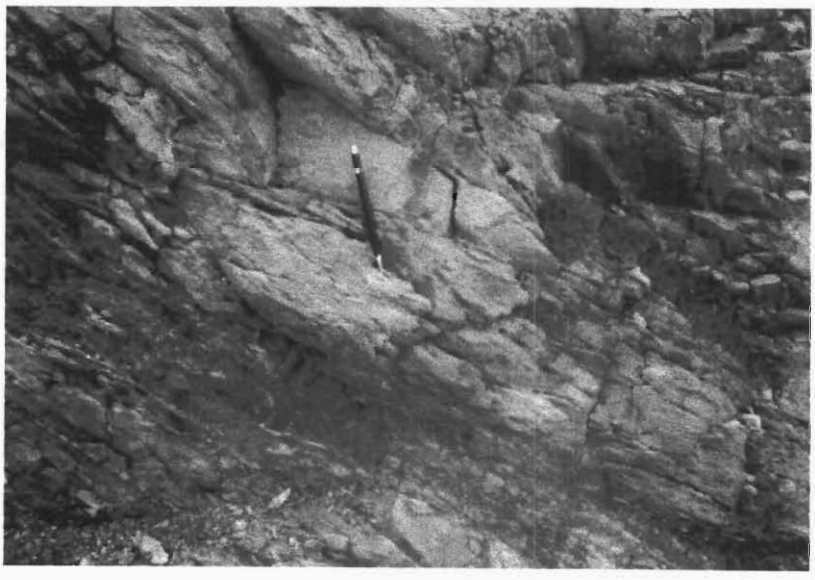

B

Plate 9.9

Foliation trends predominantly to the E–W and dips steeply to the north to northwest (Figs. 9.74A and B). Locally, the micrographic granite shows steep southerly dips. The quartz-sericite schist developed in the Esibhudeni Granitoid trends E–W to WNW–ESE and dips steeply to the north, NE and SSW. D^{G}_{3} open to close folds have been observed in the quartz-sericite schists. They plunge steeply to the north or south and are inclined steeply to the west (Fig. 9.74B). The lack of foliation in the Impisi Granitoids suggests that these granites (Nkandla and Zietover Granites) were intruded very late during D^{G}_{3} deformation or even after D^{G}_{3} deformation. This implies that the Umgabhi Granitoid Suite can be regarded as synkinematic granitoids whereas the Impisi Granitoid Suite can be regarded as post-kinematic granites.

9.3.4.2 ANALYSIS AND INTERPRETATION OF D^{G}_{3} STRUCTURES

Compilations of D^{G}_{3} structural data on the orientations of F^{G}_{3} fold axes and axial planes of the migmatitic and mylonitic gneisses (including the Nkwalinye Tonalitic Gneiss) are shown in Figs. 9.75A and B. The combined plot is shown in Fig. 9.75C. Fig. 9.75A shows that the Nkwalini mylonites and, to a lesser extent, the Amazula Gneiss have a bimodal distribution about the vertical plane with azimuth 351°. One set of fold axes plunges to the north to NNW at 40° to 90° and the other set plunges to the south to SSE at 50° to 70°. The axial planes are inclined steeply to the west with minor inclinations to the east (Fig. 9.75B). The post-Nondweni Nkwalinye Tonalitic Gneiss shows a unimodal distribution with steep (60° to 80°) plunges to the north (Fig. 9.75A).

Comparison of Figs. 9.67 and 9.75C shows that the steep westerly-dipping N–S trending F^{G}_{3} axial planes (Fig. 9.75C) are subperpendicular to the steep northerly-dipping E–W trending F^{G}_{2} axial planes (Fig. 9.67). This implies that the direction of compression of the D^{G}_{3} deformation was E–W. This compression produced open to close F^{G}_{3} folds. The mechanism of folding was probably flexural-slip. Fig. 9.76 is a diagrammatic representation of the F^{G}_{3} deformation. This is in line with the characteristic feature of polyphase deformation in which earlier generations of folds tend to be tight to isoclinal structures with well-developed schistosity parallel to their axial planes, while the later generations of folds (F^{G}_{3} in this case) are more open structures.

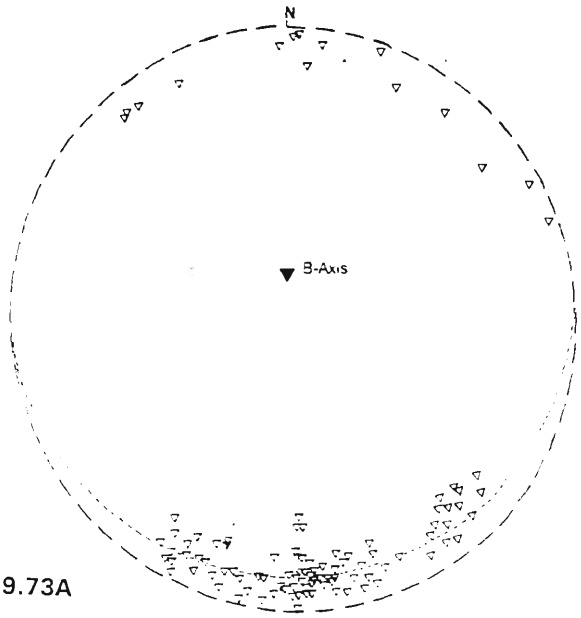

Fig. 9.73A

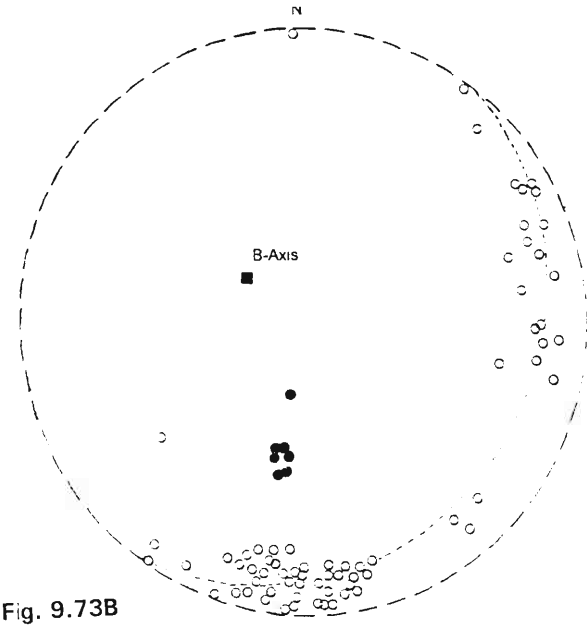

Fig. 9.73B

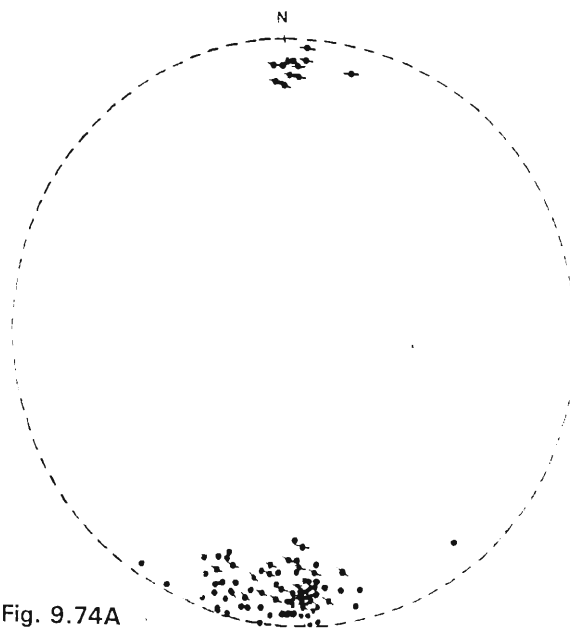

Fig. 9.74A

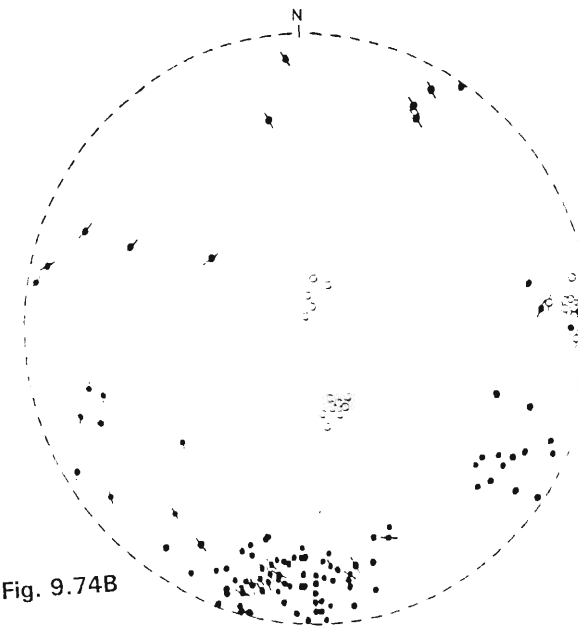

Fig. 9.74B

Fig. 9.73A : Distribution of undifferentiated foliation in the Nsengeni Granitoid Gneiss.
- Δ = Poles to foliation in the Nsengeni Granitoid Gneiss (n=120).

Fig. 9.73B : Distribution of undifferentiated foliation and orientation of L^G_3 lineations in the Ntshiweni Augen Gneiss.
- o = Poles to foliation in the Ntshiweni Augen Gneiss (n=69).
- ● = Plunge of L^G_3 lineation (n=7).

Fig. 9.74A : Distribution of D^G_3 foliation in the Umgabhi Granitoid.
- = Poles to foliation in the Umgabhi Granitoid (n=81).
- = Poles to foliation in the Umgabhi Micrographic Granite (n=29).

Fig. 9.74B : Orientation data D^G_3 structures in the Esibhudeni Granitoid and the Quartz-sericite schist of the Southern Granitoid Complex.
- ● = Poles to foliation in the Esibhudeni Granitoid (n=73).
- = Poles to foliation in the Quartz-sericite schist (n=38).
- o = Plunge of F^G_3 fold axes in the Quartz-sericite schist (n=13).
- = Poles to F^G_3 axial planes in the Quartz-sericite schist (n=8).

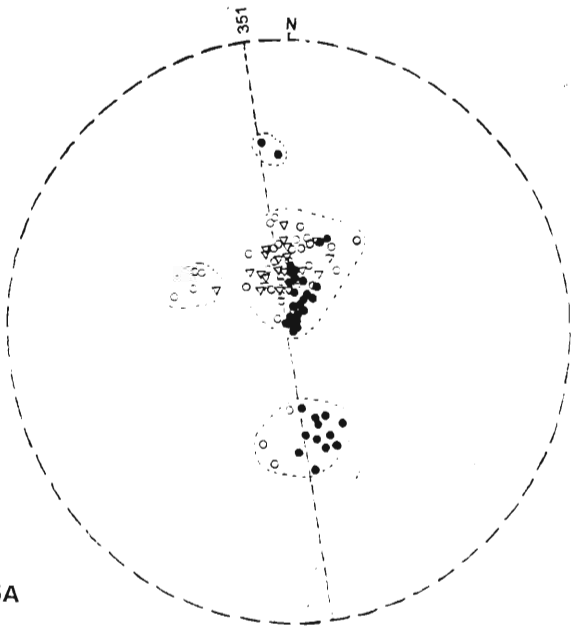

Fig. 9.75A

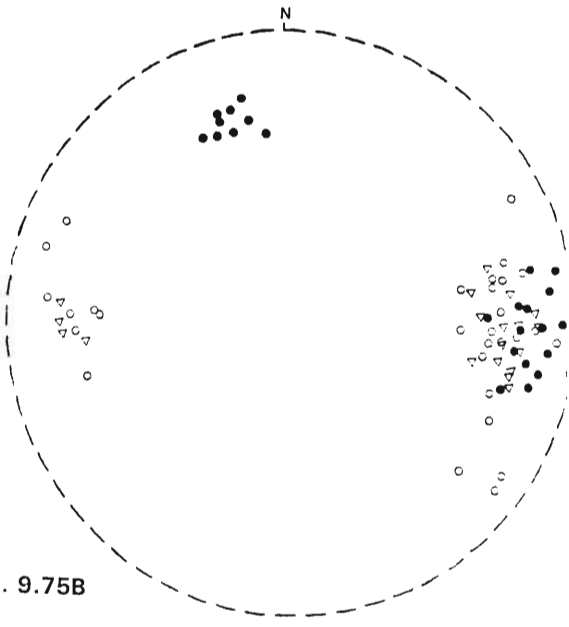

Fig. 9.75B

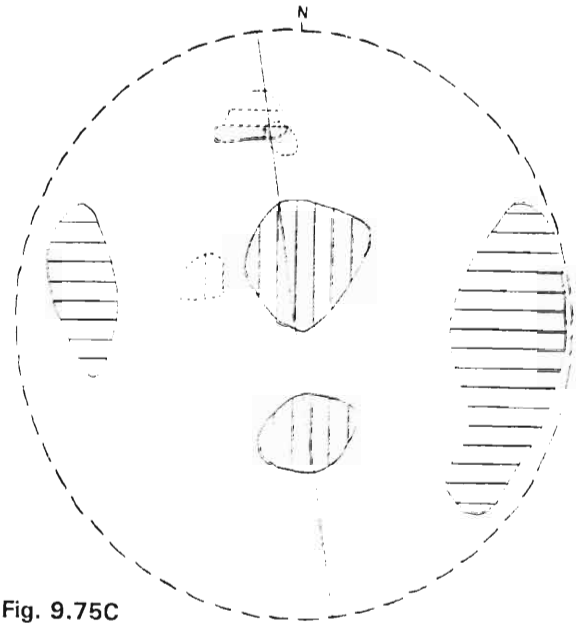

Fig. 9.75C

Fig. 9.75A : Compilation of structural data on the F^G_3 fold axes of the granitoids of the Ilangwe Complex.

- ● = Plunge of fold axes in the Nkwalini Mylonitic Gneiss.
- ○ = Plunge of fold axes in the Amazula Gneiss.
- △ = Plunge of fold axes in the Nkwalinye Tonalitic Gneiss.

Fig. 9.75B : Compilation of structural data on the F^G_3 axial planes of the granitoids of the Ilangwe Complex.

- ● = Poles to axial planes in the Nkwalini Mylonite Gneiss.
- ○ = Poles to axial planes in the Amazula Gneiss.
- △ = Poles to axial planes in the Nkwalinye Tonalitic Gneiss.

Fig. 9.75C : A combined plot of F^G_3 structural data on the Ilangwe granitoids.

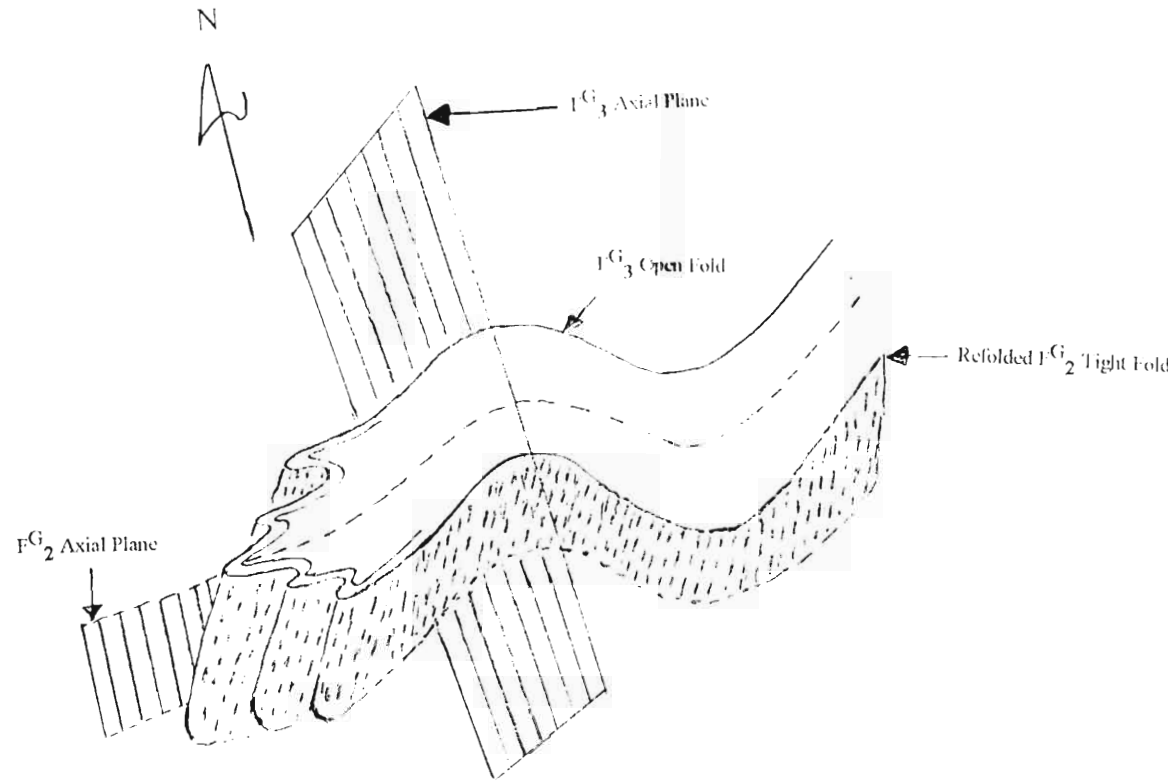

Fig. 9.76 : Exaggerated and simplified diagrammatic representation of the relationship between F^{G}_{2} and F^{G}_{3} fold elements.

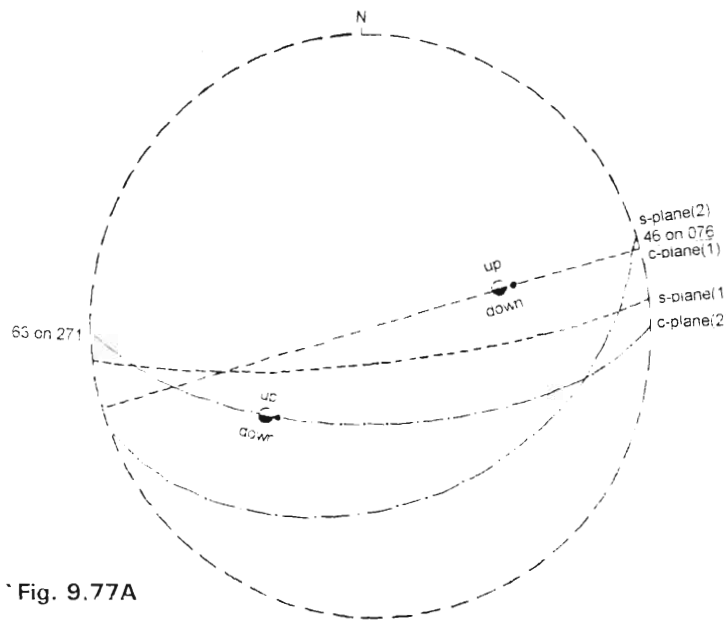

Fig. 9.77A

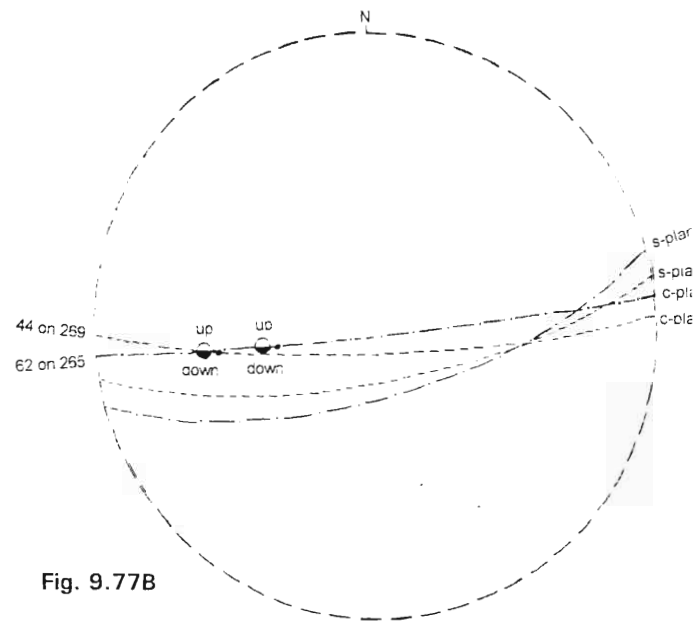

Fig. 9.77B

Fig. 9.77A and B : Orientation of ductile shear zones in the Nkwalini Mylonitic Zone of the Northern Granitoid Complex.

9.3.4.3 SHEAR ZONES IN THE GRANITOIDS

A number of shear zones, mostly D^{G}_{3} age, occur within the granitoids of the Ilangwe Complex. The most prominent shears occur in the Nkwalinye–Nkwalini area (4,5/KK,LL,MM,NN), Ntshiweni–Spelonk area (1,2/N,O,P,Q), Vumanhlamvu area (1/D), Esibhudeni area (7,8/G,H), Umhlathuze River area near the gorge (8/U,V,W) and in the Amazula River area (6,7,8/AA,BB,CC,DD).

In the Nkwalini Mylonite zone of the Nkwalini–Mzilikazi Peak area (4,5/NN,OO), there occur thin (±20cm) steep southerly dipping ductile shear zones with s–c planes showing a north over south sense of shear (Fig. 5.3; Plate 5.5A; Plate 5.5C). Some of these shear zones have been intruded by weakly foliated metagabbro (Fig. 5.3). Figs. 9.77A and B show the orientation of the ductile shear zones.

In the Nkwalinye River (4/KK,LL) and within the Nkwalinye Tonalitic Gneiss, there occurs the thin but extensive Nkwalinye River shear zone which is about 40-50 cm wide and shows a dextral sense of shearing (Plate 9.7C). It contains sigmoidal en echelon tension gashes formed parallel to the maximum principal compression and which became rotated with progressive deformation (Price and Cosgrove, 1990). Plate 9.7C shows that maximum shear stress occurred in the region just below the red knife.

At the confluence of the Safube and Nkwalinye Rivers (4.450/LL.155), intense foliation transposition in the tonalitic gneiss occurred due to shearing. It resulted in the formation of natural back-rotated layer segments (Type IIb asymmetrical pull-aparts – Hanmer and Passchier, 1991; Hanmer, 1986) (Plate 6.1A) and natural back-rotated pinch-and-swell structures (Type IIa asymmetrical pull-aparts – Hanmer and Passchier, 1991; Hanmer, 1986) (Plate 6.1B). Similar structures are found in the Amazula Gneiss (Plate 5.1A and C).

In the Amazula River area, there occurs the ductile Amazula River Shear Zone which is a ±300 metre long and ±75 metre wide E–W trending zone of intense deformation. The northern boundary of this shear zone is highly incised by the E–W flowing Amazula River. To the north and south of the shear zone, the rocks are less deformed. It can be clearly seen that the increase in strain occurs from the surroundings into the zone which consists of converging and diverging layers of subparallel lithologies enclosing less deformed augen rock (Plate 5.2B). Kinematic indicators such as anastomosing foliations, deformation of quartzo-feldslpathic veins and the crenulation cleavage formed by compression of the

shear zone fabric all show the sense of movement to be sinistral (Fig. 5.1; Plate 5.2B). The shear zone is obscured by deep weathering both to the east and west. The amphibolitic variety of the Amazula Gneiss shows a well-developed s–c fabric (Plate 9.5A; Plate 5.2B; Fig. 5.1; Berthé et. al., 1979; Lister and Snoke, 1984). The c-plane trends 087° and has an inclination of 85°N whilst the s-plane strikes 102° and is inclined steeply (70°) to the north. The angle between the s- and c-plane is 23°. The c-plane parallels the shear zone boundaries (Plate 5.2B). This is a Type I s-c fabric (Lister and Snoke, 1984). In reality the c-plane is a composite surface of mylonitic foliation (the CS surface of Berthé et. al., 1979) which is a foliation parallel to transposed earlier structures that have been developed in a high strain zone (Fossen and Rykkelid, 1990; Rykkelid and Fossen, 1992). The s-plane is a foliation structure oblique to the CS foliation and was formed by local rotation of the latter (Fossen and Rykkelid, 1990; Rykkelid and Fossen, 1992).

In the Esubhudeni area a number of thin shear zones are associated with the development of quartz-sericite schists. Kinematic indicators show a right-lateral sense of movement. A similar sense of movement is shown by shear zones in the Vumanhlamvu area which were developed near the contact of the Nomangci quartz-sericite schists and the Nkandla Granite.

PART 4

9.4 TECTONIC CORRELATION AND SYNTHESIS

9.4.1 INTRODUCTION

The aim in this section is to synthesise the structural data of the Ilangwe granite-greenstone complex and to attempt to correlate the different deformational episodes in the granitoids with those in the greenstones. To achieve this, the structural history or development of the Ilangwe Greenstone Complex will be discussed first. This will be followed by the structural correlation of the deformation events in the granitoids with those in the greenstones.

9.4.2 STRUCTURAL HISTORY OF THE ILANGWE GREENSTONE COMPLEX

Basement to the Ilangwe rocks is not known. The Amazula Gneiss, the oldest gneiss in the study area is regarded as the ***foundation*** to the Ilangwe rocks mainly because it contains mafic and ultramafic enclaves which are possibly fragments of earlier recycled simatic basement (oceanic crust). However, no evidence has been found to suggest that it is older than the Sabiza mafic and ultramafic rocks which are regarded as having been derived from mantle sources. The migmatitic and mylonitic gneisses ***and*** the Sabiza amphibolites are here regarded as forming a major crustal framework upon which younger rocks were deposited.

The Ilangwe rocks were laid down in shallow submarine environments similar to the Barberton and Pietersburg belts (de Ronde and de Wit, 1994; de Wit, et. al., 1992; Jones, 1990). Geochemical evidence presented in Chapter 10 shows that the mafic rocks are tholeiites of oceanic affinity and are derived from volcanic activity as supported by pillow structures; whilst the ultramafic rocks are regarded as altered equivalents of komatiites. The metasediments range from volcanic exhalative to shallow marine deposits. Three phases of deformation (D_1, D_2 and D_3) have affected the Ilangwe rocks.

The early Archaean Ilangwe oceanic crust was probably very thin and it grew (or thickened) as a result of the combined processes of recumbent and isoclinal folding together with tectonic stacking and repetition. This process of "continental growth" began during the first-phase of deformation with the deposition of the rocks of the Umhlathuze and Nkandla Subgroups in oceanic environments.

During D_1, there was development of a penetrative tectonic foliation (S_1) parallel to the S_0 primary layering and bedding. As was mentioned in Section 9.2.2.2, D_1 was characterized by transpositional layering, recumbent and isoclinal folding [with fold axes aligned in a more-or-less ENE (60°) direction] together with shearing and thrusting.

Evidence for transpositional layering is in the occurrence of intrafolial folds and rootless intrafolial folds in the Sabiza amphibolites and in the Olwenjini and Entembeni metasediments. Evidence for F_1 recumbent folding is provided by the Type 3 interference folds in the Sabiza amphibolites (Plate 9.1A). Evidence for early shearing and thrusting is postulated from the occurrence of the Sabiza banded amphibolites and the Amazula Gneiss in juxtaposition within the D_3 Umhlathuze River Shear Zone which is thought to be a

reactivated thrust or shear zone. These units were juxtaposed during D_1 deformation as a result of subhorizontal thrusting (and stacking).

Another evidence of early bedding parallel shearing or thrusting is provided by the occurrence of the quartz-biotite-cordierite-fuchsite gneiss within the metasediments of the Olwenjini Formation in the Sabiza River area (5.180/V.800). This gneiss was probably formed as a result of dislocation metamorphism at medium pressures (Winkler, 1979).

In the western sector, there is also evidence of repetition and stacking of lithological units of the Simbagwezi and Nomangci Formations. Firstly, around Simbagwezi Peak (5,6/H,I,J,K,L,M), there is extensive wedging of the Simbagwezi Formation between the Sabiza Formation to the south and the Olwenjini Formation to the north, Secondly, further westwards near the Nkandla forest, there is interfingering and repetition of Nomangci quartzites and Simbagwezi phyllites. This repetition is suggestive of normal dip-slip duplexes (Woodstock and Fischer, 1986) as shown on Fig. 2 at locality (4,5,6/C,D,E,F,G). All these associations suggest that D_1 was dominated by the formation of fold nappes and thrusts.

The important characteristic of D_1 deformation is that it took place in an essentially horizontal, regional high strain tectonic regime. The analysis presented in Section 9.2.2.3 suggests that the inferred direction of compression of the D_1 deformation was NNW–SSE. D_1 deformation was accompanied by prograde M_1 amphibolite facies medium-grade metamorphism.

By this time (post-D_1 folding), the Ilangwe crust had thickened considerably and partial melting was initiated at depth. This resulted in the generation of the post-Nondweni Nkwalinye tonalitic magma which intruded the greenstones mainly along lithological layering and during the early stages of D_2 deformation. Also, by this time the western sector of the greenstone belt had emerged as evidenced by the occurrence of clean white quartzites and metacherts of the Nomangci Formation which are regarded as being deposited in an emerging submarine to subaerial environment and are probably syndepositional to a collision event similar to the Moodies Group of the Barberton Greenstone Belt (de Ronde and de Wit, 1994).

The D_1 recumbent and isoclinal folds were refolded by new structures with steeply inclined axial planes during D_2 deformation (see Fig. 9.46B). In the Sabiza amphibolites, the new

D_2 structures were isoclinal and similar folds which resulted in Type 3 interference structures (Plate 9.1A). In the Olwenjini and Entembeni metasediments, the new steep structures resulted in the formation of large-scale doubly-plunging periclinal folds which generally trend E-W with steeply inclined and overturned limbs and have narrow, closed elliptical outcrops forming a typical pattern of right-hand en-echelon folding (Plate 9.2C). Flattening normal to the axial planes produced a penetrative axial planar foliation (S_1 // S_2).

Anticlinal and synclinal forms of the periclinal folds have been recognized in the Ilangwe Peak area. However, in general, the recognition of these forms is limited by lack of abundant way up indicators; difficulty in the establishment of the plunge of folds as a result of recrystallization and brecciation around fold closures (Plate 9.2); and the near vertical dip of the fold limbs and the associated cleavage (see Plate 9.9C and Plate 9.2B).

Evidence presented in Section 9.2.3.2 suggests that the D_2 phase of deformation was a major compressional event which produced the large-scale upright flattened flexural folds which are well-defined by banded ironstones and metacherts.

D_2 deformation was accompanied by regional M_2 greenschist facies metamorphism. This is supported by the dominant occurrence of muscovite/fuchsite and chlorite in the metasediments, especially cherty quartzites. Some of the fuchsite is thought to be due to K-metasomatism which probably took place during the waning stages of greenschist metamorphism.

Partial melting of the now thickened Ilangwe crust resulted in the formation of the potash-rich Nsengeni magma which intruded along the margins of the Ilangwe greenstones during post-D_2 folding event. In the northern part of the western sector, the greenstones were intruded by the Ntshiweni Augen Gneiss, the first phase of the Nsengeni Granitoid Suite. The Nsengeni Granitoid Gneiss intruded on either side of the greenstone belt in the central and eastern sectors.

The final stages of the D_2 deformation resulted in the formation of the subvertical greenstone boundary faults – the Matshansundu and Entembeni Faults and the Vungwini River shear. These lineaments contain complex internal structures like breccias and mylonites and show a curvilinear geometry. The brecciated material and the mylonitized nature of the Nsengeni granitoids in some places suggest that the boundary faults are post-Nsengeni Granitoid Gneiss in age.

The D_3 phase of deformation was dominated by formation of moderately to steeply plunging small-scale folds on the limbs and axial planes of the pre-existing D_2 perclinal folds (see Fig. 9.46C). The fold axes of these D_3 folds plunge NW and SE at about 40°-70°. This bimodal distribution of fold axes conforms with a well-known model of superposed folding in which the axes of the later folds are generated parallel to the lines of intersection of the later XY tectonic plane with the limbs and the axial planar foliation of the earlier folds. The axial planes of these folds are subvertical and are oblique to the E–W orientation of the D_2 periclinal folds. In Section 9.2.4.3, this oblique relationship was attributed to a D_3 transpressional deformation with a sinistral component of shear in response to a slight clockwise rotation of the regional compressive stress. This rotation is thought to have been further enhanced by the D^G_3 intrusion of the late post-Nondweni granitoids which caused the greenstone belt to buckle and thus assume an arcuate shape as shown in Fig. 2.

A diagrammatic representation of the deformation phases in the greenstone belt is shown in Fig. 9.46. At this stage, the Ilangwe crust was considerably thicker and partial melting at depth resulted in the generation of the "late post-Nondweni magma" which was potassic in composition.

The late post-Nondweni granitoids are divided into two suites. The Umgabhi Granitoid Suite intruded the greenstone belt along the southern boundary whereas the Impisi Granitoid Suite intruded along the northern boundary in the western sector. In the eastern and central sectors, the Umgabhi granitoid and the Umgabhi Micrographic Granite forcefully intruded the greenstones to form re-entrant extensions. In the Ndloziyana Peak area this diapiric intrusion of the micrographic granite further deformed the Ndloziyana angular unconformity. In the western sector, the Nkandla Granite also formed re-entrant extensions into the Nomangci Formation.

D_3 deformation was accompanied by M_3 low grade metamorphism. In the Mandaba and Makhanyezi areas (2,3,4/G,H,I,J), intrusion of the Nkandla Granite resulted in prograde M_3 upper greenschists metamorphism of the Nomangci quartz-sericite-schists and formed kyanite. In the Esibhudeni area (7,8/G,H,I,J,K,L,M), thin phyllonite zones of quartz-sericite-schists occur within the Esibhudeni Granitoid. These schists are associated with shear zones in the granitoids and contain retrograde assemblages related to the M_3 dislocation metamorphism. Within these schists, small-scale D_3 folds have been found.

The post-D_3 period in the Ilangwe greenstones is dominated by the intrusion of metagabbroic bodies and the occurrence of late-stage faulting.

9.4.3 STRUCTURAL CORRELATION OF THE GRANITOID DEFORMATION WITH THE ILANGWE GREENSTONE DEFORMATION

Just like in the greenstones, three episodes of deformation (designated D^G_1, D^G_2 and D^G_3) have been recognized in the older gneisses of the Ilangwe granitoid complex. These deformation events differed somewhat from those in the greenstones in that :

(i) no primary layering (S^G_0) has been unequivocally established in the granitoids (except the remnants of S^G_0 displayed by small-scale intrafolial folds);

(ii) unlike in the greenstones, no large-scale D^G_2 folds have been recognized in the granitoids;

(iii) sheath folds of D^G_2 age have been recognized in the Amazula Gneiss but not in the greenstones; and

(iv) the deformation sequence in the older granitoid gneisses was interrupted, and probably modified, by younger granitoid intrusions.

The earliest recognizable fabric in the migmatitic and mylonitic gneisses (older gneisses) is an S^G_1 gneissic banding denoted by elongate minerals like hornblende and biotite which lie parallel to D^G_1 segregation layering (which is the dominant structure) and hence a tectono-metamorphic origin is inferred for the layering. Thus, the S^G_1 foliation represents the finite flattening plane (Hobbs, et. al., 1976).

The first phase of deformation (D^G_1) is characterized by isoclinal intrafolial folding and transpositional layering together with migmatitization and mylonitization. These migmatites and mylonites together with the intense transpositional layering are a product of extreme deformation involving high strain, elongation and associated high grade of metamorphism. Elongation of the competent layers led to the development of pinch-and-swell boudinage structures which are thought to be common in crustal and small-scale shear or thrust zones at very high strains (Cobbold and Quinquis, 1980; Lister and Snoke, 1984; Fossen and Rykkelid, 1990; Rykkelid and Fossen, 1992).

Similar to the greenstones (especially the Sabiza banded amphibolites), the first phase of deformation was accompanied by prograde medium-grade M_1 middle amphibolite facies metamorphism. The analysis presented in Section 9.3.2.3 shows that there is a close correspondence between D_1 and D^G_1 elements (see Figs. 9.19; 9.20 and 9.56) which are aligned about a vertical plane with a northeasterly azimuth. This suggests that the first phase of deformation in the granitoids is synchronous with the first phase of deformation in the greenstones and these deformations can possibly be correlated. This deformation took place in a horizontal high strain tectonic regime characterized by isoclinal and recumbent folding with associated thrusting. Unfortunately, the analysis presented in Sections 9.2.2.2 and 9.2.2.3 does not indicate a direction of tectonic transport. However, the analysis showed that the inferred direction of compression of the first phase of deformation was NNW–SSE.

The post D^G_1-folding period is characterized by the intrusion of the Nkwalinye Tonalitic Gneiss possibly along lithological layering of the greenstones and the older gneisses. The tonalite gneiss was deformed together with the older gneisses during D^G_2. The salient features of this deformation (D^G_2) are :

(i) the occurrence of tight to isoclinal composite similar folds which plunge steeply to the WNW and rarely to the ESE – a weak bimodal distribution about a vertical plane with an easterly azimuth (094°) which contrasts sharply with the strong bimodal distribution in the greenstones;

(ii) the occurrence of sheath folds in the Amazula Gneiss of the Southern Granitoid Complex. In the Amazula River area, sheath folds plunge shallowly to the WSW and ENE and show a bimodal distribution about a vertical plane with azimuth 080° (see Fig. 9.67). These folds are not coaxial with the F^G_2 folds but are rather coaxial with the F^G_1 folds. In the Umhlathuze River area near the gorge, sheath folds plunge to the WNW and ESE at about 55° and show a symmetric bimodal distribution about a vertical plane with azimuth 115°. They are coaxial with the F^G_2 folds; and

(iii) in the Mooiplaas Forest Plantation area, the F^G_2 folds plunge steeply to the NW and show a unimodal distribution about a vertical plane with azimuth 139°.

In comparison with the D_2 deformation in the greenstones, the orientation of the F^G_2 folds is similar to that of the F_2 folds in the greenstones (i.e. being oriented about a vertical plane with a predominantly ESE (100°) azimuth but the bimodal distribution is not well-developed in the granitoids – probably due to the absence of large-scale folds.

Of particular interest however, is the orientation of the F^G_2 folds in the Sappi Mooiplaas Forest Plantation which is rather identical to that of the D_3 folds in the greenstones which give a NW plunge about a vertical plane with azimuth 135° (compare Figs. 9.44A and 9.45 with Fig. 9.67). This change in orientation in the Sappi Mooiplaas Forest Plantation Area can be attributed to clockwise rotation of F^G_2 fold elements during the intrusion of the Nsengeni Granitoid Suite.

In section 9.3.3.2, the F^G_2 folding was attributed to heterogeneous simple shear whereas the F_2 folding is consistent with the flexural fold model (see Section 9.2.3.3). The second phase of deformation in both the greenstones and granitoids was characterized by intense compression, flattening and rotation. It was superimposed at right angles to the first deformation and was accompanied by regional greenschist facies metamorphism. D_2 and D^G_2 are dissimilar but probably coeval. The different structures found in the Ilangwe greenstones and the Ilangwe granitoids can be attributed to competency contrast between the different lithologies in these terrains. The voluminous intrusion of the Nsengeni granitoids probably interrupted and modified the deformation in the granitoids.

The third phase of deformation (D^G_3) in the granitoids is characterized by open to close buckle folds with variable plunges to the north to NNW and south to SSE. They show a bimodal distribution about a vertical plane with a northerly azimuth (351°). They were probably initiated by oblique compressive stresses – transpression – and were further modified by the intrusion of the late post-Nondweni granitoids.

Evidence of transpression is afforded by the orientation of the folds in the D^G_3 Amazula River Shear Zone where F^G_3 folds are at a high angle to the overall zone (Fig. 9.71) and according to Sanderson and Marchini (1984), this compression is usually accommodated by crustal thickening which produces uplift. The uplifted regions are also areas of more intense strain (Plate 9.4A). Transpression is also demonstrated in Plate 9.5A where the short limbs of open folds are in the compressional field of the strain ellipse whereas the tight folds have rotated into the extensional field.

In contrast to the granitoids, D_3 folds in the greenstones are represented by chevron and close similar folds which, at some places, are tightly appressed and plunge steeply to the NW and SE (see Fig. 9.46C). In the eastern and central sectors of the Ilangwe Belt, F_3 folds occur on the limbs and axial planes of the F_2 large-scale upright periclinal folds (see Figs. 9.44A, 9.45 and 9.46). Their axial planes are subvertical and have an azimuth of 135° which is oblique to the 100° orientation of the F_2 axial planes. This obliquity of minor folds to major folds was alluded to in Section 9.2.4.3. This pattern of minor folds oblique to major folds has been observed in strike-slip zones and it is thought that it might present a useful indicator of strike-slip components of deformation (Sanderson and Marchini, 1984). In Section 9.2.4.3 this deformation was attributed to transpression with a left-lateral component of shear.

Since D_3 transpression operated over a considerable thickness of Ilangwe crust, its near-surface effect can be found in the substantially uplifted periclinal folds which now form the summits of the different peaks in the Ilangwe Belt, for example, Simbagwezi Peak, Ntabandlovu Peak, Ngcengcengu Peak, Ilangwe Peak and Ekuthuleni Peak (Fig. 2). In the Ilangwe Peak area (4,5/Y) along holostratotype 4-5, vertical uplift resulted in the production of a wedge-shaped or "keystone" uplift structure (Plate 9.9A; Section E-F in Fig. 2). Plate 9.9C and Plate 2.2A show the structures produced on the margins of the uplifted block. According to Sanderson and Marchini (1984), these structures are due to gravitational collapse and are similar to structures typical of thrust tectonic regimes.

The third phase of deformation in both the granitoids and greenstones produced structures with different geometries and slightly different orientations; however, in both terrains transpression was operative and resulted in substantial uplift of the surface. Deformation in the granitoid terrain was modified by the intrusion of the late post-Nondweni Impisi-Umgabhi Granitoid Suite and probable rotation due to transpression. This is supported by the fact that the D^G_3 structures are oriented N–S whereas the D_3 structures in greenstones are oriented in the NW–SE direction.

D_3 and D^G_3 deformations are different in terms of fold geometry and style. Although transpression was operative in both deformations, its timing was probably different. It is also possible that D_3 and D^G_3 were not coeval. This is postulated from the fact that D_3 structures are aligned about a vertical plane with azimuth 135°. It is only after D_3 folding that the greenstone assumed an arcuate shape probably as a result of granitoid intrusion. Probably this open arcuate form can be attributed to post-D_3 deformation (D_4 buckle folding

??). On the other hand, the N–S orientation of structures in the granitoid complex is related to the D^G_3 deformation. As was suggested, this is probably due to later granitoid intrusion. Therefore, this empirical evidence suggests that D^G_3 deformation is coeval with post-D_3 folding event (D_4 buckle folding ?). This is also supported by the fact that some fold structures in the greenstones are oriented N–S (see Fig. 9.44A).

Deformation and magmatism in the Ilangwe Granite – Greenstone Complex probably took place over a considerable length of time and covered a wide area. Chronostratigraphic studies will help in constraining the timing of these events; but most significantly, they will help in understanding these events in the broader context of the other Southern African granite-greenstone complexes. A logical follow-up to the study of this nature is detailed chronostratigraphy. Therefore, opportunities exist for such a study in the Ilangwe Complex.

CHAPTER 10

METAMORPHIC PETROLOGY AND GEOCHEMISTRY OF THE ILANGWE GREENSTONES AND METASEDIMENTS

10.1 INTRODUCTION

In this chapter and the following four chapters, the petrography, metamorphism and limited geochemistry of various lithologies comprising the greenstone and granitoid complexes are presented. This chapter is confined to the greenstones and metasediments of the Ilangwe Greenstone Belt. Chapters 11, 12, 13 and 14 present the data on the granitoid and gneiss complexes and Chapter 15 discusses the metabasic intrusives.

The geochemical analyses presented here record major and minor elements, loss on ignition and trace element compositions. Total iron was determined as Fe_2O_3. Owing to the numerous factors which influence the oxidation state of iron, the inherent uncertainty of any directly measured ferric/ferrous ratio and the fact that the Ilangwe rocks have been metamorphosed to varying degrees, the calculated ferric/ferrous ratio is used in this thesis.

In an attempt to arrive at a suitable and reasonable ferric/ferrous ratio, it was noted that the problem of the oxidation state of iron has been approached in various ways by different authors [for example Coombs (1963), Kay et. al., (1970), Chayes (1966), Irvine and Baragar (1971), Thompson et. al., (1972), Stice (1986), Green et. al., (1974), Brooks (1976), Hughes and Hussey (1976) and Le Maitre (1976)]. In this study, a ferric/ferrous ratio of about 0,28 was applied using the Newpet software of RAU for calculation of the CIPW norms.

The major and minor oxides have been recalculated (using Newpet) to 100% volatile-free to minimize differences amongst the rock-types caused by their variable water content and to adjust for the ferric/ferrous ratio. The anhydrous values, trace elements and CIPW norms

are given in tables in the relevant sections in the text. All plots using chemical data are based on the anhydrous values.

Amphibolites, amphibolitized pillowed metabasalts and serpentinitic talc schists occur in all the formations of the Ilangwe Greenstone Belt except the uppermost Nomangci Formation. These metabasic rocks have broadly similar mineralogy and chemistry. Thus, to avoid descriptive repetition, their petrography, metamorphism and geochemistry will be discussed under the sub-heading: "Nondweni mafic and ultramafic rocks". Differences will be mentioned where relevant.

10.2 NONDWENI MAFIC AND ULTRAMAFIC ROCKS

10.2.1 BANDED AMPHIBOLITES AND PILLOWED METABASALTS

10.2.1.1 PETROGRAPHY

Amphibolitic rocks are common within the supracrustal sequence, representing almost 70% of the Ilangwe Greenstone Belt. Whereas an amphibolite is, sensu stricto, defined as a metamorphic rock "consisting predominantly of plagioclase and hornblende" (Winkler, 1979, p 173), herein the term "amphibolite" is loosely used to denote a metamorphosed basic rock largely consisting of amphiboles and plagioclase in varying amounts and "usually showing a tectonic fabric" (Smalley, 1980). In the mapped area, the amphiboles are mainly actinolite/tremolite and minor hornblende. The plagioclase composition is usually oligoclase and andesine, however more calcic plagioclases do occur. These main constituents of the amphibolites occur together with varying amounts of quartz, rare cordierite (slightly altered to pinite), pyroxene, biotite and opaque ore (mainly magnetite and ilmenite). Talc, chlorite, sericite and epidote occur as alteration products.

In thin section they exhibit varying textures ranging from granoblastic (equigranular to seriate) to inequigranular, and are mainly nematoblastic. The nematoblastic texture is indicated by the elongate and fibrous laths of actinolite/tremolite with a preferred orientation. The amphibole laths usually show polysynthetic twinning and at times they poikiloblastically enclose plagioclase crystals. The other mineral phases show varying textures ranging from granoblastic to inequigranular. Quartz and cordierite usually show undulose extinction indicating deformation (Barker, 1990, p.71; Ehlers and Blatt, 1982, p.355). The plagioclase show twinning according to the albite, pericline and Carlsbad laws.

However, some plagioclase do not show twinning. ***Table 10.1*** is a summary of the features of the amphibolites of the Ilangwe belt.

In thin section, actinolite was differentiated from tremolite on the basis of pleochroism, extinction angle, polysynthetic twinning and high interference colours. These minerals are sometimes difficult to differentiate. They usually occur as elongate fibrous prismatic to columnar (2 - 7mm) crystals defining the foliation and having a nematoblastic texture (Plate 10.1A). However, some actinolite/tremolite crystals are idioblastic to subidioblastic, granular to equigranular, 1-3mm in length and show a granoblastic decussate to idiotropic texture (H81EB, H89EB, H90EB, H46EB, H24EB). Some samples show post-tectonic growth of actinolite laths on earlier actinolite crystals which are usually aligned along the regional foliation.

In the actinolite schist (H139EB, H140EB) of the Simbagwezi Peak, long fibrous, blade-like crystals of actinolite grow at the expense of earlier pre-tectonic subidioblastic to xenoblastic crystals which are chloritized.

In some samples, the actinolite/tremolite has grown at the expense of earlier pyroxenes. Remnant pyroxenes show schiller structures and epitaxial overgrowth of actinolite, implying uralitization, a retrograde effect (Shelley, 1993; Barker, 1990; Williams et. al., 1982). The actinolite is usually chloritized. Along fractures in some samples (e.g. H81EB), actinolite is breaking down to muscovite and calcite. This is clearly a retrograde reaction (Winkler, 1979).

Some samples show both actinolite and hornblende. Hornblende occurs as slightly elongate subidioblastic crystals which are altering along the edges to biotite. In these samples, the biotite, hornblende and cordierite are flattened along the foliation direction to give a nematoblastic texture (Plate 10.1A) whilst biotite is altered to epidote.

Where hornblende occurs as the only amphibole (e.g. H17EB, H90EB, H23EB), it is usually the blue-green and brown varieties showing pleochroism from yellow to brown to green. It has grown at the expense of orthopyroxene the remnants of which occur in a subophitic palimpsest texture with plagioclase (Plate 10.1B) and show deformation lamellae of clinopyroxene. The hornblende itself has an idiotropic texture and shows 120° triple junctions indicating stabilization and equilibrium (Ehlers and Blatt, 1982, p. 570). The hornblende piokiloblastically encloses minerals like quartz, cordierite and plagioclase.

TABLE 10.1 : ILANGWE AMPHIBOLITES : MODAL ANALYSES AND PETROLOGICAL FEATURES

SAMPLE IDENTITY	SAMPLE NO.	MINERAL MODAL COMPOSITION (%)																	GRAIN SIZE			PLAG An CONTENT %	TEXTURE Granoblastic(*); Subophitic(Sub); Ophitic(Oph); Inequigranular(In); Equigranular(Eq); Myrmekitic(Myr); Uralitization(Ur); Xenoblastic(Xen); Nematoblastic(Nem).
		Qtz	Plg	K-Fel	Hbl	Act	Pyrox	Oliv	Biot	Cord	Carb	Epid	Garn	Serp	Chlor	Ser	Mus	Ore	F	M	C		
SF	H3EB	8	13			60				10		3			3	2		1		x		nd	in.; *; cryst.
SF	H17EB	2	20		65		2			10						1		t	x	x		nd	decussate; idiobl.; suboph; traces of zir
SF	H24EB	8	24	t		60	1			2		2			1	2				x		Ab/Olig	in; idiobl.; Ur; schiller structures
EF	H38EB	t	9			65						t			25	1			x			nd	in; idiobl.;
EF	H39EB		30					65				t		5	t				x			An_{25-32}	oph.; probably oliv. basalt
SF	H42EB	1	10			78						1			5	5	t			x		An_{28}	
SF	H69EB	2	23		44				20	9	t	1				1			x			nd	in.; nem.; traces of zir. encl. in cord.
SF	H81EB	10	30			54				5	t	1					t	t	x	x		An_{30-35}	cons.; nem.; in.
SF	H89EB		2			63	2					18			15			t		x			decussate; idiobl.; ur.; *; zir. traces; dextral shearing
SF	H9OEB	5	25			60				5	t	1		4			t	t	x	x		An_{38}	
SF	H132EB	10	30		45		10			3						2				x		An_{38}	xen.
SF	H134EB	10	35	2	40		11									2				x		An_{24}	xen.; nem.
SF	H143EB	3	4			70						t			20			2	x				amph.=trem.
SF	H144EB	2	6			62								1	27		t	1	x	x			amph.=trem.
SF	H146EB	t	t		15	80						t			5				x	x			nem.
SF	H147EB	1	15			83										1				x		nd	nem.
SF	H151EB	t	2			70									28			t		x			
SF	H152EB		10			60						t			10			20	x			nd	amph.=trem. ore=mt.
SF	H158EB					81			t			1	15		2			t		x			
SBF	H139EB	5	15		75										1	2		2	x			nd	eq.; suboph.; *.
SBF	H140EB	t	1			94									5				x				post-tectonic growth of act.
SBF	H156EB	8	35			50			5						2				x			An_{33}	eq.; nem.; *.
SBF	H141EB	10	15												15	4	56			x		nd	eq.; *; lepid.

SF = UMHLATHUZE SUBGROUP EF = ENTEMBENI FORMATION SBF = SIMBAGWEZI FORMATION

PLATE 10.1 : TEXTURES IN THE AMPHIBOLITES OF THE ILANGWE BELT.

PLATE 10.1A : Nematoblastic texture in a finely banded amphibolite (see Plate 2.1) occurring in the Umhlathuze River valley (6.840/V.130). Note the quartz and cordierite (usually altered to pinite) which are flattened along the schistosity.

PLATE 10.1B : Subophitic texture in an amphibolite of the Nkwalini area (4,5/NN). Note the ill-defined nematoblastic texture indicating the schistosity and the grain boundary symplectites : myrmekitization and uralitization.

PLATE 10.1C : Schistose amphibolite showing post-tectonic over-growth of muscovite on earlier shear planes and also replacing biotite. Note the occurrence of syn-tectonic serpentine along the shear planes.

PLATE 10.1D : Garnetiferous amphibolite of the Olwenjini Formation (4.570/S.575) showing a syn-tectonic garnet (syn-tectonic porphyroblastesis - Barker, 1990). Sense of shearing is dextral. Note the "s - c" planes at the lower right-hand corner of the well-developed middle garnet grain. The "s - c" planes indicate a dextral shear sense.

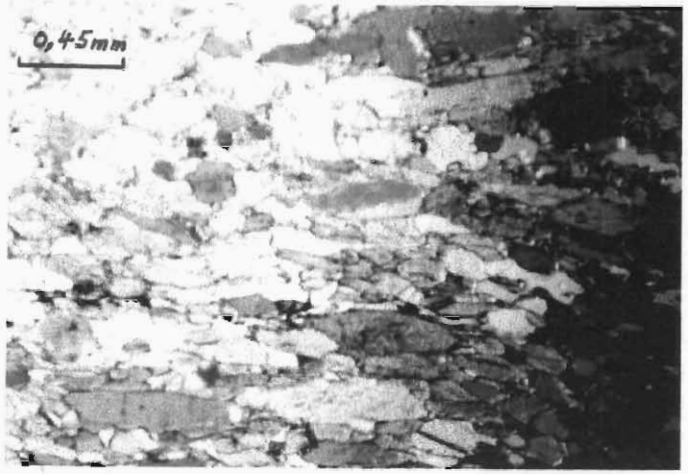

A

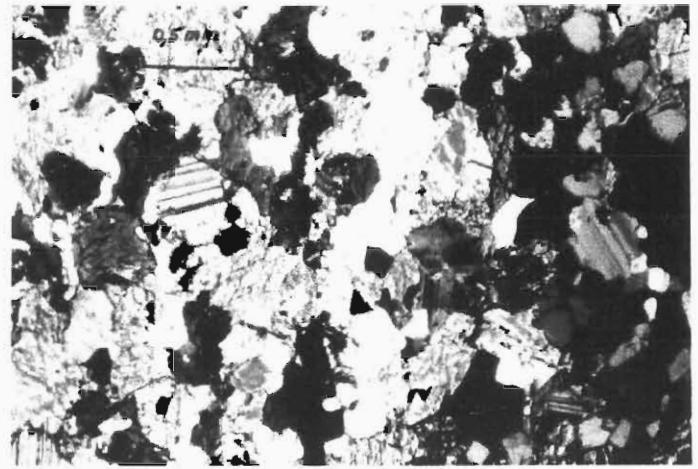

B

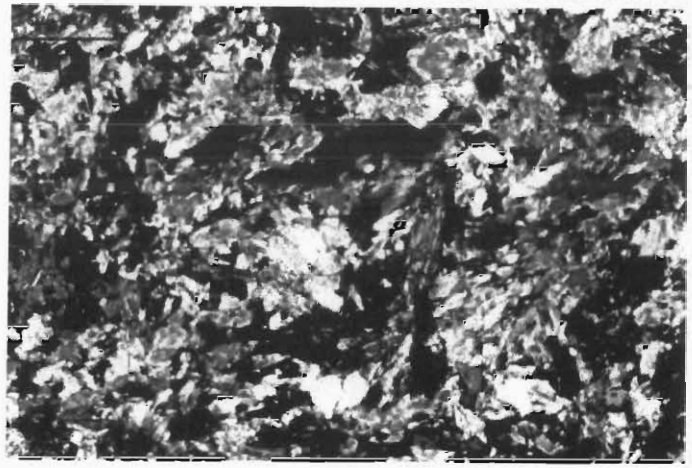

C

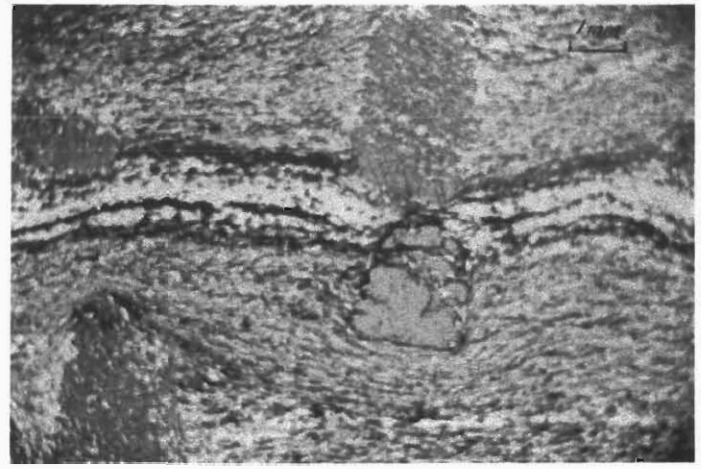

D

Plate 10.1

Plagioclase varies in amount from 0 to 40% and the grainsize is usually smaller than that of the amphiboles. The plagioclase content ranges from oligoclase to labradorite. However, the latter plagioclase is not common in the amphibolites. They occur as subidiomorphic to hypidiomorphic crystals showing, together with quartz and cordierite, a crystalloblastic fabric. Most plagioclases show varying degrees of saussaritization and are altered to sericite and minor epidote. In some plagioclase (e.g. H69EB) there occurs exsolution lamellae of biotite. Twinning, according to the albite, pericline and Carlsbad laws, is quite common but zoning was not observed.

Accessory minerals of the amphibolites include quartz, biotite, muscovite, cordierite, zircon, garnet and opaque ore. Epidote, chlorite and sericite occur as alteration products.

Quartz and cordierite occur as equant to granular grains showing a granoblastic consertal to crystalloblastic texture. Both show a wavy or undulatory extinction indicating extreme deformation. Cordierite sometimes shows polysynthetic twinning. and is commonly altered to pinite.

Biotite occurs as lathlike elongate fibrous flakes usually growing at the expense of amphiboles. It is characteristically green or brown in colour, which is typical of low-grade metamorphism (Miyashiro, 1973, p.259) and shows a mottled extinction. In sample H69EB the biotite is in equilibrium with cordierite, hornblende and plagioclase. Where the biotite is in disequilibrium it alters to epidote, calcite and chlorite. Biotite rarely occurs together with muscovite, which in samples H46EB and H78EB occurs as post-tectonic growth along earlier shear planes thus indicating post-shearing retrograde metamorphism (Plate 10.1C).

Zircon is quite rare. Where it occurs (e.g. H69EB) it is in the form of discrete euhedral cubic crystals (0,1 - 0,5mm in length) poikiloblastically enclosed in cordierite.
Garnets are not common but occur in amphibolites in the Olwenjini Valley (4/R,S) and in the amphibolites of the Amazula Gneiss in the Amazula valley (7.140/CC.470). The garnet porphyroblasts are subidioblastic to xenoblastic and range from 0,5 to 3 mm in size. They show pre-tectonic growth with later (probably syntectonic) fracturing resulting in the fractures being filled with magnetite and also rimmed by magnetite. In some thin sections, they have been rotated and indicate a dextral sense of movement (Plate 10.1D).

Opaque ore in the form of sulphides or skeletal relicts and subidioblastic crystals of magnetite or xenoblastic crystals of ilmenite with dark reddish rims is common. Some of

the ore is definitely pretectonic or even syntectonic as it has been elongated along the foliation.

As mentioned earlier, epidote, chlorite and sericite are present as retrograde minerals replacing amphiboles, biotite and plagioclase. Minor calcite occurs as alteration products of amphiboles and biotite.

10.2.1.2 METAMORPHISM

The presence of pyroxene and hornblende in some banded amphibolites and the presence of garnets in addition indicates that pressures and temperatures were appropriate for amphibolite facies metamorphism. Hornblende forms at temperatures of about 500°C (Hirschberg and Winkler, 1968 ***in*** Winkler, 1974). These temperatures and pressures indicate epidote-amphibolite facies metamorphism (Barker, 1990; Fig. 10.1), that is, lower amphibolite grade.

The presence of retrograde actinolite, chlorite and epidote in these amphibolites (e.g. H69EB) indicates that they were subsequently affected by regional greenschist facies metamorphism. The foliation defined by mafic minerals is deformed by F_2 folds and thus the lower amphibolite facies metamorphism is interpreted to have developed during D_1 deformation and, consequently, represents the first phase (M_1) of metamorphism. The retrogression event (M_2) is probably D_2 in timing as the chlorite and actinolite are aligned along the S_2 axial planar foliation.

The mineral assemblages characteristic of the M_1 event are :

Hornblende + plagioclase (oligoclase/andesine) + cordierite + quartz + biotite + epidote ..... (1)

Hornblende + oligoclase + garnets ± quartz + cordierite ....(2)

Pyroxene (→ hornblende) + andesine + quartz + cordierite ..... (3)

Hornblende (→ actinolite) + quartz + epidote + chlorite ..... (4)

Paragenesis (4) probably indicates the transition zone between lower amphibolite facies metamorphism and greenschist facies metamorphism (Barker, 1990). Winkler (1979) contends that these mineral assemblages (1 - 3) are typical of medium grade amphibolites (Fig. 10.2). The presence of cordierite is a further indication of temperatures in the region of 500 - 550°C.

The massive and pillowed metabasalts show the following mineral assemblages :

actinolite + oligoclase (or albite) ± quartz + chlorite
actinolite + oligoclase + epidote + chlorite
actinolite + chlorite + quartz + albite + epidote.

These mineral parageneses are characteristic of greenschist facies of the albite-actinolite-chlorite zone of metamorphism (Winkler, 1979; Fig. 10.3) occurring at about 350 - 450°C (Barker, 1990; Fig. 10.1).

The M_3 metamorphic event is not widespread but is mainly confined to shear zones where retrograde metamorphism has been observed. The typical mineral paragenesis is :

quartz + muscovite + sericite ± actinolite.

This assemblage is characteristic of the shear-related quartz-sericite schists (see later).

10.2.2 SERPENTINITIC TALC TREMOLITE SCHISTS

10.2.2.1 PETROGRAPHY

These schists occur as thin slices within a shear zone in the Sabiza Formation. They also occur as narrow (4 - 50m) bands within massive pillowed metabasalts of the Sabiza Formation and phyllites of the Simbagwezi Formation. The talc schists in the phyllites are quite narrow (4-10m) and do not extend for considerable distances. These schists are regarded as part of the stratigraphic sequence but it is possible that they are altered intrusives.

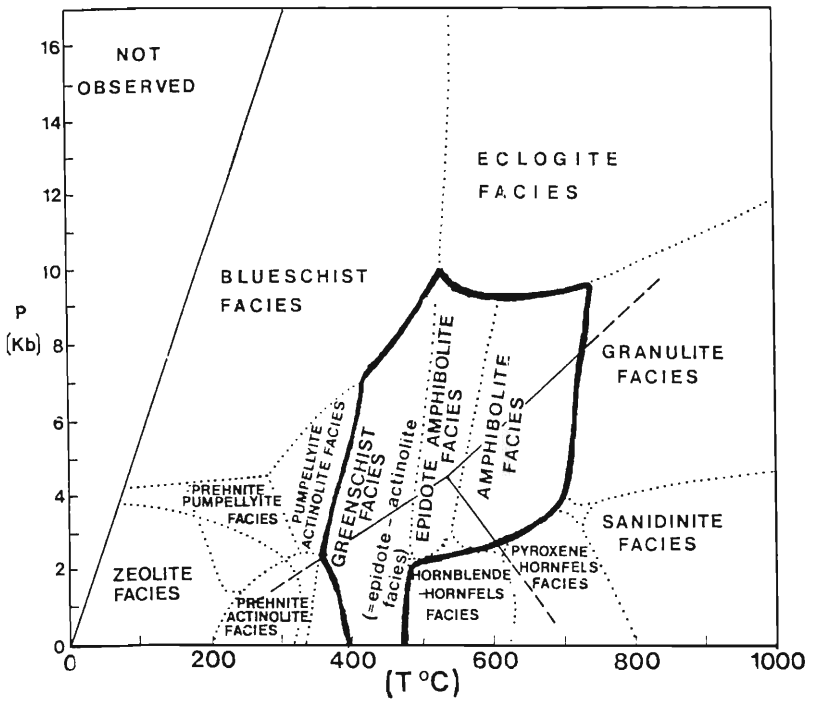

Fig. 10.1 : Illustration of different metamorphic facies in P-T space (after Barker, 1990). Solid thick lines depict the attained peak metamorphic conditions in the whole of the Ilangwe Greenstone Belt.

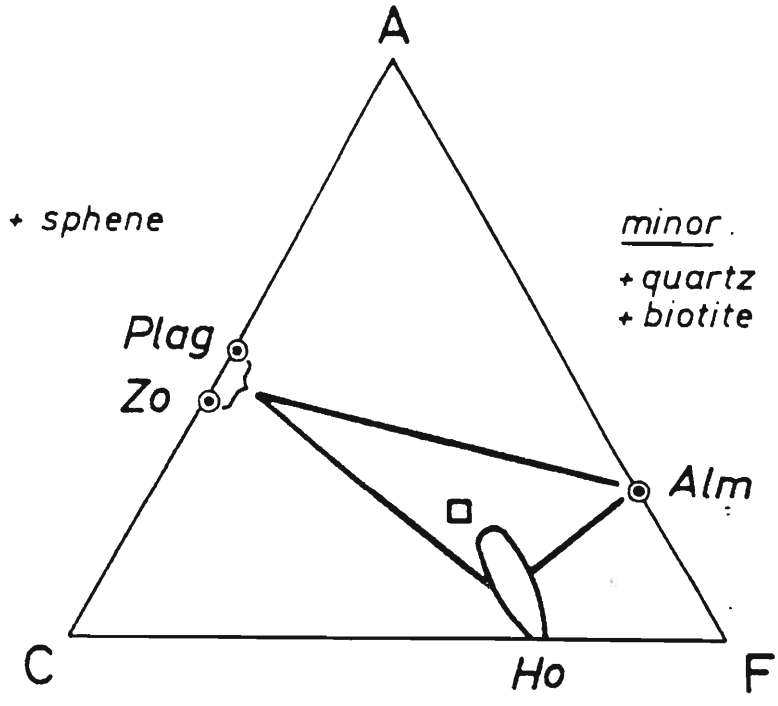

Fig. 10.2 : Medium-grade andesine- and oligoclase-amphibolite of the Ilangwe greenstones with garnets being present in the amphibolites of the Olwenjini Formation and the amphibolitic variety of the Amazula Gneiss in the Amazula River (after Winkler, 1979).

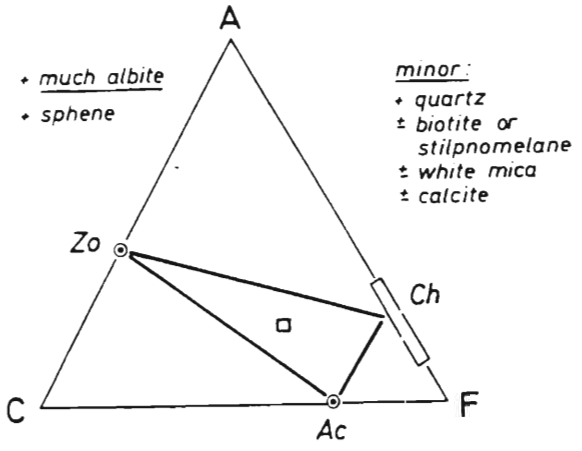

Fig. 10.3 : The albite - actinolite - chlorite zone of the lower temperature greenschist facies metamorphism of the Ilangwe greenstones (amphibolites) (after Winkler, 1979).

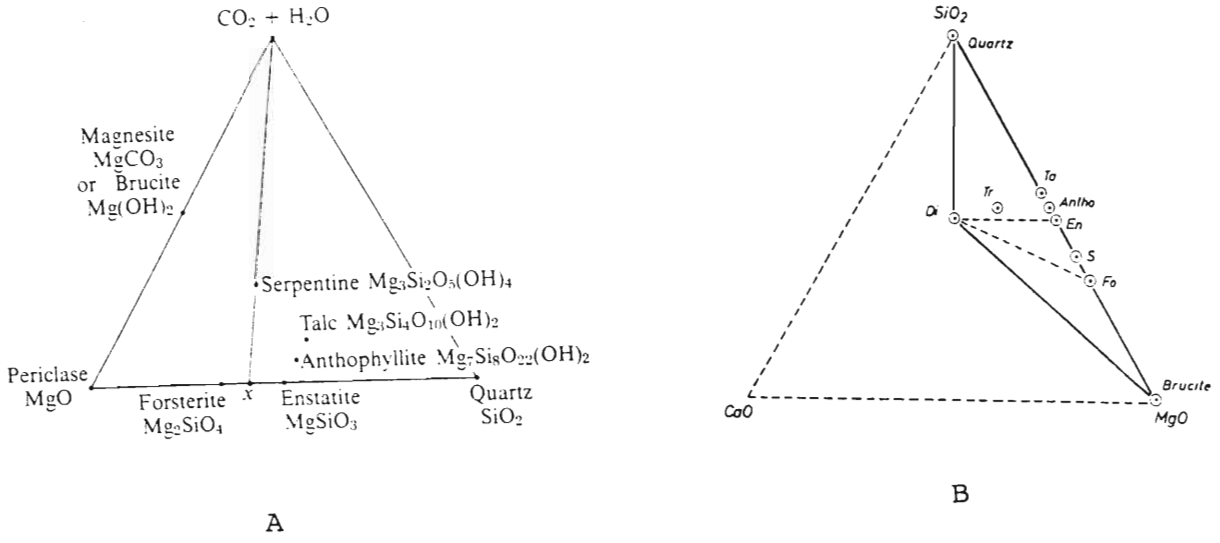

Fig. 10.4: (a) Typical minerals produced during hydration and carbonation in the system MgO - SiO_2 - (CO_2, H_2O) (from Ehlers and Blatt, 1982).

(b) Minerals produced by the metamorphism of the Entembeni Formation phyllites (after Winkler, 1979).

Table 10.2 presents the modal analyses and main mineralogical features of the serpentinitic talc schists. The schists consist mainly of long fibrous tremolite ranging from 2 to 7mm in length. In plane polarized light, tremolite is colourless and, rarely, it is pale green and non-pleochroic. The fibres are aligned along a preferred orientation. Some subidioblastic crystals of tremolite show a decussate texture. In one slide (H34EB) tremolite is forming from earlier euhedral to subhedral decussate crystals of hornblende which are also altering to chlorite; whereas in slide H37EB tremolite is intergrown with cordierite which shows undulose extinction and is slightly altered to pinite. In slide H34EB (Plate 10.2A) a cordierite porphyroblast is rotated and sheared. Tremolite rarely shows polysynthetic twinning but some faint twinning has been observed. It is usually associated with opaque ore minerals some of which have been flattened along the foliation. In H32EB tremolite poikiloblastically encloses small "inclusions" of red-rimmed opaque ilmenite. It is possible that some of the amphibole fibres identified as tremolite could possibly be anthophyllite especially those that show higher interference colours and parallel extinction.

Serpentine is another major constituent of these schists. It occurs as greyish-bluish short fibrous and, rarely, plate-like crystals which sometimes look like feathers. The most common serpentine mineral seems to be chrysotile. This is supported by observation in hand specimen where asbestiform short fibres of chrysotile have been observed. Commonly, the sheared greyish-bluish serpentine fibres are wrapped around tremolite crystals.

In most of the slides serpentine occurs as partial or complete pseudomorphs of olivine (Plate 10.2B) and sometimes occurs as massive crystals with very faint relict olivines separated by magnetite rims thus giving a mesh texture. The former occurrence is typical of disequilibrium textures (Barker, 1990). Water is required for olivine to alter to serpentine The serpentinization process is thought to proceed under differing conditions of either constant-volume hydration or hydration with volume increase (Ehlers and Blatt, 1982; Barker, 1990).

Talc occurs as foliated masses or even contorted bands. It is similar to muscovite, however the latter has a larger optic angle. The occurrence of talc as contorted bands is probably due to shearing and it is usually intergrown with chlorite (H12EB). Sometimes talc is associated with carbonate, probably magnesite, and occurs as pseudomorphs after serpentine. Ehlers and Blatt (1982) contend that these talc-magnesite pseudomorphs result from the presence of CO_2-rich fluids in the serpentinite body.

PLATE 10.2 : KINEMATIC INDICATORS AND SYMPLECTITES OF THE SABIZA FORMATION.

PLATE 10.2A : Cordierite porphyroblast indicating a dextral sense of shear. There is also an indication of shear sense reversal and the occurrence of an open fold on deformed tremolite. [Talc tremolite schist from near the Sabiza River: (5.390/V.935)]

PLATE 10.2B : Replacement of olivine by serpentine along grain boundaries. Note the occurrence of ore (magnetite) along fractures and grain boundaries. [Talcose serpentinite schist from the Sabiza River: (5.570/W.340)]

PLATE 10.2C : Feldspar porphyroblast indicating a right-lateral sense of movement in the siliceous khaki pelite showing a lepidoblastic texture. Note the flattened quartz grains which parallel the muscovite laths and the regional schistosity. [Metasiliceous khaki-coloured pelite of the Sabiza Formation: (5.440/V.875)]

PLATE 10.2D : Feldspar porphyroblast indicating a sinistral sense of movement and having a lepidoblastic texture. [Metasiliceous khaki-coloured pelite of the Sabiza Formation: (5.440/V.875)]

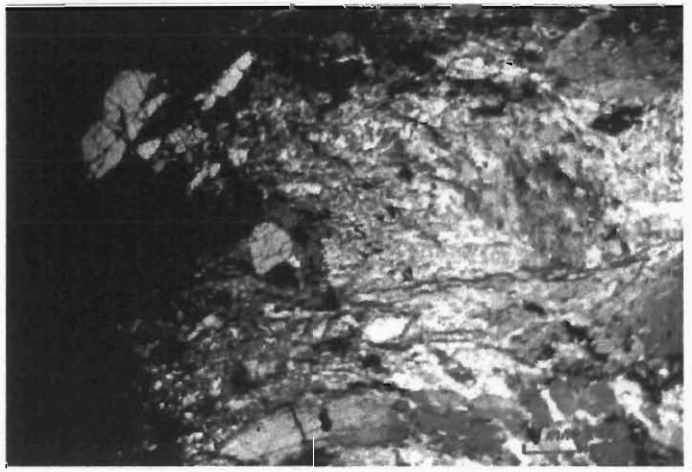

A

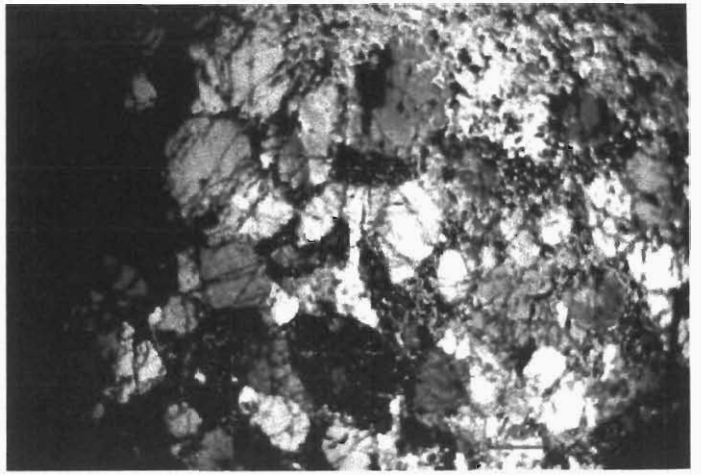

B

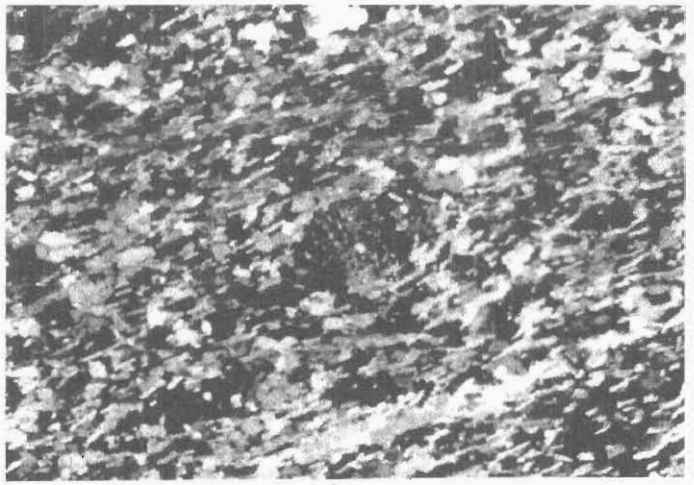

C

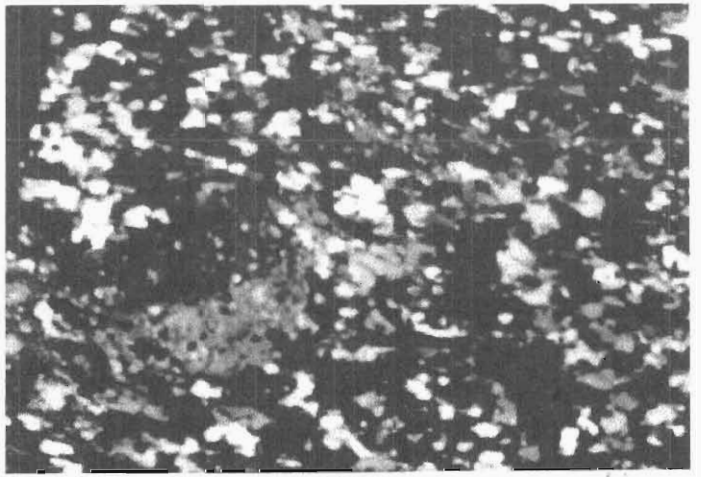

D

Plate 10.2

PLATE 10.3 : KINEMATIC INDICATORS AND TEXTURES IN THE METASEDIMENTS.

PLATE 10.3A : Rotated garnet porphyroblast indicating a dextral sense of shearing. The porphyroblast is broken and the fractures are occupied by magnetite. The quartz grains are deformed and show a consertal texture with the grain boundaries occupied by biotite. [Phyllite (H47EB): Ekuthuleni (4.675/EE.570)]

PLATE 10.3B : Lepidoblastic texture in the cherty quartzite of the Entembeni Formation. Note the flattened quartz grains and the occurrence of magnetite along bedding planes. [Cherty quartzite near Olwenjini River: (4.420/S.105)]

PLATE 10.3C : Mica fish in a sheared quartz biotite cordierite fuchsite gneiss. Note the deformed quartz and cordierite grains which are flattened along the gneissosity. The sense of shear is sinistral. [Quartz biotite cordierite fuchsite gneiss of the Sabiza River: (5.180/V.790)]

PLATE 10.3D : Folded bands of magnetite and quartz in a banded iron formation of the Entembeni Formation. Minor flakes of grunerite occur within the quartz band. [Banded iron formation near Entembeni Kraal: (5.215/EE.860)]

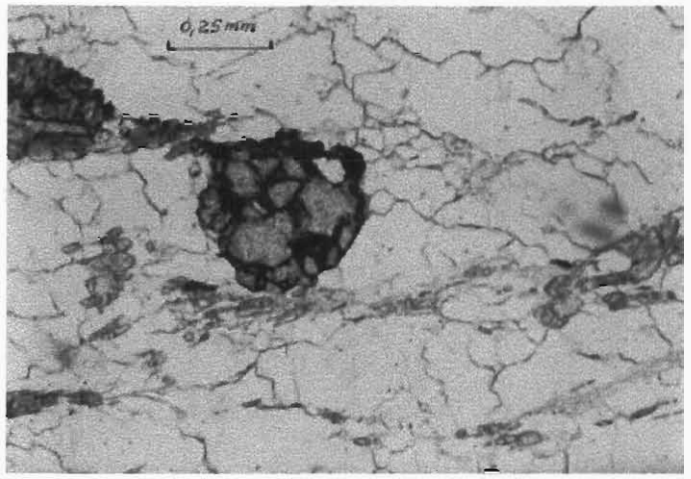

A

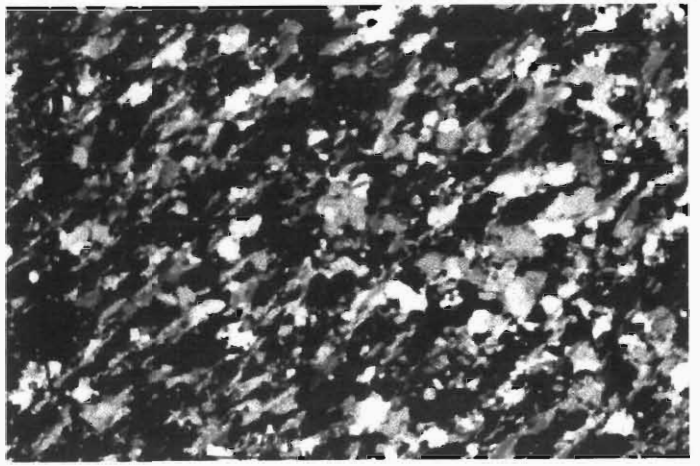

B

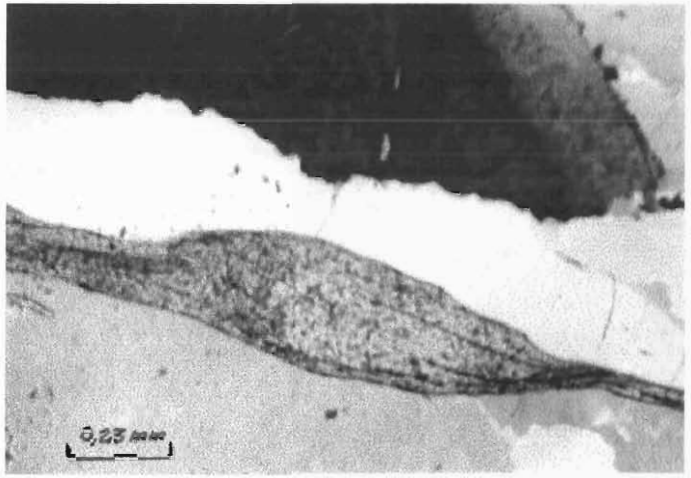

C

D

Plate 10.3

Cordierite occurs as granoblastic crystals flattened in the direction of schistosity. It occurs in variable proportions up to a maximum of 30 vol.%. In H34EB cordierite is slightly pleochroic, implying it is Fe^{2+}-rich (Heinrich, 1965) and sector and lamellae twinning is common. It is slightly altered to pinite.

Other common accessory minerals occurring in various proportions are chlorite, minor muscovite, minor plagioclase and epidote. The latter occurs as idioblastic to hypidioblastic crystals showing a decussate to idiotropic texture and usually having a lower 2V implying an increase in Fe^{3+} (Heinrich, 1965).

10.2.2.2 METAMORPHISM

The ubiquitous occurrence of pseudomorphs after olivine, completely altered relict olivine in a mesh structure and the widespread serpentinization of the talc tremolite schists indicates that these schists are derived from ultramafic rocks of probably komatiitic or dunitic affinity. The main chemical constituents of these rocks (***Table 10.3***) are MgO and SiO_2, with lesser amounts of FeO and CaO (Winkler, 1979; Ehlers and Blatt, 1982).

Metamorphism of high-temperature minerals of the ultramafic rocks usually involves reaction with H_2O or occasionally CO_2 (Winkler, 1979; Ehlers and Blatt, 1982; Mason, 1986; Barker, 1990). The typical minerals produced as a result of hydration and carbonation are shown in Fig. 10.4.

The typical parageneses observed in thin section are :

tremolite ± talc + serpentine + chlorite + olivine .....(1)

clinopyroxene (→ tremolite) + serpentine + magnestie + talc ± quartz ..... (2)

olivine (→ serpentine) + tremolite +pinite (after cordierite) ± ore ±chlorite ..... (3)

talc + pinite (after cordierite) + epidote + chlorite + calcite ..... (4)

Assemblage (2) shows that CaO is a significant component in the metamorphism of ultramafic rocks. To a lesser extent, FeO is also significant and this is supported by the occurrence of magnetite rimming olivine and occurring in the fractures within olivine. On the basis of assemblages (2) and (3), Fig. 10.4 (b) realistically represents the minerals formed from the hydration and carbonation of ultramafic rocks.

Several metamorphic reactions suggested by the above assemblages (Winkler 1979) are pertinent here:

5 serpentine + 2 diopside = 1 tremolite + 6 forsterite + $9H_2O$ .....(A)

4 forsterite + 1 H_2O + 5 CO_2 = 1 talc + 5 magnesite .....(B)

2 forsterite + 2 H_2O + 1 CO_2 = 1 serpentine + 1 magnesite.....(C)

11 diopside + 2 forsterite + 5 CO_2 + 3 H_2O = 3 tremolite + 5 calcite.....(D)

5 diopside + 3 CO_2 + 1 H_2O = 1 tremolite + 3 calcite + 2 quartz.....(E)

2 serpentine + 3 CO_2 = 1 talc + 3 magnesite + 3 H_2O.....(F)

1 serpentine + 3 CO_2 = 2 quartz + 3 magnesite + 2 H_2O.....(G)

1 serpentine + 2 quartz = 1 talc + 1 H_2O..... (H)

These reactions can be divided into two groups :

(i) Group 1 consists of reactions A to E which are considered prograde metamorphic reactions. In metamorphosed serpentinites, diopside forms at relatively low temperatures (reaction A) and with prograde metamorphism and an increase in temperature, reaction A takes place (Winkler, 1979). Reactions B and C take place at temperatures of 400 - 550°C, fluid pressures of 2Kb and intermediate to very low ranges of X_{CO2} respectively. Finally, reactions D and E take place at very low X_{CO2}, constant fluid pressure and slightly higher temperatures. These prograde metamorphic reactions are indicative of an early phase (M_1) of medium grade metamorphism.

(ii) Group 2 consists of reactions F to H which are considered retrograde metamorphic reactions. Winkler (1979) is of the opinion that the presence of serpentine in a rock indicates that the hydration fluids contained very little CO_2. In the event that the X_{CO2} increases, then reactions F and G occur at temperatures between 250 - 450°C and fluid pressures of 2KB. Reaction H takes place in quartz-bearing serpentinites at temperatures between 300 and 360°C and fluid pressures of 2Kb (Winkler, 1979). These reactions are indicative of retrograde metamorphism (M_2) occurring at greenschist facies temperatures. Retrogression is further indicated by partial and complete pseudomorphs of serpentine after olivine and those of tremolite after pyroxene thus pointing to disequilibrium conditions. Low grade metamorphic temperatures are supported by experimental and isotopic data showing that lizardite-chrysotile serpentinites formed below about 350 - 400°C (Ehlers and Blatt, 1982).

10.2.3. SABIZA KHAKI- TO CREAM-COLOURED SILICEOUS PELITIC ROCK

10.2.3.1 PETROGRAPHY

The light-coloured "silty" siliceous rocks of narrow widths (1 - 7m), intercalated within the pillowed metabasalts, occur towards the top of the Sabiza Formation and are also intercalated within the phyllites of the Entembeni Formation. The occurrence of these rocks in the Sabiza Formation is thought to be indicative of periods of quiescence when there was no volcanic activity.

In thin section, the siliceous pelitic member consists of quartz, K-feldspars, plagioclase (dominantly albite), muscovite and minor carbonate, epidote and sericite. Modal analyses of these rocks are shown in ***Table 10.2***.

Quartz occurs as granoblastic inequigranular grains that have been flattened and stretched to assume a preferred orientation parallel to the foliation direction (Plate 10.2C). It shows a wavy extinction and most grains contain dust trails. K-feldspars are predominantly cloudy orthoclase up to 2mm in diameter. The plagioclase composition is albite (An_{6-13}) showing albite and pericline twinning. Muscovite occurs as elongate flakes and columnar laths aligned along the foliation and showing a lepidoblastic texture (Plate 10.2C). There is evidence of post-tectonic overgrowth of second generation muscovite. Accessory minerals

are epidote, carbonate (calcite) and sericite/chlorite which occur as alteration products. Kaolin is present in low amounts, which indicates the later weathering effects.

There is evidence of extensive ductile shearing of the siliceous pelitic rock as shown by kinematic indicators (Plate 10.2 D or C).

10.2.3.2 METAMORPHISM

The siliceous pelitic rocks show the following paragenesis:

quartz + K-feldspar + albite + muscovite ± calcite ± epidote ± chlorite.

This paragenesis is typical of low grade regional metamorphism (Winkler, 1979; Best, 1982; Mason, 1978) of pelitic rocks in the typical Barrovian Chlorite Zone (Shelley, 1993 p.96).

10.2.4 GEOCHEMICAL CLASSIFICATION OF THE MAFIC AND ULTRAMAFIC ROCKS

To augment the field relationships and the petrographic observations, eleven (11) metabasaltic amphibolites and six (6) serpentinitic talc-tremolite schists were chemically analysed (***Table 10.3***). The aim of the geochemical analyses was to further assist in the classification and the determination of the origin of these rocks. The geochemical data is quite limited and insufficient to warrant an extended discourse. Therefore, only a tentative classification will be attempted here and any conclusions drawn from this discussion will be of a tentative nature.

In the field, it was determined from pillow structures that the Ilangwe metabasaltic amphibolites and greenstones are of volcanic origin. It is important therefore, to establish whether these ortho-amphibolites have a tholeiitic or calc-alkaline magmatic affinity. The terms tholeiitic and calc-alkaline were introduced by Kennedy (1933) and Tilley (1950) to define distinctive rock series. In order to classify the Ilangwe metalavas on this basis, the classification scheme devised by Irvine and Baragar (1971) is used, as it was designed for both unaltered and altered volcanic rocks.

TABLE 10.2 : ILANGWE TALC SCHISTS AND PELITES : MODAL ANALYSES AND PETROLOGICAL FEATURES

SAMPLE IDENTITY	SAMPLE NO.	MINERAL MODAL COMPOSITION (%)																GRAIN SIZE			PLAG An CONTENT %	TEXTURE Granoblastic(*); Subophitic(Sub); Ophitic(Oph); Inequigranular(In); Equigranular(Eq); Myrmekitic(Myr); Uralitization(Ur);Xenoblastic(Xen); Nematoblastic(Nem).
		Qtz	Plg	K-Fel	Hbl	Trem	Oliv	Cord	Carb	Epid	Talc	Serp	Chlo	Ser	Mus	Pyrox	Ore	F	M	C		
A	H2EB					30				t	35	27	8				t	x				faint decussate; schistose; no oliv. relicts
A	H12EB	t	t				5		20		39	21	10				5	x	x			porphyroblastic; oliv. relicts altered to serp
A	H18EB							30		8	60		2					x				dec.; idiobl.
A	H27EB					56		t			10	29	5					x	x			dec.; schistose; relict oliv.
A	H28EB					50		1		t	10	30	9					x	x			
A	H32EB					63					2	5	30					x				
A	H33EB					50	2	6			t	39	3				t	x	x			
A	H34EB	t			t	50	t	5			14	30	t		t			x				*; nem.
A	H35EB					52	1	25		t	1	15	5		t		1	x				nem.; relict oliv.; pinite alteration
A	H37EB					20		20				60	t				t	x				Ore aligned along foliation
A	H43EB	t				32			28		25	10	3				2	x	x			
A	H46EB		2			70				t	t		23		5		t		x			dec.; post-tectonic growth of musc.
A	H74EB					60					15	20	5					x	x			dec.; relict oliv. completely replaced
A	H78EB					60		1		20	t		15		4	t	t	x				in.; nem.; post-tectonic growth of musc. along shear bands
A	H145EB		2			58					20	5	15				t	x	x			nem.; schistose
A	H150EB		t			60					28	1	10				1	x				
B	H36EB	40	15	23					3					1	18				x			lepid.; sinistral shearing
B	H142EB	45		25						t				1	29			x	x			lepid.; kaolin on weathered k-feldspar

A = SERPENTINITIC TALC TREMOLITE SCHIST **B = SILICEOUS KHAKI-COLOURED PELITIC ROCK**

The silica content of the Ilangwe ortho-amphibolitic rocks falls within basaltic rocks and according to Irvine and Baragar (1971) the common volcanic rocks can be sub-divided into sub-alkaline and alkaline rock-types. The sub-alkaline series can further be sub-divided into tholeiitic and calc-alkaline series (Kennedy, 1933, Tilley, 1950). The total alkalis-silica plot (Fig. 10.5A) separates the sub-alkaline rock-types from the alkaline rock-types (Irvine and Baragar, 1971). Ilangwe mafic and ultramafic rocks plot on the sub-alkaline field and lie in the "Basalt", "Basaltic Andesite" and "Andesite" compositional fields of Le Bas et. al., (1986) (Fig. 10.5A).

Irvine and Baragar (1971) suggest the further sub-division of sub-alkaline suites into calc-alkali and tholeiitic series by either a plot of Al_2O_3wt.% vs normative plagioclase or by the AFM ternary diagram (Figs. 10.5B and 10.6). In the former plot, the Ilangwe rocks plot in the tholeiitic field (Fig. 10.5B) whereas in the AFM diagram (Fig. 10.6), the ortho-amphibolites plot in the tholeiitic field and the talcose serpentinites plot in the calc-alkaline field.

The ortho-amphibolites do not show any marked iron enrichment and show moderate alkali content (Fig. 10.5C and D). The talc-serpentine schists on the other hand show an enhanced MgO enrichment and an associated iron and total alkali depletion (Fig. 10.5C and D). Fig. 10.7A, which is a plot of $(Fe_2O_3 + FeO)/(Fe_2O_3 + FeO + MgO)$ versus SiO_2, further shows this characteristic of iron depletion of the talc schists.

Tholeiitic rocks generally have elevated TiO_2 compared to the calc-alkaline suite (Miyashiro and Shido, 1975). Fig. 10.7B, which is a plot of TiO_2 versus $(Fe_2O_3 + FeO)/MgO$, shows a trend of TiO_2 enrichment from the talc serpentine schists (ultramafic rocks) to the metabasaltic amphibolites (mafic tholeiitic rocks). The moderate TiO_2 concentrations and the moderate TiO_2 enrichment trend (Fig. 10.7B) further supports the tholeiitic character of the ortho-amphibolites and a calc-alkaline affinity for the talc serpentine schist.

Tilley (1950) suggested that tholeiitic rocks have higher Total FeO/MgO ratios than the calc-alkaline types. This ratio, plotted against Total FeO (i.e. $Fe_2O_3 + FeO$) can be used to separate the calc-alkaline and tholeiitic compositional fields (Miyashiro and Shido, 1975; Fig.10.7C). On such a diagram (Fig. 10.7C) the ortho-amphibolites plot on the tholeiitic field whereas the talc serpentine schists plot on the calc-alkaline field. Miyashiro (1974) defined the calc-alkaline and tholeiitic fields on an $(Fe_2O_3 + FeO)/MgO$ versus SiO_2 diagram (Fig. 10.7 D). The tholeiitic series show lower SiO_2 contents than the calc-alkaline series.

TABLE 10.3 : ILANGWE AMPHIBOLITES AND TALC SCHISTS : MAJOR AND TRACE ELEMENTS

SAMPLE	H18EB	H42EB	H69EB	H81EB	H89EB	H90EB	H132EB	H134EB	H159EB	H161EB	H162EB	H37EB	H43EB	H46EB	H74EB	H78EB	H163EB
	AMPHIBOLITES											TALC SCHISTS					
SiO_2	50.80	50.80	56.50	50.80	54.30	51.50	55.68	54.16	54.72	55.17	52.28	54.10	54.80	51.30	59.60	54.90	57.64
TiO_2	1.30	1.43	1.10	1.41	1.33	0.96	0.68	1.36	1.01	0.70	1.01	0.21	0.22	0.30	0.22	0.16	0.20
Al_2O_3	13.60	14.30	14.60	14.30	13.90	14.40	9.37	13.90	14.67	9.42	14.33	4.55	4.93	7.97	1.50	4.88	4.26
Fe_2O_3	3.01	3.04	2.16	3.05	2.69	3.07	2.75	2.69	2.60	2.76	2.72	1.69	1.54	2.13	1.71	1.55	1.67
FeO	10.90	10.90	7.78	11.00	9.70	11.00	9.89	9.68	9.36	9.93	9.81	6.10	5.56	7.67	6.14	5.60	6.01
MnO	0.21	0.30	0.19	0.24	0.20	0.22	0.23	0.22	0.18	0.21	0.19	0.21	0.20	0.18	0.16	0.17	0.16
MgO	6.98	6.34	4.86	6.40	5.62	6.17	9.36	5.38	5.07	9.32	8.56	24.80	24.10	25.70	24.50	24.10	22.98
CaO	10.80	9.51	7.98	9.59	9.07	9.27	9.60	9.29	8.25	9.95	7.85	7.46	7.89	4.11	5.67	7.83	6.61
Na_2O	1.97	2.12	2.33	2.11	1.84	2.06	1.53	1.93	2.27	1.03	1.86	0.74	0.57	0.48	0.39	0.61	0.34
K_2O	0.34	0.87	1.81	0.80	1.01	0.83	0.77	0.93	1.36	1.00	1.00	0.12	0.19	0.11	0.04	0.17	0.05
P_2O_5	0.21	0.40	0.72	0.35	0.42	0.54	0.13	0.47	0.52	0.50	0.40	0.08	0.07	0.06	0.04	0.07	0.08
TOTAL	100.00	100.00	100.00	100.00	100.00	100.00	99.99	100.00	100.00	99.99	100.00	100.00	100.00	100.00	100.00	100.00	100.00
Rb	12.90	13.70	61.00	15.90	17.10	14.90	15.90	29.00	22.70	18.30	20.60	6.90	7.70	5.70	4.90	8.70	9.20
Sr	249.00	311.00	511.00	152.00	290.00	366.00	100.30	130.90	259.80	249.60	189.60	15.30	21.20	20.50	11.90	10.30	17.90
Zr	50.60	80.30	199.00	100.00	107.00	99.70	65.30	137.70	115.30	102.90	96.80	44.80	45.90	53.00	35.40	32.60	48.90
Nb	2.50	3.80	14.30	5.00	4.20	7.00	6.90	15.10	7.60	6.30	3.90	5.30	6.10	6.30	4.90	1.30	7.10
Y	17.10	21.20	28.60	26.60	19.80	22.90	41.20	44.50	33.90	19.60	18.90	0.90	13.00	143.00	0.20	0.00	6.00
Th	6.70	5.90	5.00	5.70	4.90	8.00	7.10	7.00	4.70	5.90	5.20	9.30	10.10	9.90	8.60	11.00	7.80
U	11.30	10.00	6.30	9.40	12.30	11.90	9.40	9.30	12.00	10.30	11.10	14.00	13.70	12.00	13.70	13.30	11.90
Ni	81.70	96.50	59.70	93.60	99.20	107.00	215.00	92.50	135.20	99.80	103.90	1753	1527	1456	2934	1486	2110
C.I.P.W. NORMS (ANHYDROUS; IN Wt %)																	
Q	3.30	3.08	11.00	3.18	10.20	4.42	9.30	10.09	8.85	10.65	4.43	0.00	0.21	0.00	9.71	0.14	7.71
Or	2.04	5.13	10.70	4.71	5.97	4.93	4.56	5.49	8.01	5.92	5.89	0.74	1.12	0.63	0.25	1.00	0.31
Ab	16.70	17.90	19.70	17.80	15.50	17.40	12.97	16.32	19.17	8.74	15.75	6.23	4.83	4.05	3.34	5.19	2.90
An	27.20	27.00	24.00	27.10	26.60	27.60	16.42	26.52	25.85	18.10	27.79	8.75	10.30	19.30	2.19	10.10	9.93
Di	20.60	14.60	8.96	15.00	13.00	12.40	24.75	13.68	9.73	22.83	7.02	21.90	22.40	0.55	20.30	22.40	17.65
Hy	22.90	24.30	18.70	24.20	21.40	25.80	26.42	20.34	21.49	27.28	32.33	54.70	58.30	61.50	61.20	58.50	58.51
Ol	0.00	0.00	0.00	0.00	0.00	0.00	0.00	0.00	0.00	0.00	0.00	4.59	0.00	10.20	0.00	0.00	0.00
Mt	4.37	4.40	3.14	4.41	3.91	4.45	3.99	3.90	3.77	4.00	3.95	2.46	2.24	3.09	2.47	2.25	2.42
Il	2.47	2.72	2.09	2.68	2.52	1.82	1.29	2.58	1.92	1.32	1.91	0.39	0.42	0.57	0.41	0.30	0.37
Ap	0.50	0.94	1.70	0.82	0.99	1.27	0.32	1.11	1.22	1.19	0.94	0.20	0.18	0.15	0.10	0.18	0.20

The limited trace element chemistry of these mafic and ultramafic rocks (***Table 10.3)*** does not characterize them so well. Generally the ortho-amphibolites have higher concentrations of Sr, Zr, Nb and Th than the talc schists. The latter have higher concentrations of Ni than the metabasalts. On the plot of Ni ppm versus (FeO + Fe_2O_3)/MgO (Miyashiro and Shido, 1975), the metabasalts and talc schists plot in the tholeiitic field (Fig. 10.8A).

The serpentinitic talc schists have a higher SiO_2 content (>53%) than the metabasalts. They also have MgO>9% and CaO/Al_2O_3 >1. Such rocks are termed "komatiitic andesites" (Wilson and Versfeld, 1994). However, no spinifex texture has been observed in the talc schists of the Ilangwe Belt. When plotted on an Al_2O_3 versus (FeO + Fe_2O_3)/(FeO + Fe_2O_3 + MgO) (Arndt et. al., 1977), the talc schists occupy the komatiite field (Fig. 10.8B) similar to the Gorgona and Munro komatiites (Echeverria, 1982) whereas the amphibolites occupy the tholeiitic field, similar to the Barberton and Nondweni tholeiites (Wilson and Versfeld, 1994) and the Gorgona and Munro tholeiitic basalts (Echeverria, 1982). The talc serpentine schists have a lower Al_2O_3 content (***Table 10.3***). Nesbitt et. al., (1979) recognized some komatiites as being alumina-depleted and others alumina-undepleted. Depletion of Al results in elevated values for CaO/Al_2O_3 (Fig. 10.8C) and low values for Al_2O_3/TiO_2 (Wilson and Versfeld, 1994). Fig. 10.8B further shows that the talc schists have similar Al_2O_3 contents to the Barberton komatiites but lower Al_2O_3 content than the Nondweni komatiites (Wilson and Versfeld, 1994). They have CaO/Al_2O_3 values >1 and are therefore similar in this respect to the Barberton and Nondweni komatiites (Fig. 10.9B) (Wilson and Versfeld, 1994).

Major element chemistry (Pearce et. al., 1975; 1977) and trace element chemistry can be used to discriminate basalts from different tectonic environments. Pearce et. al., (1975) use the TiO_2 - K_2O - P_2O_5 ternary diagram to separate oceanic and non-oceanic basalts, provided the total alkali content is less than 20% in an AFM ternary diagram. Fig. 10.9A shows that most of these rocks fall in the oceanic field. This origin is strengthened by the fact that metamorphism of basaltic rocks should enrich them in K_2O. In this regard, the negative slope shown in Fig. 10.8D, which is a plot of Na_2O + K_2O against Na_2O/K_2O (Miyashiro, 1975), indicates K_2O mobility in these rocks and therefore confirms that they are of probable oceanic origin. It is also significant to note that in Fig. 10.9A amphibolites plot

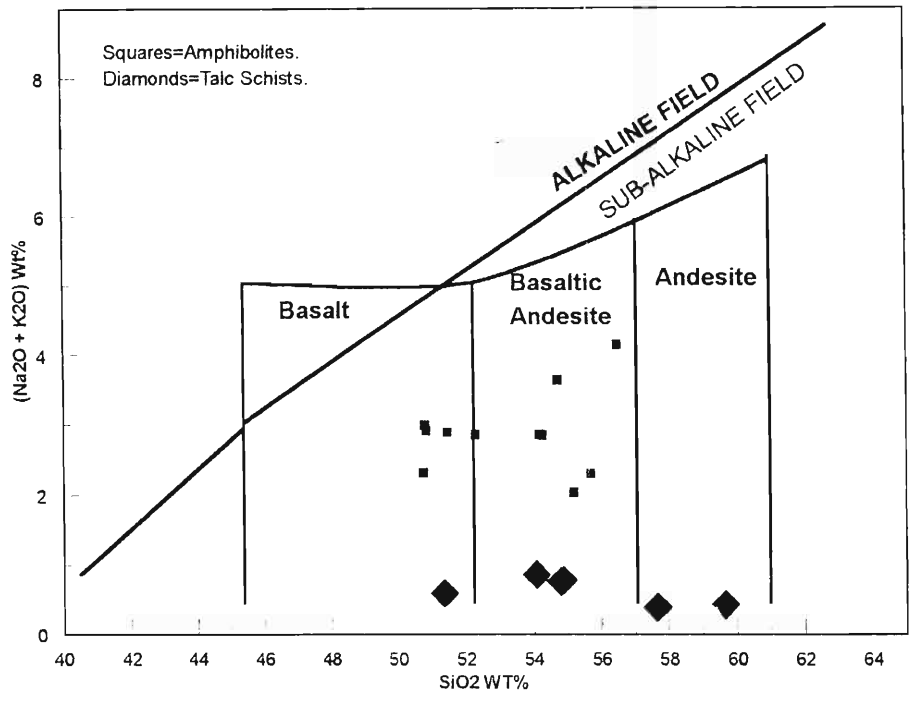

Fig.10.5 A : TAS (total alkalis vs silica) diagram depicting the sub-alkaline affinity of the amphibolites and talc schists of the Ilangwe Belt.The line separating the alkaline and sub-alkaline fields is after Irvine and Baragar (1971) and the different basaltic fields are from Le Bas et. al (1986).

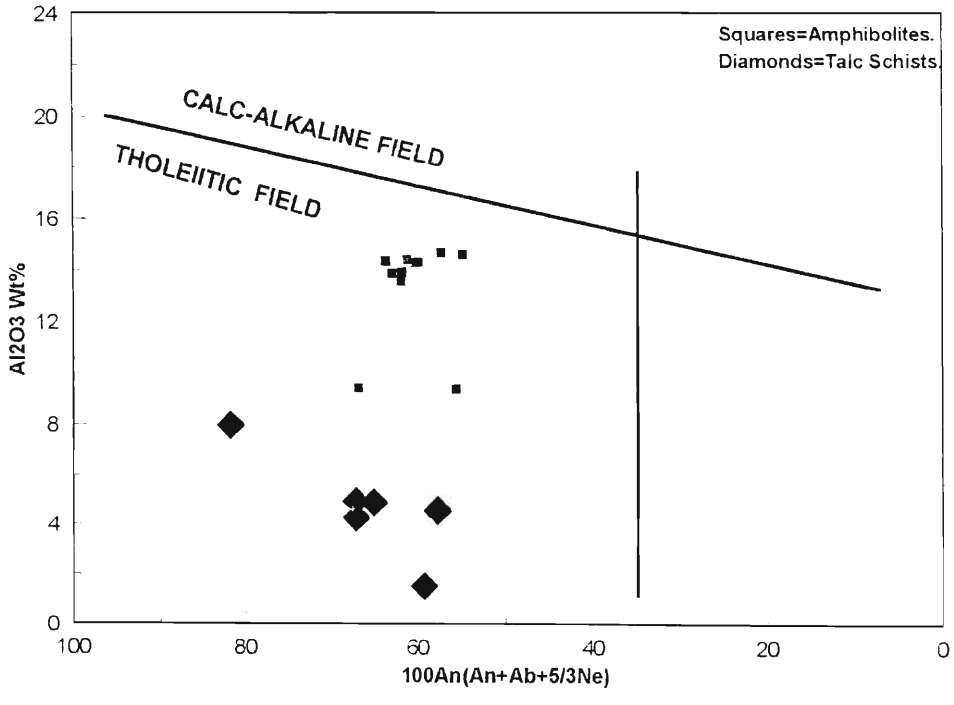

Fig.10.5 B : Plot of Al_2O_3 Wt% against normative plagioclase for the analysed amphibolites and talc schists of the Ilangwe Belt. The line separating the calc-alkaline and tholeiitic fields is from Irvine and Baragar (1971).

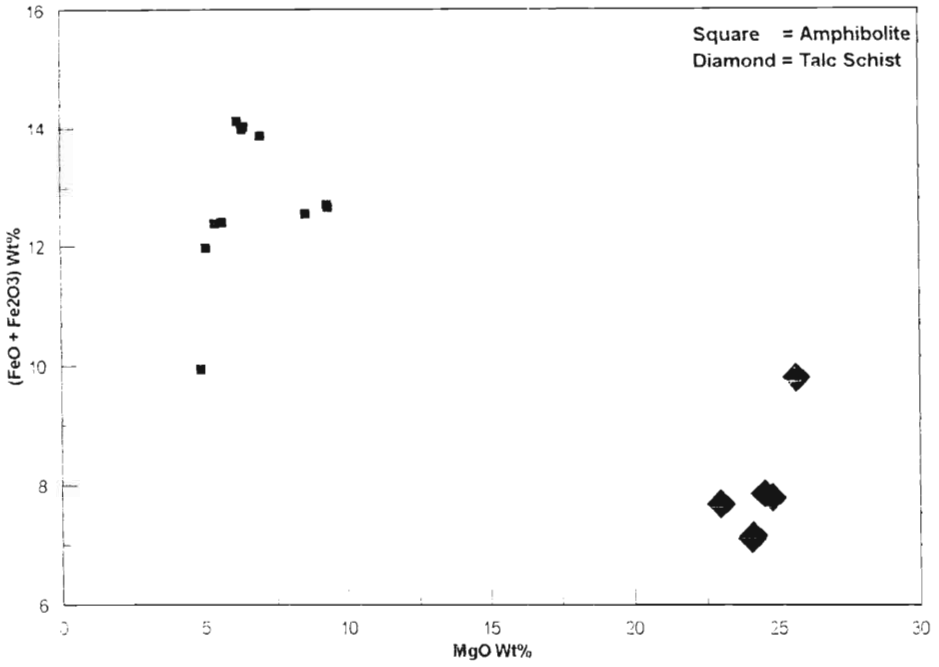

Fig. 10.5 C : Variation of total Fe with MgO for the amphibolites and talc schists of the Ilangwe Belt. There is a separation between the amphibolites and the talc schists and the latter show a total Fe depletion.

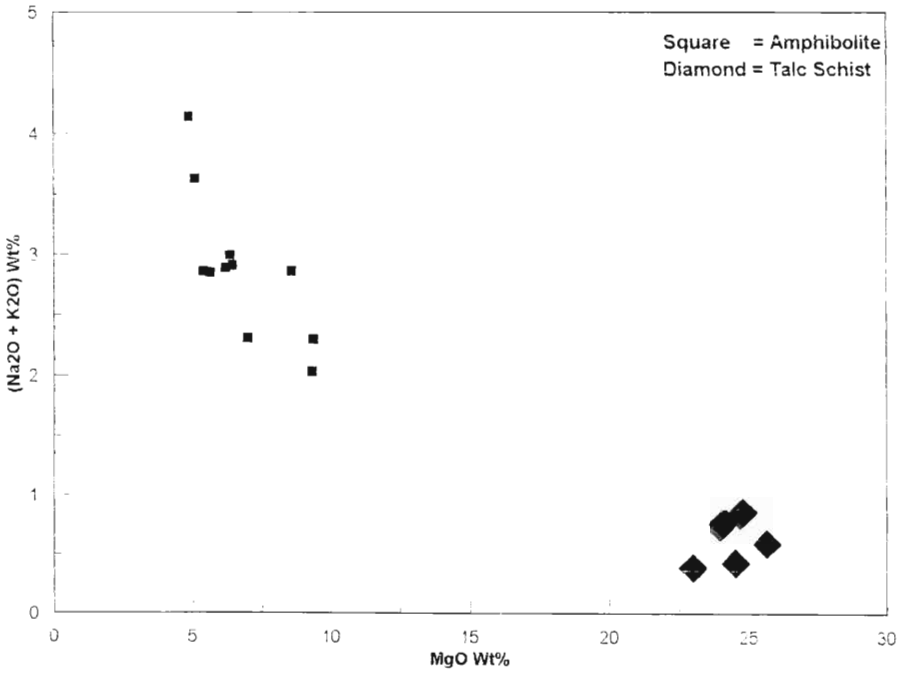

Fig. 10.5 D : Variation of total alkalis with MgO for the amphibolites and talc schists of the Ilangwe Belt showing a clear separation between the two types of suites and with the talc schists being depleted in total alkalis.

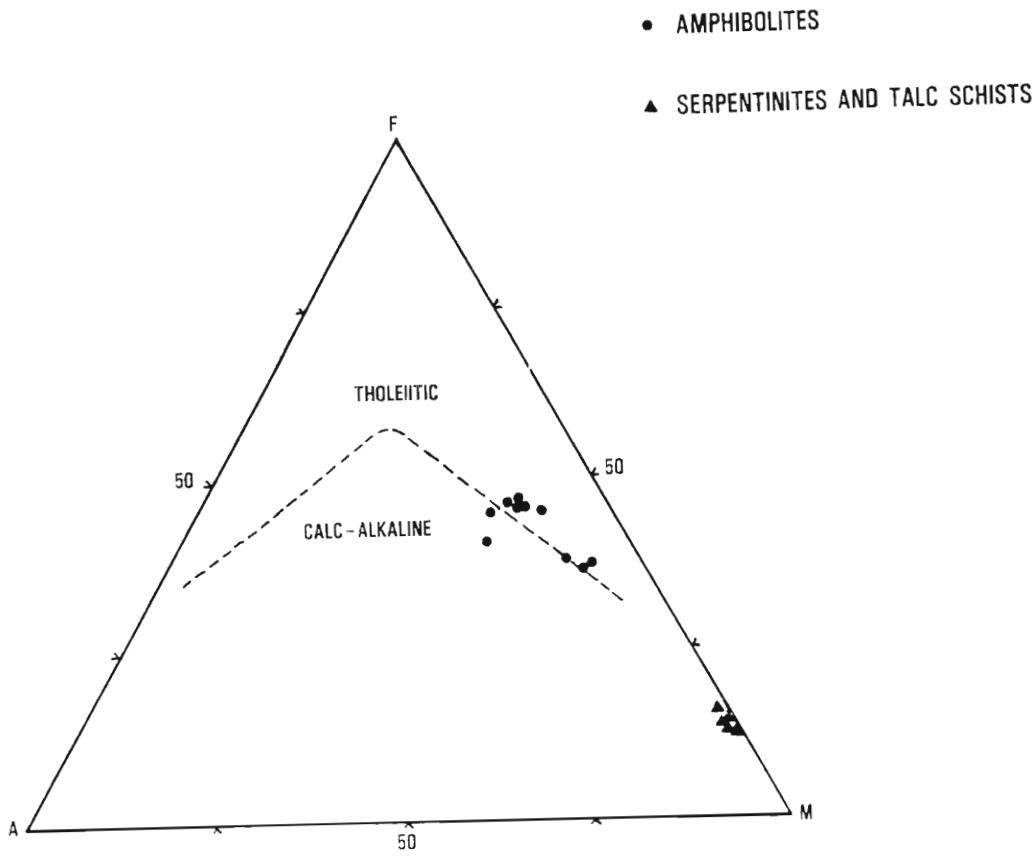

Fig. 10.6: AFM ternary plot of the amphibolites and talc schists. The dashed line separating the tholeiitic and calc - alkaline fields is after Irvine and Baragar (1971).

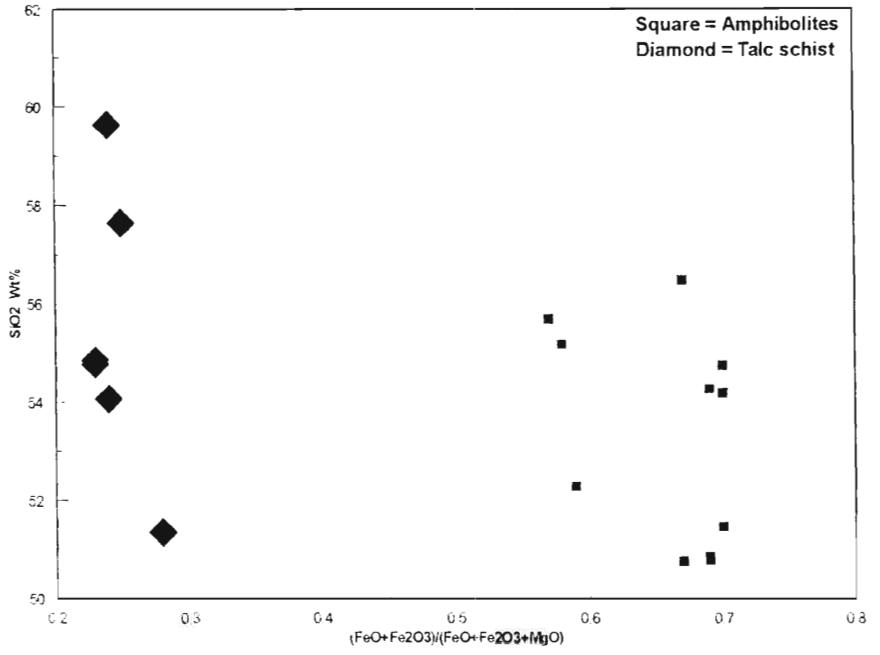

Fig. 10.7 A : Plot of total Fe/total Fe+MgO against SiO_2 showing that the talc schists of the Ilangwe Belt are depleted in Fe.

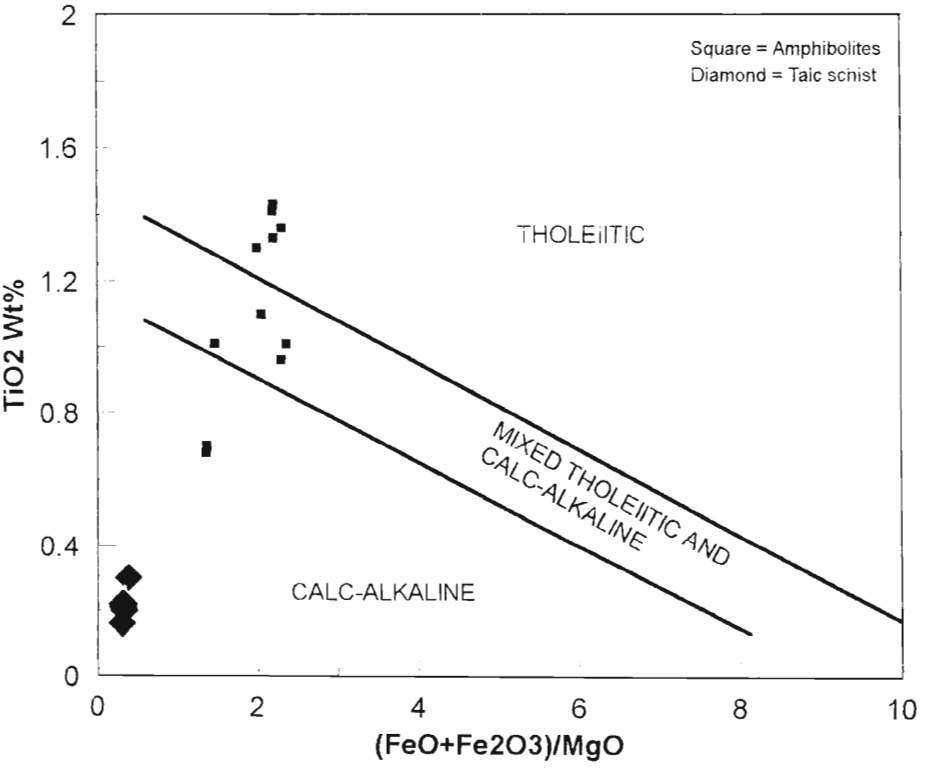

Fig. 10.7 B : Plot of total Fe/MgO against TiO_2 showing gradual TiO_2 enrichment with the increase in the $(FeO+Fe_2O_3)/MgO$ ratio. The different compositional fields are from Miyashiro and Shido (1975).

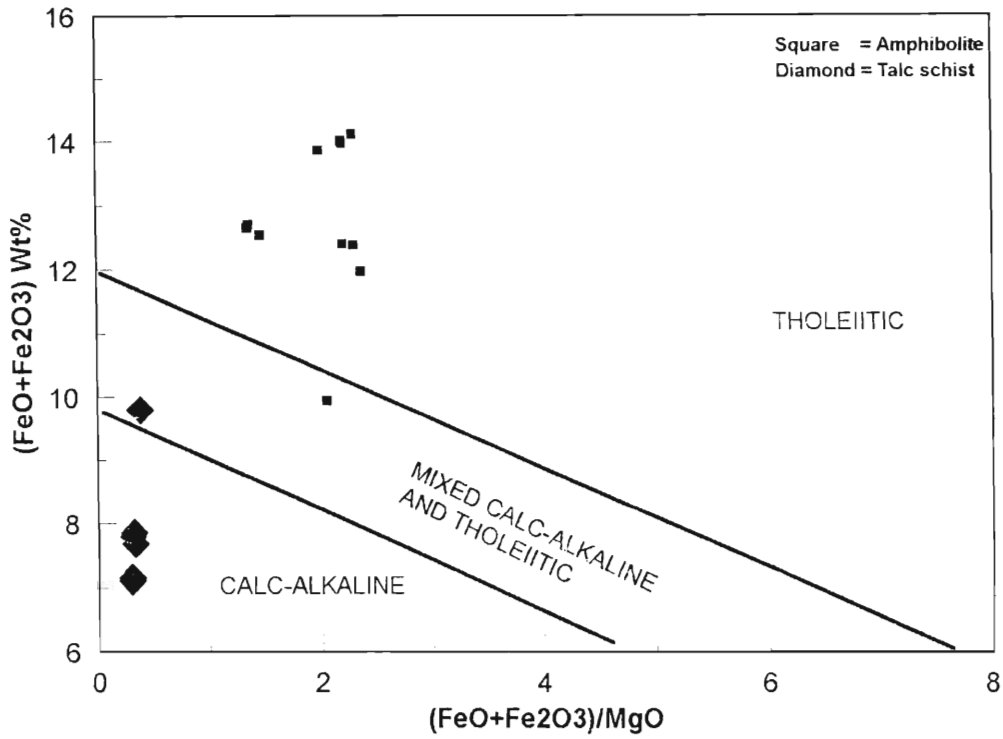

Fig. 10.7 C : Plot of total Fe/MgO against total Fe showing the iron-depleted nature of the talc schists. The different compositional fields are from Miyashiro and Shido (1975).

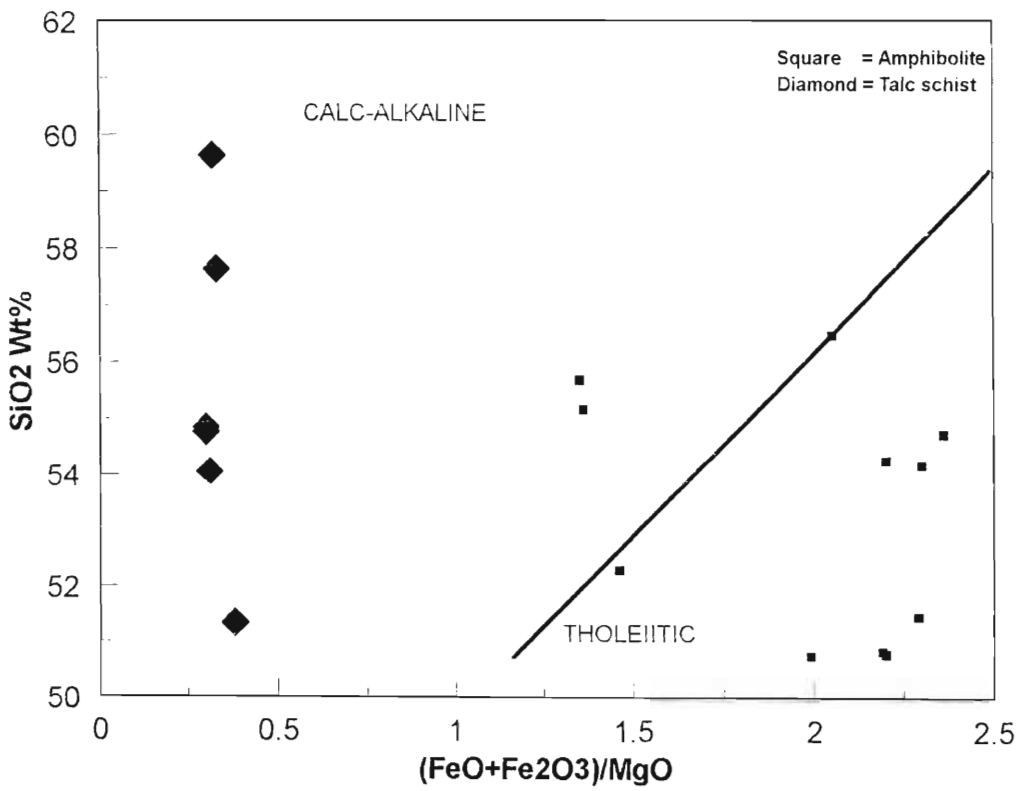

Fig. 10.7D : Plot of total Fe/MgO against SiO_2 showing the iron-depleted nature of the talc schists.The line separating the calc-alkaline and tholeiitic fields is from Miyashiro (1974).

on the island-arc tholeiitic field of Garrison (1981), thus suggesting an Archaean tectonic setting similar to a Phanerozoic island-arc setting.

From the foregoing brief discussion of the geochemical classification of the mafic and ultramafic rocks, it is clear that the pillowed and banded metabasalts were probably formed in an oceanic environment. The banded amphibolites are thought to represent strongly flattened pillows similar to the amphibolites at Torsholmsören in Finland (Ehlers, 1976) and are of tholeiitic affinity similar to the pillowed amphibolitic metabasalts. The serpentinitic talc-tremolite schists are thought to represent altered high magnesium - high silica komatiites, probably komatiitic andesites. The Archaean ultramafic komatiites are thought to be products of the partial melting (<50%) of the mantle (Herzberg, 1992; Burke and Kidd, 1978) due to hot rising plumes (Miller et. al., 1991a,b; Campbell et. al., 1989; Arndt, 1986). The Barberton- and Munro-type komatiites are thought to have formed in plumes that were hotter than in the present-day mantle by 500° and 300° respectively (Herzberg, 1992). Storey et. al., (1991) suggest that the Archaean plume-related komatiite-tholeiite sequences could represent overthrust fragments that were generated in oceanic plateau settings.

10.3 METASEDIMENTS OF THE ENTEMBENI AND OLWENJINI FORMATIONS

10.3.1 PETROGRAPHY

10.3.1.1 PHYLLITES

Ilangwe belt phyllites consist largely of quartz, alkali feldspars, cordierite, muscovite and minor carbonate (calcite?), biotite, garnets and ore as indicated by the modal analyses in ***Table 10.4***. Some minor amounts of plagioclase (of indeterminate composition) have been observed in some specimens. These show sericitized albite twinning.

Quartz, feldspars and cordierite occur as hypidioblastic inequigranular crystals in a consertal texture. Relict garnet porphyroblasts have been rotated (Plate 10.3A). Sheared ore trails bordered by muscovite and minor biotite flakes indicate a right-lateral sense of movement in thin section. The sheared nature of the ore shows that the ore mineralizing system pre-dates the shear deformation episode. Quartz, cordierite and feldspar are flattened along the foliation direction and the former two minerals show undulose extinction

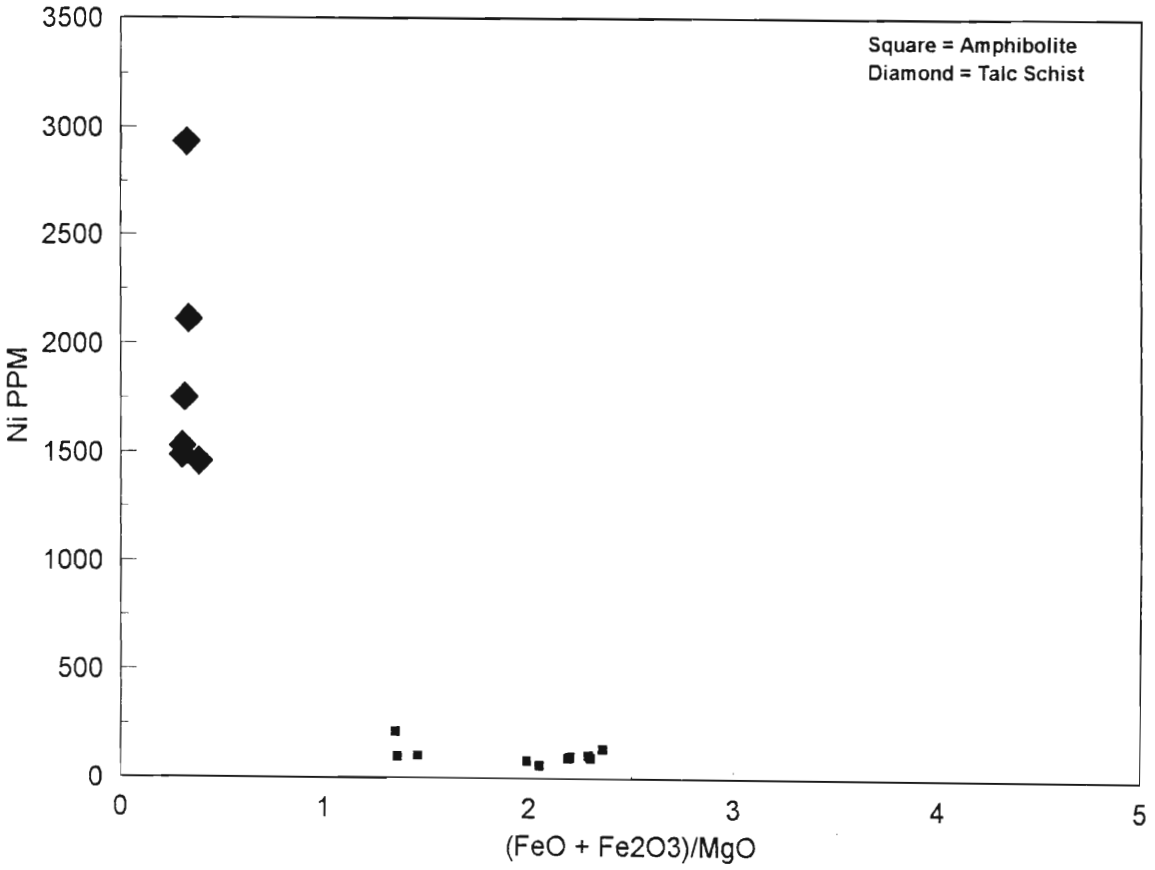

Fig. 10.8 A : Plot of total Fe/MgO against Ni ppm showing anomalous Ni concentrations for the talc schists - typical of suites of komatiitic affinity.

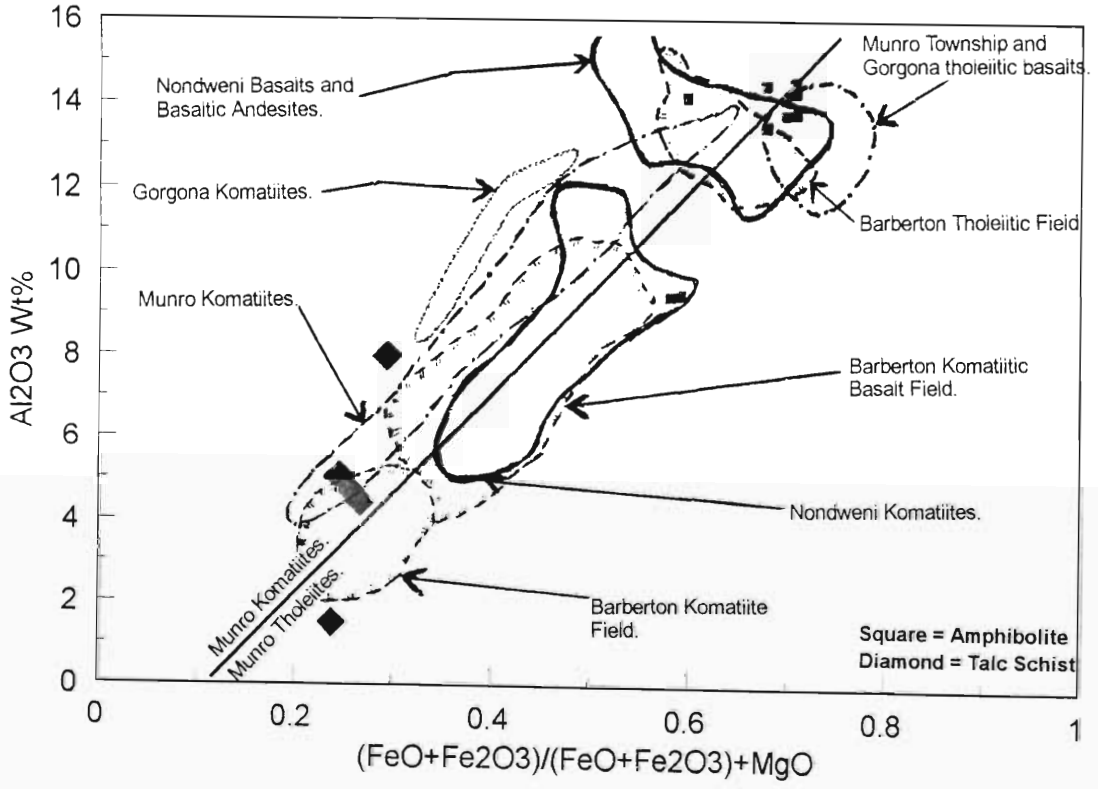

Fig. 10.8 B : Plot of total Fe/total Fe+MgO against Al_2O_3 comparing Ilangwe Belt amphibolites and talc schists with the Barberton, Nondweni and Munro Township rocks (after Wilson and Versfeld, 1994b; Echeverria, 1982; Arndt et. al. 1977).

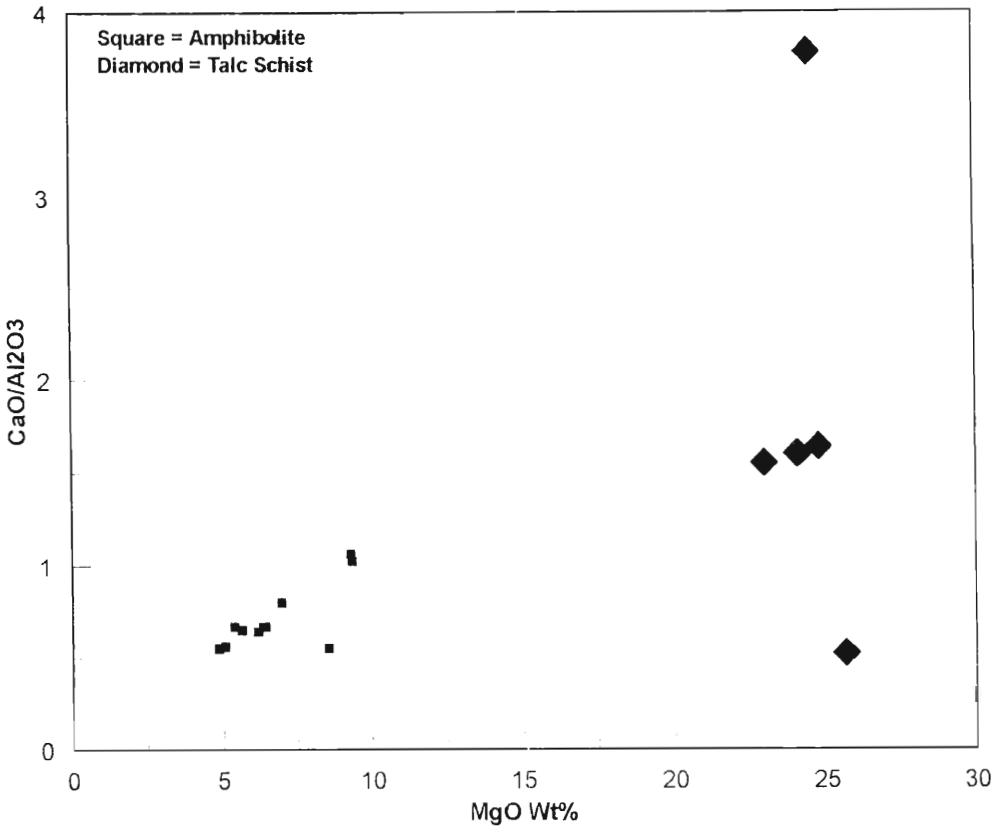

Fig. 10.8 C : Plot of MgO against CaO/Al_2O_3 showing most of the talc schists having $CaO/Al_2O_3 > 1$ as a result of the corresponding depletion in Al whereas most of the amphibolites have $CaO/Al_2O_3 < 1$.

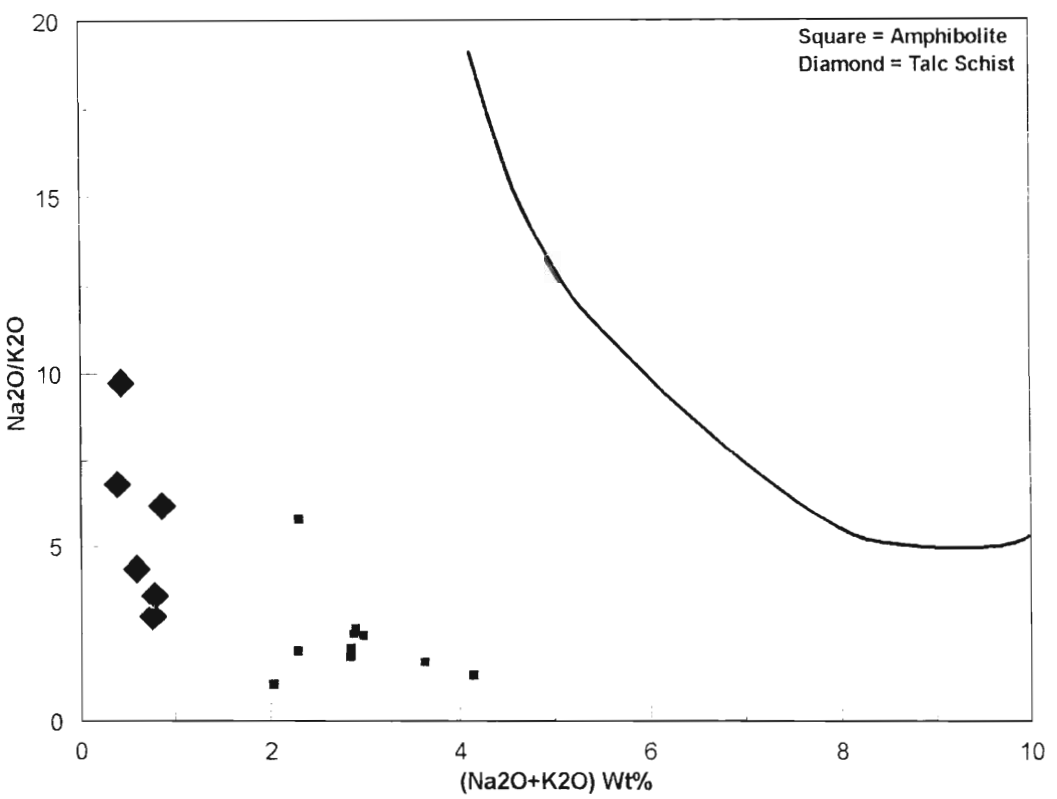

Fig. 10.8 D : Plot of total alkalis vs Na_2O/K_2O showing a negative slope thus confirming K_2O mobility during the metamorphism of amphibolites and talc schists. The solid curve is the suggested upper limit for natural unaltered volcanic rocks (after Miyashiro, 1975).

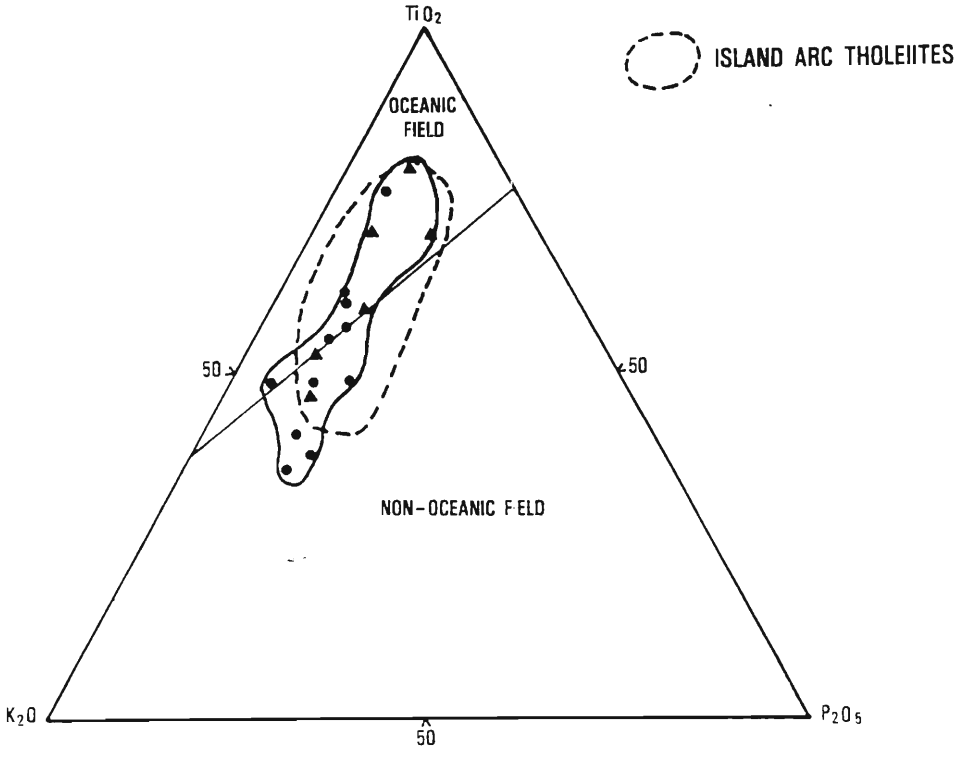

Fig. 10.9A: TiO_2 - K_2O - P_2O_5 ternary plot of the amphibolites and talc schists of the Ilangwe Belt (after Pearce et. al., 1975). The field of Island - arc tholeiites is from Garrison (1981). Symbols as in Fig. 10.6.

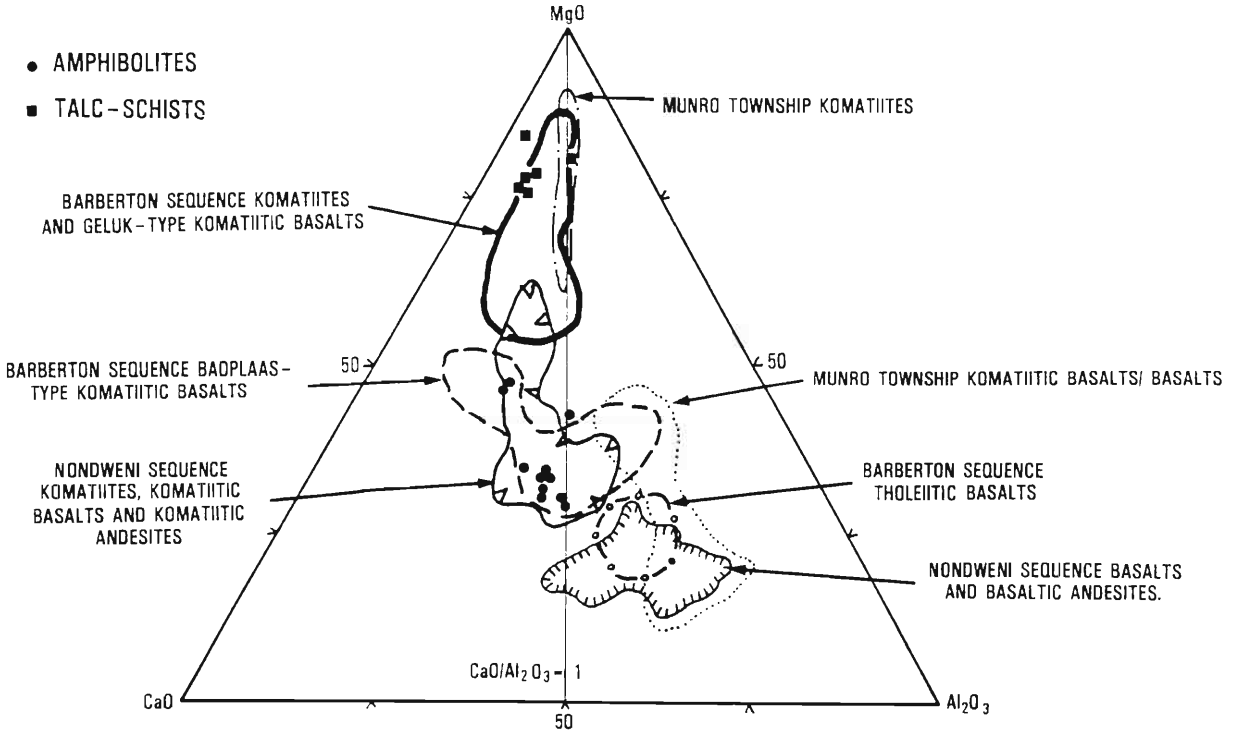

Fig, 10.9B: MgO - CaO - Al_2O_3 ternary plot of the amphibolites and talc schists compared to the Barberton, Nondweni and Munro Township rocks (after Wilson and Versfeld, 1994; Viljoen et. al., 1982; and Arndt et. al., 1977).

with some dust trails occurring within some cordierite crystals. Muscovite occurs in between the quartz, cordierite and feldspar grains thus indicating unstable grain boundaries. Less than 2% of actinolite crystals have been observed and these are altered to muscovite and carbonate. Minor sericitization of cores of feldspars occurs.

In sample H44EB there is evidence of post-tectonic growth of a second generation muscovite and epidote. It is impossible to determine mineral stretching lineations in the field because of the fractured (cataclastic) and schistose nature of these rocks. Oriented specimen did not help either. The schistose nature of the rock is thought to arise from differential movement on closely-spaced slip surfaces (Williams et. al., 1982; see Plate 5.4A).

The phyllonites are typical Type II S - C mylonites (Lister and Snoke, 1984) with the C-planes subparallel to foliation/schistosity (Plate 5.4A). Such mylonites develop during conditions of decreasing pressure and temperature (Lister and Snoke, op. cit.).

10.3.1.2 METACHERTS AND CHERTY QUARTZITES

The metacherts and cherty quartzites have simple but quite varied mineralogy as shown by the modal analyses in ***Table 10.4***. In hand specimen they range from recrystallized banded cherts with distinct thinner black bands and thicker white bands (Plate 5.4B) to massive uniform white/cream-white to buff-coloured metacherts and cherty quartzites. The cherty quartzites usually have a distinct light green coloration of fuchsite and can thus be termed fuchsitic cherty quartzites.

In thin section, these rocks consist dominantly of quartz, alkali feldspars, plagioclase, muscovite/fuchsite, cordierite, actinolite, stilpnomelane, biotite, minor carbonate, sericite, chlorite, ore, epidote/piedmontite, and trace amounts of apatite and zircon.

Quartz (30-90% by vol.) occurs as granoblastic subhedral to anhedral inequigranular grains showing a consertal to crystalloblastic fabric. Where recrystallization is evident, quartz and cordierite occur as small-sized (<0,15mm) crystalloblastic mosaic of polygonal grains. Some of the quartz is flattened along foliation and shows undulose extinction.

Cordierite (2-30% by vol.) shows bright yellow pleochroism with dust trails, undulose extinction, a moderate 2V and is biaxial negative. In recrystallized samples, it occurs in

polygonal triple-junction boundaries with quartz. Some grains are also flattened along a preferred orientation that defines the foliation.

Actinolite occurs as long fibrous to columnar laths with bright interference colours whereas muscovite/fuchsite occurs as brightly coloured laths or plates showing the characteristic mottled extinction. Both actinolite and muscovite/fuchsite assume a preferred orientation parallel to foliation and give a nematoblastic and lepidoblastic texture respectively (Plate 10.3B). Both these minerals occur between bands of quartz and feldspars and show the original S_{O1} bedding planes. Some actinolite crystals show compositional zoning.

The alkali feldspars are mainly cloudy microcline with the typical tartan twinning and some have deformed dust trails. Plagioclase is of albitic composition and has faint albite twinning. There is evidence of incipient myrmekitic texture between quartz and feldspars (e.g. H58EB) and muscovite/fuchsite surrounds or borders the incipient myrmekite. The occurrence of myrmekite points to infiltration of fluids into the rock during M_2 retrograde metamorphism (Shelley, 1993). Simpson and Wintsch (1989) have shown that myrmekite preferentially develops on the strained borders of the feldspars usually in direct response to stress-induced K-feldspar replacement.

Accessory ore (0 - 3% by vol.) is either ilmenite with red rims or magnetite. In sample H41EB the ore is as much as 10% by volume and occurs as small (<0,1mm) cubic crystals of sulphides (pyrite?) occurring along the bedding planes, showing that it crystallized from sulphidic fluids injected along bedding planes. Of particular interest is the occurrence of two forms of ores. The earlier ones are deformed and aligned along the bedding/foliation and the later ones are perfectly cubic and probably related to the M_2 retrograde metamorphism.

Stilpnomelane (0 - 7% by vol.) occurs as fibrous crystals and epidote (0 - 8%) occurs as euhedral to subhedral crystals. In sample H21EB the epidote grades to a yellowish coloured iron-rich piedmontite. Piedmontite results from the substitution of Mn^{3+} and Fe^{3+} for Al in epidote (Heinrich, 1965).

PLATE 10.4 : REPLACEMENT TEXTURES IN METASEDIMENTS AND THE AMAZULA GNEISS.

PLATE 10.4A : Phyllite of the Simbagwezi Formation showing a distinct cleavage refraction and a faint rodding lineation. [Phyllite from Simbagwezi Peak: (6.020/K.390)]

PLATE 10.4B : Large muscovite books in a sheared quartz muscovite schist of the Nomangci Formation. Grey chlorite has replaced muscovite at some places. Note the flattened quartz grains due to shearing. [Quartz muscovite schist west of Simbagwezi Peak: (6.430/H.000)]

PLATE 10.4C : Lepidoblastic texture in the quartzitic flaser gneiss. the leucosome of the Amazula Gneiss in the Umhlathuze River nappe structure (5.035/Q.330). The quartz and biotite are aligned along the foliation and define the gneissosity. There is incipient alteration of biotite to calcite along grain boundaries.

PLATE 10.4D : Reaction rim in the Amazula Gneiss showing deformed biotite, hornblende and ortho-pyroxene with lamellae of clinopyroxene. Note uralitization with pyroxene being replaced (along grain boundaries) by hornblende and hornblende is in turn replaced by biotite. Biotite is also altering to chlorite. [Sheared contact of amphibolite gneiss and a Type B xenolith, Amazula River: (6.880/BB.195)]

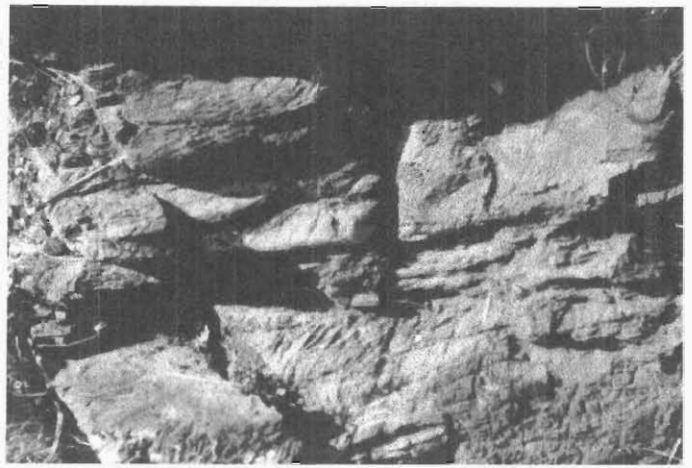

A

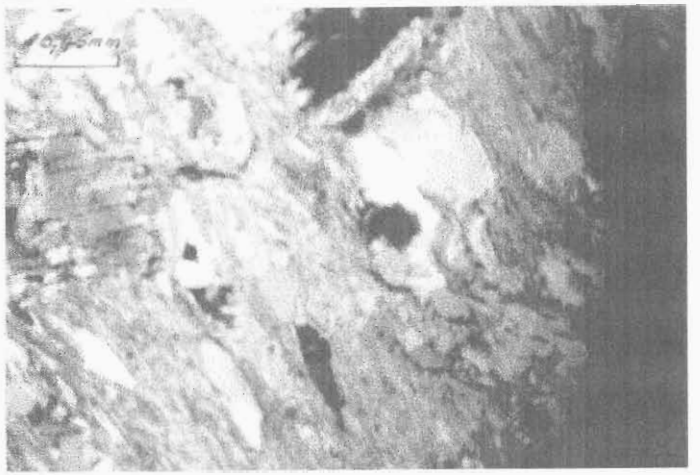

B

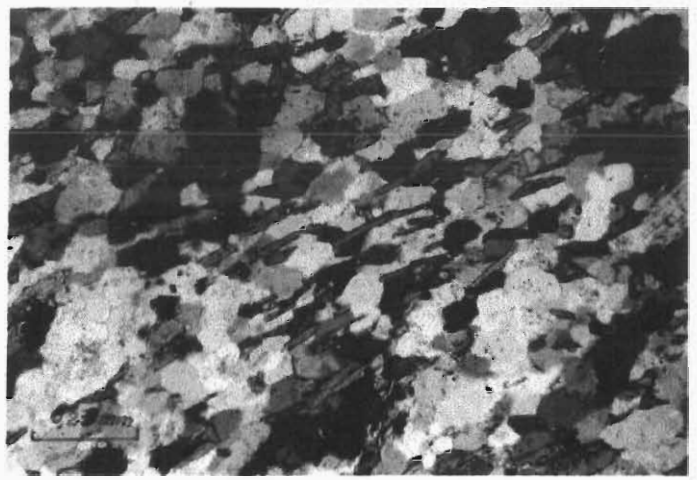

C

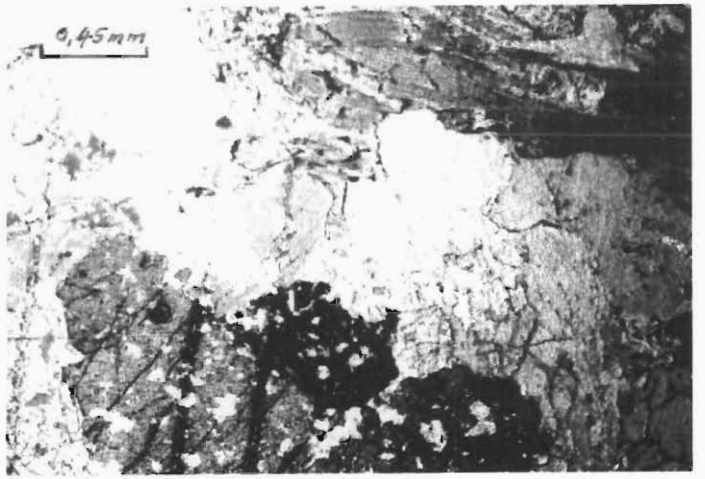

D

Plate 10.4

TABLE 10.4 : METASEDIMENTS OF THE ILANGWE BELT : MODAL COMPOSITIONS AND PETROLOGICAL FEATURES

SAMPLE IDENTITY	SAMPLE NO.	MINERAL MODAL COMPOSITION (%)																	GRAIN SIZE			PLAG An CONTENT %	TEXTURE
		Qtz	Plg	K-Fel	Act	Stilp	Grun	Cord	Biot	Garn	Carb	Epid	Zir	Chlo	Ser	Mus	Ore	Pyrox	F	M	C		Granoblastic(*); Subophitic(Sub); Ophitic(Oph); Inequigranular(In); Equigranular(Eq); Myrmekitic(Myr); Uralitization(Ur); Xenoblastic(Xen); Nematoblastic(Nem).
A	H44EB	35	35		1			15			1			3		10				x		An_5	
A	H47EB	30	40		1			10		5	3			1		10			x	x		An_7	In.; cons.; schistose
B	H10EB	30	25		20			20			t			5		t			x			An_{10}	In.; cons; dextral shearing
B	H20EB	75						25								t			x	x		nd	In.; cons.
B	H21EB	55	2		28	7						8								x			In.; nem.
B	H41EB	65		20								t				5	10			x			Slightly fuchsitic
B	H57EB	40	15	20	6			15			t		t	1	1	2	t		x	x		An_{6-10}	*; in.; nem.
B	H58EB	35	10	20				10			t	t			4	20	t			x		An_9	Myr.; *; In.; 20% Musc.=Fuchsite
B	H76EB	42	20	25				10	3								1		x	x			*; cons.
B	H79EB	25	20	15				12			t				1	24	3		x	x			In.; cons.; lepid.; 24% Musc=Fuchsite; dextral shear
B	H80EB	35	40	5				15							t	5	t			x			In., cons.; lepid.
B	H153EB	90		10					t							t				x			In., cons.
C	H48EB	10				40											50			x			Banded; Ore=Mt.
C	H83EB	40					5										55			x			In.; xen.; Ore=Mt.
C	H122EB	60		3			1									1	35			x			In.; xen.; Ore=Hm.
C	H127EB	45		2		3										t	50			x			Xen.; banded; ore=Hm.
C	H128EB	45		4		1											50			x			Ore=Hm.
C	H137EB	50				5	5									t	40		x	x			Ore=Hm.
D	H11EB	25						35	15			t		10		15					x		In.; lepid.; 15% Musc.=Fuchsite
E	H141EB	15	10											15	4	56				x		An_{9-17}	Eq.; lepid.; slightly schistose

A = PHYLLITE B = METACHERTS AND CHERTY QUARTZITES C= BIF D= QUARTZ BIOTITE CORDIERITE FUCHSITE GNEISS E = QUARTZ MUSCOVITE SCHIST

10.3.1.3 BANDED IRON FORMATIONS

The banded iron formations of the Ilangwe belt are intensely contorted and consist of finely alternating millimetre scale bands of boudinaged chert (cherty quartz) and magnetite altered to haematite (Type I iron formation) or bands of cherty quartz and mainly grunerite and stilpnomelane associated with iron-rich chlorite (Type II iron formation). Type I occurs in the eastern and central parts of the belt whereas Type II is confined to the western part of the belt especially in the Olwenjini Valley - Ngcengcengu Peak area (4/Q,R,S) where it occurs in close contact with the garnetiferous amphibolite of the Sabiza Formation and the folded metacherts and cherty quartzites of the Entembeni Formation.

Table 10.4 gives the modal analyses and a summary of the features of the iron formations. In thin section, Type I iron formations consist of various amounts of cherty quartz, magnetite, haematite (after magnetite), and subordinate K-feldspar and stilpnomelane. Minor chlorite also occurs. Quartz occurs as inequigranular grains with polygonal to interlobate granoblastic textures. It shows intense undulose extinction and recrystallization into a mosaic of polygonal grains occurring along thin 1,5 to 2,5mm long fractures or microfaults (H48EB; H127EB; H128EB). Magnetite occurs as bands of subidioblastic to xenoblastic interlocking grains showing triple-point grain boundaries. It alters to a brick-red haematite which in some thin sections occurs as ghost-like wisps.

Type II iron-formations consist of inequigranular to equigranular granoblastic quartz grains stained reddish-black by iron-bearing minerals. It shows an undulose extinction and has deformed dust trails. Magnetite occurs as interlocking subidioblastic grains associated with stilpnomelane which has a fibrous to plate-like habit. Some magnetite grains are poikiloblastically enclosed in stilpnomelane or in grunerite which occurs as asbestiform to columnar parallel aggregates defining the banded nature of the rock.

10.3.1.4 QUARTZ-BIOTITE-CORDIERITE-FUCHSITE GNEISS

A thin sliver or wedge of quartz-biotite-cordierite-fuchsite gneiss occurs within amphibolites and metacherts of the Olwenjini Formation in the Sabiza River (5.180/V.800). It is about 10-25m wide and is cut by a gabbro-noritic sill in the east just above the river. To the west, it can be traced for about 100 to 150m before it disappears. The rock occurs only in this area. It consists of bands of quartz alternating with large crystals of dark green to black biotite wrapping light-bluish ribbon-like crystals of cordierite and quartz. Minor fuchsite and

chlorite is associated with biotite. ***Table 10.4*** (sample H11EB) shows the modal composition of this rock.

In thin section, the quartz is oblate and flattened along a preferred orientation. Cordierite (slightly altered to pinite) occurs as deformed subidioblastic (pseudo hexagonal) to ribbon-like grains bounded by biotite which, seemingly, has been squeezed into the grain boundaries. Both quartz and cordierite show a wavy extinction. Biotite occurs as long columnar to fibrous crystals aligned along a preferred orientation and giving the rock its gneissose texture. Biotite is associated with fuchsite and it is altered to iron-rich chlorite.

The rock is thought to have formed as a result of low to medium pressure (Winkler, 1979) dislocation metamorphism initiated by high strains due to intense shearing. The confinement of this rock to this locality is an enigma.

10.3.2 METAMORPHISM

10.3.2.1 PHYLLONITES

Phyllonites are end-products of dislocation metamorphism. Their protolith was a phyllite which was metamorphosed to medium grade and then later experienced retrogressive greenschist metamorphism. The following parageneses were observed:

Quartz + K-feldspar + garnet + actinolite + cordierite (pinite) + plagioclase± biotite.....(1)

Quartz + feldspar + muscovite + chlorite ± cordierite (pinite).....(2)

Quartz + muscovite + chlorite + carbonate.....(3)

The first two assemblages have been observed in the same thin section (e.g. H47EB), implying that (1) is an M_1 high temperature medium grade metamorphic paragenesis which as altered to (2) during low grade M_3 retrograde metamorphism associated with the late dislocation metamorphism.

It is significant to note that in (1) cordierite and garnet co-exist. Such a co-existence is known in medium grade rocks belonging to the cordierite-almandine zone which "occurs invariably in some higher temperature part of medium grade metamorphism" (Winkler, 1979; Fig. 10.10). The possibility that (1) could represent high-grade metamorphism is negated by the presence of actinolite and the fact that the co-existence of cordierite and garnet can only occur over a limited pressure-temperature range in high grade metamorphic conditions [Hensen and Green (1971) quoted in Winkler (1979)].

It is, further, worth noting that sillimanite was not observed in thin sections. Winkler (1979, p. 233) notes that the paragenesis

cordierite + garnet + sillimanite + biotite

is not considered to be stable in the presence of plagioclase. Parageneses (2) and (3) are typical of low grade pelitic rocks. Muscovite and chlorite were probably formed from the retrograde metamorphism of actinolite and biotite.

10.3.2.2 METACHERTS AND CHERTY QUARTZITES

The following four dominant mineral assemblages have been observed in the various metacherts and cherty quartzites of the Ilangwe Belt :

Quartz + cordierite + muscovite/fuchsite ± ore.

Quartz + K-feldspar + cordierite + actinolite + chlorite + calcite ± albite ± fuchsite.

Quartz + actinolite + stilpnomelane + Epidote + albite.

Quartz + K-feldspar + albite + muscovite/fuchsite + cordierite + myrmekite.

Williams et. al., (1982) suggests that the grade of metamorphism for the quartzites "can be inferred from the nature of associated rocks of other lithology, reinforced in some cases by the minor mineral components of the quartzites themselves". Judging from the above four

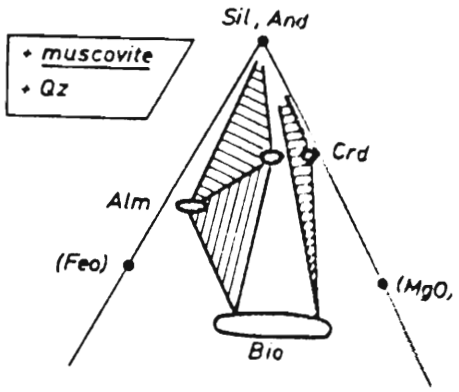

Fig. 10.10: Cordierite - (garnet) - medium-grade metamorphism of the rocks of the Olwenjini and Entembeni Formations (from Winkler, 1979).

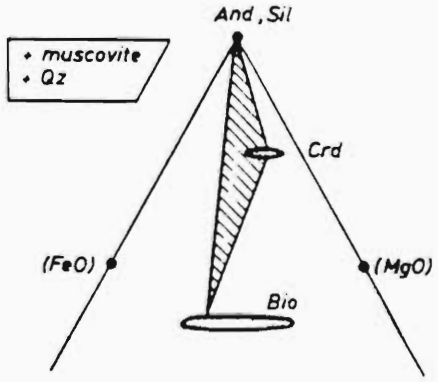

Fig. 10.11: Cordierite medium-grade metamorphism of the Ilangwe metacherts and cherty quartzites (staurolite is absent) (from Winkler, 1979).

mineral components of the metacherts and cherty quartzites and the preceding discussion on the phyllites, these rocks seem to have been subjected to two phases of metamorphism. The early M_1 phase is that of the cordierite medium grade metamorphism (Fig. 10.11) which suffered retrogression during the M_2 low grade greenschist metamorphism dominated by muscovite/fuchsite and some chlorite. These phyllosilicates show a lepidoblastic texture in these rocks (Plate 10.3B). A common texture in the fuchsitic cherty quartzites is one of anastomosing schistocity planes rich in green fuchsite separated by microlithons of quartz or chert with minor green fuchsite. Similar textures have been described by Martyn and Johnson (1986) for the fuchsite-bearing rocks near Menzies, Western Australia. Commonly, the Ilangwe Belt fuchsitic cherts and cherty quartzites are mylonitic. In the Barberton Greenstone Belt, fuchsite is characteristic of zones interpreted as mylonites of early generation thrust planes (de Wit, 1982).

Fuchsite is thought to be an indication of potash metasomatism of ultramafic rocks (Martyn and Johnson, 1986) which, in the Ilangwe Belt, are represented by talc-tremolite schists occurring in the vicinity of the cherts and cherty quartzites. Potassium metasomatism is supported by the elevated K_20 contents (***Table 10.5***), especially in samples H57EB, H58EB and H79EB which are fuchsitic. The K-metasomatism probably took place during the waning stages of the M_2 low-grade retrograde metamorphism. De Wit et. al. (1987, 1982) consider the bright green fuchsitic chert fragments occurring in felsic intrusions in the Barberton Mountainland to represent silicified mafic-ultramafic rocks (komatiites).

Ilangwe metacherts and cherty quartzites have high SiO_2 contents (***Table 10.5***) ranging between 78 and 98%. Generally, Al, Fe and Mg are low whereas K_2O is slightly elevated, as mentioned earlier. Rb ranges between 5 and 74, Sr ranges between 7 and 119 and Zr ranges between 25 and 104. Th, U and Y are very low.

10.3.2.3 BANDED IRON FORMATION

The banded iron formations have the following simple parageneses:

Magnetite + haematite + quartz ± chlorite ± stilpnomelane.....(1)
Quartz + stilpnomelane + grunerite + magnetite ± actinolite.....(2)

These mineral assemblages seem to show the early M_1 prograde metamorphism which probably retrogressed to low grade assemblages during M_2 regional greenschist

metamorphism. These parageneses are indicative of low grade to medium grade metamorphic conditions (Winkler, 1974). Charlesworth (1981) observed the assemblage magnetite + haematite + quartz for the banded ironstones of the Esibhudeni area of the Natal Mobile Belt just west of the present study area. Smalley (1980) observed assemblages similar to paragenesis (2) in the Halambu Valley of the Natal Mobile Belt ± 20km southwest of the present study area.

Magnetite is stable under a wide range of pressure and temperature conditions and its reaction with quartz is mainly due to a change in redox conditions (Eugster and Ming Chou, 1973). The generation of grunerite in the iron formations is the result of the reaction between quartz and magnetite :

$$96SiO_2 + 28Fe_2O_3 + 3H_2O = 12Fe_7Si_5O_{22}(OH) + 17O_2.$$

quartz + magnetite = grunerite.

Removal of the surplus oxygen to allow the reaction to proceed is apparently problematic due to low oxygen mobility under greenschist facies conditions (Mel'nik, 1982, pp. 206 - 207; Miyashiro, 1973, p. 54). On the other hand, Fyfe et. al., (1978, pp.115 - 117) who examined the diffusion coefficients for oxygen through feldspar, contend that the passage of oxygen is not more radically impeded than the passage of most cations. The buffering effect of magnetite and the problematic kinetics of oxygen and cation diffusion alluded to by the aforementioned authors helped preserve the original layering in the Precambrian banded iron formations. Fig. 10.12 shows the pressure-temperature conditions for grunerite stability. ***Table 10.6*** gives the chemical analyses of the banded iron formations and are compared with the analysis of the magnetite quartzite from the Kraaipan Greenstone Belt (BU1 in Table 10.6).

Table 10.6 shows that the Ilangwe BIFs have SiO_2 contents ranging between 26 and 60%. Kraaipan magnetite quartzite has 64% SiO_2. The iron content of the Ilangwe BIFs is slightly more elevated than that of the Kraaipan magnetite quartzite. Trace element contents are relatively low; however, U and Th contents are slightly higher than that of the Ilangwe metacherts and cherty quartzites.

TABLE 10.5
ILANGWE METACHERTS AND CHERTY QUARTZITES : MAJOR AND TRACE ELEMENTS

SAMPLE	H57EB	H58EB	H76EB	H79EB	H80EB
SiO_2	80.52	86.72	94.56	78.74	98.04
TiO_2	0.23	0.19	0.05	0.39	0.02
Al_2O_3	4.62	6.99	0.54	11.44	0.10
Fe_2O_3	0.65	0.21	0.87	0.38	0.23
FeO	2.35	0.75	3.13	1.35	0.84
MnO	0.15	0.13	0.05	0.06	0.04
MgO	4.21	0.96	0.40	1.94	0.51
CaO	3.05	0.79	0.09	1.57	0.10
Na_2O	0.61	1.65	0.18	1.41	0.09
K_2O	3.56	1.60	0.12	2.64	0.02
P_2O_5	0.03	0.01	0.00	0.08	0.00
TOTAL	99.98	100.00	99.99	100.00	99.99
Rb	74.30	37.20	9.60	60.40	5.60
Sr	44.00	79.20	13.40	119.80	7.60
Zr	104.10	44.30	76.40	33.80	25.10
Nb	6.40	4.30	2.80	2.60	2.50
Y	6.30	0.00	0.00	0.00	0.00
Th	0.20	6.80	11.50	0.00	9.50
U	1.90	8.70	14.50	4.30	13.70

TABLE 10.6
ILANGWE BANDED IRONSTONES AND MAGNETITE QUARTZITE (BU1)
OF THE KRAAIPAN BELT : MAJOR AND TRACE ELEMENTS

SAMPLE	H48EB	H83EB	H122EB	H127EB	H128EB	H137EB	BU1
SiO_2	51.95	60.32	55.80	26.08	53.77	35.13	64.02
TiO_2	0.09	0.18	0.09	0.06	0.47	0.10	0.03
Al_2O_3	1.08	2.18	0.93	2.55	11.41	1.51	1.39
Fe_2O_3	10.15	7.94	9.26	15.33	2.29	13.67	7.38
FeO	36.53	28.59	33.33	55.17	8.25	49.20	25.56
MnO	0.09	0.17	0.23	0.47	0.18	0.26	0.11
MgO	0.00	0.24	0.03	0.13	10.14	0.00	0.05
CaO	0.05	0.23	0.26	0.05	9.71	0.04	0.14
Na_2O	0.00	0.04	0.00	0.00	1.92	0.00	0.04
K_2O	0.02	0.05	0.04	0.02	1.69	0.04	0.08
P_2O_5	0.03	0.04	0.02	0.13	0.16	0.05	0.21
TOTAL	99.99	99.98	99.99	99.99	99.99	100.00	100.01
Rb	4.00	4.30	4.50	4.70	54.90	4.30	37.00
Sr	5.30	5.90	8.20	9.20	142.20	6.20	6.00
Zr	30.20	35.30	30.00	21.30	48.80	28.30	1.00
Nb	1.00	0.80	0.30	0.60	3.00	0.00	0.00
Y	0.00	0.00	2.00	8.10	11.00	3.70	2.00
Th	12.10	11.30	11.00	26.30	2.10	28.90	20.00
U	8.50	8.20	13.30	4.70	5.40	6.80	11.00

10.3.2.4 QUARTZ-BIOTITE-CORDIERITE-FUCHSITE GNEISS

This rock which occurs within the Olwenjini Formation in the Sabiza River (5.180/V.800) has the following stable mineral assemblage :

quartz + cordierite + pyroxene + biotite + fuchsite + epidote.

This is typical of the cordierite medium grade metamorphism as described by Winkler (1979) (Fig. 10.11). As mentioned earlier, this rock was probably formed as a result of dislocation metamorphism at low to medium pressures (Winkler, 1979 p.224).

10.4 SIMBAGWEZI FORMATION

10.4.1 INTRODUCTION

This formation consists mainly of green phyllites (Plate 10.4A) intercalated with thin bands of pillowed metabasalts and thinner units of talc schists. Towards the top of the sequence the greenschists occur together with thin layers of dark banded cherty quartzite.

The pillowed metabasalts and the talc schists were discussed in Section 10.2. In this section, a brief petrographic description of the Simbagwezi phyllites together with the peak metamorphic conditions they attained, will be given. No geochemical analyses of the phyllites were done.

10.4.2 PHYLLITES

10.4.2.1 PETROGRAPHY

In thin section, these phyllites consist of white mica, pale green or olive green chlorite, quartz, minor biotite, epidote and opaque ore. Idioblastic to subidioblastic polygonal quartz grains show a granoblastic texture especially where there are thin quartz micro-veins oblique to schistosity. These oblique quartz veins are probably related to the thin E - W trending quartz fault-fills occurring in the Simbagwezi Peak area. One thin section showed fine lenticular quartz lenses or ribbons composed of sutured grains set in a fine-grained matrix of sericite and granoblastic quartz with minor greenish-brown biotite. The deformed

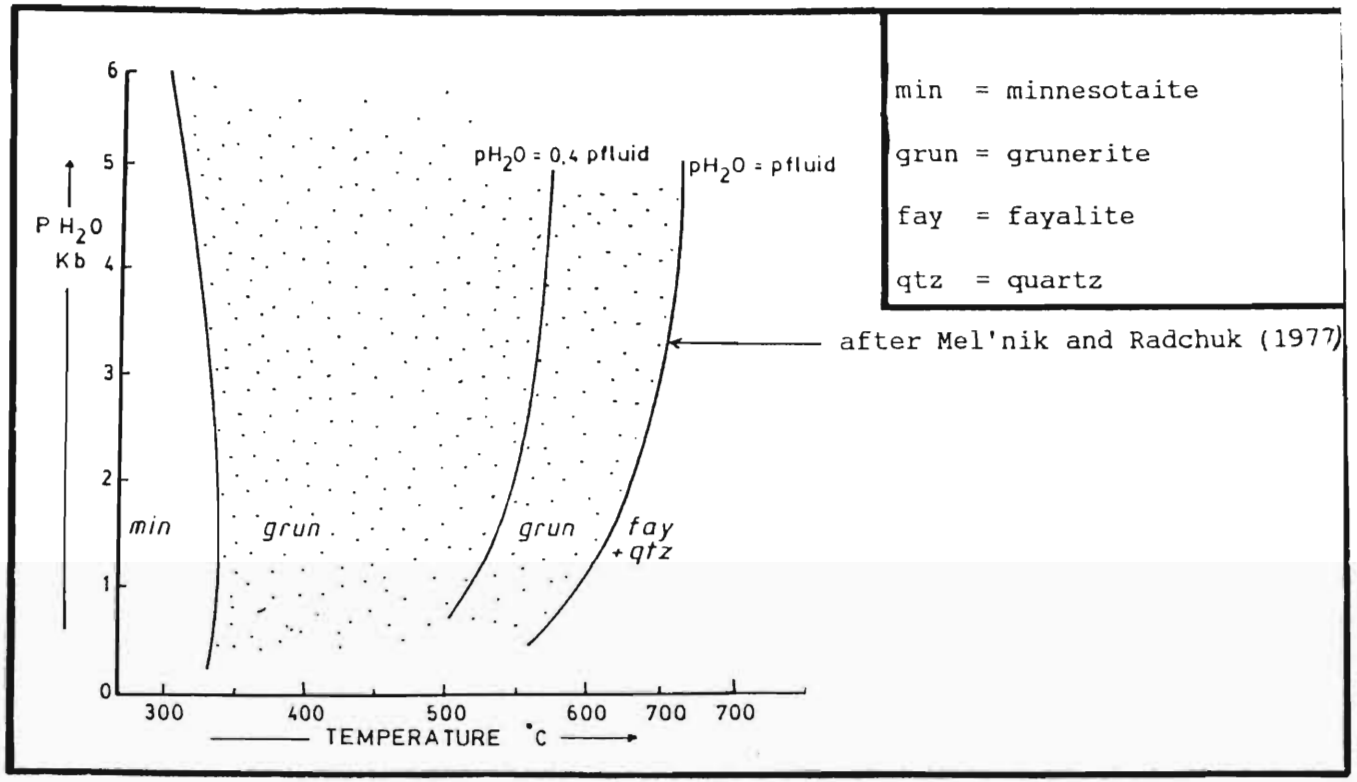

Fig. 10.12: Pressure-temperature conditions for grunerite stability (from Mel'nik and Radchuk, 1977).

nature of the quartz is shown by its undulatory extinction.

White mica occurs as elongate flakes or plates which are aligned along a preferred orientation defining schistosity. In hand specimen these micas impart a silky to silvery sheen to the surface of schistosity (Plate 10.4A). Minor brown fibrous to columnar biotite occurs in some thin sections and indicates that metamorphic temperatures rose appreciably during regional metamorphism of these rocks. Green chlorite flakes tend to parallel schistosity. Some chlorite replaces biotite and its orientation is oblique to schistosity. This denotes retrogression which took place locally during the prolonged regional low grade metamorphism. Some chlorite flakes show an hour glass structure implying that this could be chloritoid rather than chlorite. Minor epidote occurs zoned, probably with clinozoisite in the core. Plagioclase could probably occur in phyllites, however it is not twinned and identification was difficult as it is similar to quartz.

10.4.2.2 METAMORPHISM

The phyllites have a paragenesis of :

quartz + sericite + chlorite + epidote ± biotite ± ore ± plagioclase

which is indicative of low-grade greenschist metamorphism (Winkler, 1974). Where slightly higher temperatures were reached brown biotite was formed. Incipient retrogression has been observed with biotite altering to chlorite or chloritoid. This kind of retrogression is thought to have been of local occurrence within the phyllites.

10.5 NOMANGCI FORMATION

10.5.1 INTRODUCTION

This formation consists of thick units of quartzites intercalated with a distinctive quartz-muscovite schist or quartz schist and minor black and white banded cherts. The quartz-muscovite schist is a light-greenish-white rock with large muscovite books together with quartz and plagioclase. One thin section of this rock was made and it will be briefly described here.

10.5.2 QUARTZ-MUSCOVITE SCHIST AND QUARTZ-SERICITE SCHIST

10.5.2.1 PETROGRAPHY

The dominant constituent of the quartz-muscovite schist is lepidoblastic muscovite (56% by volume) occurring as long plates aligned with a preferred orientation that defines the foliation (Plate 10.4B). It has bright interference colours and shows the characteristic mottled extinction. At some places it is associated with green chlorite and it is not certain whether chlorite replaces muscovite or not. Bundles of muscovite occur. These bundles are probably thin section mimicking of muscovite books observed in hand specimen.

Quartz (15% by volume) occurs as granular to equigranlar grains giving a granoblastic texture. Minor quartz lenses are flattened and aligned along the muscovite preferred orientation and these lenses show intense wavy extinction.

Plagioclase (10% by volume) occurs as subidioblastic to xenoblastic crystals showing predominantly albite twinning. Plagioclase composition is An_{6-28} ranging between albite and oligoclase, though a number of grains are biaxial negative indicating that they are oligoclase. Some of these have been slightly altered to sericite (4% by volume).

Greenish-grey chlorite (15% by volume) occurs as aggregates and also as subhedral plates some of which are slightly curved (due to deformation?). Where it occurs in close association (parallel growth or replacement growth?) with muscovite, it has a fibrous habit (Plate 10.4B). Traces of epidote were observed.

The quartz-muscovite-(sericite) schists have very complex textures characterized by partially transposed fabrics and the occurrence of several s-surfaces. Quartz (up to 57% by volume) is the principal mineral in these schists occurring as thin ribbon-like lenses and veins set in a silvery-green chlorite-sericite-quartz matrix displaying a lenticular texture. Sericite (up to 25% by volume) occurs in association with flakes of muscovite (up to 8%) aligned along a preferred orientation and being partially replaced by interlocking aggregates of chlorite and minor chloritoid metacrysts. Muscovite, sericite and chlorite envelope lenses of quartz thus forming discrete sheared bundles. A second generation muscovite occurs as post-tectonic overgrowths on chlorite. Accessory minerals include epidote, calcite, chloritoid and traces of subidioblastic apatite crystals. Feldspars were not observed in these schist.

These schists are intruded by the Nkandla Granite and the Ntshiweni Augen Gneiss in the northwestern part of the study area. The intrusion of these granitoids resulted in the formation of kyanite in the schists. This is a classic effect of M_3 prograde metamorphism.

Disequilibrium conditions in these rocks are displayed by the myrmekitization (both incipient and advanced) (Plate 12.1B) of quartz and feldspars, the zoned plagioclase inclusions (in K-feldspars) with a core of oligoclase and a distinct but rather diffuse rim of albite, zoned epidote with allanite cores and, finally, by the replacement of hornblende by biotite or biotite by chlorite.

These rocks exhibit stress and strain effects that are manifest in quartz undulose extinction, dust trails, fractured margins and elongation of quartz and plagioclase feldspars parallel to foliation. Such effects in plagioclase are shown by bent twin lamellae and incomplete wedge-like twins.

10.5.2.2 METAMORPHISM

Quartz-muscovite schist has the following simple mineral assemblage :

quartz + muscovite + plagioclase + chlorite + epidote.

This assemblage is typical of low grade greenschist facies metamorphism (Winkler, 1974, 1979; Mason, 1978). Where there is M_3 prograde metamorphism, kyanite occurs in these schists, and the following mineral assemblage is found :

chlorite + kyanite + muscovite + quartz.

This paragenesis shows that there is virtually no plagioclase in the presence of kyanite (Winkler, 1979). Kyanite is stable throughout the range of low-grade metamorphism but Winkler (1979) argues that kyanite has been observed occasionally in the higher temperature range.

CHAPTER 11

METAMORHPHIC PETROLOGY AND GEOCHEMISTRY OF THE MIGMATITIC AND MYLONITIC GNEISSES

11.1 INTRODUCTION

In this chapter, the metamorphic petrology and geochemistry of the Amazula Gneiss, Nkwalini Mylonitic Gneiss and Nkwalini quartzo-feldspathic flaser Gneiss (which are referred to as ***older gneisses*** in this study) will be discussed. The petrography and metamorphism of each gneissic unit will be described first and then the last section will be devoted to a combined geochemical classification of all the migmatitic and mylonitic gneisses.

11.2 AMAZULA GNEISS

11.2.1 PETROGRAPHY

This gneiss is migmatitic and was described in the field as a quartzitic-amphibolitic gneiss. The amphibolitic melanosome consists of pyroxenes (aegirine-augite), hornblende, actinolite, plagioclase and minor amounts of quartz, biotite, sericite, talc, carbonate, epidote and sulphides. This gneiss shows the effects of intense deformation (Plates 2.1 and 5.2).

Table 11.1 gives the modal analyses and summary features of the Amazula Gneiss. The most abundant mineral is the blue-green variety of hornblende (30 - 62% by volume) forming idioblastic to subidioblastic crystals with textures ranging from gneissose granoblastic to strongly nematoblastic. The grains vary in size from 0,5mm to greater than 1mm. Hornblende shows the common pleochroic scheme of ∀: yellow-green to honey-brown; ∃: olive-green; (: dark green to blue green. In some thin sections, hornblende occurs together with actinolite. Generally, hornblende seems to have developed by epitaxial growth from Na-bearing pyroxenes of aegerine-augite composition (2 - 20% by volume) which are diagnostic with their green-to brownish-yellow colour and pleochroism.

Most grains show only one of the perfect {110} cleavages with minor grains showing both. Those that show both have lower interference colours. They are subidioblastic to xenoblastic and range in length from a few mm up to 5mm. Aegirine seems to abound with a 2V . 90°. The pyroxenes are zoned with aegerine on the outside. There are minor exsolution lamellae of orthopyroxene associated with the remnant clinopyroxene.

Plagioclase (10 - 35% by volume) of the composition An_{19-35} (oligoclase-andesine) occurs as subidioblastic to xenoblastic crystals showing granoblastic texture with some grains poikiloblastically enclosing pyroxene in a subophitic texture. The plagioclase are altered to sericite (1 - 8% by volume).

Quartz (2 - 10% by volume) occurs as equant to inequigranular granoblastic grains showing strong undulose extinction. The grains have perfect polygonal triple-junction boundaries indicating recrystallization.

Minor accessory minerals like epidote, carbonate, quartz and opaque ore are common as poikiloblastic enclosures in hornblende. Epidote, the most common accessory mineral, appears as small subidioblastic grains or granular aggregates ranging from 0,1mm to 0,7mm in diameter. It probably represents an alteration product of calcic plagioclase according to the reaction :

An-rich plagioclase = less An-rich plagioclase + epidote (Winkler, 1974).

Winkler (1974) contends that the amount of secondary epidote or zoisite is related to the initial An-content of the plagioclase and the metamorphic grade.

The type B xenoliths in the Amazula Gneiss consist of pyroxenes (up to 40% by volume), hornblende (45 - 97% by volume), biotite (1 - 5%) and traces of quartz, carbonate, talc and epidote. The pyroxenes are replaced by hornblende (uralitization) which in turn is replaced by biotite (Plate 10.4D). This is characteristic of retrograde metamorphism. The contact of the amphibolitic melanosome and the Type B xenolith in sample H138EB is sheared and consists of highly altered amphiboles breaking down to green-brown biotite, talc and carbonate which have been serpentinized (Plate 10.4D).

TABLE 11.1 : MIGMATITIC AND MYLONITIC GNEISSES : MODAL ANALYSES AND MINERALOGICAL FEATURES

SAMPLE IDENTITY	SAMPLE NO.	MINERAL MODAL COMPOSITION (%)																GRAIN SIZE			PLAG An CONTENT %	TEXTURE
		Qtz	Plg	K-Fel	Hbl	Pyrox	Biot	Cord	Apat	Zir	Carb	Epid	Chlo	Ser	Mus	Talc	Ore	F	M	C		Granoblastic(*); Subophitic(Sub); Ophitic(Oph); Inequigranular(In); Equigranular(Eq); Myrmekitic(Myr); Uralitization(Ur);Xenoblastic(Xen); Nematoblastic(Nem).
AG	H60EB	30	15	25			15	10			1			4					x		nd	Crystallobl.; *
AG	H73EB	35	15	30	5		t				5	t		10					x		An_{7-13}	Nem.; in.
AG	H77EB	35	18	30			15							2					x	x	An_{8-17}	Lepid.; in.' *
AG	H85EB	20	35	20	15	5							5	t					x		An_{35}	In.; nem.; oph.
AG	H87EB	40	10	30	1	5	10		t		2	2	t						x		nd	In.; lepid.
AG	H93EB	20	30	7	25	15						t		3						x	nd	Nem.; blue-green hbl.
AG	H101EB	10	35	10	30	10	2				1			2					x		An_{22}	Nem.; blue-green hbl.
AG	H111EB	15	30	5	30	15						1		4			t		x		An_{11-25}	Suboph.; eq.; blue-green hbl.
AG	H120EB	2	35		55	2								6					x		An_{36}	Eq.; *; nem.; blue-green hbl.
AG	H138EB	3	15		62	20													x		nd	Nem.; schistose blue-green hbl.
AGX	H138AEB	t			55	40	4				t	t							x			In.; schistose; blue-green hbl.
AGX	H148EB	1			98	1						t				t	t		x			In.; blur-green hbl.
FG	H54EB	25	25	38			2					1		4	5					x	An_{21}	*; in.
FG	H100EB	20	30	42										5	3				x		An_{11-16}	*; eq.
FG	H113EB	25	30	40			1					t		t	4					x	An_{6-17}	Eq.; cons. to *.
FG	H114EB	35	15	45			2					t		3					x		An_{11}	Eq.; *.
FG	H121EB	30	20	42										6	2				x		nd	In.; cons.
NM	H62EB	35	10	41	8		2					1		3					x		nd	In.; *; blue-green hbl. and brown biot.
NM	H64EB	44	5	35	15							t							x	x	nd	Nem.; in.; *; minor act.
NM	H133EB	35	10	48			<2					1		5			t		x		nd	In.; cons.
NM	H135EB	37	12	47					t			1		3			t		x		An_{12}	In.; *; sheared
NM	H136EB	40	7	50								1		2					x	x	nd	Porphyrobl.; sinistral shearing

AG = AMAZULA GNEISS AGX = MAFIC XENOLITH OF THE AMAZULA GNEISS NM = NKWALINI MYLONITES FG = NKWALINI QUARTZO-FELDSPATHIC FLASER GNEISS

The quartzitic leucosome of the Amazula Gneiss consists of quartz, alkali feldspar, plagioclase and varying amounts of actinolite, cordierite, biotite, epidote, apatite and sericite. Quartz (24 - 44% by volume) consists of subidioblastic interlocking grains of up to 1mm in diameter and define the gneissosity. Quartz together with minor cordierite (up to 10% by volume) shows a crystalloblastic fabric. Some microgranular grains of quartz are poikiloblastically enclosed in feldspars.

K-feldspars (20 - 40% by volume) occur as large xenoblastic grains which sometimes poikiloblastically enclose grains of plagioclase (with albite twinning) and quartz.

Plagioclase (10 - 30% by volume) show faint albite twinning and are of albite to oligoclase composition. The plagioclase is more easily recognisable in plane polarized light where sericite alteration has occurred along the albite twin planes.

Biotite (up to 15% by volume) occurs as elongate flakes and columnar laths aligned parallel to the foliation and showing a lepidoblastic texture (Plate 10.4C).

Some biotite shows incipient alteration to calcite. In H73EB, actinolite (up to 8% by volume) is present and defines a nematoblastic texture. Apatite occurs as idioblastic to subidioblastic grains. Traces of epidote and opaque ore are present. The ore is represented by sulphides (mainly pyrite - observed in hand specimen) and ilmenite with reddish rims around the opaque ore. In general, the quartzitic leucosome commonly shows a flaser texture (Plate 10.4C).

11.2.2 METAMORPHISM

Several distinct mineral parageneses can be recognized in the Amazula Gneiss and its Type B xenoliths :

Pyroxene + hornblende + plagioclase + quartz ± sphene + ore.....(1)
Hornblende + biotite + plagioclase + epidote + sericite ± sphene + ore.....(2)
Pyroxene + hornblende + biotite + epidote + carbonate + talc + serpentine.....(3)
Quartz + K-feldspar + plagioclase + biotite + cordierite + carbonate + sericite.....(4)
Quartz + K-feldspar + plagioclase + actinolite + sericite.....(5)

The first two assemblages are typical of the amphibolitic melanosome of the Amazula Gneiss. Assemblage (3) is typical of the sheared contact between the amphibolitic melanosome and Type B mafic xenoliths. Assemblages (4) and (5) belong to the quartzitic leucosome.

In assemblage (1) the pyroxene, usually aegirine-augite or hypersthene, contain exsolution lamellae of orthopyroxenes and, together with the hornblende, have piokiloblastic character. They are thus considered to be of metamorphic origin. In metamorphosed amphibolites, pyroxenes, hornblende and plagioclase (of oligoclase to andesine composition) are products of high temperature, medium grade metamorphism (Winkler, 1979, pp 169 - 172). Accordingly, assemblage (1) represents metamorphic conditions of middle to upper amphibolite facies M_1 metamorphism (see Fig. 11.1).

Assemblage (2) is out of equilibrium with assemblage (1). Hornblende has replaced pyroxenes and the hornblende is itself being replaced by biotite. Quartz-epidote symplectites and oligoclase have probably been produced by the reaction of pyroxenes, hornblende, opaques and andesine. These reactions and the produced symplectites indicate retrogression under M_2 lower amphibolite or greenschist conditions.

Assemblage (3) is confined to the sheared rim of the melanosome and Type B xenolith. This assemblage is a shear-related retrograde metamorphism here referred to as the M_3 dislocation metamorphism.

The quartzitic leucosome of the Amazula Gneiss contains biotite or actinolite aligned along a preferred orientation defining the foliation (Plate 10.4C). It also contains cordierite usually showing polysynthetic twinning and undulose extinction. Some cordierite and quartz grains are flattened and stretched and define a strong tectonic fabric parallel to that defined by biotite and actinolite. The strong alignment of biotite, actinolite and cordierite suggests that they are products of prograde syntectonic metamorphism probably similar to the M_1 medium grade metamorphism. (Refer to the cordierite-medium grade metamorphism in Fig. 10.11, Winkler, 1979). Incipient M_2 retrograde conditions in the leucosome are represented by the breakdown of biotite and actinolite to epidote and carbonate and the sericitization of feldspars.

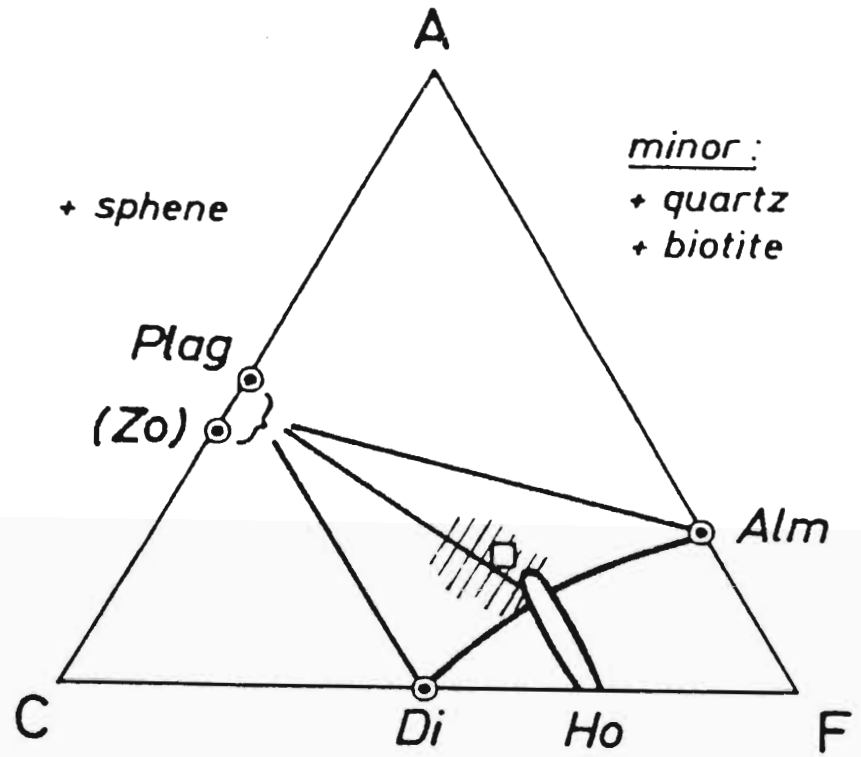

Fig. 11.1: Middle to upper amphibolite facies M_1 metamorphism of the amphibolitic variety of the Amazula Gneiss (from Winkler, 1979).

11.3 NKWALINI MYLONITIC GNEISS AND NKWALINI QUARTZO-FELDSPATHIC FLASER GNEISS

11.3.1 PETROGRAPHY

The ***Nkwalini mylonites*** are well preserved in the Nkwalini area (4,5/MM,NN,OO), Mfanefile area (3/W,Y) and in the Mooiplaas area just east of Spelonk (1,2,3/P,Q,R,S). They occur in a zone of intense ductile deformation (Hobbs et. al., 1976; Berthé et. al., 1979; Lister and Snoke, 1984; Ramsay, 1980; Ramsay and Huber, 1987). Fig. 5.3 and Plate 5.5A - C and Plate 9.1A - C show the composition and deformed nature of these rocks.

Modal analyses of the Nkwalini Mylonitic Gneisses and the Nkwalini Quartzo-feldspathic Flaser Gneisses are shown in Table 11.1. In thin section, the pink mylonitic variety consists of crystalloblastic quartz (40% by volume) occurring as lenses or ribbons ±5mm long, stretched and flattened parallel to foliation. The quartz grains show signs of recrystallization and polygonization. These ribbons alternate with K-feldspars (up to 58% by volume) mainly orthoclase and minor microcline with tartan twinning. Some large porphyroblasts of K-feldspar have been rotated in a delta-type stair-step geometry (Passchier and Simpson, 1986; Hanmer and Passchier, 1991) Minor plagioclase (7%), epidote (1%) with allanite cores, muscovite (2%) and traces of ore are present. The muscovite is aligned along and defines the foliation.

The amphibolitic variety consists of hornblende and actinolite (up to 50% by volume) xenoblastic grains stretched and aligned parallel to foliation. They alter to a brown variety of biotite (10%) which is columnar to fibrous and also parallels foliation. These minerals alternate with deformed granoblastic ribbon-like quartz (up to 10% by volume) and plagioclase (up to 30% by volume) which are deformed and show preferred orientation parallel to foliation. Accessory minerals include chlorite, epidote, sericite and minor carbonate. Plate 5.5C shows the amphibolitic variety of the mylonites (see also Plate 9.1A - C).

The ***Nkwalini Quartzo-feldspathic Flaser Gneiss*** is pinkish-red and contains pink K-feldspars alternating with streaked elongated transparent quartz ribbons or lenses and creamy to milky white plagioclase giving the rock its intense foliated and flaser texture. Where it is intensely mylonitic, it also contains flaky biotite and muscovite. This rock is a

product of shearing and dislocation metamorphism. it is similar to the quartzo feldspathic gneisses of the Godthabsfjord area of Greenland (Bridgewater et. al.,1974).

In thin section, quartz (up to 35% by volume) occurs as deformed lenses recrystallized and having an undulatory extinction. K-feldspars (up to 41% by volume) consists of orthoclase and microcline showing dust trails and minor sericitization. Plagioclase (up to 30% by volume) are mainly oligoclase with albite twinning and forming wedge-like twins with the gridiron twins of microcline, implying deformation (Barker, 1990; Smalley, 1980). The feldspars form large (± 10mm in size) porphyroblasts some of which are broken due to dislocation and are enveloped by biotite and muscovite thus giving flaser textures preserved in this gneiss.

11.3.2 METAMORPHISM

The Nkwalini mylonites have the following two mineral parageneses:

Quartz + K-feldspar + plagioclase + muscovite + epidote + sericite.....(1)
Amphiboles + biotite + quartz + plagioclase + chlorite + epidote.....(2)

The first paragenesis belongs to the pink mylonitic variety whereas the second one is that of the amphibolitic schist/mylonite variety. The presence of hornblende in the amphibolitic variety indicates that peak M_1 medium grade conditions were attained by these rocks. The subsequent replacement of hornblende by biotite is testimony to the later M_2 retrograde metamorphism. Further breakdown of biotite to chlorite and epidote in assemblage (2) and the formation of muscovite, sericite and epidote in assemblage (1) is due to the M_3 dislocation metamorphism as a result of the intense shearing of these rocks.

The pink quartzo-feldspathic flaser gneiss has similar assemblages to the pink mylonitic variety of the Nkwalini mylonites except that biotite and not muscovite is the dominant phyllosilicate. This rock was affected by dislocation metamorphism as a result of intense deformation. Where this rock is not deformed, it does not show any flaser textures and is similar to a pink micrographic granite. A similar retationship exists for the Amitsoq quartzo-feldspathic gneisses of Greenland (Bridgewater et al, 1974).

11.4 ORIGIN AND GEOCHEMICAL CLASSIFICATION OF MIGMATITIC AND MYLONITIC GNEISSES

Major and trace element analyses of the Amazula Gneiss, Nkwalini Mylonitic Gneiss and Nkwalini Quartzo-feldspathic Flaser Gneiss are given in ***Table 11.2***.

According to the ternary Q.A.P diagram (Streckeisen, 1973) these gneisses show a modal composition plotting in the quartz diorite, tonalite, granodiorite and granite fields (Fig. 11.2). This is supported by the normative An-Ab-Or ternary diagram (Fig. 11.3; Barker, 1979) which also shows that these gneisses have a varied composition. The Amazula Gneiss has a composition ranging from tonalitic to granodioritic, whereas the Nkwalini mylonites and the Nkwalini quartzo-feldspathic flaser gneisses have a granitic composition. It is worth noting that the quartzitic leucosome variety of the Amazula Gneiss plots in the granitic field (Figs. 11.2 and 11.3). These compositions are also supported by the binary diagram of Na_2O against K_2O (Fig. 11.4; Harpum, 1963). However, the binary plot shows the melanocratic variety of the Amazula Gneiss to have a composition ranging from granitic to tonalitic (Fig. 11.4). This suggests that the Amazula Gneiss is a bimodal migmatitic gneiss. This is supported by field evidence, as the Amazula Gneiss is a grey quartzitic-amphibolitic gneiss. The leucosome of the Amazula Gneiss has SiO_2 values >75% whereas the melanosome has SiO_2 values <60%. Hunter (1979) quotes values of 70% and 55% respectively for the Ancient Gneiss Complex of Swaziland.

The pink Nkwalini Quartzo-feldspathic Flaser Gneiss and most of the Nkwalini mylonites are peraluminous (Fig. 11.5; Shand, 1947 quoted ***in*** Clarke, 1992) and have the ratio A/CNK [i.e. molar $\{Al_2O_3/(CaO + Na_2O + K_2O)\}$] being greater than unity (Clarke, 1992). The Amazula Gneiss and two samples of the Nkwalini mylonites are metaluminous and have the ratio A/CNK <1 (Fig. 11.5). Fig. 11.5 also shows the possible origin (Chappell and White, 1974; White and Chapell, 1983; Barbarin, 1990) and possible tectonic setting (Barbarin, 1990; Roberts and Clemens, 1993) of these migmatitic and mylonitic gneisses. The binary plot of P_2O_5/TiO_2 against MgO/CaO (Fig. 11.6) shows most of these gneisses falling in the magmatic field. The fact that the other samples fall in the sedimentary field does not imply that they are of sedimentary origin, but rather that they are of mixed origin. The magmatic origin is also supported by the binary total alkalis ($Na_2O + K_2O$) against silica (SiO_2) diagram (Fig. 11.7) which shows that these gneisses plot on the sub-alkaline field of

TABLE 11.2 : MIGMATITIC AND MYLONITIC GNEISSES : MAJOR AND TRACE ELEMENT ANALYSES

SAMPLE	AMAZULA GNEISS						NKWALINI MYLONITES			NKWALINI QUARTZO-FELDSPATHIC FLASER GNEISS					
	H77EB	H85EB	H87EB	H111EB	H111AEB	H120EB	H62EB	H64EB	H100EB	H113EB	H114EB	H121EB	H133EB	H135EB	H136EB
iO_2	75.80	65.10	84.30	59.30	57.00	57.00	90.50	84.50	76.50	75.50	73.10	76.20	73.90	76.80	85.10
iO_2	0.70	0.37	0.18	0.83	0.90	0.97	0.00	0.20	0.08	0.12	0.11	0.12	0.02	0.03	0.02
l_2O_3	7.07	7.58	3.38	16.50	15.78	15.80	3.05	4.12	12.90	13.20	15.40	13.40	14.80	13.40	8.92
e_2O_3	1.56	1.88	10.30	1.43	1.73	2.22	0.63	0.81	0.18	0.21	0.23	0.25	0.06	0.11	0.12
eO	5.60	6.75	3.70	5.16	6.24	8.00	2.26	2.92	0.65	0.75	0.84	0.90	0.22	0.41	0.43
nO	0.13	0.23	0.13	0.17	0.19	0.35	0.35	0.14	0.04	0.03	0.03	0.05	0.02	0.03	0.04
gO	3.04	3.79	2.74	2.98	3.94	3.10	0.54	2.33	0.42	0.46	0.51	0.45	0.27	0.32	0.31
aO	2.04	12.60	2.01	7.55	8.94	7.67	0.84	2.58	0.57	0.76	1.21	0.73	0.55	0.63	0.49
a_2O	0.94	1.01	0.27	2.15	2.09	2.11	0.30	0.40	2.71	2.35	3.51	2.86	3.22	2.73	0.96
O	3.03	0.61	2.25	3.63	2.80	2.37	1.49	1.98	5.87	6.61	5.06	4.99	6.90	5.56	3.64
O_5	0.07	0.17	0.01	0.37	0.39	0.40	0.00	0.00	0.03	0.03	0.07	0.05	0.03	0.02	0.00
OTAL	100.00	100.00	100.00	100.00	100.00	100.00	100.00	100.00	100.00	100.00	100.00	100.00	100.00	100.00	100.00
	116.00	28.50	84.80	163.00	129.20	5.40	73.50	46.00	137.00	198.00	115.00	115.00	171.00	165.00	130.00
	58.30	104.00	19.90	166.00	163.70	1.60	75.70	78.90	121.00	101.00	215.00	174.00	224.00	125.00	193.00
	253.00	102.00	86.40	141.00	153.90	38.80	39.00	105.00	65.80	40.20	105.00	93.40	8.00	38.00	52.80
	12.00	9.60	6.00	15.10	13.50	1.30	4.30	8.00	6.10	8.30	10.70	11.70	2.60	3.80	4.80
	20.40	19.30	3.40	24.50	28.60	6.70	9.50	9.40	0.00	0.00	2.50	0.00	0.00	0.00	0.00
	0.00	2.90	0.00	0.00	0.00	39.70	0.00	6.40	0.00	0.00	52.50	3.20	0.00	0.00	0.00
	0.00	13.10	0.90	0.00	0.00	7.30	1.70	8.60	0.00	0.00	0.00	0.00	0.00	0.00	0.00
I.P.W. NORMS (ANHYDROUS; IN Wt %)															
	47.20	30.00	64.90	12.20	9.70	12.30	78.90	65.50	36.10	33.80	29.60	37.80	27.10	37.60	63.70
	17.90	3.62	13.30	21.50	16.56	14.00	8.82	11.70	34.70	39.00	29.90	29.50	40.80	32.80	21.50
	7.93	8.54	2.26	18.20	17.65	17.90	2.56	3.40	22.90	19.90	29.70	24.20	27.30	23.10	8.11
	6.15	14.40	1.40	24.60	25.42	26.50	2.55	3.59	2.65	3.59	5.55	3.32	2.54	3.01	2.45
	0.00	0.00	0.00	0.00	0.00	0.00	0.00	0.00	1.14	0.90	2.10	2.07	1.07	1.76	2.50
	2.90	38.90	7.00	8.64	13.51	7.45	1.38	7.57	0.00	0.00	0.00	0.00	0.00	0.00	0.00
	14.20	0.79	9.26	10.40	12.04	15.90	4.93	6.70	2.03	2.21	2.50	2.46	1.04	1.46	1.51
	2.26	2.72	1.49	2.08	2.51	3.22	0.91	1.17	0.26	0.30	0.34	0.36	0.09	0.16	0.17
	1.33	0.70	0.35	1.57	1.71	1.84	0.00	0.38	0.15	0.23	0.21	0.23	0.04	0.06	0.04
	0.17	0.41	0.02	0.87	0.92	0.96	0.00	0.00	0.07	0.07	0.17	0.12	0.07	0.05	0.00

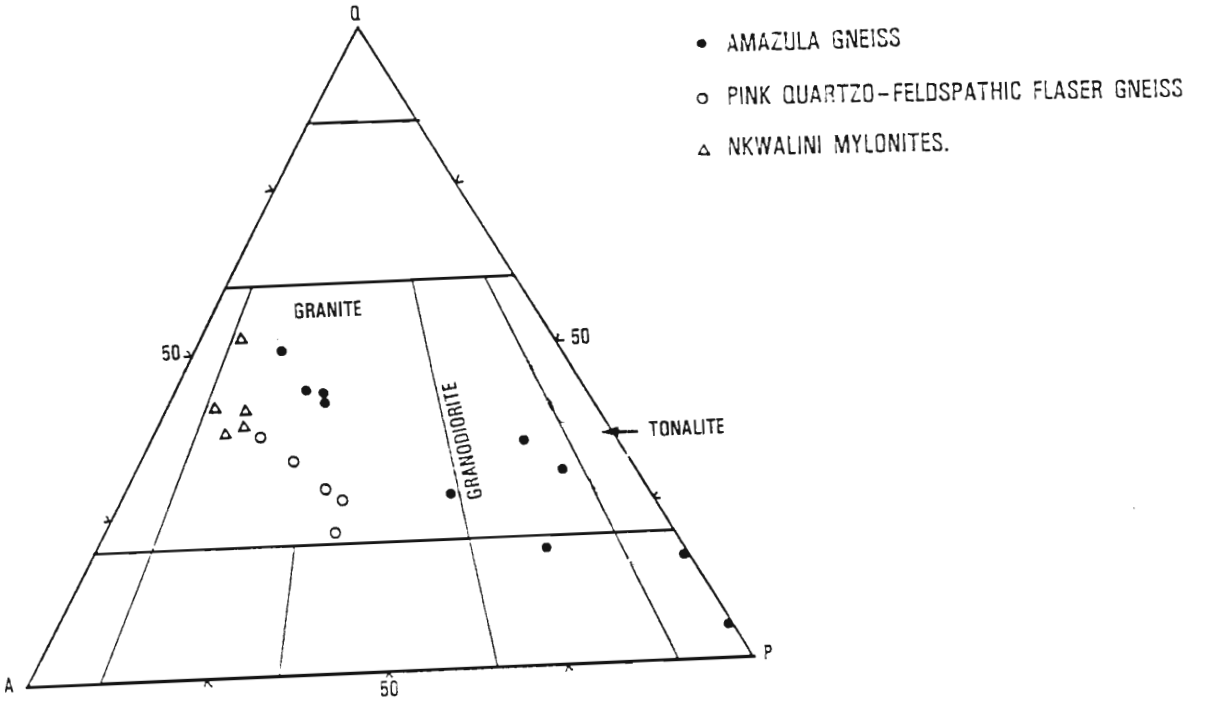

Fig. 11.2: Ternary QAP diagram (after Streckeisen, 1973) showing the composition of the migmatitic and mylonitic gneisses.
Q = quartz; A = alkali feldspar; P = plagioclase.

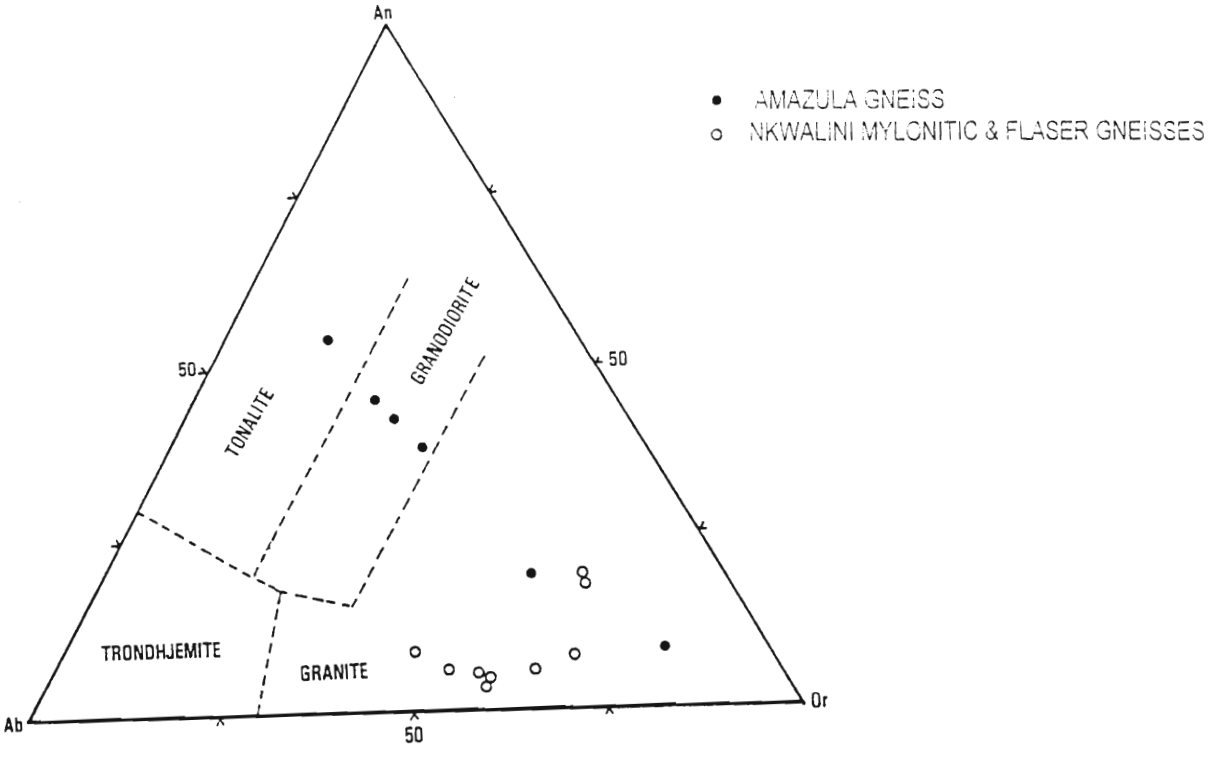

Fig. 11.3: Normative An - Ab - Or plot of the migmatitic and mylonitic gneisses. Fields of various granitoids after Barker (1979).

Irvine and Baragar (1971)and follow a calc-alkalic trend as depicted by the ternary Na_2O - (CaO + MgO) - K_2O plot (Fig. 11.8A). For comparison, Nockolds (1954) calc-alkalic suite from the Cascade Province is shown (Fig. 11.8A). Corroborative evidence for a calc-alkaline igneous origin is illustrated in Fig. 11.9A which is a binary plot of TiO_2 versus SiO_2 (Tarney, 1975) showing a Ti - Si negative correlation (similar to that obtained by Tarney (1975) for the Archaean gneisses in high-grade terranes of Scotland and Greenland) and depicting the Ilangwe migmatitic and mylonitic gneisses plotting below the cut-off line defined by Tarney (1975). The calc-alkaline affinity is also supported by the Irvine and Baragar (1971) ternary AFM diagram (Fig. 11.8B) where all the gneisses plot on the calc-alkaline field except the amphibolitic variety of the Amazula Gneiss which plots in the tholeiitic field. Fig. 11.8B separates the migmatitic gneisses very well with the Amazula Gneiss and the mylonitic gneisses depicting a possible "andesite gap" of Barker and Peterman (1974) (Fig. 11.8B).

These gneisses show a wide spread of SiO_2 contents (57,00 -90,54 wt %). As a result, the major elements show a moderate geochemical trend (Figs. 11.9 and 11.10). Fig. 11.9 shows that there is a general decrease in TiO_2, Al_2O_3, P_2O_5, MgO and CaO with an increase in SiO_2 content. However, the Nkwalini mylonites and the Nkwalini quartzo-feldspathic flaser gneisses show no detectable trend for MgO and CaO - the MgO and CaO content seems to be more-or-less similar with the corresponding increase in SiO_2. Fig. 11.10 shows a similar relationship for total Fe, MnO, Na_2O and K_2O. However, the Nkwalini mylonites and the Nkwalini quartzo feldspathic flaser gneiss show a variable trend for the total iron content and show an increase in the MnO content with an increase in SiO_2. All these gneisses have Na_2O/K_2O ratios of less than unity.

All these layered gneisses show variable trace element ratios. The Rb/Sr ratio for the Amazula Gneiss ranges between 0,27 and 4,26. Such Rb/Sr ratios are typical of tonalitic to granodioritic suites (Hunter, 1979; Hunter et. al., 1980). The Nkwalini mylonitic and Nkwalini quartzo-feldspathic flaser gneisses have ranges between 0,53 and 1,96, similar to the Tafelkoppies granitoid of the Piet Retief area (Sleigh, 1988). Further, these gneisses have very low Nb, Y and U values. Of particular interest in all these migmatitic and mylonitic gneisses (except the Amazula Gneiss) is the weak exponential increase of Rb with decreasing MgO (Fig. 11.11B) which Clarke (1992) attributes to "either the MgO concentration becoming stagnated at some pseudo-eutectic point where Rb is still free to increase in late-stage differentiates, or to the action of fluid phases or both" for the South Mountain Batholith of southern Nova Scotia.

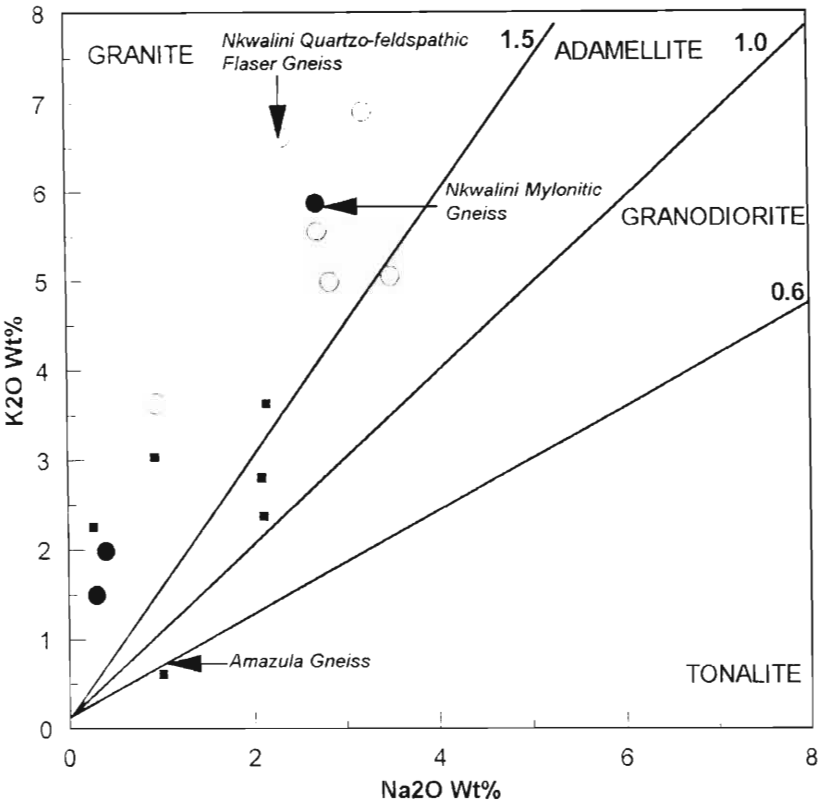

Fig. 11.4 : Binary Na_2O against K_2O plot showing the composition of the migmatitic and mylonitic gneisses of the Ilangwe Belt (after Harpum, 1963).

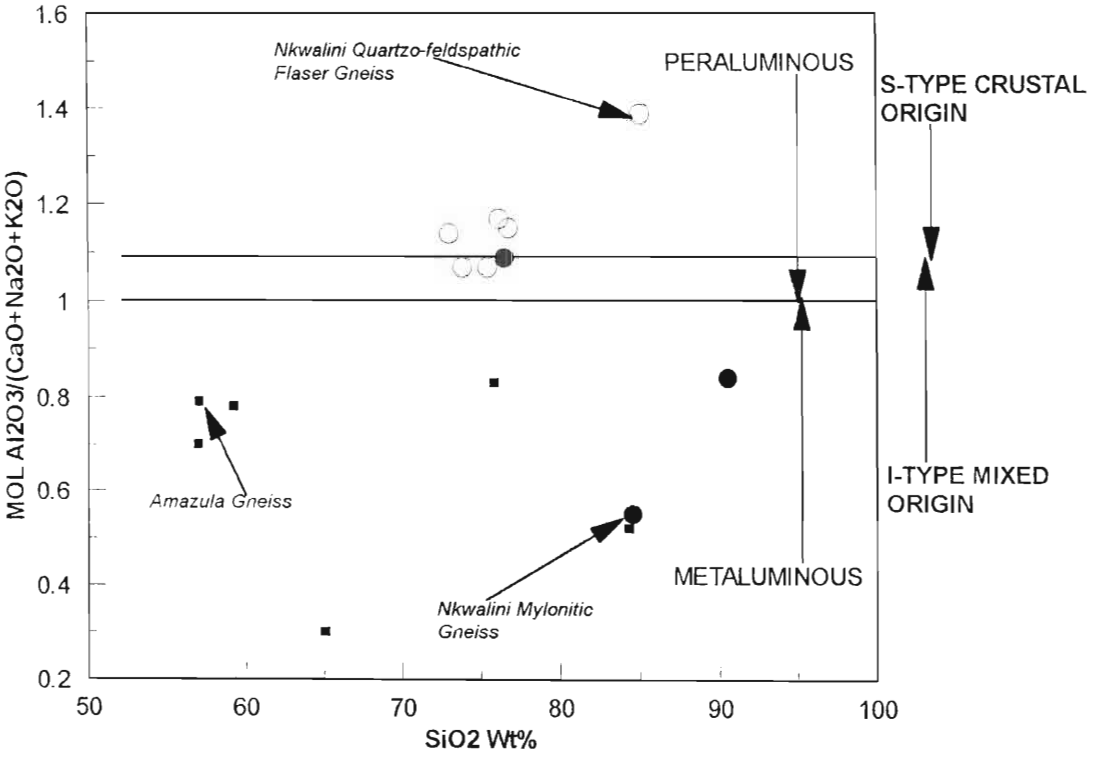

Fig. 11.5 : Binary SiO_2 against A/CNK plot (after Clarke, 1992) showing the composition of the migmatitic and mylonitic gneisses and their probable origin (after Chappell and White, 1974; White and Chappell, 1983; Barbarin, 1990).

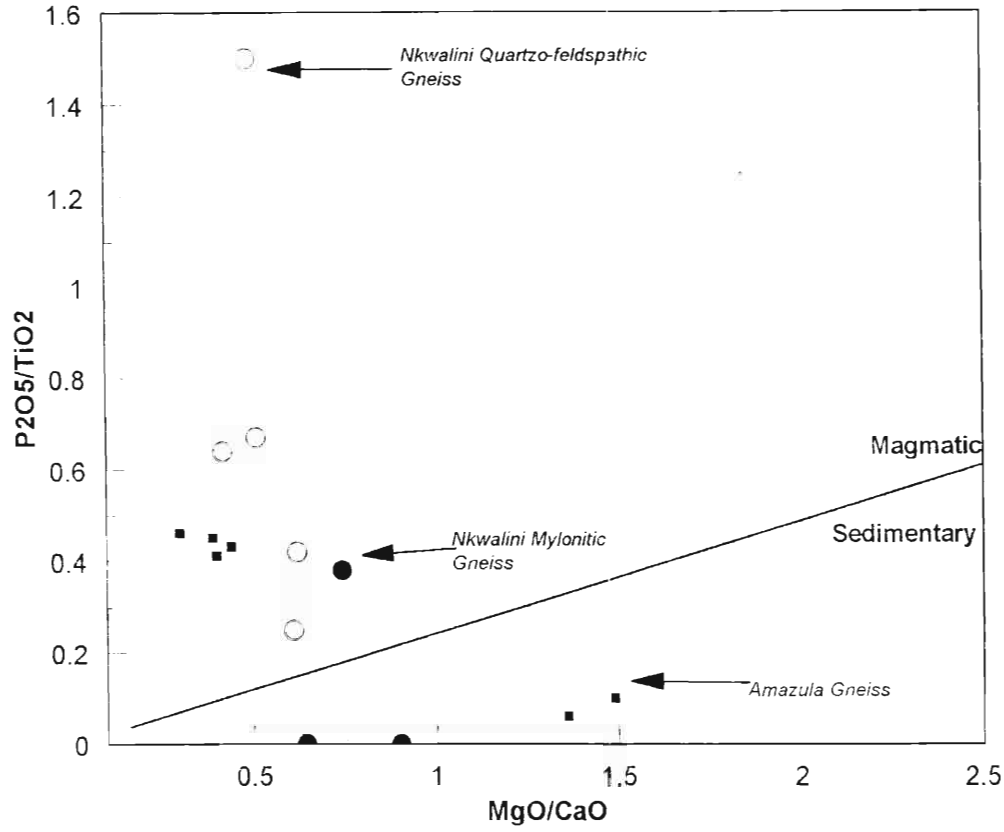

Fig. 11.6 : Binary P_2O_5/TiO_2 vs MgO/CaO plot showing the majority of the migmatitic and mylonitic gneisses to be of magmatic origin.

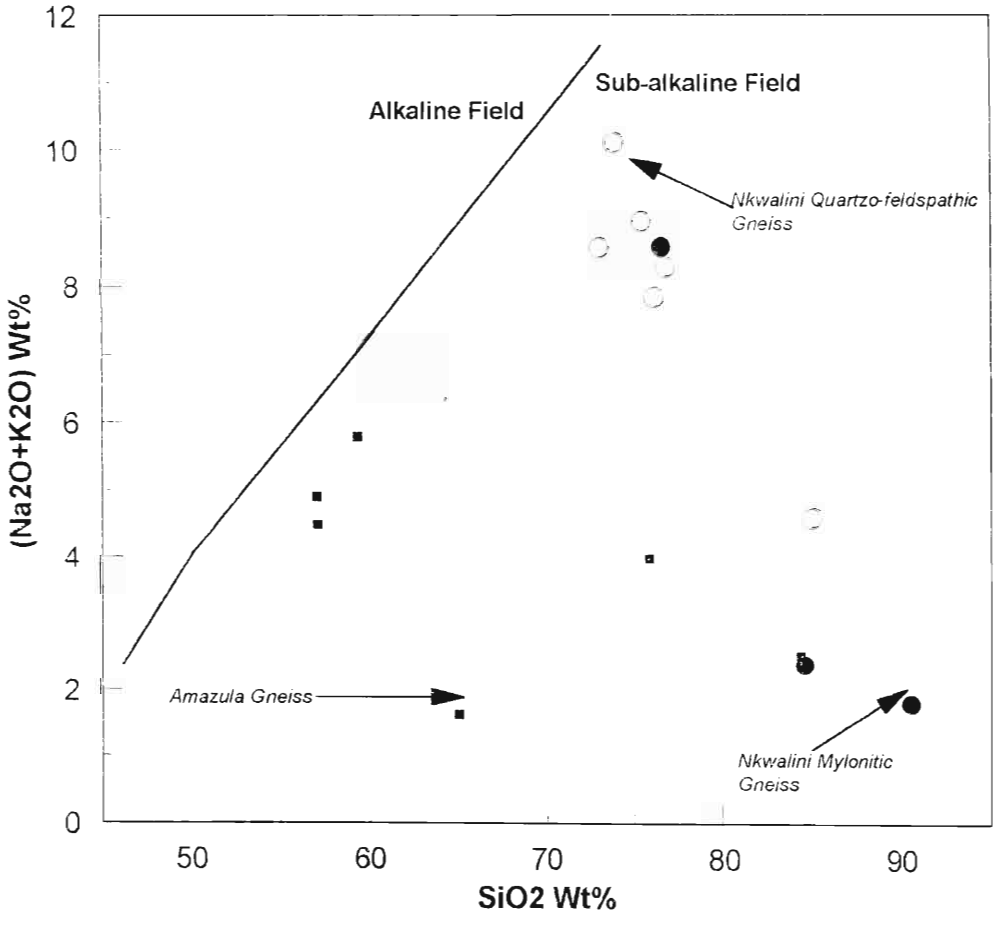

Fig. 11.7 : TAS (total alkali vs silica) plot of the migmatitic and mylonitic gneisses depicting their sub-alkaline affinity (after Irvine and Baragar, 1971).

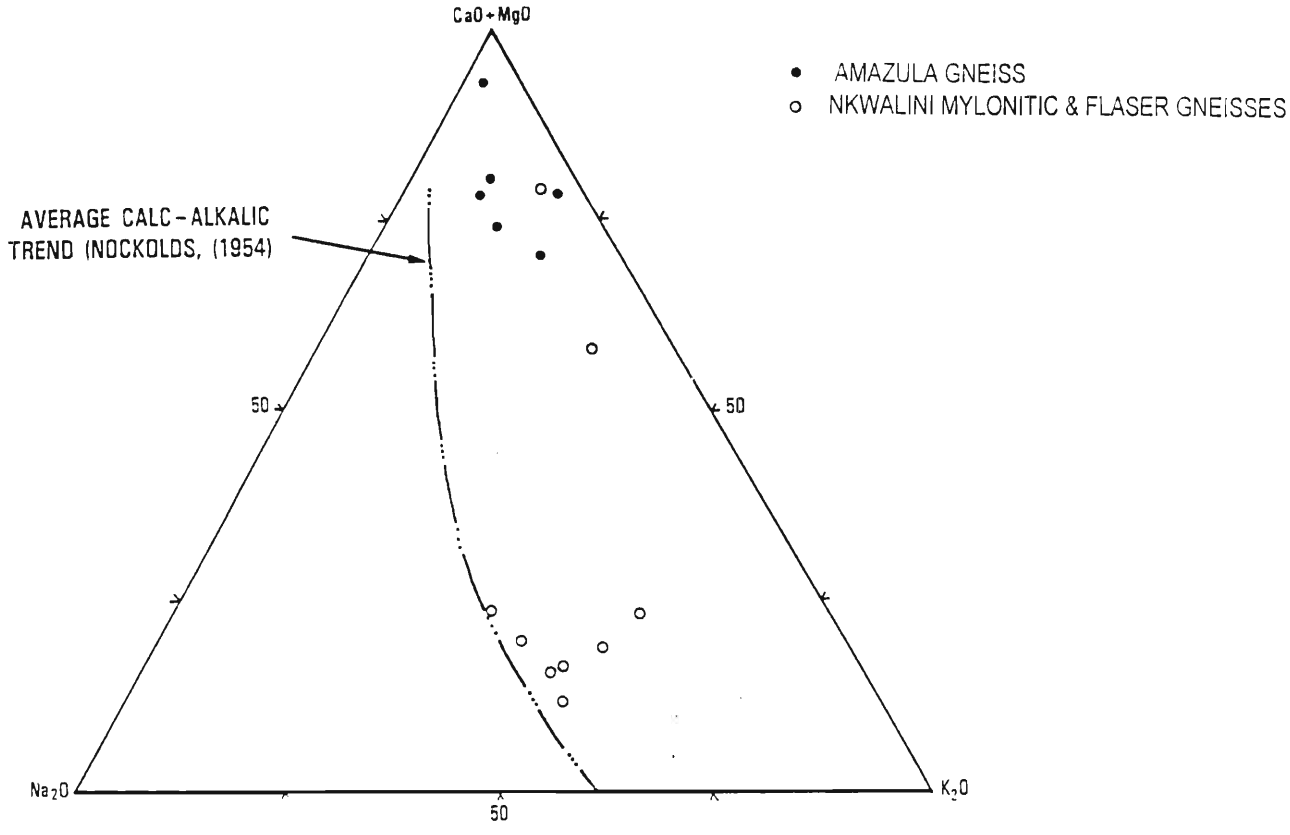

Fig. 11.8A: Ternary Na_2O - (CaO + MgO) - K_2O plot of the migmatitic and mylonitic gneisses showing a calc - alkalic trend. For comparison, Nockolds (1954) average calc - alkalic suite from the Cascade Province is shown.

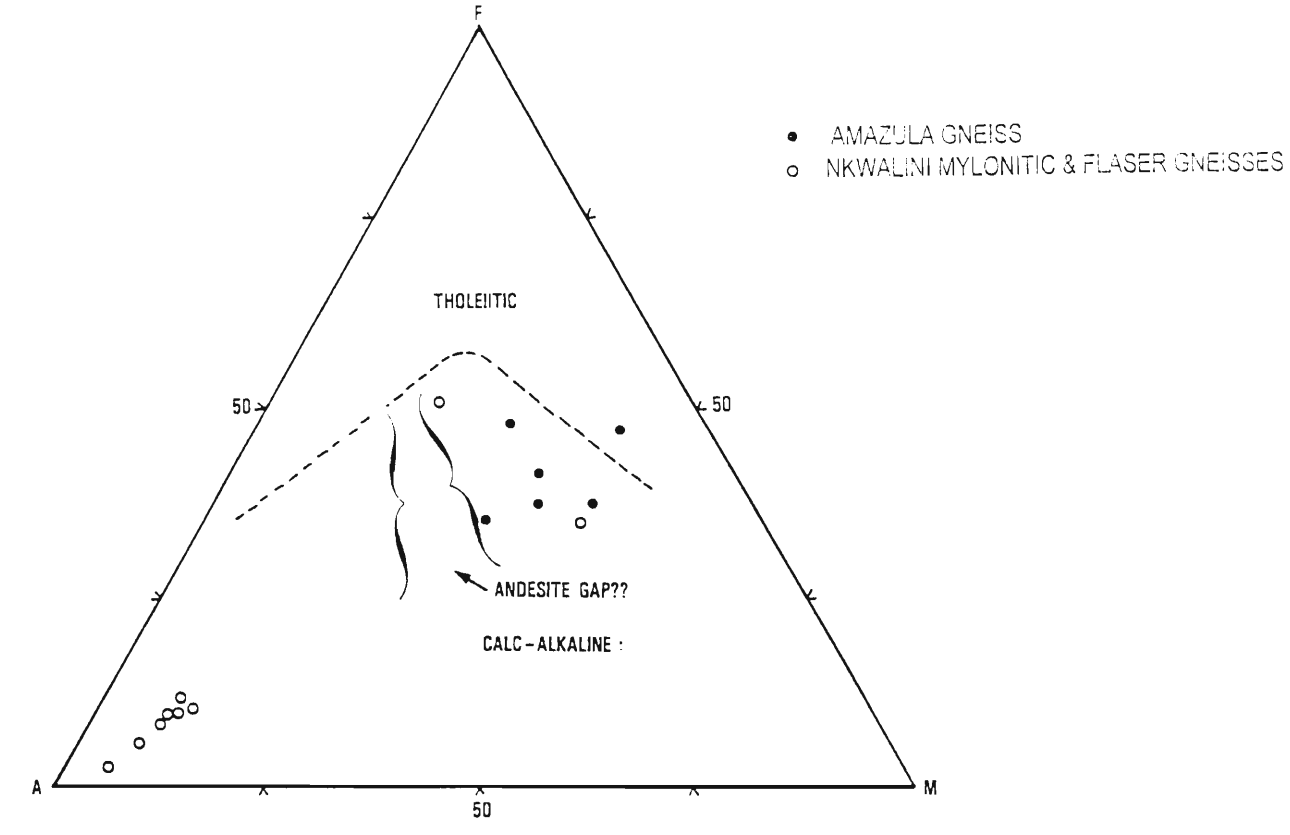

Fig. 11.8B: AFM ternary plot of the migmatitic and mylonitic gneisses showing the "andesite gap" of Barker and Peterman (1974). The dashed line separating the tholeiitic and calc - alkaline fields is after Irvine and Baragar (1971).

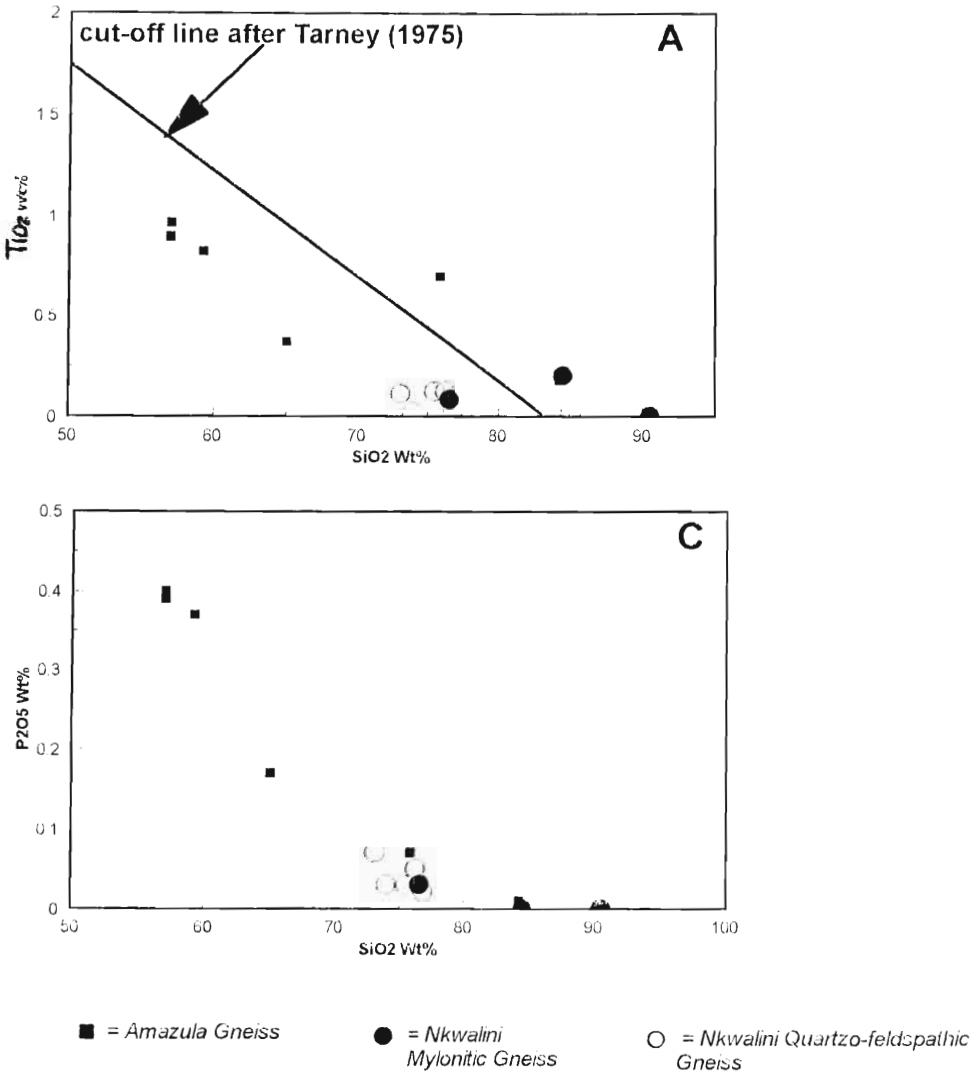

Fig. 11.9 A-E : Harker diagrams of the migmatitic and mylonitic gneisses of the Ilangwe Belt.

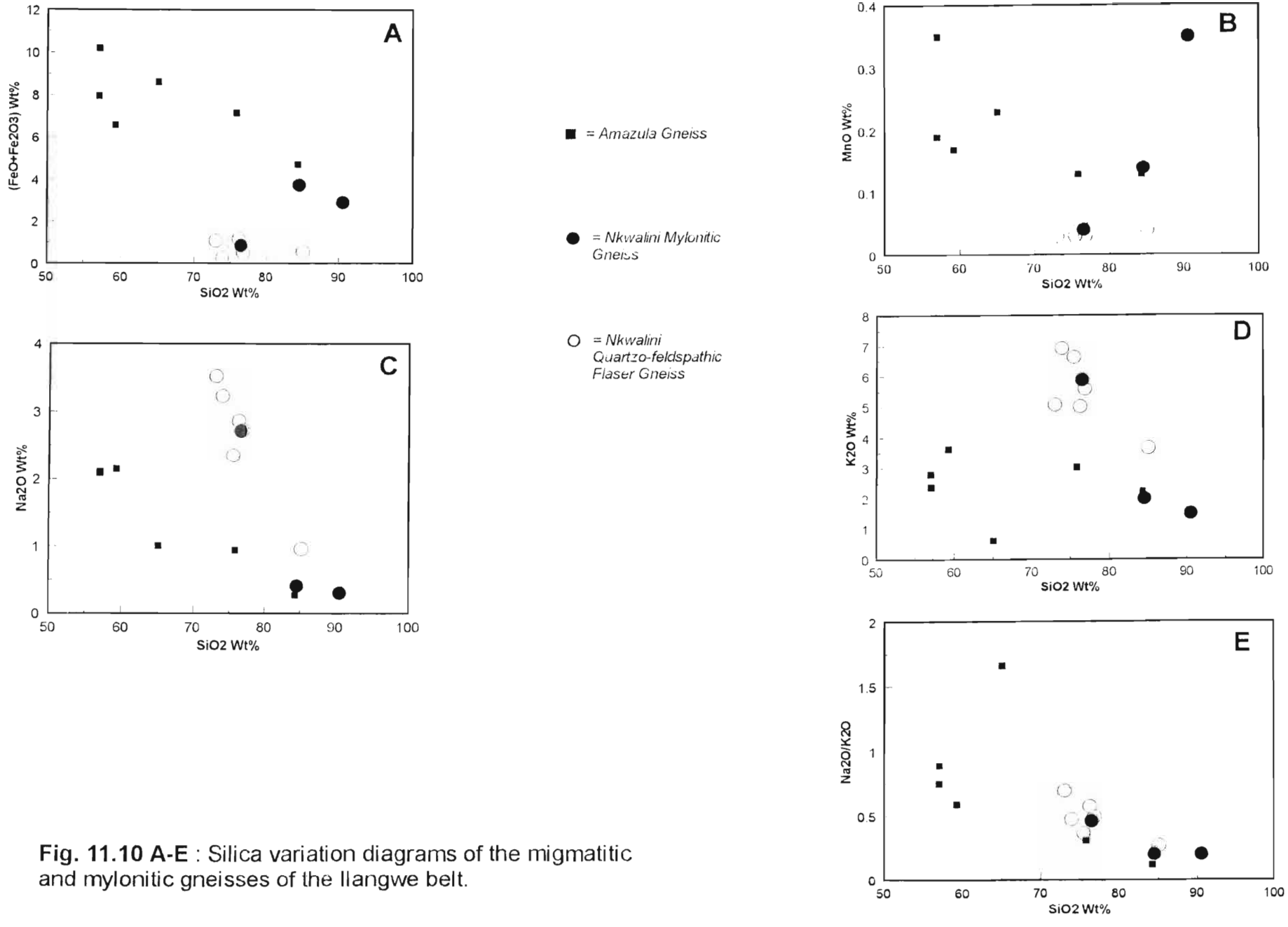

Fig. 11.10 A-E : Silica variation diagrams of the migmatitic and mylonitic gneisses of the Ilangwe belt.

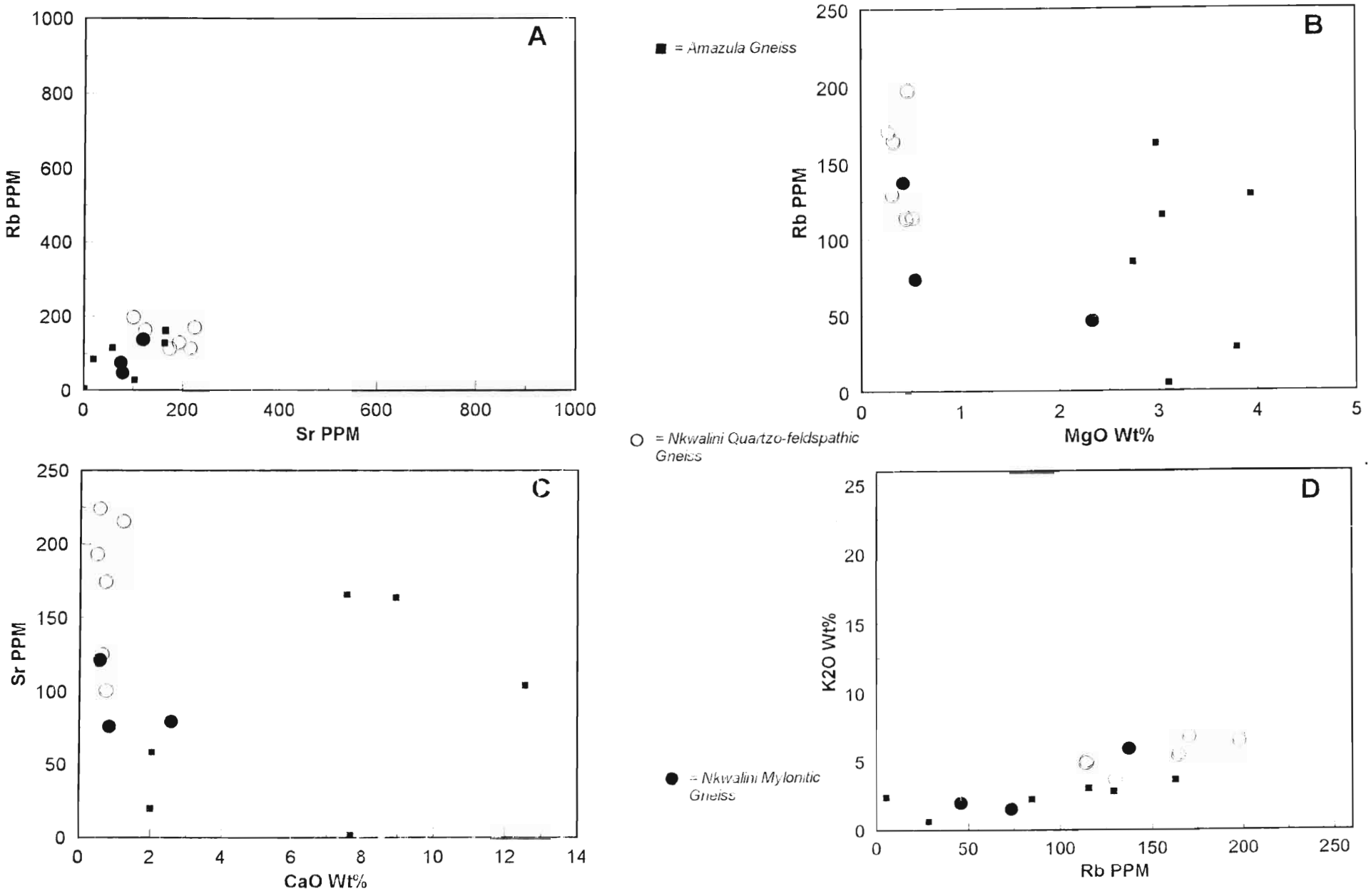

Fig. 11.11 A-D : Trace element variation diagrams of the migmatitic and mylonitic gneisses.

Fig. 11.12 depicts the migmatitic and mylonitic gneisses on a Q - Ab - Or ternary diagram. Also shown are the approximate positions of the 670°C, 700°C and 720°C isotherms at 5kb, 7kb and 2kb isobars, the Ab/An ratios and the cotectic line and eutectic points in the SiO_2 - $NaAlSi_3O_8$ - $KAlSi_3O_8$ - H_2O system at 5kb water pressure (Winkler, 1974; 1979). The fact that most of these gneisses plot both within and outside of the isotherms may indicate a possible origin by anatexis of pre-existing rocks for some of these gneisses (Winkler, 1974).

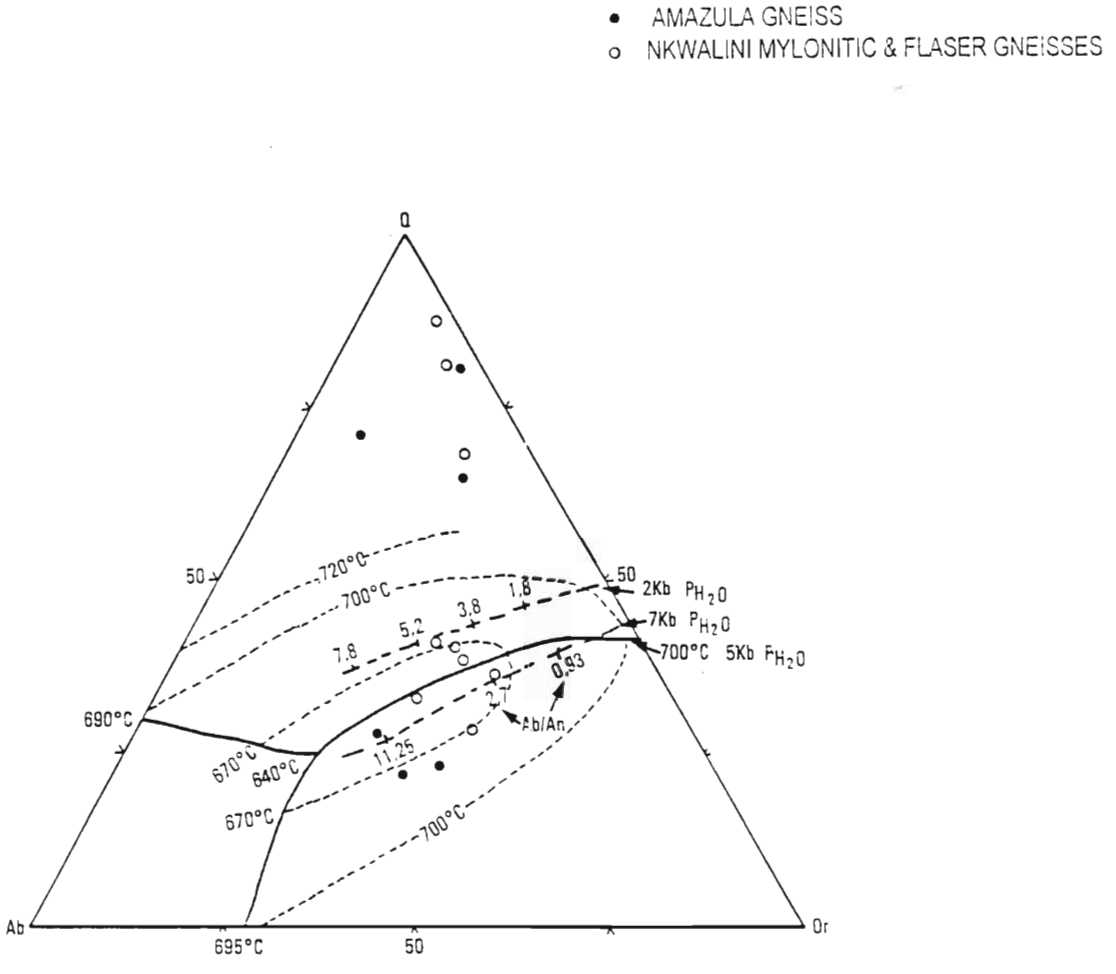

Fig. 11.12: Ternary Q - Ab - Or diagram showing the composition of the migmatitic and mylonitic gneisses relative to cotectic boundaries at various temperatures, pressures and Ab/An contents (after Winkler, 1979).

CHAPTER 12

METAMORPHIC PETROLOGY AND GEOCHEMISTRY OF THE EARLY POST-NONDWENI GRANITOIDS

12.1 INTRODUCTION

The early post-Nondweni granitoids comprise the Nkwalinye Tonalitic Gneiss and the Nsengeni Granitoid Suite association (***Table 4.1***). The latter suite consists of three granitoids (viz. the Ntshiweni Augen Gneiss, the Nsengeni Granitoid Gneiss and Ekuthuleni Granite) which show similar geochemical and mineralogical characteristics and occur to the north and south of the Ilangwe Greenstone Belt.

In this chapter, the petrography and metamorphism of both the Nkwalinye Tonalitic Gneiss and the Nsengeni Granitoid Suite will be discussed separately. To avoid unnecessary repetition, a broad all-inclusive petrographic description of the granitoids of the Nsengeni suite will be given and where there are differences these will be highlighted.

12.2 NKWALINYE TONALITIC GNEISS

12.2.1 PETROGRAPHY

Typically, this gneiss consists of a leucosome of microcrystic to megacrystic quartz and feldspars and a melanosome of foliated biotite and minor hornblende. Minor minerals include sericite, carbonate, apatite and epidote. ***Table 12.1*** gives the representative modal composition and features of these rocks.

This contorted gneiss is medium- to coarse-grained, well-foliated and exhibit equigranular interlobate granoblastic to strongly gneissic texture. Transposed foliation, isoclinal folds and natural back-rotated layer segments (Hanmer and Passchier, 1991; Plate 6.1A-C) are testimony to the extreme degree of deformation experienced by this gneiss.

In thin section, quartz is subidioblastic to xenoblastic and ranges between 0,5mm and 1,5mm in diameter. It has been modified by strain and shows deformation effects such as wavy extinction, fractured margins and elongation parallel to the foliation.

Plagioclase occurs as subidioblastic to xenoblastic grains up to 2mm in length. It does not show any zonation and the composition is An_{20-30} (oligoclase). Twinning is according to the albite, carlsbad and pericline laws. Some twins shcw strain effects of being curved. It poikiloblastically enclose minerals such as quartz, K-feldspars, biotite and epidote. The K-feldspars are present as xenoblastic microcline up to 1,5mm in size and showing tartan twinning. It, together with quartz, can also occur in the matrix.

Subidioblastic brown biotite occurs as laths showing mottled extinction. It, together with hornblende/actinolite, is aligned parallel to the foliation and seems to grow at the expense of hornblende. Calcite traces associated with biotite are present.

Sericite, the alteration product of feldspars, occurs in the cores of plagioclase grains or along cleavage traces. Traces of idioblastic small grains of epidote are present. One epidote grain contained a core of allanite. Discrete idioblastic grains of apatite occur piokiloblastically enclosed in plagioclase.

12.2.2 METAMORPHISM

Two mineral assemblages characterize the grey Nkwalinye Tonalitic Gneiss :

Plagioclase + K-feldspar + quartz + hornblende ± sphene.....(1)
Plagioclase + K-feldspar + quartz + biotite + epidote ± muscovite + sericite.....(2)

In assemblage (1), quartz and hornblende define a strong foliation. Hornblende could be a product of early prograde M_2 metamorphism probably due to the intrusion of the Nsengeni Granitoid Suite. Hornblende is abundant near the contact with the Nsengeni granitoids. In assemblage (2), biotite is after hornblende and does not define a new fabric but is rather developed in the same orientation as hornblende. This suggests that boitite was either a product of M_2 syntectonic retrogression when the strain orientation was similar to that when the original fabric developed, or of M_2 post-tectonic retrogression. The occurrence of epidote after biotite indicates that the M_2 retrograde event was prolonged to the greenschist facies.

However, the breakdown of biotite to give hornblende, epidote and sphene and the replacement of plagioclase by K-feldspar can also be interpreted as having occurred under anatectic conditions in an original rock composed of biotite, quartz and plagioclase (Winkler, 1974, 1979). This is so because hornblende is not a common constituent of the contorted gneisses. It is therefore possible that the hornblende of assemblage (1) is a product of the breakdown of biotite rather than biotite being the product of the breakdown of hornblende.

In the presence of quartz and plagioclase, biotite melts incongruently, giving a component of K-feldspar when the rock is heated beyond the temperature of the commencement of anatexis (Winkler, 1974). This is represented by the reaction :

biotite + plagioclase + quartz = hornblende + K-feldspar + sphene
(Busch, 1966;1970 in Winkler, 1974)

The formation of epidote could be an extension of the above reaction rather than a retrogressive effect. Winkler (1974) contends that provided sufficient water is available (P_{H2O} >3,5kb), conditions denoting the beginning of anatexis may be as low as the upper medium-grade field. The presence of abundant K-feldspar and the absence of primary muscovite suggests that anatectic conditions may have prevailed in these rocks. This is supported by the field observation that the grey contorted gneiss is intruded by a pink K-feldspar-rich quartzo-feldspathic sheet which could be the result of the anatectic melt (see Plate 6.1B).

12.3 NSENGENI GRANITOID SUITE

12.3.1 PETROGRAPHY

Table 12.1 gives the representative modal analyses and main mineralogical features which show the granitoids of the Nsengeni Suite having variable textures ranging from granoblastic inequigranular lobate to gneissose. In some thin sections quartz (up to 2,4mm in length) may occur in two modes :

(i) as deformed megacrystic subidioblastic to xenoblastic grains showing a consertal texture and aligned along the foliation and often showing deformed dust trails at

an oblique angle to the general foliation displayed by biotite, hornblende and quartz preferred orientation and normally showing undulose extinction;

(ii) as granoblastic small polygonal grains in the matrix or sometimes occurring along microfaults or fractures within the section. The quartz matrix occurs together with granoblastic interlocking plagioclase and K-feldspar grains.

Quartz usually occurs in triple-point boundary contact with microcline and biotite (Plate 12.1).

The K-feldspars are mainly microcline with tartan twinning. Minor orthoclase does occur. They also occur in two modes. The megacrystic poikiloblastic varieties usually enclose quartz, small plagioclase grains, biotite, epidote and minor apatite. They can be up to 3,0mm in size and are sometimes intergrown with plagioclase megacrysts. Orthoclase megacrysts can be up to 3,5mm in size and have a cloudy appearance. They usually contain exsolution lamellae of microperthitic plagioclase - normally albite. The K-feldspar megacrysts are abundant in the less deformed or rather less gneissose granitoids. In the more strongly gneissose granitoids, the megacrysts seem to be dominantly plagioclase. Incipient myrmekite and grain boundary symplectites are quite common in these granitoids (Plate 12.1B and C).

Plagioclase also occurs in two modes. The composition ranges from albite to andesine (An_{0-6} and An_{19-46}). However, oligoclase seems to be the most abundant plagioclase. Multiple albite twinning and minor carlsbad twinning occurs. The more altered (saussaritized) and deformed plagioclase show very faint twinning which is more visible in plane polarized light where the twin planes are occupied by sericite/saussarite. The megacrystic plagioclase occur as xenoblastic grains up to 2,5mm in size and often granulated on the margins. The microcrystic plagioclase interlock with K-feldspar and quartz and usually show triple-point junctions in a crystalloblastic fabric and thus indicating annealing, recrystallization and stabilization (Barker, 1990; Vernon, 1983) (Plate 12.1). In the Ntshiweni Augen Gneiss, the plagioclase megacrysts have a porphyroblastic texture with plagioclase porphyroblasts extended in the foliation planes and ferromagnesian minerals (mainly biotite) wrapped around the porphyroblasts.

The ferromagnesian minerals include biotite, muscovite, minor hornblende and actinolite. Some thin sections show both amphiboles. The principal ferromagnesian mineral is brown

biotite defining the foliation and occurring as columnar flakes up to 2,5mm in length or sometimes as irregular flakes poikilitically enclosed in feldspars. It shows polysynthetic twinning and in plane polarized light it is pleochroic from yellow-brown to dark green. It shows the typical mottled or birds eye extinction. In the Nsengeni granitoids, biotite occurs in association with muscovite and epidote. Muscovite occurs as flakes up to 3,5mm long and seems to grow at the expense of biotite. Biotite is more abundant (up to 30% by volume) in the Umgabhi granitoid and it often alters to brightly coloured epidote and calcite. Some biotite is not necessarily aligned parallel to the foliation.

Amphiboles (up to 15% by volume) are mainly hornblende and actinolite occurring as subidioblastic to xenoblastic crystals which, together with biotite, define the foliation. Hornblende shows the normal pleochroism whereas actinolite is faintly pleochroic in pale greens. They both show the typical amphibole cleavage and polysynthetic twinning. In some thin sections, hornblende breaks down to biotite and epidote.

Accessory minerals include apatite, epidote, allanite, zircon, chlorite, sericite, sphene and opaque ore. Apatite (trace - up to 1% by volume) occurs as euhedral crystals ± 0,5mm in size and sometimes poikilitically enclosed in feldspars and rarely in biotite. Some apatite occurs in grain boundary contact with opaque ore - usually ilmenite or magnetite. Epidote occurs as lath-like idioblastic crystals which are at times zoned with allanite core. The occurrence of allanite cores in epidote indicates some immiscibility within the epidote-allanite solid solution series (Deer et. al., 1966; 1985). In H91EB allanite crystals have exsolution lamellae of an unidentifiable material [probably radioactive? as allanite is weakly radioactive (Heinrich, 1965)] which also extend to the adjacent quartz grains. The allanite crystals are also rimmed by opaque ore (Plate 12.1D). Sericite is an alteration product of feldspars occurring especially on twin planes. In H110EB, the sericite trails on feldspar occur at an oblique angle to the deformed dust trails in quartz thus indicating that sericitization is post-deformation. Chlorite (up to 3% by volume) occurs as crystal aggregates resulting from the alteration of biotite and to some extent hornblende. Sphene and ore occur in trace amounts.

Garnets are not common constituents of these granitoids. According to the classification of Streckeisen (1973), these rocks plot in the granite field (Fig. 12.1).

12.3.2 METAMORPHISM

The typical mineral assemblage of the granitoids of the Nsengeni Suite is :

quartz + plagioclase + K-feldspar + biotite ± hornblende ± muscovite ± chlorite.

These granitoids are broadly similar both chemically and mineralogically. The Nsengeni Granitoid Gneiss and the Ekuthuleni Granite are in mutual contact with each other. No contact relationships between the Nsengeni Gneiss and the Ntshiweni Augen Gneiss have been observed. But it is possible that the augen gneiss is a less evolved earlier phase of the Nsengeni Granitoid Gneiss. The above paragenesis generally represents the mineral constituents present in these granitoids in various amounts. Incipient symplectites have been observed, thus indicating that minor retrogression has occurred in these rocks, probably during the cooling stages of the batholith and before the emplacement of the late post-Nondweni granitoids. The fact that some biotite (and to a lesser extent amphiboles) is not aligned parallel to foliation indicates that biotite is a product of syntectonic recrystallization. During the waning stages of intrusion, some biotite became re-aligned sub-parallel to foliation. However, this re-alignment could have also taken place during the emplacement of the late post-Nondweni granitoids which caused the regional deformation in the Nsengeni granitoids, the product of which is a uniform foliation in the Nsengeni Granitoid Gneiss and the associated augen gneissic layering in the Ntshiweni Augen Gneiss.

There is no evidence to indicate that these foliated granitoids were subjected to amphibolite or even upper greenschist facies metamorphic conditions. The weakly developed retrogression of biotite to chlorite or epidote and plagioclase to sericite are the only metamorphic reactions observed in these rocks. It is thought that these metamorphic reactions took place in the waning stages of M_2 greenschist facies metamorphism.

PLATE 12.1 : PHOTOMICROGRAPHS OF GRAIN BOUNDARY SYMPLECTITES IN NSENGENI GRANITOIDS AND SHEARING IN PHYLLITE.

PLATE 12.1A : Phyllite of the Entembeni Formation in the Ilangwe Peak (5.820/Y.755) showing lepidoblastic texture and sinistral shear sense indicated by the stair-step structure (Hanmer and Passchier, 1991; Barker, 1990) of the porphyroblast.

PLATE 12.1B : Incipient myrmekite in the Nsengeni granitoid in the Nkwalinye River (5.300/MM.185). Note the occurrence of biotite along grain boundaries of quartz and microcline. Also note the faint dust trails in the grey quartz grains. Quartz occurs in a consertal texture.

PLATE 12.1C : Grain boundary symplectites in Nsengeni granitoid. Biotite replaces pyroxene. The quartz shows an inequigranular crystalloblastic texture with polygonal grains showing 120° triple junctions. {Sample from Mfanefile: (3.380/Y.890)]

PLATE 12.1D : Zoned allanite poikilitically enclosing a quartz grain. Biotite, occurring along quartz and microcline boundaries, is altering to epidote. [Nsengeni-type granitoid from Mfanefile area: (3.380/Y.890)]

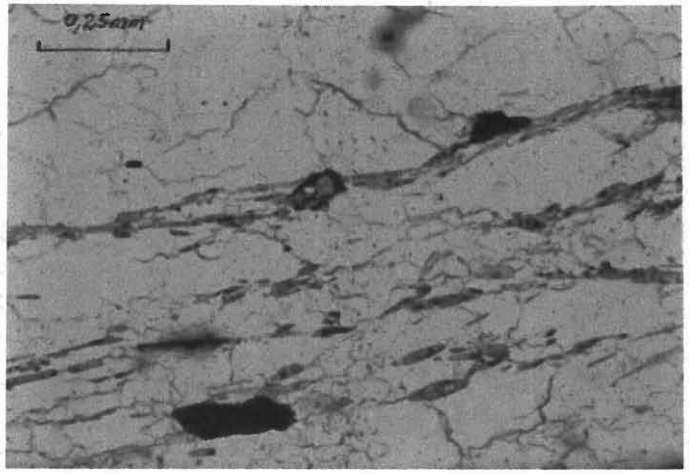

A

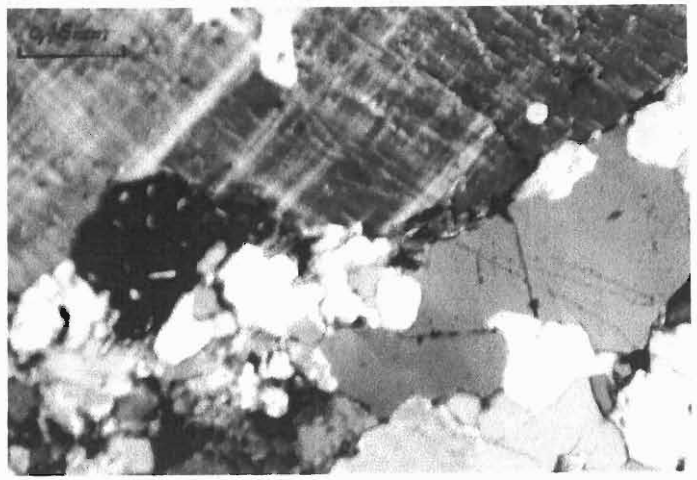

B

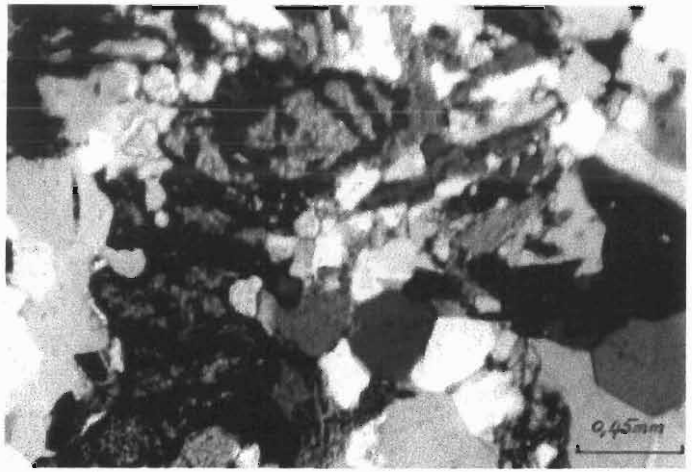

C

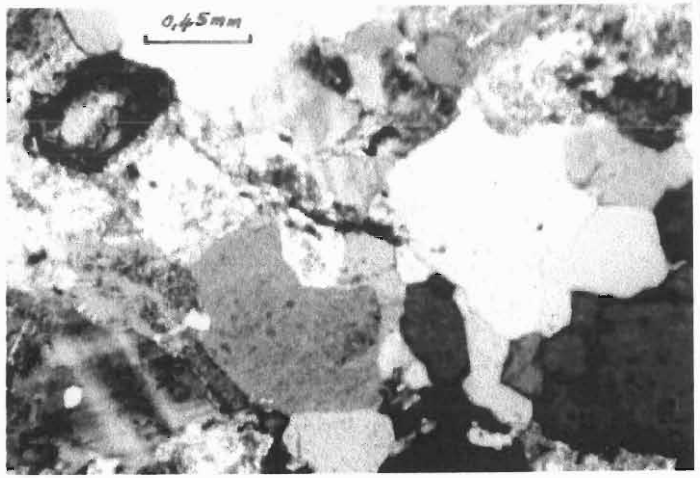

D

Plate 12.1

TABLE 12.1 : THE EARLY POST-NONDWENI GRANITOIDS : MODAL ANALYSES AND PETROLOGICAL FEATURES

SAMPLE IDENTITY	SAMPLE NO.	MINERAL MODAL COMPOSITION (%)															GRAIN SIZE			PLAG An CONTENT %	TEXTURE
		Qtz	Plg	K-Fel	Biot	Hbl	Pyrox	Mus	Apat	Zir	Carb	Epid	Ser	Ore	Allan	Chlrd	F	M	C		Granoblastic(*); Subophitic(Sub); Ophitic(Oph); Inequigranular(In); Equigranular(Eq); Myrmekitic(Myr); Uralitization(Ur); Xenoblastic(Xen); Nematoblastic(Nem).
NGG	H7EB	15	5	75	3			2				t						x		nd	In.; subidiobl.
NGG	H9EB	30	12	50	2							1	5					x		nd	Eq.; *.
NGG	H15EB	20	15	45	8								10	2				x		nd	Subidiobl.; poikilobl.
NGG	H16EB	22	13	48	7			2	t			1	5	1				x		Albite	In.; consertal
NGG	H23EB	25	17	43	10			2				1	2					x		Albite	
NGG	H25EB	15	20	55	2							1	7						x	An_{22}	In.; *.
NGG	H30EB	25	10	54	2							1	8						x	nd	Eq.; *.
NGG	H52EB	27	25	35	6				t	t		2	4	t	1			x		An_{23}	In.; *; zoned allanite
NGG	H55EB	29	20	43	2			t				t	6						x	An_{8}	In.; consertal
NGG	H65EB	22	15	42	9				t			1	10					x		An_{46-50}	In.; *; traces of zoned allanite
NGG	H7OEB	20	15	48	10	2			t			1	3	1	1			x		An_{9-23}	In.; cons.; equant
NGG	H86EB	31	41	24	2			t					2						x	An_{28}	Myr.; in.; *.
NGG	H86AEB	28	25	40	5								2					x		An_{25}	In.; *; myr.
NGG	H91EB	17	23	45	6				t	t		t	7	2					x	An_{25}	In.; equant., traces of allanite
NGG	H92EB	20	35	40	1							1	3						x		In.; *; myr.
NGG	H98EB	25	31	40	1			t			t		3					x		An_{29}	In.; *.
NGG	H110EB	20	28	30	10			1				1	10					x		An_{6-15}	* to cons., myr.
NGG	H123EB	25	28	36	5			1					5					x		An_{6-27}	In.; *.
EG	H51EB	26	20	40	6							1	7						x	An_{12-16}	In.; equant.
EG	H94EB	30	20	45	2							t	3					x		An_{15}	Myr.
EG	H165EB	31	15	42	4				t			1	5	t					x	nd	
NAG	H8EB	25	17	50	8							t						x		An_{5-13}	Suidiobl.; crystallobl.; myr.
NAG	H67EB	25	20	40	10		2		1			2		t					x	An_{14}	Xen.; crystall.; myr.; allanite traces
NAG	H71EB	26	28	40	2			1					3					x		An_{6-17}	Subidiobl.; myr.

NAG = NTSHIWENI AUGEN GNEISS EG = EKUTHULENI GRANITE NGG = NSENGENI GRANITOID GNEISS

TABLE 12.1 : THE EARLY POST-NONDWENI GRANITOIDS : MODAL ANALYSES AND PETROLOGICAL FEATURES (CONTINUED)

SAMPLE IDENTITY	SAMPLE NO.	MINERAL MODAL COMPOSITION (%)																GRAIN SIZE			PLAG An CONTENT %	TEXTURE
		Qtz	Plg	K-Fel	Hbl	Pyrox	Biot	Cord	Apat	Zir	Carb	Epid	Chlo	Ser	Mus	Talc	Ore	F	M	C		Granoblastic(*); Subophitic(Sub); Ophitic(Oph); Inequigranular(In); Equigranular(Eq); Myrmekitic(Myr); Uralitization(Ur);Xenoblastic(Xen); Nematoblastic(Nem).
NTG	H14EB	25	30	5	20	10						2		8					x	x	An_{6-21}	*; in.
NTG	H19EB	30	52	3	t		12					t		3	t		t			x	An_{13-21}	*; eq.; lepid.
NTG	K84EB	25	60	7	t		5					t		2					x		nd	In.; lepid.; blue-green hbl.
NTG	H96EB	35	48	5	t		10							2						x	Ab_{18}	In.; *.
NTG	H99EB	31	60	2	t		3		t			2		2						x	An_{25-29}	Eq.; *; poikilobl.
NTG	H105EB	30	35	10	1		14						10						x		An_{30}	Eq.; poikilobl.
NTG	H115EB	20	70	3			2			t				5					x		An_{26-29}	In.; poikilobl.; lepid.
NTG	H116EB	15	72	7	1		3		t			t		1			t		x		An_{17-24}	Poikilobl.; lepid.
NTG	H129EB	40	42	5	t		10					t		3					x		An_{10}	Lepid.
NTG	H130EB	35	53	5			5					1		1					x		An_{27}	Lepid.; in.; *; brown biot.

NTG = NKWALINYE TONALITIC GNEISS

12.4 GEOCHEMICAL CLASSIFICATION OF THE EARLY POST-NONDWENI GRANITOIDS

In this section, all the early post-Nondweni granitoids, that is the Nkwalinye Tonalitic Gneiss and the Nsengeni Granitoid Suite, will be combined together for the purpose of geochemical classification. This will aid in the determination of any compositional change in the evolution of the early post-Nondweni magma which generated these foliated granitoids. This may also elucidate any structural change that the granitoids were subjected to during the evolution of the early post-Nondweni magma.

According to the Q.A.P. diagram (Streckeïsen, 1973) the early post-Nondweni granitoids show a modal composition plotting in the tonalite, granodiorite and granite fields (Fig. 12.1). This is supported by the normative An-Ab-Or ternary diagram (Fig. 12.2; Barker, 1979) which shows this varied composition. This diverse composition is also corroborated by the binary plot of Na_2O against K_2O (Harpum, 1963) wherein these rocks are shown to have a composition ranging from granitic to tonalitic (Fig. 12.3), are of calc-alkaline affinity (Fig. 12.4; Irvine and Baragar, 1971), and show a very strong trend towards the total alkali ($Na_2O + K_2O$) apex (Fig. 12.4).

The Nkwalinye Tonalitic Gneiss has a composition ranging from tonalitic to granodioritic whereas the Nsengeni Suite of granitoids has a granitic composition. All the early post-Nondweni granitoids are peraluminous (Fig. 12.5; Shand, 1947 quoted ***in*** Clarke, 1992) with the ratio A/CNK [i.e. molar $\{Al_2O_3/(CaO + Na_2O + K_2O)\}$] greater than unity (Clarke, 1992), are mostly of magmatic lower crustal or even mantle origin (Fig. 12.6; Fig. 12.5; Roberts and Clemens, 1993; Barbarin, 1990; White and Chappell, 1983; Chappell and White, 1974) and have a sub-alkaline character when plotted on the TAS diagram (Fig. 12.7) of Irvine and Baragar (1971).

The early post-Nondweni granitoids have SiO_2 values ranging between 65% and 78% (***Table 12.2***). Although the SiO_2 spread is restricted, the silica variation diagrams (Harker diagrams) show some discernible geochemical trends (Figs. 12.8 and 12.9). Generally, TiO_2, P_2O_5, MnO, MgO, CaO and total Fe decrease with increasing SiO_2 (Fig. 12.8). Al_2O_3, Na_2O and K_2O show a scatter of values with increasing SiO_2 for the granitoids of the Nsengeni Suite (Fig. 12.9) whereas the Nkwalinye Tonalitic Gneiss shows no variation in the Na_2O and K_2O content with increasing SiO_2 (Fig. 12.9). The granitoids of the Nsengeni Suite have Na_2O/K_2O ratios of less than unity whereas the Nkwalinye Tonalitic Gneiss has

TABLE 12.2
THE EARLY POST-NONDWENI GRANITOIDS : MAJOR AND TRACE ELEMENT ANALYSES

MPLE	NSENGENI GRANITOID GNEISS														NTSHIWENI AUGEN GNEISS		EKUTHULENI GRANITOID	
	H23EB	H52EB	H55EB	H56EB	H61EB	H65EB	H70EB	H86EB	H86AEB	H91EB	H92EB	H98EB	H110EB	H123EB	H67EB	H71EB	H51EB	H94EB
$_2$	74.20	68.80	73.20	78.10	74.00	72.60	65.60	71.50	74.78	69.00	73.20	71.50	73.23	78.11	68.60	75.10	74.31	73.72
$_2$	0.24	0.74	0.20	0.03	0.20	0.52	0.61	0.59	0.32	0.79	0.30	0.41	0.34	0.19	0.83	0.04	0.24	0.22
O_3	13.80	14.00	12.80	13.00	14.70	13.70	11.50	13.20	11.62	14.00	13.70	13.50	13.58	11.60	13.00	14.40	13.23	13.17
O_3	0.47	0.97	0.53	0.07	0.33	0.71	1.10	0.92	0.91	1.13	0.47	0.60	0.56	0.42	1.27	0.13	0.44	0.44
)	1.70	3.49	1.92	0.26	1.19	2.54	3.97	3.33	3.28	4.07	1.69	2.16	2.02	1.49	4.56	0.46	1.60	1.57
O	0.04	0.10	0.06	0.03	0.04	0.07	0.12	0.06	0.08	0.10	0.06	0.06	0.07	0.04	0.10	0.03	0.05	0.04
O	0.69	1.64	2.12	0.23	0.64	0.74	7.17	1.28	2.23	1.15	0.70	1.34	0.85	0.55	1.99	0.36	0.49	0.63
O	0.80	2.69	0.88	1.08	1.20	1.29	3.25	1.24	2.17	2.04	1.10	1.57	1.51	0.66	2.96	0.46	0.95	1.22
O	2.64	2.63	2.86	3.21	3.82	2.37	2.09	2.13	2.10	2.96	2.67	2.39	3.23	2.13	2.43	3.20	1.52	1.98
)	5.34	4.73	5.34	3.98	3.88	5.33	4.35	5.49	2.46	4.55	6.02	6.32	4.49	4.77	3.85	5.82	7.12	6.96
$_5$	0.08	0.26	0.07	0.02	0.10	0.09	0.20	0.24	0.04	0.24	0.09	0.15	0.11	0.04	0.43	0.04	0.03	0.06
TAL	100.00	100.00	100.00	100.00	100.00	100.00	100.00	100.00	99.99	100.00	100.00	100.00	99.99	100.00	100.00	100.00	99.98	100.01
	39.70	116.00	257.00	49.60	122.00	139.00	111.00	112.00	88.60	100.00	219.00	171.00	180.70	187.10	112.00	126.00	161.20	173.00
	470.00	268.00	68.90	315.00	229.00	330.00	115.00	476.00	337.40	750.00	144.00	133.00	103.70	153.10	704.00	147.00	161.80	126.40
	54.30	393.00	128.00	3.40	144.00	337.00	375.00	345.00	442.70	332.00	190.00	272.00	241.00	182.80	254.00	163.00	161.50	145.90
	5.20	25.20	22.90	1.90	8.10	16.40	25.80	13.40	14.20	28.60	15.00	12.60	32.70	16.40	17.10	3.50	20.90	14.60
	0.70	177.00	18.00	0.00	0.00	23.30	42.60	12.10	0.00	44.50	0.00	0.00	12.70	1.90	21.50	0.00	24.70	1.60
	7.00	4.30	0.00	1.10	3.90	60.30	0.00	11.80	0.00	46.50	5.10	12.10	31.90	10.40	2.80	15.20	55.10	18.00
	8.60	0.00	0.00	7.60	0.00	15.00	0.00	0.00	0.50	14.60	0.00	0.00	0.00	0.00	0.00	0.00	12.00	0.00
.W. NORMS (ANHYDROUS; IN Wt %)																		
	34.80	25.90	30.00	41.30	32.90	33.30	18.40	32.20	43.07	26.50	30.50	27.20	31.76	44.39	28.90	32.50	34.49	31.18
	31.60	27.90	31.60	23.50	22.90	31.50	25.70	32.40	14.55	26.90	35.60	37.30	26.55	28.18	22.80	34.40	42.11	41.15
	22.40	22.20	24.20	27.20	32.30	20.10	17.70	18.00	17.75	25.10	22.60	20.20	27.35	17.99	20.50	27.10	12.84	16.73
	3.43	11.60	3.90	5.22	5.28	5.82	9.23	4.55	10.49	8.54	4.85	6.79	6.77	2.99	11.90	2.04	4.54	5.66
	2.39	0.32	0.85	1.52	2.23	1.90	0.00	2.10	1.66	1.06	0.99	0.25	0.92	1.85	0.49	2.07	1.36	0.30
	0.00	0.00	0.00	0.00	0.00	0.00	4.46	0.00	0.00	0.00	0.00	0.00	0.00	0.00	0.00	0.00	0.00	0.00
	4.11	8.65	8.16	1.00	3.25	5.21	21.30	7.67	10.44	8.29	4.08	6.25	4.92	3.54	11.10	1.63	3.49	3.79
	0.68	1.41	0.77	0.11	0.48	1.02	1.60	1.34	1.32	1.64	0.68	0.87	0.81	0.60	1.84	0.18	0.64	0.63
	0.46	1.40	0.38	0.06	0.38	0.98	1.16	1.12	0.62	1.50	0.57	0.77	0.65	0.36	1.57	0.08	0.46	0.42
	0.19	0.62	0.17	0.05	0.24	0.22	0.48	0.58	0.10	0.57	0.21	0.36	0.26	0.10	1.03	0.10	0.07	0.14

TABLE 12.2
THE EARLY POST-NONDWENI GRANITOIDS : MAJOR AND TRACE ELEMENT ANALYSES
(CONTINUED)

NKWALINYE TONALITIC GNEISS							
SAMPLE	**H84EB**	**H96EB**	**H99EB**	**H115EB**	**H116EB**	**H129EB**	**H130EB**
SiO_2	71.30	72.80	74.70	69.80	73.40	70.40	69.10
TiO_2	0.40	0.42	0.22	0.36	0.28	0.45	0.51
Al_2O_3	15.10	14.30	13.80	13.60	14.50	15.50	15.20
Fe_2O_3	0.72	0.66	0.51	1.63	0.53	0.73	0.91
FeO	2.59	2.37	1.82	5.87	1.92	2.63	3.26
MnO	0.05	0.06	0.06	0.07	0.06	0.07	0.08
MgO	1.12	1.48	1.14	0.98	0.98	1.25	1.55
CaO	2.80	2.72	3.20	2.53	2.19	3.08	3.47
Na_2O	3.97	3.34	3.35	3.22	3.48	3.89	3.86
K_2O	1.73	1.79	1.20	1.74	2.54	1.78	1.88
$_2O_5$	0.18	0.10	0.07	0.15	0.13	0.20	0.21
TOTAL	100.00	100.00	100.00	100.00	100.00	100.00	100.00
Rb	74.90	68.90	55.30	69.20	79.80	68.30	70.80
Sr	306.00	650.00	445.00	310.00	254.00	366.00	344.00
Zr	159.00	160.00	157.00	189.00	94.30	159.00	166.00
Nb	13.60	10.10	13.80	15.20	15.20	11.70	12.50
Y	4.30	11.00	14.60	6.50	0.00	13.20	12.40
Th	11.30	29.70	26.70	8.60	4.10	7.80	4.80
U	4.50	11.80	10.30	4.50	3.00	6.10	4.80
C.I.P.W. NORMS (ANHYDROUS; IN Wt %)							
Q	32.80	37.30	41.00	33.90	36.40	31.40	28.20
Or	10.20	10.60	7.11	10.30	15.00	10.50	11.10
b	33.60	28.30	28.30	27.20	29.40	32.90	32.70
An	12.70	12.90	15.40	11.50	10.00	14.00	15.80
C	2.04	2.12	1.31	2.22	2.33	2.10	0.97
Di	0.00	0.00	0.00	0.00	0.00	0.00	0.00
Hy	6.38	6.91	5.52	11.40	5.16	6.72	8.40
Mt	1.04	0.95	0.73	2.36	0.77	1.06	1.31
Il	0.77	0.80	0.42	0.68	0.54	0.86	0.97
Ap	0.43	0.24	0.17	0.36	0.31	0.48	0.51

$Na_2O/K_2O>1$ (Fig. 12.9). The relatively high Na_2O/K_2O ratios of the tonalitic gneiss suggest derivation by partial fusion of pre-existing meta-igneous rocks (Roberts and Clemens, 1993). The Nsengeni Suite rocks show variable MgO/CaO ratios ranging between 0,21 and 2,41 whereas the tonalitic gneiss shows constant ratios averaging 0,43 (Fig. 12.9).

The early post-Nondweni granitoids show variable trace element ratios. The Nsengeni Suite granitoids have Rb/Sr ratios of 0,08 to 1,74 whereas the tonalitic gneiss has Rb/Sr ratios ranging between 0,11 and 0,31 — typical of tonalitic to granodioritic suites (Hunter, 1979; Hunter et. al., 1980). Zr values range between 3,5 and 443 for the Nsengeni Suite rocks ***and*** range between 94,30 and 189 for the tonalitic gneiss. All the early post-Nondweni granitoids show very low values for Y, Th and U. In the binary MgO versus Rb plot, a weak exponential increase in Rb with a decrease in MgO content is shown (Fig. 12.10A), whereas the binary CaO versus Sr plot shows a positive steep linear trend (Fig. 12.10C).

It is concluded from the Q-Ab-Or ternary diagram (Fig. 12.11) that crystallization of the early post-Nondweni granitoids took place at temperatures of about 650-750°C and pressures of between 2kb and 5kb and with the crystallization of quartz and k-feldspar probably taking place close to the Q-Or cotectic (Winkler, 1979).

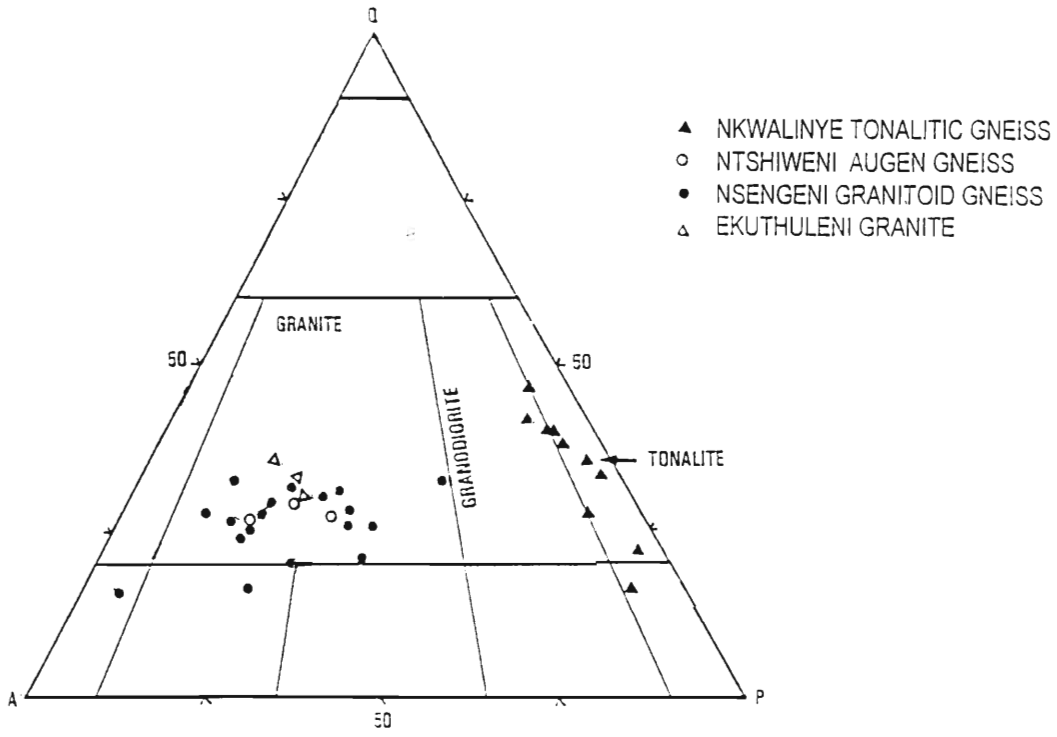

Fig. 12.1 : QAP ternary diagram (after Streckeisen, 1973) showing the granitic to tonalitic composition of the **early post-Nondweni granitoids**. Q = quartz; A = alkali feldspar; P = plagioclase

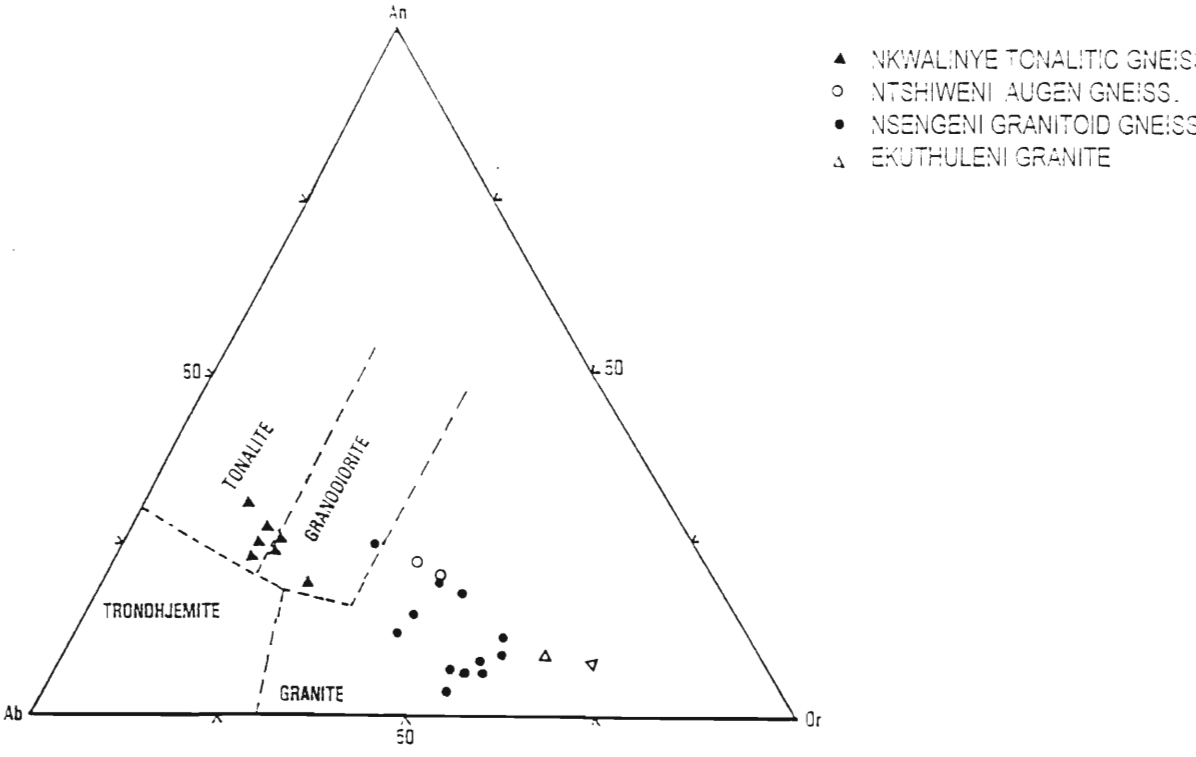

Fig. 12.2 : Normative An - Ab - Or ternary plot of the **early post-Nondweni granitoids**. Compositional fields are after Barker (1979).

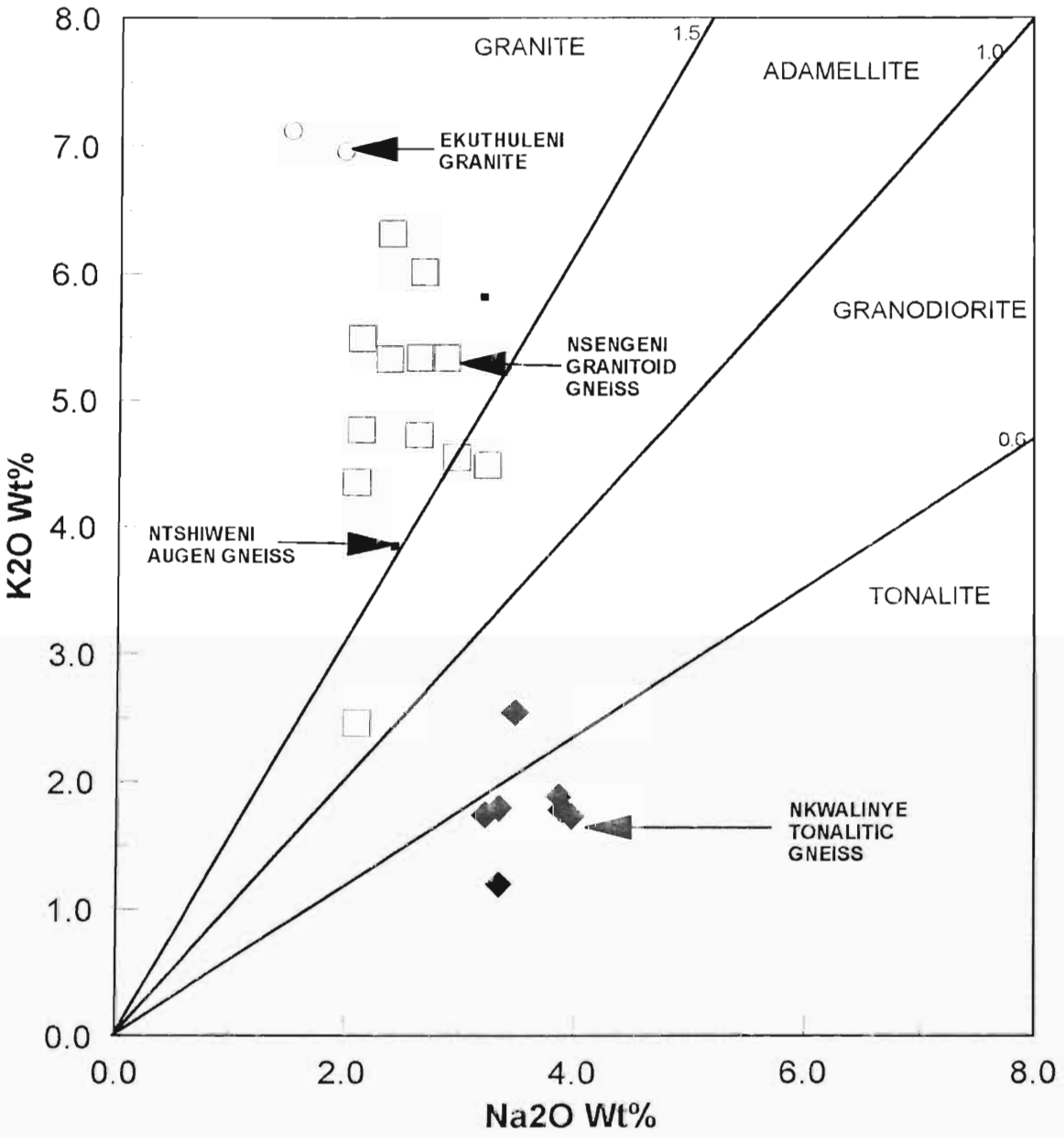

Fig. 12.3 : Binary Na_2O against K_2O plot showing a granitic to tonalitic composition for the early post-Nondweni granitoids (after Harpum, 1963).

▲ NKWALINYE TONALITIC GNEISS
o NTSHIWENI AUGEN GNEISS
• NSENGENI GRANITOID GNEISS
△ EKUTHULENI GRANITE

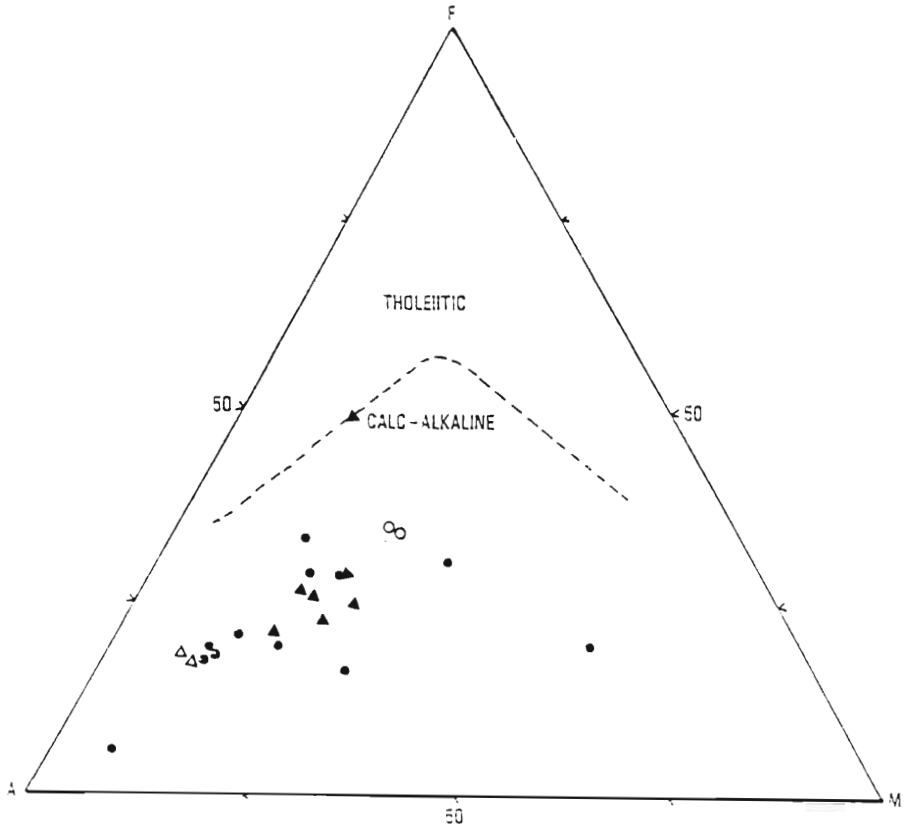

Fig. 12.4 : AFM ternary plot of the **early post-Nondweni granitoids** showing their calc-alkaline nature. The dashed line separating the tholeiitic and calc-alkaline fields is after Irvine and Baragar (1971).

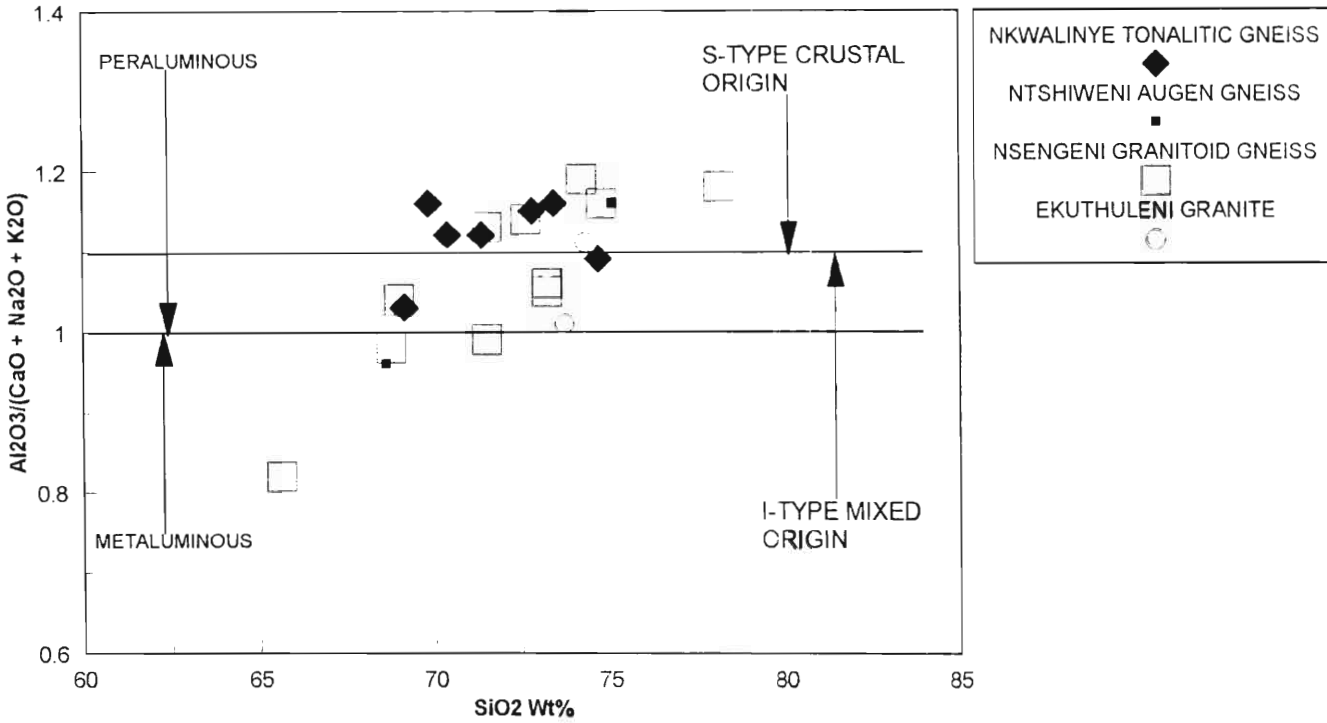

Fig. 12.5 : Binary SiO_2 vs A/CNK plot (after Clarke, 1992) showing the composition and probable origin of the early post-Nondweni granitoids (after Chappell and White, 1974: White and Chappell, 1983: Barbarin, 1990).

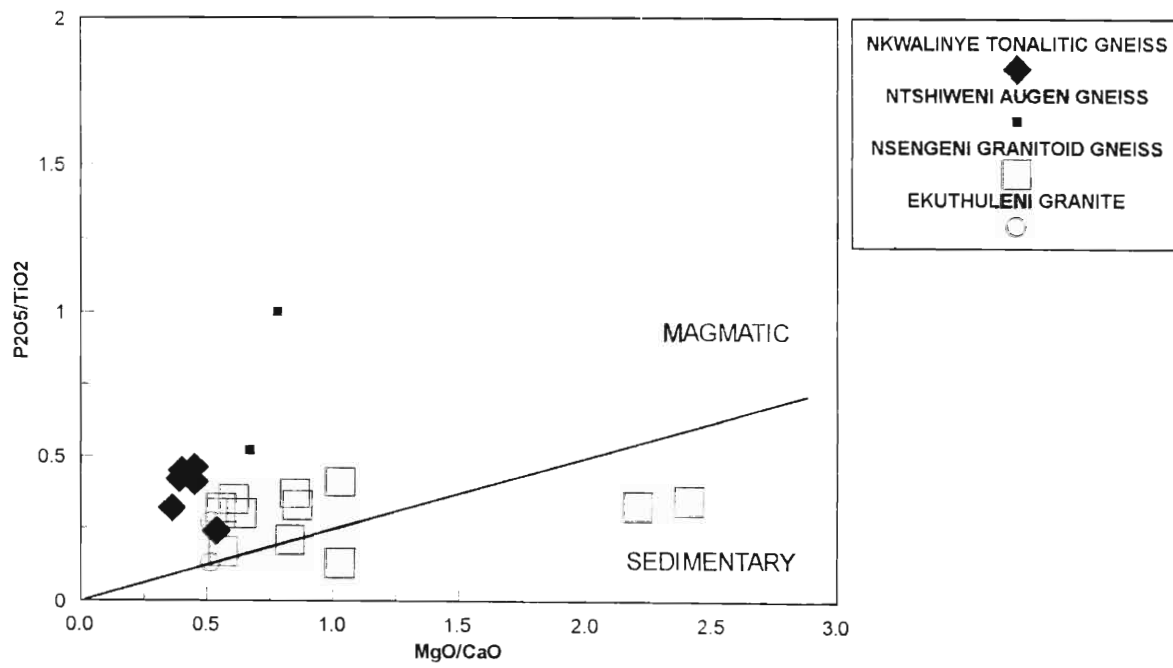

Fig.12.6 : Binary P_2O_5/TiO_2 vs MgO/CaO diagram showing the majority of the early post-Nondweni granitoids plotting in the magmatic field.

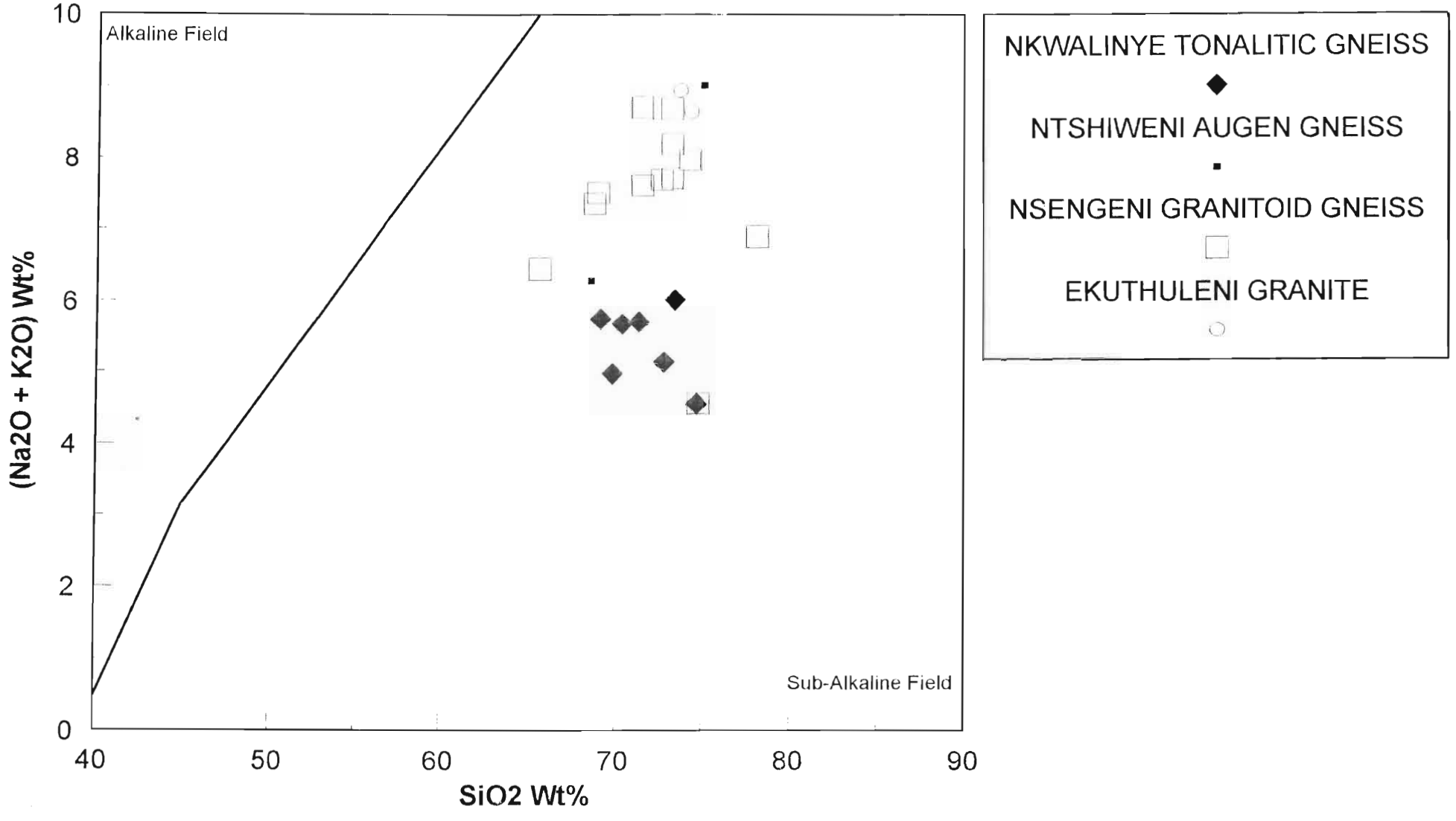

Fig. 12.7 : TAS (total alkali against silica) diagram of the early post-Nondweni granitoids showing their sub-alkaline affinity. The solid line separating the alkaline and sub-alkaline fields is after Irvine and Baragar (1971).

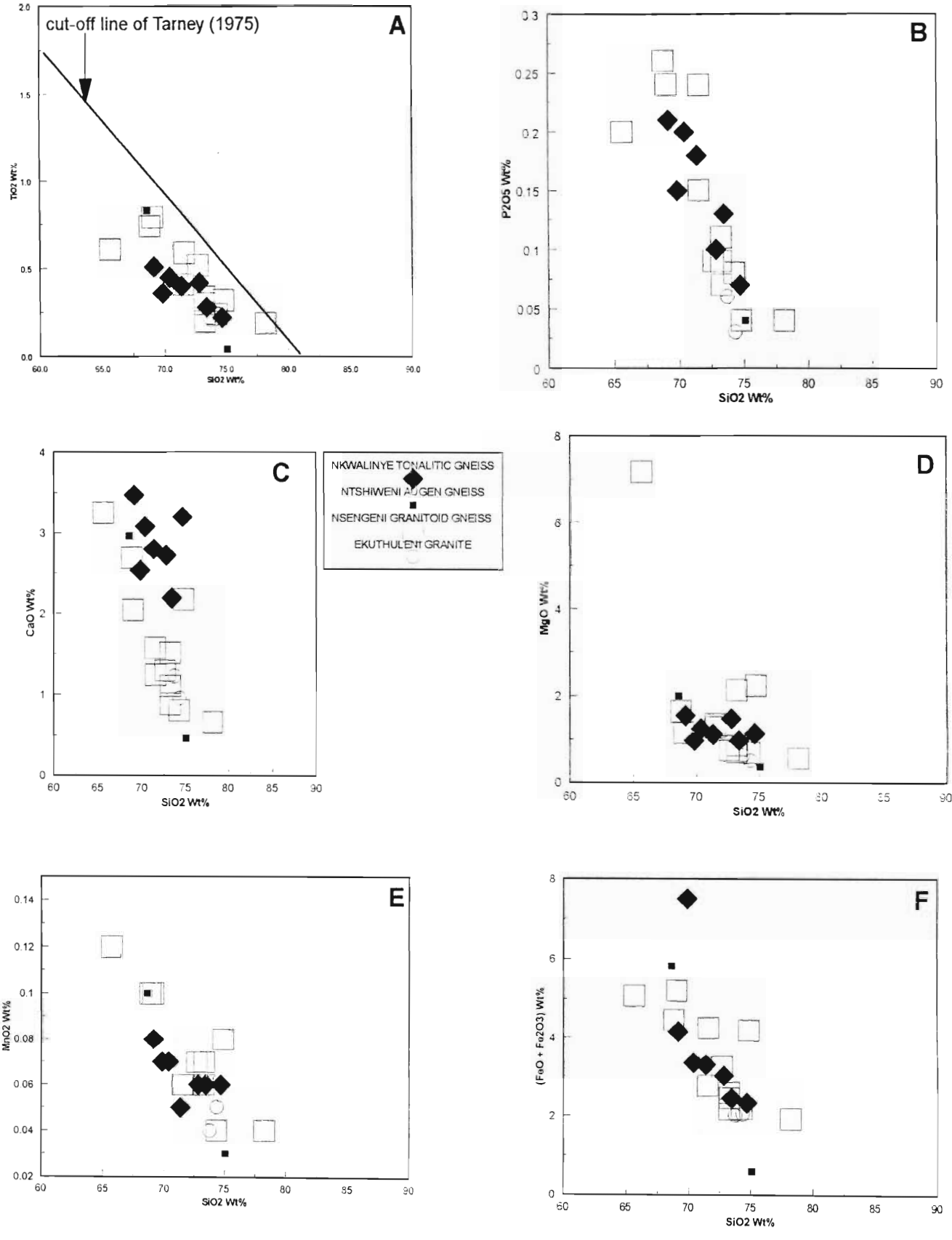

Fig. 12.8 A-F : Harker variation diagrams of the major element oxides against silica for the early post-Nondweni granitoids.

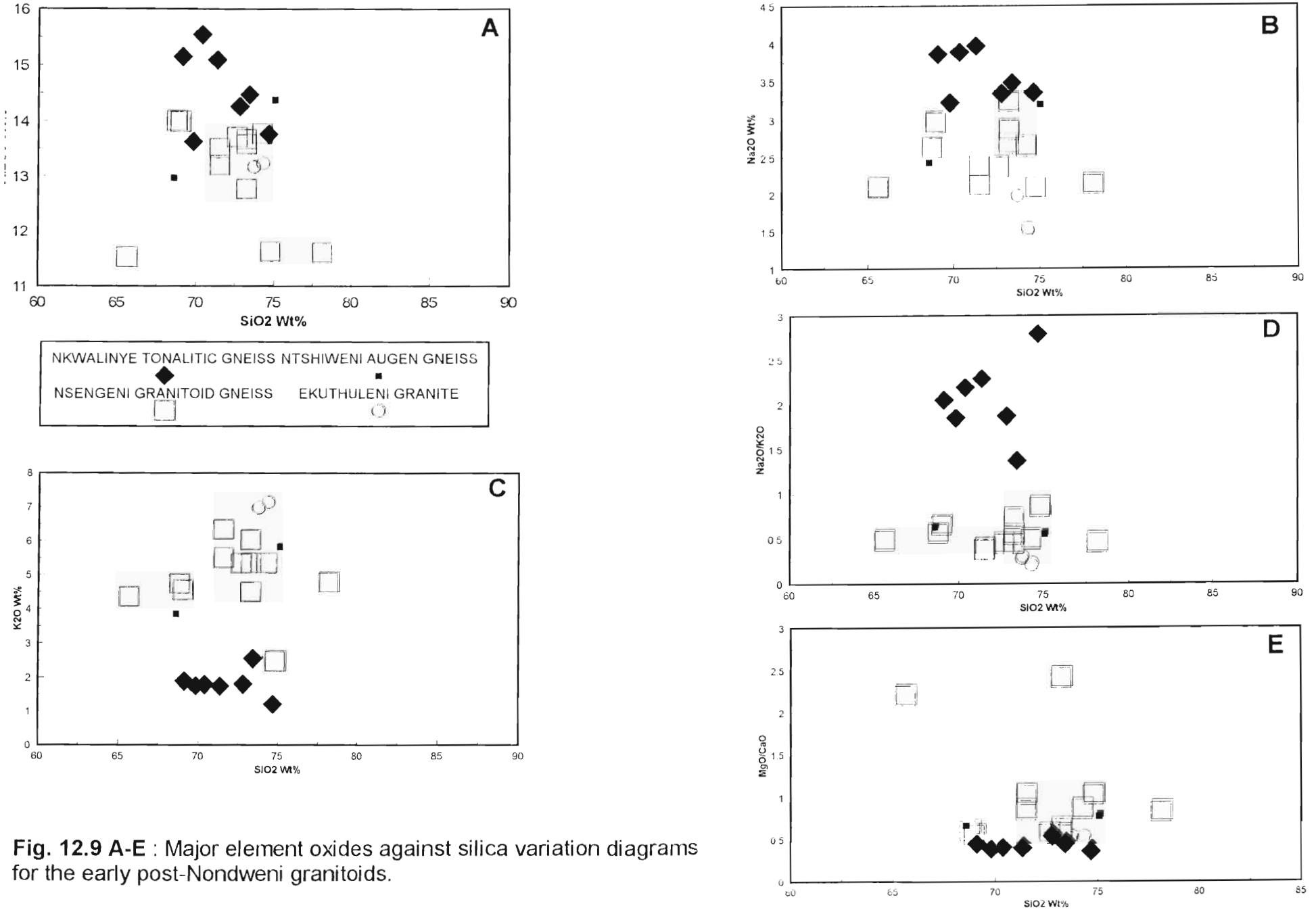

Fig. 12.9 A-E : Major element oxides against silica variation diagrams for the early post-Nondweni granitoids.

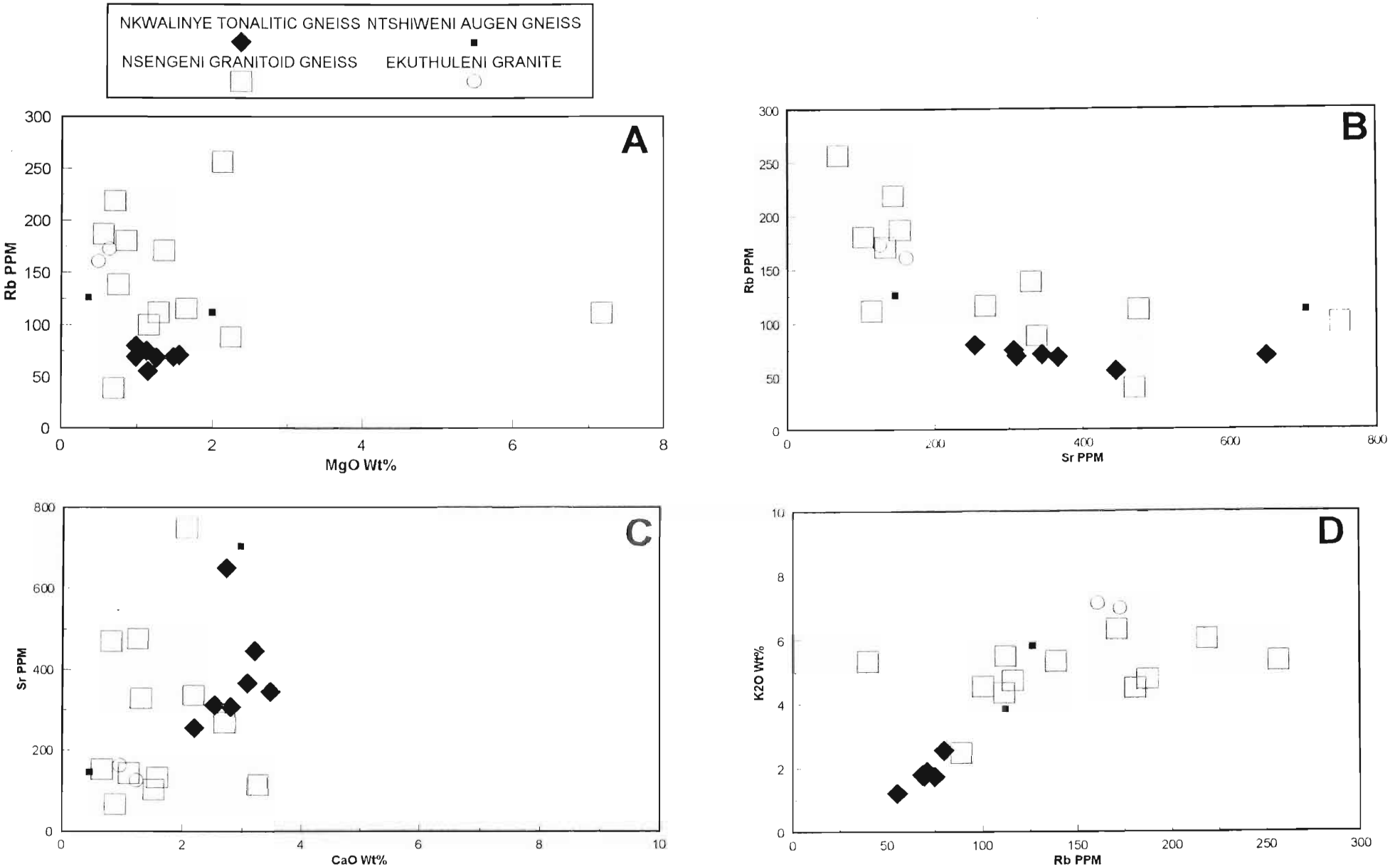

Fig. 12.10 A-D : Trace element variation diagrams of the early post-Nondweni granitoids.

▲ NKWALINYE TONALITIC GNEISS
o NTSHIWENI AUGEN GNEISS
• NSENGENI GRANITOID GNEISS
△ EKUTHULENI GRANITE

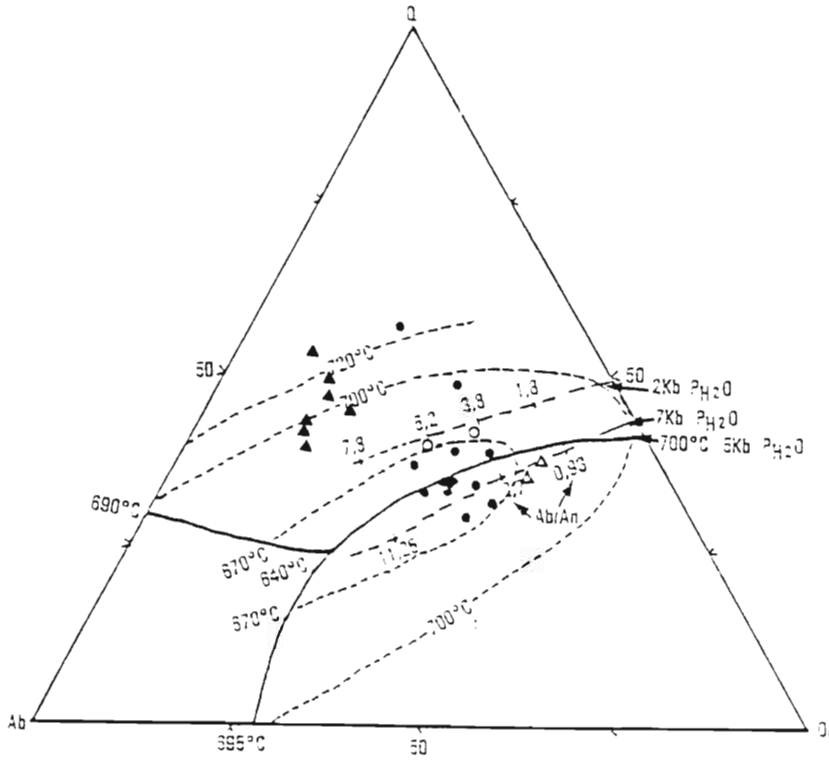

Fig. 12.11 : Q - Ab - Or ternary diagram showing the composition of the **early post-Nondweni granitoids** relative to cotectic boundaries at various temperatures, pressures and Ab/An contents (after Winkler, 1979).

CHAPTER 13

METAMORPHIC PETROLOGY AND GEOCHEMISTRY OF THE LATE POST-NONDWENI GRANITOIDS

13.1 IMPISI-UMGABHI GRANITOID SUITE

13.1.1 INTRODUCTION

The late post-Nondweni granitoids comprise two granitoid suites which have been discussed in this thesis as separate units but geochemical and mineralogical evidence supported by field observations suggest that these units are possibly a combined single association of granitic rocks. These late post-Nondweni granitoids are here referred to as the Impisi-Umgabhi granitoid suite consisting of five granitoid units, viz. :

(i) Umgabhi Granitoid;
(ii) Esibhudeni Granitoid;
(iii) Umgabhi Micrographic Granite;
(iv) Nkandla Granite;
(v) Zietover Granite.

The first three granitoids occur in the Southern Granitoid Complex, have mutual contacts, are megacrystic to microcrystic, have a weakly developed foliation or lack it totally, intrude the older gneisses, greenstones and the boundary fault and have an elongate sheet-like shape. The latter two granitoids occur to the north of the greenstone belt in the Northern Granitoid Complex and show similar characteristics to the former three. The only significant difference between the two granitoid suites is their distribution relative to the Ilangwe Greenstone Belt.

In this chapter, an all-inclusive description of the petrography and metamorphism of these granitoids will be given. Similarities and differences will be highlighted where it is appropriate.

13.1.2 PETROGRAPHY

Modal analyses and a summary of the mineralogical features of these late post-Nondweni granitoids are shown in ***Table 13.1***. Quartz, K-feldspar and plagioclase in varying amounts occur as megacrystic inequigranular subhedral to anhedral grains showing consertal to granoblastic textures. Both K-feldspars and plagioclase poikilitically enclose small grains of quartz and other accessory minerals - notably biotite and epidote. Quartz shows some faint undulose extinction and occurs in triple-point boundary contact with K-feldspar and rarely with biotite. It is usually in two modes :

(i) as megacrystic subidioblastic to xenoblastic grains showing a consertal texture; and

(ii) as granoblastic microcrystic polygonal grains in the matrix or enclosed in feldspars.

K-feldspars are mainly microcline and orthoclase. The former occurs more abundantly and shows the characteristic gridiron twinning. Orthoclase shows the Carlsbad twinning. Plagioclase, mainly oligoclase and some albite, occur as ± 2mm anhedral grains and as microperthites of albite in orthoclase and microcline. It occurs in two modes. The megacrystic plagioclase occurs as xenoblastic grains showing some incipient granulation along the margins. The microcrystic plagioclase usually encloses microcrystic polygonal grains of quartz. The plagioclase feldspars are slightly altered to sericite

Biotite occurs as columnar laths up to 1mm in length. In hand specimen it is dark green to black but in thin section it is dark brown. In the Nkandla Granite, biotite is often altered to chlorite and is locally replaced by hornblende. Some biotite is associated with muscovite.

Accessory minerals include allanite, epidote, apatite, zircon, sericite, chlorite, sphene and opaque ore. Traces of allanite are usually associated with epidote forming zoned crystals. Epidote and sphene occur as euhedral to subhedral (and occasionally anhedral) crystals whilst apatite occurs as euhedral crystals poikilitically enclosed in feldspars or occasionally, in grain boundary contact with magnetite ore. Traces of enhedral crystals of zircon have only been observed in the thin section of Esibhudeni Granitoid (H102EB). Sericite is an alteration product of plagioclase feldspars, usually occurring on twin planes, whilst chlorite occurs as aggregates resulting from the alteration of biotite — especially in samples of

TABLE 13.1 : THE LATE POST-NONDWENI GRANITOIDS : MODAL ANALYSES AND PETROLOGICAL FEATURES

SAMPLE IDENTITY	SAMPLE NO.	MINERAL MODAL COMPOSITION (%)													GRAIN SIZE			PLAG An CONTENT %	TEXTURE Granoblastic(*); Subophitic(Sub); Ophitic(Oph); Inequigranular(In); Equigranular(Eq); Myrmekitic(Myr); Uralitization(Ur); Xenoblastic(Xen); Nematoblastic(Nem).
		Qtz	Plg	K-Fel	Hbl	Garn	Biot	Carb	Epid	Mus	Apat	Zir	Ore	Chlo	Ser	F	M	C	
UG	H1EB	15	5	74						1					5		x		An_{7-15}	In.; *.
UG	H4EB	20	20	53						3					4		x		An_{7}	In.; *.
UG	H26EB	20	6	65						1					8		x		nd	In.; equant to *.
UG	H72EB	25	20	45			1			3					6			x	An_{5}	Myr.; In.; *.
UG	H117EB	25	15	50			2		1	t	t		t		6			x	nd	In.; *.
UG	H118EB	22	25	45			2		t	1					5		x		An_{6}	In.; *; myr.
UG	H124EB	25	20	48			t		1	2	t		t	t	2		x		An_{11}	Subidiobl.; myr.
UG	H126EB	28	15	45			2		1	3	t		t	t	5		x		nd	
UG	H131EB	29	19	50		t	t								2			x	An_{4-11}	Myr.; *; in.
UG	H139AEB	30	10	47		t	t		1	1	t				10			x	nd	In.; myr.
ZG	H95EB	25	27	38			3		2				t		5		x		An_{4-12}	In.; subidiobl.; equant.
ZG	H97AEB	25	20	40			4		1	2		t	t		7		x		nd	In.; *.
ZG	H164EB	23	10	50			3	t	2	1	t		t		10		x	x	nd	In.; equant.
NG	H155EB	30	19	50			1	t	t		t		t					x	An_{12}	In.; *
NG	H166EB	30	20	47			t		t		t				2		x		nd	*; myr.
NG	H166AEB	25	25	40		t	1	t	t	2	t		t		6			x	An_{15}	In.; *.
UGG	H5EB	45		53			2		t	t							x			In.; *.
UGG	H6EB	12	26	30			25		2		t		t		5			x	nd	In.; myr.; *.
UGG	H45EB	30	20	28			15		2				t		5		x		nd	Myr.
UGG	H56EB	23	27	40			4		2		t				4		x			In.; * to cons.
UGG	H61EB	18	25	47			5		1						4			x	nd	Eq.; * to cons.; allanite traces.
UGG	H149EB	15	20	35			25	2	1				t		2			x	An_{17-19}	
EGG	H102EB	20	30	35			2		t	7	t	t	t		5			x	An_{8-18}	Subidibl.; porphyrobl.

GG = UMGABHI GRANITOID GNEISS EGG = ESIBHUDENI GRANITOID GNEISS ZG = ZIETOVER GRANITE
NG = NKANDLA GRANITE UG = UMGABHI MICROGRAPHIC GRANITE

Umgabhi and Esibhudeni Granitoids. Ore traces usually occur in contact with biotite, quartz and feldspars. The ore grains are normally subhedral magnetite often poikilitically enclosing small quartz grains.

Garnets are not common constituents of these granitoids. However, in sample H131EB, a single fractured crystal of almandine garnet was observed. The fractures contain traces of biotite. This could be some form of retrograde metamorphic effect on an essentially primary garnet. Northeast of Esibhudeni (7,8/G to M), a zone of fine- to medium-grained quartz-sericite schists occurs within the Esibhudeni Granitoid Gneiss, mainly associated with thin shear zones in the granitoid. These schists have very complex textures characterized by partially transposed fabrics and the occurrence of several s-surfaces. Quartz (up to 57% by volume) is the principal mineral occurring as thin ribbon-like lenses and veins set in a silvery-green sericite-chlorite-quartz matrix displaying a lenticular texture.

Sericite (up to 25% by volume) occurs in association with flakes of muscovite (up to 8% by volume) aligned along a preferred orientation and being partially replaced by interlocking aggregates of chlorite and minor chloritoid metacrysts. Sericite, chlorite and muscovite envelope lenses of quartz thus forming discrete sheared bundles. A minor second generation muscovite occurs as post-tectonic overgrowths on chlorite. Accessory minerals include epidote, calcite, chloritoid and traces of subidioblastic apatite crystals. No feldspars were observed in these schists.

From the modal classification (Streckeïsen, 1973), the Impisi-Umgabhi granitoids plot on the granite field (Fig. 13.1).

13.1.3 METAMORPHISM

The Impisi-Umgabhi granitoids have the following general mineral assemblage :

quartz + K-feldspar + plagioclase + biotite + sericite ± muscovite ± epidote.

There is no evidence to indicate that these granitoids were subjected to any intense regional greenschist metamorphism. Minor incipient symplectic reactions have been observed in thin section. However, it is not easy to distinguish incipient retrogressive or even progressive metamorphic effects from deuteric effects in the alteration of primary igneous minerals (Shelley, 1993).

The quartz-sericite schists have the following paragenesis :

quartz + sericite + muscovite + chlorite + chloritoid ± epidote.

This paragenesis is typical of assemblages associated with shearing and dislocation (see Section 11.3.2) and is related to M_3 dislocation metamorphism. Charlesworth (1981) referred to these schists as diapthoritic phyllonites due to their partially transposed fabrics and several foliation surfaces.

Normative Q - Ab - Or contents of these granitoids (***Table 13.2***) shows that K-feldspar crystallized prior to plagioclase (Fig. 13.2).

13.1.4 GEOCHEMICAL CLASSIFICATION OF THE LATE POST-NONDWENI GRANITOIDS

Major and trace element analyses of the Impisi-Umgabhi granitoids are given in ***Table 13.2***. These rocks plot on the granite field of the ternary An - Ab - Or diagram (Fig. 13.3; Barker, 1979). They are normative An-poor. This is borne out by the ternary Q.A.P. diagram (Streckeïsen, 1973; Fig. 13.1). The granitic composition is also depicted in the binary Na_2O versus K_2O Harpum diagram (Fig. 13.4). On the binary SiO_2 versus A/CNK diagram, these granitoids occur on the peraluminous field (Clarke, 1992) indicating that they are from a magmatic source (Figs. 13.5 and 13.6) but are of a mixed origin (Barbarin, 1990; Roberts and Clemens, 1993) being derived from both the crust and the mantle. These granites plot on the sub-alkaline field (Fig. 13.7) of Irvine and Baragar (1971) and are of calc-alkaline affinity (Fig. 13.8; Irvine and Baragar, 1971). They show a very strong trend towards the total alkali apex (Fig. 13.8).

Because of the limited geochemical data of the Impisi granitoids (Nkandla and Zietover Granites) and the extremely restricted spread of the SiO_2 values (74,00% to 80,63%), the Harker variation diagrams do not show a clear geochemical trend. A very weak decrease with increasing SiO_2 is shown by Al_2O_3, K_2O, Na_2O and P_2O_5 (Fig. 13.9). The other major elements show a wide scatter. MgO/CaO ratios range between 0,21 and 0,85 whilst the Na_2O/K_2O ratios range between 0,35 and 0,98 (Fig. 13.9F and G).

TABLE 13.2
THE LATE POST-NONDWENI GRANITOIDS : MAJOR AND TRACE ELEMENT ANALYSES

SAMPLE	ZIETOVER GRANITE	NKANDLA GRANITE	UMGABHI GRANITOID		ESIBHUDENI GRANITOID	UMGABHI MICROGRAPHIC GRANITE				
	H95EB	H155EB	H56EB	H61EB	H102EB	H117EB	H118EB	H124EB	H126EB	H131EB
SiO_2	74.34	75.56	78.10	74.00	75.20	79.25	80.63	78.74	76.44	75.56
TiO_2	0.17	0.04	0.03	0.20	0.16	0.33	0.12	0.07	0.09	0.04
Al_2O_3	13.67	13.87	13.00	14.70	14.80	10.10	9.37	11.52	12.90	13.87
Fe_2O_3	0.56	0.09	0.07	0.33	0.26	0.60	0.47	0.20	0.18	0.09
FeO	2.01	0.34	0.26	1.19	0.95	2.16	1.69	0.71	0.64	0.34
MnO	0.13	0.03	0.03	0.04	0.04	0.11	0.04	0.04	0.04	0.03
MgO	0.62	0.26	0.23	0.64	0.51	0.68	0.57	0.29	0.38	0.26
CaO	1.85	0.67	1.08	1.20	0.67	0.80	0.82	0.51	0.59	0.67
Na_2O	2.84	3.14	3.21	3.82	3.55	1.56	1.62	2.32	2.57	3.14
K_2O	3.77	5.97	3.98	3.88	3.86	4.32	4.67	5.58	6.13	5.97
P_2O_5	0.04	0.03	0.02	0.10	0.00	0.08	0.01	0.02	0.03	0.03
TOTAL	100.00	100.00	100.00	100.00	100.00	99.99	100.00	100.00	99.99	100.00
Rb	100.50	139.90	49.60	122.00	78.60	120.60	119.60	178.10	186.50	139.90
Sr	275.70	155.60	315.00	229.00	271.10	202.30	166.80	120.50	185.50	155.60
Zr	94.40	46.90	3.40	144.00	102.10	715.50	161.20	56.50	49.10	46.90
Nb	17.70	3.40	1.90	8.10	11.00	10.10	7.00	6.90	7.20	3.40
Y	25.90	5.90	0.00	0.00	11.60	20.40	0.00	0.00	0.00	5.90
Th	24.00	0.00	1.10	3.90	25.40	131.50	0.00	0.00	0.00	0.00
U	9.30	0.00	7.60	0.00	6.40	1.40	0.00	0.00	0.00	0.00
C.I.P.W. NORMS (ANHYDROUS; IN Wt %)										
Q	37.17	32.48	41.30	32.90	37.00	49.72	49.59	41.93	35.82	32.48
Or	22.28	35.26	23.50	22.90	22.81	25.54	27.62	32.97	36.23	35.26
Ab	24.03	26.55	27.20	32.30	30.01	13.19	13.67	19.60	21.76	26.55
An	8.91	3.14	5.22	5.28	3.31	3.44	3.99	2.42	2.74	3.14
C	1.66	1.10	1.52	2.23	3.58	1.60	0.19	0.79	1.03	1.10
Hy	4.72	1.18	1.00	3.25	2.60	4.82	4.00	1.83	1.91	1.18
Mt	0.81	0.14	0.11	0.48	0.38	0.87	0.68	0.29	0.26	0.14
Il	0.33	0.08	0.06	0.38	0.31	0.63	0.23	0.13	0.17	0.08
Ap	0.10	0.07	0.05	0.24	0.00	0.19	0.02	0.05	0.07	0.07

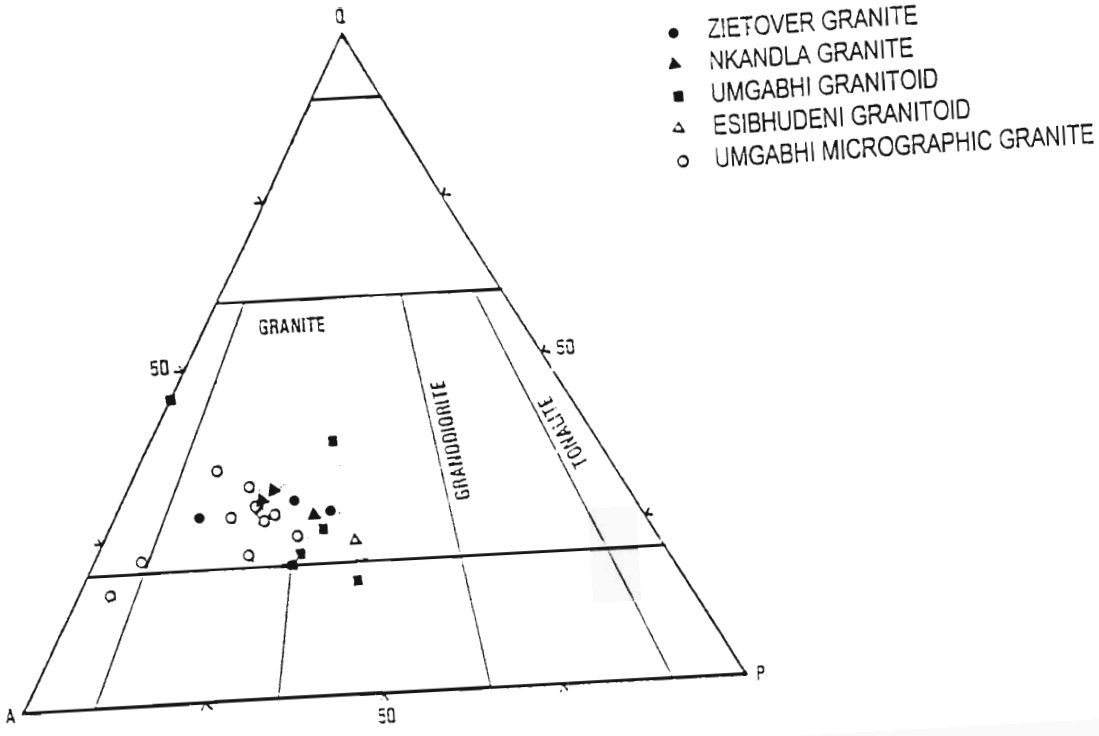

Fig. 13.1 : QAP ternary diagram showing the granitic composition of the **late post-Nondweni granitoids** (after Streckeisen, 1973).
Q = quartz; A = alkali feldspar; P = plagioclase

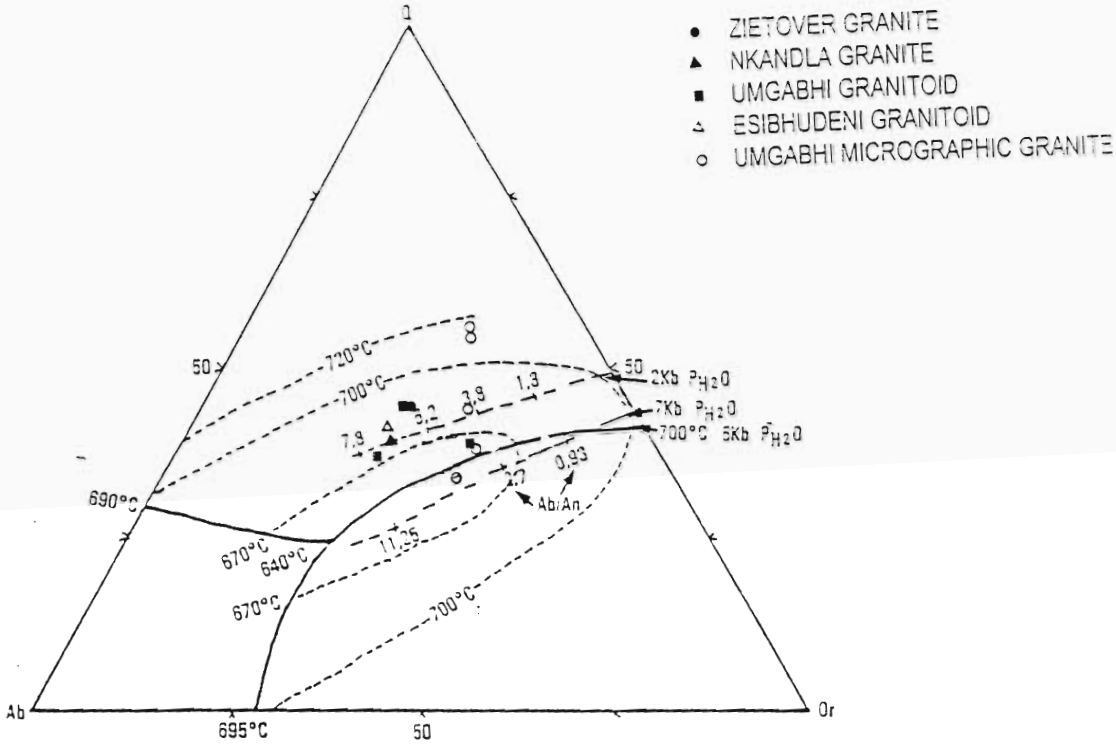

Fig. 13.2 : Q - Ab - Or ternary diagram showing the composition of the **late post-Nondweni granitoids** relative to cotectic boundaries at various temperatures, pressures and Ab/An contents (after Winkler, 1979).

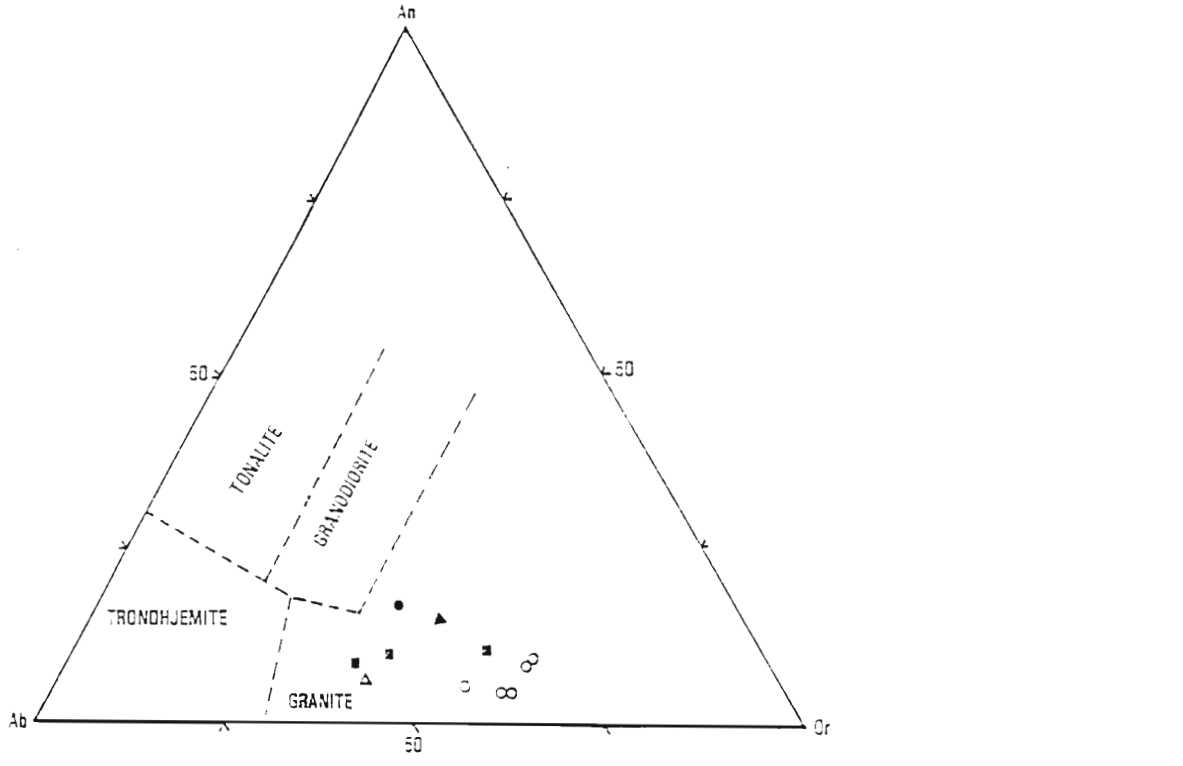

Fig. 13.3 : Normative An - Ab - Or ternary plot of the **late post-Nondweni granitoids.** Compositional fields after Barker (1979).

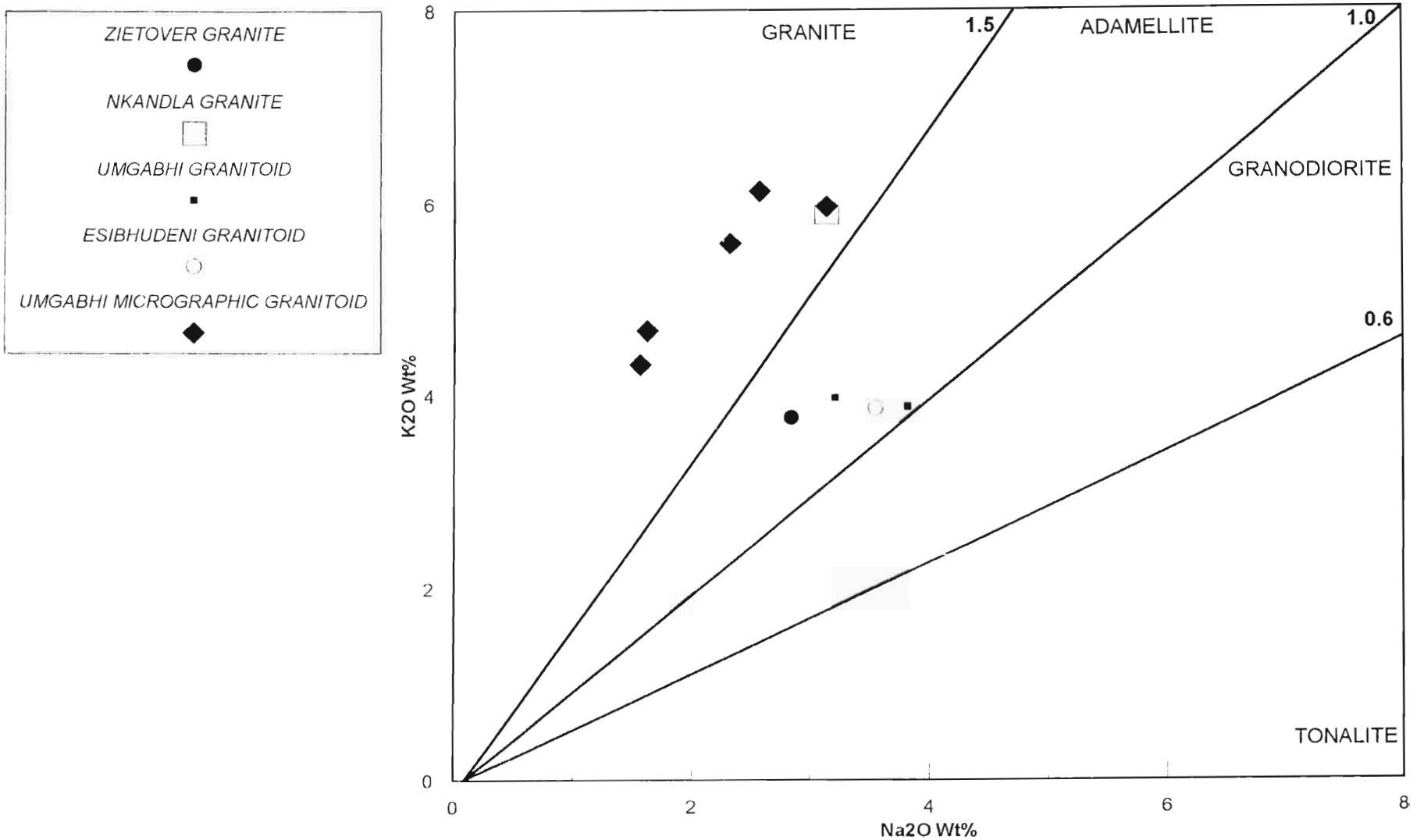

Fig. 13.4 : Binary Na_2O against K_2O plot showing the composition of the late post-Nondweni granitoids (after Harpum, 1963).

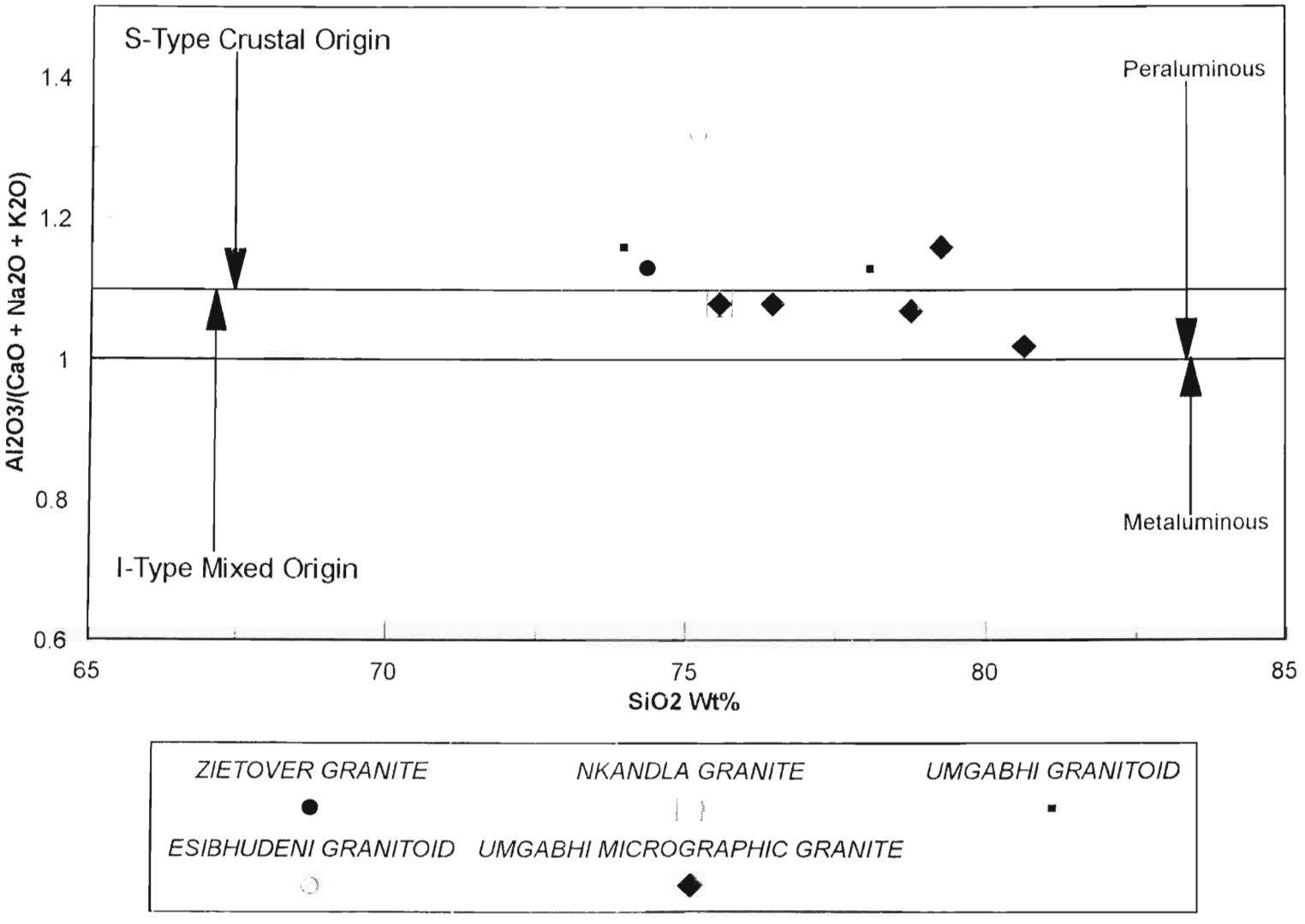

Fig. 13.5 : Binary silica against A/CNK plot (after Clarke, 1992) showing the composition of the late post-Nondweni granitoids and their probable origin (after Chappell and White, 1974; White and Chappell, 1983; Barbarin, 1990).

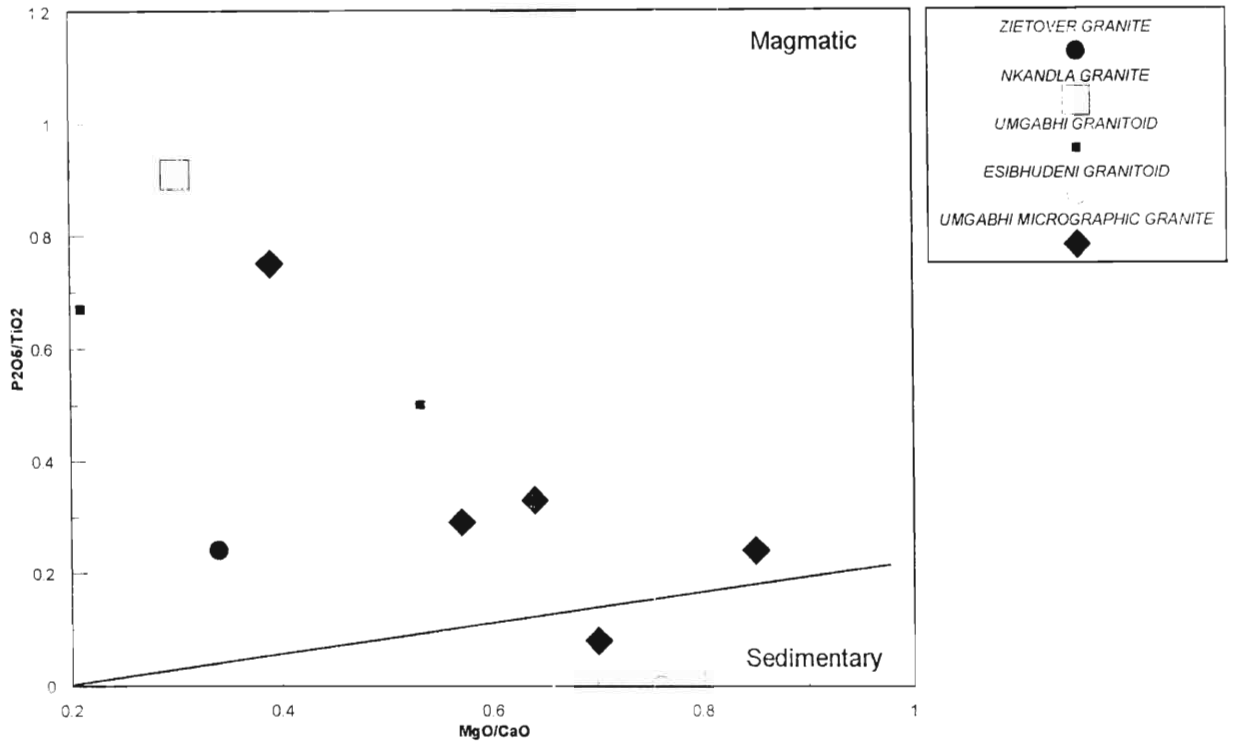

Fig.13.6 : Binary plot of P_2O_5 against MgO/CaO showing that the late post-Nondweni granitoids are of magmatic origin.

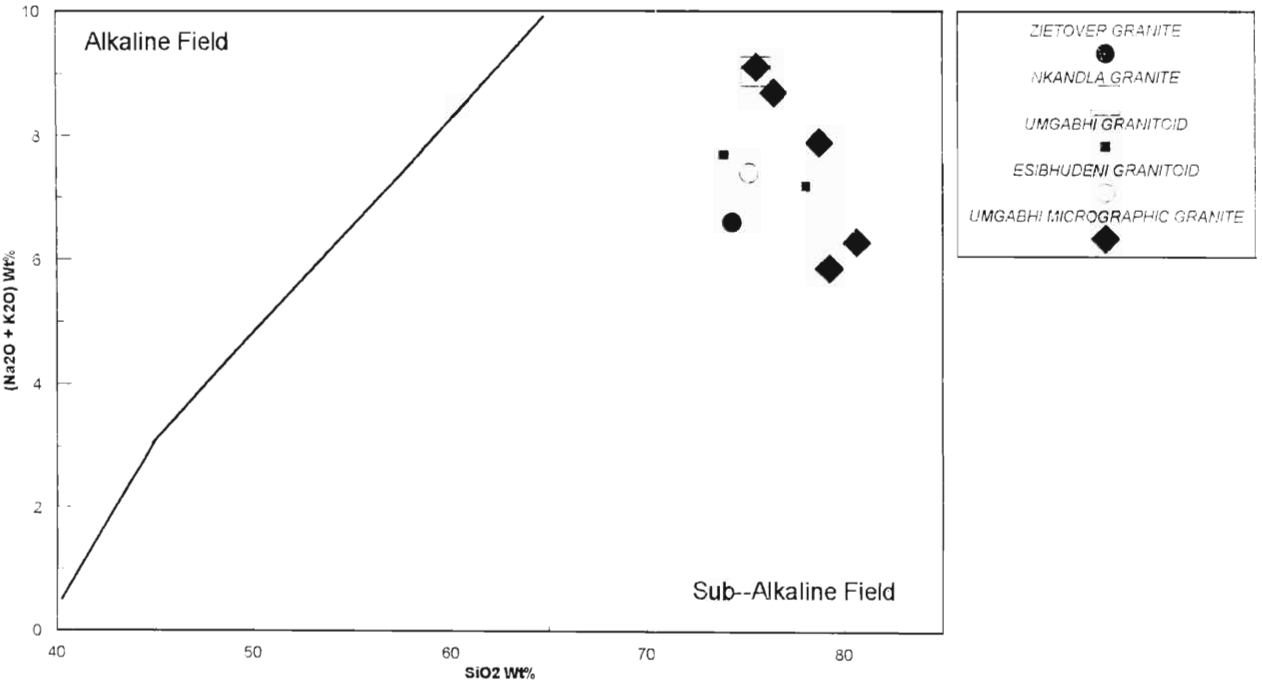

Fig. 13.7 : TAS diagram showing the sub-alkaline nature of the late post-Nondweni granitoids. The solid line dividing the alkaline and sub-alkaline fields is after Irvine and Baragar (1971).

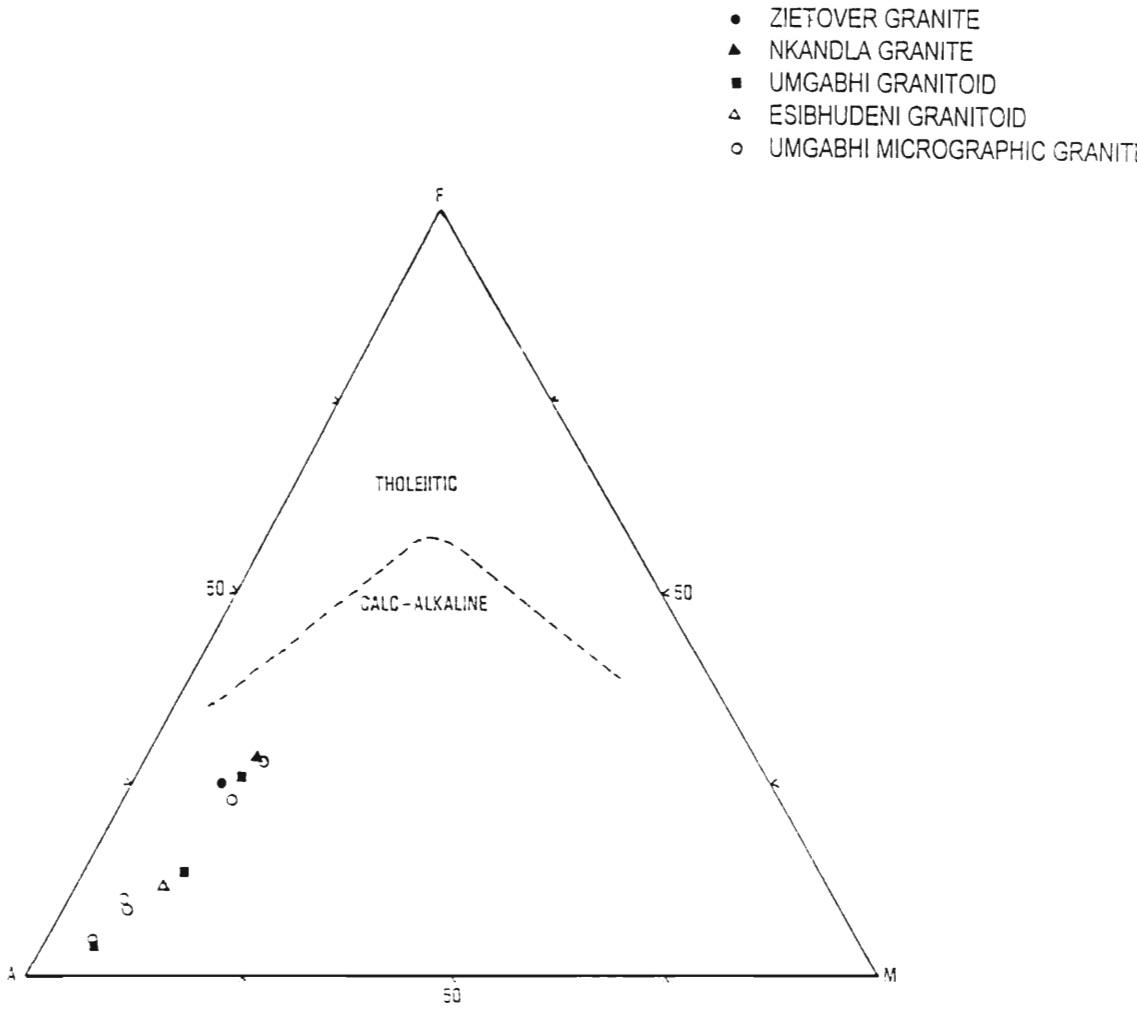

Fig. 13.8 : AFM ternary diagram showing the calc-alkaline nature of the **late post-Nondweni granitoids.** The dashed line separating tholeiitic and calc-alkaline fields is after Irvine and Baragar (1971).

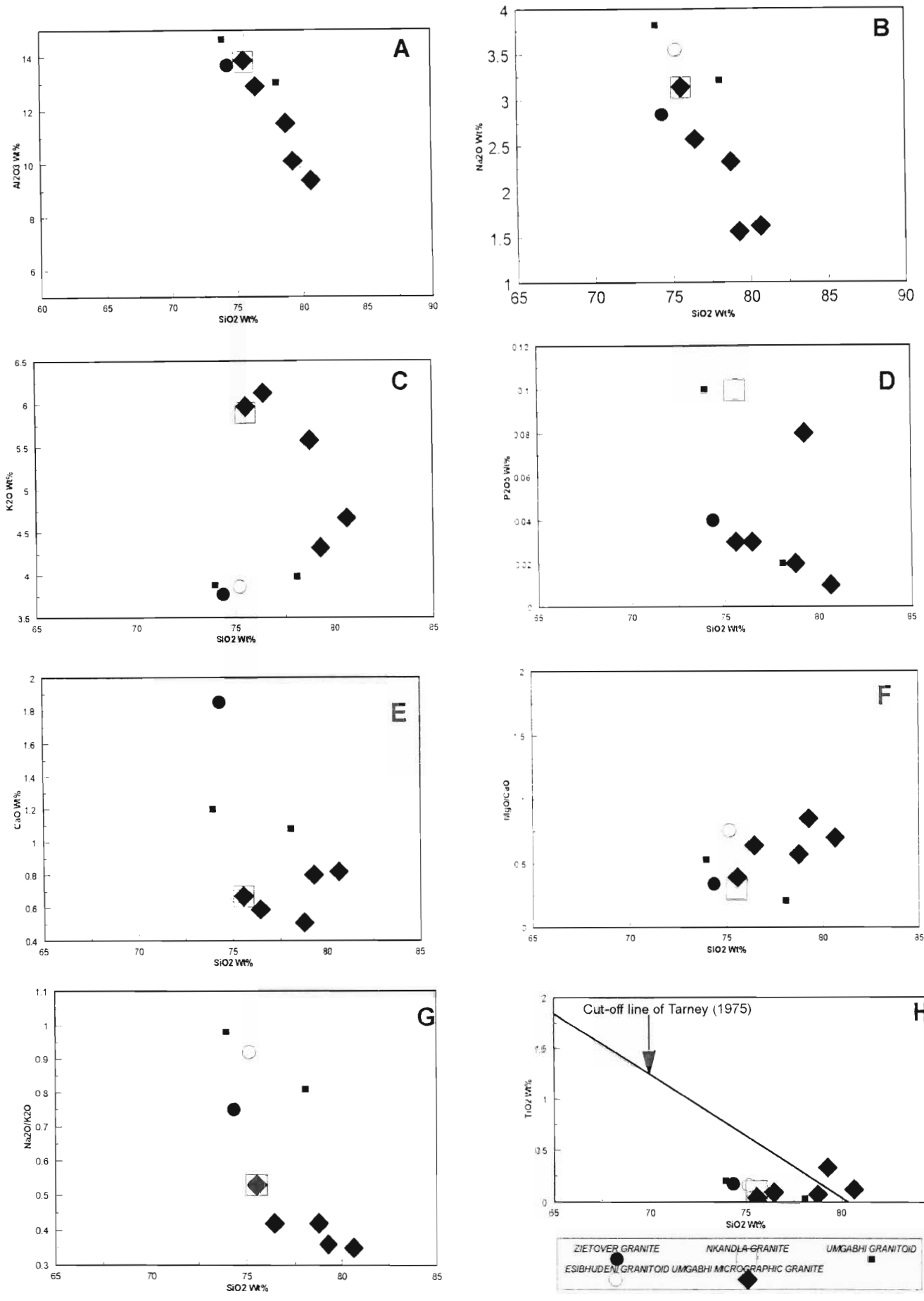

Fig. 13.9 A-H : Major element oxides against silica Harker diagrams of the late post-Nondweni granitoids.

The trace element chemistry of these granitoids shows 49,60 - 186,5 ppm Rb, 155,60 - 315,00 ppm Sr and Rb/Sr ratios ranging between 0,16 and 1,48. Zr values range from 3,40 ppm to 715,50 ppm whereas Nb, Y, Th and U show low values.

The ternary Q - Ab - Or diagram (Fig. 13.2) shows that these granites crystallized at temperatures of 650 - 680°C and pressures of 2 to 5kb (Winkler, 1979), similar to the Nsengeni Granitoid Gneisses (Fig. 12.11).

CHAPTER 14

COMPARISON OF THE ILANGWE GRANITOIDS WITH OTHER ARCHAEAN GRANITOIDS

14.1 INTRODUCTION

In this short chapter, the Ilangwe granitoids will be compared and contrasted with those of Swaziland, Eastern Transvaal (Mpumalanga) and Zimbabwe. This is significant in that detailed geochemical and geochronological studies have been undertaken on the granitoids of these Archaean terranes (Hunter, 1979; Matthews, 1985; Martin, 1987; Sleigh, 1988; Matthews, 1990; Hunter et. al., 1992) whereas only tentative geochronological studies have been attempted on the Nsengeni Granitoid Gneiss of the Ilangwe Northern Granitoid Complex (Reimold et. al., 1993). Zircon chronology for the Nsengeni gneiss indicates strong resetting to dates ranging from ±2,3 to 2,65 Ga which represent minimum ages for the formation of this granitoid gneiss (Reimold et. al., 1993). These authors suggest that this disturbance could have been caused by the Natal Thrust Front which is in direct contact with the Ilangwe Granite-Greenstone Belt. Detailed field relationships of Ilangwe rocks presented in this thesis, together with the limited geochemical data, strongly suggest a pre- 3,0 Ga age for the emplacement of the Ilangwe granitoids.

Briefly, the Ilangwe granitoids can be divided into three associations, viz. :

(i) An association of ***older gneisses*** comprising the Amazula Gneiss, Nkwalini Mylonitic Gneiss and Nkwalini Quartzo-feldspathic Flaser Gneiss. They have a composition ranging from tonalitic to granitic and are highly deformed — being mylonitic to migmatitic. Together with the Ilangwe greenstones, they form the early crustal framework onto which the later granitoids were emplaced.

(ii) The early post-Nondweni granitoid association comprising the Nkwalinye Tonalitic Gneiss and the Nsengeni Granitoid Suite. The latter consists of three foliated granitoids which are intrusive into the older gneisses, greenstones and Nkwalinye Tonalitic Gneiss. The early phase of the early post-Nondweni granitoids — the

Nkwalinye Tonalitic Gneiss — is mostly tonalitic to granodioritic in composition whereas the later phase of the early post-Nondweni granitoids — the Nsengeni Suite — is mostly potash-rich and granitic. The early phase is highly deformed and migmatitic whereas the later phase is well-foliated to augen gneissic.

(iii) The late post-Nondweni granitoid association comprising two similar suites, located on either side of the Ilangwe Greenstone Belt, which probably evolved from a single magmatic batholith. These two granitoid suites consist of five granitoid units which lack foliation or are weakly foliated especially at their boundaries. They are granitic in composition and are potash-rich. They are intrusive into the older gneisses, the Ilangwe greenstones and metasediments and the early post-Nondweni granitoids.

14.2 DISCUSSION

The granitoids of the Ilangwe Belt show a strong trend towards the K-apex of the K -Na - Ca ternary diagram (Fig. 14.1) and depict a trend which compares and coincides very well with the calc-alkaline field enclosing the granitic rocks of 3.1 Ga and younger in Swaziland and the Eastern Transvaal, the granodiorite suite, and the Mushandike granite of Zimbabwe (Hunter, 1979). This trend contrasts remarkably with the Na-trend of the trondhjemitic field enclosing the granitoids of the Ancient Gneiss Complex of Swaziland, the diapiric tonalite plutons of the Eastern Transvaal and the granitoid gneisses of Zimbabwe (Hunter, 1979). What is noticeable on Fig. 14.1 is that the Amazula Gneiss shows a trend towards the Ca-apex. Also noticeable is the fact that the granitoids of the Ilangwe Belt do not show a strong trend towards the Na-apex. This implies that, with the available limited geochemical data, there seems to be no granitoids of trondhjemitic composition. However, more detailed geochemical studies are required to prove or disprove this.

On the plot of Na_2O against K_2O (Fig. 14.2), the Amazula Gneiss does not compare with any of the granitoids of the Piet Retief and Barberton area of the Eastern Transvaal (Sleigh, 1988). The Nkwalinye Tonalitic Gneiss compares well with the Witrivier and Witkloof gneissic leucotonalites whereas the Nkwalini mylonites and the Nkwalini Quartzo-feldspathic Flaser Gneiss compare somewhat with the granitic dykes, Mpuluzi phase of the Lochiel Granite, the Tafelkoppies and Vrede granites (Sleigh, 1988; Hunter et. al., 1992).

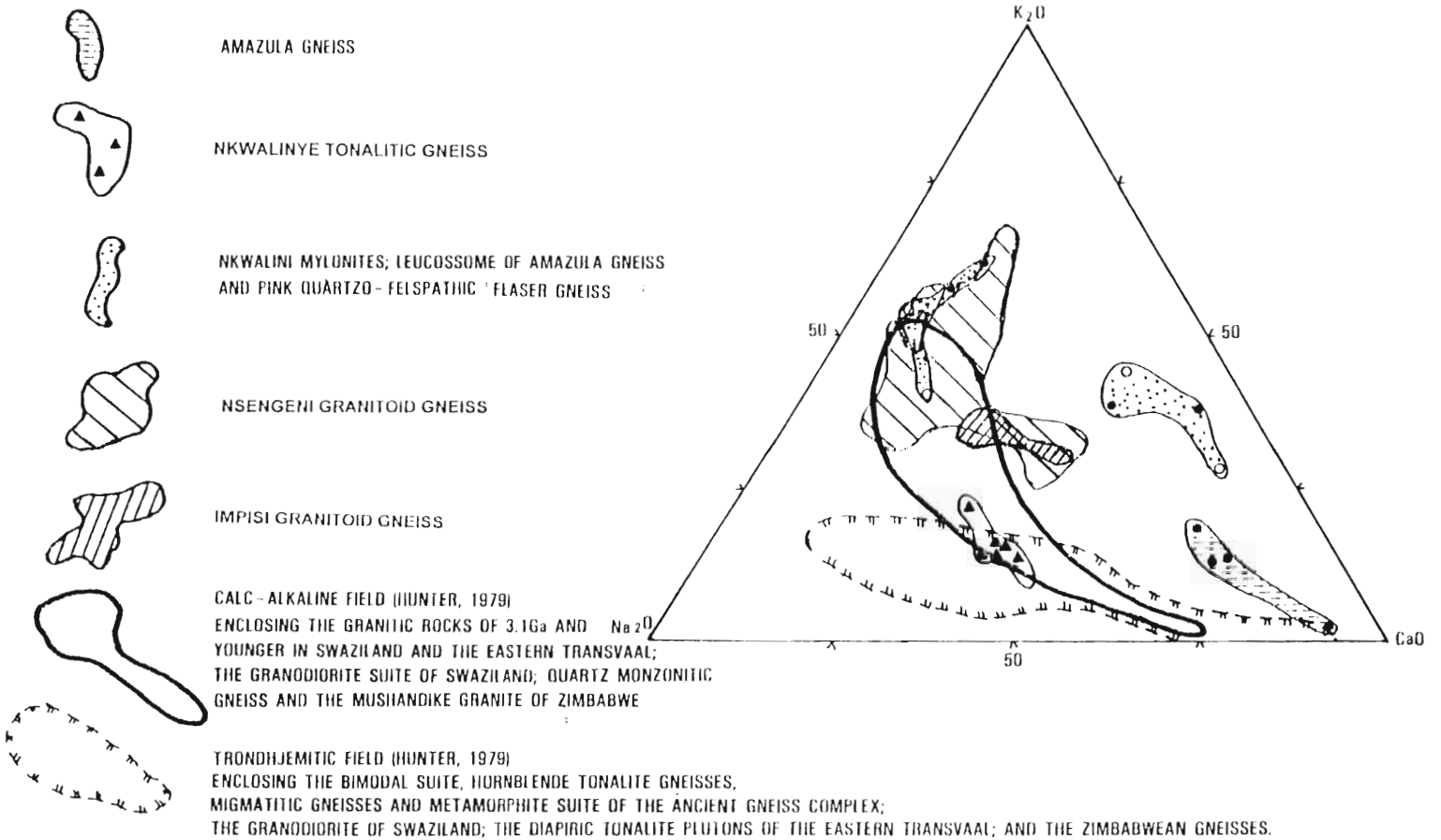

Fig. 14.1 : K - Na - C ternary plot comparing the Ilangwe granitoids with the Ancient Gneiss Complex of Swaziland and some of the granitoid gneisses of the Mpumalanga Province (Eastern Transvaal) and Zimbabwe (after Hunter, 1979).

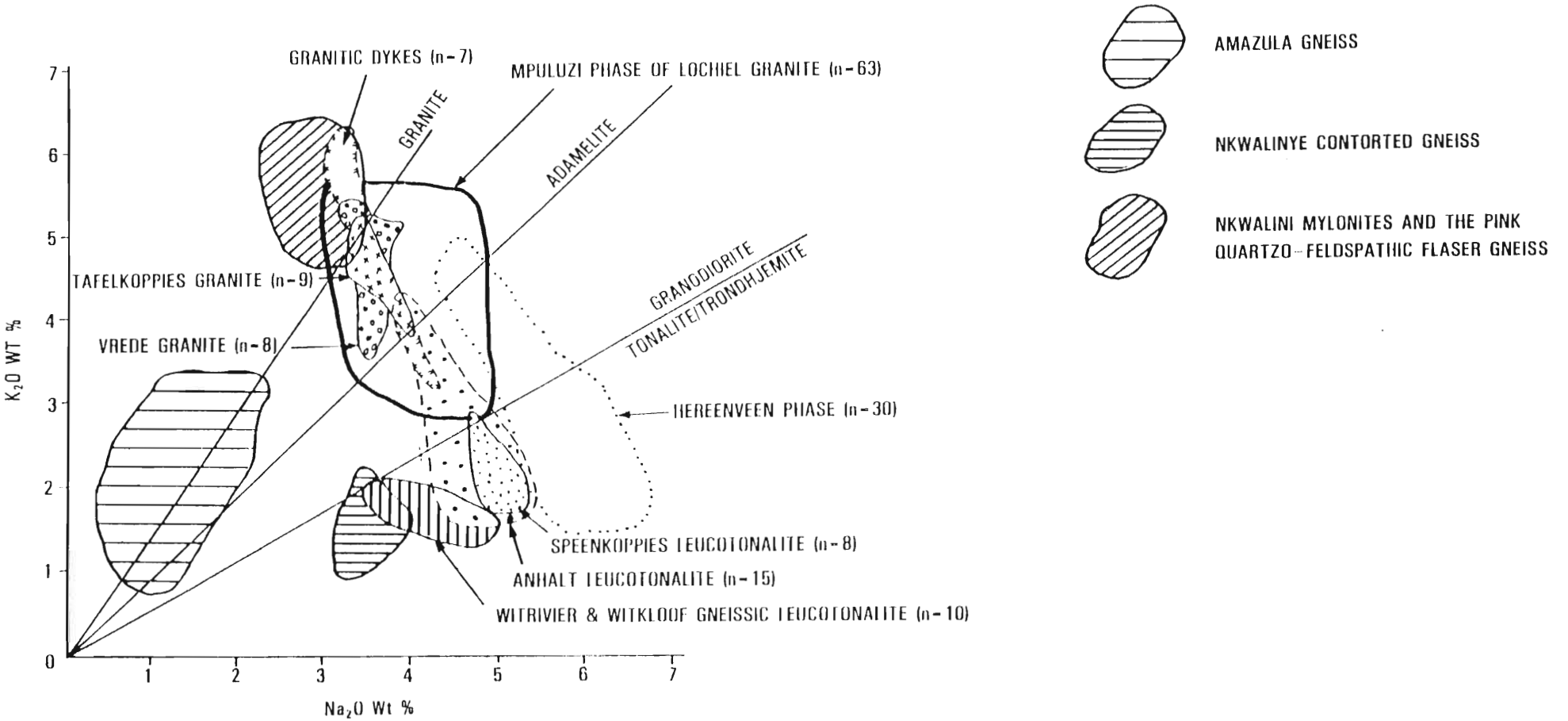

Fig. 14.2 : Comparison of the Ilangwe migmatitic and mylonitic gneisses with other granitoids of the Mpumalanga Province (Eastern Transvaal) (after Sleigh, 1988).

The Nsengeni granitoids compare very well with the Mpuluzi phase of the Lochiel Granite, the granitic dykes, the Tafelkoppies and the Vrede granites (Fig. 14.3; Sleigh, 1988; Hunter et. al., 1992) whereas the Impisi granitoids do not compare so well (Fig. 14.3).

The ternary AFM diagram (Fig. 14.4) compares the Ilangwe granitoids with the granitoids of the Superior Province, Manitoba (Ermanovics, et. al., 1979).

Similar to most Archaean granitoids, the trace element concentrations of the Ilangwe granitoids show no regular trends. They show random or near constant values versus SiO_2. Rb has average concentration of 120ppm whilst those for Zr and Sr are 200 and 350ppm respectively. Th and U have very low concentrations whereas Nb and Y have overall concentrations of <20ppm, which is characteristic of Archaean granitoids (Martin, 1987; Hunter et. al., 1992).

Generally, the Ilangwe granitoids are similar to most Archaean granitoid terranes. To further constrain the similarities of the other Archaean granitoids with the Ilangwe granitoids, detailed age determination studies (which are beyond the scope of this thesis) would be essential.

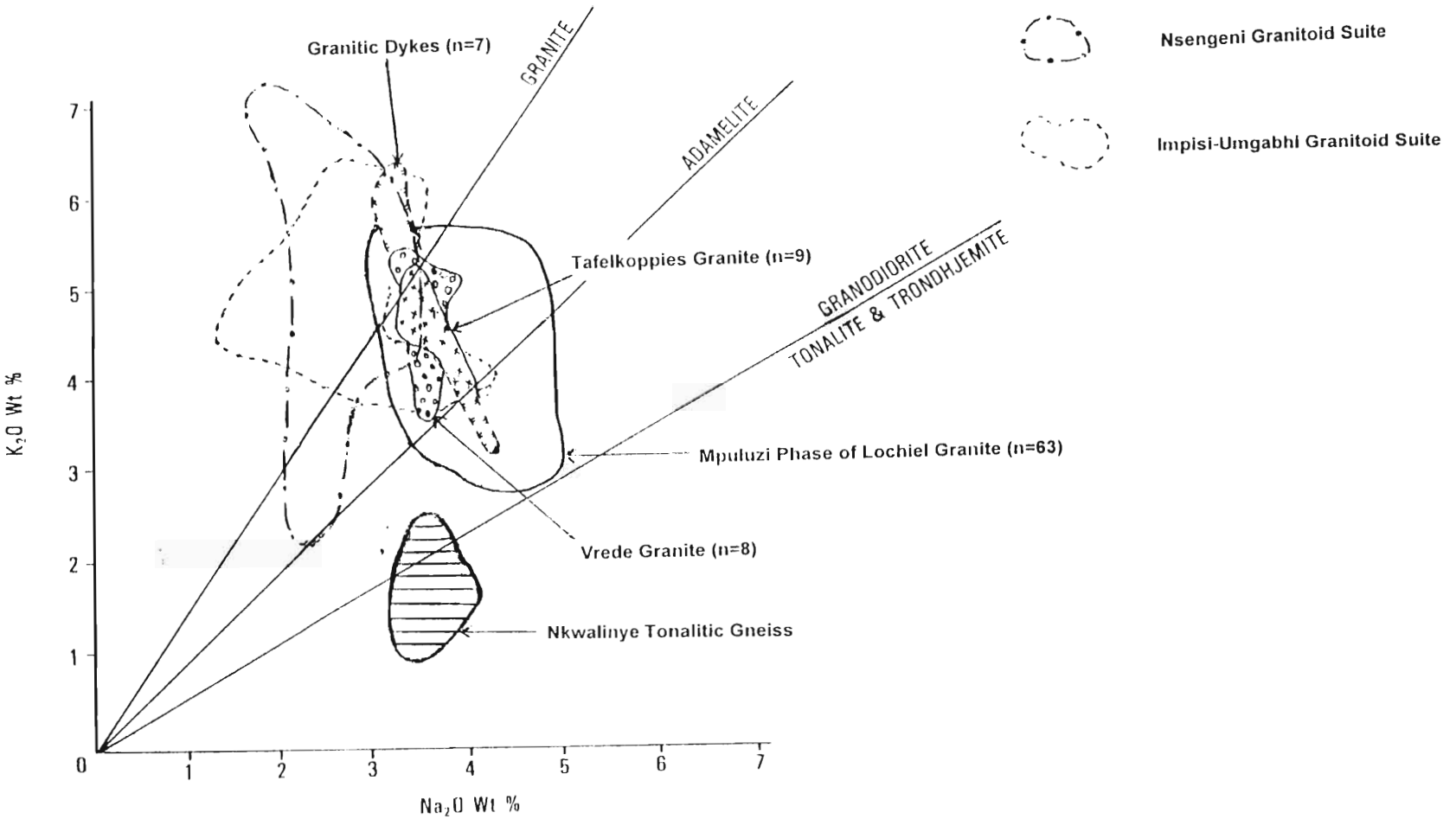

Fig. 14.3 : Comparison of the Ilangwe post-Nondweni granitoids with other granitoids of the Mpumalanga Province (Eastern Transvaal) (after Sleigh, 1988).

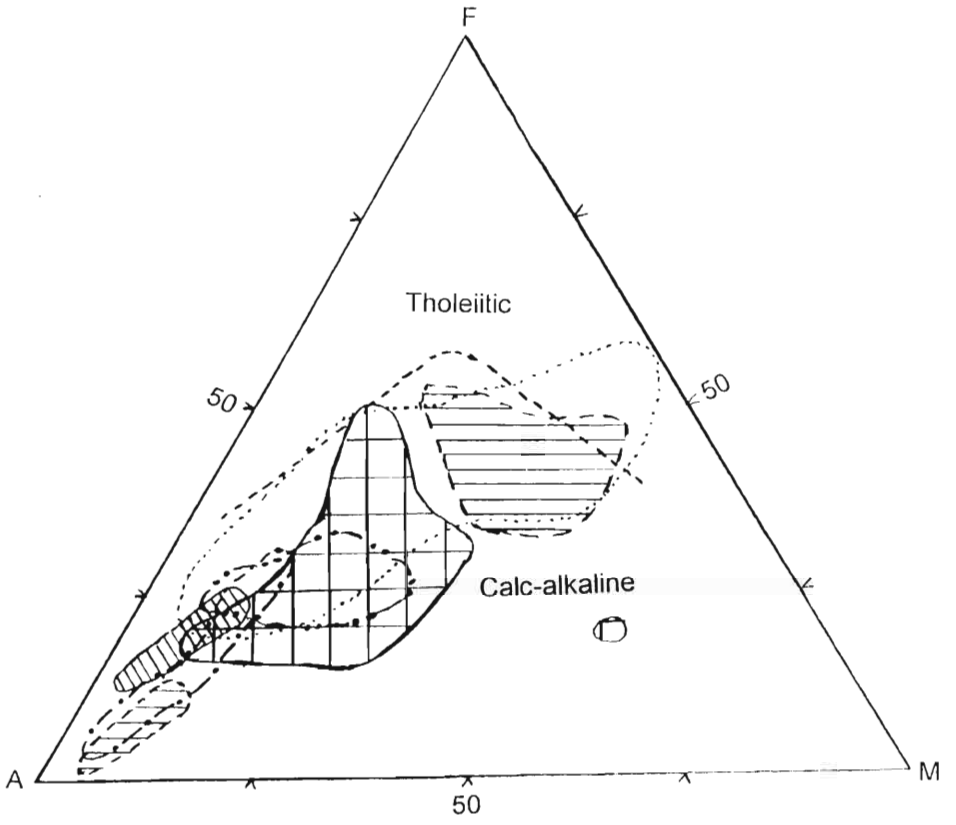


Migmatitic and mylonitic gneisses.

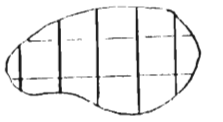
Early post-Nondweni granitoids.


Late-post-Nondweni granitoids.

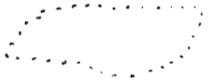
Tonalite and trondhjemite
(Black Island area, Uchi belt).

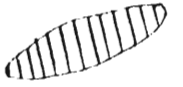
Granite (Lac du Bonnet, English River subprovince).


Tonalite (Ross River Pluton, Uchi subprovince).

Fig. 14.4 : The ternary AFM diagram comparing the Ilangwe granitoids with the granitoids of the Superior Province in Manitoba (Ermanovics et. al., 1979). The dashed line separating tholeiitic and calc-alkaline fields is after Irvine and Baragar (1971).

CHAPTER 15

ILANGWE METABASIC INTRUSIVES

15.1 INTRODUCTION

The Ilangwe belt metabasic/basic intrusions are of three types :

(i) medium- to coarse-grained dark green metagabbroic rocks;

(ii) medium- to coarse-grained dark-greenish-black norite;

(iii) fine- to medium-grained porphyritic amphibolitic dyke with cubic light-green microcline porphyrocrysts.

The first two types occur mainly as sills and sheets intrusive into the granite-greenstone belt. They range in size from a few centimetres to hundreds of metres. The thinner sheets are usually fine-grained and show a very faint foliation mimicking that of the country rock they intrude, for example the metagabbros intruding the Nkwalini mylonites (Fig. 5.3). This faint foliation is shown at the scale of a thin section as a nematoblastic texture (Plate 15.1A). Subordinate dyke-like metagabbros do occur. The last type (i.e. [iii] above) occurs in the form of dykes cutting across the Amazula Gneiss and the Nkwalinye Tonalitic Gneiss, especially in the Nkwalinye River. The porphyritic dykes have not been observed to cut across the greenstones and related metasediments. These dykes are usually very thin - not more than 5m wide.

15.2 PETROGRAPHY

A gabbro (sensu stricto) is a medium- to coarse-grained rock consisting of basic plagioclase and augitic clinopyroxene (Moorhouse, 1959; Shelley, 1993). The gabbros of the Ilangwe belt have a varied composition, consisting mainly of hornblende, actinolite, pyroxene (hypersthene and augite) and minor olivine and biotite.

Table 15.1 gives the modal composition and a summary of the features of the various Ilangwe metabasic rocks. The plagioclase composition varies from andesine to labradorite. Bytownite is uncommon. Blue-green to brown hornblende (up to 70% by volume) is the most common amphibole, occurring as subidioblastic to xenoblastic crystals some of which enclose small subidioblastic plagioclase in a subophitic texture. Usually hornblende is associated with long fibrous to lath-like crystals of actinolite. In some thin sections the actinolite seems to be growing at the expense of hornblende but in others the association is not clear-cut. In the fine-grained variety of sills, the amphiboles are aligned along a preferred orientation defining the foliation and thus giving a nematoblastic texture (Plate 15.1A). Hornblende also occurs in the matrix as interlocking aggregates. It alters to biotite, epidote and chlorite.

Pyroxenes (up to 70% by volume) occur as xenoblastic crystals enclosed in plagioclase in an ophitic texture (Plate 15.1A). Larger xenoblastic crystals usually show exsolution lamellae of orthopyroxene. Some of the lamellae are slightly bent due to deformation. In H40EB the pyroxenes show a zonal structure with the zones being more marked at the grain boundaries (Plate 15.1C). Here, the pyroxenes are replaced by hornblende (up to 5% by volume) and chlorite as a result of uralitization (Shelley, 1993; Barker, 1990). Hypersthene has also been observed with exsolution lamellae of augite. However, no schiller structures were observed.

Plagioclase (up to 45% by volume) occurs as subidioblastic to xenoblastic crystals or as long laths (± 10mm). The composition ranges from oligoclase to labradorite and twinning is quite common. The plagioclase partially or completely enclose the pyroxenes and/or the hornblende. In some thin sections the hornblende porphyroblasts enclose plagioclase. That is, both ophitic and subophitic textures do occur.

Olivine (up to 3% by volume) occurs as fractured idioblastic to subidioblastic grains with the fractures sometimes lined by magnetite or ilmenite. Brown biotite usually replaces hornblende and occurs as laths or fibres. Epidote (up to 2% by volume) occurs as zoned bright coloured crystals. Quartz (up to 5% by volume) occurs as equigranular to inequigranular crystals which seem to occur in the matrix and also poikilitically enclosed in plagioclase. Other minor constituents of metagabbros are cordierite, calcite and sericite.

PLATE 15.1 : PHOTOMICROGRAPHS OF REPLACEMENT TEXTURES IN META-GABBROS.

PLATE 15.1A : Photomicrograph showing the development of a weak nematoblastic texture in the amphibolites (hornblende) of the metagabbros. (Meta-gabbro of Matshansundu near Ndloziyana Peak: (6.420/GG.640)]

PLATE 15.1B : Ophitic and subophitic textures in the metagabbros. Note the development of grain boundary symplectites and magnetite-filled fractures in olivine. [Metagabbro from southeast of Ilangwe Peak: (5.950/Z.195)]

PLATE 15.1C : Zonal structure of pyroxenes occurring in plagioclase in a subophitic texture. Grain boundary symplectites occur on the lower left corner of the photomicrograph. {Metagabbro from southeast of Ilangwe Peak: (5.950/Z.195)]

PLATE 15.1D : Photomicrograph showing subophitic texture in the metanorite of Ilangwe, west of Ilangwe Peak (5.570/Y.120). A euhedral hornblende crystal shows polysynthetic twinning. There is development of magnetite/ilmenite ore along the grain boundaries. Plagioclase crystals are large (±2mm) and are mainly bytownite.

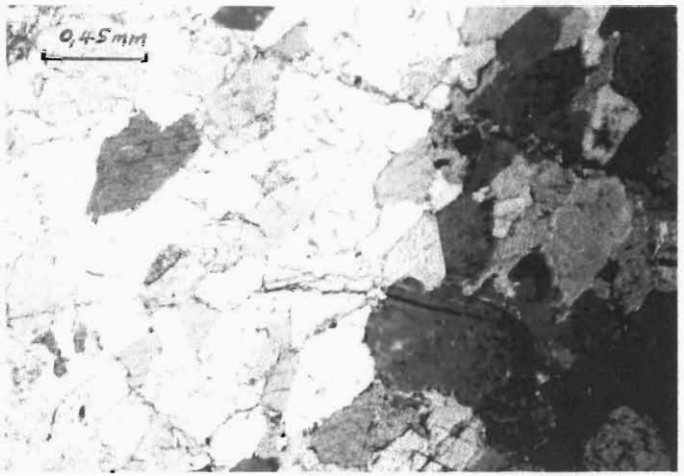

A

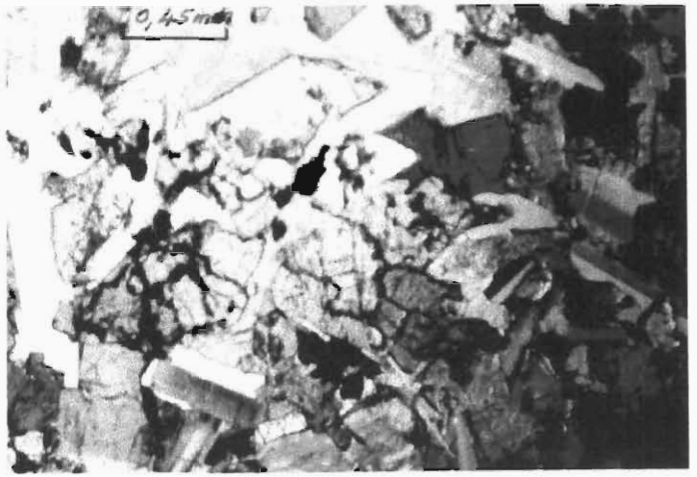

B

C

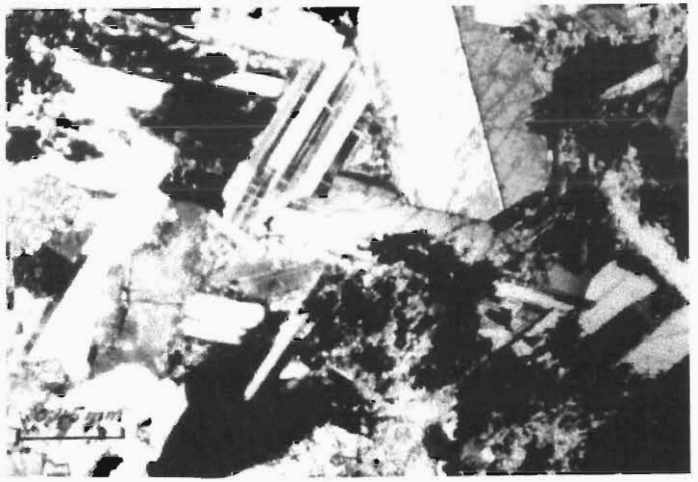

D

Plate 15.1

Norites occur as large sills for example the Ilangwe norite body (Fig. 2). They usually consists of hypersthene (up to 40% by volume) poikiloblastically enclosed in laths of plagioclase to give an ophitic texture and have bright reaction rims (zonation?). Some hypersthene enclose plagioclase and minor olivine in a subophitic texture (Plate 15.1D). Exsolution lamellae of augitic clinopyroxene sometimes do occur.

Plagioclase (up to 45%) is the next abundant mineral in the norites. The composition is usually An_{53-68} (labradorite). It usually encloses or is enclosed in pyroxenes. Twinning follows the albite, pericline and carlsbad laws.

Subidioblastic olivine (up to 10% by volume) occurs fractured and rimmed by magnetite. It is altered to serpentine and talc. Other accessory minerals are biotite, sericite and minor carbonate. In hand specimen these rocks seem unaltered and unmetamorphosed. It is only in thin sections that alteration and metamorphic replacement reactions are revealed.

The porphyritic dyke is very fine-grained in texture and it consists of cube-like porphyroclasts of feldspar embedded in a fine-grained matrix. The porphyroclasts vary in size and are usually absent or very small near the chilled contact with the country rock (see Plate 5.1A). In outcrop, the phenocrysts are aligned subparallel with the weak foliation developed near the contact with the country rock.

In thin section, the porphyritic dyke consists of fine-grained idioblastic to subidioblastic amphiboles (hornblende or actinolite - up to 45% by volume) enclosed poikiloblastically in plagioclase (up to 40% by volume) in an ophitic texture. Some of the plagioclase laths are intergrown and can be up to 10mm in length. The matrix consists of amphiboles, plagioclase, saussarite and minor quartz. Big (± 8mm)porphyroclasts of microcline have been completely altered to sericite and they are characterized by faint gridiron twinning visible through the sericite.

Accessory minerals include small interlocking idioblastic quartz grains, skeletal relics and subidioblastic ore and traces of carbonate.

TABLE 15.1 : METAGABBROIC ROCKS : MODAL ANALYSES AND MAIN PETROLOGICAL FEATURES

SAMPLE NO.	MINERAL MODAL COMPOSITION (%)																	GRAIN SIZE			PLAG An CONTENT %	TEXTURE Granoblastic(*); Subophitic(Sub); Ophitic(Oph); Inequigranular(In); Equigranular(Eq); Myrmekitic(Myr); Uralitization(Ur); Xenoblastic(Xen); Nematoblastic(Nem).
	Qtz	Plg	K-Fel	Hbl	Act	Pyrox	Oliv	Biot	Cord	Carb	Epid	Talc	Serp	Chlo	Ser	Mus	Ore	F	M	C		
H13EB	10	35			40				5		2			8			t	Vx			nd	Eq.; nem.
H22EB	5	30		55	t			t		t	2			5	2		t	x			An_{26-35}	Eq., *.
H29EB	3	20		65					t		2			7	3		t		x		An_{40}	Eq.
H40EB		20		5		65	3		1		1				5		t		x		An_{29}	Eq.; *; oph.
H59EB	t	25		6		60	4			t	1				4		t	Vx			nd	Ur.; oph.
H63EB	5	30		45		15					1			1	2		1	x	x		An_{37}	Ur.; sub.; oph.; idiobl.
H68EB	5	32		60					2		t						1	Vx			nd	Xen.; in.
H88EB	2	25		3		65		1						2	2					x	An_{45}	Xen.; oph.; myr.
H97EB	2	40	2	45											10		1	x	x			Sub.; oph.
H154EB		42		1		35	10	t				3	4		3		2		x		An_{55}	Sub.

15.3 METAMORPHISM

From the foregoing petrographic description and the summary of the features of these rocks, it is evident that they are altered to varying degrees. In thin sections, complete alteration or replacement was only observed in the thin metagabbroic sills, that, for example, intrude the Nkwalini mylonites (Fig. 5.3), that is, sills occurring in or associated with shear zones. Partial or incomplete replacement is quite common in the widespread metagabbroic/noritic sills of the Ilangwe belt. The following mineral assemblages characterise the metabasic intrusions in general :

Actinolite + plagioclase + quartz ± cordierite ± biotite + chlorite + epidote.....(1)

Hornblende (sometimes together with actinolite/tremolite) + plagioclase + quartz ± biotite ± chlorite ± epidote + sericite + ore.....(2)

Pyroxene ± olivine + tremolitic hornblende ± biotite + plagioclase ± cordierite + epidote + chlorite + sericite + ore.....(3)

Hypersthene + olivine + hornblende ± biotite + serpentine + talc + sericite.....(4)

Hornblende + plagioclase + K-feldspar + quartz + sericite ± ore.....5)

Assemblage (1) is characteristic of thin sills occurring in shear zones and usually displaying faint foliation, depicted by nematoblastic hornblende, mimicking that of the country rock they intrude. This foliation is also parallel to the C-planes of the shear zones i.e. Type II S - C mylonites (Lister and Snoke, 1984). In these sills, alteration is complete and extensive retrogression has occurred due to shearing. The retrogression is from medium grade metamorphic conditions to greenschist facies metamorphism characterized by chlorite and epidote (Winkler, 1979; Barker, 1990; Shelley, 1993).

Assemblages (2) and (3) are typical of the huge metagabbroic sills. These assemblages are characterized by partial or incomplete replacement reactions. Grain boundary symplectites (Plates 15.1B and C) are quite common. This partial alteration is characterized by uralitization of pyroxenes, the occurrence of magnetite along the rims and

fractures of olivine, replacement of hornblende by biotite, chloritization of biotite and sericitization or saussaritization of plagioclase. From the thin sections, it was not easy to distinguish whether these replacement reactions are due to incipient retrograde metamorphic effects or whether they are due to deuteric alteration effects. A detailed study of these relationships in these rocks (which is beyond the scope of this thesis) could be of particular interest in that it can further elucidate the timing of the intrusion of these rocks, i.e. whether they are pre- or post-peak metamorphic conditions.

Assemblage (4) is typical of the noritic bodies. It is basically similar to assemblage (3) except that the main pyroxene is hypersthene. Further, olivine is altered along the grain boundaries, to serpentine and talc. Uralitization of hypersthene is common and hornblende alters to biotite. Chloritization of biotite is not common. It is also not clear whether the replacement reactions in the norites are due to incipient retrograde metamorphism or deuteric alteration effects. In this regard, it is interesting to note that Harley et. al., (1990) describe on the one hand partial replacement reactions (symplectites) of cordierite mantling orthopyroxene and garnet and cordierite+ sapphirine symplectite replacing sillimanite ***and***, on the other, cordierite + orthopyroxene symplectite between biotite and plagioclase + quartz from the granulites of Forefinger Point, Enderby Land, Antarctic and ascribe these relationships to retrogressive metamorphism. These authors further constructed a PTt curve of retrogressive metamorphism based on textural evidence and geothermobarometry. However, in the case of the Ilangwe metabasic rocks, further research is warranted before these replacement reactions can be ascribed to incipient retrograde metamorphic effects.

Assemblage (5) is characteristic of the porphyritic dykes which cut the older migmatitic granitoids. The most common alteration product in these dykes is sericite. It is worth noting that the minor quartz occurring in these rocks is mostly granoblastic and shows intense undulose extinction. There seems to be evidence of recrystallization and metamorphism in these dykes. The assemblage is typical of medium to low grade metamorphism (Winkler, 1979).

15.4 GEOCHEMICAL CLASSIFICATION

Table 15.2 shows the chemical analyses of six samples of the metabasic rocks including one sample of the porphyritic dyke.

Insufficient analyses are presently available to distinguish the quantitative geochemical variations that may exist in these rocks. However, all of the samples fall in the sub-alkaline field in the binary total alkali against SiO_2 diagram (Irvine and Baragar, 1971; Fig. 15.1). The ternary AFM diagram (Fig. 15.2) shows that the majority of the samples fall in the tholeiitic field. On the ternary TiO_2 - K_2O - P_2O_5 diagram (Fig. 15.3) of Pearce et. al., (1975) half of the samples fall in the oceanic field and half fall in the non-oceanic field. Samples falling on the non-oceanic field are sheared and enriched in K_2O. In fact one sample is a porphyritic dyke containing microcline phenocrysts.

The limited geochemical data suggests that the basic rocks are theoleiitic and of oceanic affinity

TABLE 15.2
METAGABBROIC ROCKS :
MAJOR AND TRACE ELEMENT ANALYSES

SAMPLE	H29EB	H63EB	H68EB	H112EB	H119EB	H125EB
SiO_2	51.15	51.70	51.83	51.69	51.58	50.88
TiO_2	1.35	2.19	0.73	1.01	1.06	1.52
Al_2O_3	13.31	12.16	19.33	15.03	14.95	12.75
Fe_2O_3	3.16	3.61	1.94	2.67	2.57	3.38
FeO	11.36	13.01	6.98	9.62	9.25	12.18
MnO	0.22	0.22	0.19	0.21	0.20	0.24
MgO	6.62	4.93	4.56	6.65	7.27	6.62
CaO	10.12	8.84	9.92	9.95	9.72	9.95
Na_2O	1.77	2.18	2.03	2.07	2.09	1.50
K_2O	0.60	0.69	2.23	0.83	1.04	0.63
P_2O_5	0.33	0.47	0.27	0.29	0.28	0.35
TOTAL	99.99	100.00	100.01	100.02	100.01	100.00
Rb	22.00	20.00	110.80	36.30	43.00	22.30
Sr	127.00	117.80	216.00	132.00	185.00	94.10
Zr	95.50	184.10	77.80	78.40	73.30	106.10
Nb	4.70	7.80	5.20	4.10	3.60	5.60
Y	32.30	53.40	16.40	22.20	22.10	39.50
Th	4.80	6.60	0.00	2.20	3.10	6.70
U	6.50	8.50	0.00	5.30	5.20	9.30
Ni	94.80	51.40	67.30	89.60	128.50	104.60

C.I.P.W. NORMS (ANHYDROUS; IN Wt %)

Q	5.07	7.54	1.73	3.54	2.31	6.08
Or	3.55	4.08	13.16	4.92	6.15	3.71
Ab	14.97	18.47	17.18	17.48	17.70	12.70
An	26.62	21.33	37.07	29.29	28.33	26.21
Di	17.76	16.29	8.59	14.96	14.79	17.28
Hy	24.13	21.78	17.45	23.35	24.33	25.41
Mt	4.58	5.24	2.81	3.87	3.73	4.91
Il	2.57	4.17	1.39	1.91	2.02	2.89
Ap	0.77	1.11	0.63	0.68	0.66	0.83

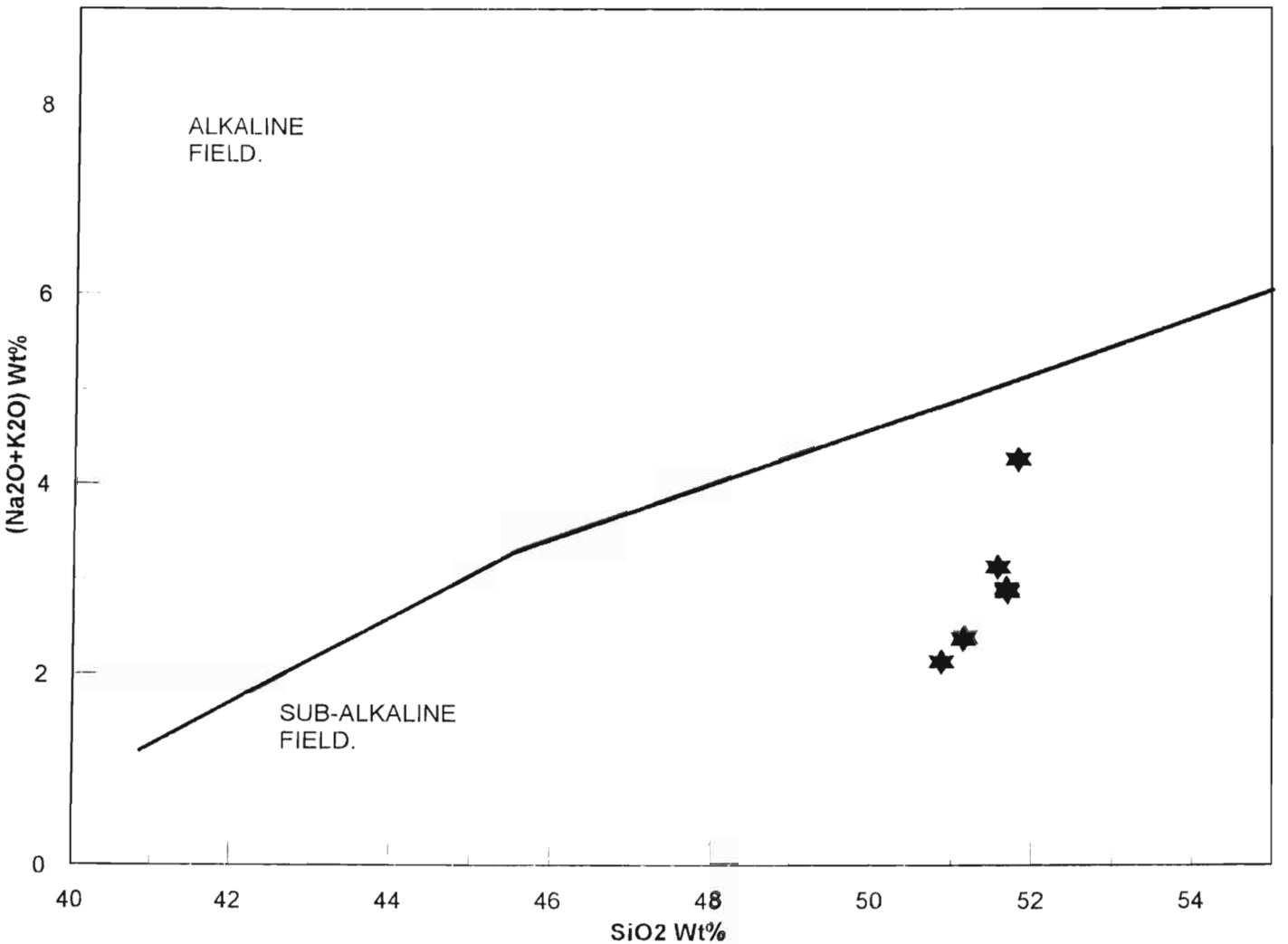

Fig. 15.1 : TAS diagram depicting the metagabbroic rocks of the Ilangwe Belt plotting on the sub-alkaline field of Irvine and Baragar (1971).

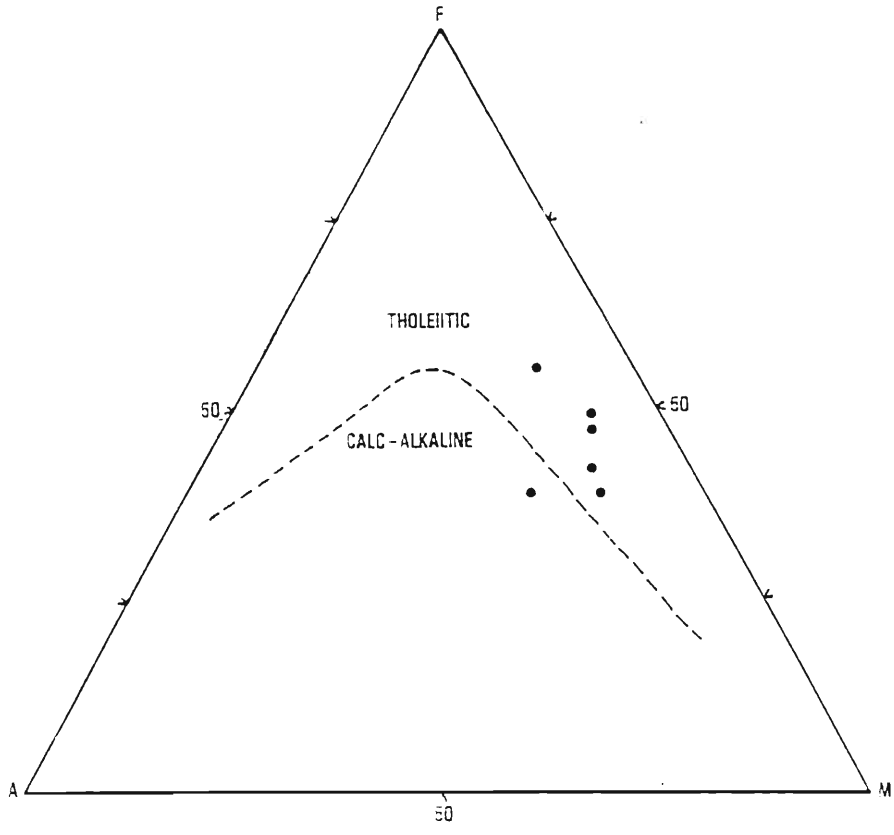

Fig. 15.2 : AFM ternary diagram of the metagabbroic rocks of the Ilangwe Belt showing a tholeiitic affinity. The dashed line dividing the tholeiitic and calc-alkaline fields is after Irvine and Baragar (1971).

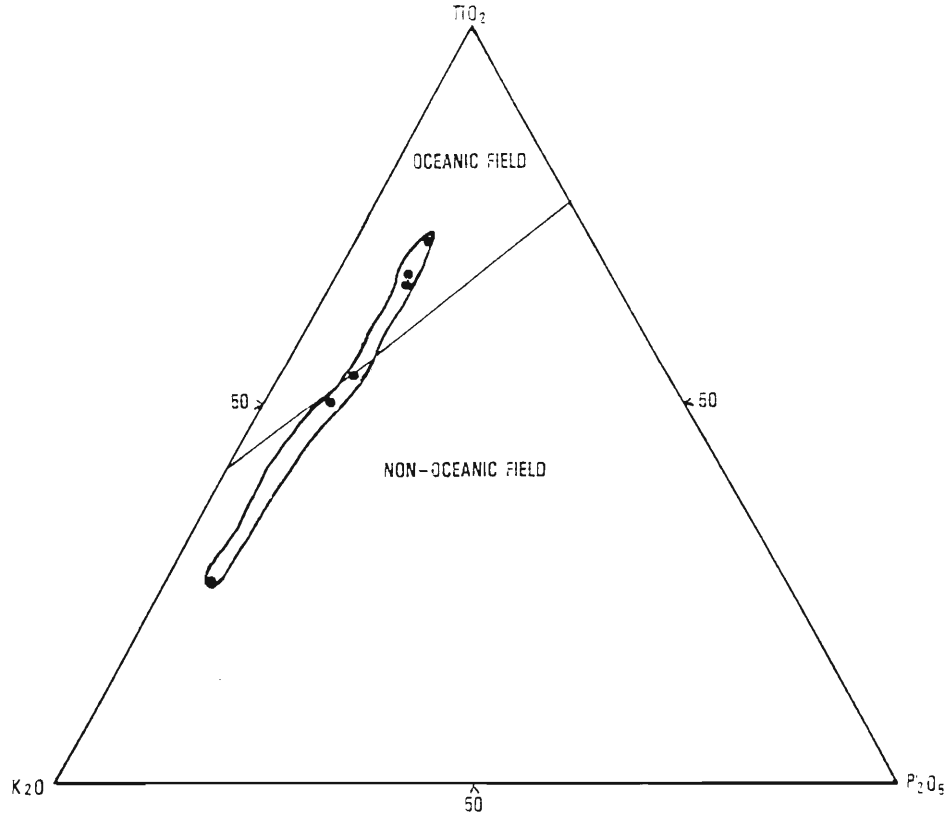

Fig. 15.3 : TiO_2 - K_2O - P_2O_5 ternary plot showing most of the metagabbroic rocks falling on the oceanic field (after Pearce et. al., 1975).

CHAPTER 16

DISCUSSION AND CONCLUSIONS

16.1 INTRODUCTION

In this chapter, all the available data on the Ilangwe Granite-Greenstone Complex will be synthesized. To achieve this, a brief overview of the setting of the Ilangwe Complex will be given. This will be followed by a discussion of the possible foundation to the Ilangwe supracrustals and the related migmatitic and mylonitic gneisses. A brief overview of the tectonostratigraphy and the tectono-structural synthesis of the supracrustals will be discussed. Finally, the tectonomagmatic episodes of the post-Nondweni granitoids will be reviewed. In conclusion, a brief summary of the possible sequence of geological events in the study area will be given. This will obviously be constrained by lack of geochronological data. However, herein lies future research opportunities.

16.2 TECTONIC SETTING

The Ilangwe granite-greenstone complex in the study area is ±35km long and ±11.5km wide. It occurs along the southern margin of the Kaapvaal Craton and is bounded by the Mid-Proterozoic migmatite-gneiss terrane of the Natal Structural and Metamorphic Province to the south and the Early Proterozoic Pongola Supergroup to the west. The boundary with the Natal Province is a thrust whereas the boundary with the Pongola Supergroup is an unconformity. The granite-greenstone complex disappears below a cover of Late Ordovician to Early Devonian Natal Group sandstones in the north and the Late Palaeozoic to Mid-Mesozoic Karoo Supergroup in the east.

It can be divided into three broad zones, viz.

(i) the Northern Granitoid Complex;
(ii) the Ilangwe Greenstone Belt; and
(iii) the Southern Granitoid Complex.

These zones are separated by shears, faults, sharp semi-concordant intrusive contacts or sharp transgressive intrusive contacts.

The Northern Granitoid Complex is separated from the Ilangwe Greenstone Belt by the extensive (post-Nsengeni granitoids) Entembeni Fault in the eastern and central portions of the study area. In the western parts of the study area, the Northern Granitoid Complex has a sharp transgressive intrusive contact with the Ilangwe Greenstone Belt. In some places, the granitoid complex forms re-entrant extensions into the greenstones.

The Southern Granitoid Complex is separated from the Ilangwe Greenstone Belt by the post-Nsengeni granitoids Matshansundu Fault in the eastern parts of the belt and by the Vungwini River shear in the western parts. In the central parts of the belt (6,7/V,W), the contact is semi-concordant and intrusive. Small xenoliths of greenstones occur in the granitoids not very far from the contact. In some places, the granitoids are quite mylonitic near the contact.

The Ilangwe Greenstone Belt is divided into two subgroups and six formations which have tectonic contacts (see ***Table 2.1***). The overall structural trend of the Ilangwe Belt is east-west. This contrasts with the ENE to NE trend of the Barberton, Pietersburg and Sutherland Greenstone Belts (Jones, 1990; de Wit, 1987, 1991; de Ronde and de Wit, 1994), but is similar to the trend of the Nondweni Greenstone Belt (Linström, 1987; Versfeld, 1988; Wilson and Versfeld, 1992a) and the Melmoth greenstone fragment (Linström, 1987).

16.3 FOUNDATION TO THE ILANGWE LITHOLOGIES

Basement to the Ilangwe rocks is not known. The migmatitic Amazula Gneiss, the oldest gneiss in the study area, is regarded as the possible ***foundation*** to the Ilangwe greenstones. However, it must be noted that there is no evidence to suggest that it is older than the banded amphibolites of the Sabiza Formation which is the lowermost unit of the Umhlathuze Subgroup. Three important relationships have been observed between the Amazula Gneiss and the Sabiza banded amphibolites, viz.:

(i) They are both intruded by the Nkwalinye Tonalitic Gneiss, the first phase of the early post-Nondweni granitoids. The intrusion is sheet-like and was possibly emplaced along fault zones [Fig. 2; (4.300/S 540)] or lithological layering.

(ii) Together with the Nkwalinye Tonalitic Gneiss, they are intruded by younger post-Nondweni granitoids.

(iii) They occur as tectonic slices within the Umhlathuze River Shear Zone in the Sabiza Formation. The shear zone mélange is intensely deformed and contains sheath folds of the migmatitic gneiss. In the Umhlathuze River locality (4,5/Q), the Amazula Gneiss occurs as northward thrusted slices emplaced on amphibolites of the Sabiza Formation. This tectonic slice of Amazula Gneiss was probably emplaced during the early stages of D^{G}_{1} deformation.

In these dislocation areas, which are either thrust zones or transcurrent shear zones, it is difficult to determine the age relationships between the Amazula Gneiss and the banded amphibolites of the Sabiza Formation. However, what is clear is that they, together with the Nkwalini mylonitic and quartzo-feldspathic flaser gneisses, form the Nondweni major crustal framework that represents the oldest recognizable metamorphic complex in this region.

The Amazula paragneiss comprises a quartzitic leucosome and an amphibolitic melanosome. It occurs as rafts in various post-Nondweni intrusive granitoids and contains mafic to ultramafic enclaves which are possibly fragments of ***simatic basement*** material (see Fig. 5.1 and Plate 5.3A and B). The mafic enclaves are well-foliated and hornblendic in composition whereas the ultramafic enclaves show no fabric and are pyroxenitic in composition.

The limited geochemical data suggests that the Amazula Gneiss is a metaluminous I-type granitoid with a composition ranging from granitic to tonalitic (Chapter 11; Fig. 11.4). The quartzitic variety is of calc-alkaline affinity and the amphibolitic variety is tholeiitic. The possible mechanisms of origin for the Amazula Gneiss were outlined in Section 5.2.1 and it can be concluded that it is of mixed origin, derived from pre-existing rocks by diatexis (Ashworth, 1985).

The Amazula Gneiss records middle to upper amphibolite facies prograde M_1 metamorphism. Retrogression to M_2 lower amphibolite to greenschist facies has been observed. In the sheared rim between the amphibolitic melanosome and the Type B xenolith, retrogression due to dislocation metamorphism occurs. The M_1 prograde metamorphism is associated with the first phase of deformation which resulted in intense

transpositional layering and isoclinal intrafolial folding. Pre-F_1 deformation is thought to have been dominated by horizontal tectonics but very little evidence is preserved.

Complex superimposed folding (Plat 9.4A) has been observed in the Amazula Gneiss of the Amazula River where F^G_2 tight to isoclinal folds plunge moderately to steeply to the WNW and rarely to the ESE. They are associated with a strong $S^G_1//S^G_2$ foliation inclined steeply to the north or south. Sheath folds (Plates 5.4 and 9.6B) occur in ductile shear zones and their presence indicates a local history of plastic non-coaxial deformation (Passchier, 1986; Passchier et. al., 1990; Hanmer and Passchier, 1991).

D^G_3 deformation in the Amazula Gneiss was observed in the Amazula River and Umhlathuze River. In these localities, the orientation of the folds differs slightly. In the former locality, D^G_3 folds plunge moderately to steeply to the NNW whereas in the latter locality, they plunge steeply to the NNE. F^G_3 axial planes are predominantly inclined to the west. No penetrative S^G_3 foliation is present.

The Nkwalini mylonitic and quartzo-feldspathic flaser gneisses are also regarded as ***older gneisses*** (see ***Table 4.1***) and are associated with the Amazula Gneiss. They occur in two widely separated areas and are confined to the Northern Granitoid Complex. In the Nkwalini – Mzilikazi Peak area (5/NN,OO) they are in tectonic contact with the deeply weathered amphibolite schists of the Matshansundu Formation. The E-W trending tectonic contact is transgressively truncated by the post-Karoo Tugela Fault. In the Sappi Mooiplaas forest plantation area (3/R,S), the Nkwalini Mylonitic Gneiss is in tectonic contact with the amphibolites of the Olwenjini Formation and they are both intruded by the Nsengeni Granitoid Gneiss. The orientation of the structures in the Nkwalini mylonitic and quartzo-feldspathic flaser gneisses is similar to that of the Amazula Gneiss in the different localities.

It is significant to note that the orientation of D^G_1 structures in the older gneisses is closely similar to that of the supracrustal formations of the Umhlathuze and Nkandla Subgroups. This supports the conclusion that these lithologies formed the Archaean crustal framework upon which later granitoids were emplaced. The size of this crustal framework must have been quite extensive judging from the occurrence, in widely separated areas, of the migmatitic and mylonitic gneisses and the extensive nature of the Ilangwe greenstones.

16.4 THE ILANGWE SUPRACRUSTAL ROCKS

16.4.1 INTRODUCTION

The Ilangwe Greenstone Belt is a narrow linear belt which disappears below Karoo cover in the east and is unconformably overlain by the Pongola Supergroup in the west. Its size (35km by ±3.5km) falls within the greenstone belt dimensions of Condie (1981). It consists of a lower predominantly mafic – ultramafic component (the Umhlathuze Subgroup) and an upper metasedimentary – minor metavolcanic unit (the Nkandla Subgroup). This is similar to most Archaean greenstone complexes (Condie, 1981; Lemon, 1990; Jones, 1990; de Wit, 1991). The Umhlathuze Subgroup is divided into three formations of dominantly amphibolite and minor metasedimentary lithostratigraphic units. The Nkandla Subgroup also consists of three formations of metasedimentary and minor metavolcanic lithostratigraphic units. The boundaries between all these formations are tectonic (see ***Table 2.1***).

The approximate stratigraphic thicknesses shown on ***Table 2.1*** include thicknesses of sequences structurally repeated by isoclinal folding (see Plates 9.1 and 9.7) and by probable tectonic stacking due to layer-parallel shearing (Martyn, 1986) or imbricate thrusting (Vearncombe et. al., 1986).

Evidence of possible tectonic stacking in the Ilangwe Belt can be found in the Umhlathuze River Shear Zone in the Umhlathuze River (6.000/U,V) where rocks of amphibolite grade metamorphism (Amazula Gneiss and Sabiza banded amphibolite) are juxtaposed with rocks of greenschist facies metamorphism (massive amphibolite schists and chloritic schists). The juxtaposition of the granitoid gneisses and the mafic rocks may also be related to the unroofing of the metamorphic core complex due to extensional tectonics.

Another evidence of possible tectonic stacking is found in the Umhlathuze River southwest of Ngcengcengu Peak (4,5/Q) where slices of the quartzitic variety of the Amazula Gneiss have been thrusted onto Sabiza pillowed amphibolites (Fig. 5.2).

16.4.2 GREENSTONE LITHOLOGIES

The oldest greenstone rocks are those of the Sabiza Formation, which has been informally divided into the ***lower*** and ***upper*** banded and massive amphibolites and has been described in detail in section 2.3.2. The upper and lower parts of the Sabiza Formation are separated by the 150m to 300m wide Umhlathuze River Shear Zone, a tectonic mélange consisting of deformed blocks of Amazula Gneiss and Sabiza metavolcanic assemblages. This shear zone is probably a D_1 thrust zone which was reactivated during D_3 deformation.

Occurring to the east of the Sabiza Formation is the Matshansundu Formation which is an amphibolite – BIF association comprising tremolite schists, actinolite schists, massive metabasalts, amphibole-mica-schists and a silicate-rich cherty BIF. Two rafts of amphibole-mica-schist and BIF occur in the Nsengeni Granitoid Gneiss and the Nkwalinye Tonalitic Gneiss respectively [Fig. 2; (1,2,3,4/EE)]. These rafts possibly suggest that the Matshansundu Formation was once quite extensive or, alternatively, it was disrupted and dismembered by granitoid intrusion.

To the north of the Sabiza Formation and overlying it, occurs the Olwenjini Formation, an amphibolite-banded chert – BIF association. It consists of pillowed metabasalts overlain by massive metabasalts and garnetiferous amphibolite. Minor actinolite schists and tremolite schists occur. The metasediments overlying the metavolcanics include metacherts, cherty quartzites, BIF and a thin discontinuous magnetite quartzite lens. A thin lens of quartz-biotite-cordierite-fuchsite gneiss occurs in the Sabiza River (5.180/V.820) and is thought to represent a shear zone.

The lowermost metasedimentary unit structurally overlying the Sabiza, Matshansundu and Olwenjini Formations is the Entembeni Formation comprising deformed phyllites, banded metacherts, cherty quartzites, BIF and minor pillowed metabasalts.

The Simbagwezi Formation occurs in the western portion of the study area. It structurally overlies and underlies the lowermost and uppermost formations of the Umhlathuze Subgroup. It consists of phyllites, metachert bands, actinolite schists, pillowed metabasalts and minor talc-chlorite schists.

The Nomangci Formation, the uppermost metasedimentary unit, is the only formation which lacks metavolcanics. It consists predominantly of quartzite, quartz schists, phyllite, quartz-muscovite-(sericite) schists and minor metachert bands.

Amphibolitic rocks form a greater percentage (>60%) of the Ilangwe rocks whereas the serpentinitic talc-tremolite schists (altered komatiites) form a minor percentage (2-5%). Geochemical evidence presented in section 10.2.4 indicates that the ortho-amphibolites are of tholeiitic affinity whereas the serpentinitic talc-tremolite schists are of calc-alkaline affinity.

The tholeiitic ortho-amphibolites display a pronounced iron enrichment and show no alumina enrichment whereas the serpentinitic talc-tremolite schists lack iron enrichment and have slightly elevated alumina. These characteristics are thought to be produced by low-pressure fractionation of plagioclase, clinopyroxene and olivine (Lowe and Byerly, 1986; Laflèche et. al., 1992).

Geochemical evidence further indicates that the Ilangwe ortho-amphibolites are of oceanic affinity and field evidence shows that they are of volcanic origin. The serpentinitic talc-tremolite schists are also derived from an oceanic environment and resulted from komatiitic igneous activity. They are altered equivalents of komatiites. The alteration was probably due to a seafloor-type hydrothermal system (de Wit and Hart, 1993; de Ronde and de Wit, 1994).

No spinifex textures were observed in the altered komatiites of the Ilangwe Belt. To the north-northwest of the belt, in the Nondweni Greenstone Complex, spinifex textures in komatiites have been observed (Versfeld, 1988; Versfeld and Wilson, 1992a, b; Wilson and Versfeld, 1994b).

The compositionally variable Precambrian mafic and ultramafic rocks are thought to have been derived from a depleted upper mantle source and in this regard resemble recent mid-ocean ridge basalts (Lowe and Byerly, 1986; de Wit et. al., 1987; Laflèche et. al., 1992; de Ronde and de Wit, 1994). Their close association with calc-alkaline rocks suggests a probable emplacement in a back-arc setting (de Wit, 1991; Laflèche et al., 1992; de Ronde and de Wit, 1994; Lowe, 1994). It is also possible that these rocks could have formed in an Archaean plume-related oceanic environment (Storey et. al., 1991) or a rift-related oceanic environment (Groves and Batt, 1984; Vearncombe et. al., 1986).

16.4.3 METASEDIMENTS

Metasediments comprise about 40 to 45% of the Ilangwe Belt. They occur mostly in the Olwenjini, Entembeni, Simbagwezi and Nomangci Formations. Minor metasedimentary units are found in the Sabiza and Matshansundu Formations.

In the Sabiza Formation, thin lenses (±5m) of fine-grained khaki-coloured siliceous pelitic rock occur intermittently towards the top of the sequence. These laterally discontinuous units consist of thin layers of sheared quartz ribbons alternating with K-feldspars. These lenses clearly represent a break in volcanic activity.

In the Ndloziyana Peak area, the Matshansundu Formation contains an extensive contorted silicate-rich cherty BIF horizon folded into an easterly-closing synform. In the Zietover area (1,2/EE) a detached cherty BIF unit similar to the Ndloziyana one occurs as a raft within Nkwalinye Tonalitic Gneiss. This BIF is thought to be part of the Matshansundu Formation. The amphibolite – BIF association of this formation is similar to the metavolcanic – BIF association of the Rietvley area in the Pietersburg Greenstone Belt which is thought to have been formed in an oceanic-like spreading centre (Jones, 1990).

The top half of the Olwenjini Formation contains a slightly greater percentage of the Metasediments. It consists of banded metacherts, cherty quartzites, BIF and phyllite intercalated with metavolcanics. These metasedimentary lithologies are similar to those of the Entembeni and Simbagwezi Formations. However, the Olwenjini cherty quartzites are fuchsitic whereas the metacherts and cherty quartzites of the Entembeni Formation have black carbonaceous bands (Plate 2.2B). Similar greyish-black layers within banded metacherts of the Pietersburg greenstone belt are known to contain graphite (Maarten de Wit, pers. comm., July, 1995). The banded metacherts and cherty quartzites of the Simbagwezi Formation have a distinctive vitreous charcoal-grey to black colour with muscovite and sericite flakes.

The white and clean quartzites of the Nomangci Formation are massive and blocky. They are highly recrystallized units which are intercalated with thin quartz schists, quartz-muscovite-(sericite) schists, kyanite schists and minor chert bands. In less recrystallized areas, they show steep northerly-inclined dips. They are laterally extensive but wedge eastward into the phyllites of the Simbagwezi Formation. The Nomangci Formation is

analogous to the Moodies Group of the Barberton greenstone belt which is regarded as syndepositional to a collision event (de Ronde and de Wit, 1994).

The phyllites of the different formations of the Nkand'a Subgroup are similar. However, those of the Entembeni Formation are weathered and extremely phyllonitic at the contacts with the other lithologies and at the tectonic contact with the Nsengeni Granitoid Gneiss. The Simbagwezi phyllites are bottle green cleaved rocks consisting of quartz, sericite and chlorite. They are intercalated with a number of thin concordant quartz veins representing cleavage/bedding parallel faults, especially close to the contact with the structurally underlying Sabiza Formation.

The grunerite-rich BIF of the Olwenjini Formation is similar to the Matshansundu BIF. The BIFs of the Entembeni Formation are finely-laminated, strong to moderately magnetic rocks consisting of bands of micro-crystalline cherty quartz and bands of haematite and magnetite (Plate 2.2C). The quartz layers are boudinaged and intensely contorted, implying an intense extensional deformation pre-dating or syntectonic with the D_1 isoclinal folding. The Entembeni BIFs occur along the northern or outer flank of the large synformal fold and are in contact with the structurally underlying phyllites and metacherts, thus suggesting that they occur at the base of the Entembeni Formation.

In section 2.5.1 it was suggested that the metacherts and cherty quartzites probably originated by shallow water chemical precipitation of colloidal silica in a manner analogous to those of the Barberton and Pietersburg greenstone belts (Jones, 1990; de Ronde and de Wit, 1994). The BIFs are thought to have been derived from seafloor hydrothermal processes taking place in a relatively shallow body of water (Kimberley, 1989). The spatial association of BIFs, metacherts, cherty quartzites and metavolcanics suggests deposition in an emerging marine to subaerial environment.

16.4.4 METABASIC BODIES

The greenstones and, to a lesser extent, the Amazula Gneiss are closely associated with a number of small metabasic bodies which were described in Chapter 4 and Chapter 15. They occur close to tectonic contacts of various lithologies. They are predominantly gabbroic and are, to a lesser extent, associated with serpentinite, which could have been a peridotite, pyroxenite or harzburgite – probably a layered intrusion. The metabasic body occurring to the northwest of Ilangwe Peak is a metanorite.

Limited geochemical analyses indicate that these bodies are tholeiitic and of oceanic affinity. Their close association with the Ilangwe greenstones suggests that they were emplaced in a mid-oceanic ridge-like setting.

Gabbroic bodies intruding the Amazula Gneiss show a weak S_1 foliation which is associated with an M_1 medium-grade metamorphism. Both the D_1 foliation and the M_1 metamorphism are not penetrative in these rocks. Retrogression from medium-grade to greenschist facies metamorphism is quite common. The larger gabbroic bodies are characterized by partial or incomplete replacement reactions. Grain boundary symplectites are quite common. The partial alteration was described in Chapter 15 and it was concluded that incipient retrograde metamorphic effects cannot be easily distinguished from deuteric alteration effects.

In hand specimen, these gabbroic bodies show no foliation. In thin section, a weak incipient foliation characterized by nematoblastic actinolite was observed. The timing of this foliation is not clear.

The metabasic bodies intruding the Amazula Gneiss are probably of D_1 age because of their weak S_1 foliation. However, no folds were identified in these rocks. The timing of the larger metabasic bodies is unclear. They could probably be pre-late post-Nondweni granitoids in age as they contain a weak foliation (observed in thin section) which is absent in the late post-Nondweni granitoids. Further, some bodies occur as rafts in these granitoids.

The metabasic bodies can be regarded as remnants of disrupted layered mafic intrusions. They were probably emplaced along tectonic contacts. As was suggested in Chapter 15, a detailed study of these bodies can elucidate the timing of their emplacement.

16.4.5 STRUCTURAL SUCCESSION

The Umhlathuze and Nkandla Subgroups show complex structural relationships. The rocks of these sub-groups are complexly deformed and show primary layering and foliation to be sub-vertical to vertical. Moreover, field mapping has provided evidence for polyphase folding.

In Chapter 3, it was argued that due to this high degree of deformation, all initial angular discordances will have been obliterated by rotation parallel or sub-parallel to the regional steep axial planar foliation. As a result, any direct evidence of original angular unconformities will be circumstantial.

As mentioned previously, the Sabiza Formation is the oldest greenstone formation in the Ilangwe Belt. To the east of it but not in contact with it, occurs the Matshansundu Formation. Although no contact relationships between the two formations have been observed, it is thought that the Matshansundu either structurally overlies the Sabiza or it is contemporaneous with it. Way up evidence as indicated by pillow structures in the Sabiza Formation together with the distinct lithological compositions of the two formations suggests the former.

In the central parts of the study area, the Sabiza Formation is structurally overlain by the Olwenjini Formation, which is thought to be the uppermost formation of the Umhlathuze Subgroup. The Olwenjini Formation does not occur in contact with the Matshansundu Formation. However, the latter is thought to be older mainly on the basis of the compositional variations in their lithologies and on the abundance of metasediments in the Olwenjini Formation. These metasediments closely resemble those of the Entembeni Formation which structurally overlies it.

In the central sector of the Ilangwe Belt, very interesting contact relationships exist between the three formations of the Umhlathuze Subgroup and the Entembeni Formation. West of Ndloziyana Peak (6.200/FF), the Entembeni Formation is in a sharp tectonic contact with the Sabiza and Matshansundu Formations. The Matshansundu Formation trends NNE–SSW and dips to the NW, the Sabiza Formation trends E–W and dips to the north whereas the Entembeni Formation is complexly folded in this locality. This discordant contact between the three formations therefore represents a major deformed angular unconformity which can be referred to as the ***Ndloziyana angular unconformity***. All three formations in this locality are transgressively intruded by the Umgabhi Micrographic Granite.

Another interesting contact relationship exists between the Sabiza Formation, Olwenjini Formation and the Entembeni Formation in the Sabiza locality (4,5/V,W) west of Ilangwe Peak. The Entembeni Formation transgressively overlaps the Olwenjini Formation, All three formations trend NW–SE and are steeply inclined to the NE. Their contact, which is

partly intruded by a metanoritic body, trends roughly NNW–SSE. This contact is regarded as a deformed local angular unconformity.

Further to the west, in the Simbagwezi Peak area (5,6/J,K,L,M), complex contact relationships exist between the Sabiza Formation, Olwenjini Formation and the Simbagwezi Formation. The latter occurs as a structural wedge between the former two formations of the Umhlathuze Subgroup. This relationship suggests overthrusting from the north by a segment of the Umhlathuze Subgroup.

Finally, the Simbagwezi and Nomangci Formations of the Nkandla Subgroup also show complex structural relationships. The Nomangci Formation occurs as a series of wedges within the Simbagwezi Formation. These relationships were described in section 3.3. It can thus be concluded that these Nomangci wedges occurred as a result of overthrusting. The cyclical repetitive nature of the Nomangci and Simbagwezi Formations (Fig. 2) is suggestive of normal dip-slip duplexes (Woodcock and Fischer, 1986).

16.5 BRIEF OVERVIEW OF THE STRUCTURAL AND METAMORPHIC HISTORY

Three major deformation episodes (D_1 to D_3) have been recognized in the Ilangwe complex. Similarly, three deformation events (D^G_1 to D^G_3) were observed in the granitoid complex. Deformation in the granitoids was interrupted by younger granitoid intrusions. The three deformation episodes were accompanied by three metamorphic events (M_1 to M_3).

The first phase of deformation in the granitoids was probably synchronous with the first phase of deformation in the greenstones. It was characterized by recumbent and isoclinal folds with the associated transpositional layering and thrusting. D_1 folds plunge steeply to the WSW and ENE with subvertical axial planes aligned along a vertical plane with a northeasterly azimuth.

Analyses of structural data shows that the first phase of deformation took place in a horizontal tectonic regime characterized by high strain and possible formation of fold nappes and thrusts which thickened the Ilangwe crust considerably.

D_1 deformation was accompanied by prograde M_1 medium-grade middle amphibolite facies metamorphism probably taking place in temperatures ranging between 500° and 550°C as

indicated by the presence of cordierite in some mineral assemblages (Winkler, 1979; Barker, 1990). Typical mineral assemblages characteristic of the M_1 event were discussed in sections 10.2.1.2, 11.2.2 and 11.3.2. Widespread retrogression was observed. Initial retrogression was due to dislocation metamorphism associated with early shearing or thrusting (see Figs. 5.1 and 5.3).

The post D_1-folding event was dominated by the emplacement of the Nkwalinye Tonalitic Gneiss along lithological boundaries of the pre-existing greenstone and granitoid lithologies. The tonalite was deformed together with the older rocks during the second phase of deformation which was superimposed at right angles to the first phase.

Competency contrast between the different lithologies in the greenstones and older gneisses resulted in different geometrical structures. In the older gneisses and in the Sabiza amphibolites, the structures were composite similar folds, with sheath folds occurring in the Amazula Gneiss. In the greenstones, these structures plunge to the WNW and ESE and show a bimodal distribution about a vertical plane with azimuth 100°. In the older gneisses, the folds plunge predominantly to the WNW. In the formations dominated by metacherts, quartzites and banded ironstones, D_2 structures comprise upright doubly-plunging en-echelon periclinal folds which generally trend E–W with steeply inclined overturned limbs. Flattening normal to the axial planes produced a penetrative axial planar foliation. The folding mechanism in the greenstones was largely flexural slip whereas heterogeneous simple shear was the mechanism in the older gneisses.

Although the second phase of deformation in both the greenstones and granitoids was dissimilar, evidence suggests that it was coeval. It was characterized by compression, flattening and rotation.

The post D_2-folding period was dominated by the intrusion of the late D_2 Nsengeni Granitoid Suite. The final stages of D_2 deformation resulted in the formation of the post-intrusive Entembeni and Matshansundu Faults which bound the Ilangwe Greenstone Belt.

D_2 deformation was accompanied by the regional M_2 greenschist facies metamorphism. This albite–actinolite–chlorite zone of metamorphism (Winkler, 1979) took place at temperatures between 350° – 450°C (Barker, 1990). Minor retrogression to lower greenschist facies metamorphism was observed in the Simbagwezi and Nomangci lithologies and is thought to be related to the overthrust event.

The third phase of deformation in the greenstones was characterized by moderately to steeply plunging small-scale folds occurring on the limbs and axial planes of D_2 upright periclinal folds. The axes of these folds plunge to the NW and SE and show a bimodal distribution about a vertical plane with azimuth 135°. In the granitoids, D^G_3 folds have an open to close geometry with variable plunges to the north to NNW and south to SSE. Their axial planes are steeply inclined to the west and rarely to the east. No penetrative S_3 foliation occurs.

The D_3 minor folds are oblique to the D_2 large-scale periclinal folds. This oblique relationship was attributed to a D_3 transpressional deformation with a sinistral component of shear in response to a slight clockwise rotation of the regional compressive stress. In both the greenstone and granitoid terrains, transpression was operative and resulted in substantial uplift of the surface.

In the Mandaba and Makhanyezi areas (3,4/G,H,I,J,K) where kyanite schists occur, D_3 deformation was accompanied by prograde greenschist facies metamorphism which is probably related to the intrusion of the Nkandla Granite in this area.

In the Esibhudeni area (7,8/G,H,I,J), D_3 deformation was accompanied by a localized M_3 retrograde dislocation metamorphism in the quartz sericite schists.

16.6 POST-NONDWENI MAGMATISM

16.6.1 EARLY POST-NONDWENI GRANITOIDS

Post-Nondweni magmatism was dominated by the emplacement of calc-alkaline granitoids during D_2 and D_3. During the early stages of D_2 deformation, the Nkwalinye Tonalitic Gneiss, the first phase of the ***early post-Nondweni granitoids***, was emplaced along lithological layering and along F_1 axial planar regions in the older gneisses and greenstones. The tonalitic gneiss was folded together with the older lithologies into F_2 tight to isoclinal folds plunging to the WNW and ESE. D_3 dextral shearing in the tonalitic gneiss resulted in the formation of natural back-rotated layer segments and natural back-rotated pinch-and-swell structures (Plate 6.1A and B) (Hanmer, 1986; Hanmer and Passchier, 1991).

The later stages of D_2 deformation were characterized by the emplacement of the Nsengeni Granitoid Suite, the second phase of the early post-Nondweni granitoids, consisting of three phases/units. This resulted in the further deformation of the older gneisses, greenstones and the Nkwalinye Tonalitic Gneiss.

The Nsengeni granitoids show sharp transgressive intrusive contacts with the older gneisses and the Nkwalinye Tonalitic Gneiss whereas they have post-intrusive tectonic contacts with the greenstones. The individual granitoid units have gradational contacts. It is essential to emphasize that the early post-Nondweni granitoids ***pre-date*** the development of the ***greenstone boundary faults*** (Entembeni and Matshansundu Faults). Evidence of this effect has been presented in the text. Moreover, and most significantly, the fact that the early post-Nondweni granitoids occur on either side of the greenstone boundary faults which show strike-slip displacement, suggests that the boundary faults post-date the emplacement of the early post-Nondweni granitoids.

These granitoids have similar characteristics. They are megacrystic to microcrystic well-foliated leucocratic granitoids. Chemical analyses show that they range from tonalitic to granitic in composition, are of calc-alkaline affinity and indicate a very strong trend towards the total alkali apex. The limited geochemical data indicates an igneous origin and a probable derivation from the lower crust or upper mantle, possibly by partial melting of pre-existing material.

Mineral assemblages of the Nkwalinye Tonalitic Gneiss suggest that its deformation was accompanied by M_2 prograde medium grade (lower amphibolite facies) metamorphism. These assemblages are similar to some of those of the M_1 metamorphism. This suggests that the M_1 event outlasted the D_1 deformation event. M_2 syntectonic retrogression has been observed.

The Nsengeni granitoids, on the other hand, do not show any evidence of having been subjected to lower amphibolite or even upper greenschist facies metamorphic conditions. Mineral assemblages are consistent with those of the regional M_2 greenschist facies metamorphism. Biotite in these granitoids shows incipient retrogression to chlorite or epidote whilst plagioclase is altered to sericite. These retrogressive reactions are thought to have occurred during the waning stages of the regional M_2 greenschist facies metamorphism.

The early post-Nondweni granitoids were emplaced as passive batholithic sheets probably along pre-existing tectonic contacts (shear zones) or lithological layering. Their emplacement mechanism is probably similar to that of the Wyangala Batholith of SE Australia (Paterson et. al., 1990) or the Archaean gneisses of the Fiskenaesset region, West Greenland (Myers, 1976).

Several features are consistent with structurally-controlled passive emplacement. These granitoids lack well-developed contact aureoles; their strong E–W foliations are consistently parallel to those of the wall rocks; they occur as linear sheet-like or tabular bodies which parallel the regional trend of structures in the wall rocks; they are spatially associated with the complex D_2 deformation in the Ilangwe Belt; and finally, they pre-date the greenstone boundary faults, which suggests that post-emplacement deformation progressed from ductile to brittle-ductile (in the Nkwalinye Tonalitic Gneiss) to brittle (on the contacts of the Nsengeni granitoids with the greenstones).

16.6.2 LATE POST-NONDWENI GRANITOIDS

As mentioned previously, D_3 deformation was dominated by the intrusion of the ***late post-Nondweni granitoids***. The Umgabhi Granitoid Suite was emplaced along the southern boundary with the greenstones whereas the Impisi Granitoid Suite was emplaced along the northwestern boundary with the greenstones. The emplacement of these granitoids probably resulted in superimposed deformation in the earlier lithologies.

The late post-Nondweni granitoids have similar chemical and mineralogical characteristics, they are in mutual contact and show gradational relationships with each other.

They are mostly megacrystic and lack any foliation except near the contacts with older lithologies or where they are sheared, in which case they show weak foliations mimicking the foliation of the wall rocks.

They are intrusive into the greenstones, migmatitic and mylonitic gneisses and the early post-Nondweni granitoids. The intrusive contacts range from transgressive discordant to semi-concordant. In some localities, they form re-entrant extensions into the greenstones.

Sparse geochemical data indicates that they are of calc-alkaline affinity, are exclusively granitic in composition and show a strong trend towards the total alkali apex. They are igneous in origin, probably derived from the lower crust.

They were emplaced as batholithic sheets. The emplacement mechanism is probably similar to that of the Doctor's Flat Pluton of Australia (Morand, 1992) and the Mortagne Pluton in France (Guineberteau et. al., 1987) which are interpreted as having been emplaced into a pull-apart in a strike-slip fault. Consistent with this mechanism, a jog in the Matshansundu Fault or in the Vungwini River shear probably initiated a pull-apart into which Umgabhi granitic magma intruded.

Several characteristics of the Umgabhi granitoids such as the elongate shape, steep foliations along the boundaries and intrusive mylonitic margins suggest this mode of emplacement.

Similarly, the Impisi Granitoid Suite in the northwest portion of the study area was probably emplaced along the terminations of the Entembeni and Makhanyezi Faults, to the northwest of Simbagwezi Peak. The Umgabhi Micrographic Granite shows evidence of forceful emplacement in the Ndloziyana Peak area (5,6/GG,HH). This is the only place in the entire Ilangwe complex where evidence of diapirism is found.

16.7 POSSIBLE SEQUENCE OF EVENTS

The Ilangwe Belt, just like the Barberton greenstone belt (de Ronde and de Wit, 1994), represents a crustal remnant of an Archaean orogenic belt which was once part of a much larger orogenic system occurring on the southern edge of the Kaapvaal craton.

Basement to the Ilangwe rocks is not known but is thought to have been simatic in composition, judging from the mafic and ultramafic enclaves contained in the Amazula paragneiss. The latter, together with the Nkwalini mylonitic and flaser gneisses, was probably derived from the partial melting of this simatic basement. The Amazula Gneiss and the Nkwalini mylonitic and flaser gneisses together with the Ilangwe greenstones form the earliest recognizable gneissic metamorphic complex in this region.

The greenstones occur in all the formations of the Umhlathuze Subgroup and to a lesser extent in the lower formations of the Nkandla Subgroup. They, together with the older

gneisses, were subjected to intense D_1 deformation. This deformation was broadly similar in the five tectonostratigraphic units and in the older gneisses. The D_1 structures can be attributed to horizontal shortening in either a fore-arc or back-arc environment (de Ronde and de Wit, 1994; de Wit, 1991; de Wit et. al., 1987).

The greenstones and older gneisses were intruded by the Nkwalinye Tonalitic Gneiss during the early stages of D_2 deformation. The gneiss was emplaced in the eastern and central portions of the belt. In the western part of the belt, syntectonic deposition of the Nomangci Formation quartzites and metacherts took place, probably in an emerging marine to subaerial environment. D_2 deformation resulted in tight to isoclinal folding.

During the late stages of D_2, the Nsengeni Granitoid Suite was emplaced on either side of the greenstone belt. The Ntshiweni Augen Gneiss intruded first in the northwestern portion of the belt. This was followed by the emplacement of the Nsengeni Granitoid Gneiss in the eastern and central parts of the study area and on either side of the greenstone belt.

Emplacement of the Nsengeni Granitoid Suite resulted in complex superimposed deformation. The terminal stages of D_2 deformation are also associated with the deformation of the Ndloziyana and Sabiza angular unconformities, the overthrusting of the Simbagwezi and Nomangci Formations thus resulting in tectonic wedges of these formations in older lithologies and finally, the development of the post-intrusive greenstone boundary faults. Minor metabasic bodies were probably intruded during this period.

Emplacement of the early post-Nondweni granitoids was followed by the emplacement of the late post-Nondweni granitoids during D_3. This resulted in the formation of D_3 northerly trending upright structures and the continued deformation of the older lithologies. The Ndloziyana angular unconformity was deformed by the diapiric intrusion of the Umgabhi Micrographic Granite in the Ndloziyana Peak area. D_3 transpression caused considerable uplift of the Ilangwe thick crust and resulted in the present topography of the Ilangwe complex.

16.8 SUMMARY OF MAIN CONCLUSIONS

1. The Ilangwe granite-greenstone complex can be divided into three broad zones, viz., the Northern Granitoid Complex, the Ilangwe Greenstone Belt and the Southern Granitoid Complex.

2. The granitoids of the Northern and Southern Complexes have been differentiated for the first time in this study and can be divided into :

2.1 older gneisses comprising the Amazula Gneiss – Nkwalini Mylonitic and flaser gneisses association;

2.2 the early post-Nondweni granitoid association;

2.3 the late post-Nondweni granitoid association.

3. Geological mapping has revealed that the Ilangwe Greenstone Belt can be divided into the Umhlathuze and Nkandla Subgroups :

3.1 the mafic – ultramafic – minor metasedimentary Umhlathuze Subgroup comprises the Sabiza, Matshansundu and Olwenjini Formations;

3.2 the metasedimentary – minor metavolcanic Nkandla Subgroup comprises the Entembeni, Simbagwezi and Nomangci Formations.

4. Limited geochemical data suggests that the ortho-amphibolites have a tholeiitic affinity and are of volcanic origin. The serpentinitic talc-tremolite schists are of calc-alkaline affinity and were probably formed in plume-related environments.

5. Geochemical data of the granitoids suggest that they are of calc-alkaline affinity and of igneous derivation, probably from the lower crust or upper mantle.

6. Three major phases of deformation accompanied by associated metamorphic events have been identified.

7. Evidence suggests that the Ilangwe granite – greenstone complex represents a middle to upper crustal remnant which was once part of a much larger Archaean orogenic system (de Wit and Ashwal, 1993).

ACKNOWLEDGEMENTS

I want to express my sincere gratitude and indebtedness to the following people who supported me throughout this difficult project :

1. My supervisors Prof P E Matthews and Prof M K Watkeys. Special gratitude to Prof P E Matthews my mentor for his guidance and many hours spent in the field. His assistance with the structural analysis and interpretation of the Ilangwe Greenstone Belt is greatly appreciated.

2. My friends John Dixon, Sam Mokoka and Louis Selekane for their help, encouragement and many fruitful discussions in the field.

3. The technical staff of the University of Natal, Durban, for the preparation of thin section slides.

4. Dr Barta and his staff at the former Bophuthatswana Geological Survey for geochemical analyses and thin section preparation.

5. The Department of Geology, University of Zululand for logistical support during my tenure as lecturer. Special thanks to Prof Vos Coetzee and J W J Rheeder (JR.).

6. Dr Andrew Mitchell of the University of Durban-Westville Geology Department for allowing me to use facilities in the petrographic laboratory and for his assistance with the geochemical data.

7. Prof Chris Roering of the Randse Afrikaans Universiteit for allowing me access to the Geology Department and Prof Lewis Ashwal for his assistance with the Newpet software and for his encouragement.

8. The Randse Afrikaans Universiteit for allowing me access to the library facilities.

9. The Minerals Division of Shell SA (Pty) Limited for financial assistance during my unpaid leave. Sincere gratitude to John Dreyer and Kowie Strauss for motivating the financial assistance and to Gavin Whitfield and Ciaran Halpin for their encouragement and support.

10. Sappi Forests (Pty) Limited Mooiplaas Plantation for giving me permission to map their Mooiplaas (Hillside Block D) properties.

11. All the people of Ilangwe, especially Mr Shandu, the late Mr Khuzwayo, and their families for their hospitality during the field work.

12. Lynwood Hannie, Laurie Lavis and Matt Daubermann for their professional work in drafting the Ilangwe map and other figures. Lisa Bureau, for her scanning of all the photographs which appear as plates in this thesis.

13. Adam Fleming, Ted Grobicki, Vaughan Armstrong and Geoff Mowatt of West Rand Consolidated Mines Limited for encouraging and motivating me.

14. Roleen Vorster for typing the first draft of the thesis.

15. Rosemary Taylor for typing subsequent drafts and for the professional layout of the thesis. To her I say: "ukwanda kwaliwa umthakathi".

16. My mother, Mukile, brothers and sisters, Sibongile, Simangele, Mduduzi, Zandile, Sizwe and Fouzia for the support and encouragement.

17. Last but not least, my wife Nomxolisi and my children Siyabonga, Thoba, Thobeka and Thobile for their love, patience and understanding.

REFERENCES

ANHAEUSSER, C R, MASON, R, VILJOEN, M J and VILJOEN, R P (1969): A reappraisal of some aspects of Precambrian shield geology. *Geol. Soc. Am. Bull., **80**: pp 2175-2200.*

ANHAEUSSER, C R (1973): The evolution of the early Precambrian crust of southern Africa. *Phil. Trans. Rey. Soc., London, Ser.* **A273***: pp 359-388.*

ARNDT, N T, NALDRETT, A J and PYKE, D R (1977): Komatiitic and iron-rich tholeiitic lavas of Munro Township, Northeast Ontario. *J. Petrol, **18**: pp 319-369.*

ARNDT, N T (1986): Komatiites: a dirty window to the Archaean mantle. *Terra Cognita, **6**: pp 59-66.*

ARNDT, N T and NISBET, E G (1982): What is a komatiite? ***In*** Komatiites edited by N T Arndt and E G Nisbet. *George Allen & Unwin, London: 526p.*

ASHWORTH, J R (1985): Introduction. ***In*** Migmatites. *Editor J R Ashworth (1985), Blackie, London: 293p.*

BARBARIN, B (1990): Granitoids: main petrogenetic classifications in relation to origin and tectonic setting. *Geol. Journal,* **25***: pp 227-238.*

BARKER, F (1979): Trondhjemite : definition, environment and hypotheses of origin. ***In:*** *Trondhjemites, Dacites and Related Rocks (edited by F Barker), Elsevier, Amsterdam.*

BARKER, A J (1990): Introduction to Metamorphic textures and microstructures. *Blackie. Published in the USA by Chapman and Hall, New York: 162p.*

BATES, R L and JACKSON, J A (EDITORS) (1980): Glossary of Geology. 2nd Edition. *American Geological Institute, USA.*

BELL, T H (1978): Progressive deformation and reorientation of fold axes in a ductile mylonite zone: the Woodroffe Thrust. *Tectonophysics, **44**: pp 285-320.*

BELL, T H and HAMMOND, R L (1984): On the internal geometry of mylonite zones. *J. Geol., **92**: pp 667-686.*

BERNSTEIN-TAYLOR, B L, BROWN, K M, SILVER, E A and KIRCHOFF-STEIN, K S (1972): Basement slivers within the New Britain accretionary wedge: Implications for the emplacement of some ophiolitic slivers. *Tectonics, **11**: pp 753-765.*

BERTHÉ, D, CHOUKROUNE, P and JEGOUZO, P (1979): Orthogneiss, mylonite and non-coaxial deformation of granites: the example of the South Armorican Shear Zone. *J. Struct. Geol.* **2***: pp 119-126.*

BEST, M G (1982): Igneous and Metamorphic Petrology. *W H Freeman and Company, New York: 630p.*

BESWICK, A E (1982): Some geochemical aspects of alteration, and genetic relations in Komatiitic suites. ***In*** Komatiites, edited by N T Arndt and E G Nisbet. *George Allen & Unwin, London: 526p.*

BICKLE, M J, NISBET, E G and MARTIN, A (1994): Archaean Greenstone Belts are not oceanic crust. *J. Geol., **102**: pp 121-138.*

BOYER, S E and ELLIOTT, D (1982): Thrust Systems. *The American Association of Petroleum Geologists Bulletin **66**: No.**9**: pp 1196-1230.*

BRIDGEWATER, D, McGREGOR, V R and MYERS, J S (1974): A horizontal tectonic regime in the Archaean of Greenland and its implications for early crustal thickening. *Precambrian Res. **1**: pp 179-197.*

BROOKS, C K (1976): The Fe_2O_3/FeO ratio of basalt analyses: an appeal for a standardised procedure. *Bull. Geol. Soc., Denmark, **25**: pp 117-120.*

BURKE, K and KIDD, W S F (1978): Were Archaean continental geothermal gradients much steeper than those of today? *Nature, **272**: pp 240-241.*

BUTLER, R W H (1982): The terminology of structures in thrust belts. *J. of Struct. Geol. **4**: pp 239-245.*

CAMPBELL, J D (1958): En Echelon Folding. *Economic Geology, **53**: pp 448-472.*

CAMPBELL, I H , GRIFFITHS, R W and HILL, R I (1989): Melting in an Archaean mantle plume : heads it's basalts, tails it's komatiites. *Nature, **339**: pp 697-699.*

CARRERAS, J, ESTRADA, A and WHITE, S (1977): The effect of folding on the c-axis fabrics of a quartz mylonite. *Tectonophysics, **39**: pp 3-24.*

CHAKRABORTY, K L and MAJUMDER, T (1992): An unusual diagenetic structure in the Precambrian banded iron formation (BIF) of Orissa, India and its interpretation. *Mineral Deposita, **27**: pp 55-57.*

CHAPPELL, B W and WHITE, A J R (1974): Two contrasting granite types. *Pacific Geology, **8**: pp 173-174.*

CHAPPELL, B W, WHITE, A J R and WYBORN, D (1987): The importance of residual source material (Restite) in granite petrogenesis. *J. Petrol., **28**: pp 1111-1138.*

CHARLESWORTH, E G (1981): Tectonics and Metamorphism of the Northern Margin of the Namaqua-Natal Mobile Belt, near Eshowe, Natal. *Ph.D thesis (unpubl.) Univ. of Natal, Durban: 433p.*

CHAYES, F (1966): Alkaline and subalkaline basalts. *Am. J. Sci., **264**: pp 128-147.*

CLARKE, D C (1992): Granitoid rocks. Topics in the Earth Sciences 7. *Chapman & Hall, London: 283p.*

COBBOLD, P R and QUINQUIS, H (1980): Development of sheath folds in shear regimes. *J. Struct. Geol., **2**: pp 119-126.*

CONDIE, K C (1981): Archaean Greenstone Belts. *Elsevier Scientific Publishing Company, Amsterdam: 434p.*

COOMBS, D S (1963): Trends and affinities of basaltic magmas and pyroxene as illustrated on the diopside-olivine-silica diagram. *Min. Soc. Amer. Spec. Pap.* ***1****: pp 227-250.*

COUSINEAU, P A and ST-JULIEN, P (1992): The Saint Daniel Melangè: Evolution of an accretionary complex in the Dunnage Terrane of the Quebec Appalachians. *Tectonics,* ***11****: pp 898-909.*

COWARD, M P and POTTS, G J (1983): Complex strain patterns developed at the frontal and lateral tips to shear zones and thrust zones. *J. Struct. Geol.,* ***5****: pp 383-399.*

DALZIEL, I W D and BAILEY, S W (1968): Deformed garnets in a mylonitic rock from the Grenville front and their tectonic significance. *Am. J. Sci.,* ***266****: pp 542-562.*

DAVIS, G H (1984): Structural Geology of rocks and Regions. *John Wiley & Sons, Inc., USA: 492p.*

DAVIS, R A JNR (1983): Depositional Systems: A genetic approach to sedimentary geology. *Prentice-Hall Inc., Englewood Cliffs, New Jersey: 669p.*

DE LEON, M I P and CHOUKROUNE, P (1980): Shear zones in the Iberian Arc. *J. of Struct. Geol.,* ***2****: pp 63-68.*

DEER, F R S, HOWIE, W A and ZUSSMAN, J (1985): An Introduction to the rock-forming minerals. *Longman Group Ltd.*

DE RONDE, C E J and DE WIT, M J (1994): Tectonic history of the Barberton greenstone belt, South Africa: 490 million years of Archaean crustal evolution. *Tectonics,* ***13****: pp 983-1005.*

DE RONDE, C E J, DE WIT, M J and SPOONER, E T C (1994): Early Archaean (>3,2 Ga) Fe-oxide-rich, hydrothermal discharge vents in the Barberton greenstone belt, South Africa. *Geol. Soc. of Amer. Bull.,* ***106****: pp 86-104.*

DESROCHERS, J P, HUBERT, C, LUDDEN, J N and PILOTE, P (1993): Accretion of Archaean oceanic plateau fragments in the Abitibi greenstone belt, Canada. *Geology,* ***21****: pp 451-454.*

DE WIT, M J, HART, R A, MARTIN, A and ABBOTT, P (1982): Archaean abiogenic and probable biogenic structures associated with mineralized hydrothermal vent systems and regional metasomatism, with implications for greenstone belt studies. *Econ. Geol.,* ***77****: pp 1783-1802.*

DE WIT, M J, FRIPP, R E P and STANNISTREET, I G (1983): Tectonic and stratigraphic implications of new field observations along the southern part of the Barberton greenstone belt. *Spec. Publ. Geol. Soc. S.Afri.,* ***9****: pp 21-29.*

DE WIT, M J, ARMSTRONG, R, HART, R J and WILSON, A H (1987a): Felsic Igneous Rocks within the 3,3 to 3,5 Ga Barberton Greenstone Belt: High Crustal level equivalent to the surrounding tonalite-trondhjemite terrain emplaced during thrusting. *Tectonics, **6**: pp 529-549.*

DE WIT, M J, HART, R and HART, R (1987b): The Jamestown Ophiolite Complex, Barberton Mountain Belt: A composite section through 3.5 Ga oceanic crust. *J.Afr. Earth Sci., **5**: pp 681-730.*

DE WIT, M J (1982): Gliding and overthrust Nappe tectonics in the Barberton greenstone belt. *J. Struct. Geol. **4**: pp 117-136.*

DE WIT, M J (1991): Archaean greenstone belt tectonism and basin development: some insights from the Barberton and Pietersburg greenstone belts, Kaapvaal Craton, South Africa. *J. Afr. Earch Sci., **13**: pp 45-63.*

DE WIT, M J, ROERING, C, HART, R J, ARMSTRONG, R A, DE RONDE, C E J, GREEN, R W E, TREDOUX, M, PEBERDY, E and HART, R A (1992): Formation of an Archaean Continent. *Nature, **357**: pp 553-562.*

DE WIT, M J and HART, R A (1993): Earth's earliest continent lithosphere, hydrothermal flux and crustal recycling. *Lithos, **30**: pp 309-335.*

DE WIT, M J and DE RONDE, C E J (1994): Tectonic history of the Barberton greenstone belt, South Africa: 490 million yeas of Archaean crustal evolution. *Tectonics, **13**: pp 983-1005.*

DIMROTH, E (1977): Models of physical sedimentation of iron formations. *Geosc. Can., **4**: pp 23-30.*

DIXON, J (in prep): Geology of the Buffalo Gorge Complex. *PhD thesis, University of Natal, Durban.*

DU TOIT, A L (1931): The geology of the country surrounding Nkandhla, Natal. An explanation to sheet No. 109 (Nkandla): *Geol. Surv. S.Africa.*

ECHEVERRIA, L M (1982): Komatiites from Gorgona Island, Colombia. ***In*** N T Arndt and E G Nisbet (eds) (1982): Komatiites. *George Allen & Unwin (Publ) Ltd., London: 526p.*

EHLERS, C (1976): Homogeneous deformation in Precambrian supracrustal rocks of Kumlinge area, southwest Finland. *Precam. Res., **3**: pp 481-504.*

EHLERS, E G and BLATT, H (1982): Petrology: Igneous, Sedimentary and Metamorphic. *W H Freeman & Co., San Francisco: 732p.*

ERMANOVICS, I F, McRITCHIE, W D and HOUSTON, W N (1979): Petrochemistry and tectonic setting of plutonic rocks of the Superior Province in Manitoba. ***In*** Barker, F (Editor); Trondhjemites, Dacites and Related Rocks. *Elsevier, Amsterdam.*

ESCHER, A and WATTERSON, J (1974): Stretching fabrics, folds and crustal shortening. *Tectonophysics, **22**: pp 223-231.*

EUGSTER, H P and MING CHOU, I (1973): The depositional environments of Precambrian Banded Iron-Formations. *Econ. Geol., **68**: pp 1144-1168.*

FOSSEN, H and RYKKELID, E (1990): Shear zone structures in the Øygarden area, West Norway. *Tectonophysics, **174**: pp 385-397.*

FRIPP, R E P (1976): Stratabound gold deposits in Archaean banded iron formation, Rhodesia. *Econ. Geol., **71**: pp 58-75.*

FYFE, W S, PRICE, N J and THOMPSON, A B (1978): *Developments in geochemistry, **1**: pp 115-117.*

GARRISON, J R (1981): Metabasalts and metagabbros from the Liano Uplift, Texas: Petrologic and geochemical characterisation with emphasis on tectonic setting. *Contrib. Mineral. Petrol., **78**: pp 459-475.*

GORMAN, B E, PEARCE, T H and BIRKETT, T C (1978): On the structure of Archaean Greenstone Belts. *Precambrian Res., **6**: pp 23-41.*

GREEN, D M, EDGAR, A D, BEASLEY, P, KISS, E and WARE, N G (1974): Upper mantle source for some hawaiites, mugearites and benmoreits. *Contrib. Mineral. Petrol., **48**: pp 33-43.*

GRIFFITHS, R W and CAMPBELL, I H (1990): Stirring and structure in mantle starting plumes. *Earth and Planetary Science Letters, **99**: pp 66-78.*

GROENEWALD, P B (1984): The lithostratigraphy and petrogenesis of the Nsuze Group northwest of Nkandla, Natal. *M.Sc Thesis (unpubl) Univ. Natal, Pietermaritzburg, S Africa: 316p.*

GROVES, D I and BATT, W D (1984): Spatial and Temporal Variations of Archaean Metallogenic Associations in Terms of Evolution of Granitoid-Greenstone Terrains with particular Emphasis on the Western Australian Shield: *pp 73-98. **In*** Kröner, A; Hanson, G N and Goodwin, A M (Editors) : Archaean Geochemistry: The Origin and Evolution of the Archaean Continental Crust. *Springer-Verlag Berlin Heidelberg: pp 73-98.*

GUINEBERTEAU, B, BOUCHEZ, J L and VIGNERESSE, J L (1987): The Mortagne granite pluton (France) emplaced by pull-apart along a shear zone: structural and gravimetric arguments and regional implication. *Bull. Geol. Soc. Am., **99**: pp 763-770.*

HANMER, S (1986): Asymmetrical pull-aparts and foliation fish as kinematic indicators. *J. Struct. Geol., **8**: pp 111-122.*

HANMER, S and PASSCHIER, C (1991): Shear-sense indicators: A review. *Geol. Survey of Canada, Paper 90-17.*

HARLEY, S L, HENSEN, B J and SHERATON, J W (1990): Two-stage decompression in orthopyroxene-sillimanite granulites from Forefinger Point, Enderby Land, Antarctica: implications for the evolution of the Archaean Napier Complex. *J Metam. Geol., **8**: pp 591-613.*

HARPUM, J R (1963): petrographic classification of granitic rocks in Tanganyika by partial chemical analyses. *Records Geol. Surv. Tanganyika,* **10***: pp 80-88.*

HEINRICH, E Wm (1965): Microscopic identification of minerals. *McGraw-Hill, Inc., USA: 414p.*

HENDERSON, J R (1981): Structural analysis of sheath folds with horizontal X-axes, northeast Canada. *J. Struct. Geol., **3**: pp 203-210.*

HERZBERG, C (1992): Depth and degree of Melting of Komatiites. *J. Geophys. Res., **97**: No. B4, pp 4521-4540.*

HESSE, R (1988): Diagenesis 13 : Origin of chert : diagenesis of biogenic siliceous sediments. *Geosci. Can., **15**: pp 171- 193.*

HOBBS, B E, MEANS, W D and WILLIAMS, P E (1976): An outline of structural geology. *Wiley International Edition. J Wiley & Sons, New York, NY: 571p.*

HOWELL, D G (1995): Principles of Terrane Analysis. New Applications for Global Tectonics. *2nd Edition. Chapman and Hall, London: 245p.*

HUGHES, C J and HUSSEY, E M (1976): Mn and Mg values in igneous rocks: proposed usage and a comment on currently employed Fe_2O_3 corrections. *Geochim. Cosmochim. Acta., **40**: pp 485-486.*

HUNTER, D R, SMITH, R G and SLEIGH, D W W (1992): Geochemical studies of Archaean granitoid rocks in the Southwestern Kaapvaal Province: implications for crustal development. *Journ. Afr. Earth Sci., **15**: pp 127-151.*

HUTTON, D H W and REAVY, R J (1992): Strike-slip tectonics and granite petrogenesis. *Tectonics, **11**: pp 960-967.*

HUTTON, D H W, DEMPSTER, T J, BROWN, P E and BECKER, S D (1990): A new mechanism of granite emplacement: intrusion in active extensional shear zones. *Nature, **343**: pp 452-455.*

HUTTON, D H W (1988): Igneous emplacement in a shear zone termination: biotite granite at Strontian, Scotland. *Geol. Soc. Amer. Bull., **100**: pp 1392-1399.*

HYNDMAN, D W (1985): Petrology of igneous and metamorphic rocks. 2nd Edition. *McGraw-Hill Book Company, New York: 786p.*

IRVINE, T N and BARAGAR, W R A (1971): A Guide to the Chemical Classification of the Common Volcanic Rocks. *Can. Jour. of Earth Sci., **8**: pp 523-548.*

ISLEY, A E (1995): Hydrothermal Plumes and the delivery of iron to Banded Iron Formations. *J. Geol., **103**: pp 169-185.*

JANECKY, D R and SEYFRIED, W E (1986): Hydrothermal serpentinisation of peridotite within the oceanic crust: experimental investigations of mineralogy and major element geochemistry. *Geochim. et Cosmochim. Acta., **80**: pp 1357-1378.*

JARVIS, G T and CAMPBELL, I H (1983): Archaean komatiites and geotherms: Solution to an apparent contradiction. *Geophysical Research Letters, **10**: pp 1133-1136.*

JONES, M G 1990): The geology of the Mt Mare area, Pietersburg Greenstone Belt, South Africa. *Unpubl. Ph.D thesis, Univ. of London: 297p.*

KAY, R W, HUBBARD, N J and GAST, P W (1970): Chemical characteristics and origin of oceanic ridge volcanic rocks. *J. Geophys. Res., **75**: pp 1585-1613.*

KENNEDY, W Q (1933): Trends of differentiation in basaltic magmas. *Amer. J. Sci., **25**: pp 239-256.*

KIMBERLEY, M M (1978): Palaeo-environmental classification of iron formations. *Econ. Geol., **73**: pp 215-229.*

KIMBERLEY, M M (1979): Geochemical distinctions among environmental types of iron formations. *Chemical Geology: **25**: pp 185-212.*

KIMBERLEY, M M (1989): Exhalative origins of iron formations. *Ore Geology Reviews, **5**: pp 13-145.*

KUSKY, T M (1989): Accretion of the Archaean Slave Province. *Geology, **17**: pp 63-67.*

KUSKY, T M (1993): Collapse of Archaean orogens and the generation of late- to post-kinematic granitoids. *Geology, **21**: pp 925-928.*

KUSKY, T M and KIDD, W S F (1992): Remnants of an Archaean oceanic plateau, Belingwe greenstone belt, Zimbabwe. *Geology, **20**: pp 43-46.*

LACASSIN, R and MATTAUER, M (1985): Kilometre-scale sheath folds at Mattmark and implications for transport directions in the Alps. *Nature, **315**: pp 739-741.*

LAFLÈCHE, M R, DUPUY, C and DOSTAL, J (1992): Theoleiitic volcanic rocks of the late Archaean Blake River Group, southern Abitibi greenstone belt: origin and geodynamic implications. *Can. J. Earch Sci., **29**: pp 1448-1458.*

LE MAITRE, R W (1976): A new approach to the classification of igneous rocks using the basalt-andesite-dacite-rhyolite suite as an example. *Contrib. Mineral. Petrol., **56**: pp 191-203.*

LEMON, R P (1990): Principles of Stratigraphy. *Merrill Publishing Company, Columbus.*

LINSTRÖM, W (1987): The geology of the Dundee Area. *Expl. of Sheet 2830, Scale 1:250 000. Geol. Surv. of S.Africa.*

LINSTRÖM, W and MATTHEWS, P E (1990a): Hlathini Formation. ***In*** M R Johnson (Editor): Catalogue of South African Lithostratigraphic Units. *S.A. Committee for Stratigraphy.*

LINSTRÖM, W and MATTHEWS, P E (1990b): Mabaleni Formation. ***In:*** *M R Johnson (Editor): Catalogue of South African Lithostratigraphic Units. S A Committee for Stratigraphy.*

LISTER, G S and SNOKE, A W (1984): S-C mylonites. *J. Struct. Geol.,* ***6****: pp 617-638.*

LOWE, D R, BYERLY, G R, RANSOM, B L and NOCITA, B W (1985): Stratigraphic and sedimentological evidence bearing on structural repetition in early Archaean rocks of the Barberton greenstone belt, South Africa. *Precambrian Res.,* ***27****: pp 165-186.*

LOWE, D R and BYERLY, G R (1986): Archaean flow-top alteration zones formed initially in a low-temperature sulphate-rich environment. *Nature,* ***324****:* pp 245-248.

LOWE, D R (1994): Accretionary history of the Archaean Barberton Greenstone Belt (3.55 - 3.22 Ga), Southern Africa. *Geology,* ***22****: pp 1099-1102.*

MACKENZIE, W S and GUILFORD, C (1981): Atlas of rock-forming minerals in thin section. *Longman Group Ltd., USA: 98p.*

MACKENZIE, W S, DONALDSON, C H and GUILFORD, C (1982): Atlas of igneous rocks and their textures. *Longman Group Ltd., USA: 148p.*

MANIAR, P D and PICCOLI, P M (1989): Tectonic discrimination of granitoids. *Geol. Soc. Am. Bull.,* ***101****: pp 635-643.*

MARTIN, H (1987): Petrogenesis of Archaean trondhjemites, tonalites and granodiorites from eastern Finland: major and trace element geochemistry. *J. Petrol.,* ***28****: pp 921-953.*

MARTYN, J E (1986): Evidence for structural stacking and repetition in the Greenstones of the Kalgoorlie District, Western Australia. ***In*** M J de Wit and L D Ashwal; (Editors): Workshops on the Tectonic Evolution of Greenstone Belts (Abstracts). *LPI Technical Report 86-10.*

MARTYN, J E and JOHNSON, G I (1986): Geological setting and origin of fuchsite-bearing rocks near Menzies, Western Australia. *Austr. J. Earth Sciences,* ***33****, pp 1-18.*

MASON, R (1985): Petrology of the Metamorphic rocks. 5th Impression. *George Allen & Unwin, London: 254p.*

MATTAUER, M, FAURE, M and MALAVIEILLE, J (1981): Transverse lineation and large-scale structures related to Alpine obduction in Corsica. *J. Struct. Geol.,* ***3****: pp 401-409*

MATTHEWS, P E (1958): The succession, metamorphism and tectonics of the pre-Cape formations in southwest Zululand, Natal. *Ph.D thesis (unpubl) Univ. of Natal, Durban: 173p.*

MATTHEWS, P E (1959): The metamorphism and tectonics of the pre-Cape formation in the post-Ntingwe Thrust Belt, S W Zululand, Natal. *Trans. Geol. Soc. S.Africa,* ***62****: pp 258-322.*

MATTHEWS, P E (1972): Possible Precambrian obduction and plate tectonics in Southeast Africa. *Nature, **240**: pp 37-39.*

MATTHEWS, P E (1981): Eastern or Natal sector of the Namaqua-Natal mobile belt in Southern Africa. ***In*** D R Hunter (Editor) (1981): Precambrian of the Southern Hemisphere. Developments in Precambrian Geology. *Elsevier Scientific Publishing Company, Amsterdam.*

MATTHEWS, P E and CHARLESWORTH E G (1981): National Geodynamics Project: northern margin of the Namaqua-Natal Mobile Belt in Natal: Geol. Map Scale 1:140 000. *Univ. of Natal, Durban.*

MATTHEWS, P E, CHARLESWORTH, E G, EGLINGTON, B M and HARMER, R E (1989): A minimum 3.29 Ga age for the Nondweni greenstone complex in the southeastern Kaapvaal Craton, South Africa. *J. Geol., **92**: pp 272-278.*

MEL'NIK, Yu P (1982): Precambrian Banded Iron Formations. *Elsevier Scientific Publishing Company, Amsterdam.*

MEL'NIK, Yu P and RADCHUK, V V (1977): The stability of grunerite - $Fe_7Si_8O_{22}(OH)_2$. *Geokhimiya (Geochemistry), **5**: pp 693-704.*

MIES, J W (1993): Structural analysis of sheath folds in the Sylacauga Marble Group, Talladega Slate Belt, southern Appalachians. *J. Struct. Geol, **15**: pp 983-993.*

MILLER, G H, STOLPER, E M and AHRENS, T J (1991a): The equation of state of a molten komatiite, 1, shock wave compression to 36 GPa. *J. Geophys. Res., **96**: pp 11831-11848.*

MILLER, G H, STOLPER, E M and AHRENS, T J (1991b): The equation of state of a molten komatiite, 2, application to komatiite petrogenesis and the Hadean mantle. *J. Geophys. Res., **96**: pp 11849-11864.*

MINNIGH, L D (1979): Structural analysis of sheath folds in a meta-chert from the Western Italian Alps. *J. Struct. Geol., **1**: pp 275-282.*

MITRA, G (1978): Ductile deformation zones and mylonites: the mechanical processes involved in the deformation of crystalline basement rocks. *Am. Jour. Sci., **278**: pp 1057-1084.*

MIYASHIRO, A (1973): Metamorphism and metamorphic belts. *George Allen and Unwin, London: 492p.*

MIYASHIRO, A (1975): Classification, characteristics and origin of ophiolites. *J. Geol., **83**: pp 249-281.*

MIYASHIRO, A and SHIDO, F (1975): Tholeiitic and calc-alkalic series in relation to the behaviours of titanium, vanadium and nickel. *Am. Jour. Sci., **275**: pp 265-277.*

MOORHOUSE, W W (1959): The study of rocks in thin section. *Harper and Row Publishers, New York, USA: 514p.*

MORAND, V J and GRAY, D R (1991): Major fault zones related to the Omeo Metamorphic Complex, northeastern Victoria, Australia. *Jour of Earth Sciences, **38**: pp 203-221.*

MORAND, V J (1992): Pluton emplacement in a strike-slip fault zone: the Doctors Flat Pluton, Victoria, Australia. *J. Struct. Geol., **14**: pp 205-213.*

MYERS, J S (1976): Granitoid sheets, thrusting, and Archaean crustal thickening in West Greenland. *Geology, **4**: pp 265-258.*

NOCKOLDS, S R (1954): Average chemical composition of some igneous rocks. *Geol. Soc. Am. Bull., **65**: pp 1007-1032.*

PARIS, I, STANISTREET, I G and HUGHES, M J (1985): Cherts of the Barberton Greenstone Belt interpreted as products of submarine exhalative activity. *J.Geol., **93**: pp 111-130.*

PASSCHIER, C W (1986): Flow in natural shear zones. *Earth Planet. Sci. Lett., **77**: pp 70-80.*

PASSCHIER, C W, MYERS, J S and KRÖNER, A (1990): Field Geology of high-grade Gneiss Terrains. *Springer-Verlag, Berlin Heidelberg, Germany: 150p.*

PATERSON, S R, TOBISCH, O T and MORAND, V J (1990): The influence of large ductile shear zones on the emplacement and deformation of the Wyangala Batholith, S.E. Australia. *J. of Struct. Geol., **12**: pp 639-650.*

PEARCE, J A, HARRIS, N B W and TINDLE, A G (1984): Trace element discrimination diagrams for the tectonic interpretation of granitic rocks. *J. Petrol. **25**: pp 956-983.*

PEARTON, T N (1982): Gold and antimony mineralization in altered komatiites of the Murchison greenstone belt, South Africa. ***In*** Komatiites, edited by N T Arndt and E G Nisbet. *George Allen & Unwin, London: 526p.*

PHILPOTTS, A R (1989): Petrography of Igneous and Metamorphic Rocks. *Prentice-Hall Inc., Englewood Cliffs, New Jersey: 178p.*

PHILPOTTS, A R (1990): Principles of Igneous and Metamorphic Petrology. *Prentice- Hall, Englewood Cliffs, New Jersey: 498p.*

PLATT, J P (1983): Progressive refolding in ductile shear zones. *J. Struct. Geol., **5**: pp 619-622.*

PLATT, J P and VISSERS, R L M (1980): Extensional structures in anisotropic rocks. *J. of Struct. Geol. **2**: pp 397-410.*

PRICE, N J and COSGROVE, J W (1990): Analysis of Geological Structures. *Press Syndicate Publisher, University of Cambridge: 502p.*

QUINQUIS, H, AUDREN, C, BRUN, J P and COBBOLD, P R (1978): Intense progressive shear in Ile de Croix blueschists and compatibility with subduction or obduction. *Nature, **273**: pp 43-45.*

RAMSAY, J G (1967): Folding and Fracturing of Rocks. *McGraw-Hill Book Company, New York: 569.*

RAMSAY, J G (1980): Shear Zone geometry: a review. *J. Struct. Geol., **2**: pp 83-99.*

RAMSAY, J G and HUBER, M I (1983): The techniques of Modern Structural Geology Vol. 1: Strain analysis. *Academic Press Inc., London: 307p.*

RAMSAY, J G and HUBER, M I (1987): The techniques of Modern Structural Geology, Vol. 2: Folds and Fractures. *Academic Press Inc., London: pp 309-700.*

READING, H G (EDITOR) (1982): Sedimentary Environments and Facies. *Blackwell Scientific Publications, Oxford: 569p.*

REIMOLD, W U, MEYER, F M, WALRAVEN, F and MATTHEWS, P E (1993): Geochemistry and chronology of pre- and post-Pongola granitoids from northeastern Natal. *16th Colloquium of African Geology, Extended Abstracts, Vol. 2. Compiled by R Maphalala and M Mabuza, Geol. Surv. and Mines, Mbabane, Swaziland: 382p.*

RHODES, S and GAYER, R A (1977): Non-cylindrical folds, linear structures in the X-direction, and mylonite developed during translation of the Caledonian Kalak Nappe Complex of Finnmark. *Geol. Mag., **114**: pp 329-342.*

RIDLEY, J (1986): Parallel stretching lineations and fold axes oblique to the shear displacement direction - a model and observations. *J. Struct. Geol., **8**: pp 647-653.*

RIDLEY, J R and KRAMERS, J D (1990): The evolution and tectonic consequences of a tonalitic magma layer within Archaean continents. *Can. J. Earth Sci., **27**: pp 219-228.*

ROBERTS, J L (1984): Introduction to Geological Maps and Structures. *Pergamon Press, Oxford, England: 332p*

ROBERTS, M P and CLEMENS, J D (1993): Origin of high-potassium, calc-alkaline, I-type granitoids. *Geology, **21**, pp 825-828.*

ROGERS, J W and GREENBERG, J K (1990): Late-orogenic, post-orogenic and anorogenic granites: distinction by major-element and trace-element chemistry and possible origins. *J. Geol., **98**: pp 291-309.*

RYKKELID, E and FOSSEN, H (1992): Composite fabrics in mid-crustal gneisses: observations from the Øygarden Complex, West Norway Caledonides. *J. Struct. Geol., **14**: pp 1-9.*

SANDERSON, D J and MARCHINI, W R D (1984): Transpression. *J. Struct. Geol., **6**: pp 449-458.*

SHELLEY, D (1993): Igneous and Metamorphic Rocks under the Microscope. 2nd Edition. *Chapman & Hall, London: 445p.*

SIMPSON, C and WINTSCH, R P (1989): Evidence for deformation-induced K-feldspar replacement by myrmekite. *J. Metamorphic Geol., **1**: pp 261-275.*

SKJERNAA, L (1989): Tubular folds and sheath folds: definitions and conceptual models for their development, with examples from the Grapesvare area, northern Sweden. *J. of Struct. Geol.*, ***11***: *pp 689-703.*

SLEIGH, D W W (1988): The geology of the Archaean Terrane in the Piet Retief district, Transvaal. *M.Sc. Thesis (unpubl), Univ. Natal, Pietermaritzburg, S Africa: 208p.*

SMALLEY, T J (1980): Structure and Metamorphism of the Tugela Group within the Northern Zone of the Natal Mobile Belt. *Ph.D thesis (unpubl), Univ. of Natal, Durban: 220p.*

SPEER, J A, McSWEEN, Jr. H Y and GATES, A E (1994): Generation, Segregation, Ascent and Emplacement of Alleghanian Plutons in the southern Appalachians. *Jour. Geology,* ***102****: pp 249-267.*

STERN, R A and HANSON, G N (1991): Archaean high-Mg granodiorite: a derivative of light rare earth element-enriched monzodiorite of mantle origin. *J. Petrol.,* ***32****: pp 201-238.*

STICE, G D (1968): Petrography of the Manuá Islands, Samoa. *Contrib. Mineral. Petrol.,* ***19****: pp 343-357.*

STOREY, M, MAHONEY, J J, KROENKE, L W and SAUNDERS, A D (1991): Are oceanic plateaus sites of komatiite formation? *Geology,* ***19****: pp 376-379.*

STRECKEISEN, A L (1973): Plutonic Rocks. Classification and nomenclature recommended by the I.U.G.S. Subcommission on the Systematics of Igneous Rocks. *Geotimes,* ***18****: pp 26-30.*

SUWA, K, MIZUTINI, S and TSUZUKI, Y (1974): Proposed optical twinning method of determining the laws of plagioclase. *Mem. Geol. Soc., Japan,* ***11****: pp 167-250.*

TAIRA, A, PICKERING, K T, WINDLEY, B F and SOH, W (1992): Accretion of Japanese Island Arcs and implications for the origin of Archaean greenstone belts. *Tectonics,* ***11****: pp 1224-1244.*

TARNEY, J (1975): Geochemistry of Archaean high-grade gneisses, with implications as to the origin and evolution of the Precambrian crust. ***In*** Windley, B F (Editor): The early history of the Earth. *John Wiley and Sons, London, 619p.*

TERRY, R D and CHILLINGAR, G V (1955): Charts for estimating percentage composition of rocks and sediments. *Jour. Sed. Petr.,* ***25****: pp 229-234.*

THOMPSON, R N, ESSOU, J and DUNHAM, A C (1972): Major element chemical variation in the Eocene lavas of the Isle of Skye, Scotland. *J. Petrol.,* ***13****: pp 219-252.*

TILLEY, C E (1950): Some aspects of magmatic evolution. *Quart. J. Geol. Soc., London,* ***106****: pp 37-61.*

TOBISCH, O T (1966): Large-scale basin-and-dome pattern resulting from the interference of major folds. *Geol. Soc. Am. Bull.* ***77****: pp 393-408.*

TREAGUS, J E and TREAGUS, S H (1981): Folds and the strain ellipsoid: a general model. *J. of Struct. Geol.* ***3****: pp 1-17.*

TULLIS, J T, SNOKE, A W and TODD, V R (1982): Significance of petrogenesis of mylonitic rocks. *Geology* ***10****: pp 227-230.*

TURNER, F J (1981): Metamorphic Petrology: Mineralogical, Field and Tectonic Aspects. Second Edition. *McGraw-Hill Book Company, New York: 524p.*

TURNER, F J and WEISS, L E (1963): Structural analysis of Metamorphic tectonites. *McGraw-Hill Book Company, San Francisco, USA: 545p.*

VEARNCOMBE, J R, BARTON, Jr. J M and VAN REENEN, D D (1986): Greenstone Belts: their components and structure. *pp 214-220.* ***In*** *M J de Wit and L D Ashwal (Editors): Workshop on the tectonic evolution of greenstone belts (abstracts), LPI Technical Report 86-10.*

VERNON, R H (1983): Metamorphic processes: reactions and microstructure development. 2nd Impression. *George Allen and Unwin, London: 247p.*

VERSFELD, J A (1988): The geology of the Nondweni Greenstone Belt, Natal. *Ph.D thesis (unpubl.) Univ. of Natal, Pietermaritzburg: 298p.*

VERSFELD, J A and WILSON, A H (1992a): Nondweni Group. ***In:*** *M R Johnson (Editor): Catalogue of South African Lithostratigraphic Units. SA Committee for Stratigraphy: pp 19-20.*

VERSFELD, J A and WILSON, A H (1992b): Magongolozi Formation. ***In:*** *M R Johnson (Editor): Catalogue of South African Lithostratigraphic Units. SA Committee for Stratigraphy: pp 7-9.*

VERSFELD, J A and WILSON, A H (1992c), Toggekry Formation. ***In:*** *M R Johnson (Editor): Catalogue of South African Lithostratigraphic Units. SA Committee for Stratigraphy: pp 29-30.*

VERSFELD, J A and WILSON, A H (1992d): Witkop Formation: ***In:*** *M R Johnson (Editor): Catalogue of South African Lithostratigraphic Units. SA Committee for Stratigraphy: pp 35-37.*

VILJOEN, M J, VILJOEN, R P and PEARTON, T N (1982): The nature and distribution of Archaean komatiite volcanics in South Africa. ***In:*** *N T Arndt and E G Nisbet (Editors), Komatiites. Allen and Unwin, London: pp 53-79.*

WAHLSTRÖM, E E (1966): Optical Crystallography. 3rd Edition. *John Wiley & Sons, Inc., USA: 356p.*

WALKER, R G (1978): A critical appraisal of Archaean basin-craton complexes. *Can. J. Earth Sci.* ***15****: pp 1213-1218.*

WALL, V J, CLEMENS, J D and CLARKE, D B (1987): Models for granitoid evolution and source compositions. *J. Geol.,* ***95****: pp 731-749.*

WELLS, G, BRYAN, W B and PEARCE, T H (1979): Comparative morphology of ancient and modern pillow lavas. *J. Geol.* ***87****: pp 427-440.*

WHITE, A J R and CHAPPELL, B W (1983): Granitoid types and their distribution in the Lachlan Fold Belt, southeastern Australia. ***In*** A J Roddick (Editor): Circum - Pacific Plutonic Terranes, *Mem. Geol. Soc. Am., **159**: pp 21-34.*

WILLIAMS, G D (1978): Rotation of contemporary folds into the X-direction during overthrust processes in Laksefjord, Finnmark. *Tectonophysics, **48**: pp 29-40.*

WILLIAMS, H, TURNER, F J and GILBERT, C M (1982): Petrography: An introduction to the study of rocks in thin sections. 2nd Edition. *W H Freeman & Co., USA: 626p.*

WILSON, A H and VERSFELD, J A (1994a): The early Archaean Nondweni greenstone belt, southern Kaapvaal Craton, South Africa, Part I. Stratigraphy, sedimentology, mineralization and depositional environment. *Precambrian Research, **67**: pp 243-276.*

WILSON, A H and VERSFELD, J A (1994b): The early Archaean Nondweni greenstone belt, southern Kaapvaal Craton, South Africa, Part II. Characteristics of the volcanic rocks and constraints on magma genesis. *Precambrian Research, **67**: pp 277-320.*

WINKLER, H G F (1974): Petrogenesis of Metamorphic Rocks. *Springer Verlag, 254p.*

WINKLER, H G F (1979): Petrogenesis of Metamorphic Rocks. Fifth Edition. *Springer Verlag, 348p.*

WOODCOCK, N H and FISCHER, M (1986): Strike-slip duplexes. *J. of Struct. Geol., **8**: pp 725-735.*

YAMAGASHI, H (1985): Growth of pillow lobes: Evidence from pillow lavas of Hokkaido, Japan, and North Island, New Zealand. *Geology **13**: pp 499-502.*